

Author's declaration

At no time during the registration for the degree of Doctor of Philosophy has the author, Luis Felipe Opazo Mella, been registered for any other University award without prior agreement of the Graduate Committee.

This study was financed with the aid of CONICYT, an official body of the Chilean government and the ALBAN Program of European community scholarships. A programme of advanced study was undertaken, which included the extensive reading of literature relevant to the research project and attendance at international conferences on:

NATIONAL SCIENCE FOUNDATIONS, Paleobiology Database Summer Course in Analytical Paleobiology, National Center for Ecological Analysis and Synthesis University of California, Santa Barbara, USA.

Opazo, L.F., R. Twitchett, & L. Mander, 2008. Mass extinction: Triassic-Jurassic (Tr-J) example of one biotic crisis in marine ecosystems. 1ra Reunión de la Sociedad de Paleontología de Chile, Museo de Historia Natural, Santiago, Chile.

Opazo, L.F., R.J. Twitchett & L. Mander. 2008. Filling the ecospace in the Mesozoic: changes in the modes of life of marine organisms, 52nd Annual meeting of the Paleontological Association, University of Glasgow, Glasgow, Scotland.

Opazo, L.F., R.J. Twitchett & L. Mander. 2009. Changes in Ecological Traits in Marine Organisms through the Early Mesozoic. 9th North America Paleontological convention, University of Cincinnati, Ohio, USA.

Opazo, L.F., R.J. Twitchett. 2009. Recovery after Triassic–Jurassic mass extinction (Tr-J): An evaluation of the richness, composition, and ecological traits in the marine fauna. 53rd Annual meeting of the Paleontological Association, University of Birmingham, Birmingham, England.

Buono, G., L.F. Opazo, B. Metcalfe, M. Schemm-Gregory & R.J. Twitchett. 2009. Palaeobiogeographical and palaeoecological brachiopod trends during the Permian–Triassic (P–Tr) and Triassic–Jurassic (Tr–J) mass extinction events. 53rd Annual meeting of the Paleontological Association, University of Birmingham, Birmingham, England.

Opazo, L.F., R.J. Twitchett, A.J. Jeram, I. Enlander & M. Simms. 2010. Using rank-abundance curves to evaluate the palaeoecological response of marine benthic communities to the Late Triassic mass extinction event. The 3th International Palaeontological Congress (IPC3), Imperial College and The Natural History Museum, London, England.

Twitchett, R.J., L.F. Opazo, A. Rubilar, G. Chong, F. A. Mourgues. 2010. Temporal and spatial variation in the paleocommunity structure of Late Triassic coral reefs from Northern Chile, Annual Meeting of the Geological Society of America, Denver, Colorado, USA.

Opazo, L.F., R.J. Twitchett, A. Rubilar, G. Chong, F.A. Mourgues. 2010. Temporal and spatial variation in the palaeocommunity structure of Late Triassic coral reefs from Northern Chile. 2da Reunión de la Sociedad de Paleontología de Chile, Universidad de Concepción, Concepción, Chile.

The author has engaged in learning and teaching at the University of Plymouth in courses such as: EOE 1102 - Earth History; and EOE 2103 - The Evolving Earth. School of Geography, Earth and Environmental Sciences (Faculty of Science and Technology).

COPYRIGHT © 2012 Luis Felipe Opazo Mella, this copy of the thesis has been supplied on the condition that anyone who consults it recognises that its copyright belongs to its author and that no quotation from the thesis and no information derived from it may be published without referencing the source.

Paragraphs or larger bodies of text may not be published without the author's prior consent.

Word count of the main body of the thesis: 55,664.

A handwritten signature in blue ink, appearing to be 'Luis Felipe Opazo Mella', written over a light blue grid background.

Signed :

.....

Date : 27/01/2012

**EXTINCTION AND RECOVERY DYNAMICS OF TRIASSIC-
JURASSIC MACRO-INVERTEBRATE COMMUNITIES**

By

LUIS-FELIPE OPAZO MELLA

A thesis submitted to the University of Plymouth
In partial fulfilment of the degree of

DOCTOR OF PHILOSOPHY

Faculty of Science and Technology
School of Geography, Earth and Environmental Sciences

January 2012

Table of Contents

AUTHOR'S DECLARATION	1
ACKNOWLEDGEMENTS	1
ABSTRACT	2
CHAPTER 1 INTRODUCTION	4
1.1 BRIEF HISTORY OF MASS EXTINCTIONS	4
<i>Figure 1.1</i>	4
<i>Figure 1.2</i>	5
1.2 THE TRIASSIC–JURASSIC (TR/J) BOUNDARY: STRATIGRAPHICAL FRAMEWORK	7
1.3 PALAEOGEOGRAPHY AND CLIMATE ACROSS THE TR/J BOUNDARY	10
<i>Figure 1.3.</i>	11
<i>Figure 1.4.</i>	20
1.4 POTENTIAL CAUSES OF TR/J MASS EXTINCTIONS	21
CLIMATIC CHANGES.....	22
BOLIDE IMPACT	23
CAMP VOLCANISM	24
<i>Figure 1.5</i>	25
SEA LEVEL CHANGE	26
1.5 PALAEOENVIRONMENTAL SCENARIO DURING THE TR/J BOUNDARY: CO₂ OUTGASSING	28
1.6 FAUNAL EXTINCTIONS	30
<i>Figure 1.6</i>	30
<i>Figure 1.7</i>	31
1.7 IMPORTANT FAUNAL GROUPS	32
1.8 ECOLOGICAL EFFECTS, SELECTIVITY, EXTINCTION AND RECOVERY	34
1.9 STATEMENT AND OBJECTIVES	40
CHAPTER 2 METHODOLOGY	45
2.1 STUDY APPROACH	45
2.2 STUDY SITES	45
2.2.1 SOUTHWEST UK	45
<i>Figure 2.1</i>	46
<i>Figure 2.2</i>	47
2.2.2 NORTHERN IRELAND	48
2.2.3 NORTHERN CHILE	48
2.3 METHODOLOGY OF SAMPLING	49
2.4 DATA ANALYSIS	50
2.4.1 RICHNESS	50
2.4.2 ABUNDANCE	52
<i>Figure 2.3.</i>	54
2.4.3 COMPOSITION	55
2.4.4 ECOSPACE.....	56
2.4.5 TRACE FOSSILS	57
<i>Figure 2.4</i>	59
<i>Figure 2.5</i>	60
<i>Figure 2.6</i>	61
2.4.6 BODY SIZE.....	61
<i>Figure. 2.7.</i>	62
<i>Figure 2.8</i>	64

CHAPTER 3 ECOSPACE AND ECOLOGICAL TRENDS OF MARINE ORGANISMS THROUGH THE LATE PALAEOZOIC AND EARLY MESOZOIC	65
3.1 INTRODUCTION.....	65
<i>Table 3.1</i>	66
3.2 DATABASE AND METHODS	68
<i>Figure 3.1</i>	70
<i>Table 3.2</i>	71
3.3 RESULTS AND DISCUSSION.....	72
<i>Figure 3.2</i>	72
3.3.1 ECOSPACE THROUGH THE PHANEROZOIC.....	73
<i>Figure 3.3</i>	73
<i>Figure 3.4</i>	74
3.3.2 LATE PERMIAN	75
3.3.3 EARLY TRIASSIC.....	76
<i>Figure 3.5</i>	77
<i>Figure 3.6</i>	80
3.3.4 MIDDLE TRIASSIC	81
3.3.5 LATE TRIASSIC	82
3.3.6 EARLY JURASSIC	83
3.4 DIVERSITY AND ECOLOGICAL DIVERSITY	84
<i>Figure 3.7</i>	85
<i>Figure 3.8</i>	87
3.5 MASS EXTINCTION EVENTS AND ECOLOGICAL SPACE	93
3.5.1 PERMIAN/TRIASSIC MASS EXTINCTION.....	94
<i>Figure 3.9</i>	95
3.5.2 END TRIASSIC MASS EXTINCTION	97
<i>Figure 3.10</i>	100
<i>Figure 3.11</i>	101
3.6 MASS EXTINCTION AND ECOSPACE	105
3.7 CONCLUSIONS	110
CHAPTER 4 ST AUDRIE'S BAY SECTION.....	112
4.1 GEOLOGICAL SETTING	112
4.1.1 THE WESTBURY FORMATION.....	112
4.1.2 THE COTHAM MEMBER.....	113
<i>Figure 4.1</i>	114
4.1.3 THE LANGPORT MEMBER	113
4.1.4 THE BLUE LIAS FORMATION	114
4.2 RICHNESS.....	115
4.2.1 LIMESTONE SAMPLES	115
<i>Figure 4.2</i>	117
<i>Figure 4.3</i>	118
<i>Figure 4.4</i>	119
4.2.2 MUDSTONE SAMPLES.....	119
<i>Figure 4.5</i>	121
4.3 ABUNDANCE	122
4.3.1 LIMESTONE SAMPLES	122
<i>Figure 4.6</i>	124
4.3.2 MUDSTONE SAMPLES.....	126
<i>Figure 4.7</i>	127
<i>Table 4.1</i>	128
<i>Figure 4.8</i>	129
4.4 COMPOSITION	131

4.4.1	LIMESTONE SAMPLES	131
	<i>Figure 4.9</i>	132
4.4.2	MUDSTONE SAMPLES.....	134
	<i>Figure 4.10</i>	135
4.4.3	MUDSTONE AND LIMESTONE COMPARISON.....	136
4.5	ECOSPACE	136
	<i>Figure 4.11</i>	139
	<i>Figure 4.12</i>	140
4.6	BODY SIZE	142
	<i>Figure 4.13</i>	143
	<i>Figure 4.14</i>	147
	<i>Figure 4.15</i>	148
	<i>Table 5.2</i>	149
	<i>Figure 4.16</i>	151
4.7	TRACE FOSSILS	151
	<i>Figure 4.17</i>	152
	<i>Figure 4.18</i>	154
4.8	SUMMARY	155
CHAPTER 5	PINHAY BAY SECTION	157
5.1	GEOLOGICAL SETTING	157
5.1.1	THE LANGPORT MEMBER	157
	<i>Figure 5.1</i>	158
5.1.2	THE BLUE LIAS FORMATION	159
5.2	RICHNESS	161
5.2.1	LIMESTONE SAMPLES	161
	<i>Figure 5.2</i>	162
5.2.2	MUDSTONE SAMPLES.....	163
	<i>Figure 5.3</i>	164
	<i>Figure 5.4</i>	165
	<i>Figure 5.5</i>	166
5.3	ABUNDANCE	167
5.3.1	LIMESTONE SAMPLES	167
	<i>Figure 5.6</i>	169
	<i>Figure 5.7</i>	170
5.3.2	MUDSTONE SAMPLES.....	170
	<i>Table 5.1</i>	172
	<i>Figure 5.8</i>	173
5.3.3	SPECIES DOMINANCE INDEX.....	174
5.4	COMPOSITION	174
5.4.1	LIMESTONE SAMPLES	174
	<i>Figure 5.9</i>	175
5.4.2	MUDSTONE SAMPLES.....	176
	<i>Figure 5.10</i>	177
5.5	ECOSPACE	178
	<i>Figure 5.11</i>	179
	<i>Figure 5.12</i>	181
5.6	BODY SIZE	183
	<i>Figure 5.13</i>	184
	<i>Figure 5.14</i>	185

Figure 5.15	186
Figure 5.16	188
Table 5.2	189
Figure 5.17	190
5.7 TRACE FOSSILS	191
Figure 5.18	192
5.8 SUMMARY	193
CHAPTER 6 LARNE SECTION	195
6.1 GEOLOGICAL SETTING	195
6.1.1 THE WESTBURY FORMATION	195
6.1.2 THE COTHAM MEMBER	195
6.1.3 THE LANGPORT MEMBER	196
6.1.4 THE LIAS GROUP	197
6.2 RICHNESS	197
Figure 6.1	198
Figure 6.2	199
Figure 6.3	201
Figure 6.4	202
Figure 6.5	203
6.3 ABUNDANCE	203
Figure 6.6	204
Figure 6.7	205
Table 6.1	206
Figure 6.8	208
6.4 COMPOSITION	208
Figure 6.9	209
Figure 6.10	211
6.5 ECOSPACE	212
Figure 6.11	213
Figure 6.12	214
6.6 BODY SIZE	216
Figure 6.13	217
Figure 6.14	218
Figure 6.15	219
Table 6.2	220
Figure 6.16	222
Figure 6.17	223
6.7 SUMMARY	223
CHAPTER 7 PORTEZUELO PROVIDENCIA SECTION	225
7.1 GEOLOGICAL SETTING	225
Figure 7.1	225
Figure 7.2	226
Figure 7.3	227
7.2 SPECIES RICHNESS	230
Figure 7.4	231
Figure 7.5	232
Figure 7.6	232

7.3 ABUNDANCE	233
<i>Figure 7.7</i>	233
<i>Figure 7.8</i>	234
<i>Table 7.1</i>	235
<i>Figure 7.9</i>	236
7.4 COMPOSITION	236
<i>Figure 7.10</i>	237
7.5 ECOSPACE	237
<i>Figure 7.11</i>	238
<i>Figure 7.12</i>	239
CHAPTER 8 DISCUSSION.....	240
8.1 TIMING, RECOVERY AND SPECIES RICHNESS PATTERNS THROUGH THE TR/J MASS EXTINCTION EVENT.	240
8.2 ABUNDANCE AND SPECIES COMPOSITION	247
8.3 ECOSPACE	254
8.4 ENVIRONMENTAL FACTORS RELATED TO THE EXTINCTION EVENT: SEA LEVEL FALL, CO₂ INCREASE, OR FACTOR COMBINATIONS.....	257
8.5 BODY SIZE	259
8.6 TR/J IN CHILE.....	263
8.7 GEOGRAPHICAL VARIATION OF THE TR/J EXTINCTION EVENT.....	266
CONCLUSIONS.....	269
REFERENCES	272
APPENDIX 1.1.....	300
APPENDIX 1.2.....	301
APPENDIX 1.3.....	302
APPENDIX 2.1.....	305
APPENDIX 2.2.....	306
APPENDIX 2.3.....	307
APPENDIX 2.4.....	308
2.41 <i>Species dominance index estimation:</i>	308
2.42 <i>Kurtosis:</i>	308
2.43 <i>Null Models:</i>	308
2.44 <i>Randomisation (permutation):</i>	309
2.45 <i>Non-metric Multidimensional scaling (nMDS):</i>	309
APPENDIX 3.1.....	310
APPENDIX 3.2.....	311
APPENDIX 3.3.....	319
APPENDIX 3.4.....	320
APPENDIX 4.1.....	321
APPENDIX 4.2.....	322
APPENDIX 4.3.....	323
APPENDIX 4.4.....	324
APPENDIX 4.5.....	325

APPENDIX 4.6.....	326
APPENDIX 4.7.....	327
APPENDIX 4.8.....	328
APPENDIX 4.9.....	329
APPENDIX 4.10.....	330
APPENDIX 4.11.....	331
APPENDIX 4.12.....	334
APPENDIX 4.13.....	335
APPENDIX 4.14.....	341
APPENDIX 4.15.....	343
APPENDIX 4.16.....	347
APPENDIX 4.17.....	352
APPENDIX 4.18.....	353
APPENDIX 5.1.....	355
APPENDIX 5.2.....	357
APPENDIX 5.3.....	358
APPENDIX 5.4.....	359
APPENDIX 5.5.....	360
APPENDIX 5.6.....	361
APPENDIX 5.7.....	362
APPENDIX 5.8.....	363
APPENDIX 5.9.....	364
APPENDIX 5.10.....	367
APPENDIX 5.11.....	368
APPENDIX 5.12.....	371
APPENDIX 5.13.....	373
APPENDIX 5.14.....	374
APPENDIX 5.15.....	377
APPENDIX 5.16.....	378
APPENDIX 6.1.....	380
APPENDIX 6.2.....	382
APPENDIX 6.3.....	383
APPENDIX 6.4.....	384
APPENDIX 6.5.....	385
APPENDIX 6.6.....	386
APPENDIX 6.7.....	387
APPENDIX 6.8.....	390
APPENDIX 6.9.....	391
APPENDIX 6.10.....	397

APPENDIX 6.11.....	398
APPENDIX 6.12.....	400
APPENDIX 6.13.....	401
APPENDIX 7.1.....	403
APPENDIX 7.2.....	404
APPENDIX 7.3.....	405
APPENDIX 7.4.....	406
APPENDIX 7.5.....	407
APPENDIX 7.6.....	408
APPENDIX 7.7.....	409
APPENDIX 7.8.....	412
APPENDIX 8.1.....	413

ACKNOWLEDGEMENTS

I would like to express my gratitude to a number of people, without whom the endeavour of writing this dissertation would have been much harder to accomplish.

First and foremost I would like to offer my sincerest gratitude to my supervisors, Dr. Richard Twitchett and Professor Malcolm Hart who have supported me throughout the process of writing my thesis with their patience and knowledge whilst allowing me the room to work in my own way.

Dr. Kevin Page deserves a special mention for his friendship as well as his useful comments in the field.

I would like to express my tremendous gratitude to Dr. Andrew Jeram for his assistance in the field and especially to the Dr. Ian Elander by his advices in the field and made a more pleasant my stay in North of Ireland.

Also, I would like to thank you to the Dr. Alfonso Rubilar and the Dr. Amaro Mourgues for their support in the fieldwork performed in Chile and the institution which they are part, Servicio Nacional de Geología y Minería, SERNAGEOMIN.

A big thank you to the friendly and cheerful group of individuals who I have had the pleasure to work with in my daily environment and who have helped me in various ways: Matt, Martha, el Loco Rob, Andy, Nikita, James and Sam. Invaluable support has also come from my PhD colleagues and friends Silvia Danise, Marie-Emilie Clemence, Marco Maffione and Chinwendu Elenwa: thank you!

Outside the university, there are others who deserve my gratitude Francois Chantret, Douwa Matt and Frederic Verret. My Chilean friends; Sebastian, Fabio, Hector, Christian, Arturo, Pelao, Karen, Karen Chica and Jose, and more locally, the members and extended members of the "Alien House": Musaab, Fred, Pepe, Martin, Claudio, Paul, Rob, Bill and Stephen.

My family, for international assistance, practical or other.

I want to thank specially to Claudy Op den Kamp, for her patience, understanding and unconditional support to carry on this work.

This works was supported by the Programme Alβan, the European Union Programme of High Level Scholarships for the Latin America, scholarship No (E07D402767CL) and CONICYT, Beca de Doctorado en el Extranjero por Gestión Propia 2007, given by the Chilean Government.

Abstract

This work is focused on characterising and evaluating the intensity and selectivity of the marine fauna during the Tr/J mass extinction and recovery of the ecosystem in different localities throughout Pangaea. To address this, four localities were studied: St. Audrie's Bay, Larne and Pinhay Bay in the UK, and Portezuelo Providencia in Chile. From each locality, samples were taken at approximately 1m intervals throughout the Tr/J sections. Species abundance per sample was estimated and each species was classified according to autoecological information derived from the literature. In order to assess changes in the structure and composition of the assemblages, NMDS and beta diversity index were performed, dominance and richness were estimated and the data were tested against five rank abundance (RAD) models. Ecospace modelling was used to estimate the loss in ecological diversity. Measures of the body size of bivalves and ichno-parameters were recorded on each section. Through the UK sections, the richness, dominance and the composition rate shifted abruptly during the extinction event. A geometric model shows the best fit during extinction events and, in contrast, a log-normal model best fits the pre-extinction and recovery event. The body size of the bivalves did not decrease during the Tr/J, while the coverage, richness and body size of ichnofossils increased during the recovery. The Chile Tr/J section records low richness, but the ecological complexity and richness decreases through the interval and composition records high turnover, while the dominance increases. The results indicate that the Tr/J disruption changed species composition in a relatively short time period, which decreased the ecological functionality of the invertebrate marine assemblage. In spatial terms, the UK fauna show a clear response to the extinction effect, but the diversity response of the Chilean assemblage is not clear at all, which may be related to taphonomical bias.

Alternatively, this work analysed stage-by-stage occupation of ecospace of 3181 genera recorded from Sepkoski`s compendium for the marine fauna from the Late Permian to Early Jurassic. The ecospace can be represented as a combination of the three axes of tiering, motility and feeding, each divided into six subcategories. From the Cambrian to Recent, ecospace utilisation has tripled, however the trend through the Phanerozoic remains unclear. This result indicates that from the Guadalupian to Sinemurian the number of modes of life did not increase significantly, but the ecospace packing does. There was a significant positive correlation between abundance of predators and both infaunalisation and motility. However, the ecospace utilisation decreased 35% and 16% at the end of Permian and Triassic, respectively. During the extinction events, non-motile animals, organisms with little physiological control of biocalcification and the epifaunal forms, were heavily affected. This indicates that the mass extinction had a particular ecological effect on the biota and is an important episode of ecological changes due to ecological selectivity. Parallel, the appearance of adaptations to new trophic niches during the Triassic, like durophagy, presumably increased predation pressure and drove the increase in benthic infaunalisation. This series of adaptation could be potentially associated with the Marine Mesozoic Revolution.

Chapter 1 Introduction

1.1 Brief history of mass extinctions

The Phanerozoic generic diversity curve shows discontinuity over time resulting from changes in both origination and extinction dynamics, which play a significant role in the restructuring of ecosystems (Fig.1.1). Cuvier introduced the notion of discontinuity in the 18th century. He proposed that the history of the biosphere had known periods of creation, stasis and catastrophe. Nevertheless, some geologists considered all gaps or discontinuities in the fossil record to correspond only to stratigraphic hiatuses and therefore rejected Catastrophism in favour of Lyellian uniformitarianism and Darwinian evolution. Consequently, the discovery of large changes through the Mesozoic period as described by Phillips (1860) and Chamberlin and Moulton (1909) did not generate much interest.

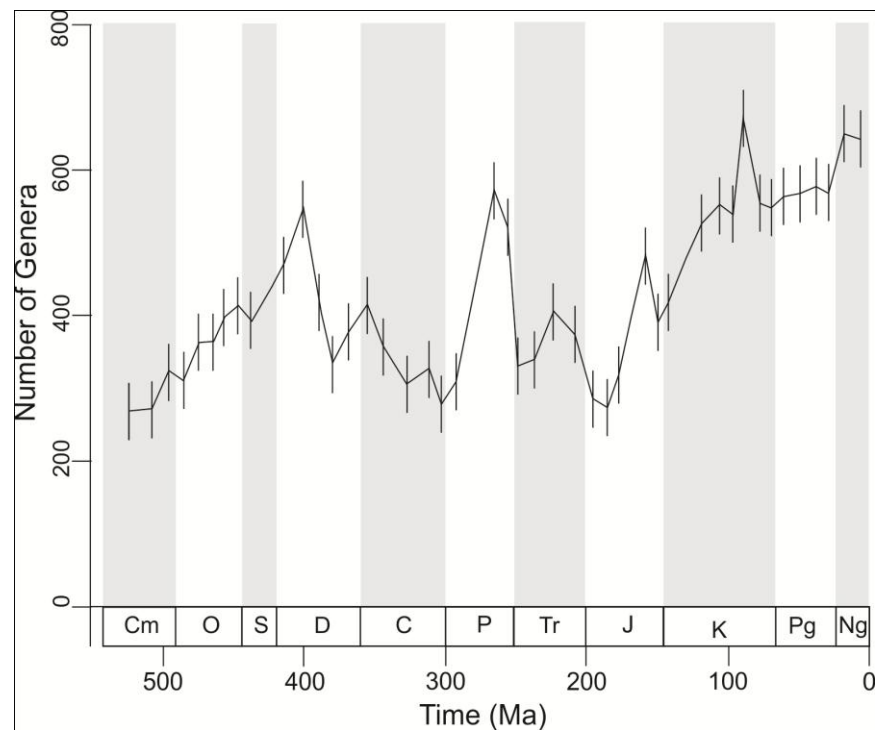


Figure 1.1 Diversity curve (Genus-level) of marine invertebrates through the Phanerozoic. The data plotted are based on a sampling-standardized analysis of the Paleobiology Database. From Alroy (2008).

A number of papers were published in the 20th century, which focused on changes in species composition during the Palaeozoic and Mesozoic (Newell 1962; Schindewolf 1963). However, it was not until Newell's (1967) work that the "discontinuity" in diversity during the Phanerozoic was reviewed and six events were recognised to be different from the normal or background extinctions and which were characterised as mass extinctions. Finally, this idea took hold in Raup and Sepkoski's (1982) work. They suggested that there had been five mass extinction events, estimated through a parametric 95% confidence interval around linear regressions that describe the Phanerozoic decline in extinction rates (Fig. 1.2).

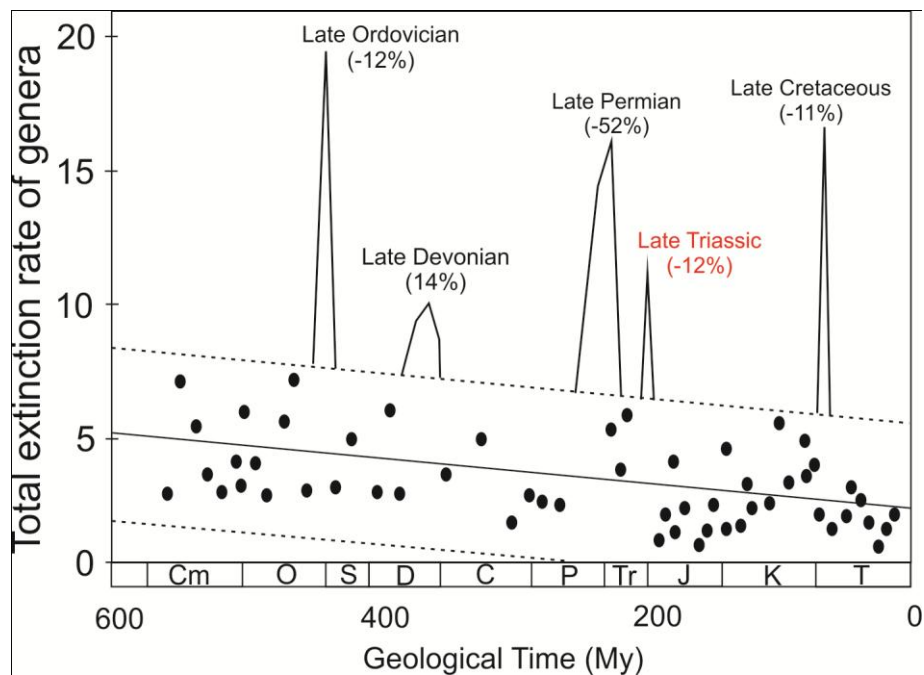


Figure 1.2 The "big five" mass depletions are numbered. In red is indicated the Tr/J mass extinction event. Modified from Raup and Sepkoski (1982).

A mass extinction may be defined as a substantial loss of biodiversity of wide geographic and taxonomic extent and relative short duration (Jablonski 1986; Raup 1995; Hallam and Wignall 1997). This kind of event is an important component of the evolutionary process (Jablonski 1989). It characterises an extreme biodiversity crisis that not only had evolutionary consequences arising from the termination of clades, but

potentially also had severe ecological effects (Brenchley *et al.* 2001). The ecological and evolutionary patterns during a mass extinction are significantly different from the normal background, because they mark the termination of a period of ecologic stability—an Ecologic Evolutionary Unit (EEU)—and precede a period of recovery (Sheehan 1996b). The recovery stage is generally characterised by the occupation of new ecospace as well as a large pulse of evolutionary radiation and an evolutionary tendency toward new ecological features (Erwin and HuaZhang 1996; Erwin 1998a; Erwin 1998b; Erwin 2001). Understanding the extinction process is, therefore, crucial in understanding the evolution of the biosphere, because it may provide insight into today's biodiversity crisis.

Of the five mass extinction events previously mentioned, the Tr/J boundary is one of the most controversial, in term of the causes, duration, and selectivity (Hesselbo *et al.* 2007; Ruhl *et al.* 2010).The evidence for this event comes from the fossil record of bivalves, brachiopods, ammonites, corals, radiolarians, ostracods and foraminiferas of marine habitats, and plants and tetrapods of terrestrial environments (Hallam 1981; McRoberts and Newton 1995; Olsen *et al.* 2002; Kiessling and Aberhan 2007; Kiessling *et al.* 2007b; McElwain *et al.* 2007; Tomašových and Siblík 2007; Wignall and Bond 2008; McElwain *et al.* 2009; Thorne *et al.* 2011). The Tr/J mass extinction is ranked in third place (23%), in terms of ecological impact and fourth in terms of the number of species lost (McGhee *et al.* 2004). The extinction event is strongly marked at specific level but is more complicated at generic and family levels (Deng *et al.* 2005).

During this interval, dramatic changes of the environment, such as temperature rise due to the greenhouse effect (McElwain *et al.* 1999; McElwain 2004; Ruhl *et al.* 2009; Belcher *et al.* 2010; Bacon *et al.* 2011; Ruhl *et al.* 2011; Ruhl and Kurschner 2011),

marine anoxic habitats caused by a sudden transgression after the regression at the end of Triassic (Hallam and Wignall 1999; Hallam and Wignall 2000; Wignall 2001b; Hallam 2002; Barras and Twitchett 2007; Clemence *et al.* 2010; Paris *et al.* 2010), have been claimed to be the main causes of the extinction. Many hypotheses have been suggested to account for the environmental changes, however, the most plausible is volcanic eruption (Hallam and Wignall 1999; Palfy *et al.* 2001; Wignall 2001a; Hesselbo *et al.* 2004; Hesselbo *et al.* 2007; Wignall 2009). This triggered one of the largest turnovers in global biogeochemical cycles (Hesselbo *et al.* 2002), all possibly attributed to large-scale carbon release caused by a major volcanic episode, namely development of the Central Atlantic Magmatic Province (CAMP) during the break-up of Pangaea (Deenen *et al.* 2010; Ruhl *et al.* 2011). This led to an increased flux of CO₂, SO₂, and CH₄ into the oceans and atmosphere, which generated extreme greenhouse conditions, which impacted on ocean chemistry, generating a substantial decrease of seawater pH that slowed down or inhibited precipitation of calcium carbonate minerals (Hautmann 2004; Hautmann *et al.* 2008a; Crne *et al.* 2011). The cessation of carbonate sedimentation affected organisms with aragonitic or high-Mg calcitic skeletons and little physiological control of biocalcification, which generated one of the biggest biological crises to have affected tropical reef systems (Hallam 1981; Hallam 2002; Hautmann 2004; Kiessling and Aberhan 2007; Kiessling *et al.* 2007a; Hautmann *et al.* 2008a; Mander *et al.* 2008; Crne *et al.* 2011).

1.2 The Triassic–Jurassic (Tr/J) boundary: stratigraphical framework

At the first Jurassic colloquium in Luxemburg in 1962, the scientific community recommended that the Rhaetian Stage were placed at the top of the Triassic and that the zone of first appearance (FA) of the ammonite *Psiloceras planorbis* (J. de C. Sowerby) (Bed 13 in Fig. 1.3) correlate the basal unit of the Hettangian Stage at the base of the

Jurassic (Maubeuge 1964; Lloyd 1964 ; Cope *et al.* 1980). In 1968 the British National Committee for Geology proposed that the base of the Planorbis Zone, and hence the Tr/J boundary in UK, should be defined at the base of the Blue Lias Formation in St Audrie's Bay, in West Somerset (south west England; George 1969; Morton 1974: see Palmer (1972) and Whittaker and Green (1983) for descriptions of the Triassic-Jurassic succession in this area). In doing so, it was believed that correlation with sections internationally was facilitated (Cope *et al.* 1980; see also Warrington *et al.* 2008).

Older, but poorly preserved *Psiloceras* spp. was recorded by Hodges (1994), however, in St Audrie's Bay. In contrast, better-preserved ammonites from Doniford Bay, to the east of St Audrie's Bay, and from boreholes in north west England, allowed Page and Bloos (1998) and Bloos and Page (2000) to establish a new ammonite succession in UK, as later reviewed by Page (2004). In Somerset, this included the recognition of the earliest ammonite species recorded in the UK, *P. erugatum* (Phillips), in Bed 8 (of Whittaker and Green (1983)), with “*Neophyllites*” in the lower part of Bed 9 and *Psiloceras* sp. cf. *planorbis* in the upper part – all below the first occurrence of *P. planorbis* as recorded previously in Bed 13. *P. planorbis* is abundantly represented in Beds 13 to 19. The base of Bed 23 above comprises at least 2 m of hard, laminated mudstone that contains abundant crushed “iridescent” (i.e. with preserved shell aragonite) specimens of *P. planorbis*, followed by *P. sampsoni* (Portlock), *P. plicatulum* (Quenstedt) and ultimately *P. bristoviense* Donovan (Fig. 1.3; Page, 2005). The Planorbis Subzone extends up to the base of Bed 25 (Page 2005; Clémence *et al.* 2010).

The FA of *Psiloceras* has been identified in Nevada (USA; Guex *et al.* 2004) as the species *Psiloceras spelae* Hillebrandt *et al.* (2007) a member of the *Psiloceras tilmanni*

Lange group, and in Austria as *P. spelae* (Hillebrandt *et al.* 2007). These early species display characteristic small primary tubercles on their juvenile stages (Guex *et al.* 2004). Initially, many localities were proposed as the Global Boundary Stratotype Section and Point (GSSP) for the Tr/J boundary, including in the USA, Canada, Peru, Hungary, England, the north of Ireland and Austria (Palfy *et al.* 2000; Ward 2001; Guex *et al.* 2004; Hillebrandt *et al.* 2007; Simms and Jeram 2006; Warrington *et al.* 2007) (Fig. 1.3). However, there were initially many problems with agreeing on a definition for the GSSP, resulting from the provincialism of the ammonite faunas (Hallam and Wignall 1997; Bloos and Page 2000; Page 2008) and because the FA of *Psiloceras* is demonstrably diachronous across Western Europe and often separated by up tens of metres from the last appearance (LA) of the ammonoid *Choristoceras marshi*, which characterises the uppermost Triassic ammonoid zone (Tanner *et al.* 2004). Finally, in 2009, the Kuhjoch section, in the Northern Calcareous Alps, Austria, was accepted by vote of the members of the Tr/J Boundary Working Group (TJBWG) of the International Subcommittee on Jurassic Stratigraphy (ISJS) as the GSSP for the base of the Hettangian Stage and hence the Jurassic System, and correlated with the FA of the *P. spelae* (Fig. 1.3).

However, *Psiloceras spelae* has not been found in UK, probably due to more pronounced shallow-water conditions that made environments either unsuitable for this taxon during this time interval or prevented it from arriving, or alternatively, this could suggest the presence of a hiatus (Page 2010, Clémence *et al.* 2010). As a result, it is necessary to apply an integrated stratigraphical approach using ammonites and two negative Carbon Isotope Excursions (CIE), which are widely recorded at this level (Hesselbo *et al.* 2002; Clémence *et al.* 2010; Page 2010).

Figure 1.3 shows the biostratigraphical framework for the Tr/J boundary in the UK and Europe as updated by Page (2010), who included a Pre-Planorbis Zone (Tilmanni Zone) at the base of the Jurassic, below the Planorbis Zone, as established by Hildebrandt *et al.* (2007) - and corresponding to levels previously referred to as Pre-planorbis Beds in the UK. The figure indicates that the beginning of the first CIE approximates to the top of the *Choristoceras crickmayi* Zone of the Rhaetian. The second negative CIE begins close to FA of *Neophyllites* (Bed 7), while the FA of *P. spelae* occurs within the positive CIE between the two negative CIEs (Page *pers. com.* 2010). This suggests that the Tr/J boundary could be located within the upper part of Bed 1 of the St Audrie's Bay section.

1.3 Palaeogeography and climate across the Tr/J boundary.

The Tr/J boundary occurs around $201.31 \pm 0.18/0.38/0.43$ Ma (Schoene *et al.* 2010; Whiteside *et al.* 2010). At this time almost all landmass was concentrated in the supercontinent Pangaea, which was centred across the equator (from 80°N to 80°S) (Fig. 1.3A). On the eastern border of Pangaea was the Tethys Ocean, a vast gulf that was surrounded by coasts that are now located in Antarctica, north eastern Africa, Eastern Europe, and southern Asia (Baltica). The vast ocean Panthalassa surrounded the supercontinent (Scotese 2002; Golonka 2004, 2007) and showing almost hemispherically symmetrical circulation patterns composed of two large subtropical gyres that rotated clockwise in the northern hemisphere and anti-clockwise in the southern hemisphere (Arias 2008). Pangaea comprised two large continental masses, Laurasia and Gondwana (Fig.1.4A) (Arias 2008).

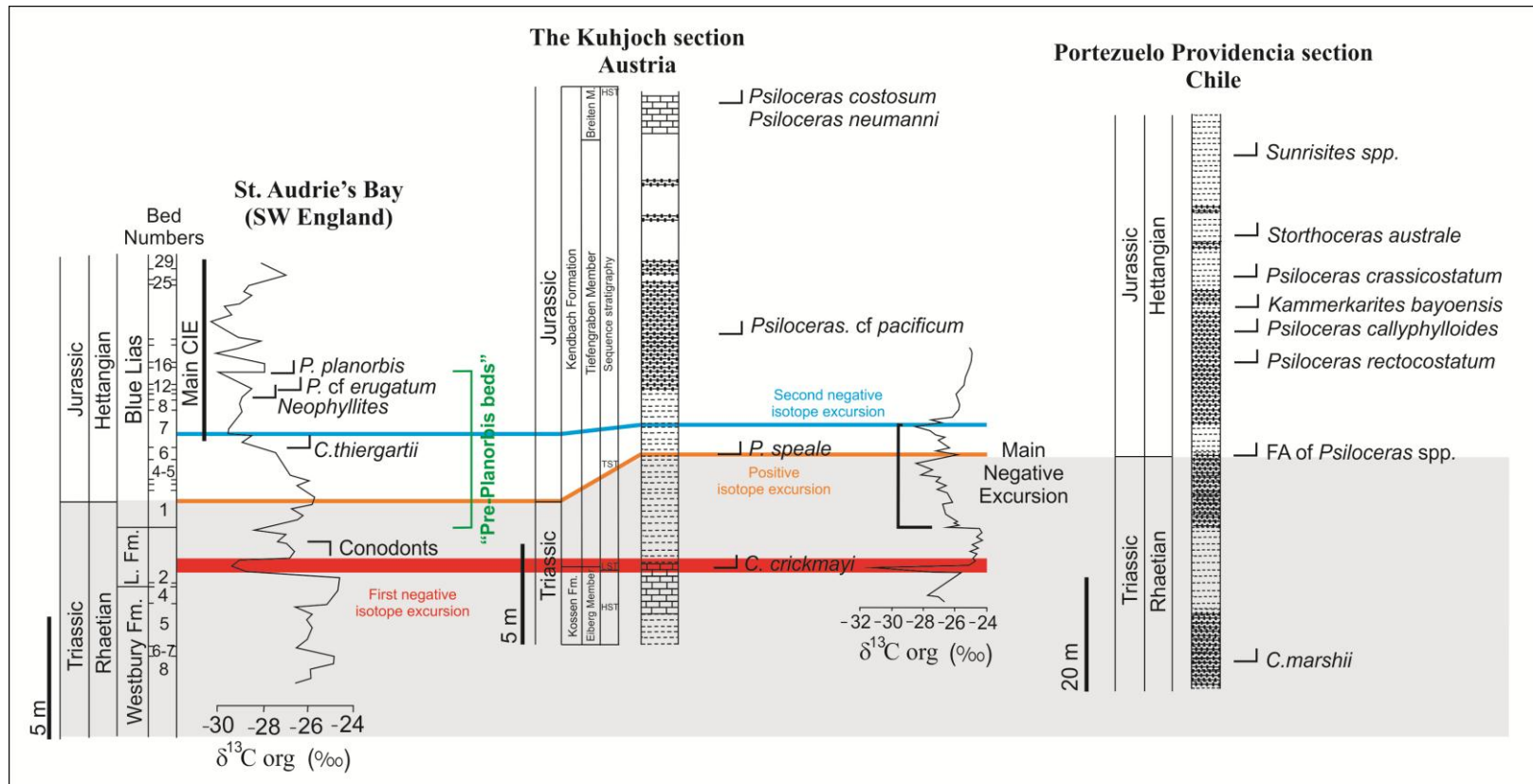


Figure 1.3. Correlation between sections in Austria, England and Chile. The red arrow show the first negative excursion, which coincided with the last occurrences of *C. crickmayi*. The orange line indicates the positive excursion, which peaks at 7 m, coincident with the first appearance of *P. speale* and which marks the Tr/J boundary. This boundary is correlated to Bed 1 of the Blue Lias Formation in SW England. (See appendix 1.1 for ammonite correlations). The FA of *Psiloceras* spp. in the Portezuelo Providencia section is correlated to the FA of *P. speale* in the Kuhjoch section. (from Hillebrandt *et al.* 2007, Page 2010 and Clemence *et al.* 2010). The St Audrie's Bay section was obtained from Clemence *et al.* (2010). The Kuhjoch section was modified from Hillebrandt *et al.* (2007). While the Chilean profile was constructed by R. Twitchett and the ammonite determinations was performed by A. Mourgues.

The climate during the Late Triassic period was generally hot and dry and there is no evidence of glaciations at or near either pole. The polar regions were apparently humid and/or temperate (Frakes *et al.* 1992) (Fig. 1.4A) (Shubin and Sues 1991; Frakes *et al.* 1992; Belcher *et al.* 2010; Ezcurra 2010; Whiteside *et al.* 2011).

Pangaea was formed by the Carboniferous, due to a large number of collisions of many smaller continental masses in different time intervals. In particular, Pangaea was ultimately formed due to the collision of the two supercontinents of Laurasia (to the north) and Gondwana (to the south) (Golonka 2007; Stanley 2008). However, from the Triassic through to the early Jurassic, Pangaea suffered a series of modifications that were determined mainly by the kinetics of the continental mass and which led to drastic changes in the biosphere. One of the first events was the formation of the “Rim of Fire” along the coast of Pangaea, which was active during the Triassic and Jurassic and generated active volcanism, terrain accretions, and back-arc basin development (Golonka 2007; Arias 2008) (Fig. 1.4B).

The closure of the Palaeotethys, which had existed between Gondwana and Laurasia, generated the development of large carbonate platforms along the Neotethys and Palaeotethys margins. The later separation of North America from Gondwana, which was initiated by the Triassic stretching and rifting phase, continued during Early-Middle Jurassic time (Golonka 2007). This activity produced a volcanic belt around Africa-North America known as the Central Atlantic Magmatic Province (CAMP)(Fig. 1.5): one of the largest known Phanerozoic flood basalt provinces (Olsen 1997; Marzoli *et al.* 1999; Knight *et al.* 2004). Once the rift was open, a system of deltas developed on the

marine shelves. Pangaea was under stress during Late Triassic-Early Jurassic times due to the subduction zones surrounding the supercontinent (Fig.1.4B).

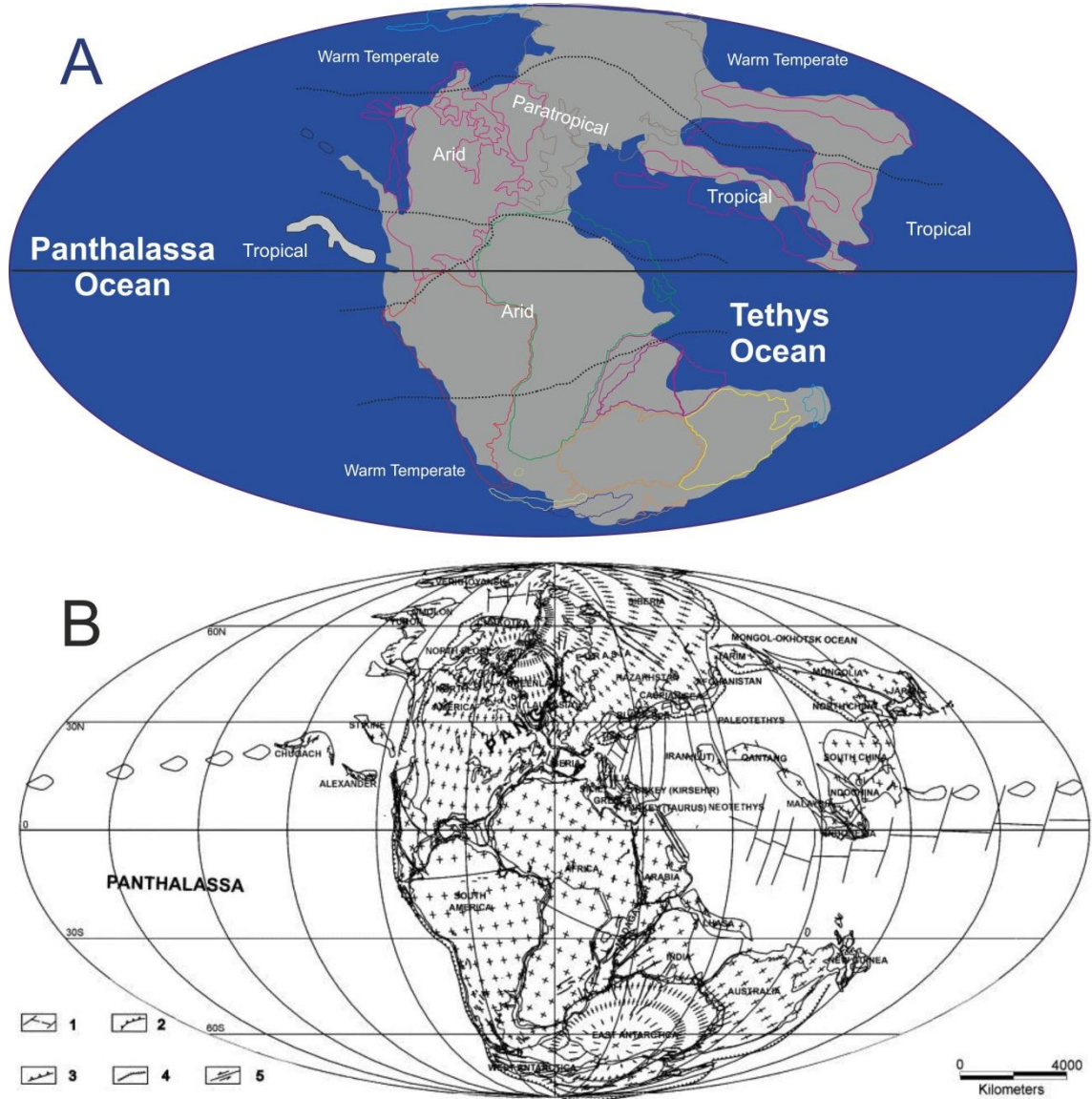


Figure 1.4. (A) Late Triassic climate was apparently warm, without evidence for ice at either North or South Poles. The warm temperate conditions extended towards the poles. (modified from Scotese (2002) <http://www.scotese.com>, PALEOMAP website). (B) Global plate tectonic map of Late Triassic. 1—oceanic spreading centres and transform faults, 2—subduction zone, 3—thrust fault, 4—normal fault, 5—transform fault. (from Golonka (2004)).

1.4 Potential causes of Tr/J mass extinctions

The evidence in the fossil record that suggested an accelerated biotic turnover during the Tr/J boundary has led to the idea of that a mass extinction event occurring during this period (Hallam 1981; Raup 1982; Olsen *et al.* 1987; Hallam 1990; Benton 1995; Sepkoski 1996; Hallam 1997; Sepkoski 1997; Olsen *et al.* 2002; Olsen and Rainforth 2002; Bambach *et al.* 2004)

Various mechanisms have been proposed to explain these diversity depletions, but two mechanisms have been identified as the most likely causes: gradualism (Tucker and Benton 1982; Hallam 1990; Hallam and Wignall 1999) and catastrophism (Olsen *et al.* 1987; Marzoli *et al.* 1999; Mcelwain *et al.* 1999; McHone 2000; Palfy *et al.* 2001; Wignall 2001c; Olsen *et al.* 2002; Olsen and Rainforth 2002; Simms 2003).

Nevertheless, some have suggested that this event may be the result of the interaction of both components (Tanner *et al.* 2004).

The sea level changes during the Rhaetian are an example of a gradualist mechanism (Hallam 1990; Hallam and Wignall 1999; Hesselbo *et al.* 2004). They caused a reduction in habitat for marine organisms, in particular for those that lived on the shelves. Other gradualist mechanisms include anoxia resulting from transgression, and climatic changes, specifically widespread aridification (Tucker and Benton 1982).

Catastrophic events offered as an explanation for the observed biological changes include: extraterrestrial impact (Olsen *et al.* 1987; Hodych and Dunning 1992; Spray *et al.* 1998; Olsen *et al.* 2002; Olsen and Rainforth 2002; Simms 2003; Tanner *et al.* 2004), associated with a sudden opacity of the atmosphere; the release of huge volumes of CO₂ and SO₂, resulting from volcanic activity (Marzoli *et al.* 1999; Mcelwain *et al.*

1999; McHone 2000; Palfy *et al.* 2000; Palfy *et al.* 2001; McElwain *et al.* 2007; McElwain and Punyasena 2007); and the release of methane hydrates associated with instabilities in the sea floor (Palfy *et al.* 2001; Hesselbo *et al.* 2002).

In summary, all these mechanisms produced significant physical and chemical changes in the atmosphere and played a significant role in the ecological changes through the Tr/J extinction in either a local or a global context. The precise cause and effect relationships, however, remain unproven. In the next section, the potential causal mechanisms that led to the mass extinction event are summarised.

Climatic changes: Climate change was one of the first gradualist mechanisms proposed as an explanation for the deep biotic change at the end of the Triassic (Colbert 1958). Tucker and Benton (1982) proposed that the climatic changes induced vegetation changes, which then triggered extinction among the tetrapods. Later, Simms and Ruffell (1990) suggested that a series of events occurred during the Carnian/Norian, and established that the change from humid to dry conditions happened during the latest Carnian. Lucas (1999) confirmed the changes between warm and dry, conditions. However, he established that those conditions were restricted to the high latitudes and that there was no evidence of glaciation.

Similar aridity-related trends have been associated with southern Pangaea, ranging from southern Africa and Madagascar to the lower regions of Argentina. Olsen (1997) and Kent and Olsen (2000) were able to confirm the increase in aridity from their interpretations of facies changes, evaporite occurrences, and paleosols in the Upper Triassic to Lower Jurassic formations of the Newark Supergroup, but alternatively established that these conditions were restricted to central Pangaea, spanning 15°

palaeolatitude. This interpretation of zonal climatic gradients is supported by the interpretation of increasing humidity in low latitude zones. For example, humidity levels increased in Australia and Greenland during the Late Triassic (Clemmensen *et al.* 1998).

Models of the Late Triassic Pangaea climate suggest a largely azonal climatic pattern with mostly dry equatorial and continental interior regions and humid belts in higher regions and around the Tethyan margin (Dubiel *et al.* 1991; Parrish 1993). Nevertheless, more sedimentological evidence in support of this azonal model is required. Apparently, the climatic changes affected the terrestrial systems more severely than marine ecosystems and likely affected regions in Pangaea in different ways. Lastly, McElwain *et al.* (1999), and McElwain *et al.* (2007) suggested that CO₂ concentration increases significantly across the Tr/J boundary and that global temperatures increased by up to 4°C. Belcher *et al.* (2010) suggested that temperatures were much higher, which led to a drastic compositional floral change. They concluded that global warming probably led to increased storm activity and this coupled with a climate-driven increase in vegetation flammability led to a significant rise in fire activity at the Tr/J boundary.

Bolide impact: Similar to the K/T boundary, an asteroid impact has been suggested as a causal mechanism for the mass extinction. The first to propose this were Olsen *et al.* (1987), who used a crater with a 100-km diameter, found in Manicouagan, Quebec, as an argument in favour of this theory. However, support for this theory has declined since radiometric data suggested that this record may be associated with an older boundary: the Norian/Carnian (216.5 ± 41 ma) (Hodych and Dunning 1992).

Additionally, a multiple impact theory has been associated with the Tr/J boundary (Gerhard *et al.* 1982; Kohn *et al.* 1995; Kelly and Spray 1997; Masaitis 1999). It has been suggested that chains of craters were formed by multiple impacts in a matter of hours (Tanner *et al.* 2004). However, this hypothesis has been rejected due to the incongruence of the palaeomagnetic record (Kent and Olsen 1998). Finally, Simms (2003) showed suggestive evidence of a bolide impact in the Cotham Member of the Penarth Group, which is of Late Triassic (Rhaetian) age. His argument is based on the presence of extensive horizons (e.g. $> 250,000 \text{ km}^2$) showing evidence of contorted, soft sediments that can be interpreted as “seismite”. However, Nomade *et al.* (2007) proposed that these sedimentary structures resulted from tectonic activities associated with CAMP. Therefore, in spite of some claims of the presence of features such as craters of appropriate age and extensive alteration in some sedimentary layers, their chronological relation to the Tr/J boundary and the low Iridium concentration (<0.4 ppb) (McLaren 1990) makes extraterrestrial impact an unlikely causal mechanism for the Tr/J mass extinction.

CAMP volcanism: One of the first associations between volcanism and extinctions was established by McHone (1996), who proposed that early Jurassic eruptions created a flood basalt province that covered at least $5 \times 10^5 \text{ km}^2$ of north-eastern America. This was based on similarities between compositions and ages of tholeiitic basalts within the Newark Supergroup. Marzoli *et al.* (1999) enlarged the extent of this basaltic flood province and applied the name Central Atlantic Magmatic Province (CAMP) (Fig. 1.5).

They included regions in North America, South America, North Africa and south-western Iberia (Marzoli *et al.* 1999; Knight *et al.* 2004), which meant an area increase of

$7 \times 10^6 \text{ km}^2$ and an added volume of approximately $2.5 \times 10^6 \text{ km}^3$ (McHone 2000; Nomade *et al.* 2007). Verati *et al.* (2007), revealed that pulses of volcanic activity probably occurred between 197.8 ± 0.7 and 201.7 ± 2.4 Ma, with a peak at 199.1 ± 1 Ma and with an estimated duration of 1 myr (Schubert *et al.* 1992; Marzoli *et al.* 1999; 2004; Verati *et al.* 2007).

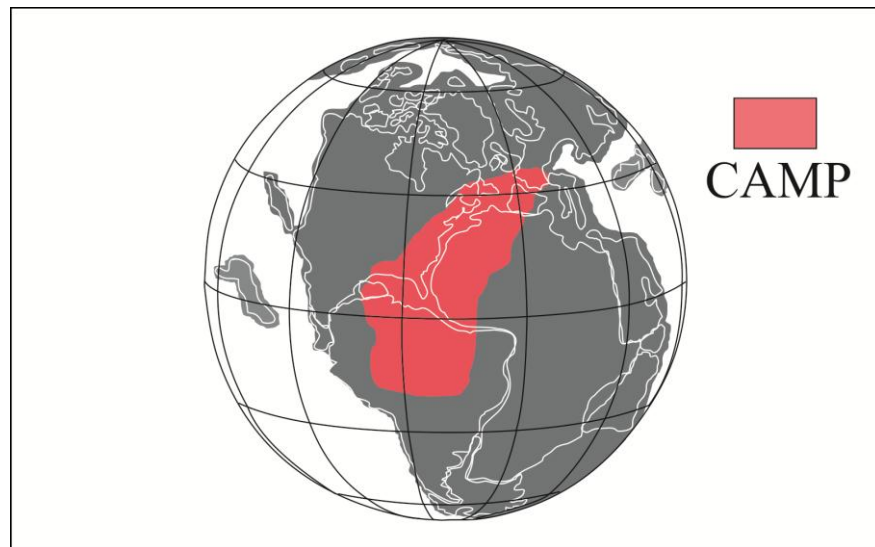


Figure 1.5 Original extent of the CAMP inferred from locations of extant outcrops of lava flows, dykes and sills with radioisotopic age dates of Hettangian (adapted from Whiteside *et al.* 2010).

Many studies have suggested the relationship between CAMP and the Tr/J boundary (Marzoli *et al.* 1999; Olsen 1999; McHone 2000; Beerling and Berner 2002; Marzoli *et al.* 2007; Nomade *et al.* 2007). Palfy *et al.* (2000) have estimated the age of the Tr/J boundary at 199.6 ± 0.3 Ma, using U-Pb zircon geochronology, and suggested an age of 200.6 Ma for the extinction on land. A similar estimation was obtained by Mundil *et al.* (2005). Schaltegger *et al.*, (2008), made a more recent age estimation for the Tr/J boundary, also based on U-Pb zircon. They suggest that the Tr/J boundary is older (201.58 ± 0.17 Ma). However, recent studies by Schoene *et al.* (2010), Whiteside *et al.* (2010) and Ruhl *et al.* (2011), placed the Tr/J boundary at 201.33 ± 0.13 Ma with the

FA of *P. spelae* (Schoene *et al.* 2010). The first negative carbon excursion was located at 201.4 Ma with a duration of 10 to 20 ky (i.e. the onset of CAMP), which also serves as an estimate for the duration of the mass extinction event - although CAMP had a duration of around ~600 ky (Ruhl *et al.* 2011). The relationship between the biological extinction and the volcanic events, therefore, is still under debate. Nevertheless, the timing of the massive CAMP magmatic event seems to fall within the error ranges of modern estimates for the age of the Tr/J boundary, which supports the possibility of a connection with the extinction event.

Sea level change: Marine regression had been for long time considered as a possible cause of biotic turnover as it reduces the available shallow marine habitat (Hallam and Wignall 1999). Global eustasy results from a variety of processes, including continental uplift due to thermal underplating (e.g. by a mantle plume) or changes in volumes or rates of mid-ocean ridge production, but these processes occur on time scales longer than 1 my (e.g. Miller *et al.* 2005). Latest Triassic regression-transgression is recognized in numerous sections in Europe and North America and is likely to be the result of global sea-level change (Hallam and Wignall 1999).

There is very good evidence that extensive sea level changes occurring around the Tr/J boundary. Rapid sea level fall is quickly followed by abrupt rise, which is clearly indicated by a marked lithological changes from carbonates to mudrock facies (Hallam 1997). There was extensive shallowing across northern Europe in the latest Rhaetian, which is marked by a widespread progradation of sandstone in Germany (Bloos 1990), while in the earliest Hettangian (Planorbis Zone) there was an evidently rapid sea level rise. This rise lasted throughout the Hettangian Stage and reached a maximum in the early Sinemurian (Bloos 1990).

The regressive pulse at the end of the Rhaetian can also be recognised in the Northern Calcareous Alps of Austria, southern Sweden, and northwest Poland. In England, however, the Tr/J boundary may be accompanied by a sedimentary hiatus between the Penarth Group (Lilstock Formation) and Blue Lias Formation (See Chapter 4, 5 and 6) (Hallam 1995; Hesselbo *et al.* 2004). In the Muller Canyon Member at New York Canyon in Nevada, the regression is marked by an upper Rhaetian siltstone unit that separates Norian-Rhaetian and Hettangian-Sinemurian calcareous units. In South America in the Utcubamba Valley, Peru, Hillebrandt (1994) reported a facies change from the north to the south, in which silty shales indicative of deeper water grade southwards into shallow-water siltstones and limestones.

Records from Africa, Australasia and Asia are generally poor because of the paucity or absence of marine successions across the system boundary (Tanner *et al.* 2004). Hallam and Wignall (1997; 1999) suggested that the reduction of habitat and the consequent loss of species might have been regional rather than global, and was driven by thermal uplift of the region surrounding the Atlantic rift prior to the initiation of magmatism. From this evidence, they concluded that sea-level changes were not likely to be one of the principal mechanisms that caused the biotic changes during the Tr/J boundary. On the other hand, Guex *et al.* (2004), suggested a model with several triggering factors, in which the negative $\delta^{13}\text{C}$ excursion is associated with extinction and primary productivity collapse caused by volcanic SO_2 and heavy metal emissions and acid rain. They also proposed, however, a cooling and glacial event that caused a short but major drop in sea level.

1.5 Palaeoenvironmental scenario during the Tr/J boundary: CO₂ outgassing

The Tr/J mass extinction event is associated with a major perturbation in the carbon cycle recorded in stable carbon isotopes (McElwain *et al.* 1999; van de Schootbrugge *et al.* 2008). The immense activity of CAMP associated with volcanic outgassing has been suggested by some authors to be responsible for the environmental deterioration at the end of Triassic (McElwain *et al.* 1999; McHone 2000; 2003). The sudden release of CO₂ has been considered to be one of the main factors, in that it triggered an interval of intense greenhouse warming conditions that resulted in the extinction (McElwain *et al.* 1999; Olsen 1999; McHone 2000).

One of the first studies that showed the CO₂ anomalies across the Tr/J boundary was carried out by McElwain *et al.* (1999) who studied the stomatal characteristics of fossil leaves, which at the same time also provided a palaeoclimatic evidence for the semi-arid conditions during the Late Triassic. Their estimations indicated that at the end of the Triassic atmospheric CO₂ averaged approximately 1400 ppmv. However, most estimations centre around 1500 ppmv and compilations of all available CO₂ estimates suggest that on average CO₂ increased 2- to 3-fold across the Tr/J boundary (Royer *et al.* 2001; Beerling and Berner 2002), which probably produced an environmental temperature increase of 3° to 4°C.

For the same time interval, Tanner *et al.* (2004) alternatively proposed a steady increase of CO₂ from ~250 ppmv to Late Triassic levels four times as high, based on isotopic composition studies using carbonates. However, the relative stability suggested by Tanner *et al.* (2004) has been rejected on the basis that the temporal resolution of the paleosol samples may have been inadequate to detect a rapid, transient rise in

atmospheric CO₂ and that the carbon isotopic composition of terrestrial organic matter within the paleosol was not considered (Retallack 2002).

Beerling and Berner (2002) recalibrated the CO₂ estimations to the natural isotopic variation and estimated a 1032 ppmv rise of CO₂ during the end Triassic, based on biogeochemical modelling of carbon cycle perturbations. They suggested that the CO₂ degassing alone could not produce the substantial negative carbon isotopic excursion (as much as -3.5 ‰) recorded in marine carbonates, organic matter, and terrestrial wood (McElwain *et al.* 1999; Palfy *et al.* 2001; Hesselbo *et al.* 2002). They established that volcanic CO₂ triggered the release of massive amounts of CH₄ into the ocean-atmosphere system by destabilizing methane hydrate reservoirs. The oxidation of CH₄ to CO₂ could then have raised atmospheric CO₂ values to about 2500 ppmv during the Early Jurassic (Hodych and Dunning 1992). The most recent studies carried out by Ruhl *et al.* (2010) using compound-specific C-isotopes, showed that the initial carbon isotope excursion recorded a depletion of ~8.5 per mil (‰) atmospheric ⁻¹³C, suggesting a total injection of ~12,000 to 38,000 Gt of carbon as methane in just 10-12 kyr, from three mechanisms: CAMP, a marine methane-hydrate reservoir and through volcanic sill intrusions and flood basalt emplacement. They suggest that these mechanisms triggering a strong warming event and an enhanced hydrological cycle directly coinciding with the marine and terrestrial assemblage changes and extinction event.

1.6 Faunal extinctions

At the close of the Triassic, about 80 % of all species went extinct (Sepkoski 1997) and massive biotic turnover occurred in both the marine and terrestrial realms. Benton (1995) estimated that average familial extinction rates were as high as 15.2–23.9% for all organisms, 10.6–23.4% for continental organisms, and 12.7–16.9 % for marine organisms (Fig. 1.7).

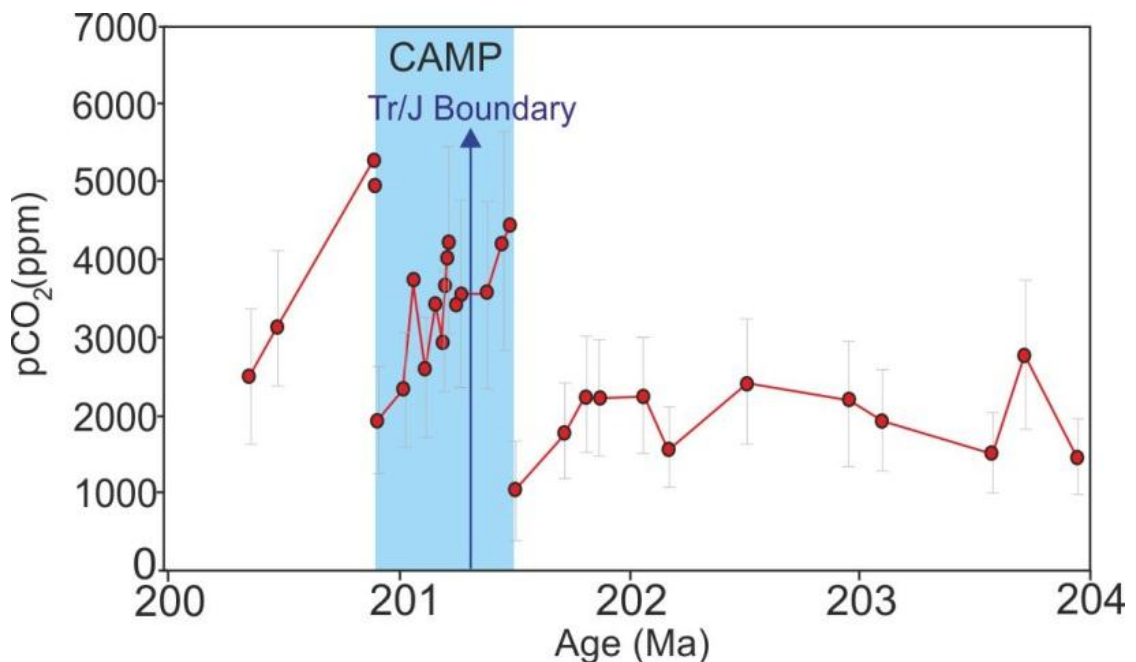


Figure 1.6 Atmospheric pCO₂ through the Late Triassic to Early Jurassic. [Error bars are $S(z) = 3000$ to 1000 ppm]. Pre-CAMP pCO₂ values of ~2000 parts per million (ppm), increasing to ~4400 ppm immediately after the first volcanic unit, followed by a steady decrease toward pre-eruptive levels over the subsequent 300 thousand years. pCO₂ increase as a direct response to magmatic activity (primary outgassing or contact metamorphism). Adapted from Schaller *et al.* (2011).

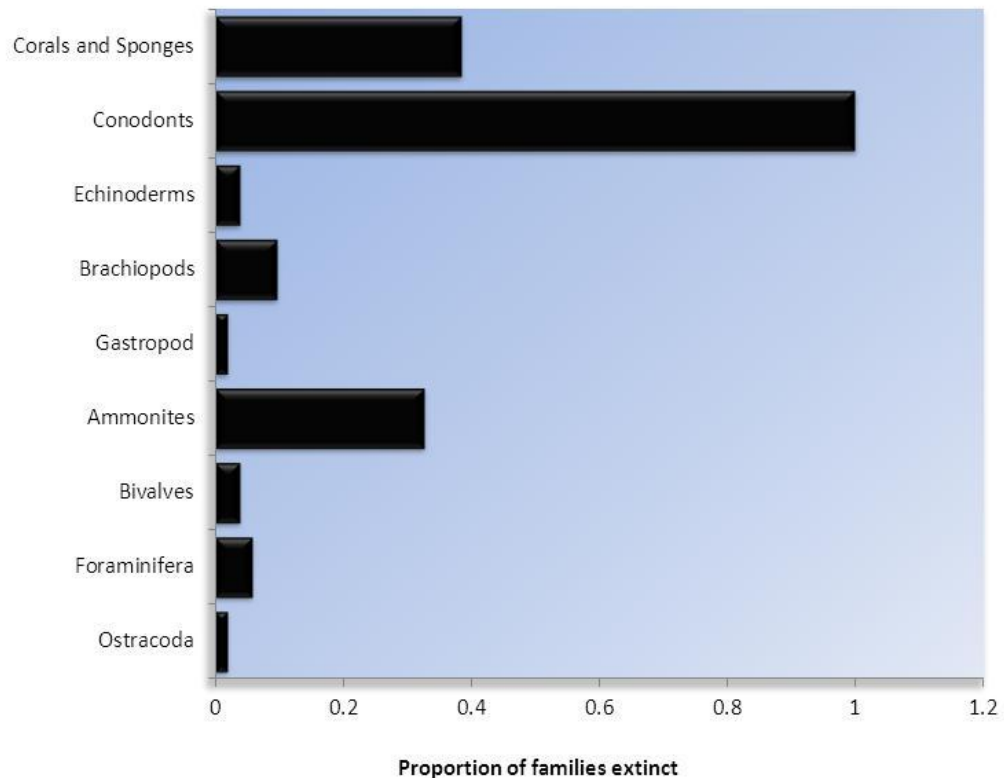


Figure 1.7 Proportion of important benthic families becoming extinct during the Tr/J mass extinction event. Based on Benton (1993) and Hallam (2002) data.

Recently, Kiessling *et al.* (2007a) analysed the diversity and abundance patterns of organisms throughout the Tr/J boundary based on the Paleobiology Database (<http://paleodb.org/cgi-bin/bridge.pl>). They reported that 41% of all mesobenthic and macrobenthic genera that crossed the Norian-Rhaetian boundary became extinct during the Rhaetian. With this extinction, they noted a significant reduction in origination and strong diversity depletion in the Early Hettangian. At the same time, they observed a selective extinction of certain taxa when separating species according to environmental setting. They suggested that reef dwellers had a significantly higher extinction risk than bottom dwellers, that near shore taxa suffered more than offshore taxa; that taxa with a preference for carbonate substrates were more strongly affected than taxa that preferred siliciclastic substrates, and that taxa that inhabited high latitudes showed lower extinction rates than taxa at intermediate and low latitudes.

There are many studies that report the loss of diversity across the Tr/J boundary, but the information they provide varies between them and also depends on the time these studies were done (Benton 1993; Sepkoski 1996; Hallam and Wignall 1997; Hallam 2002; Kiessling *et al.* 2007a). However, they all agree on that the Tr/J extinction event resulted from the intensification of background extinctions, that the risk of extinction was selective for certain taxa, and that this mass extinction is not the result of a decrease in origination rates (Kiessling *et al.* 2007a).

1.7 Important faunal groups

***Mollusca*:** The traditional definition of the Tr/J boundary is based on the ammonoid record. Teichert (1988) indicated that more than 150 genera and subgenera existed during the Carnian, but were reduced to 90 during the Norian and finally to 6 or 7 during the Rhaetian. Some authors suggested that the extinction occurred at the end of the Norian and not at the end of the Rhaetian. This is based on the studies of Taylor *et al.* (2000; 2001), who plotted the ammonoid distribution for the Gabbs and Sunrise formations in Nevada, USA. They reported that only 11 species lived through the Norian and just one crossed the Tr/J boundary. These results and the conclusion based on them are shared by Hallam (2002), although Page (2008) considered that the Late Triassic Phylloceratina that crossed the boundary into the Jurassic, actually gave rise to the first *Psiloceras* immediately above. Nevertheless, the most obvious change in ammonoid faunas across the Tr/J boundary is the replacement of *Choristoceras* of the Rhaetian by the earliest Jurassic *Psiloceras*.

Bivalves are one of the most abundant and diverse macro-invertebrates in the early Mesozoic shallow marine facies and their stratigraphic distributions through the Tr/J boundary are relatively well known. They were not much affected at the family level by

the End-Triassic extinction, as only 2 out of 52 families went extinct (the Myophoridae and Mysidiellidae) (Benton 1993). However, there was a much higher extinction rate at the generic level, as was established by Hallam (1981) at 92%, although Skelton and Benton's (1993) global compilation of bivalve family ranges showed a Tr/J extinction of only 5 families at the boundary. McRoberts and Newton (1995) established a selective and stepwise extinction through high resolution analysis, with the highest rates (percentage of species extinguished) occurring during the early (51%) and middle (71%) Rhaetian, and a significantly lesser extinction at the end of the Rhaetian.

Later, Hallam and Wignall (1997) re-examined the bivalve record for the Tr/J boundary interval in north-western Europe and the northern Calcareous Alps in considerable detail. They found an extinction of only 4 out of 27 genera in northwest Europe and 9 out of 29 genera in the Calcareous Alps across the boundary. Later, Hallam (2002) concluded that the biggest extinction in bivalves occurred during the Rhaetian with extinction close to 31% of genera and suggested that the gradual pattern in the disappearance of bivalves could be associated with an environmental bias related to changes of facies (Fig. 1.7). For gastropods, Tracey *et al.* (1993) suggested that no significant extinction occurred at the family level across the Tr/J boundary, with four families going extinct at the Norian-Rhaetian boundary, and only one at the Tr/J boundary, with 42 surviving (Fig. 1.7).

Echinoderms: Only one crinoid family became extinct at the end of the Rhaetian (Somphocrinidae) (Fig. 1.7).

Brachiopods: This group shows a series of stepwise extinctions and diversifications through different stages of the Triassic. However, 17 brachiopod families went extinct

at the end of the Triassic. A recent compilation of brachiopods at the generic level (Manceñido 2000) does not indicate a substantial loss or turnover. Alternatively, Austrian studies indicated the disappearance of 6 species in the Marshi Zone with just one species persisting in the top of the section (Ulrichs 1972). This fails to provide evidence of a sudden mass extinction (Fig. 1.7).

Sponges and corals: At the end of the Triassic, there was a dramatic decline in reef corals and sponges, which appears to reflect mass extinctions on a global scale.

Kiessling (2001) recognised the strong effect of this mass extinction in the fact that the global distribution of reef-building corals and sponges was restricted to a zone around 30°N. According to Benton (1993), three families of corals went extinct during the Rhaetian. At the generic level, however, the extinction was more pronounced: Beauvais (1984) reported that of the 50 scleractinian genera in the Upper Triassic only 11 survived into the Jurassic. The sponges were most severely affected by the decline in the demosponge sphinctosoids, of which 16 families went extinct at the end of the Rhaetian. Similarly, the spongiomorphs were another reef-building group that went extinct at the end of the Triassic (Fig. 1.7).

1.8 Ecological effects, selectivity, extinction and recovery

The Tr/J mass extinction represents the collapse of biological systems, reducing the ecological complexity to more simple levels of organisation and changing the species dominance, the ecological structure, complexity, and functionality of marine communities (Sheehan 1996a; Droser *et al.* 2000; Brenchley *et al.* 2001; Bambach *et al.* 2004; McGhee *et al.* 2004; Layou 2009). It has been ranked third in terms of its ecological impact (Sheehan 1996a), which involves the collapse of the reef systems, turnover of the evolutionary subunits, and deep structural changes in ecology (Droser *et*

al. 2000; McGhee *et al.* 2004). One of the most recent compilations developed by Kiesling *et al.* (2007), indicated that 41% of the genera that crossed the Norian-Rhaetian became extinct at the end of the Triassic, and that tropical systems, calcareous organisms, and reef systems were preferentially affected (Kiesling and Aberhan 2007; Kiesling *et al.* 2007).

The effects of the extinction on the ecosystems did not just result in species loss (diversity), but also included loss of modes of life or ecological traits (Fig. 1.8). Modes of life can be defined as the ways in which species groups use particular resources (Fig. 1.8). These relate species traits to habitat characteristics and provide important insights into the structure and functioning of palaeocommunities.

Alternatively, the ecological traits of the fauna have the potential to indicate changes in community structure that relate to function as an alternative to using traditional taxonomic descriptors (Bush *et al.* 2007; Novack-Gottshall 2007). The Tr/J mass extinction is known to have exerted selective pressure on ecological traits (Kiesling *et al.* 2007a; Mander and Twitchett 2008). For example, Hallam (1981) indicated that there is a smooth transition in the number of epifaunal and infaunal occurrences and feeding mode. Similarly, Aberhan (1994) recognised 10 ecological traits in the Late Triassic to Early Jurassic bivalve communities that are characterised by specific turnover in the relative contribution of each group through time. McRoberts and Newton (1995) concluded that burrowing suspension-feeders suffered high extinction rates (92%) compared to epifaunal suspension-feeders and attributed this pattern to differences in efficiency rates of feeding in periods of low productivity. Finally, Mander and Twitchett (2008) confirmed the pattern of differential selection in favour of

epifaunal suspension-feeding through bias control of lithofacies. They established the necessity of fine-resolution studies in order to obtain a more convincing pattern.

Alternatively, Kiessling *et al.* (2007a) used compiled data and sample-standardised analysis of occurrences. They established that only a few ecological traits are significantly associated with extinction risk during the End Triassic extinction. They found that the probability of survival increased with mobility, mainly due to the extinction of reef builders and brachiopods, and that there is a tendency towards increased survival of epifaunal rather than infaunal bivalves.

The selective changes in the modes of life were not the only ecological modification to the benthic communities across the Tr/J boundary. The trace fossils showed a severe decrease in the number of ichnotaxa, as well as in burrowing depth and size. Twitchett and Barras (2004) and Barras and Twitchett (2007) analysed records from three localities in southern England, which included the former candidate GSSP at St Audrie's Bay. Their data reveals how eight ichnogenera show significant patterns of infaunal changes through the interval, with a notable gap in the "Pre-Planorbis Beds". Although this study only involved the Jurassic recovery phase, it clearly shows the selective extinction (infaunalisation) and the almost complete disappearance of burrowing organisms, which is likely as result of marine anoxia.

The ecological impact can also be observed in community reorganisation. Tomasovych and Siblík (2007) evaluated the compositional changes in the brachiopod communities in the Northern Calcareous Alps (Austria) using multivariate techniques. They demonstrated a marked effect of the Tr/J extinction on the composition, indicating that there was a high extinction rate and large species turnover, which led to fundamental

reorganisation of the community structure. Similarly, Mander *et al.* (2008) studied the turnover in benthic assemblages in two sites in the southwest of the United Kingdom (St Audrie's Bay and Lavernock Point). They reported a 73% species loss in taxa at the end of the Rhaetian, with just 6 species surviving into the Hettangian. These changes caused a severe depletion in diversity, dominance, and evenness, and a small turnover in species composition. This constitutes good evidence of a real biotic crisis occurring in the marine ecosystem during the short stratigraphic interval spanning the uppermost Westbury Formation and the lower Lillstock Formation (both Rhaetian).

It has been shown that altered palaeoenvironmental conditions, such as carbonate undersaturation (Hautmann 2004), anoxia in benthic ecosystems (Wignall 2001c), and a productivity decrease in marine ecosystems (Twitchett 2006) resulted in substantial changes in the functional communities.

These changes in the organisation of the assemblage are not the only feature from which the Tr/J extinction can be recognised. Morphological changes (shape and size) in individuals of different species have also been observed (Urbanek 1993; Twitchett 2001; Hautmann *et al.* 2008b; Mander *et al.* 2008). Although there are no direct surveys focusing on this phenomenon for the Tr/J mass extinction, some studies have reported a change in body size. For example, Dommergues *et al.* (2002) recorded a temporal increase in the shell size of ammonites, including a significant size increase through the Early Hettangian. Although the aim of their survey was to correlate the trend with Cope's rule, they considered that the size increase in the beginning of the Jurassic was linked to the nutrient scarcity during the latest Triassic.

In contrast, Hautmann (2004; 2006) analysed the evolutionary response of 8 bivalve families to changes in sea water chemistry. He found a strong decrease in shell size in the earliest Jurassic (from 108-420 mm in the Rhaetian to 34-60 mm in the Hettangian). This phenomenon was most obvious in the family Megalodontoidea, which he associated with problems resulting from their inability to adapt their shell mineralogy to seawater chemistry.

Similarly, analysis of the trace fossil record (Twitchett and Barras 2004; Barras and Twitchett 2007) in the “Pre-Planorbis beds” showed a significant reduction in body size in the ichnofauna. Although some authors related this size reduction to low oxygen concentrations, e.g. Rhoads and Morse (1971), it is very likely that other factors such as decreased food supply, productivity reduction, and suboptimal salinity are also involved. Despite all this, it is still not clear which factors are of greatest importance and why this phenomenon was selective across the Tr/J boundary.

After the extinction event, other phenomena that can be related to the recovery of ecosystems can be observed. These types of phenomena involve the reorganisation of all community components. Typical characteristics include an increase in the complexity of the ecological structure, which results from the appearance of new clades that diversify rapidly, and the re-establishment of old clades that survived the mass extinction. In summary, modification of the life strategy in life history (generalist versus specialist), an increase in complexity, dominance, and species size, and the filling of new ecospace are all part of the recovery process (Twitchett 2006; Layou 2009).

Although certain indications of recovery processes taking place after the Tr/J mass extinction are well-studied, such as the re-appearance of ichnofauna, increasing

infaunalisation, increasing species size, composition turnover, increasing diversity, and the diachronous recovery of benthic and reef systems (Stanley 2006; Tomašových 2006; Barras and Twitchett 2007; Hautmann *et al.* 2008b; Mander *et al.* 2008), insufficient attention is given to understanding the ecological re-organisation processes or the dynamics of changes between stages and co-evolving taxa (Twitchett *et al.* 2004; Twitchett 2006). Recently, Clémence *et al.* (2010) attempted to construct a “local versus regional” extinction model for the Tr/J interval, integrating geochemical and sedimentological data. However, as these studies were based on calcareous nannofossils and foraminiferal assemblages, they may not be representative of the complete ecological succession process. In fact, the study places more emphasis on productivity and does not record a descriptive component relevant to the structure of the palaeocommunities (e.g. compositional change, rank abundance, richness).

Recently there has been increasing interest in studying the Tr/J boundary interval and more information regarding the causes of this mass extinction is continuously being gathered. However, there are a restricted number of marine sections available for study and knowledge of the time interval and the ecological and taxonomical effects on marine ecosystems is incomplete. The lack of knowledge basically relates to elements associated with structure, functionality, and complexity of benthic communities. These elements include extinction and origination rates, geographical effects (deep versus shallow water), selective extinction of certain guilds (including trophic level), changes in the modes of life, and morphological changes.

1.9 Statement and objectives

During the Late Triassic, about 80 % of all species went extinct (Sepkoski 1997) and massive biotic turnover occurred in both the marine and terrestrial realms (Hallam and Wignall 1997). This extinction event was concurrent with the onset of environmental changes associated with the appearance of CAMP and one of the biggest drops in the sea level (Hesselbo *et al.* 2002; 2004; 2007). Although the loss of taxonomic diversity is well-documented through the extinction, the trajectory of the marine fauna through the extinction and recovery period has not been studied in detail, specifically in the context of a quantitative, community-level palaeoecological approach. Hitherto, there has been greater emphasis on understanding the environmental scenario that triggered this extinction event (Section 1.5). However, knowledge of the exact timing of changes in the structure of communities and the function of ecosystems relative to this environmental disruption is currently poor, which suggests that more research needs to be done. Finally, as result of a small number of outcrops, mainly located in the northern hemisphere, there is no clear understanding of the palaeoecological response over different spatial scales (local-regional).

The overall aims of this study are (1) to evaluate the ecological changes of marine assemblages through the Tr/J mass extinction event and (2) to compare patterns of ecological changes at local and regional scale, in order to estimate the timing, intensity, and geographical dispersion of the changes in marine palaeocommunities. To achieve these aims, a series of questions regarding the effects of the Tr/J mass extinction over different ecological elements, such as diversity, ecological complexity, and changes in body size, will be addressed.

1.9.1 Richness, abundance and composition

In terms of diversity, there is limited knowledge about the changes in richness, abundance and composition across the Tr/J boundary (Hallam 2002). Additionally, most previous work on the Tr/J mass extinction has focused on compilations (e.g. Kiessling *et al.* 2007) or is restricted to the evaluation of a single higher taxonomic group, rather than quantitative palaeoecological approaches that incorporate palaeocommunity-level data (Droser *et al.* 2000; Bottjer 2001) (See section 1.8). To improve our understanding in this area, the following questions were addressed:

- 1) How does species richness in a local community change through the Tr/J mass extinction? Do different Tr/J sections record the same patterns?
- 2) Is the abundance of certain species higher during the extinction event? Is species abundance more evenly distributed before or after the Tr/J extinction event?
- 3) Does species composition change drastically after the extinction? If so, does it happen in a short period of time? And which species survived and which ones did not?
- 4) Are the extinction and recovery dynamics during the Tr/J mass extinction event comparable to other mass extinctions? Are ecological parameters (richness, abundance and composition) associated with environmental changes?

1.9.2 Ecological Complexity

Complexity can be defined as a “function of the number of different types of parts or interactions” that characterizes a system (McShea 1996). A complex ecosystem is characterized by organisms that perform many functions and by numerous types of ecological interactions. In contrast, organisms in a simple ecosystem would fill fewer ecological roles and would interact in fewer ways (Bush and Bambach 2011).

Ecological complexity is related to taxonomic diversity; therefore any decrease in

species richness will affect ecological complexity. Ecological studies have demonstrated that the loss of biodiversity can imperil ecosystem services and functions (Erwin 2008). Consequently, is expected that during a regime of mass extinction the community will suffer a loss of functional richness.

A more operational measure of ecological complexity is the Ecospace concept (as described in detail by Bambach *et al.* 2007, Bush *et al.* 2007 and Novack-Gottshall 2007), which employs a series of categories, or life styles, to describe the way in which available resources are divided among a group of species (see section 3.1 for details).

Although, this concept has been applied mainly to studies of megatrends, the ecospace concept has not commonly been used to study extinction events (Erwin 2008; Layou 2009) and there are even fewer studies of Tr/J marine assemblages (Hallam 2000; Aberhan *et al.* 2006; Kiessling *et al.* 2007; Mander *et al.* 2008). Most Tr/J studies describe the selective impact of a mode of life such as infaunal, suspension-feeding marine taxa (Section 1.7). Despite this, the ecospace changes before, during and after the Tr/J extinction are totally unknown. In order to better understand changes in ecological complexity through the Tr/J interval, the following questions were addressed:

- 1) How does the ecological complexity in a local community change through the Tr/J mass extinction?
- 2) There is a decrease in the density of each mode of life during the extinction event?
- 3) There is a selective extinction of the infaunal, suspension-feeding marine taxa?
- 4) Do different Tr/J sections record the same patterns?
- 5) How is the recovery pattern in the ecospace after Tr/J extinction event?

1.9.3 Reduction in body size

Body size is an important morphometric measure, since it influences almost every aspect of the biology of a species and is considered one of the single most important attributes of an organism (Roy *et al.* 2000). Body size spectra are widely used to assess the state of marine ecosystems at regional and global scales (Shin *et al.* 2005).

Measurements from a range of fossil marine taxa and trace fossils demonstrate that the majority of animals suffered a reduction in body sizes through the biotic crisis (i.e. the Lilliput effect in the strict sense) (Twitchett *et al.* 2004; Twitchett 2006; Twitchett 2007; van de Schootbrugge *et al.* 2007).

However, this phenomenon has been little studied in the Tr/J extinction event. Some studies had described small body size of bivalves and ammonites in the Early Hettangian (Hallam 1960; Kennedy 1977; Dommergues *et al.* 2002). Additionally, Hautmann (2004) indicates that just one family of bivalve (Megalodontidae) is affected across the Tr/J boundary, suggesting that this reduction could be a response to changes in seawater chemistry (e.g. under-saturation of dissolved carbonate) (Section 1.9). More recently, Mander *et al.* (2008) suggested a size reduction in bivalves in bivalve communities. Although their study records a good temporal resolution of changes in body size through two Tr/J sections in England, their analysis did not separate out individual families, genera or species of bivalve.

Although these studies possibly demonstrate a global change in body size, the trends are still not clear. In order to better understand changes in body size through the Tr/J interval three questions are addressed:

- 1) Is there a reduction of the body size of marine bivalves through the studied interval?

- 2) If there is a size reduction, does it affect all bivalves?
- 3) If there is a size reduction, does it occur before, during or after the Tr/J mass extinction event?

1.9.4 Trace fossils

Trace fossils are good indicators of environmental conditions and evidence the composition and behaviour of the marine fauna (Droser and Bottjer 1991). Studies of mass extinction events have recorded a severe decrease in the number of ichnotaxa, as well as in burrowing depth and diameter, which has mostly been attributed to the result of marine anoxia (Twitchett and Wignall 1996; Wignall 2001; Twitchett and Barras 2004; Twitchett 2006; Barras and Twitchett 2007).

The Tr/J extinction event does not escape to this pattern. Twitchett and Barras (2004) and Barras and Twitchett (2007), analysed carefully the records of three Tr/J boundary sections in southern England. Their data reveals a notable gap immediately after the extinction events but a rapid reappearance during the recovery stage. Using parameters such as the number of ichnotaxa, burrowing depth and diameter, this work intends to answer the following questions:

- 1) Is there a correlation between the trace fossil and body fossil records?
- 2) If so, do their respective recoveries take place simultaneously?

Chapter 2 Methodology

2.1 Study approach

This research focuses on the effects of the mass extinction on different organizational levels (individuals, species, and communities). High resolution spatial-temporal analysis was performed to describe and evaluate the timing, the intensity, and the amplitude of the changes in marine palaeocommunities through the Tr/J boundary. For this, four locations were selected with the aim of evaluating the changes in the marine fauna through the Tr/J in different locations of Pangaea. Three localities are in the United Kingdom and one in northern Chile. Those localities were selected for their high quality fossil record and high stratigraphic resolution, allowing a good comparison between the sites (Hillebrandt 1990; 1994; McRoberts *et al.* 2007; Lucas *et al.* 2007; Simms and Jeram 2006; 2007; Longridge *et al.* 2007; Hillebrandt *et al.* 2007).

2.2 Study sites

2.2.1 Southwest UK

The sequences of Upper Triassic and Lower Jurassic strata in Southwest UK are exposed continuously in sea cliffs widespread over 300 metres. The sediments were deposited in a series of east – west trending extensional basins (Mander *et al.* 2008). Throughout the Late Triassic and Early Jurassic, Palaeozoic basement rock cropped out along the northern margin of the depositional area and formed an elongated region of high ground that was not finally buried until the Mid-Jurassic. The depositional environments in the Norian were lacustrine and commonly evaporitic; however conditions became generally marine through the Rhaetian (Hesselbo *et al.* 2004).

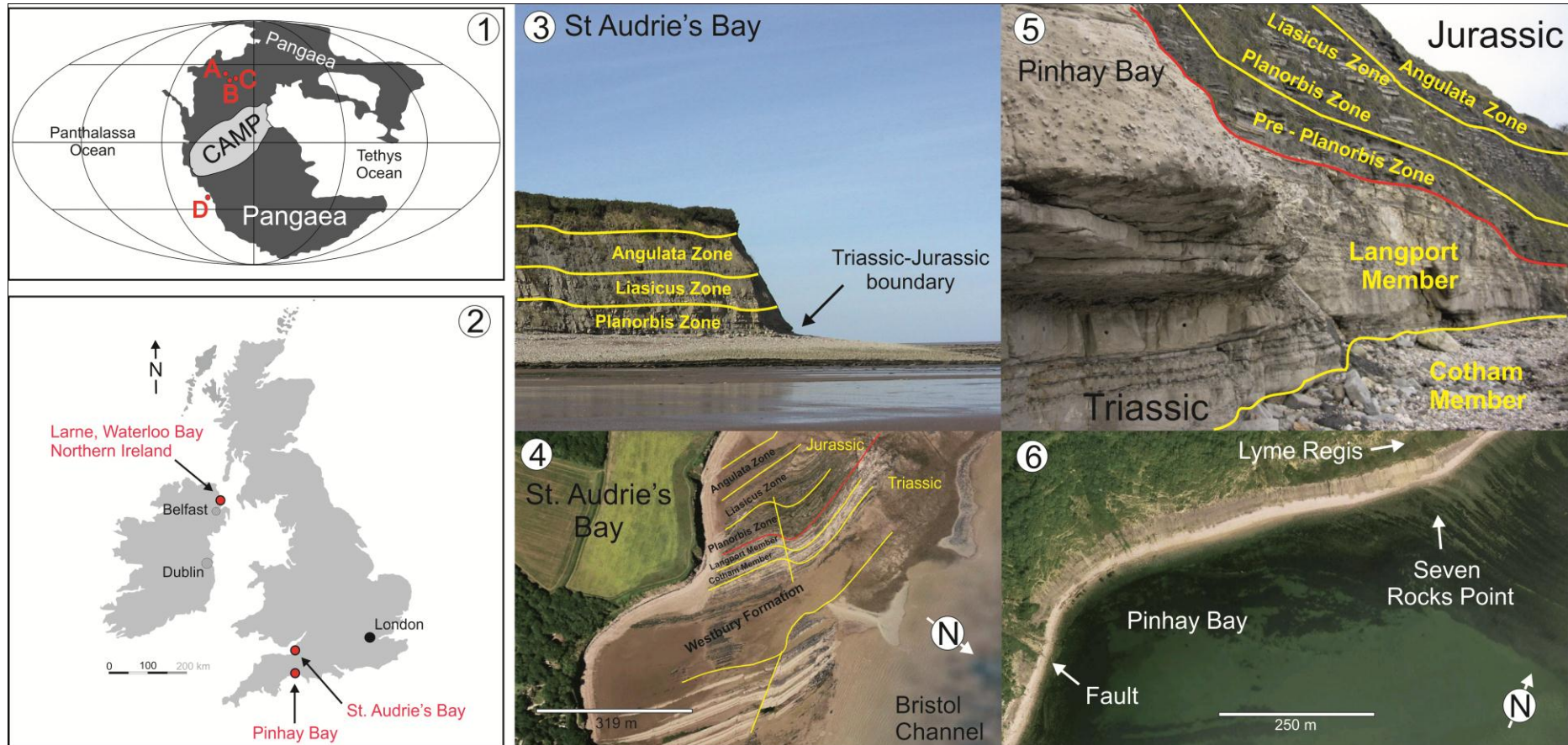


Figure 2.1 Geological setting of studied sections. (1) Triassic-Jurassic palaeogeography (modified from Scotese 2002). CAMP, Central Atlantic Magmatic Province. A: Larne, Northern Ireland (See fig. 2.2), B: St Audrie's Bay; C: Pinhay Bay; and D: Northern Chile. (2) Maps of the locations sampled in UK, the dots and the red letters indicate the three localities. Figures 3 and 4 show the section of St. Audrie's Bay. Figures 5 and 6 show the section of St. Audrie's Bay. Each pictures show their lithostratigraphy (Larne is shown in the figure 2.2).

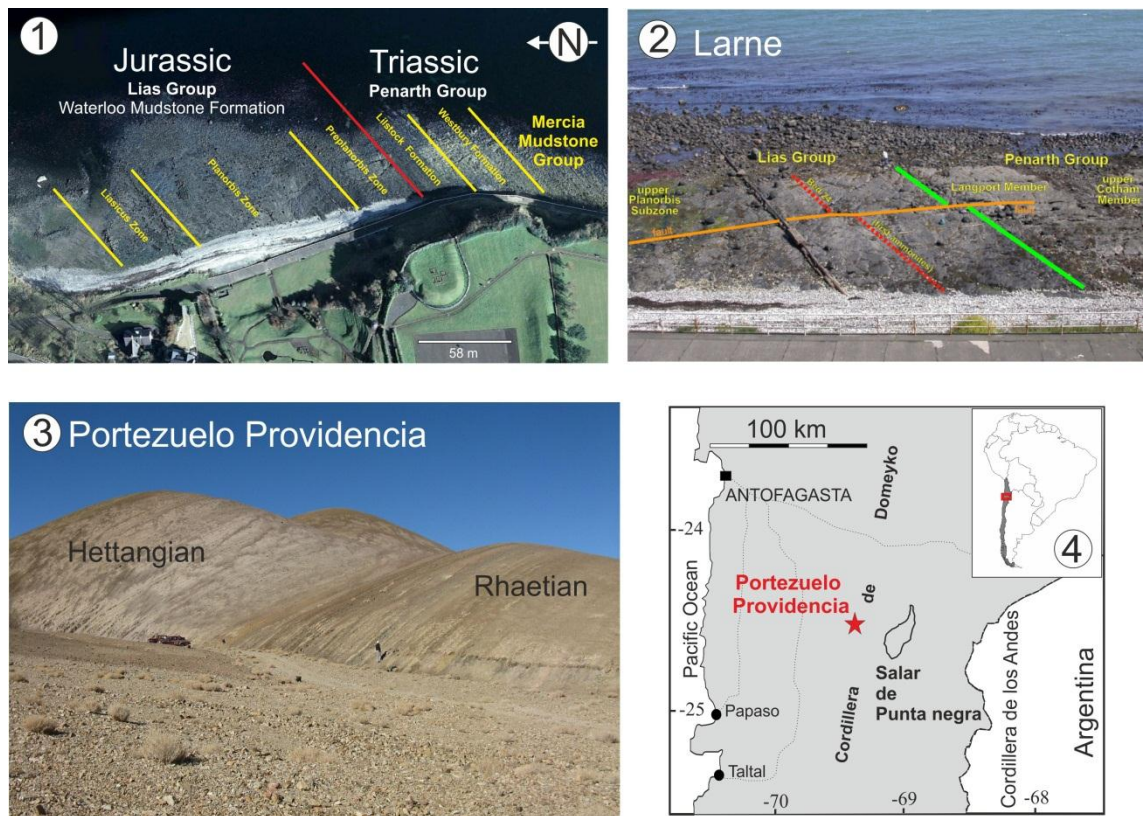


Figure 2.2 Geological setting of studied sections. (1 and 2) Map of the Triassic-Jurassic strata exposed on the foreshore at the Waterloo Bay, Larne. (3 and 4) Strata exposed on Portezuelo Providencia, Northern Chile. Each pictures show their lithostratigraphy.

The Tr/J boundary has been studied for 200 years and many of studies have focused on the localities of St Audrie's Bay and Lyme Regis. Both sections are of international importance, since they incorporate one of the former candidate global stratotype sections for the base of the Hettangian Stage (Warrington *et al.* 2008) and the GSSP of the Sinemurian base (Bloos and Page 2002).

St Audrie's Bay section, is located at the north end of the sea cliff on the west side of St Audrie's Bay, west Somerset, England (51°10'53.99"N; 3°17'9.37"W) (Fig. 2.1). The site is a headland located to the south side of the Bristol Channel, separating St Audrie's Bay, to the east, from Doniford Bay, to the west. Exposure of the succession seen here in vertical section continues south-eastwards for 200 m in a strike section in the cliff (Fig. 2.1) at the west side of the St Audrie's Bay, and westwards, into Doniford Bay.

The same vertical section is exposed on the adjacent foreshore. The stratigraphic succession is continuous downwards, to the east in St Audrie's Bay, and upwards, to the west, in Doniford Bay.

The Pinhay Bay section is located in a broad embayment 2.45 km west of Lyme Regis round to Seven Rock Point (50°42'44.94"N; 2°58'2.81"W). Hallam (1960) described the cliff sections as "incomparably the best section in the country". The Pinhay Bay section is a vertical succession which extends from the Rhaetian to Sinemurian in an eastward direction (Fig. 2.1). Pinhay Bay records the uppermost Triassic Penarth Group (Rhaetian Stage) (Lord 2010). Due to the regional dip, the White Lias descends to beach level in the centre of the bay and passes onto the foreshore at the eastern end of the bay.

2.2.2 Northern Ireland

Larne is located on the east coast of county Antrim, Northern Ireland, 28 km NNE of Belfast (Fig. 2.1). The section is very well exposed and is located on a wave-cut platform on the foreshore at Waterloo Bay (54°51' 26''N; 54°8'18''W) (Fig. 2.1). The section is continuously exposed from the Norian to the Sinemurian (Bucklandi Zone), covering approximately 115 m (Ivimey-Cook 1975). The strata dipping to beach level in the centre of the bay between 20° and 30° to the NW and are cut by a few minor faults (Fig. 2.1) (Simms and Jeram 2007).

2.2.3 Northern Chile

Portezuelo Providencia is located 164 km from Antofagasta, Northern of Sierra Argomedo, North of Chile (24°43'29.93"S; 69°18'45.50"W) (Fig.2.1). The Portezuelo Providencia strata are relatively well expose, and represent continuous marine sedimentation. This section mostly consists of sandstones, siltstones and calcareous intercalations. The section is approximately 60 m thick, spanning from the Norian to

uppermost Hettangian. Through the section the benthic fauna is relatively poor, although ammonites are found in many horizons, which allows a good correlation with other sections through the world (Hillebrandt 1994; 2000). Previous studies in this area have been done by Hillebrandt (1990) and Hillebrandt and Chong (1985) and more recently by Sansom (2000). This investigation is, however the first ecological characterisation of the marine fauna through the Tr/J boundary in Chile.

2.3 Methodology of sampling

Sedimentary logs were produced for each locality in the field. In each section bed numbers were the same as those used by Hesselbo *et al.* (2004) for St Audrie's Bay; Simms and Jeram (2007) for Larne; Lang (1924) and Page (2002) for Pinhay Bay. The beds in the section in Chile do not have bed numbers. The correlation between localities was made through ammonite zone (e.g. Hillebrandt 1994; Hillebrandt *et al.* 2007).

To decrease the lithological bias and capture the spatial and temporal variation in the marine fauna, one random sample of 1.5 ± 0.2 kg of each lithofacies encountered (limestone, mudstone) was taken approximately every 1 ± 0.5 m. Lastly, each sample was wrapped in plastic bags and transported to the laboratory.

The samples from different lithologies were processed in two ways. The limestone rock samples were cut perpendicular to the bedding plane surface, generating slabs of approximately 2.5 cm thickness. Later each slab was polished with wet emery paper (three steps from 200 grit, 400 grit and then 800 grit), and afterwards the polished surfaces were soaked in 37% hydrochloric acid for about 10 seconds and washed under water. This technique allowed the precise recognition of fossil features and the identification of trace fossils. However, when the slabs showed poor preservation of the fossils, it was broken in to pieces for a more precise identification of the fossils.

Each sample of mudstone was broken into 45 cm² chips. Water was used to soak the rock and separate the fossils without damaging them. In both cases the macrofauna of marine invertebrates was identified as far as possible and the number of individuals per species was counted. All the specimens were classified according to Hallam (1960), Chong and Hillebrandt (1985), Swift and Martill (1999), Moghadam and Paul (2000), Hodges (2000), Simms & Jeram (2007), Mander *et al.* (2007), Paul *et al.* (2008), Warrington *et al.* (2008) and Lord and Davis (2010).

Additionally, other measurements were made in the field, such as the body-size of the organisms and the number and size of ichnofossils (see 2.4.4 and 2.4.5). In this case, all the observations and the measurements were performed at the same horizons where samples were taken. Finally, richness, dominance, composition, abundance, ichnometric and morphometric indices were calculated to document the ecological changes in the marine palaeocommunities.

2.4 Data analysis

2.4.1 Richness

Richness is a fundamental property of any biotic assemblage. It is defined as the number of different categories observed in one collection (any unit e.g. area, volume, weight) (Olszewski 2010). Richness characterises the assemblage and gives information about ecosystem condition (Gaston 1996). Many techniques have been developed for estimating the richness in one sample (Magurran 2004). Here, to evaluate the changes in richness in the palaeocommunities through the Tr/J boundary, the number of species was estimated through individual-based and sample-based rarefaction techniques (Gotelli and Cowell 2001).

Individual-based rarefaction is a sequential sampling of the individuals of each sample, or the expected number of species in a random sub-sample of individuals from a single, large collection (Gotelli and Cowell 2001). The advantage of this technique is that it avoids the biases due to differences in sample effort between sampling (Gotelli and Cowell 2001). Sample-based is the mean value of repeated re-sampling of all pooled samples (Gotelli and Cowell 2001; Appendix 2.1).

Rarefaction curves of each sample were estimated as sampling size (SaS) increases, where SaS was defined by sequentially increasing the number of individuals from 1 to N (Gotelli and Cowell 2001). In the analysis, for each SaS (from 1 to N) the sample was randomly resampled 5000 times and the followed parameters were estimated: the number of species (species richness); Shannon-Wiener H' diversity index (Hayek & Buzas, 1997); and the fraction of the collection that is represented by the most abundant species (a species dominance index). After 5,000 rarefactions were performed, species richness at each SaS was estimated as the average number of species calculated from the 10,000 re-samples obtained for each SaS (Gotelli and Entsminger 2006). Richness estimators like Mao Tau (Colwell *et al.* 2004), $Chao_1$ (Chao 1984), and $Jackknife_1$ (Burnham and Overton 1978; 1979) were calculated to confirm the observed patterns (Appendix 2.1).

The Shannon-Wiener H' diversity index of each SaS was calculated using the natural logarithm as:

$$H = \sum p_i \ln[p_i] \quad (2.1)$$

Where p_i is the proportion of the sample represented by the species i th in the sample (Gotelli & Colwell 2001); then, these 5,000 values of this index obtained for each sample were averaged to estimate the mean diversity of the respective SaS. In all procedures richness was estimated for the whole locality, for each bed and for the

different stratigraphic units. The stratigraphic units considered were the Westbury Formation, Cotham Member, Langport Member, Pre-Planorbis Zone, Planorbis Zone, Liasicus Zone and Angulata Zone.

All the rarefaction analyses were performed with software EcoSim 7.72 (Gotelli and Entsminger 2006) and Estimates 7.5 (Colwell 2005). The values of species richness and Shannon-Wiener H' diversity index were plotted against SaS to assess variation as the number of individuals included in the samples increased. The statistical differences between different samples, localities and stratigraphic units were evaluated through the estimation of 95% confidence intervals at each SaS. Significant differences were considered when the confidence intervals did not overlap.

2.4.2 Abundance

Abundance is defined as the number of entities (individuals) of a specific category (species) and represents the structure and complexity of the community (Begon *et al.* 2006). Its properties are estimated by evenness, which quantifies how equal the community is numerically, or by dominance, which shows that one species is particularly abundant or controls a major portion of the resources in a community.

Three methods were used to calculate temporal differences in abundance. The first is kurtosis (see Appendix 2.4.2 for definitions), which is a measure of whether species abundance is peaked or flat relative to a normal distribution. If the kurtosis is positive it indicates assemblages with high dominance; more even communities record negative kurtosis (Webb *et al.* 2010). This measure was plotted against stratigraphic height and lithostratigraphic units. The kurtosis values were estimated with the program Statistica 6.0 (Statsoft, Inc. 2001).

The second method applied is the Rank Abundance Distribution Curve (RADs) (Whittaker 1965). This method displays the logarithmic species abundances against species rank order. Different RADs reflect specific ecological scenarios (environmental gradients or disturbance). Five of the most popular RADs models following Wilson (1991) were tested against the palaeoecological data: Broken stick, Geometric series, Log normal, Zipf and Zipf – Mandelbrot (Appendix 2.2).

The Figure 2.3 shows the five main rank abundance models, which reflect different ecological scenarios (Magurran 2004). The geometric model is interpreted to reflect a situation in which the majority of the resource is dominated by one to few species within the community (Harnik 2009). The plot of the geometric model is a straight line with a high slope, which represents the ranking from the most to the least abundant species. Field data have shown that the geometric model is found primarily in species-poor (and often harsh) environments or in the very early stages of a succession (low ecological complexity) (Bastow 1991).

The log normal model is one of the most common patterns that appear in large assemblages studied by ecologists (Magurran 2004). The log normal distribution has a shallower slope, which is associated with the highest evenness, and is generally associated with more “stable” ecosystems (Magurran 2004). Associated with the log normal distribution is the Zipf-Mandelbrot model, which reflects successional processes in which the later colonists have more specific requirements and hence are rarer than the first species that arrive. Finally, the broken stick model represents a more uniform distribution of abundance and is the most uniform distribution ever found in natural communities (Bastow 1991). The model could be viewed as representative of a group of

species of equal competitive ability jostling for niche space (Tokeshi 1993; Magurran 2004).

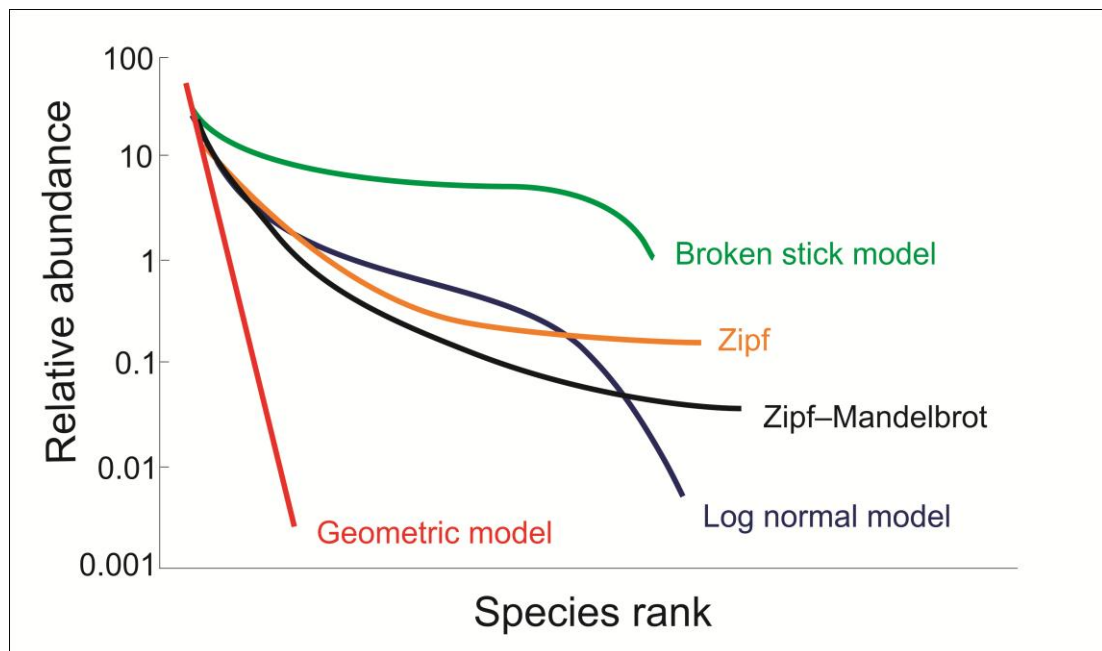


Figure 2.3. Rank/abundance plot illustrating the typical shape of three well-known species abundances models: the geometric, log normal and broken stick models.

During the extinction event the rank abundance distribution will best fit to the geometric model, because the expectation is that the assemblages will be dominated by few species, showing low ecological structure (Magurran 2004). Or could also, fits to Broken Stick model, which predicts a very uniform RADs, where the group of species have the same competitive ability jostling for niche space (Magurran 2004).

Before the extinction (i.e. the Westbury Formation) and from late recovery onwards (i.e. the Angulata Zone) assemblages should reflect a mature and stable system (Barras and Twitchett 2007), represented by a more even abundance of species, and should conform to Zipf or Zipf - Mandelbrot model (Harnik 2009). During the post-extinction recovery stages assemblages should fit to a log normal distribution.

The choice of the best fit model is based on maximum-likelihood-estimation, performed through the Akaike Information Criterion (AIC), which balances the goodness-of-fit against model complexity (Johnson and Omland 2004; Wang 2010). Briefly, the likelihood is defined as the probability of obtaining the observed data given a specific model. The objective of this metric is to choose values for parameters that maximise the likelihood i.e. that yield the highest probability of producing the data at hand.

Summarising the models with higher AICc (Akaike weights) are the best candidates to represent an assemblage through the Tr/J extinction event.

Finally the third method consisted of estimating a dominance index by lithology, locality and stratigraphic unit. This index was calculated as the fraction of the (re-sampled) collection that is represented by the most common species (a species dominance index) at each run (Gotelli and Entsminger 2011; Appendix 2.4.1). The dominance was estimated in the same way as described for the Shannon-Wiener index (as SaS increases). The statistical differences between different samples, localities and stratigraphic units were evaluated through the estimation of 95% confidence intervals at each SaS. Differences were considered significant when the confidence intervals did not overlap. All data were analysed using R programming (R Development Core Team., 2006), EcoSim version 7 (Gotelli and Entsminger 2011) and Statistica 6.0 (Statsoft, Inc. 2001).

2.4.3 Composition

Composition refers to the different “taxonomical entities” that constitute an assemblage (Magurran 2004). One of the measurements is beta diversity (β), which measures the difference in species composition either between two or more local assemblages through any gradient, e.g. spatial or temporal (Koleff *et al.* 2003). In this work two

different β diversity indices were estimated with the aim of observing the turnover of the fossils organisms through the Tr/J boundary. Whittaker (β_w) (Whittaker 1960) and Wilson and Shmida's index (β_T) (Wilson and Shmida, 1984) (Appendix 2.3). Both indices are the most robust against sample size and changes in α -diversity, but overall, they are sensitive enough to detect gradients in composition (Wilson and Shmida 1984, Magurran 2004). The indices were estimated by using the statistical program PAST Version 2.07 (Hammer and Harper 2006).

To observe composition patterns in the assemblage, multivariate analysis was performed on the square root transformed abundance data. Additionally, Euclidian distance was calculated (McCune and Grace 2002) (Appendix 2.3). Non-metric Multidimensional scaling (nMDS) (Appendix 2.4) ordination was used to identify whether the samples are strongly grouped by lithologies, stratigraphic unit, or localities. Statistical differences between groups were analysed by means of analysis of similarity (one and two way ANOSIM) (Clark 1993) (Appendix 2.3). The relative importance of each group with the highest dominance was identified by similarity of percentage (SIMPER procedure). All multivariate analyses were performed by using the Program PRIMER 5.2.2 computer package (Plymouth Routines in Multivariate Research).

2.4.4 Ecospace

Ecospace is a combination of 3 elements; tiering, motility and feeding. Each of these categories is subdivided into 6 subcategories (See Figure 3.1), which generate a cube with 216 combinations that synthesise organism performance in the environment (Bambach *et al.* 2007; Bush *et al.* 2007). In this work, species were categorised sample-by-sample in terms of tiering, motility and feeding using the autecological information derived from Mander & Twitchett (2008) and from the Paleobiology Database

(<http://paleodb.org/cgi-bin/bridge.pl>). The proportion of each mode of life used by the fauna was estimated based on the total number of species recorded in each stratigraphic unit. This was repeated for each lithology and study site. To test patterns of selective extinction: e.g., the selective extinction of infaunal bivalves hypothesis (McRoberts and Newton 1995), the proportion of each ecological trait was correlated by Spearman rank-order and Pearson product-moment. The significance of each correlation was evaluated by a student's *t* test with a $\alpha = 0.05$.

2.4.5 Trace fossils

In palaeoecological studies, trace fossils provide important palaeoenvironmental information and evidence of the composition and behaviour of the macrofauna (Droser and Bottjer 1991). In order to characterise and evaluate the bioturbation recorded through the Tr/J boundary; this work assessed the trace fossil response through three methodologies estimating the degree of bioturbation using the vertical section of each bed sampled. For that, the slabs or “cores” obtained from each cut limestone sample were analysed in three ways.

The first method was the utilisation of a vertical ichnofabric index (Droser and Bottjer 1993). The ichnofabric index is a semi-quantitative ranking of the extent of bioturbation (Droser and Bottjer 1986). The ichnofabric index is based on 6 categories that measure the percentage of the original sedimentary fabric that has been disturbed (Droser and Bottjer 1986; 1993). The index can be represented by schematic diagrams such as those shown in Figure 2.4. Each sample obtained from the field could be categorised by visual recognition of similarities of pattern. In this way it, it is possible to give a percentage value to each sample from each specific stratigraphic horizon.

The second method estimates the relative abundance of each ichnotaxa through the random placing of three quadrats of 5×5 cm on the vertical cross section area of each plate. This method reported information of the richness, relative abundance per ichnotaxa, and the bioturbation percentage per specific unit area (Fig. 2.5C).

The third method consisted of estimating various ichnometric parameters. The most simple and informative measure is the burrow diameter (McIlroy 2004). For that, the diameter of each ichnotaxa found on the vertical cross section area of each plate from each stratigraphic horizon was measured by electronic callipers (Fig. 2.5). Also, measurements of composition and diameter were obtained from the field by using a tape measure (standard error $\pm 0.1\text{mm}$) (Fig. 2.5). Finally, the ichnofabric index, percentage covered and burrow diameter were plotted against their stratigraphic setting. Several models were fitted into the data (linear, exponential and logistic) in order to observe a general trend. The ichnotaxonomic determination was performed following the work of Swift and Martill (1999), McIlroy (2004), Twitchett and Barras (2004), Barras and Twitchett (2007) and Lord and Davis (2010).

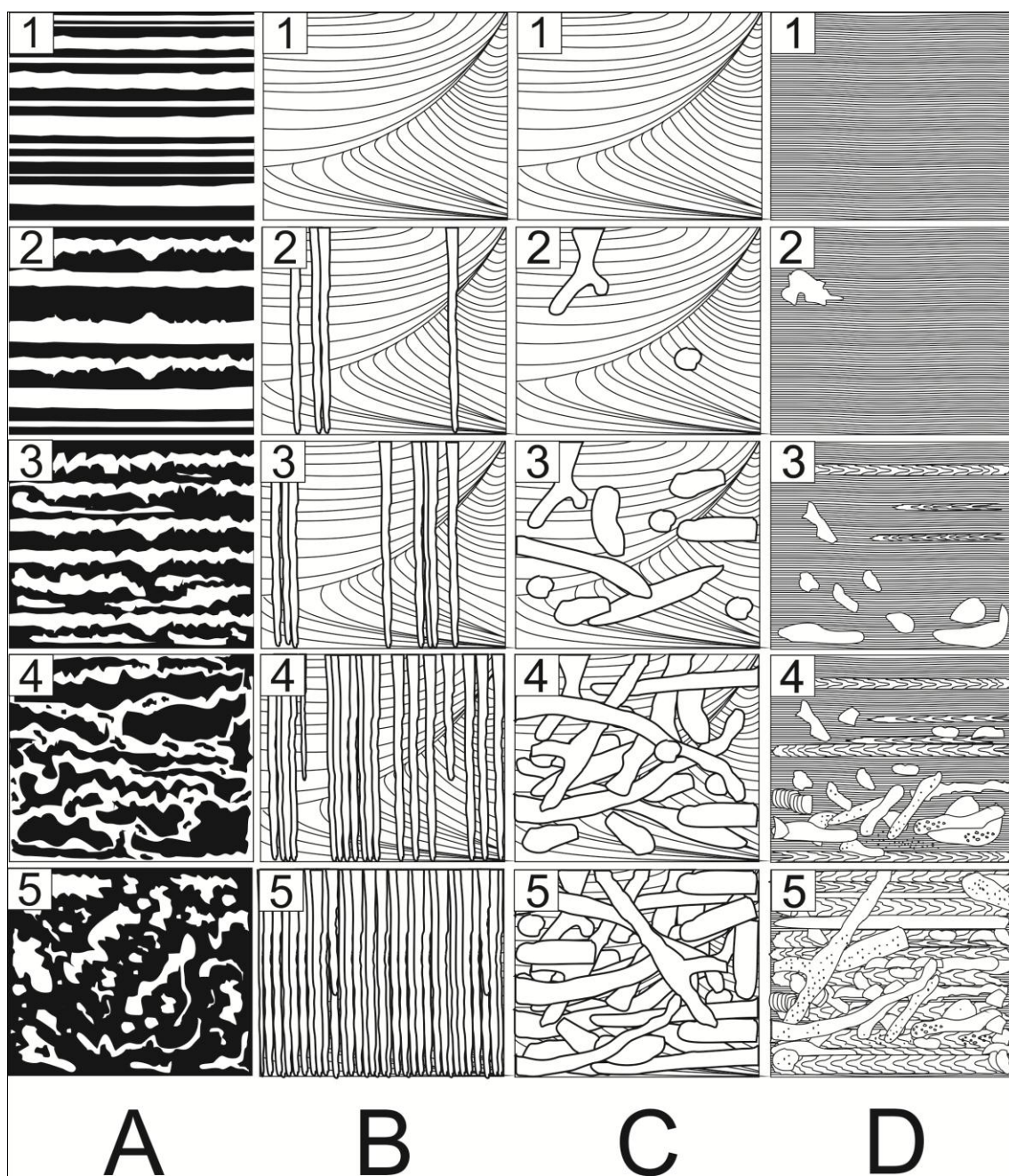


Figure 2.4 Schematic diagrams of ichnofabric indices represented by five categories in four different environments. A) Shelf environments, B) High-energy near-shore sandy environments dominated by *Skolithos*, C) High-energy near-shore sandy environments dominated by *Ophiomorpha*; D) Deep-sea deposits. 1. No bioturbation recorded. 2. Discrete, isolated trace fossils up to 10% of the original bedding disturbed. 3. Approximately 10-40% of original bedding disturbed. 4. Last vestiges of bedding discernible; approximately 40-60% disturbed. 5. Bedding is completely disturbed. Modified from Droser & Bottjer (1986; 1991; 1993).

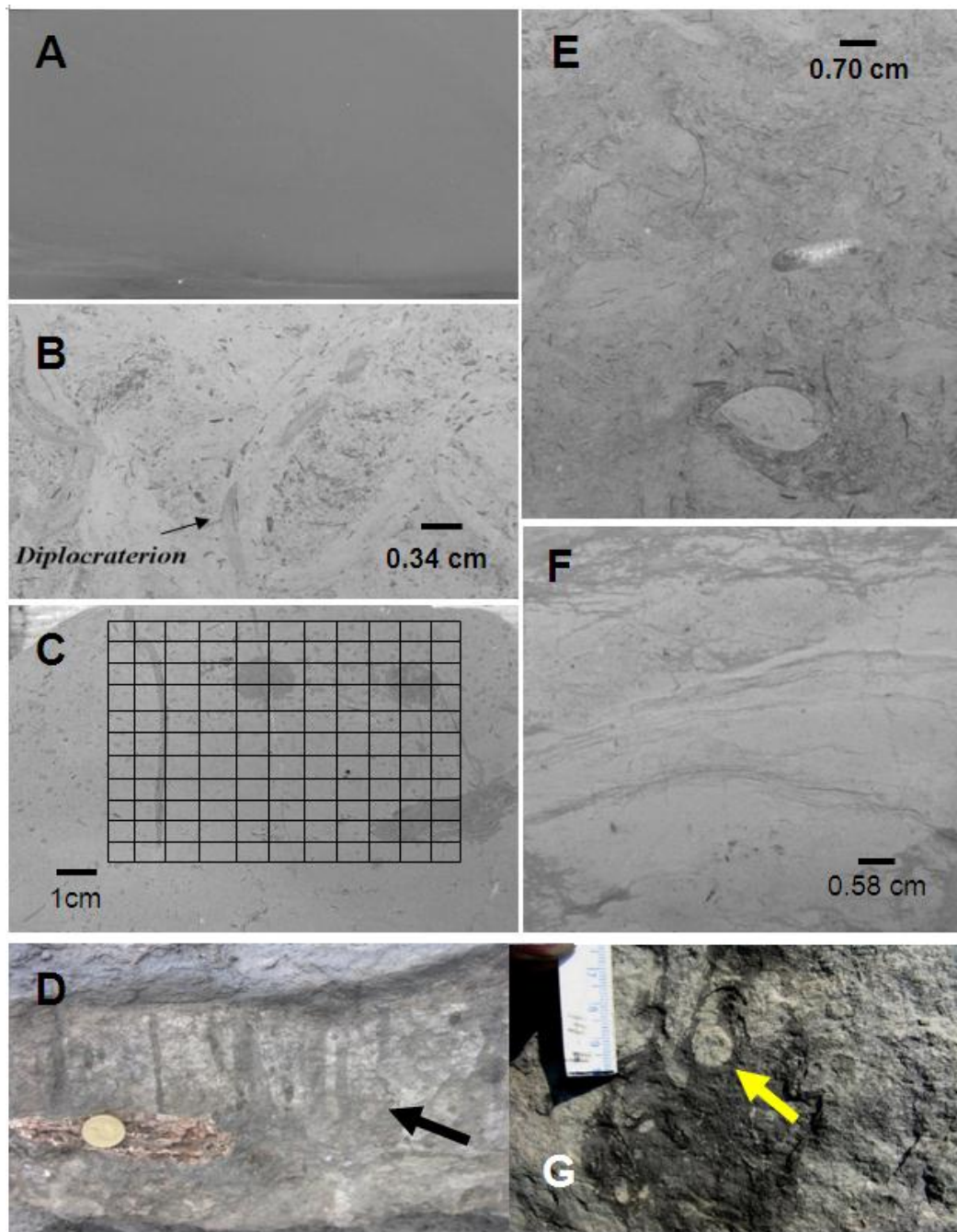


Figure 2.5 Cross section plates that show a perpendicular view to bedding plane surface. (A) Shelf environments, with no-bioturbation. (B) And (E) Shelf environmental, highly disturbed, the black arrow shows *Diplocraterion*; *Thalassinoides* is also observed. (C) Cover quadrant of 5×5 cm on the vertical cross section area. (F). A vertical cross section, with approximately 10 % disturbance, apparently the sediment was deposited under high-energy near-shore sandy environment. (D) and (G) show a cross vertical view of one bed horizon; *Skolithos* is indicated by a black arrow and *Arenicolites* by a yellow arrow.

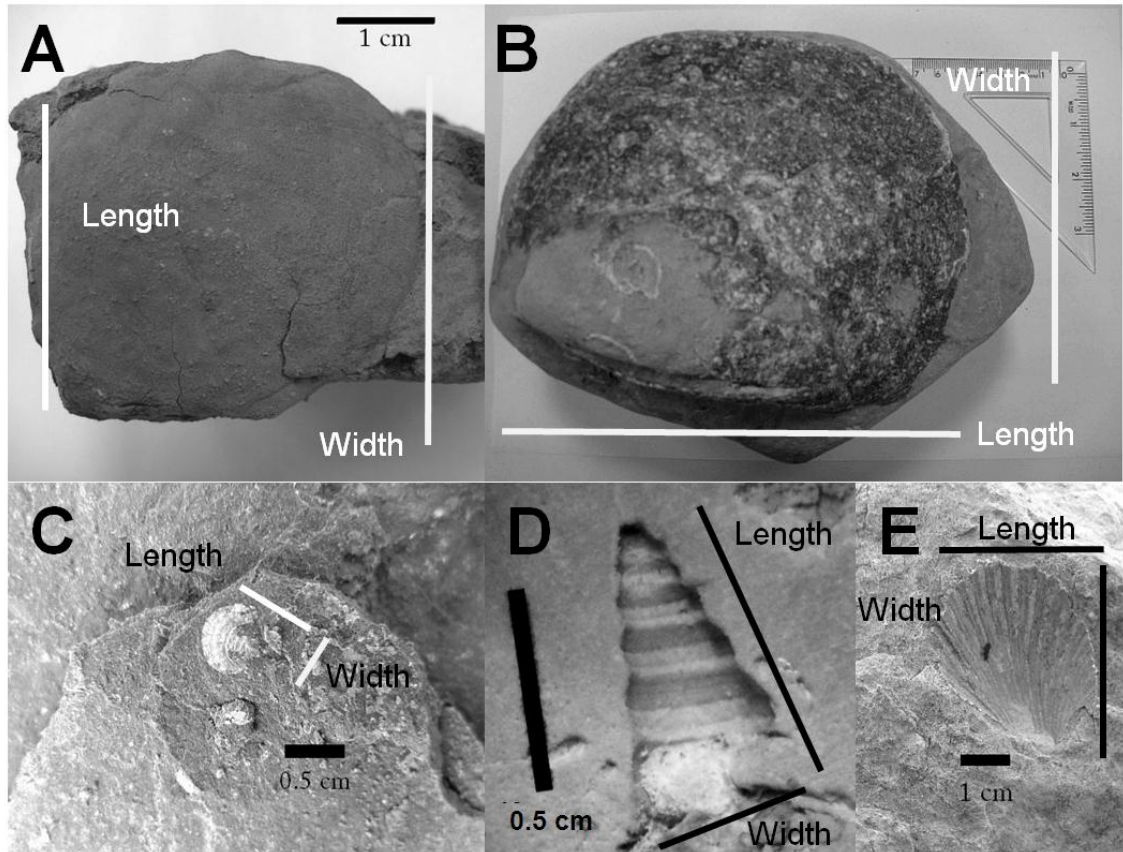


Figure 2.6 Photographs showing the variables measured to estimate the geometric mean. A) *Pteromya langportensis* (Richardson and Tutcher 1916). B) *Plagiostoma giganteum* (J. Sowerby 1815). C) *Modiolus minimus* (J. Sowerby 1818). (D) *Promathildia rhaetica* (Moore 1861). (E) *Chlamys valoniensis* (DeFrance 1825).

2.4.6 Body size

In each sample, the width and length of complete individuals of groups such as bivalves, gastropods, brachiopods and ammonites were measured by electronic calliper (standard error ± 0.01 mm) (Fig. 2.6). In addition, in order to increase the sample size per each stratigraphic horizon, individual measurements were made in the field from bedding plane exposures using a tape measure (standard error ± 0.5 mm) (Fig. 2.6). Later, the size was calculated as the geometric mean of the length and width following Jablonski (1996), which represents the square root of the product of length and width and/or height:

$$\text{Geometric mean} = \left(\prod_{i=1}^n a_i \right)^{1/2} = \sqrt[n]{a_1 a_2 \cdots a_n} \quad (2.2)$$

In order to determine whether any significant interspecific changes in the body size occurred in the section, four quantitative analyses were performed. The first is based on a scatter plot of the % changes in the maximum and minimum body size (Jablonski 1996) (Fig. 2.7).

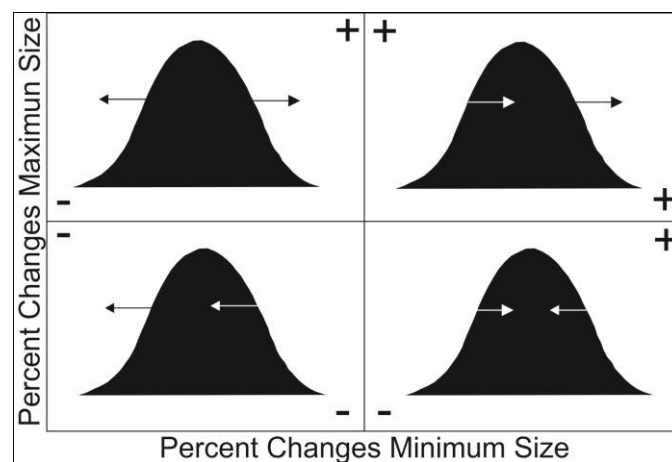


Figure. 2.7. Graphical approach to the analysis of evolutionary changes in body size. Modified from Jablonski (1996).

Through this plot it is possible to represent different evolutionary patterns. The right upper quadrant represents Cope’s Rule which is an active and directional trend of size increase (Fig. 2.7). The lower left quadrant indicates a strong pattern of size decrease, for example “The Lilliput Effect” (Twitchett 2007; Metcalfe *et al.* 2010; He *et al.* 2010). The upper left quadrant represents an increase in the variance; the range of the adult body size has expanded through the time, which means an increase in the largest size and a decrease in the smallest size. Finally, the lower right quadrant (Fig. 2.7) represents a decrease in the variance, the evolutionary loss of both extremes, resulting in a constriction of the sizes contained within the group or clade (Jablonski 1996). In order

to perceive passive evolutionary changes in size through the Tr/J boundary, Jablonski target plots were produced for each stratigraphical unit and study site.

The second methodology was to perform size-frequency distribution plots of the genera with the most extensive stratigraphic ranges through the Tr/J boundary pooled by stratigraphic unit. The third method was to estimate a simple size rate change through successive samples. This was developed by pooling all the individuals' sizes per species per sample, and then the rate was estimated as follows:

$$\text{Size rate of change} = \left[\frac{\log(r_2 - r_1)}{\log(t_2 - t_1)} \right]$$

Where, r_2 represents the average size of all individuals measured in t_2 , while that r_1 , represents the average size of all individuals measured in t_1 , and $(t_2 - t_1)$ indicate the difference in time or the stratigraphic distance between sample two and one. The objective of this metric is to observe if the rate of change in body size shows a directional trend, whether they are negative rates through extinction events or positive values through recovery.

Finally, the data were compared to a “null model” in body size. A null model is designed with respect to some ecological or evolutionary process of interest. A null model is a pattern-generating model that is based on randomisation of ecological data. Certain elements of the data are held constant and others are allowed to vary stochastically to create new assemblage patterns. The randomization is designed to produce a pattern that would be expected in the absence of a particular ecological mechanism (Gotelli and Graves 1996).

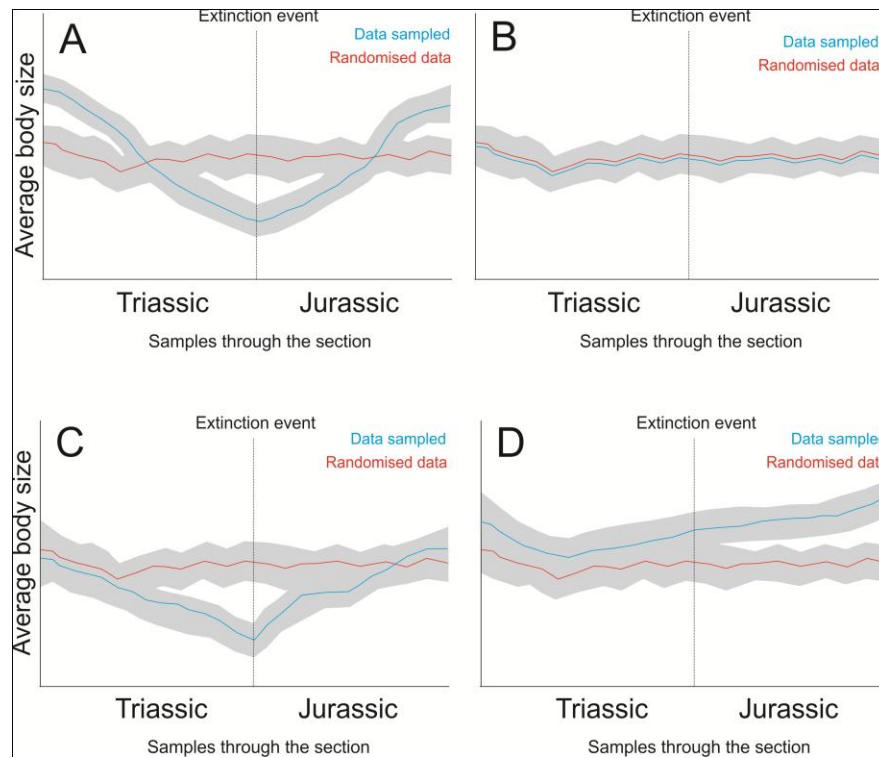


Figure 2.8 Null model in body size through the Tr/J boundary. The null model is expressed as randomised data (red line), the grey shadow represents the 95% confidence intervals. The blue line represents four possible size change scenarios. A) A decrease of average body size spanning the extinction event with significant increase following. B) No-changes in body size. C) No-changes before and after the extinction event and a significant decrease in body size during the event and D) The mean size observed is higher than expected by chance and trend to increase through the time.

The reason for generating null models is that they emphasise the potential importance of stochastic mechanisms in producing natural patterns (Gotelli and Graves 1996). A matrix of individual body sizes was obtained from the samples, and these values were randomised 10,000 times by individuals and samples. The idea of this randomisation is to produce patterns of body size generated just by chance. This “randomised data” was contrasted with data observed in field. The mean, confidence intervals and density distributions were plotted. A t test was calculated, in order to evaluate the differences between constraints-data (randomised) and sampled-data (Zar 1999). Finally, four hypothetical scenarios are proposed (see Figure 2.8) for more explanations. All the analyses were performed using R programming (R DEVELOPMENT CORE TEAM., 2006).

Chapter 3 Ecospace and ecological trends of marine organisms through the late Palaeozoic and early Mesozoic

3.1 Introduction

The publication of the Sepkoski diversity curve (1979; 1984; 1997) led to a clearer understanding of the dynamics of marine diversity throughout the Phanerozoic.

Nevertheless, the patterns of change are still widely debated, e.g. Stanley (2007), Alroy *et al.* (2008), Alroy (2010). The material compiled since the 1970s has demonstrated: (1) how diversity changes, (2) the different phases of diversification, and (3) the structure of the fossil record throughout the Phanerozoic.

The diversity curve through time does not just represent a secular increase in species richness but also demonstrates a continuous increase in ecological diversity: this means that complex ecosystems are generated through the incorporation of new species with new morphological adaptations to exploit new ecological spaces, which give rise to new ecological interactions (Bambach *et al.* 2007). One of the ways to study the evolutionary trends of ecological interactions is through ecomorphology. Morphological adaptations can be used as a proxy for the ecological traits of an organism and can consequently be pooled into ecological groups (e.g. microhabitat, mobility, reproduction, diurnal activity, and ecomorphology) (Schoener 1974; Bambach 1983, 1985; Simberloff and Dayan 1991; Winemiller 1991; Wainwright 1994; Novack-Gottshall, 2007).

Bambach (1977; 1983 and 1985) presented one of the first ecological approaches to the classification of organisms, developing the idea of *ecospace* or *ecological space*, using the morphology of marine fossil taxa to generate mega-guilds. The ecospace model reveals adaptive strategies in the marine community over time, describing how

organisms exploit the resources on which competition develops or are limited in their attempts to do so (Bambach 1983; 2007; Bush *et al.* 2007; Novack-Gottshall 2007).

According to Bambach's model, ecospace consists basically of three attributes that describe the autoecology of an organism (Fig. 3.1; Table 3.1). **Tiering** is the relationship of the organism with the substrate and the water column; the **feeding mechanism** is the manner in which the organism feeds; and **motility** is the organism's capacity to move on its own. Bambach divided each of these axes into six subcategories, the combinations of which generate a cube with 216 possible combinations for describing the performance of each species (see Bambach *et al.* 2007; Bush *et al.* 2007).

Table 3.1 Examples of fossil organisms which display determinate modes of life (from Bush *et al.* 2007).

Number	Modes of life	Representative groups
Tiering		
1	Pelagic	<i>Chondrichthyes, Amphibia, Cephalopoda</i>
2	Erect	<i>Crinoidea</i>
3	Surficial	<i>Gastropoda, Echinoidea, Polyplacophora</i>
4	Semi infaunal	<i>Bivalvia, Asteroidea, Echinoidea</i>
5	Shallow infaunal	<i>Bivalvia, (clams)</i>
6	Deep infaunal	<i>Bivalvia (clams), Annelida</i>
Motility		
1	Freely, Fast	<i>Osteichthyes, Reptilia, Mollusca</i>
2	Freely, Slow	<i>Echinoidea, Asteroidea, Polychaeta</i>
3	Facultative, unattached	<i>Bivalvia (mussels, Pectinidae)</i>
4	Facultative, attached	<i>Holothuroidea, Bivalvia</i>
5	Non motile, unattached	<i>Rostroconchia, Bivalvia</i>
6	Non motile, attached	<i>Cirripedia, Crinoidea, Rhynchonellata</i>
Feeding		
1	Suspension	<i>Bivalvia, Crinoidea, Holothuroidea</i>
2	Surface deposit	<i>Bivalvia, Echinoidea, Gastropoda</i>
3	Mining	<i>Echinoidea, Gastropoda</i>
4	Grazing	<i>Gastropoda, Echinoidea, Polyplacophora</i>
5	Predatory	<i>Cephalopoda, Osteichthyes, Reptilia</i>
6	Chemotrophic, parasites	<i>Bivalvia, Nematoda</i>

The ecospace model offers a way to approach the changes in community structure over time, identifying the factors that influence the life modes of organisms and evaluating changes in the community on both spatial and temporal scales. For example, Bambach (1983) and Bambach *et al.* (2007) described the adaptive strategies of the major faunal turnovers documented by Sepkoski (1981), who reported that the Cambrian fauna consisted mainly of epifauna, with no deep-infauna or passive shallow forms and few pelagic forms. Epifaunal forms increased during the Mid and Late Palaeozoic and, at the same time, pelagic and infaunal forms began to expand. In the Mid-Cenozoic, diversity is concentrated in infaunal and pelagic habitats, which replaced the epifaunal life mode, and the well documented increase in predation.

Bush *et al.* (2007) also used this tool from a biogeographic perspective. These authors performed a temporal comparison of the life modes from Mid-Palaeozoic and Cenozoic and compared communities of the same age from tropical and temperate regions from the Late Cenozoic. Their results showed that the categories associated with infaunalisation, motility and predation increase from the Palaeozoic to Cenozoic and from temperate to tropical zones.

Extinction events can also be evaluated using the ecospace model, since massive extinctions reduce ecosystems to simpler organization levels. Fraiser and Bottjer (2005) used ecospace to observe the recovery of benthic palaeocommunities after the extinction in the Late Permian. They reported a severe contraction of the ecospace: only four life modes were in use in the Early Triassic and eight in the Mid-Triassic. Layou's (2009) recent use of ecospace to evaluate spatial-temporal changes after the mass extinction event in the Late Ordovician indicates that ecospace is sensitive enough to identify transitional changes in ecological traits on a regional scale.

The Bambachian ecospace model was designed to observe ecological components from an evolutionary perspective. It is a flexible, informative tool that synthesizes the life modes of organisms in a few variables, allowing us not just to detect and evaluate changes in the community structure, but also to apply the ecospace model to observed radiation or extinction events. This work focuses on the Late Permian, Triassic and Early Jurassic in terms of assessing the total number of life modes occupied, correlating richness with ecological space, the observation of contraction and ecospace expansion through the Late Triassic mass extinction event (Tr/J event) and a comparison of the magnitude of the mass extinction in question compared to the Permian-Triassic event (P/Tr).

Biologically, the Late Palaeozoic and Early Mesozoic (i.e. Triassic) constituted a transition period (cf. Payne and Van de Schootbrugge 2008) during which one of the greatest faunal turnovers was generated through the mass extinctions of the Late Permian and Late Triassic. In addition, a series of evolutionary novelties appeared in the subsequent radiations, triggering a series of changes in the functioning and structure of marine systems and the beginning the Mesozoic Marine Revolution (MMR) (Stanley 1974; Vermeij 1977). This present work, therefore, will not only describes the dynamics of the changing ecospace model, it also evaluates the behaviour and relationship of the axes that construct the ecospace model in order to determine the ecological factors and evolutionary processes related to the MMR.

3.2 Database and methods

Changes in the ecospace utilisation in marine habitats from the Late Permian (Wordian-Changhsingian), Triassic (Induan-Rhaetian), and Early Jurassic (Hettangian-Sinemurian), covering a total of 80.9 ± 1.1 Myr (Gradstein *et al.* 2005), were analysed

from data obtained from Sepkoski's Online Genus Database, at the site maintained by S. E. Peters (<http://strata.geology.wisc.edu/jack/>). This is one of the most complete records of marine diversity over time. However, it does not consist strictly of sampled diversity; rather, this database lists only the first and last occurrences, deriving standing diversity estimates from taxa for time intervals in which they were not always sampled (Smith and McGowan 2007).

The geographic coverage of the Sepkoski database is not homogeneous due to geographic variations in outcrops and sampling paleontological in detail (Smith and McGowan 2007; McGowan and Smith 2008). The data from the Northern Hemisphere constitute 58% of average occurrences, with North America, Europe, Indian Ocean and Asia, respectively representing 12.6%, 23.1%, 0.59% and 21.8% of the records. Records from the southern hemisphere constitute 41.9% of the records with data from Oceania, Africa and South America (Appendix 3.1).

In contrast, the temporal coverage seems to be more homogeneous; there are no significant differences in the average number of occurrences of taxa in the fossil record for the 14 stages considered ($X^2 = 20.87$; D.F. = 12; $p > 0.05$) (Appendix 1.2). That could suggest that the stages are equally distributed temporally. This point is important, because the over-representation of any of the stages would generate spurious patterns, marred by differential sampling efforts (Vermeij and Leighton 2003).

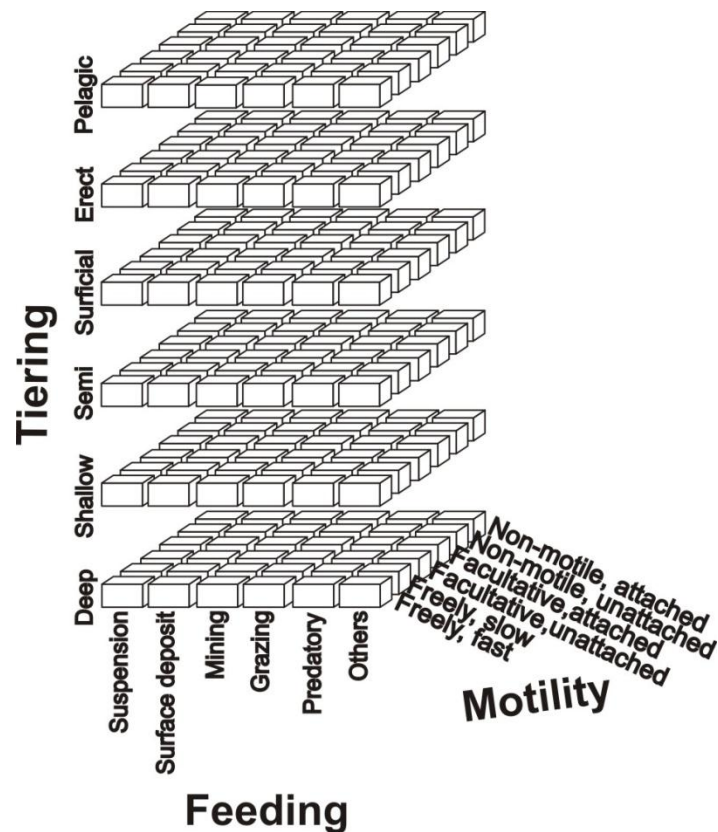


Figure 3.1 Ecospace as defined by the axes of tiering, motility level, and feeding strategy. The ecospace cube expanded, showing 216 cubes or modes of life specified by the combination of the categories on each ecospace axis (from Bambach *et al.* 2007).

Additionally, Sepkoski's database does not detail the changes in richness and the interactions of organisms in a particular environment. However, from this data base it is possible to: (1) approximate when changes (in structure, richness and ecological functionality) occur in local systems (Bambach *et al.* 2002; Aberhan *et al.* 2006); (2) observe the maximum level of potential use of ecological space, considering that different habitats present different proportions of life modes (e.g. coral reef, coastal, deep-water environments) (Bush *et al.* 2007); and (3) observe the relations between the roles and functions of species that made up the communities or ecosystems.

The Sepkoski Database was used to generate a presence-absence matrix, registering a total of 3810 genera grouped in 11 phyla. Each genus was assigned to an ecological

category (Table 3.1) according to its ecomorphological traits, using auto-ecological information derived from The Paleobiology Database (<http://www.paleodb.org/cgi-bin/bridge.pl>) and from information obtained from the literature for the different taxa (Table 3.2). In some cases, for example in genera such as *Lingularia*, *Modiolus*, *Arenicola*, *Nannastacus*, *Limulitella*, and *Goniada*, the inferences were based on current living groups.

Table 3.2 References used to categorise species into each mode of life.

Mollusca	(Hallam 1960; 1981; 2002; Rohr and Bloodgett 1985; Anderson <i>et al.</i> 1990; Aberhan 1992; 1994; Aberhan <i>et al.</i> 2006; Bambach <i>et al.</i> 2007; Mander and Twitchett 2008; Hendy <i>et al.</i> 2009).
Osteichthyes	(Carroll 1988; Tintori 1990; 1998; Arratia 1996; Arratia and Tintori 2004; Mutter and Herzog 2004).
Chondrichthyes	(Underwood 2006; Arratia and Tintori 2004).
Arthropoda	(Alessandrello <i>et al.</i> 1991; Wilson and Edgecombe 2003; Feldmann and Goolaerts 2005; Knopf <i>et al.</i> 2003; Schweigert 2007).
Brachiopoda	(Kowalewski <i>et al.</i> 2000).
Reptilia	(Carroll 1988; Rieppel 2002; Müller 2005; 2007).
Echinodermata	(Villieret <i>et al.</i> 2004; Hendy <i>et al.</i> 2009; Saucedo <i>et al.</i> 2007).
Amphibia	(Tverdokhlebov 2002).
Bryozoa	(Smith <i>et al.</i> 2006).
Annelida	(Grossmann and Reichardt 1991; Magnusson <i>et al.</i> 2003).
Ostracoda	(Lethiers and Whatley 1995).
Corals	(Turnsek 1997).

The time division used in the Sepkoski Database corresponds to a combination of stages, substages, and ages. These temporal categories were standardised at the stage level following the time scale of Gradstein *et al.* (2005). Finally, in order to identify general tendencies in the data, diversity was estimated as the total number of genera; the number of life modes derived for the categories given by Bambach *et al.* (2007) and Bush *et al.* (2007); and the relative abundance of each mode of life was estimated as the number of genera per life mode in each stage. 95% confidence intervals were estimated assuming a binomial distribution for each category per stage. The statistical significance

of the ecological tendencies was evaluated using Spearman and/or Pearson's correlation of the data transformed through logit ($\ln [p/(1-p)]$) over time (see Fig. 3.8).

3.3 Results and Discussion

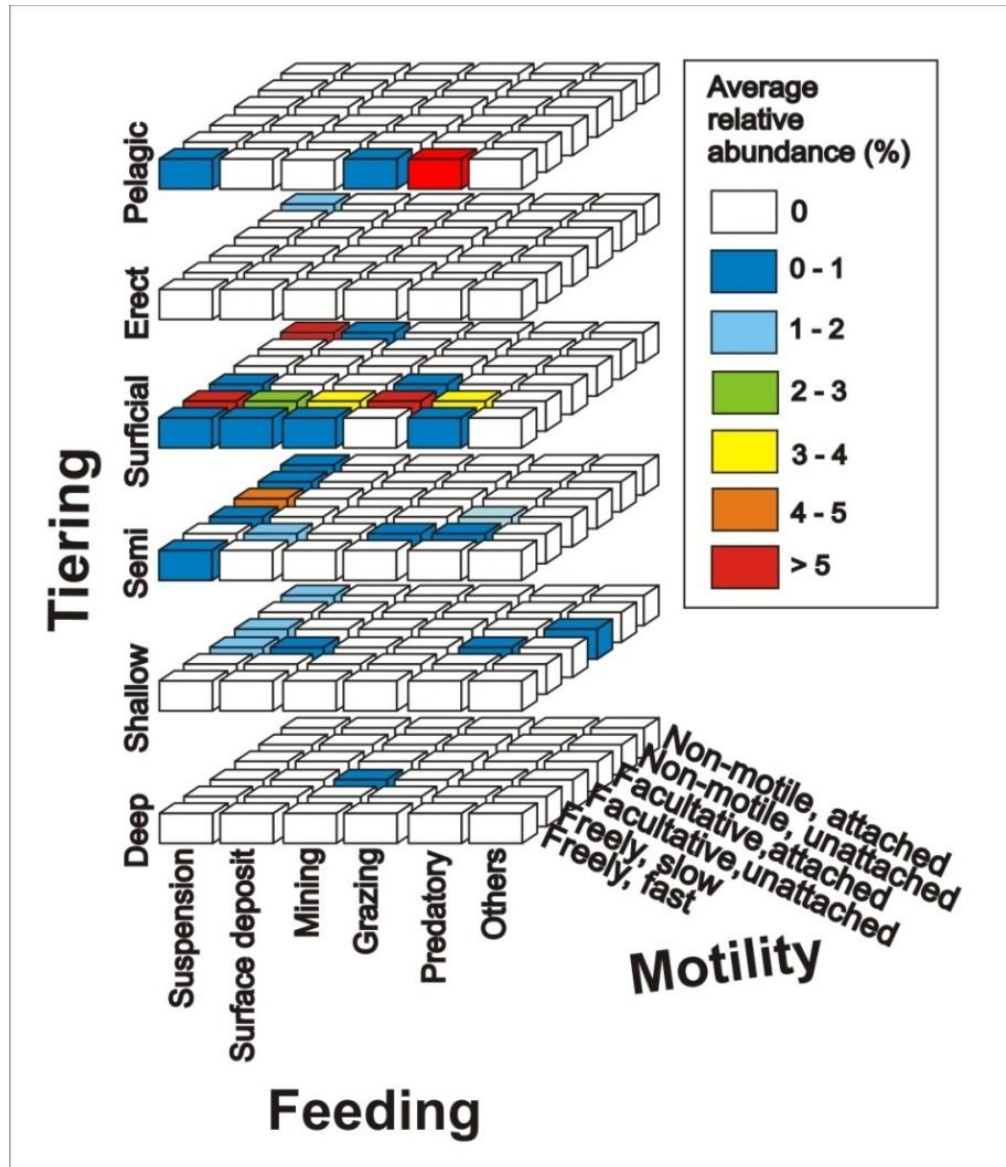


Figure 3.2 Theoretical ecospace uses by the marine fauna from the Wordian to Sinemurian. The colours indicate the relative abundance values (%) estimated as number of genera by each mode of life by stage. See Appendix 3.3 for the list of taxa. A total of 33 modes of life (15.3% of the theoretical ecospace) were recorded from the Wordian to the Upper Sinemurian (Mean: 25, range: 21 to 29). The average relative abundance per ecological trait varied greatly between modes of life. 20 life modes (60.6% of the used ecospace) recorded proportion <1%; 15.2 % of the realised ecospace has densities between 1-2%; 2 modes of life (6.1 %) contain densities among 3-4%, while just 1 mode of life represented a proportion between 2-3% and another 4-5%. Finally, only 12.1% of the realised ecospace had relative densities > 5%, spanning a proportion between 5-36 % (Appendix 3.6).

3.3.1 Ecospace through the Phanerozoic

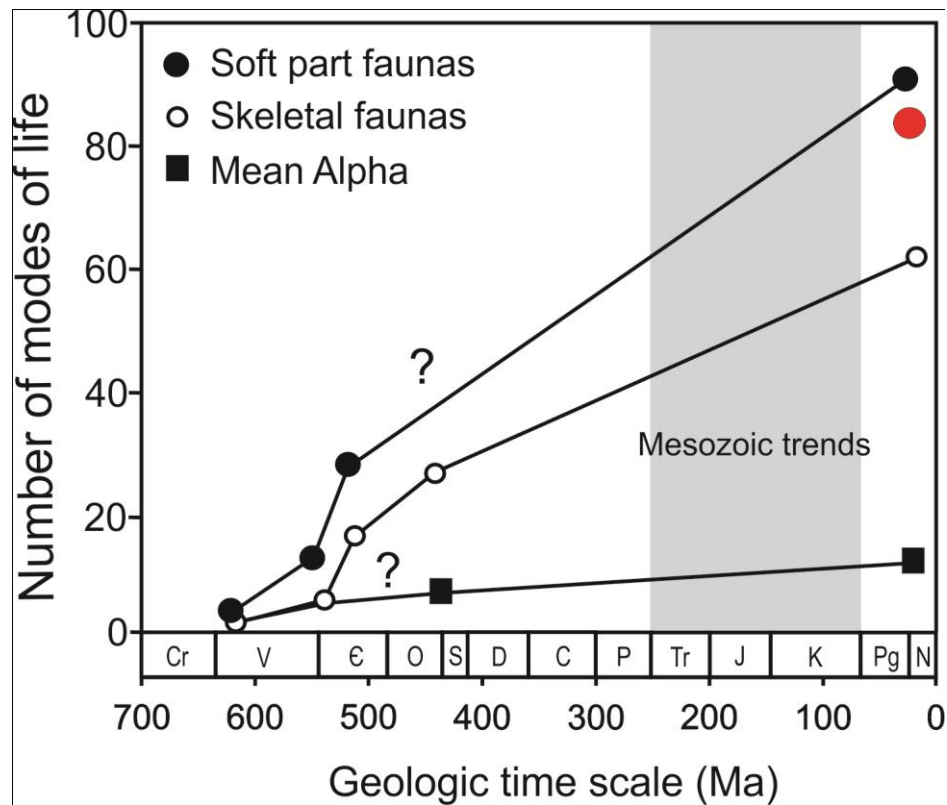


Figure 3.3 Graph of the expansion of realised ecospace representing the number of modes of life of the skeletal fauna through the Phanerozoic, plotted from Bambach *et al.* (2007). The solid circles represents all recorded modes of life, the open circles represent the skeletal fauna only; the solid square record alpha diversity (α). The red circle containing a black dot represents those modern taxa with a diverse fossil record.

Previous studies appear to indicate that the number of modes of life employed by the skeletal marine fauna through the Phanerozoic, had increased steadily and expanded across all categories through the ecological space, which has brought about the development of more complex and structured ecological systems (Clapham *et al.* 2003; Bambach *et al.* 2007; Bush *et al.* 2007; Xiao and Laflamme 2009). During the Ediacaran Period, the fauna occupied 6% of the theoretical ecospace (Fig. 3.4). The Ediacaran fauna appear to be restricted to just sessile organisms, surface deposit-feeders and grazing forms of little motility. The ecological structure appears to be similar to current deep-sea communities, with short food chains, although apparently without predators (Clapham *et al.* 2003; Bambach *et al.* 2007; Xiao and Laflamme 2009).

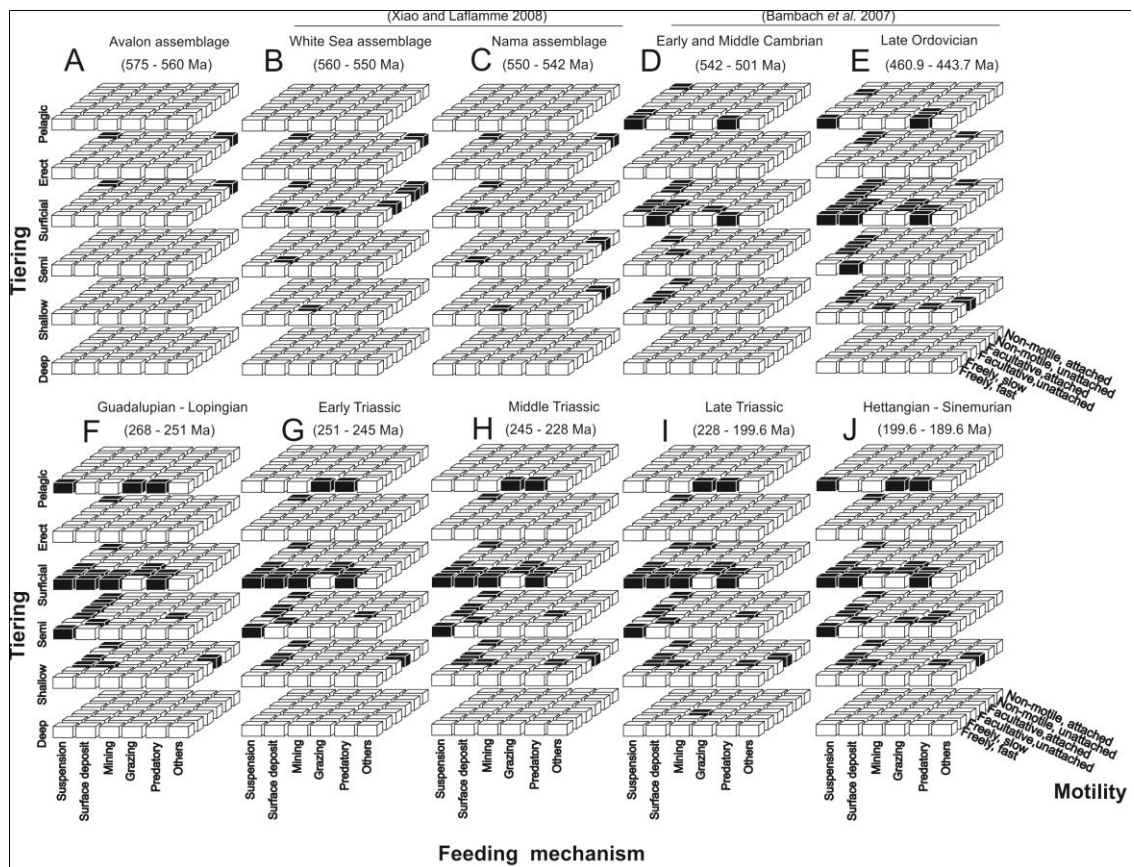


Figure 3.4 Ecospaces realized used by skeletal marine fauna through the Phanerozoic. 4A, D-E, represent data obtained from Bambach *et al.* (2007). 4B-C represents Ediacara fauna, plot by Xiao and Laflamme (2008). 4F-J, corresponded to data record from this works. The black boxes are modes of life utilised by the designated fauna.

The Cambrian represents the biggest species radiation of body plan at the beginning of the Phanerozoic and the expansion of marine organisms into new areas of ecological space (Fig. 3.4D). In terms of tiering, pelagic organisms appear for first time, the number of the surficial modes of life increases to 9 and the burrowing mode of life originates and intensifies, impacting and modifying marine ecosystems. The feeding mechanism diversifies with the appearance of herbivorous and predating forms. Although 14% of the total ecospaces was occupied, in terms of complexity, these communities are composed of simple structures as the result of a low packing (Erwin *et al.* 1987).

Thirty modes of life were recorded during the Late Ordovician (Fig. 3.4E), with 14 new modes of life recorded in just 59.9 Myr. The Ordovician is considered to be the second greatest diversification event of the marine fauna, in term of species number and at higher taxonomical levels (Munnecke *et al.* 2010). This period is characterised by the generation of new types of communities, particularly associated with deeper water and around reefs (Munnecke *et al.* 2010). In terms of their ecological complexity the communities were better structured and densely packed with an expansion of the number of ecological guilds falling into new feeding and tiering categories.

From the Guadalupian to Sinemurian, an interval of 79.6 Myr (Fig. 3.4 F-J), the skeletal marine fauna expanded into new eco-morphological areas; new pelagic, burrowing and moving forms, appear to generate more complex ecosystems with large trophic chains and greater interconnectedness, which may have intensified biotic interaction and drove the fauna towards new ecological and evolutionary scenarios. During this interval, the number of modes of life correlates significantly with taxonomic diversity and the packing tends to increase, that means that more species began to fill each mode of life (e.g. suspension feeders made up of 15 classes) (Fig. 3.5A).

3.3.2 Late Permian

Taxonomic diversity reached a peak during the Guadalupian to Lopingian (at 1253 recorded genera) (Fig. 3.4 F and 3.5A). During this interval, the occupied ecospace comprised 28 modes of life, of which 77% correspond to surficial forms. Of these, the brachiopods dominated the Palaeozoic epibenthic communities with a relative abundance of ~35% of all genera, followed by the Mollusca with 24% and the Bryozoans with 13% (Appendix 3.2). Of surficial forms, 26% have some degree of motility and were mainly represented by herbivorous classes like Patelogastropoda, Echinoidea and Polyplacophora. Concurrently, faster predators (14% of the ecospace)

invaded the pelagic realms, of which the Cephalopoda were the dominant-group (~90%), followed by key predators such as Chondrichthyes (8%) and Osteichthyes (1%).

During this period, semi - and shallow infaunal ecospace comprised 12 modes of life with a relative abundance of ~10%. Bivalvia, an incipient but highly diverse group, represented ~54% of the total infaunal guild followed by Ostracoda, Holothuroidea, Scaphopoda and Rostroconcha. Infaunal motile forms appear to have been restricted to the groups Ostracoda (Palaeocopida) and Bivalvia (Arcoidea, Trigonioidea, Pholadomyoidea and Nuculoida).

3.3.3 Early Triassic

When analysing the Late Palaeozoic to Early Mesozoic (i.e. Triassic) period, it is possible to determine that 90% of the modes of life were generated during the Palaeozoic, of which 60% pass through into the Triassic. The Late Permian mass extinction is considered to be the most devastating extinction event; decreasing diversity by more than 95% of all species, modifying ecological structure and generating one of the biggest turnovers of marine communities.

The Early Triassic records the disappearance of three pre-existent modes of life, the recovery of the marine ecosystems End-Permian mass extinction and the reorganisation of marine communities (Fig. 3.4G).

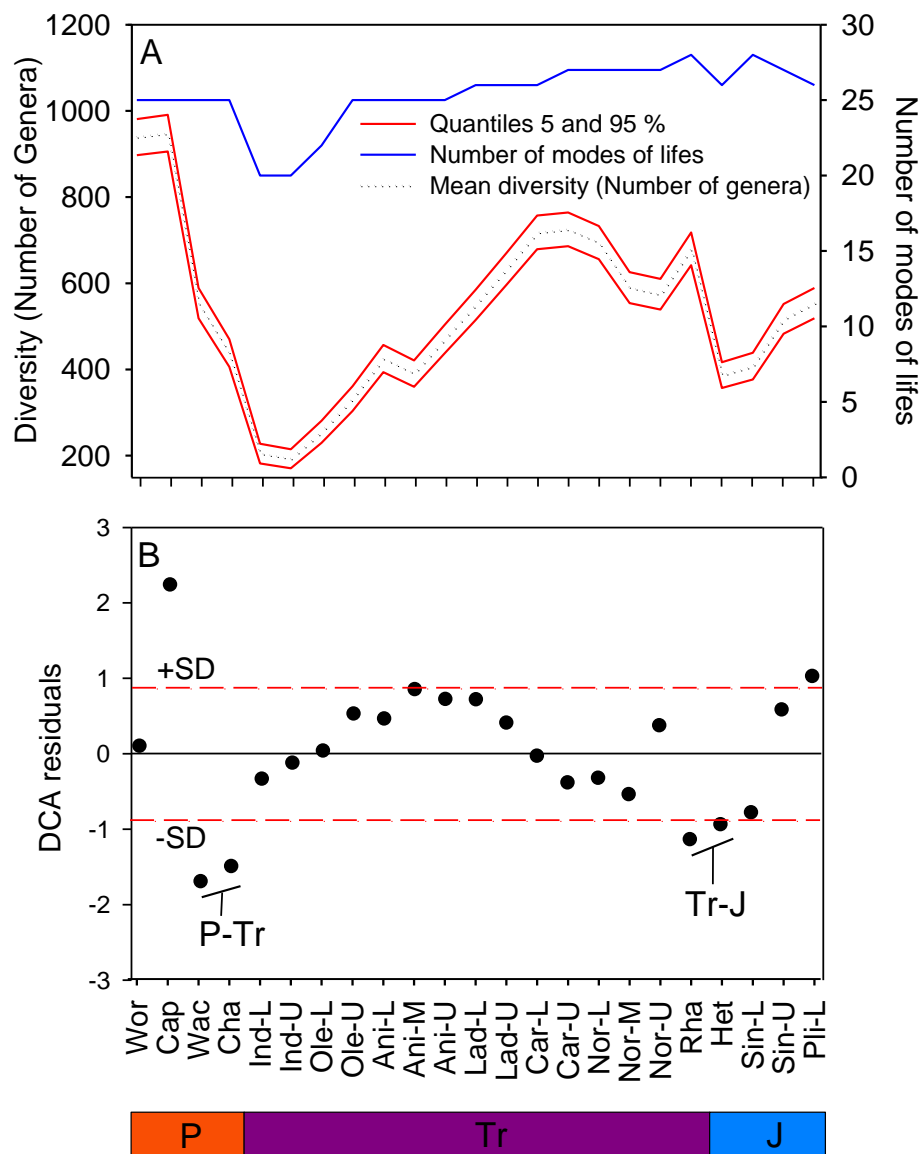


Figure 3.5 (A) Changes in marine diversity and the number of modes of life from the Wordian to the Pliensbachian. The continuous red lines represent 95% confidence intervals; calculated by bootstrap procedure (number of iterations = 50,000). (B) Plot of residuals of the first component of DCA obtained of the relative abundance per mode of life. Dashed red lines equal to two standard deviations around the mean, standard deviation was estimated through bootstrap procedure that resampled (with replacement) the number of modes of life per stage (number of iterations = 50,000). Wor = Wordian, Cap = Capitanian, Wuc = Wuchiapingian, Cha = Changhsingian, Ind = Induan, Ole = Olenekian, Ani = Anisian, Lad = Ladinian, Car = Carnian, Nor-L = Norian, Nor-M = Norian, Nor-U = Norian, Rha = Rhaetian, Het = Hettangian, Sin = Sinemurian, Pli = Pliensbachian. P = Permian; Tr = Triassic; J = Jurassic. L= Lower, M = Middle, U = Upper.

The Early Triassic recorded an average species richness of 200 ± 22 genera with 25 modes of life. Pelagic fast-moving suspension feeders, semi infaunal, non-motile unattached, suspension feeders and shallow infaunal, facultatively motile unattached, suspension feeders disappear after the extinction event. Of these, the fast-moving suspension feeders reappear in the Hettangian and semi-infaunal, non-motile, unattached suspension feeders reappear in the Middle Triassic. However the shallow infaunal facultative unattached suspension feeding mode of life became extinct never to reappear (Appendix 3.2). Through this epoch there was no appearance of new modes of life and the number of genera per mode of life decreased in average by ~47%.

At higher temporal resolution (stage level), just 168 genera cross into the Induan, reducing occupied ecospace to 20 modes of life. Erect suspension feeders (Crinoidea) disappeared completely from this database in the Induan. However, apparently *Holocrinus* (Holocrinidae, Isocrinida) is considered the only Induan forms known to cross through the Late Permian (Twitchett and Oji 2005). Erect suspension feeders increased in abundance during the Olenekian and persisted through the early Mesozoic with low proportional abundance (~5%).

Apparently the forms most affected were surficial suspension feeders, which dropped from ~53% to ~39%. The pelagic forms increased from 10% to 19% from the previous period. Semi-shallow infaunal categories increases from 11% to 17%. In terms of their ecological structure, 50% of the genera exploited filter feeder modes and just less than 10% of the genera recorded modes of life associated with predation and herbivory (Fig. 3.6). According to Fraiser *et al.* (2005) in a local scale (alpha), four modes of life were used by the benthic fauna during the Early Induan, which suggests that those communities showed a similar ecological structure to Cambrian benthic communities.

Later, on during the Olenekian, the environmental conditions improved and the organisms expanded into new ecological space (Bottjer *et al.* 2008). The reptiles appeared in marine systems with the appearance of two genera (Placodontia: *Placodus* and Ichthyosauria: *Cymbospondylus*). While the Osteichthyes proliferated quickly increasing their abundance from 2 genera in the Late Permian to 10 genera, of which 40% of them were represented by herbivorous forms.

The disappearance of large proportion of surficial life forms triggered the turnover of the Palaeozoic fauna. The brachiopods reduced their abundance progressively to ~6%, while bivalves became the most dominant surficial organisms with a relative abundance of ~45%. Motility slightly increased from the Induan (46%) to the Olenekian (~53%). This pattern was driven by the diversification of groups like Gastropoda, Echinoidea, Patelogastropoda and Polyplacophora (Fig. 3.6). Crinoids occupied the erect non-moving filter-feeder mode of life, with just two genera *Holocrinus* and *Dadocrinus*. In addition, burrowing life forms increased significantly to ~33%, following the radiation in the Bivalvia (to 9 orders) and Holothuroidea (to 4 orders). ~50% of the burrowing fauna shows some degree of motility (fast, slow and facultative unattached), in particular the bivalves, annelids and ostracods.

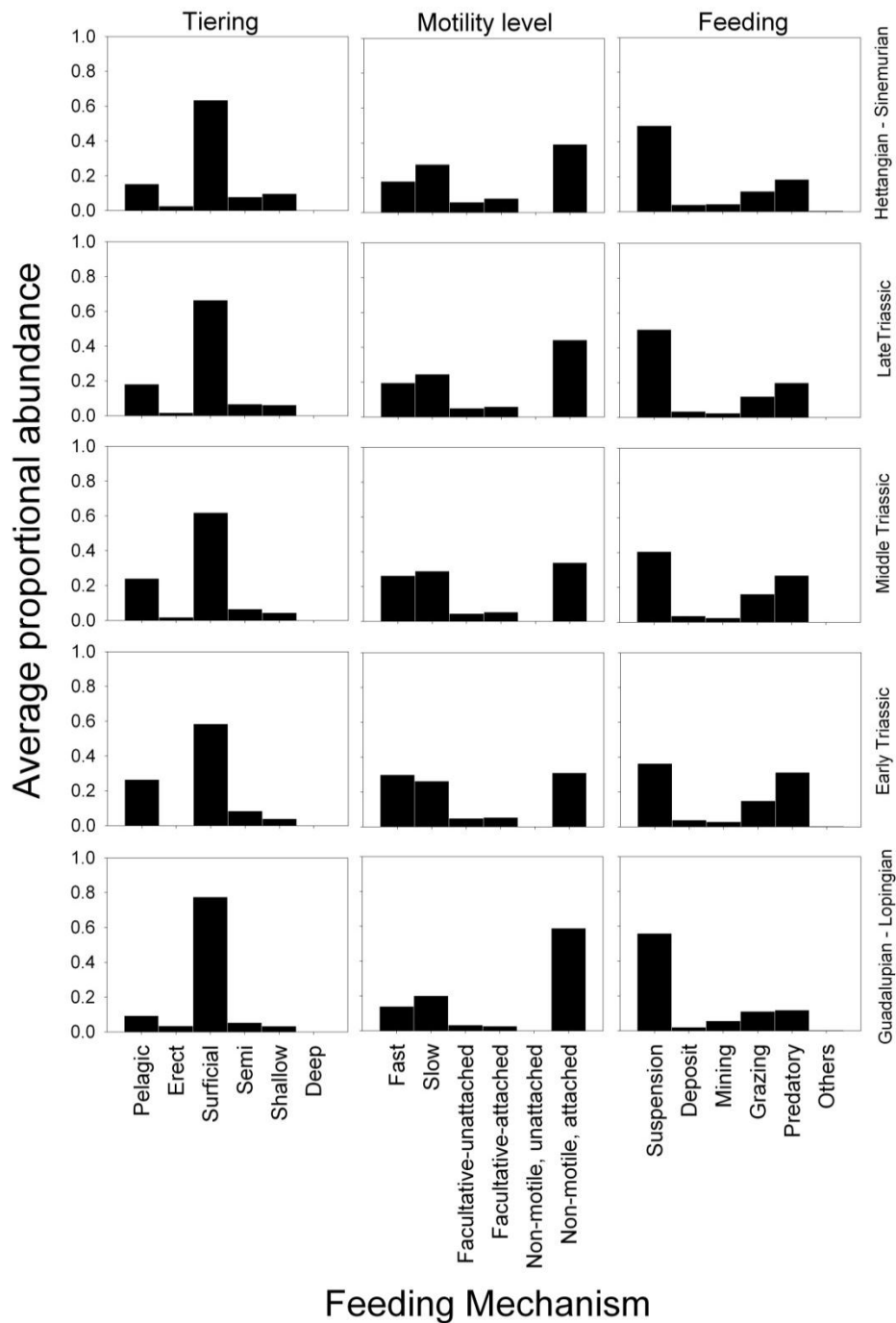


Figure 3.6. Average proportional abundance of tiering, motility and feeding mechanisms based on taxonomic occurrences from the Guadalupian to Sinemurian (268-196.5 Ma). The average proportional abundance were estimated through bootstrap procedure that resampled (with replacement) the number of modes of life per stage (number of iterations = 50,000).

3.3.4 Middle Triassic

The Middle Triassic records 27 modes of life employed by 840 recorded genera.

Through this epoch two new modes of life appeared associated with shallow forms; facultative unattached deposit feeders (Bivalvia – Nuculoida: Nuculidae) and predators (Bivalvia – Pholadomyoidea: Cuspidariidae) (Appendix 3.2) (Fig. 3.4H). During this time, surficial organisms constitute 61% of all genera of which just 40% are represented by non-motile filter-feeders and ~50% are represented by taxa with some motility level. The latter includes grazers and micro-predators. Epifaunal non-motile filter feeders were represented by 14 Classes, comprising 23% of all surficial forms (12 modes of life). 42% of epifaunal non-motile filter feeders constitute reef building organisms. Despite the fact that they are the numerically dominant group, the proportional abundance decreased to 50% from the Early Triassic (Fig. 3.6).

In contrast, burrowing forms expanded to 12 new ecological categories, with a parallel increase in relative abundance to ~10% (Fig. 3.6). 53% of the infaunal forms were represented by Bivalvia, with the rest of the infauna comprising motile facultative unattached and facultative attached modes of life represented by Holothuroidea (35%), Polychaeta (4%), Scaphopoda (4%), Ostracoda (1%), and Lingulata (1%).

Pelagic forms were represented by 270 genera, of which 69% are ammonids. Of the rest, the reptiles reach a maximum richness of 21 genera grouped in the four Orders Ichthyosauria, Notosauria, Placodontia and Thalattosauria; the Osteichthyes were composed of 40 genera from 12 orders; the Chondrichthyes were made up of 8 genera, all from the Order Ctenacanthida; finally, the Thylacocephala, which constitute four genera grouped into the orders Concavicularia and Conchyliocarida.

Through the Middle and Late Triassic, the biotic interaction intensified as a result of the high guild packing and of the highly connected trophic network. Fast moving predators spread through different ecological categories (infaunal, surficial and pelagic). More organisms began to explore benthic environments by burrowing deeply; modifying the substrate chemically and physically. Simultaneously, surficial grazers intensified the pressure on the sessile dwelling organisms.

3.3.5 Late Triassic

This epoch records the maximum richness through the Triassic, in which the reef builders become highly dominant. The ecosystems of the Middle Triassic seem to be very complex and the interrelation between species becomes more intense (Flügel 2002; Kiessling 2008). Throughout the Late Triassic, the marine fauna used 29 modes of life (Fig. 3.4I), amongst which two new modes of life appeared: surficial non-motile miners and deep facultative unattached miners.

At this time, surficial ecospace comprised 12 modes of life. Two of these were slow moving grazers and non-motile filter feeders constituted the most abundant groups with densities of 10% and 41%, respectively. Of the non-motile filter feeders ~81% were reef builders. The motility of the surficial taxa increased by ~7%, more than observed in previous periods, this trend was crowded by echinoderm and mollusc herbivores.

On other hand, semi and shallow infauna was made up of 79 genera, of which each was represented six modes of life. The deep infauna made its first appearance with the genus *Archarenicola* (Polychaeta). As the previous interval, Bivalvia still show high dominance reaching ~80% of all genera. In terms of motility, ~30% of the genera possessed a level of motility whether fast, slow or facultatively motile forms.

Predation increased from the previous period, although the relative abundance of pelagic predators dropped by ~5%, apparently driven by the almost complete disappearance of the ammonoids at the end of the Rhaetian (Fig. 3.6). In contrast, the number of orders of Osteichthyes kept steadily increasing from 5 orders in the Early Triassic to double that number in the Late Triassic and so kept proportional abundance relatively high (~10%).

The number of genera of Chondrichthyes tripled from the end of the Palaeozoic to the Late Triassic (15 genera). At the ordinal level there is little compositional turnover and just the Ctenacanthida remains through all of the Triassic and Jurassic. Finally, marine reptiles such as the Ichthyosauria, Notosauria, Placodontia, Plesiosauria and Thalattosauria had, by the Late Triassic, become key organisms in the marine seascape reaching proportions of ~5% with 16 genera.

3.3.6 Early Jurassic

The Earliest Jurassic marked the recovery following the Late-Triassic mass extinction and the collapse of reef building communities. During this time, 27 modes of life comprised the occupied ecological space (Fig. 3.4J). At the same time, three modes of life disappeared: surficial non-moving deposit feeders and deep infaunal facultative unattached miners (both from the Class Polychaeta) and surficial fast moving miners, made up by three genera of the Class Marrelomorpha (Appendix 3.2). On average, the number of species by mode of life dropped by ~42%. The groups associated with pelagic and semi, shallow and deep infauna tiers recorded a considerable loss in term of number of genera by modes of life (~65%) (Fig. 3.4J). This mass extinction drastically affected the ecosystems generating the second biggest turnover in the ecospace and overall in those organisms associated with to reef building. Even though the ecosystems were affected by this mass extinction, Early Jurassic communities are robust and highly

interconnected, in which the marine fauna colonised pelagic and deep benthic environments, with different levels of motility and a wide dietary spectrum.

3.4 Diversity and ecological diversity

The ecospace increases rapidly from the Ediacaran fauna to the Late Permian. However, through the Guadalupian to the Sinemurian the number of modes of life of the marine fauna remains relatively constant (Mean ~26) (except after the End Permian and End Triassic mass extinction) (Fig. 3.6). These results are not totally consistent with the model proposed by Bambach *et al.* (2007), which predicts a steady increase of the skeletal fauna from the Ediacaran to the Neogene (Fig.3.7).

Bambach *et al.* (2007), considered all the known modes of life represented by the marine fauna on a global scale in all environments (reef, rocky shore and pelagic realm), establishing that from the Ediacaran to the Ordovician, the skeletal fauna increased from 12 to 30 modes of life, while from the Ordovician to the Recent, the number of modes of life doubled. Similarly, Bush *et al.* (2007) although analysing the marine fauna in a local scale, showed that the ecospace increases from the Mid-Palaeozoic to Late Cenozoic from 21 to 25 modes of life. The number of modes of life used by the marine fauna recorded in this work (Guadalupian to the Sinemurian; 81 Myr) is low compared with previous periods.

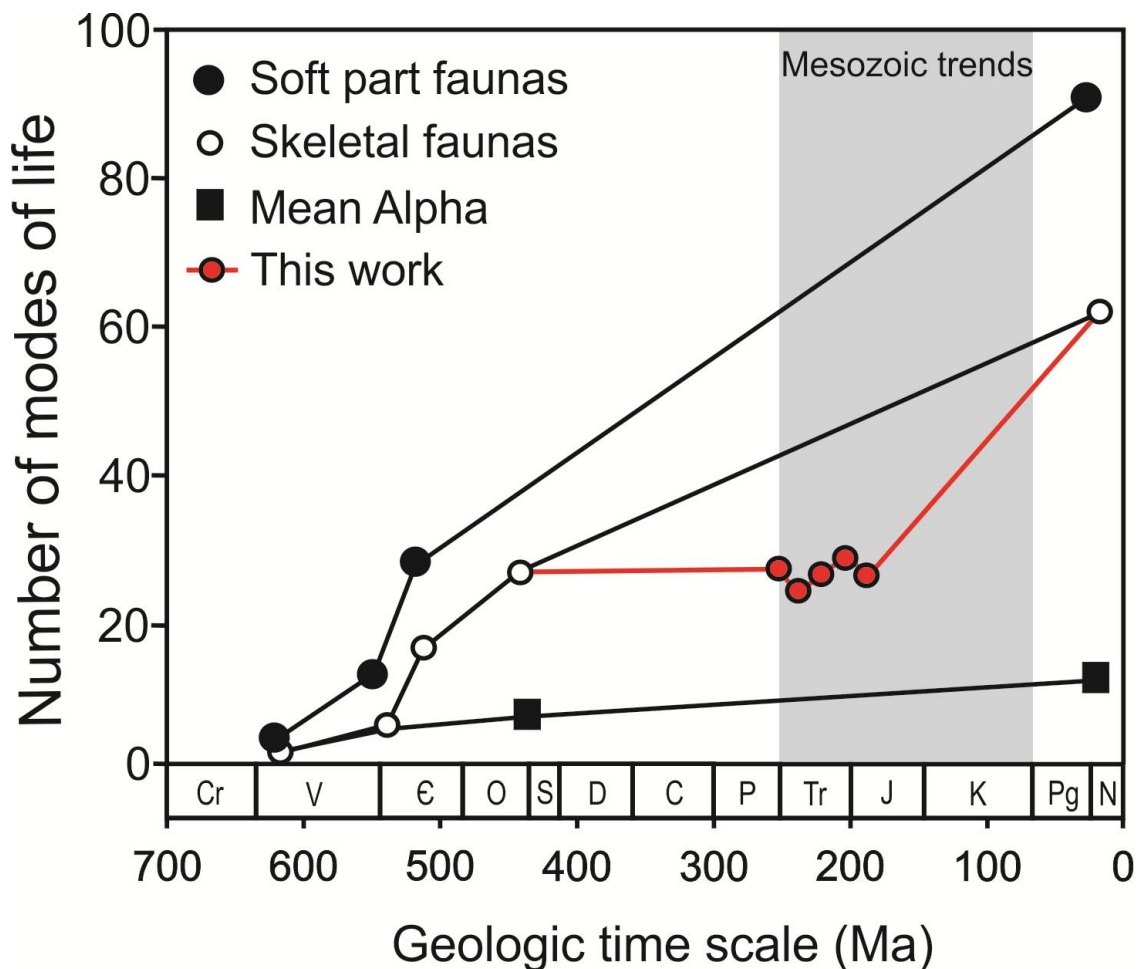


Figure 3.7 Secular trend of number of modes of life used by the skeletal fauna through the Phanerozoic. The white dots represent the secular trend hypothesised by Bambach *et al.* (2007). The red dots represent the number of modes of life recorded in this study. Shaded area indicates the Mesozoic Era.

This study focused mainly in the Triassic Period, during this period two mass extinctions affected the marine fauna, generating loss of 90% in the end Permian and 65% in the end Triassic (Fig. 3.5). Biologically, the Triassic is a period of transition from the Late Palaeozoic diversity plateau to the roughly exponential diversification in the marine realm through the Jurassic. Recent estimation by standardized diversity curves, shows that this interval has a relative low richness (maximum peak 400 genera), compared to the Permian, with 600 genera and the Jurassic with 500 genera (Alroy 2008). Despite this low richness and relatively low number of modes of life, ecospace does not fluctuate through this period. It seems that modes of life with low abundance (< 0.1%, i.e. “rare”) are more susceptible to disappearance (Fig. 3.8, Appendix 3.6) (i.e.

surficial, no motile attached, deposit feeders and deep infaunal, facultative unattached miners).

Although the ecospace did not record an expansion in the number of modes of life, the relative abundance of certain modes of life co-vary in different intensities and magnitude through this interval, which indicates that the marine ecosystems tends to increase in complexity and functionality (Fig. 3.8). These findings confirm and extend the suggestions that the Triassic represents the beginning of the Marine Mesozoic Revolution (MMR) (Tintori 1998; Bambach *et al.* 2002; Nutzelt 2002; Hautmann and Golej 2004; Aberhan *et al.* 2006; Bambach *et al.* 2007; Bush *et al.* 2007; Vermeij 2008; Bush and Bambach 2011).

Vermeij (2008) established that the Triassic has the highest average rates of production of innovation compared to the Jurassic, suggesting that the escalation began no later than the Carnian Stage. For example, between the Triassic and Early Jurassic there were two innovations in infaunalisation - obligate deep-boring bivalves (Vermeij 1987) and infaunal echinoids. In terms of predation, five innovations took place: suckered arms in squid (Vermeij 2008), fish-like marine tetrapods (Motani 2005), mineralized ammonoid jaws (Vermeij 2008), protrusible upper jaws in teleosts (Tintori 1998) and meat-cutting sharks (Underwood 2006). In term of grazing, bioerosive herbivory arose (Vermeij 1987).

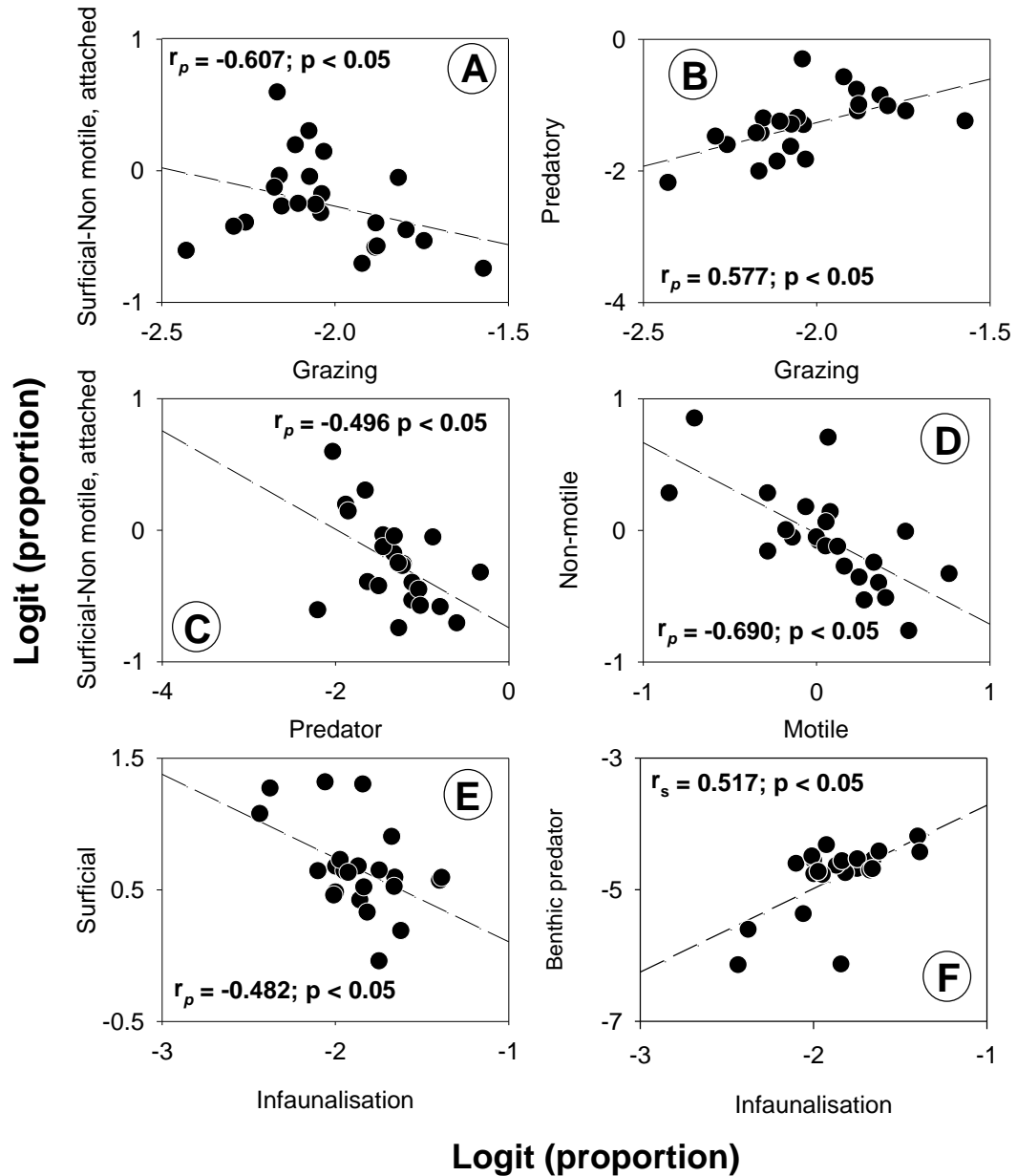


Figure 3.8 Correlations between logit-transformed proportion of occurrences of grazing vs. surficial, non-motile, attached and predatory taxa (A and B). surficial, non-motile, attached vs. predator (C), non-motile vs. motile taxa (D) and infaunalisation vs. surficial, and benthic predator (E and F). The dashed lines represent last-square lines of best fit.

The non-motile suspension feeders always showed a higher relative abundance during the Triassic, which reflects the high primary productivity of the marine habitats (Madin et al. 2006; Aberhan *et al.* 2006; Bush *et al.* 2007; Falwoski *et al.* 2004). The evolution of the epibenthic filter feeders is extensive through all phyla. After the Palaeozoic, the non-motile suspension feeders records one of the biggest turnovers in faunal

composition. Before of the P/Tr mass extinction the stationary epifaunal constituted over half of the fossilised marine genera, their diversity plunged as a result of the extinction, and they never regained dominance. Instead of expanding in the Triassic, the Late Palaeozoic fauna was hit again by the end-Triassic extinction and petered out in the Jurassic (Bush and Bambach 2011) (Fig. 3.6).

During the Triassic, the stationary epifaunal was strongly influenced by modes of life associated with bioturbation, grazing and predation (Fig. 3.8 A, C, E). The number of bioturbator organisms such as bivalves increased steadily during the Late Triassic. The burrowing and mixing of unconsolidated sediment are particularly potent agents of disturbance. This action modifies chemically and physically the upper layer of sediment. Bioturbations can structure entire communities, acting as ecosystem engineers (Berke 2010; Woodin *et al.* 2010). Additionally, the frequency of herbivores increases from the Early Triassic to the Early Jurassic (Fig. 3.8), having a negative effect on the stationary epifauna as a result of the bioerosive herbivory (Steneck 1983; Vermeij 1987; 2006 and 2008). The Osteichthyes, Gastropoda, Echinoidea and Polyplacophora are groups that potentially drove this trend. Recent studies have established that these organisms structure and modulate different ecological scenarios in marine benthic communities (Chazottes *et al.* 1995; Brown-Saracino *et al.* 2007).

Predation also impacted on epibenthic life forms (Fig. 3.8). Ammonites, marine reptiles and fishes were probably the main predators in Triassic ecosystems although groups such as mobile epifaunal predators occur with a low abundance during the Triassic (e.g. neoasterioids, neogastropod and Decapoda) (Fig. 3.8F). Predation was one of the ecological features that increased considerably in relative frequency (Fig. 3.13 B-C and F) and the effects of this group were an important ecological and evolutionary

determinant for faunas from the Late Palaeozoic to Early Mesozoic (Stanley (1977), Vermeij *et al.* (1977), Bush *et al.* (2007), Aberhan *et al.* (2006) and Bambach *et al.* (2007).

Through the Phanerozoic, 5 radiation events have been characterised by intensified predation: a) Cambrian explosion, b) Ordovician radiation, c) Devonian, d) Triassic and e) Cretaceous–Tertiary (Bambach *et al.* 2007). From the Triassic to the Jurassic the predation was by Ammonoids, Gastropoda, Reptilia, Chondrichthyes, and Osteichthyes. Predation rates, however, were also heavily influenced by the extinctions of the P/Tr and Tr/J from the Late Palaeozoic to the Early Jurassic, its relative abundance increasing from ~6% to ~13%, with a peak (~17%) in the Carnian (Fig. 3.8).

At the same time, modes of life like fast-low moving epifauna brought new adaptive strategies like shell-breaking (e.g. by decapods) and shell-drilling, which increased with the incorporation of gastropods belonging to the Heterostrophia, Cephalaspida and Neotaenioglossa. From the Early Triassic, the Merostomata, Malacostraca, Reptilia, and Thylacocephala increased steadily their relative frequency, whereas the Asteroidea and Bivalvia only started to increase from the Early Jurassic (Hettangian). According to Bush and Bambach (2011), members of the group of the solemyoids (Bivalvia) evolved successful ecological strategies in the Palaeozoic and were capable of coping with the disturbances that characterized the Mesozoic. That could explain why this group remained constant for the End Palaeozoic to the Early Jurassic without recording changes in proportions (Fig 8.4; Shallow, facultative motile attached, chemotrophic).

Aberhan *et al.* (2006) identified the Early Jurassic as the starting point of a marine diversification, and observed that the predation effect increases significantly (although as observed by Harper (2003), the major predatory taxa had already appeared in the

Triassic). This increase in predators was accompanied by a series of adaptive innovations such as predation by breakage, prying, crushing, and drilling (Vermeij 1977; 1987). For example, modern asteroids (starfish) radiated from the Jurassic (Blake and Hagdorn 2003) although they were already present in the Late Triassic. The homarid arthropods and palinurid lobsters evolved in the Triassic, giving rise to the malacostracan crustaceans with crushing chelae in the Jurassic and Early Cretaceous (Vermeij 1977; 1987) and cephalopods (ammonoids, nautiloids and coleoids) also developed as shell-breaking predators. In vertebrates, a series of reptiles from the Triassic showed a moderate increase in diversity with representatives such as chelonids, placodonts, nothosaurus, pachypleurosaurus, plesiosaurs, and ichthyosaurs, although only the latter two continued during the Jurassic (Harper 2003). Predatory bony fishes appeared in the Early Triassic with groups such as pycnodontiformes and semionotiformes, joining Chondrichthyes (mainly represented by hybodonts), which had appeared in the Devonian and radiated into the Triassic. These marine reptiles, bony fishes, and Chondrichthyes were characterized by a feeding behaviour known as “breaking predation” (Vermeij 2007).

Infaunalisation has been essential for developing structurally complex communities. Infaunalisation is positively related to primary production, as the activities of bioturbations change nutrient fluxes and improve conditions for production by the microphytobenthos (sedimentary microbes and unicellular algae) (Lohrer *et al.* 2004). Bioturbation improves the oxygen concentration, which modifies components associated with primary productivity (organic matter and/or nutrients), negatively affecting immotile and/or low-motility organisms. The same effect is observed with mechanical removal from the sediment through movement, filtering, or feeding (e.g. by mining feeders) (Thayer 1979; 1983; Vermeij, 1987; Harper 2003; Aberhan *et al.* 2006).

Irregular echinoids, decapods, gastropods, heterodont bivalves, and rays are some of the important bioturbating agents that appeared in the Late Triassic and Early Jurassic (Stanley, 2008; Baumiller *et al.* 2010; Stanley 1977; Kier 1982; Smith, 1984; Vermeij 1987; Harper 2003).

Burrowing behaviour may have been associated with the Ediacaran fauna, but it increased significantly in the Early-Middle Cambrian and into the Ordovician (Sheehan and Schiefelbein 1984). From Triassic to the Early Jurassic, is a period of intensification of major morpho-functional changes associated with infaunalisation (Baumiller *et al.* 2010). For example, veneroid bivalves under predatory pressure generated ontogenetic changes reducing the probability of attack by epifauna or nektonic predators (Stanley 2008) and expanded their ability to burrowing more deeply. Irregular echinoids evolved from regular echinoids in the Early Jurassic due to a range of morphological adaptations for a deep burrowing habit, as a direct result of the increase in predation pressure (Stanley 1977; Kier 1982; Smith 1984; Vermeij 1987; Harper 2003). Naticids and cassids among gastropods became important infaunal predators of echinoids and bivalves. Decapod crustaceans also adopted a deep burrowing habit (Vermeij 1987; Harper 2003).

There is an important turnover period between epifauna and infauna from the Late Palaeozoic to the Early Jurassic (Fig. 3.8 E, F). The benthic communities of the Late Palaeozoic were dominated by epifaunal-suspension-feeders such as crinoids, brachiopods, and molluscs. Nevertheless, after the P/Tr boundary, mostly semi- and shallow infaunal traits were led by the bivalves which were ecologically dominant (Ausich and Bottjer 2001), reaching high abundances towards the Mid-Triassic and the Early Jurassic.

The infauna included groups such as the Asteroidea, Echinoidea, Holothuroidea, Bivalvia, Lingulata, Polychaeta, Ostracoda, and Rostroconchia, whereas shallow-infaunal groups comprised mainly Bivalvia, Craniata, and Scaphopoda. In contrast, the largest proportion of the ecospace (~58%) tended to be occupied by surficial life modes. However, the rate of expansion of their relative frequency over time was lower than that observed for the semi, shallow and infaunal group (Fig. 3.8 E). The greater frequency of occurrence of infaunal taxa apparently resulted from the selective pressures associated with durophagic predation, tied to the development of more complex communities (Fig. 3.8 F).

Finally, motility is one of the categories that increased in proportion (Fig. 3.13D). The ability to control movement and manipulate the environment is critical to coping with a wide range of difficulties, including predation and disturbance. From the Late Palaeozoic to the Early Jurassic, the proportion of motile taxa increases by ~10% (Fig. 3.8). This tendency was much more pronounced for epifauna, infauna, and pelagic life forms, and correlates with higher predation, infaunalisation, and a motile epibenthic life style such as that of gastropods and echinoids, which are generally considered to be prey. Likewise, the increase in motility was much more accelerated in semi- and shallow infaunal suspension-feeders. This adaptation was developed as an escape mechanism for dealing with predation and/or environmental perturbations (e.g. the bulldozer effect) (Thayer 1979; 1983). For example, the ability of the pteroids to swim and the rapid burrowing ability of groups like Trigonioidea, Arcoida and Veneroida is associated with semi- and infaunal life modes.

The correlations found between the relative frequencies of the life modes observed, establishes the existence of a causal relationship between ecospace parameters and the

escalation hypothesis (Vermeij 1977; 1978; 1982; 1987; Signor and Brett 1984; Kowalewski *et al.* 1998, 2006; Aberhan *et al.* 2004; Kosnik 2005, Madin *et al.* 2006; Bush *et al.* 2007). These tendencies show that factors such as carnivory and disturbance follow a directional selection pressure, controlling and replacing surface non-motile benthic forms, reducing epifauna, and expanding infaunal life modes (Aberhan *et al.* 2006).

The Triassic set the scene for the MMR, leading to the reconstruction of marine communities as a result of the intensification of specific life modes and the innovation of specific morphological adaptations (Harper 2003). The latter work summarizes the most important adaptive tendencies from the Late Palaeozoic and Early Mesozoic, extending the previous observations by Bush *et al.* (2007) and Bambach *et al.* (2007) and Bush and Bambach (2011).

Regarding this issue, Vermeij (2008) determined that one of the greatest pulses of innovation, with a rate of 0.45 per million years, was generated in the Mid-Triassic and Early Jurassic. This author established that these pulses were a response to the high supply of energy incorporated into the ecosystems associated with volcanic activity and/or related phenomena (e.g. higher CO₂ and temperatures) that affected primary productivity (Vermeij 1995). Vermeij (1995; 2008) found that the break-up of Pangaea in the Late Triassic generated the energetic input for the development of this process.

3.5 Mass extinction events and ecological space.

Figure 3.5B shows the deviations of the residues of the first component of the Detrended Correspondence Analysis (DCA), calculated over the relative proportion of each life mode from the Wordian to the Pliensbachian. Positive values on this graph shows, how the morphospace reached a maximum before the extinction of the Late

Permian and in the Early Jurassic. In contrast, negative values indicate the greatest decreases in diversity associated with the highest turnovers in the ecospace. This verifies that the extinctions of the Late Permian and Late Triassic not only affected the highest number of life modes but also decreased the relative density of each ecological category, generating significant contractions in ecospace and demonstrating the coupling of ecological functionality and diversity.

3.5.1 Permian/Triassic mass extinction

Figure 3.9 (A-B) shows the effect of the Late Permian extinction (Changhsingian to Induan) in the ecospace. Five life modes disappeared, of which four were associated with the filter feeders: pelagic-fast moving (Malacostraca, Ostracoda), erect forms (Crinoidea), surficial facultatively motile unattached (Bivalvia: Hyolithida, Pterioidea, Arcoida), shallow-facultatively motile-unattached (Bivalvia, Craniata) and finally, the predatory-fast moving-surficial (Malacostraca: Decapoda).

In terms of taxonomic loss, according to this data, the number of genera dropped from 436 to 168 genera (genera that cross to the Induan stage), which represents a reduction of 61%. At the ordinal level, ~20% of the orders underwent extinction and 15 classes were affected. The mean number of genera per mode of life dropped drastically at the generic and ordinal levels, and slightly at class level, but there were no significant changes at the level of phyla. In terms of the proportional abundance, each ecological category decreased in average more than 50% (Fig. 3.10, appendix).

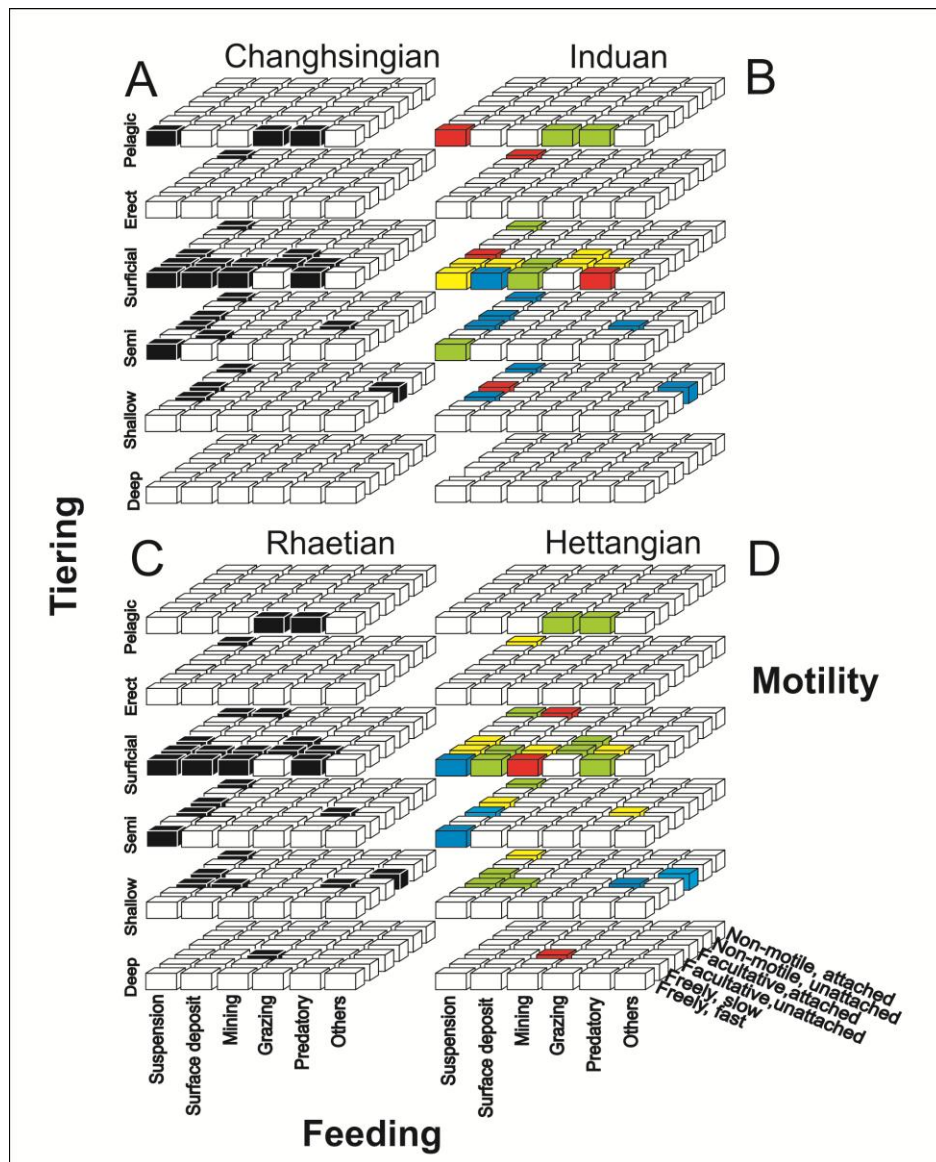


Figure 3.9 theoretical ecospace occupations for marine genera through the P/Tr and Tr/J mass extinction events. The black boxes represent the ecospace occupation prior to mass extinction events (A) Changhsingian and (C) Rhaetian. The coloured boxes represent the ecospace occupation after the mass extinction events, (B) Induan and (D) Hettangian. Red indicates the modes of life lost after the extinction event. Green indicates a > 50% decrease, yellow represent < 50% decrease and the blue indicates no change in the relative abundance of the mode of life after the extinction event.

The pelagic forms record a decrease of ~60%. This category was made up by 4 groups, Cephalopoda, Chondrichthyes, Osteichthyes, and Ostracoda, which finally disappeared in the Induan. The Cephalopoda lost 44% of its orders, of which the Anarcestida became extinct, while dominant groups like the Ceratida, Goniatitida and Nautilida decreased by > 50%. Among the Osteichthyes, the Coelocanthiformes disappeared

entirely and ~80% of the Palaeonisciformes disappeared (all grazing forms), while Semionotiformes crossed into the Induan. Finally, Chondrichthyes did not record losses, and the Ctenacanthida and Eugeneodontida crossed into the Induan.

The erect forms comprised Cladida and Monobathrida, which disappeared completely during the Late Permian. At the same time, surficial life forms suffered one of the greatest decreases, from 345 genera recorded in the Changhsingian to 125 genera in the Induan. Two modes of life disappeared, one being the facultative, unattached filter feeders – only represented by *Pernopecten* (Pteroidea) - and the other being the fast motile predatory modes of life represented by the decapod, *Protoclytiopsis*.

In addition, the average number of genera per mode of life decreased from 28.5 in the Late Permian to 10.41 in the Induan (Fig. 3.8). This means that packing decreased more than 50% by mode of life. The greatest extinction was observed in non-motile filter feeders, where 70% of the extinct taxa belong to the Brachiopoda. Porifera, Cnidaria and Bryozoa represent 30% of the extinction pool associated with the collapse of reef systems (Brayard *et al.* 2011). With the depletion of sessile filter feeding forms (primary consumers), predators and consumers in upper trophic levels also responded negatively. Groups like Decapoda (fast motile) and Gastropoda (Neotaenioglossa and Bellerophonitida) decreased significantly. Simultaneously, slow motile grazers almost disappeared, with the loss of groups such as Archeogastropoda, Neotaenioglossa, Cephalapsida and Euomphalina (Gastropoda). Fast and slow motile miners decreased by more than 50%, of this group the Trilobites and Ostracoda (Podocopida) disappeared, while Gastropoda record a loss of just 5 orders. Finally, fast motile deposit feeders made up by Isopoda and Tanaidacea, crossed through the Induan without significant variation (Fig. 3.8).

During the Changhsingian, 26 genera occupied 10 modes of life related to semi-infaunal and shallow-infaunal habits. Bivalvia represented 46%, followed by Holothuroidea 38%, Scaphopoda and Palaeocopida both with 3%. Of these taxa, the Paleocopida - shallow facultative, attached suspension feeders - dropped by >80% with the disappearance of 11 genera. The fast motile filter feeders mode of life, comprised three genera, *Pseudopermophorus* and *Gujocardia* (both veneroids), and *Orbiculoidea* (Lingulida), and was the only mode of life that became extinct through this interval. Most of the infaunal forms used suspension and deposit-feeding mechanisms, while just one form was a predators (Scaphopoda: Dentaloida) and another chemotrophic feeder (*Acharax*: Solemyoida). In terms of motility, only two modes of life were recorded as facultative, attached and just one mode showed fast motile qualities.

Apparently, these data suggest that during the P/Tr extinction taxa associated with surficial modes of life were more susceptible to extinction than those that were infaunal (Fig. 3.10). Modes of life with low packing were more susceptible to extinction than groups with more species (Fig. 3.11). Motile forms were less affected than non-motile taxa and slow motile forms, apparently, were more affected than fast-motile modes of life.

3.5.2 End Triassic mass extinction

A total of 386 recorded genera cross to the Hettangian from 682 genera recorded in the Rhaetian. At the level of the higher taxa, 57 orders went extinct, whilst no extinctions were recorded at class, or phylum level (Fig. 3.9). Compositional analysis of the taxonomic loss revealed that annelids dropped slightly with the extinction of three genera: *Microtubus*, *Palaeoaphrodite* and *Archarenicola*. Arthropoda recorded a significant loss at generic level (12 genera), with the disappearance of the Concavicularida, Tanaidacea and Cyclina. Brachiopods recorded one the largest

turnovers, with the Spiriferida, Rhynchonellida and Terebratulida recording losses of 80%, 34% and 85% of genera, respectively.

Bryozoa recorded the extinction of the classes Trepostomata and Cryptostomata.

Echinodermata recorded a generic loss of the taxa *Tulipacrinus* (Isocrinida), *Bihaticrinus*, *Lanternocrinus*, *Lotocrinus* (order uncertain), whilst at ordinal level taxa related to Encrinida and Roveacrinida (Crinoidea) disappeared. The Cnidaria record the loss of Conulariida, Pennatulacea and the almost complete disappearance of the Scleractina. In addition the Chordata recorded the loss of the orders Perleidiformes, Palaeonisciformes, Pachycormiformes, Placodontia and Squatinactida.

The Mollusca lost ~55% of all genera (682 genera records in the Rhaetian) and a significant loss at class level. For example, gastropods recorded a loss of 73 genera (45% of all recorded gastropods) with a significant decrease of the groups Neotaenioglossa, Archaeogastropoda, Bellerophontida and Euomphalina. The Bivalvia lost 43 genera (43% of all bivalve genera), with a significant impact in groups such as the Hippuritoida, Nuculoidea, Veneroidea, Trigonoida and Pholadomya. Another group that was severely affected was the Cephalopoda, of which just 6 genera (12%) cross to the Hettangian. Finally, the Porifera lost 41 genera, of which ~86% belonged to Demospongea and the rest to the Pharetronida (Calcarea).

In terms of ecological complexity, ecospace utilisation decreased by only three life modes (Fig. 3.9C-D): surficial fast-miners (Marrelomorpha), surficial non-motile deposit feeders (Polychaeta) and deep infaunal facultative, unattached miners (Polychaeta). As in the previous extinction (P/Tr), those modes were occupied by very few genera, which suggest that modes of life with low packing are more susceptible to extinction (Fig. 3.9).

The biggest decreases were observed in modes of life associated with pelagic forms, which fell ~71% with respect to the previous period. Semi and shallow infaunal modes recorded a loss of ~ 66%, while the surficial category recorded a loss of ~57%, and predatory and grazing modes of life lost 57% and 61 % of all genera, respectively (Fig. 3.10). Finally, the average number of genera per mode of life decreased from 21.89 to 9.25 genera (Fig. 3.9) (Appendix 3.3).

Pelagic forms were made up by marine reptiles, Cephalopoda, Osteichthyes, Chondrichthyes and Thylacocephala, which were fast motile predators and grazing forms (the latter, filled just by fish). In the Rhaetian, 96 genera were pelagic predators, of which the Cephalopoda were numerically dominant. Through the End Triassic extinction this group suffered the biggest decrease with an 88 % loss of genera. 50% of Chondrichthyes became extinct, of which the Squatinactida disappeared completely, the Ctenacanthid lost 3 genera and just the Chimaeriformes ranged into the through Hettangian without loss.

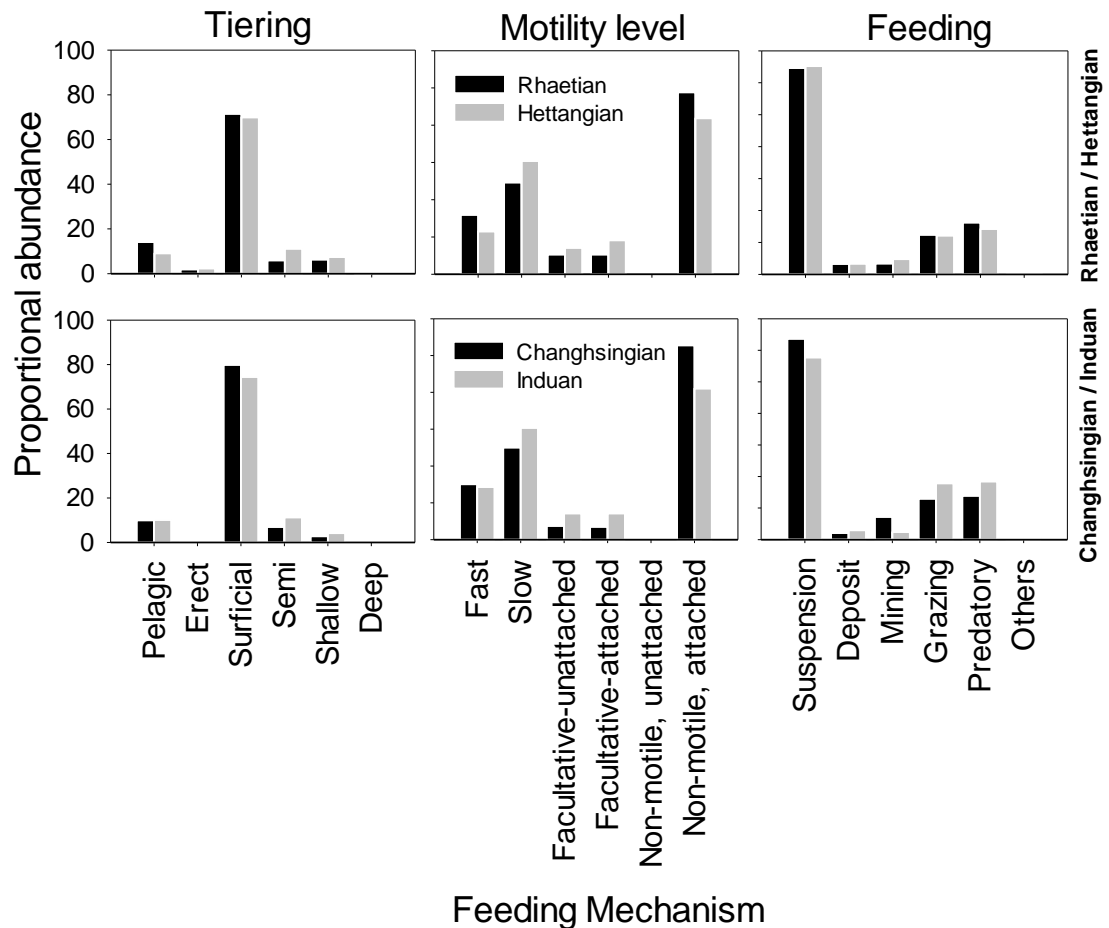


Figure 3.10 Proportional abundance of each ecological category before and after each extinction event.

Osteichthyes used two feeding mechanisms, predatory and grazing modes of life. The predators were represented by 20 genera and 8 orders in the Rhaetian and, of these, one order and 50% of genera became extinct. Grazing modes of life were made up by Palaeonisciformes, which disappear completely but the Pachycormiformes did not record any depletion. Finally, the reptiles recorded 8 genera in the Rhaetian and just 2 genera belonging to Plesiosauria and Ichthyosauria cross to the Hettangian.

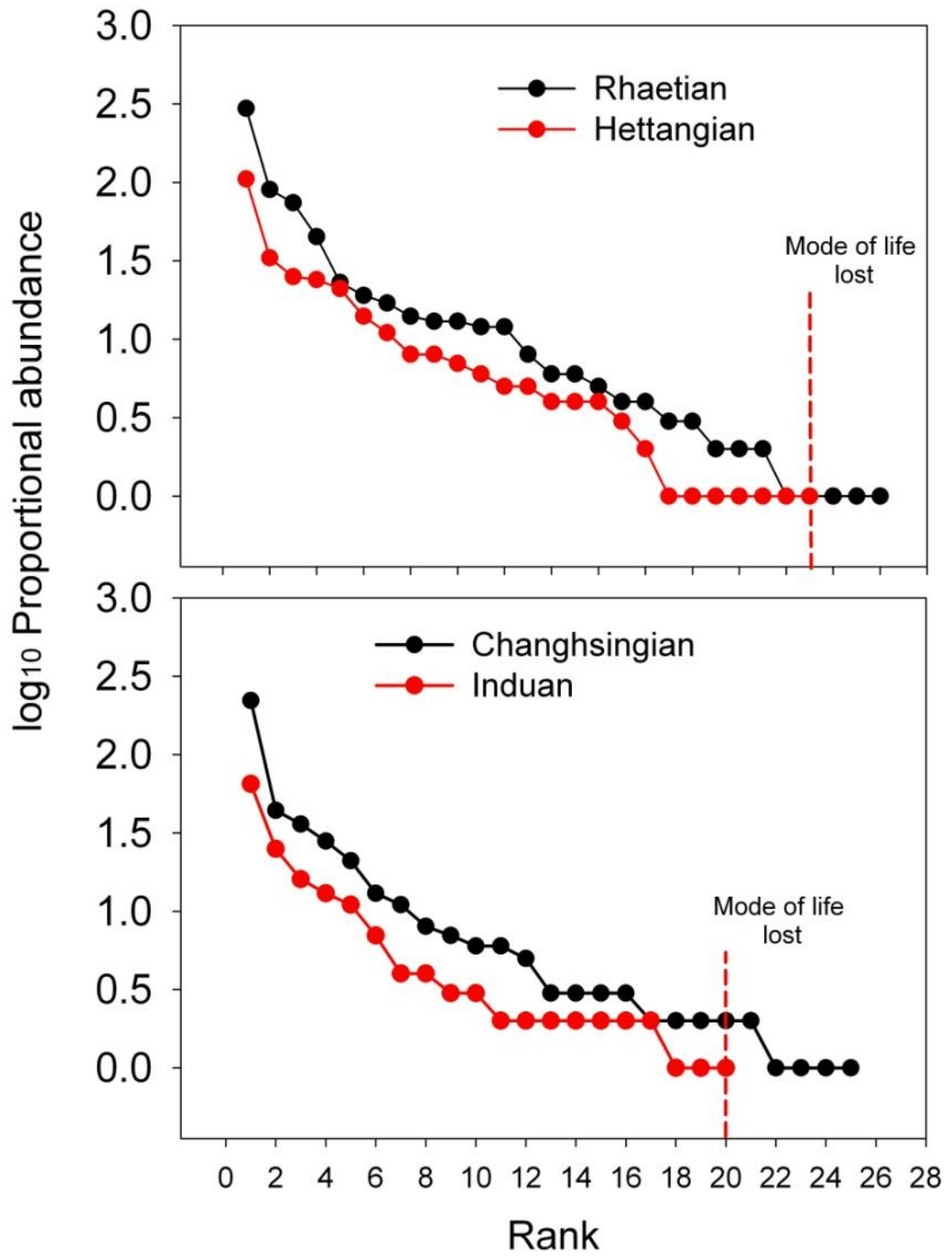


Figure 3.11 Rank abundance curve of each mode of life before and after each mass extinction event.

The End Triassic extinction event did not bring about the complete disappearance of erect forms; however they did decrease by ~50% genera, from two orders, Encrinida and Roveacrinida. Surficial modes of life were made up of 485 genera and 13 modes of life in the Rhaetian. In contrast, in the Hettangian the number of genera dropped to 207 genera, filling 11 modes of life (Fig. 3.9). This represents an average decrease of ~42% of the genera per mode of life (Fig. 3.10). Motile epifaunal miners and non-motile epifaunal deposit feeders were the only two modes of life that disappear through the Tr/J extinction. These modes were constituted by the Cyclina (3 genera) and Terebellomorpha (1 genus), respectively. In contrast, fast motile suspension feeders, which comprise the Metacopida (Ostracoda), do not record changes in abundance through the Tr/J boundary. From surficial modes, non-motile suspension feeders were the most numerous mode of life, comprising 301 genera, 29 orders and 13 families. This group recorded a loss of 65% of all genera (Fig. 3.9). The biggest decreases were observed in the Brachiopoda (~79% genera loss), Cnidaria (68%), Porifera (66%), Bryozoa (47%) and Bivalvia (42%).

Most of the marine epifauna was composed of fast, slow and facultative, unattached forms (Fig. 3.10). Slow motile forms spanned 5 of the 6 feeding categories and this group was made up mostly by Gastropoda (104 genera), Ostracoda (14 genera), Polychaeta (7 genera), Echinoidea (6 genera), Tergomya (2 genera), and one genus each of Polyplacophora and Merostomata. The modes associated with surface deposit and grazing feeding mechanisms lost >50% of this genera. The deposit-feeding surficial mode of life was made up exclusively by Gastropoda, of which the Neotaenioglossa were the most abundant, but recorded the highest taxonomic loss. Additionally, slow motile grazers form a polyphyletic group made up by 79 genera belonging to

Echinoidea, Tergomya and Polyplacophora and Gastropoda, of which cidaroids and archeogastropods recorded a loss of 2% and 39% of their genera, respectively.

Epifaunal fast motile forms were represented by the Arthropoda. The fast-motile filter-feeding Metacopida (Ostracoda) did not experience any extinction. Miners are represented by Tanaidacea and Isopoda, of which the latter crossed into the Jurassic. The genera *Aeger* and *Tropifer* (Decapoda) were the only fast moving epifaunal predators recorded in the Rhaetian, of which only *Aeger* crossed into the Hettangian.

The facultative, unattached forms represented ~2% (10 genera) of the epifaunal modes of life and recorded an average decrease of ~54% in the Hettangian. This group was composed of categories like filter feeders and grazing forms. Filter feeders were represented exclusively by the pteroid bivalves, of which just one genus went to extinction (*Tosapecten*) through the Tr/J event. Of the forms, only one genus (from Gastropoda) crosses through the Tr/J boundary.

During the Rhaetian, the shallow, deep and semi-infaunal tiers comprised 4 phyla, 6 classes, 21 orders and 84 genera, which used 12 modes of life. The semi infaunal tier was made up by 33 genera of molluscs, annelids, arthropods, echinoderms and brachiopods, which used 5 modes of life. The facultatively motile, attached suspension feeder group was the richest mode of life, and was made up by holothuroids (21 genera), bivalves (1 genus) and lingulids (1 genus). This group crossed to the Hettangian with the loss of 2 genera belong to the orders Apodida and Dendrochirotida, both from the Holothuroidea.

Non-motile filter feeder forms record the biggest loss (Fig. 3.9). This category was made up by 3 orders in the Rhaetian (Mytiloidea, Pterioidea and Hippuritoida). The

Pterioidea cross into the Hettangian without loss, the Mytiloidea suffer the extinction of one genus and the Hippuritoida disappear, which reduced the packing by more than 50%. Facultatively - attached predatory feeders record the loss of just one genus *Palaeoaphrodite* (Polychaeta), while facultatively motile and fast motile suspension feeder forms were made up by Paleocopida and Arcoida and crossed the Tr/J boundary without changes (Fig. 3.9).

The shallow infaunal forms were made up of 43 genera (all bivalves) which occupied six modes of life. Of these, three modes of life recorded the major depletions in taxonomical richness: the facultative-attached filter feeders, which lose ~50% of the veneroid bivalve; the facultative unattached filter feeders, with a reduction of ~50% of the orders Trigonioidea, Pholadomyoidea and Nuculoida; and, facultatively unattached deposit feeders, of which *Palaeonucula*, was the only genus that went through into the Hettangian (Fig. 8.9). The no motile filter feeding mode of life decreases by ~38%, and four veneroid genera and 1 genus of Nuculida disappear. In contrast, shallow infaunal facultative-attached chemotropic feeders (*Acharax*: Solemyoidea) and facultative unattached predatory feeders (*Cuspidaria*: Cuspidariidae) did not record changes through the Tr/J boundary. Finally, the deep infaunal tier was occupied by *Archarenicola* (Polychaeta) in the Rhaetian and was the only deep-infaunal group that disappears to the end Triassic extinction.

To summarise, three modes of life disappear across the Tr/J boundary. The End Triassic extinction event was intense at generic and ordinal levels. Modes of life with low numbers of species were more susceptible to extinction than modes of life with high packing. On average ~38% of the total epifauna and 65% of the total infauna cross through to the Hettangian. In parallel, 50% of the infaunal bivalves underwent

extinction through the End Triassic extinction event compared to 40% of epibenthic bivalves. Seventy-three percent of the pelagic forms disappear through the Tr/J boundary. Finally, eighty-six motile genera disappeared compared to 196 non-motile genera that became extinct, which suggests a strong selective pressure on non-motile mode of life.

3.6 Mass extinction and Ecospace

The ecospace data shows that the Late Permian and the Late Triassic extinction events affected the proportional abundance of each ecological category. In the same way the skeletal physiology seems to relate to extinction vulnerability in both extinction events. Motility apparently results in an adaptive advantage, which reduces significantly the likelihood of extinction in modes of life associated with fast, slow and facultative-unattached modes of life. Finally, dominant modes of life tended to decrease significantly, while the modes of life made up by just a few genera are most susceptible to extinction (Figure 3.10 and 3.11).

The Late Permian and the Late Triassic extinction events coincide with large volcanic events: the Siberian Traps large igneous province and CAMP (Central Atlantic Magmatic Province), respectively. In both situations hypercapnia has been suggested as a major factor that triggered the extinction in the marine ecosystems (Knoll *et al.* 2007 and Hautmann *et al.* 2008), with effects on skeletal physiology and the capacity to buffer chemical stress potentially being some of the main selectivity factors in marine organisms (Portner *et al.* 2004; 2005; Raven *et al.* 2005).

Knoll *et al.* (2007), using this approach, generated the following classification: (1) heavily calcified organisms with little physiological control over mineralization (for example, corals and calcite brachiopods), (2) calcified organisms with physiological

control with respect to the factors that govern carbonate precipitation (principally molluscs and arthropods), and (3) animals with skeletons made of materials other than calcium carbonate (lingulid brachiopods, conodonts, cartilaginous fish, etc.).

The epifaunal mode of life was the category that suffered the biggest depletion in the number of taxa. Most epifaunal organisms were heavily carbonated and without physiological buffering, with the exception of surficial, fast motile deposit feeders (occupied only by bivalves), which survived through without change (Figure 3.8). Taxa associated with shallow and semi infaunal modes of life were made up by organisms with high physiological control (Group 2 and Group 3). Of this group, 8 modes of life were recorded and only one mode of life decreased by more than 50% (made up by Ostracoda). This pattern is interesting from an evolutionary point of view, and could explain the replacement of a brachiopod-dominant fauna by a bivalve-dominant fauna.

Pelagic forms were composed physiologically of groups (2) and (3). The three largest taxonomic groups were the cephalopods (ammonites and nautiloids), cartilaginous and bony fishes. For cephalopods (moderate carbonate load-potential physiological buffering) the selectivity was apparently differential and the Nautiloidea were the only group which did not record large losses. Cartilaginous fishes do not have such physiological constraints, although predator and grazer modes of life still recorded depletion, apparently associated with trophic collapse, such as the bottom-up effect initialised by primary productivity depletion.

For the end Triassic mass extinction, Hautmann *et al.* (2008) divided the end Triassic fauna in three groups; (1) heavy calcified and little physiological control (Scleractina and Sphinctozoa), (2) heavy calcified and with physiological control, but with more susceptibility to extinction in aragonite groups (Bivalvia and Foraminifera), and (3)

non-calcareous taxa (Polychaeta and Radiolaria) (with a low extinction rate). However, it seems that physiological control is not reflected in the occupied ecospace, with the largest extinction occurring among surficial groups and only ~38% of the total epifauna crossing through to the Hettangian, of which the majority comprised brachiopods, sponges and corals. In contrast, 65% of the infauna crossed the end Triassic into the Jurassic. Only the bivalves record a selective extinction, of which 50% of the infaunal bivalves underwent extinction compared to 40% of epibenthic bivalves. This selective extinction has been widely documented (McRoberts 2001; Hallam 2002; Aberhan and Baumiller 2003; Hautmann 2004; Aberhan *et al.* 2006; Hautmann 2006; Kiessling and Aberhan 2007a; Kiessling *et al.* 2007; Hautmann *et al.* 2008; Mander and Twitchett 2008; Mander *et al.* 2008; Wignall and Bond 2008). A potential explanation is that burrowing bivalves are exclusively aragonite (Group 2), whilst most epifaunal bivalves at the time had calcitic outer shell layers suggesting that selective extinction of shell mineralogies occurred in bivalves during the end-Triassic.

The disappearance of groups of non-calcareous taxa such as Marrelomorpha and Polychaeta (group 3), which were surficial fast miners, surficial non motile deposit feeders and deep infaunal facultative, unattached miners, however, contradicts the hypothesis of physiological control. This could mean that this mode of life had a low relative abundance or the number of species per mode of life was low (i.e. low packing). This pattern is not strange and seems to repeat through the P/Tr extinction event (Fig. 3.11). Five life modes disappeared in this interval, four associated with filter feeding: pelagic fast moving (Malacostraca, Ostracoda), erect forms (Crinoidea), surficial facultative-unattached (Bivalvia: Hyolithida, Pterioidea, Arcoida), shallow facultative unattached (Bivalvia, Craniata) and fast moving surficial predators (Malacostraca:

Decapoda). All of these modes of life record an average of 2 genera per mode of life before the extinction (Fig. 3.11, Appendix 3.3).

Figure 3.11 summarises the structure of the ecospace before and after the mass extinction. Each mode of life represents a guild constituted by different clades. From the ecological view, each mode of life represents a combination of different variable of niche, where specialised rare species, use rare modes of life. Those species are associated with restrictive habitats with a narrower tolerance to change, using small areas of the potential morphospace and are characterised by a restrictive geographic range. Observations on the extinction risk of rare and abundant species have been made up by Kiessling and Aberhan (2007b). Those authors established that the Tr/J extinction event did not show a selective effect and the end-Triassic mass extinction equally affected common and rare genera. In contrast, Payne and Finnegan (2007) and Payne *et al.* (2011) studied the relationship between abundance and extinction risk in gastropods from the Palaeozoic to the Mesozoic. They established that global genus occurrence frequency is inversely associated with extinction risk (i.e. positively associated with survival) and suggest that abundance has been a more important influence on extinction risk throughout the Phanerozoic. This apparently could support the hypothesis that the probability of extinction is reduced in abundant modes of life (with high packaging).

Another factor associated with survival through each extinction event is motility.

Organisms with some degree of motility (fast, slow and facultative unattached), shows greater advantage compared to the no motile fauna. Through the P/Tr extinction event ~47% of the motile fauna and 33% of the no motile fauna survive through this event. Through the Tr/J, 86 motile genera disappeared compared to 196 non-motile genera. From the Guadalupian to the Sinemurian the motile fauna increased steadily by ~20%.

At the Tr/J boundary the ecosystem was made up by an ecologically diverse fauna, which incorporated different clades with motile modes of life and had expanded through the ecospace (e.g. Mollusca). This pattern has been documented before (Bambach *et al.* 2002; Aberhan *et al.* 2006; Bush and Bambach 2011). The ability to move is ecologically important, allowing escape against potential predators and disturbance, and as a mechanism of dispersion, which would allow expansion of the distribution range avoiding local extinction as a result of environmental stochasticity (Bambach and Bush 2011).

In summary, modes of life with a few species, combined with certain physiological constraints and a high degree of specialization seem to be more susceptible to extinction. Organisms with motile modes of life show high survivorship compared to non-motile taxa through both, the P/Tr and Tr/J mass extinctions. This is very important, because the proportion of mobile species increases greatly after each mass extinction event (Bush and Bambach, 2010). However, there is one potential question to evaluate: The relationship between abundance of species, modes of life and susceptibility to the extinction event. This question can be extended to include physiological studies on the Tr/J fauna and correlations with ecological space, and evaluation of this ecospace on a geographical scale, in terms of differences in the filling of the ecospace and/or temporal changes related to extinction and/or recovery event. Finally, in mass extinctions involving the collapse of biological systems, ecological complexity is reduced to low levels of organization. This leads to changes in the dominant species, ecological structure, and the complexity and functionality of communities. However, the pattern in the dynamic of the extinction seems to respond canonically.

3.7 Conclusions

Ecospace does not expand from the Ordovician to the Jurassic; however the proportion of genera per mode of life does increase, and generates complex marine communities in the Early Mesozoic. The use of ecological space by marine communities through time correlates with secular changes in richness, but also with turnovers in composition associated with the mass extinctions of the P/Tr and Tr/J. These mass extinctions significantly decreased the relative frequency of some ecological categories.

Physiological control was an important factor through the P/Tr event, and seems to influence patterns of selectivity in the ecospace. In addition, the Tr/J mass extinction event, shows some correlation with physiological constraints.

To generate a more precise rate of change of ecological features by community, including different extinction and origination regimens, future studies should analyse comparatively changes in ecological space between similar communities (for example between coral reef, shallow marine or deep water systems). The concept of ecospace, however, does not necessarily incorporate "*sensu stricto*" the idea of ecological guilds, although it is possible to organise each mode of life by entities belonging to trophically-similar groups (for example, for epifaunal, shallow and semi infaunal filter feeding organisms) and to evaluate the distribution of rank abundance models and the rate of changes of species, compared to neutral models (Hubbel 2001). Such studies would allow the dynamics of species turnover and distribution to be observed under different scenarios and the development of hypotheses concerning the potential factors that could determinate changes in the composition of each guild.

Initially, however, it is necessary to generate a detailed curve of the ecospace composition through the Phanerozoic, to see how different phases of adaptive radiation are related to ecological and taxonomic diversity and, crucially, observation on how

ecological complexity has increased in the communities in which the clades had participated.

Chapter 4 St Audrie's Bay section

4.1 Geological setting

The St Audrie's Bay section is one of the most complete known across the Tr/J boundary interval (see Chapter 2). This section is 89 m thick from the base of the Westbury Formation to up to a level within the Hettangian, the Angulata Zone. The Rhaetian Stage is represented by the Penarth Group, which is subdivided into the Westbury Formation and the Lilstock Formation. The Lilstock Formation is divided into the Langport and the Cotham members. The Blue Lias Formation overlies the Penarth Group, and includes the base of the Jurassic System near its base (Warrington *et al.* 2008; Clémence *et al.* 2010). Four chronostratigraphical zones comprise the Hettangian: the Tilmanni Zone, the Planorbis Zone, the Liasicus Zone and the Angulata Zone.

4.1.1 The Westbury Formation

This unit has a thickness of 10.90 m and is a marine unit, consisting predominantly of siliciclastic-rich calcareous mudstone with subordinate interbedded, calcareous sandstone, bioclastic packstone, wackestones and intraformational conglomerates (Fig. 4.1). The calcareous sandstones have been considered to represent barrier bar deposits, whilst the bioclastic packstone represents winnowed shallow marine concentrations, and the intraformational conglomerates and "bone-beds" have been variously interpreted as transgressive lag deposits, condensed horizons or storm deposits (Macquaker 1999; Warrington *et al.* 2008).

The sea was shallow and deposition took place under generally quiet-water offshore conditions, although periodically wave base impinged upon the sea floor as shown by the occurrence of wave-ripples (Macquaker 1994). The main part of the Westbury Formation, however, is interpreted as having been deposited in deeper water below

wave base. Upward-coarsening and upward-finishing successions on a stacked parasequence scale within the Westbury Formation suggest that sediment distribution was controlled by relative sea-level change (Macquaker 1999).

Bivalves are the most common and fossils within the Westbury Formation and occur predominantly in shell-beds (Ivimey-Cook *et al.* 1999). Vertebrate debris is abundant at some levels and includes fish teeth, spines and scales, and some bones and teeth from larger marine reptiles (Martill 1999). This material commonly occurs together with coarse siliciclastic sediment and phosphatic coprolites in well-defined 'bone-beds' (Macquaker 1999; Martill 1999).

4.1.2 The Cotham Member

The Cotham Member is of Rhaetian age and forms the lower part of the Lilstock Formation, The Cotham Member is 1.70 m thick and can be divided into a lower and upper unit, separated by an erosion surface characterised by desiccation cracks (Fig. 4.1). The lower part is 1.30 m thick and comprises thinly laminated siltstones and fine-grained sandstone with bands of ripple-marked limestone. The top of the unit shows a contorted, slump structures (Fig. 4.1). The upper part of the Cotham Member has a thickness of 0.6 m and comprises thinly inter-bedded mudstone, limestone and greenish grey shale.

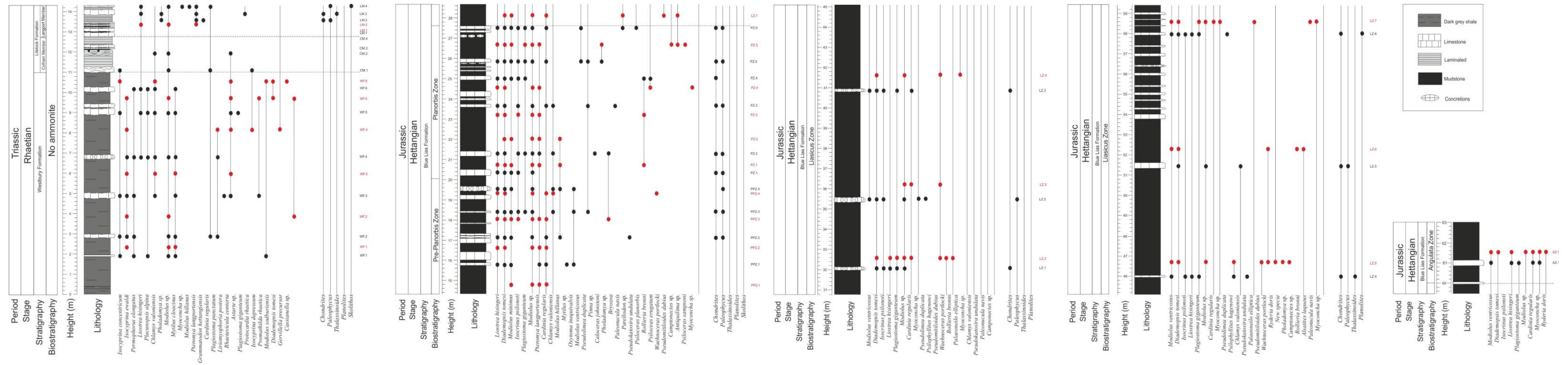


Figure 4.1 Lithostratigraphical log of the Westbury Formation, Lilstock Formation and basal Blue Lias Formation exposed at St Audrie’s Bay. Occurrences (limestone ● and mudstone ●) and ranges (black lines) of taxa recorded from 56 samples taken from the St Audrie’s Bay section.

The Cotham Member fauna typically includes only a few bivalve species, only in the lower part. The upper part of the Member, however, has yielded a few microfossil species, the ostracods *Baridia* and *Ogmoconchella* (Boomer *et al.* 1999; Hesselbo *et al.* 2004). The lower Cotham is a shallowing-upward succession, capped by a surface characterised by deep desiccation cracks that indicate a sudden fall in relative sea level (Swift 1999; Hesselbo *et al.* 2004). The deformed unit has been interpreted as a 'seismite', formed as a result of a massive regional shock caused by extra-terrestrial impact (Simms 2003). Overall, however, the upper Cotham Member represents a coastal environment which developed during a relative sea level rise (Swift 1999, Hesselbo *et al.* 2004). The initial negative carbon-isotope excursion recorded in many sections across the Tr/J boundary commences around 10 to 30 cm above the desiccation-cracked erosion surface (Fig. 4.1; 12 m above the base of the section).

4.1.3 The Langport Member

The Langport Member overlies the Cotham Member and has a thickness of 1.30 m. This unit is made up of pale grey limestone with inter-bedded grey or blue-grey mudstone. The lower part of the Langport Member comprises lenticular or nodular limestone, locally micritic or laminated, intercalated by dark grey mudstone. The higher beds include three limestones which weather to a cream colour and which form a unit with irregular base (Fig. 4.1). Deposition occurred in warm, very shallow water in a saline lagoonal environment (Gallois 2007). The fauna of the Langport Member includes bivalves, echinoderms, gastropods and corals. Ammonites have not been recorded in previous studies (Fig. 4.1).

4.1.4 The Blue Lias Formation

The base of the Blue Lias Formation of the Lias Group lies close to the base of the Jurassic System in Britain (see references in Page (2010)). The section comprises 74 m of the Blue Lias Formation, up to a level in the Hettangian Angulata Zone. The detailed stratigraphy of the Blue Lias Formation of the St Audrie's Bay area was first described by Palmer (1972) and later by Whittaker and Green (1983). The correlation of the Hettangian of the West Somerset Coast has been revised by Page (2004), with the base of the Jurassic System re-correlated by Clémence *et al.* (2010) using the carbon isotope curve to level around Beds 1-3 of Whittaker and Green (i.e. the base of the 'Pre-Planorbis Zone' – or more correctly the Tilmanni Zone according to Page 2010 after Hildebrandt *et al.* 2007, etc.). The base of the Planorbis Zone would then probably lie at the base of Bed 9 (cf. first occurrence of *Neophyllites*-like ammonites at Doniford Bay to the west– K. Page *pers. comm.* 2011) with the base of the Liasicus Zone in Bed 43 and the base of the Angulata Zone in Bed 80 (Fig. 5.1; 60 m above the base) (Page 2004).

The Blue Lias Formation comprises rhythmic sedimentary units of organic-rich shale, marl and limestone. The marl is often blocky, but sometimes more fissile, and medium to pale grey in colour. The limestone is dark bluish grey to medium grey in colour and typically hard, compact and splintery micrite, sometimes argillaceous. It occurs mostly in thin, laterally persistent beds, some of which are lenticular, but also forms laterally persistent horizons of nodules. The well-developed very fine laminations, occasional presence of pyrite and the lack of a benthic surface dwelling and burrowing fauna in the shale units, reflects anoxic sea-floor and substrate conditions. The calcareous mudstones (i.e. marls) and carbonate-rich beds with a benthic fauna reflect, in contrast, oxygenated

conditions. Similar observations have also been made by Whittaker & Green (1983), Hesselbo *et al.* (2004) and Warrington *et al.* (2008).

The lower around 5.7 m corresponds the Pre-Planorbis Zone and includes at least the higher part of Bed A1 to Bed A18 (Fig. 4.1, 14. 60 m above the base of the section). No ammonites have been recorded in this interval in the St Audrie's Bay area, although *Psiloceras erugatum* (Phillips), as Pinhay Bay section, has been placed in the upper part of the Zone (Page 2010). The base of the succeeding the Planorbis Zone is placed at the first occurrence of *Neophyllites* in Bed A18 and the zone ranges up to Bed 42, a total of 7.60 m (Fig. 4.1). The Liasicus Zone succeeds the Planorbis Zone, and is around 30.7 m thick, ranging from Bed 43-44 to Bed 80 (Fig. 4.1). Finally, the Angulata Zone spans beds 80-82 to 145 and is 21 m thick (Page 2010) (Fig. 4.1).

4.2 Richness

Two-thousand five-hundred ninety-eight macrofossil specimens corresponding to 51 species, grouped in 30 families, 17 orders, 5 classes, 2 phyla were recorded from 56 samples collected from the Tr/J section at St Audrie's Bay (Appendix 4.1). Mollusca are the dominant group, comprising Bivalvia 38 species, followed by Cephalopoda (5 species) and Gastropoda (2 species). Two classes of Echinodermata are also present, represented by one species of each of Echinoidea and Crinoidea.

4.2.1 Limestone samples

Thirty-eight species were recorded from 31 limestone samples. Around 20% of these were recorded in the Westbury Formation (15 spp.), 12% of the species disappearing at the base of the Cotham Member. From the Langport Member to the Planorbis Zone, the

number of the species increases rapidly from 10 spp. to 19 spp. Subsequently, the richness drops slightly through the Liasicus Zone, to 11 spp.

Average species richness from the 31 limestone samples through the Tr/J boundary section shows a significant decrease from the Westbury Formation to the Cotham Member (Fig. 4.2A). Between the Cotham and the Langport members the richness remains low (mean ~ 3 species). From the base of the Pre-Planorbis Zone the richness increases rapidly to 10 species at 21.2 m above the base of the studied section.

Subsequently, richness begins to decrease smoothly. From the base of the Liasicus Zone to the Angulata Zone the mean richness decreases significantly (mean ~4 species) to reach 5 species at 61 m above the base of the section (Fig. 4.2A).

Individual rarefaction performed by increasing the sample size, indicated that the lowest expected richness is recorded in the Cotham Member (mean = 5.59 ± 1.5), whilst the highest values are observed in the Planorbis Zone (mean = 19.58 ± 1.58) (Fig. 5.3A). The Westbury Formation and the Pre-Planorbis Zone do not record significant differences (14.85 ± 0.85 and 13.90 ± 0.9 , respectively). Similarly, the Langport Member and the Liasicus Zone do not record differences (~10 spp.).

In addition, the sample rarefaction estimated by three extrapolative techniques (Fig. 5.4), confirms the abrupt decrease of species number in the Cotham Member and the rapid increase in the number of the species up to the Planorbis Zone. The Shannon-Wiener diversity index shows a slightly different scenario, however (6.5A). The Cotham Member has the lowest diversity score (1.37 ± 0.13), whilst the Planorbis Zone records the highest diversity (2.06 ± 0.02), followed by, in order of decreasing diversity, the Pre-Planorbis Zone and Langport Member and the Liasicus Zone and the Westbury Formation, which have the same richness (6.5A).

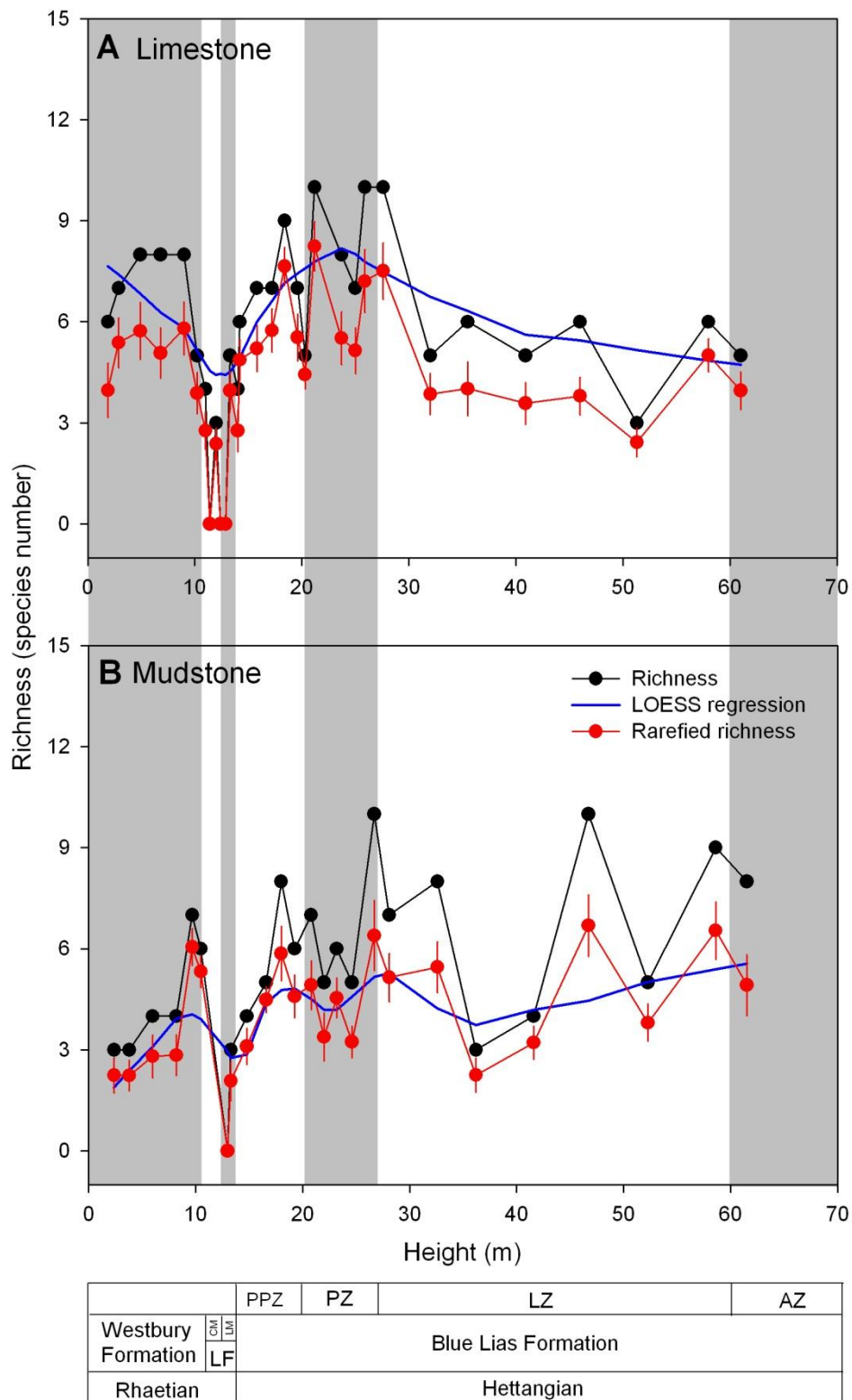


Figure 4.2 Raw (black line) and mean species richness (red line \pm 2 S.D.) recorded for each sample collected. The mean species richness represents the rarefied within-sample marine invertebrate richness estimated by 10,000 iterations. The blue line is the LOESS regression through the data point ($\alpha=0.3$). LF: Lilstock Formation, CM: Cotham Member, LM: Langport Member, PPZ: Pre-Planorbis Zone, PZ: Planorbis Zone, LZ: Liasicus Zone, AZ: Angulata zone.

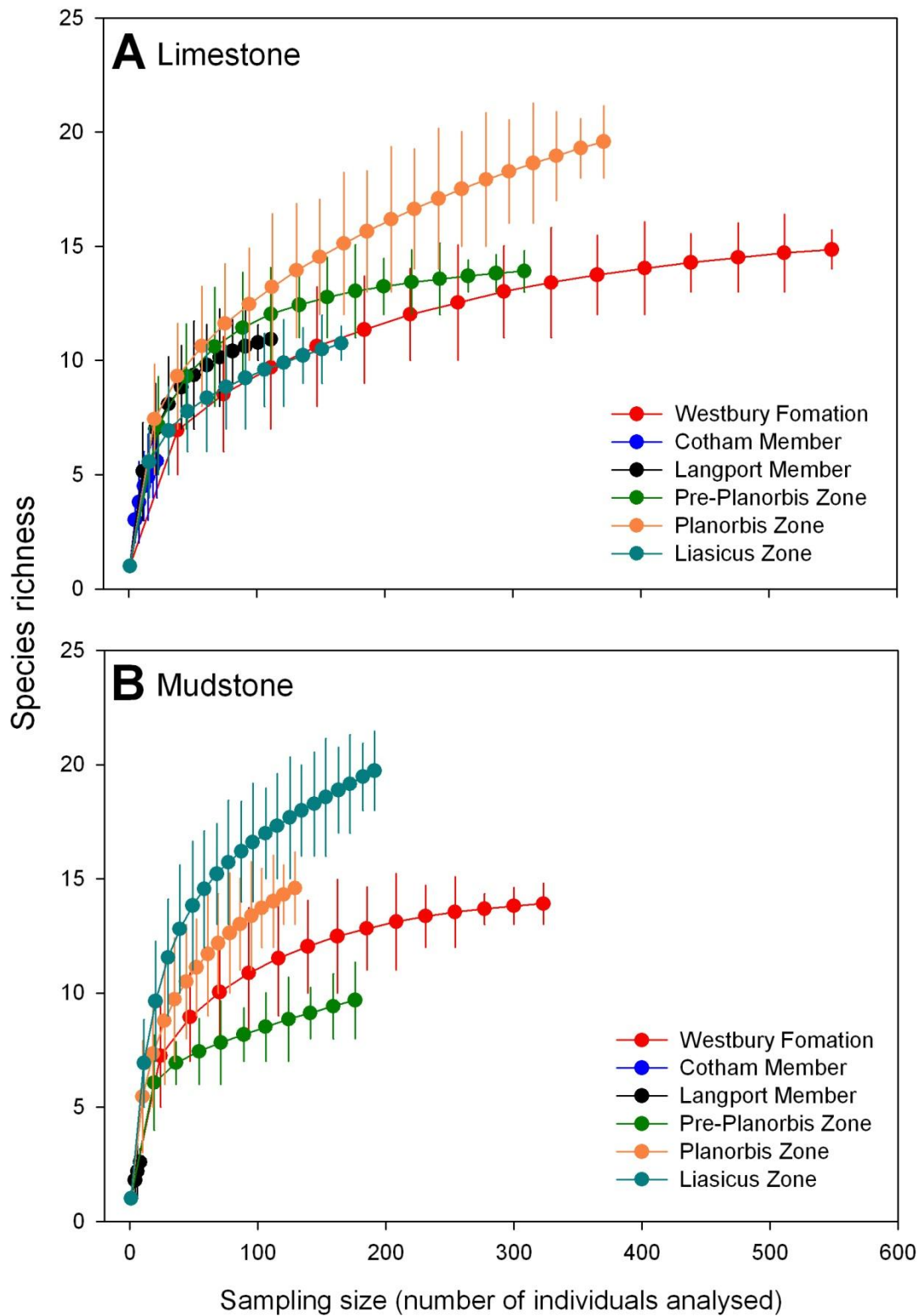


Figure 4.3 Average values (\pm 95% confidence intervals) of species richness estimated as sampling size increases through the Tr/J section in St Audrie’s Bay. Significant differences were assumed if 95% confidence intervals did not overlap.

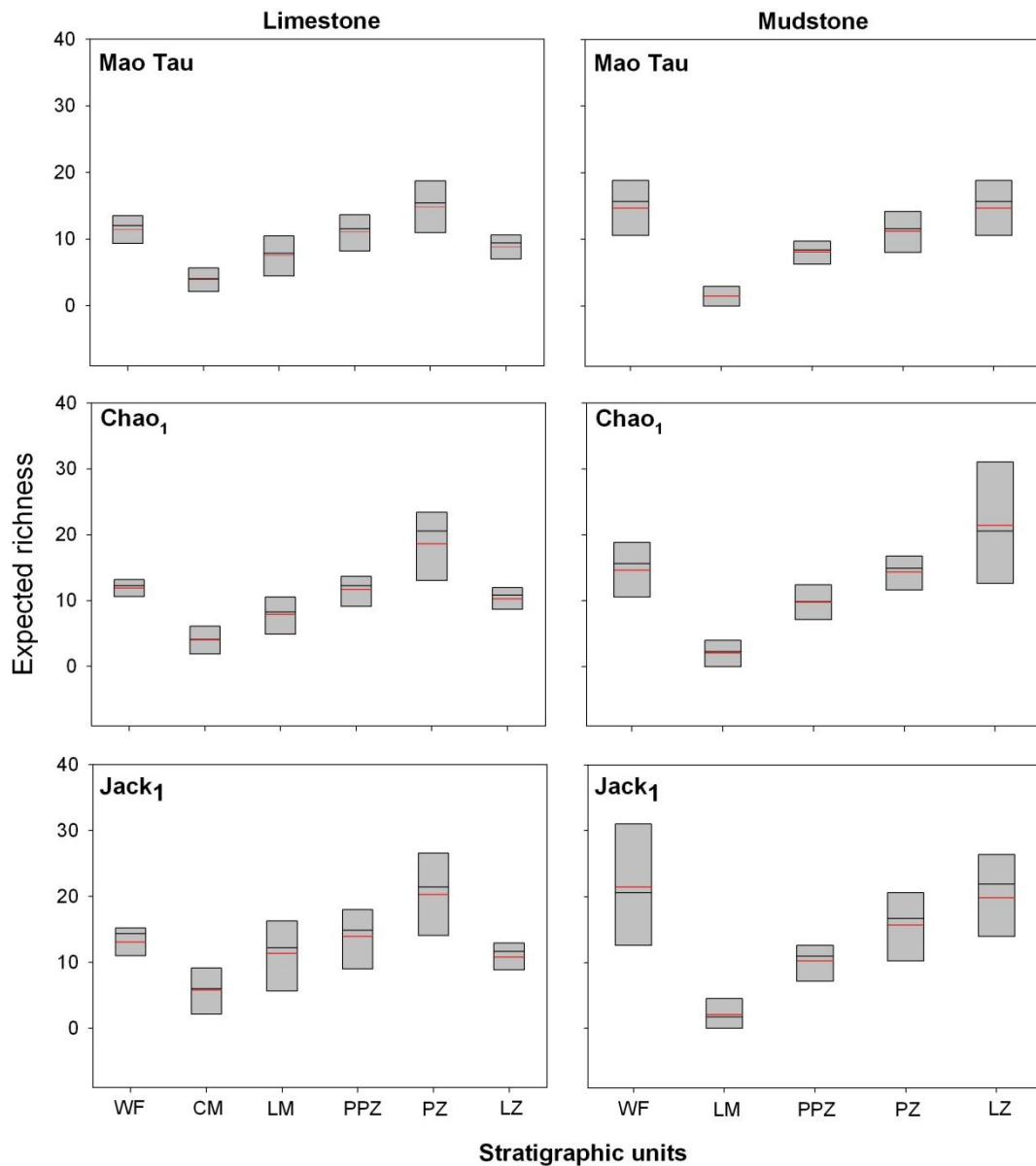


Figure 4.4 Boxplot of the rarefied within-sample marine fauna (Mao Tau, Chao₁ and Jackknife₁) during the study interval in St Audrie's Bay section. Each box represents the 95% confidence interval. The median is shown by an inner black line and the mean by a red line. WF: Westbury Formation, LM: Langport Member, CM: Cotham Member, PPZ: Pre-Planorbis Zone, PZ: Planorbis Zone, LZ: Liasicus Zone.

4.2.2 Mudstone samples

Thirty-eight species were recorded from 25 mudstone samples through the Tr/J boundary section (Appendix 4.1). In contrast to limestone samples, the highest richness was observed in the Liasicus Zone with 32% of the species, following by the Planorbis Zone and the Westbury Formation with 24%, and the Pre-Planorbis Zone with 16% of

all species recorded. In contrast, the Langport Member only records 5% (3 spp.) of the total number of species recorded in the entire Tr/J section.

The diversity curve drawn using these samples (Fig. 4.2B) shows an increase in the average richness from the base of the section to 10.05 m (sample W7). However, the richness drops sharply within the Langport Member where values of 0 and 3 species at 13 m and 13.3 m, respectively, above the base of the section (sample LM1 and LM2). Later, the richness increases rapidly to 8 species at 18 m above the base of the section (sample PPZ3). From this level in the Pre-Planorbis Zone to 24.6 m (Sample PZ4) in Planorbis Zone, although the richness fluctuates, it has a tendency to decrease (Fig. 4.2B). At 26.7 m above the base of the section the richness increases again to 10 spp. (sample PZ5) and decays gradually to 3 species (Sample LZ3) at 36.2 m above the base (Fig. 4.2B). Up to the Angulata Zone, the average richness increases slightly to 8 species at 61.5 m (Sample AZ1). The raw richness by sample, however, shows high fluctuations, recording two peaks; the first at 46.7 m (10 spp. sample LZ4) and the second at 58.6 m (9 spp. sample LZ7) above the base of the section (Fig. 4.2B, Appendix 4.1).

Individual rarefaction performed by increasing the sample size, shows that the Langport Member records the lowest expected richness through the section (2.59 ± 0.59) (Fig. 4.3B). From the Pre-Planorbis Zone to the Liasicus Zone, the richness values increase rapidly from 9.67 ± 1.67 in the Pre-Planorbis Zone to 14.58 ± 1.58 in the Planorbis Zone and 19.73 ± 1.73 in the Liasicus Zone. The Westbury Formation records slightly lower values (13.90 ± 0.90) than observed in the Planorbis Zone (Fig. 4.3B).

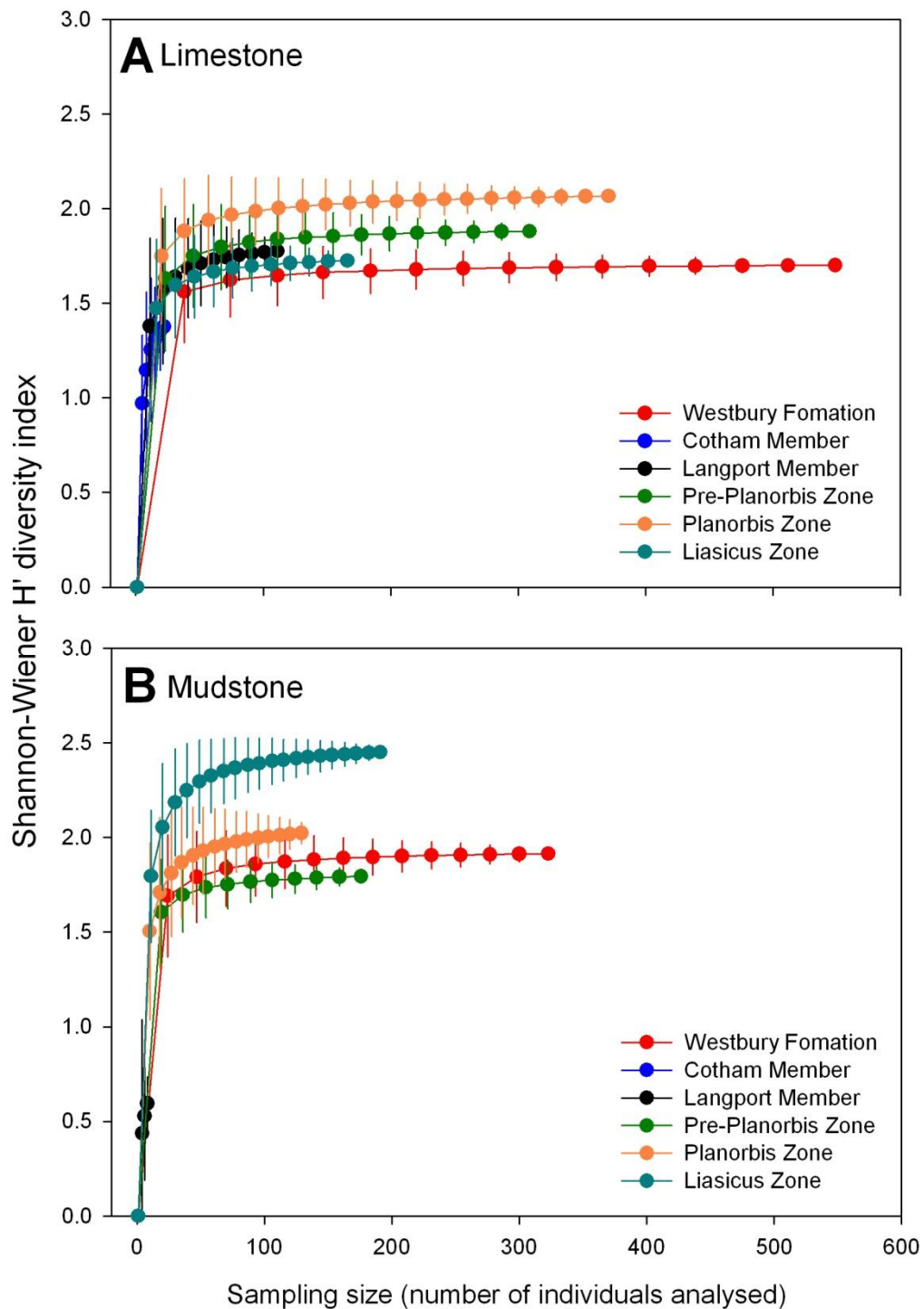


Figure 4.5 Average values ($\pm 95\%$ confidence intervals) of Shannon-Wiener diversity estimated as sampling size increased during the study interval. Significant differences were assumed if 95% confidence intervals did not overlap.

The sample rarefaction estimated by the three sampling techniques (Fig. 4.4B), confirms the sharp decrease in the number of the species from Westbury Formation to the Langport Member. From the Pre-Planorbis to the Liasicus Zone the expected

richness increases from 13 to 27 species. In addition, the Shannon-Wiener diversity index (Fig. 4.5B) confirms the richness depletion observed in the Langport Member. As with previous results, the diversity increases from the Pre-Planorbis to the Liasicus Zone. The lower Westbury Formation records intermediate values between those of the Pre-Planorbis and the Planorbis Zone.

4.3 Abundance

4.3.1 Limestone samples

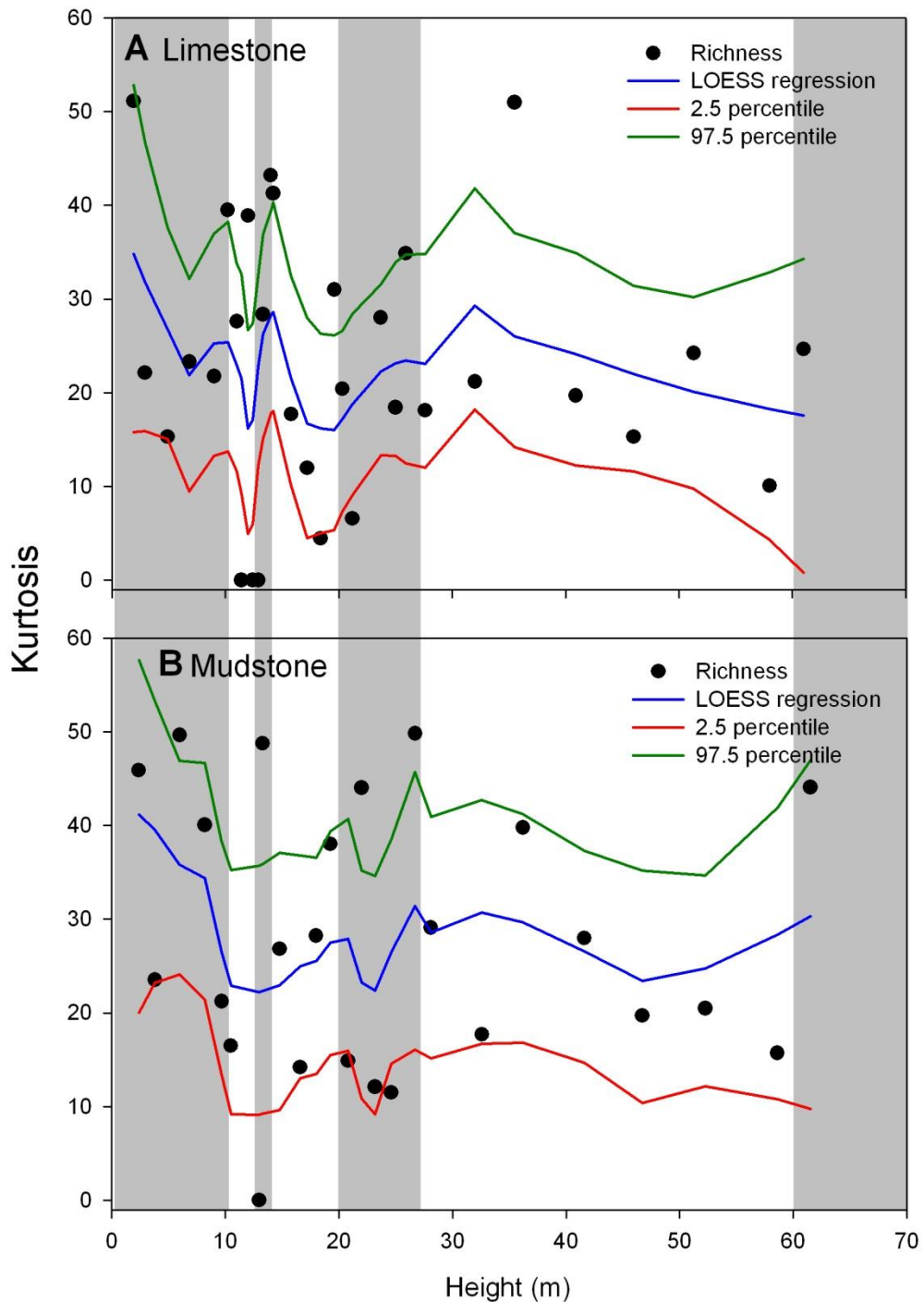
Kurtosis values estimated from limestone samples tend to decrease through the studied section. In the Westbury Formation, the kurtosis (dominance) reaches an average value of 28.85 ± 5.53 (Fig. 4.6A). The trajectory of kurtosis through the Westbury Formation tends to decrease from the base of the section to 10.2 m (Appendix 4.2). From the base of the Cotham Member to the top of the Langport Member (11 m to 14.24 m above the base of the sampled section) kurtosis increases significantly (mean = 35.83 ± 3.00) reaching a values of 41.26 at 14.2 m (sample Lang4). This gradual increase is interrupted, however, by a negative peak at 11.4 m (Fig. 4.6) due to the absence of any fauna (sample CO2), and also at 12.4 m (sample CO4) and 12.9 m (Sample LM1) above the base of the section. From the base of the Blue Lias Formation, the kurtosis values tend to increase to a maximum peak at 35.5 m (score 50.96) (Sample LZ2). From this level to the first Angulata Zone sample (61 m above the base of the section), the kurtosis (dominance) tends to decrease significantly.

The Westbury Formation records a total of 15 species, the dominant being *Isocyprina concentricum* (32.48%), followed by *Isocyprina waldi* (29.91%) and *Permophorus elongatus* with 17.26%. Two species show a rank abundance of >5% (*Placunopsis alpine* and *Chlamys valoniensis*), whilst 9 species have an abundance of < 1%. The

abundance distribution tends to decay smoothly to values under 1%. The behaviour of this curve is best explained by the Geometric model, which states that most species show a similar abundance, while few species have a low abundance (Fig. 4.7A, Table 4.1, Appendix 4.3).

The Cotham Member assemblage contains 6 species; the dominant species is *C. valoniensis* (48.15%) followed by *Modiolus* sp. and *I. concentricum* with 22.22 % and 14.81%, respectively, whilst the abundance of *Protocardia rhaetica*, *Cardinia regularis* and *Rhaetavicula contorta* falls slightly to between 8 and 3% (Fig. 4.7A, Appendix 4.3). Despite the low species number, the Rank abundance distribution fits a Broken Stick model (Table 4.1). Rank abundance models such as Zipf, Mandelbrot and Log normal generally indicate assemblages under undisrupted ecological conditions, while the Broken stick model assume a more even distribution of the species abundance.

The Langport Member assemblage comprises 10 species and the rank abundance decays gradually. In this sequence *Liostrea hisingeri* has the highest abundance (46.61%), *Pholadomya* sp. and *Myoconcha* sp. show abundances between 10-15%, whilst *Modiolus hillanus*, *Pteromya langportensis* and *Grammatodon hettangiensis* occur at between 5-9%. Three species have an abundance between 1-3% and *C. valoniensis* has the lowest abundance at <1% (Figure 4.7A, Appendix 4.3). The Zipf Model was the best fit for this assemblage (Table 4.1).



		PPZ	PZ	LZ	AZ
Westbury Formation	CM	Blue Lias Formation			
	LF				
Rhaetian		Hettangian			

Figure 4.6 Dominance (Kurtosis \pm 95% confidence intervals) of marine fossils assemblages through Tr/J section in St Audrie's Bay. The red line is the LOESS regression through the data point estimated with an alpha 0.3. LF: Lilstock Formation, CM: Cotham Member, LM: Langport Member, PPZ: Pre-Planorbis Zone, PZ: Planorbis Zone, LZ: Liasicus Zone.

L. hisingeri is the dominant species in the Pre-Planorbis Zone assemblage (35.82%) followed by *Modiolus minimus* and *Diademopsis tomesi* with abundances of 23.28 and 15.52 %, respectively. The abundance of the remaining species drops to proportions between 7 and 0.3%. Within this range, eight species record abundances between 7-1%, whilst three specimens record an abundance of <1% (Figure 4.7A, Appendix 4.3). The abundance distribution of the fifteen recorded species fits a Mandelbrot model (Table 4.1).

The Planorbis Zone records the highest richness through the study section. However, the proportional abundance between species shows the highest differences. *D. tomesi* is the dominant species with an abundance of 32.32%, the abundance of other species, however, falls to proportions between 17 and 12%, with species such as *L. hisingeri*, *I. psilonoti* and *P. giganteum*. Six species record abundances of between 10 to 1%, whilst 9 species have an abundance of less than 1% (Figure 4.7A, Appendix 4.3). Due to a rapid fall of the rank abundance and high dominance of just a few species, this assemblage fits closely with a Geometric model (Table 4.1).

As for the Planorbis Zone, the Geometric model, also explains very well the rank abundance distribution through the Liasicus Zone assemblage. Eleven species were recorded in the Zone of which *M. ventricosus* is the dominant at 34.44%, followed by *D. tomesi* at 26.67% and *I. psilonoti* at 16.67%. The rank abundance of the next four species falls sharply to between 7 to 1%, whilst three species have single occurrences with abundances of 0.56%.

Figure 4.8A shows the species dominance index computed by increasing the sample size. This plot shows 2 homogeneous groups; the first group with high dominance is represented by the assemblages of the Cotham and Langport members, whilst the

remaining assemblages show a low dominance (mean $\sim 0.32 \pm 0.01$), without significant differences between them.

4.3.2 Mudstone samples

Figure 4.6B shows the trajectory of the kurtosis (dominance) through the study section in St Audrie's Bay. Kurtosis tends to decrease from a value of 45.87 (Sample W1) at 2.5 m above the base of the recorded section, 16.50 at 10.5 m above the base (sample W7), reflecting a relatively high mean dominance through the sequence. Through the Langport Member dominance increases, although only one sample provided results, at 13.3 m above the base of the recorded section (score 48.75; Sample LM2). In the Blue Lias Formation above, the mean kurtosis fluctuates highly between zones.

Through the Pre-Planorbis Zone, kurtosis values increase from a value of 26.83 at 14.8 m to 38.0 at 19.25 m above the base of the section (samples PPZ1 to PPZ4). From 20.5 m above the base of the section (sample = PZ1), kurtosis decreases significantly to 21.20 m (sample = PZ2). From this level, the kurtosis increases to a peak at 35.5 m above the section (score = 51; sample = LZ2). From this level, the kurtosis tends to decrease smoothly to 60 m above the base of the section, with a score of 24.66 in the Angulata Zone.

Fourteen species are recorded in the Westbury Formation, with *R. contorta* showing the highest proportional abundance at 35.04 %. The abundance distribution of the remaining species drops more than 50% with *I. concentricum*, *I. ewaldi* and *P. rhaetica* having a recorded abundance of between 18 and 11%. Three species show abundances between 8 and 2% (*M. sodburiensis*, *Cassianella* sp. and *P. rhaetica*). *M. minimus* and *Astarte* sp. record abundances of around 1.02%, whilst the remaining 28% of the species in this assemblages record abundances of < 1%. Due to the high dominance of

the one species (*R. contorta*), the Geometric model is the best fit for this assemblage (Fig. 4.7B, Table 4.1, Appendix 4.3).

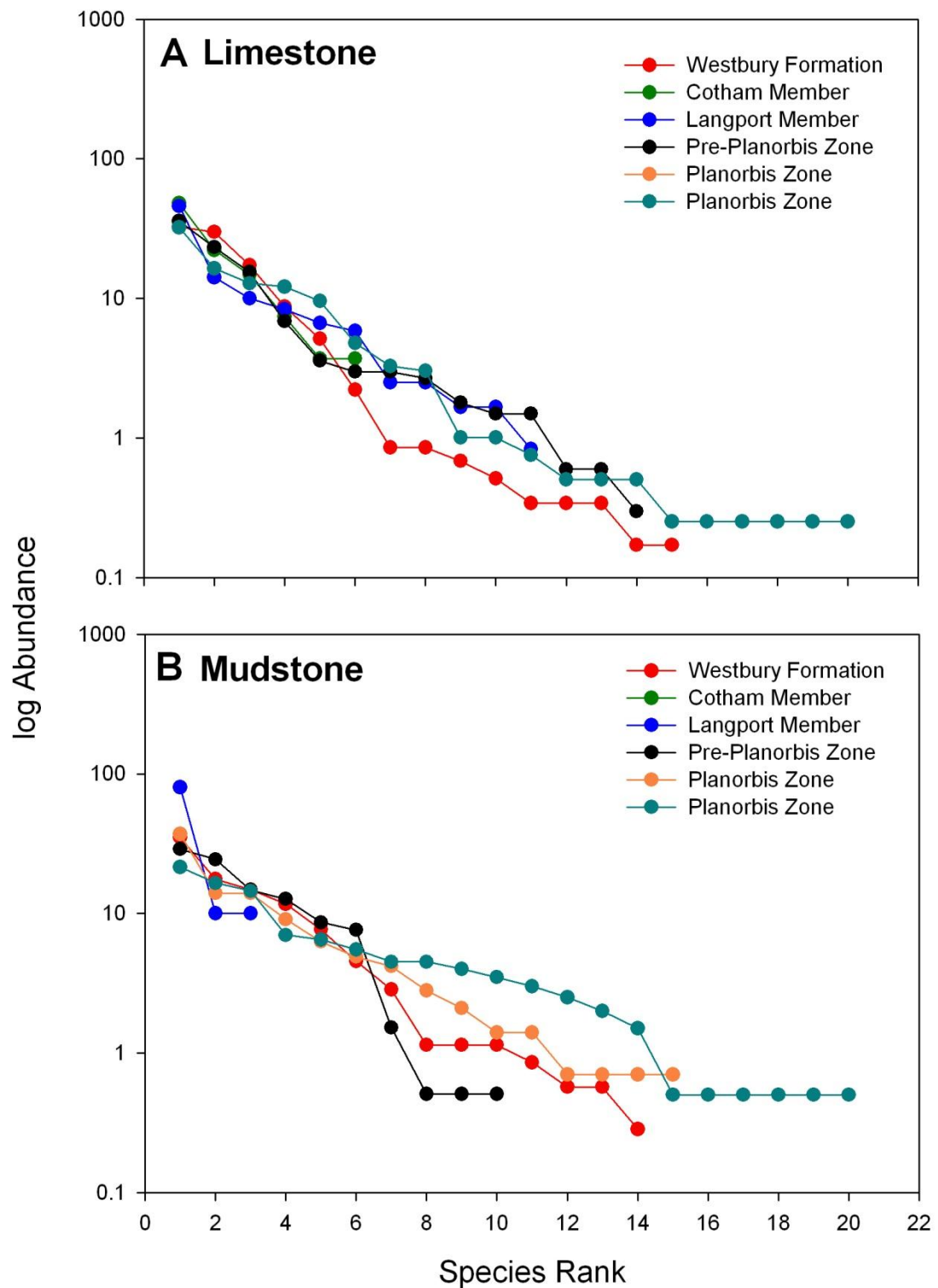


Figure 4.7 RACs derived from the abundance of marine invertebrate fossil communities through the Tr/J study interval. Y-axis on log(n) scale.

Table 4.1 Comparison of RAD models derived from abundance distribution of marine invertebrates through the Tr/J section in St Audrie's Bay. The models were ranked based on Akaike's weight (ω_i) following Burnham & Anderson's (2002) recommendation. AICc sample-size corrected was estimated as $AICc = AIC + (2K/[K+1])/(n-K-1)$. AIC is report only for completeness. K is the number of parameters; T is the number of taxa; n is the number of specimens. The highest ω_i gives the best fit (**In bold**).

Limestone								
Parameters (K)	T	n	AIC	RAD models				
				Broken stick	Geometric	Log normal	Zipf	Mandelbrot
				0	1	2	2	3
Westbury Formation	15	585	AIC	350.88	94.17	180.58	236.27	98.17
			AICc	350.88	94.18	180.60	236.29	98.21
			ω_i	1.59×10^{-19}	0.88	1.50×10^{-19}	$1. \times 10^{-31}$	0.11
Cotham Member	6	27	AIC	18.96	20.32	22.29	22.57	24.14
			AICc	18.96	20.48	22.79	23.07	25.18
			ω_i	0.560	0.261	0.082	0.072	0.025
Langport Member	11	120	AIC	59.61	55.13	47.92	47.88	49.88
			AICc	59.61	55.16	48.02	47.98	50.09
			ω_i	1.26×10^{-3}	0.01	0.41	0.42	0.14
Pre-Planorbis Zone	14	335	AIC	136.28	79.13	80.10	93.54	73.39
			AICc	136.28	79.14	80.14	93.58	73.46
			ω_i	2.09×10^{-14}	0.05	0.03	3.92×10^{-5}	0.91
Planorbis Zone	19	397	AIC	217.61	91.84	115.83	152.41	93.70
			AICc	217.61	91.85	115.86	152.44	93.76
			ω_i	3.5×10^{-28}	0.72	4.40×10^{-6}	5.02×10^{-14}	0.27
Liasicus Zone	11	180	AIC	72.94	46.67	60.36	74.57	50.67
			AICc	72.94	46.70	60.43	74.64	50.80
			ω_i	1.77×10^{-6}	0.88	9.24×10^{-4}	7.59×10^{-7}	0.11

Mudstone								
Parameters (K)	T	n	AIC	RAD models				
				Broken stick	Geometric	Log normal	Zipf	Mandelbrot
				0	1	2	2	3
Westbury Formation	14	351	AIC	125.61	68.39	81.59	108.68	71.94
			AICc	125.61	68.40	81.62	108.72	72.01
			ω_i	3.23×10^{-13}	0.85	1.15×10^{-3}	1.51×10^{-9}	0.14
Langport Member	3	10	AIC	9.99	10.91	12.90	12.38	14.38
			AICc	9.99	11.41	14.62	14.09	18.38
			ω_i	0.57	0.28	0.05	0.07	8.68×10^{-3}
Pre-Planorbis Zone	10	197	AIC	60.97	56.24	67.76	90.03	60.17
			AICc	60.97	56.26	67.82	90.09	60.30
			ω_i	0.07	0.81	2.51×10^{-3}	3.66×10^{-8}	0.10
Planorbis Zone	15	143	AIC	74.34	61.54	58.38	63.35	61.14
			AICc	74.34	61.57	58.47	63.44	61.31
			ω_i	2.33×10^{-4}	0.13	0.65	0.05	0.15
Liasicus Zone	20	200	AIC	84.80	80.18	84.27	98.74	83.34
			AICc	84.80	80.20	84.33	98.80	83.46
			ω_i	0.07	0.70	0.08	6.42×10^{-5}	0.13

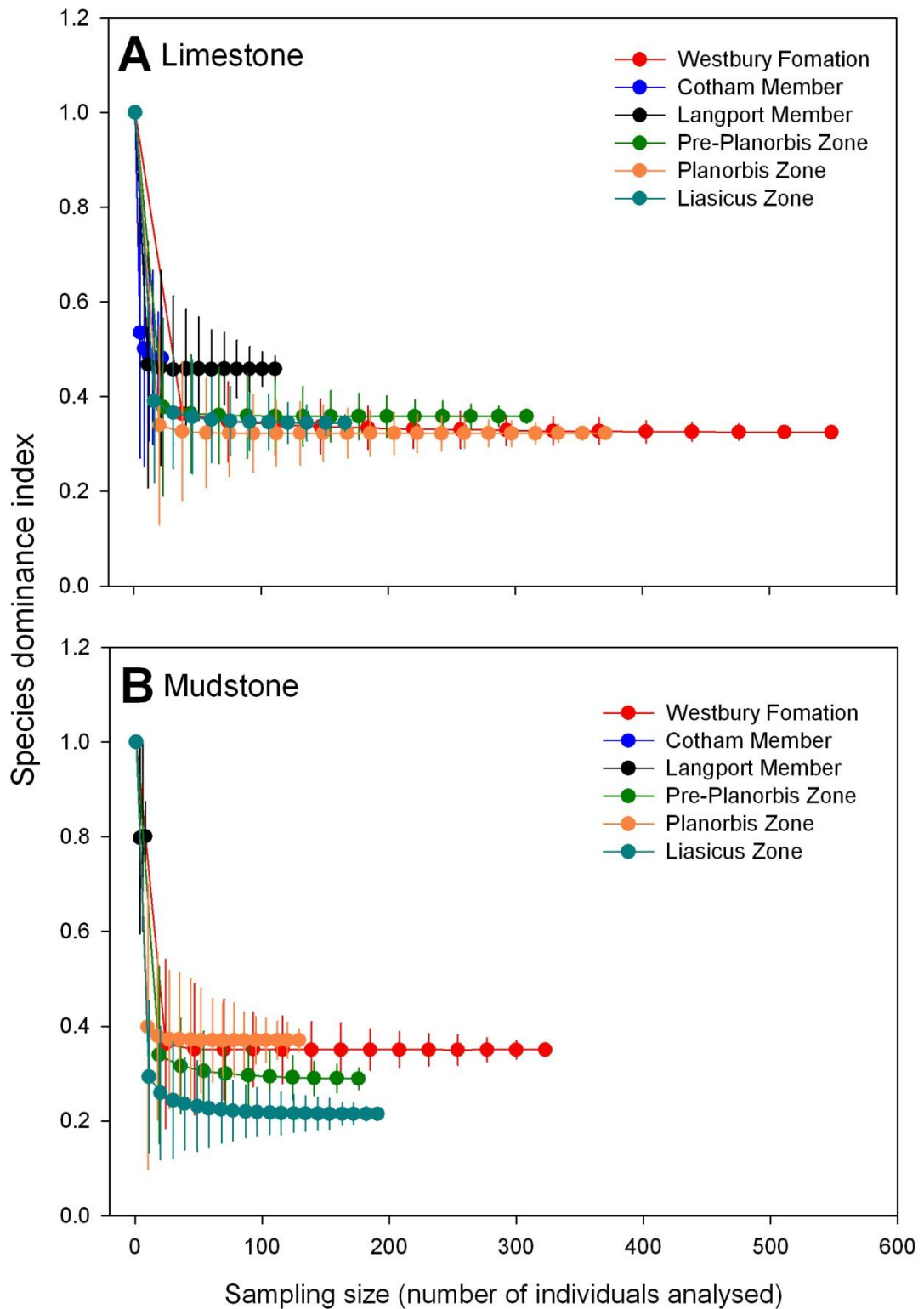


Figure 4.8 Average values ($\pm 95\%$ confidence intervals) of species dominance index estimated as sampling size increased during the Tr/J section in St Audrie's Bay. Significant differences were assumed if 95% confidence intervals did not overlap.

The Langport Member shows the lowest abundance and just 3 species were recorded: *P. langportensis* has an abundance of 80%, whilst *M. minimus* and *L. hisingeri*, both have abundances of 10% (Fig. 4.7B, Table 4.1, Appendix 4.1). Despite the low species number, the abundance distribution of this assemblage fits a Broken Stick model, which predicts an even rank abundance distribution (Fig. 4.7B, Table 4.1, Appendix 4.3).

The Pre-Planorbis Zone records 14 species, although the rank abundance by species does not exceed 30%, and the abundance distribution drops rapidly. *D. tomesi* was the most abundant species at 30%, followed by *Modiolus* sp. and *L. hisingeri*, at 19% and 15%, respectively. Seven species record abundances between 10 and 1%, whilst 4 species occurred at < 1%. Despite the high number of specimens found in the Pre-Planorbis Zone, the assemblage shows a high dominance, which fits a Geometric model (Fig. 4.7B, Table 4.1, Appendix 4.3).

The Planorbis Zone records a total of 15 species, the relative abundances of which are more equally distributed, although the rank abundance distribution tends to behave as a Log Normal model (Table 4.1). In this assemblage the ammonite *Caloceras* is the dominant species (37.07%), whilst *L. hisingeri* and *P. langportensis* both have relative abundance of 14%. Eight species show a relative abundance of between 9 and 1% (Appendix 4.3). *I. psilonoti* and *P. sampsoni* record proportions between 1-2% and four species have unique occurrences with abundances of <1% (Fig. 4.7B, Table 4.1, Appendix 4.3).

The 200 collected specimens from the Liasicus Zone can be grouped into 19 species. The rank abundance distribution tends to decay sharply, with just 3 species recording high dominance, although with a high difference between them (*D. tomesi* with a relative abundance of 21.5%, *Modiolus* spp. 6.5% and *C. regularis* with 14.55 %). The

proportional abundance of the remaining species drops an order of magnitude to 9-1%, but includes 63% of the species in the assemblage (10 spp.). The remaining six species in the assemblage show an abundance of <1%. As for the Pre-Planorbis Zone, the geometric model was the best fit for this assemblage (Fig. 4.7B, Table 4.1, and Appendix 4.3).

Figure 4.8B shows the species dominance index calculated by increasing the sample size and indicates that the dominance is relative low (< 50%). The Langport Member records the highest dominance through the section at 0.8 ± 0.07 , whilst lower values were observed within the Liasicus Zone (0.21 ± 0.01). The Planorbis Zone and the Westbury Formation did not show significant differences in dominance (0.35 ± 0.01 and 0.37 ± 0.02 , respectively) although they both recorded higher values than the Pre-Planorbis Zone (0.28 ± 0.02).

4.4 Composition

4.4.1 Limestone samples

Non-metric multidimensional scaling clearly separated the limestone samples generating three groups with similar fauna (1) Westbury Formation and the Cotham Member; (2) The Langport Member and the Pre-Planorbis Zone and (3) those from the Planorbis and Liasicus zones (Fig 4.9A). One-Way ANOSIM indicated significant and gradual differences in species composition between stratigraphic units. The Westbury Formation and the Cotham assemblages are more similar between then, however its differs from The Langport Member and the Pre-Planorbis Zone, which are in the same time, more similar between then, but differs from the Planorbis and Liasicus zones ($R=0.14$; $p = 0.0032$).

SIMPER analysis shows that the dissimilarity is higher between samples from the Westbury Formation, the Cotham Member and the Langport Member (85.97%) than between samples from higher levels in the Blue Lias Formation (Appendix 4.5). Fifteen species were recorded in the Westbury Formation, of these 5 continued into the Cotham Member, recording a dissimilarity of 87.3% between both assemblages. 3 species present become extinct globally, whilst the remainder only became extinct regionally. *L. hisingeri*, *Modiolus* spp. *C. valoniensis* and *C. regularis* pass through into the Blue Lias Formation, although *L. hisingeri* disappears through the Cotham Member and *C. valoniensis* disappears from Langport Member assemblages (Appendix 4.6).

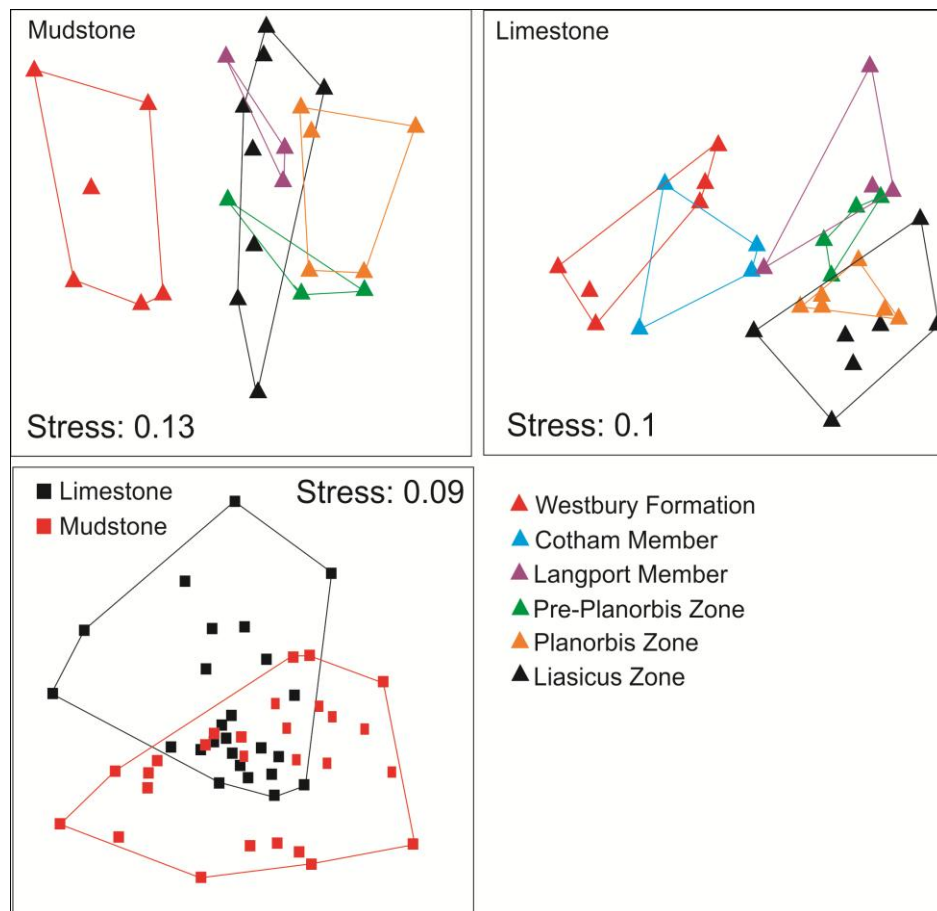


Figure 4.9 Non-metric multidimensional scaling (NMDS) plot resulting from the ordination analysis (Chord distance) of the marine invertebrate fauna from the St Audrie's Bay section, using abundance data transformed by taking the fourth root of [\times].

The Cotham Member records 6 species, from which only 3 range through to the base of the Blue Lias Formation (Appendix 4.6). Assemblages between the Cotham and the Langport members record a dissimilarity of 84.6%. *R. contorta*, *I. concentricum*, *P. rhaetica* and *C. valoniensis* disappear at this unit, although only *R. contorta* becomes globally extinct, whilst *I. concentricum* and *P. rhaetica* become regionally extinct.

The Langport Member records 9 species, seven of which appear in this assemblage, two of them recorded as single specimens (*G. hettangiensis* and *Myoconcha* sp.), whilst the remaining 5 range through to the Blue Lias Formation, although *M. hillanus* disappears in the Pre-Planorbis Zone. The Langport Member records a dissimilarity of 81% when compared with the Pre-Planorbis assemblage (Appendices 4.5 and 4.6).

The Pre-Planorbis Zone records a total of 14 species, six of which appear for the first time at this zone. *O. inequivalvis*, *Mytilus* spp. and *Parellodon* sp. are exclusive to this zone, whilst *D. tomesi*, *I. psilonoti* and *M. minimus* persist to higher levels in the Blue Lias Formation (Appendix 4.6). The Pre-Planorbis Zone and the Planorbis Zone records a dissimilarity of 50%. The Planorbis assemblage recorded a total of 20 species, nine appearing at this level, although seven are recorded as single specimens and hence have a very low abundance (< 1%). Two species from this assemblage persist upwards into the Liasicus Zone, although the ranges of three species terminate at this level (*M. minimus*, *P. langportensis* and *Pholadomya* sp.). Through the Liasicus Zone, the number of the species decreases by 11, whilst sharing a similarity of more than 50% with the Planorbis Zone assemblages. *Psilophyllites hagenowi* is unique to the Liasicus Zones and only one specimen was recorded (Appendix 4.6).

The Whittaker and Routledge beta index is used to estimate the composition turnover between pairwise samples. This indicates that the greatest compositional changes

happened between the Cotham and the Langport members, with two high peaks at 11.7 and 13.1 m above the base of the recorded section (Fig. 4.10A). In contrast to ANOSIM, another significant peak is observed at 54.65 m above the base of the section, at the end of the Liasicus Zone (Appendix 4.2).

4.4.2 Mudstone samples

Non-metric multidimensional scaling separates the mudstone samples from the Westbury Formation from those of the Langport Member and the Blue Lias Formation (Fig 4.9B). Conversely, One-Way ANOSIM indicates however, that there are no significant differences in composition between samples from the Westbury and Langport Member, and from samples taken in the Blue Lias Formation. However, there are significant differences in the species composition between samples from the Blue Lias Formation and from the Westbury Formation and the Langport Member. SIMPER analysis shows that the similarity is higher between samples from the Westbury Formation and the Langport Member (85.97%) than between those of higher levels in the Blue Lias Formation (Appendix 4.7).

Ninety-two percent of the species (13 species) disappear between the Westbury Formation and the Langport Member (no species were recorded for the Cotham Member). *Modiolus* sp. is the unique taxon that ranges through to the Blue Lias Formation. Eight per cent of the species record global extinction, whilst *Protocardia rhaetica*, *Promatilda rhaetica* and 3 species of the genus *Isocyprina* recorded regional extinction (undergone extinction on Langport Member).

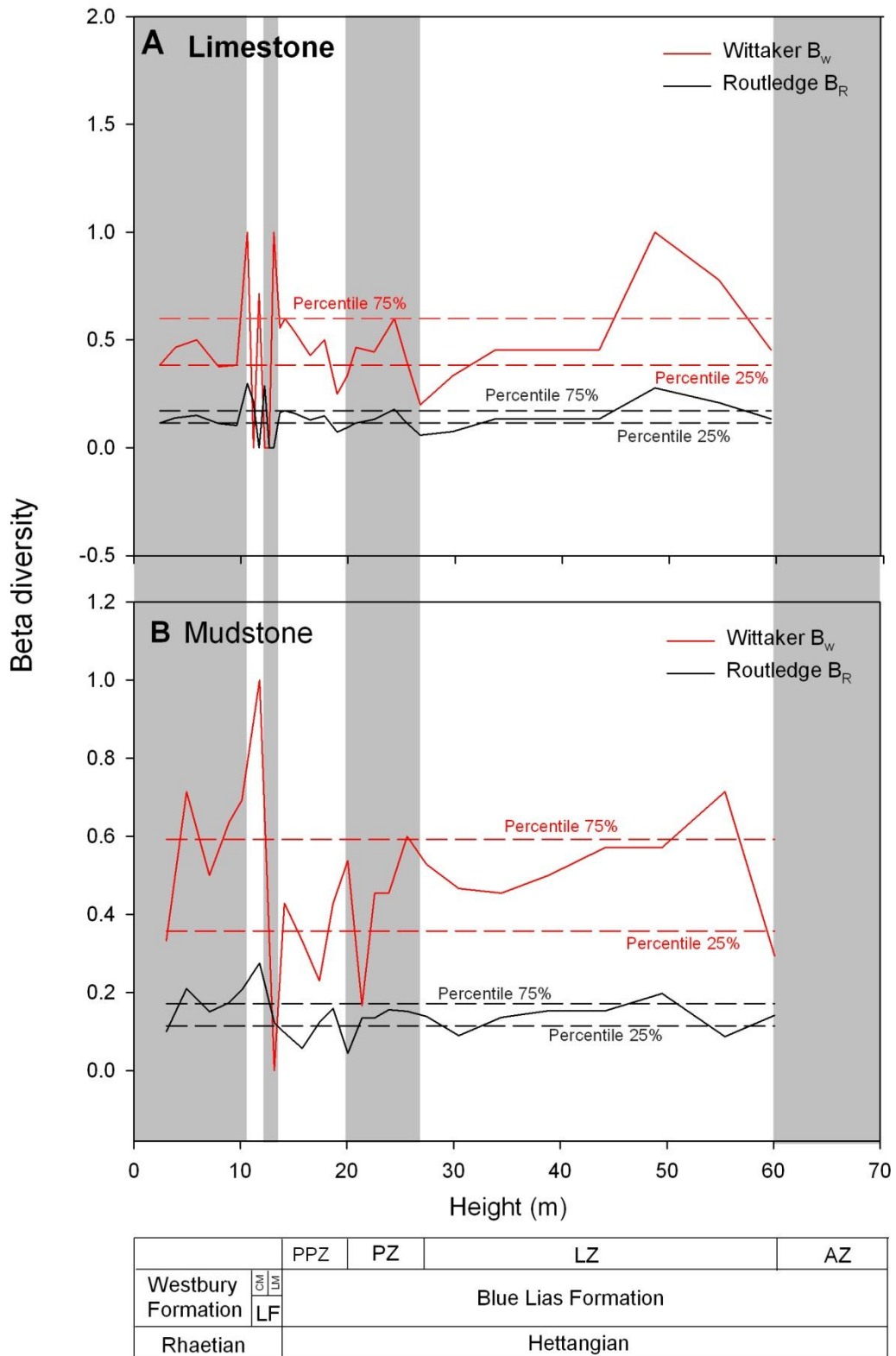


Figure 4.10 Beta diversity (β) estimated by Whittaker and Routledge indices. These indices reflect the temporal difference in species composition between samples. The percentiles represent the 95% confidence intervals calculated by bootstrap procedure (number of iterations = 10000). LF: Lillstock Formation, CM: Cotham Member, LM: Langport Member, PPZ: Pre-Planorbis Zone, PZ: Planorbis Zone, LZ: Liasicus Zone.

The Langport Member to the Pre-Planorbis Zone shares a dissimilarity of 85.54%. Five species range through the Langport Member to Pre-Planorbis Zone; *C. regularis*, *L. hisingeri*, *M. minimus* and *P. langportiensis* appears for first time in the Langport Member, whilst *Modiolus* sp. remained since the Westbury Formation assemblage (Appendix 4.8). Between the Pre-Planorbis Zone and the Planorbis Zone, nine species appear; of this, six species records a single occurrence, two species record its last appearance and eight species went through the Liasicus Zone (see Appendices 4.7 and 4.8). Through the Liasicus zone, the number of species increases slightly (14 species). 40% of this species are unique records, whilst nine species terminate at this level (Appendices 4.7 and 4.8).

4.4.3 Mudstone and Limestone comparison

Mudstone and limestone samples record a significant difference in species composition (Fig. 6.9C, $R = 0.08$, $p = 0.0092$, Dissimilarity = 79.64%). SIMPER analysis shows that fourteen taxa only appear in the mudstone samples, while thirteen are exclusively recorded in limestone samples (Appendix 4.9).

4.5 Ecospace

The marine fauna sampled from the limestone and mudstone lithologies through the Tr/J boundary at St Audrie's Bay, used fourteen modes of life, which corresponds to 7% of the total theoretical ecospace (Fig. 4.11). As for the Pinhay Bay section (see Chapter 5), samples of different lithologies were grouped by stratigraphic unit with the aim of observing potential interaction networks (e.g. predator-prey relationships) and the ecological complexity of each assemblage.

The results demonstrate that ecological complexity increases through the study section at St. St Audrie's Bay (Fig. 4.11). Six modes of life were recorded in the Westbury Formation and occupied ecospace decreases by 68% into the Cotham Member of the Lilstock Formation. Subsequently, occupied ecospace expands rapidly through the Langport Member (4 modes of life), whilst in the Pre-Planorbis Zone, the number of modes of life doubles to 8. In the Planorbis Zone, the number of modes of life occupied apparently reaches a maximum of 10, which is maintained in the Liasicus Zone.

The Westbury Formation assemblage uses 6 modes of life (Fig. 4.11, Appendices 4.10 and 4.11), although no pelagic forms were found. 45% of the modes of life used were surface types. Six of the bivalve species use a facultative-motile, attached suspension feeder mode of life; two gastropod species show slow moving grazing and predatory forms and one species, *L. hisingeri*, was a sessile-suspension feeder (Fig. 4.10, Appendices 4.8 and 4.9). 20% of the species (all bivalves) were semi-infaunal, facultatively-attached suspension feeders and 35% (also bivalves) used a shallow infaunal, facultatively motile, unattached suspension feeder mode of life. The assemblage is ecologically simple, with organisms restricted to a benthic existence, with a very short trophic network and with small predators and suspension feeder's forms with limited locomotion (45% of the species) (Fig. 4.12).

The Cotham Member assemblages occupied 3 modes of life; *C. valoniensis* and *R. contorta* were surficial, facultatively-motile, attached, suspension feeders. *Modiolus* sp. used a semi-infaunal, facultative motile attached, suspension feeder mode. *I. concentricum*, *P. rhaetica* and *C. regularis* occupied the shallow-infaunal, facultatively-motile, unattached, suspension feeders niche. From the Westbury Formation to the Cotham Member the relative abundance of surface dwelling modes of life decreases by

77%, whilst semi- and shallow infaunal modes decrease by 57% (Fig. 4.11, Appendices 4.10 and 4.11). The only feeding mechanisms recorded were the suspension feeders and motility was restrictive to facultatively motile or non-moving species (Fig.4.11, Appendix 4.10).

Although the Langport Member records the same modes of life as the previous assemblages, the species composition has changed completely. Ten species are present in this assemblage and one 'new' mode of life is added: surficial, non-moving suspension feeders, represented by *L. hisingeri* and *P. duplicata* (14% relative abundance) (Fig. 4.11). Associated semi-infaunal and shallow infaunal modes were occupied by three species (all bivalves) (Fig. 4.11, Appendices 4.10 and 4.11). Through this unit the number of species increases by 40%, with the number of species per mode of life (i.e. the packing) also increasing. The Langport Member assemblage is also, however, relatively simple and dominated by only benthic filter bivalves with restricted movement (Fig. 4.12, Appendix 4.12).

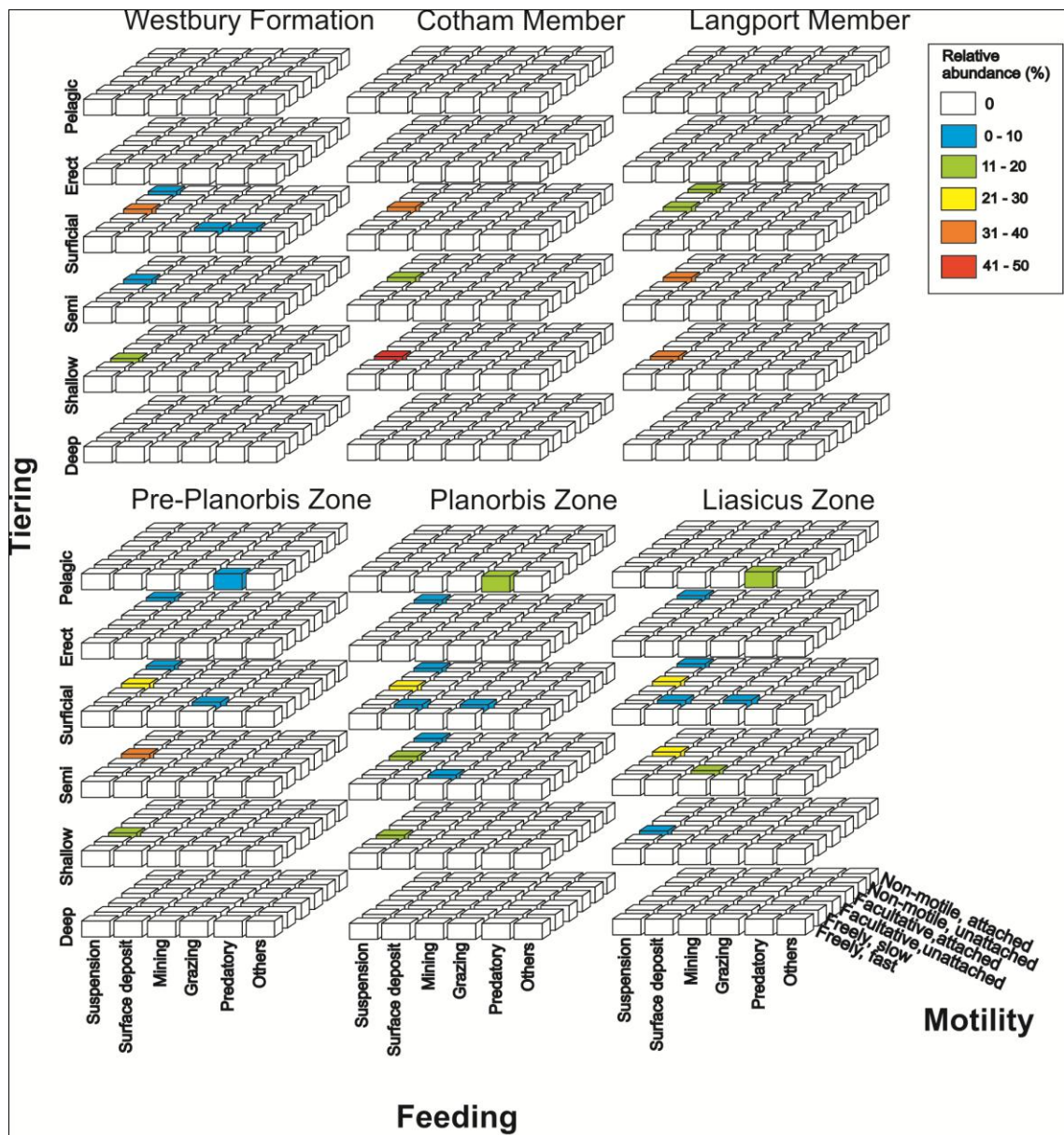


Figure 4.11 Theoretical ecospace occupations of the marine invertebrate fauna through the Tr/J interval in St Audrie's Bay.

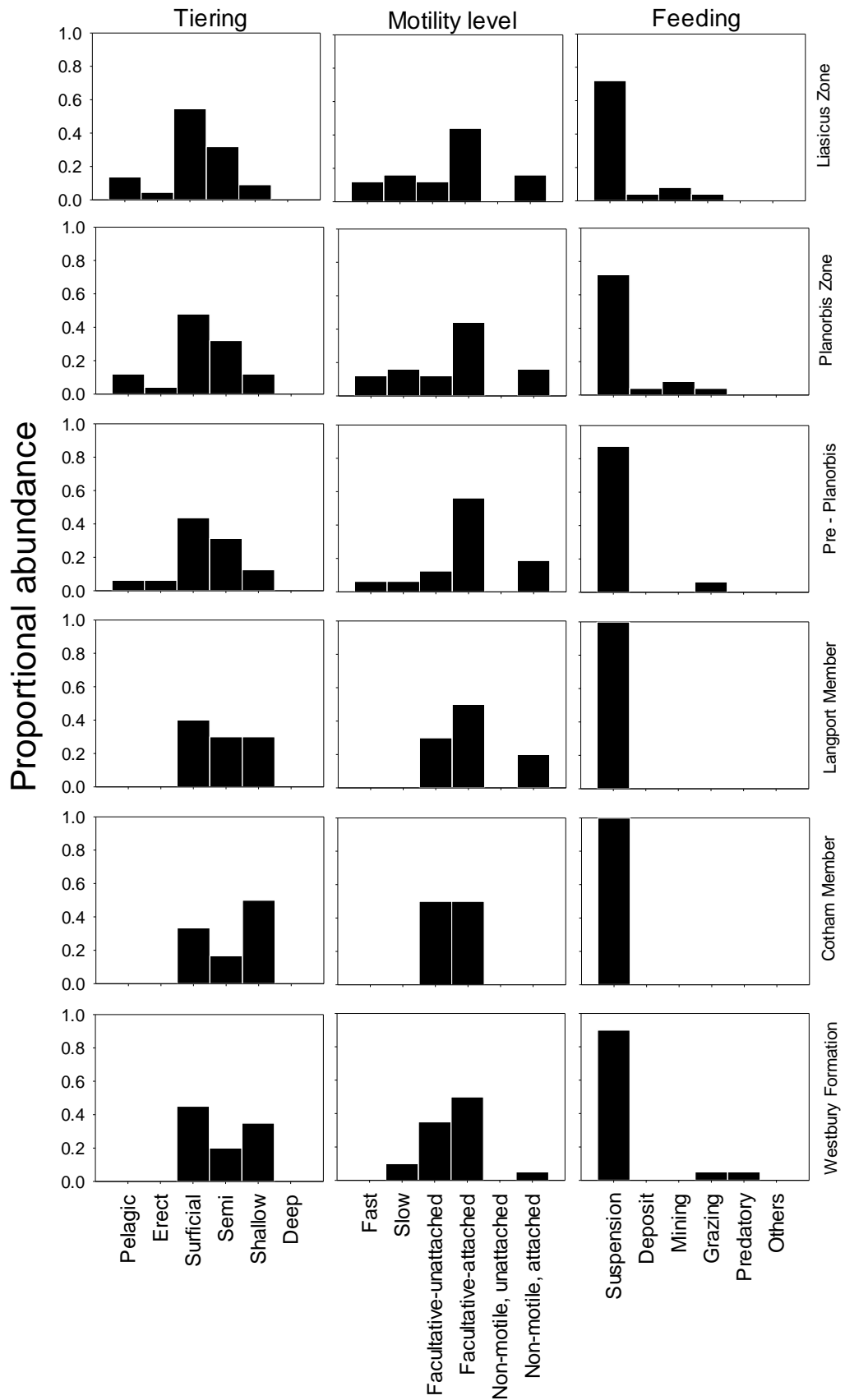


Figure 4.12 Mean proportional abundance of tiering, motility and feeding mechanisms based on number of species recorded from the Westbury Formation to the Liasicus Zone of the Blue Lias Formation.

The Pre-Planorbis Zone records a total of 16 species, occupying 7 modes of life. Pelagic predators colonised new areas of the ecospace, as represented by *P. erugatum*. Erect forms appear for the first time in the assemblage with *I. psilonoti* and surficial slow moving grazing forms reappear, although now occupied by *D. tomes* (Fig. 4.11, Appendices 4.10 and 4.11). The bivalves represent 37% of the surficial faunal, occupying two ecological categories: epifaunal non-moving suspension feeders represented by *P. duplicata* and *L. hisingeri* and epifaunal facultatively-motile, attached suspension feeders, represented by *C. valoniensis*, *P. giganteum*, *Mytilus* sp. and *O. inequivalvis*. The semi-infaunal, facultative attached and shallow infaunal, facultative unattached, suspension feeder categories continue to be used exclusively by bivalves. However, the semi-infaunal component increased by 2% (from below), now represented by 5 species, whilst the relative abundance of the shallow infaunal element decreases by 55% from the Langport Member (Fig. 4.11, Appendices 4.10 and 4.11). The Pre-Planorbis Zone assemblage records both a high richness and a high ecological complexity. The species present enhance the trophic spectrum and with them all the tier categories now being used (from pelagic to shallow infaunal), which increase the functionality of the ecosystem.

Ten species were recorded in the Planorbis Zone assemblage, with the pelagic fast moving predator modes of life increasing from the previous assemblage by 50% - three species of ammonites occupying this mode of life (Fig. 4.11 and 4.12, Appendices 4.11 and 4.12). The erect category is used by the crinoid *I. psilonoti*, although with an abundance decreasing by 4% from the Pre-Planorbis Zone. Surficial forms also decrease by 4%, despite being the group with most species (10). Four modes of life are represented by this category: surficial slow moving *P. undulata* (surface deposit); *D. tomes* (grazing); surficial, facultatively motile attached represented by 6 bivalve species

(Appendix 4.11) and surficial, non-moving stationary forms represented by *L. hisingeri* and *P. duplicata*. The semi-infaunal content increased by 2%, with the appearance of two new modes of life: slow-mining by *R. bronni* and *P. navis*, and the stationary suspension feeder, *Pinna* spp. The relative abundance of the shallow infaunal modes of life remained, nevertheless, constant when compared to earlier assemblages. The Planorbis Zone assemblage has a high complexity, redundancy and functional diversity. This indicates large trophic chains and a high motility which increases the potential for interactions between species and increases the number of species with the same ecological role, thereby conferring more ecological stability.

Twenty-two species and nine modes of life comprise the Liasicus Zone assemblages. Ecospace through this unit shows the same structure and species composition as that observed for the Planorbis Zone (Fig. 4.11 and 4.12, Appendices 4.10 and 4.11). Only the semi-infaunal categories, however, recorded large compositional changes. The semi-infaunal non-motile attached suspension feeder mode of life is no longer recorded in this assemblage.

4.6 Body size

Figure 4.13 shows mean body size of bivalves and the rate of change of body size through the study interval. Body size tends to increase slightly from the base of the section (9.79 ± 0.51 mm) to 14 m above the base into the Langport Member (17.11 ± 0.75 mm) (Sample: LM4, Appendix 4.2). From this level average size tends to decrease smoothly to reach an inflexion point at 40.9 m above the base, where 6.17 ± 0.71 mm was recorded (sample: LZ3). From 40.2 m to 61 m above the base, the body size increases to 16.17 ± 1.04 mm (Appendix 4.13).

Throughout the Westbury Formation, an average body size of 12.14 ± 1.35 mm (min.: 8.62; max.: 16.41) was recorded. Throughout this sequence, 26% of the measurements corresponded to genera as *Isocyprina* (8.09 ± 0.39 mm); 25% *P. alpina* (14.92 ± 0.82 mm); 14.17% *C. valoniensis*; 13.92% *Liostrea* sp. (11.44 ± 0.8 mm) and 9.11% *R. contorta* (7.65 ± 0.50 mm), whilst taxa, such as *Modiolus* sp. *Cassianella*, *Cardinia*, *Plagiostoma*, *P. rhaetica* and *P. elongatus*, contributed <3% to the measurements (Appendix 4.13).

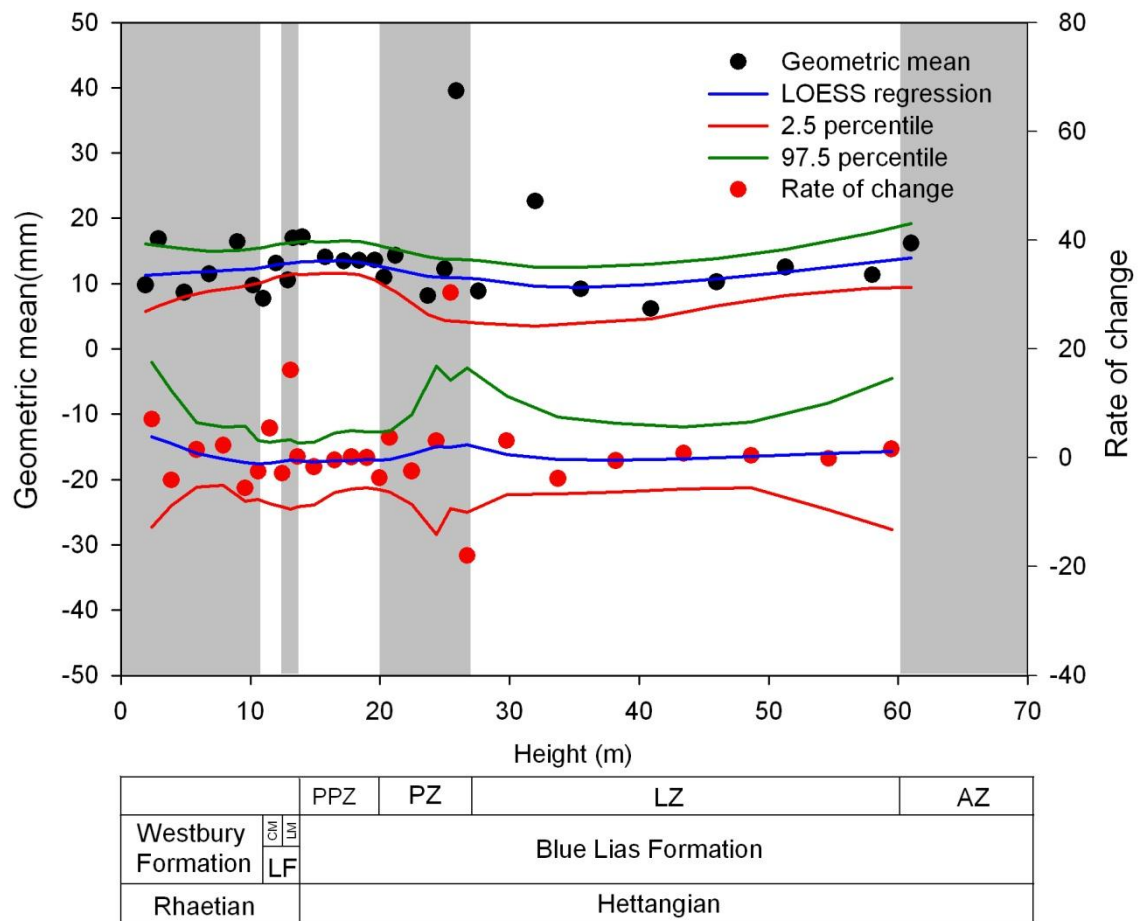


Figure 4.13 The average body size (●) and rate of change (●) of the bivalve assemblage sampled through the Triassic-Jurassic boundary at St Audrie’s Bay section. The red line is the LOESS regression through the data point estimated with an alpha 0.3. LF: Lilstock Formation, CM: Cotham Member, LM: Langport Member, PPZ: Pre-Planorbis Zone, PZ: Planorbis Zone, LZ: Liasicus Zone, AZ: Angulata zone.

Average body size throughout the Westbury Formation tends to increase although with fluctuation (Appendix 4.13). Three outlying values are observed throughout this unit; the first two are observed at 2.9 m with an average value of 16.85 mm and the third at 9 m with 16.41 mm (samples WF2 and WF5, Appendix 4.2). In both cases, three species were responsible for this size increase; *C. valoniensis* (17.34 ± 0.38 mm; min.: 4.97, max.: 40.81), *P. alpina* (14.92 ± 0.82 mm; min.: 4.24, max.: 50.20) and the species of *Plagiostoma* (21.16 ± 1.35 mm; min.: 11.7, max.: 30.72). The third outlier was recorded at 10.2 m (sample: WF6) above the base of the section where a significant decrease in body size was recorded. At this point the assemblage was mainly made up of taxa of small sizes, such as *Cassianella* sp. (3.38 ± 0.5 mm), *Modiolus* spp. (8.83 ± 0.91 mm), *R. contorta* (7.65 ± 0.5 mm) and *M. cloacinus* (8.34 ± 1.27 mm) (Appendix 6.13).

Throughout the Cotham and Langport Member, an average body size of 13.09 ± 1.67 mm was recorded. At the base of the Cotham Member (Sample: CM1), the body size decreases significantly, recording a mean value of 7.69 ± 0.37 mm. At this level the assemblage comprises *I. concentricum* (5.92 ± 0.8 mm), *P. rhaetica* (8.69 ± 1.72 mm), *C. regularis* (14.58 mm; $n = 1$) and *Modiolus* spp. (4.09 mm; $n = 1$). From 12 m into the Cotham Member (Sample: CM3) to the last sample of the Langport Member (Sample: LM3), the body size increases rapidly. At 12 m, 54% of the species is made up of *C. valoniensis* with a mean size of 19.27 ± 3.87 mm followed by *Modiolus* spp. (5.81 ± 0.35 mm) and one specimen of *R. contorta* (8.07 mm). In the Langport Member, new species with larger sizes are incorporated into the assemblage, for example, *Pholadomya* sp. (18.07 ± 1.82 mm) and *P. langportensis*. Also, some taxa experience an increase of body size throughout the sequence, compared to previous assemblages, such

as: *C. regularis* (14.96 ± 1.62 mm), *Liostrea* sp. (19.07 ± 0.76 mm) and *Mytilus* sp. (17.01 ± 1.18 mm).

Throughout the Pre-Planorbis beds, an average body size of 13.65 ± 0.11 mm was recorded, without any fluctuations. Some species during this interval increased in body size significantly; this phenomenon is well represented in taxa, such as *P. giganteum*, *Pholadomya* sp. *C. regularis*, *Liostrea* sp. *Oxytoma* sp. and *P. langportensis* (Appendix 6.13). On the other hand, more small size taxa are incorporated into the assemblage, such as *M. minimus* (7.31 ± 0.34 mm), *Mytilus* sp. (20.70 ± 0.38 mm), *Gervillella* sp. (18.87 ± 1.09 mm), *R. doris* (3.83 mm) and *Myoconcha* sp. (10.34 ± 1.09 mm). The assemblage variance is increased by both an increase in body size of the previous fauna and appearance of new taxa into the assemblage.

Throughout the Planorbis Zone, an average body size of 15.68 ± 4.86 mm was recorded for the bivalve assemblage. *Pholadomya* sp. *Chlamys* sp. *Modiolus* spp. and *P. giganteum* display a steady increase in body size (Appendix 4.13). Small-sized species, such as *P. navis* (2.45 mm) and *M. ventricosus* (4.99 mm), are incorporated into the assemblage. Some large-sizes species, such as *P. langportiensis*, *Liostrea* sp. and *M. minimus*, are highly represented in the assemblage (>50% of total specimens). They do not show a significant change in body size throughout the section, but introduce more variance into the assemblage, which therefore shows a relatively high body size value.

From the base of the Liasicus Zone to 61 m above the base of the section, the body size tends to decrease slightly (12.66 ± 2.03 mm). This trend was mainly driven by species, such as *Liostrea* sp. (14.82 ± 0.78 mm), *C. valoniensis* (12.56 ± 1.86 mm), *C. regularis* (14.64 ± 1.52 mm) and *Pholadomya* sp. (11.67 ± 3.99 mm), which represent >50% of the fauna. Additionally, more taxa are incorporated in the Liasicus Zone; however, they

are of relative small size: *P. eliptica*, *M. sodburiensis*, *Camponectes* sp. and *Myoconcha* sp. By contrast, few species tend to increase in body size throughout the sequence: *P. giganteum* (41.83 ± 4.88 mm), *Modiolus* spp. (8.28 ± 1.60 mm) and *M. ventricosus* (6.75 ± 0.90 mm) (Appendix 4.13). Finally, there is a not significant change in the rate of body size throughout the study section. A linear model fitted to the rate of change indicates an absence of any trend ($F_{1,27}$: 0.0005, $P > 0.05$) (Fig. 4.13).

Figure 4.14 shows the size-frequency distribution estimated from 969 bivalve specimens from the Tr/J St Audrie's Bay section. Throughout the St Audrie's Bay section the assemblages do not display significant changes in body size (Fig. 4.14). However, the variances tend to increase throughout the section (Fig. 4.14A, see class intervals), which is associated with the incorporation of new species in each stratigraphic unit.

The changes in the minimum and maximum body size of *Cardinia*, *Modiolus*, *Chlamys*, *Plagiostoma*, *Liostrea* and *Mytilus* throughout the Tr/J section in St Audrie's Bay are visualised using the Jablonski target plot (Fig. 4.15), which records the change in percentages between minimum and maximum size and is useful for determining whether the change is simply due to a change in variance (Jablonski, 1996). None of the genera seem to decrease in body size during the extinction event (WF-CM), except for *Chlamys*, which does decrease in body size from the Cotham Member to the Pre-Planorbis Zone and *Modiolus*, which tends to decrease in body size from the Planorbis Zone to Liasicus Zone (Fig. 4.15). In the remaining cases, the genera show three trends: (1) an increase in body size (to use the right upper corner); (2) an increase in variance (decrease of the minimum size, upper left corner) and (3) a decrease in variance (lower

right quadrant), which means a decrease of the maximum size without a change in minimum size (Table 4.2) (Appendix 4.14).

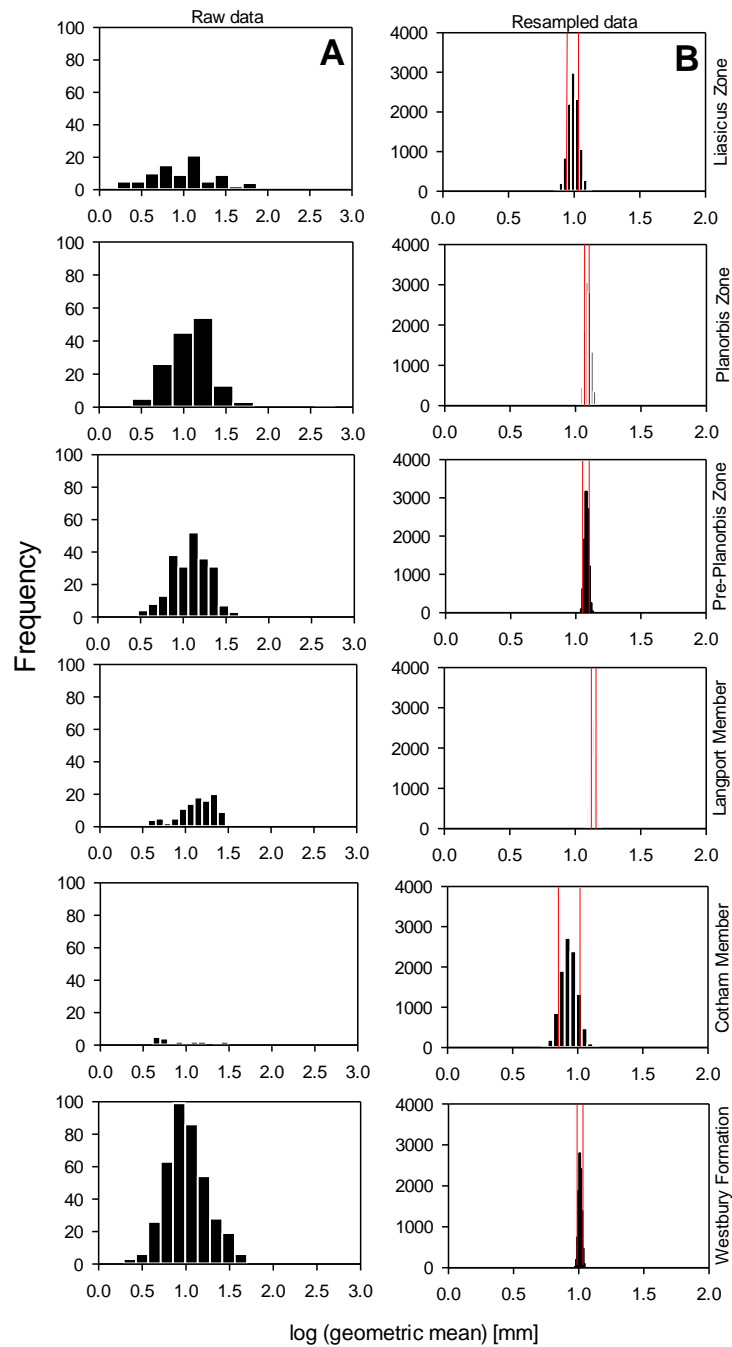


Figure 4.14 Frequency distribution of log geometric mean of bivalve size sampled through Triassic-Jurassic boundary at St Audrie's Bay section. (A) Shows the distribution frequency of raw data by each lithostratigraphy (B) Showed the distribution frequency of resampled data by bootstrapping procedure (10,000 iterations with replacement). The red lines indicate the percentiles of 2.5% and 97.5% around the mean.

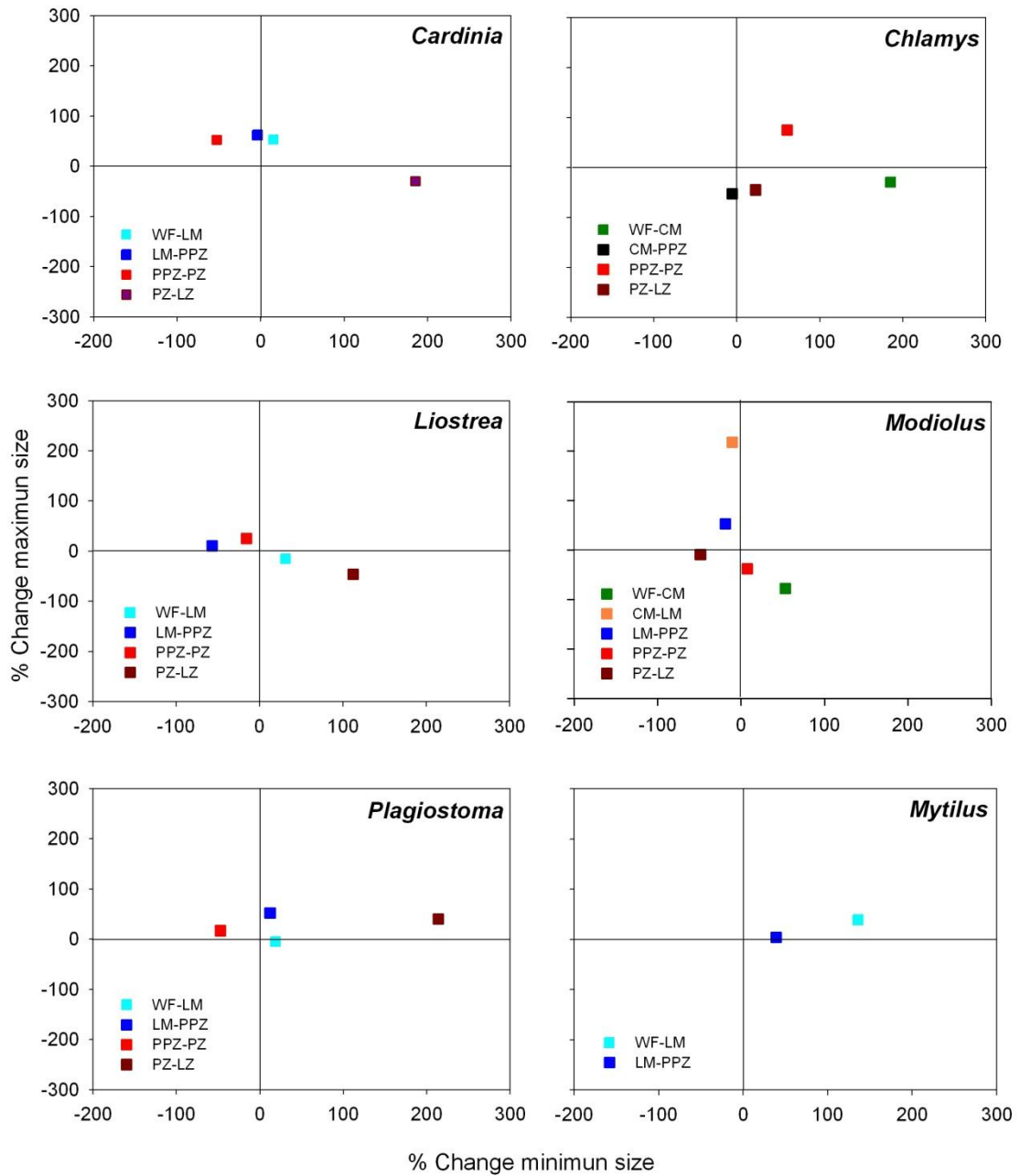


Figure 4.15 Change in size in four bivalve genera through the St Audrie's Bay section. Top left and bottom right indicate variance in size whilst the top right and lower left represent Cope's Rule and size decrease, respectively. (After Jablonski 1996). The legend indicates the pairwise combinations between stratigraphical units. WF: Westbury Formation, CM: Cotham Member, LM: Langport Member, PPZ: Pre-Planorbis Zone, PZ: Planorbis Zone, LZ: Liasicus Zone.

Table 5.2 Body size parameters of four bivalve's genera with high occurrences trough the Tr/J interval in St Audrie's Bay. LM: The Langport Member, PP: The Pre-Planorbis Zone, PZ: The Planorbis Zone, LZ: The Liasicus Zone, AZ: Angulata Zone. (*): no data point was recorded.

	WF	CM	LM	PPZ	PZ	LZ
<i>Cardinia</i>						
Mean	11.32	****	14.96	18.24	39.37	17.84
Std. error	1.79	****	1.67	1.15	2.82	1.61
<i>n</i>	4	****	9	27	25	20
Min. size	7.87	****	9.06	8.7	4.11	11.72
Max. size	15.98	****	24.49	39.81	60.9	43
<i>Chlamys</i>						
Mean	17.35	19.27	****	10.82	18.19	12.57
Std. error	1.05	3.88	****	1.49	2.82	1.87
<i>n</i>	55	6	****	6	5	2
Min. size	4.98	5.77	****	5.45	8.74	10.7
Max. size	40.48	31.16	****	14.85	26.04	14.43
<i>Liostrea</i>						
Mean	17.20	****	19.07	14.17	15.18	14.98
Std. error	1.58	****	0.78	0.53	1.01	0.76
<i>n</i>	16	****	30	77	51	17
Min. size	8.92	****	11.69	5.02	4.23	8.97
Max. size	31.38	****	26.58	29.54	37.15	20.2
<i>Modiolus</i>						
Mean	8.76	4.97	8.61	9.05	8.09	6.91
Std. error	0.64	0.35	0.82	0.58	0.61	0.70
<i>n</i>	44	5	26	59	33	32
Min. size	2.79	4.1	3.65	2.95	3.17	1.62
Max. size	26.36	5.82	18.48	28.29	17.56	15.96
<i>Plagiostoma</i>						
Mean	21.17	****	22.33	27.29	26.81	45.03
Std. error	2.20	****	3.17	5.52	3.73	5.72
<i>n</i>	8	****	4	5	13	10
Min. size	11.74	****	13.92	15.6	8.19	25.72
Max. size	30.73	****	29.32	44.69	52.46	73.82
<i>Mytilus</i>						
Mean	9.29	****	17.11	20.71	****	****
Std. error	1.00	****	1.18	0.38	****	****
<i>n</i>	9.00	****	5.00	3.00	****	****
Min. size	6.18	****	14.57	20.20	****	****
Max. size	14.80	****	20.54	21.45	****	****

The frequency distribution of the most common genera throughout the study interval was plotted to observe the trajectory of the body size (Fig. 4.16). In these histograms, *Modiolus* shows a complete trajectory of body size throughout the entire study section in St Audrie's Bay. The body size of this genus fluctuates slightly, but there is no significant difference throughout the Tr/J intervals (ANOVA one-way: $F_{(5,193)} = 1.95$; $P < 0.05$). The same trend is observed in *Cardinia* ($F_{(4,80)} = 0.52$; $p < 0.05$) and *Chlamys* ($F_{(4,69)} = 1.37$; $p < 0.05$). Conversely, *Liostrea* ($F_{(4,186)} = 4.82$; $p < 0.05$) shows a significant increase in body size from the Westbury Formation to the Langport Member; later the mean body size tends to decrease throughout the Blue Lias Formation. The body size of *Plagiostoma* remains constant from the Westbury Formation to the Planorbis Zone, however, the body size increases significantly throughout the Liasicus Zone ($F_{(4,39)} = 4.70$; $p < 0.05$), whilst *Mytilus* shows a steady increase in body size from the Westbury Formation to the Pre-Planorbis Zone ($F_{(2,16)} = 26.41$; $P = 0.001$) (Table 4.2).

Finally, the mean body size of all bivalve assemblages through the study section was significantly higher than the null model values, which presumes a random distribution of body sizes throughout the study interval. This seems to indicate that the bivalves as a whole show a directional trend towards larger body size throughout the section (t-value = 7.25, d.f. = 29; $p < 0.001$) (Fig. 4.17, Appendix 4.15).

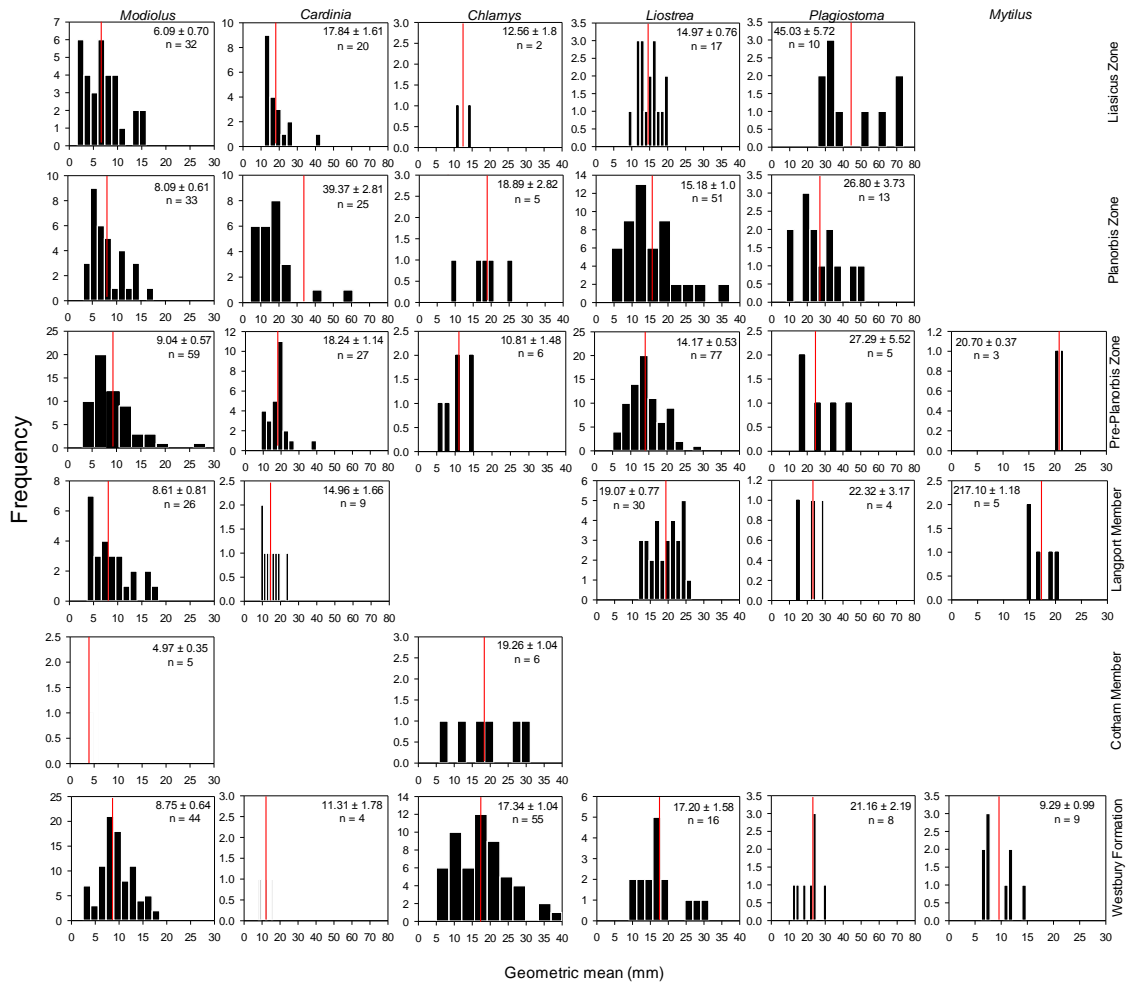


Figure 4.16 Frequency distribution of geometric mean of the four most common bivalve genera found through the study section at St Audrie's Bay. The red line indicates the average values. Average values, standard error (\pm) and sample size (n) are indicates upper corner of each histogram.

4.7 Trace Fossils

The number of ichnotaxa increases from the Langport Member to the Liasicus Zone (Fig. 5.18). Throughout the study section, five ichnogenera were identified: *Chondrites* with a total occurrence of 80%; *Palaeophycus* (60%); *Thalassionides* (20%); *Planolites* (2%) and *Skolithos* (1%).

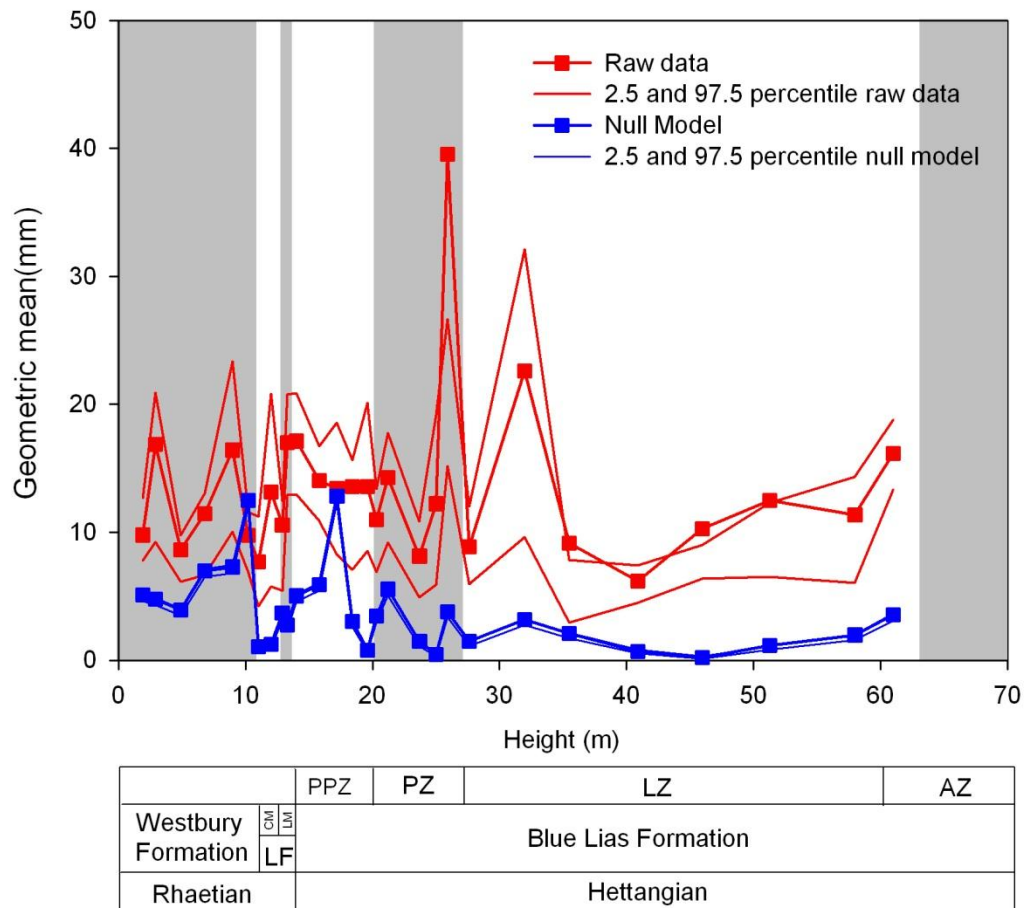


Figure 4.17 The average size of bivalves sampled through the study interval at St Audrie's Bay (Red Line: raw data \pm percentile 2.5 % and 97.5 %). Null model (blue line \pm percentile 2.5 % and 97.5 %) was calculated by row-permutation (number of iterations = 10000) of the geometric mean of each individual by specie through 36 samples (see Appendix 4.11). LF: Lillstock Formation, CM: Cotham Member, LM: Langport Member, PPZ: Pre-Planorbis Zone, PZ: Planorbis Zone, LZ: Liasicus Zone, AZ: Angulata zone.

During the Langport Member, four ichnogenera were identified; *Chondrites* and *Palaeophycus* at 17.40 m above the base of the section (Sample: PPZ2), followed by *Thalassinoides* at 18.40 m (Sample: PPZ3) and *Skolithos* at 19.6 m (sample: PPZ4). Throughout the Pre-Planorbis and Planorbis Zones three ichnogenera are presented; *Chondrites*, which is present throughout all the sequence, except at 19.6 m above the section; *Palaeophycus*, except at 23.6 m (samples: PZ2) and *Thalassinoides*, which is recorded from 23.6 m (sample: PZ3) to 25 m above the base of the section (Sample: PZ4). From the base of the Liasicus Zone to 58 m above the base of the section, four ichnogenera are recorded; *Chondrites* range throughout all the sequence; *Palaeophycus*,

with occurrences at 35.5 m and 51.5 m (samples LZ2 and LZ5). Finally, *Thalassinoides* and *Planolites* are recorded at 46 m and 58 m above the base of the section respectively (Sample LZ4 and LZ6) (Fig. 4.1).

Figure 4.18 shows the trajectory of three ichnological parameters through the study section in St Audrie's Bay. The mean cover percentage of each ichnogenera (see Chapter 2 methodology) increases rapidly from the Langport Member to the Planorbis Zone reaching the maximum value at 25.9 m (sample: PZ5). From this level, the cover decreases significantly to reach 50% in the top of the Liasicus Zone (Fig. 4.17, Appendix 4.2). The trajectory of the burrow diameter throughout the Tr/J section shows three stages. The first stage is a significant and rapid increase of the burrow diameter, which reaches its maximum size of 10.49 mm at 23.7 m above the base of the section (sample: PZ3). The second stage, spanning from 23.7 to 35.5 m above the section, comprises a decrease in burrow diameter, and finally, the third stage constitutes an increase in burrow diameter from 5.51 mm at 40.9 m to 11.21 mm at 58 m (samples: LZ3 to LZ6) (Fig. 4.17, Appendix 4.2). The ichnofabric index remains relatively constant throughout the Westbury Formation and drops throughout the Cotham Member, however, during the Langport Member, the index increases significantly to reach its maximum value during the Planorbis Zone. Later the Ichnofabric Index drops slightly to the top of the Liasicus Zone (Fig. 4.17, Appendix 4.2).

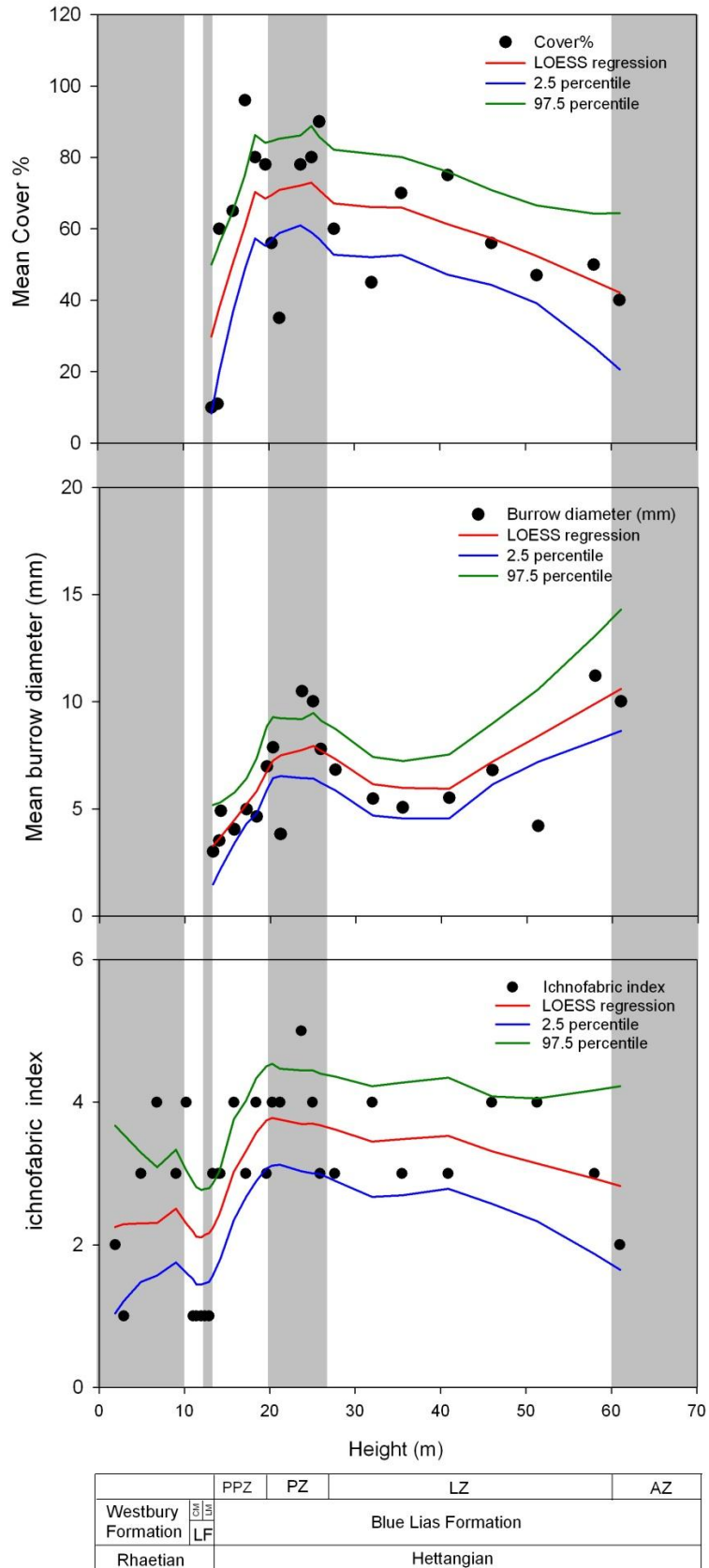


Figure 4.18 Response of bioturbation estimates through three methodologies along the Tr/J boundary at St Audrie's Bay section. LF: Lilstock Formation, CM: Cotham Member, LM: Langport Member, PPZ: Pre-Planorbis Zone, PZ: Planorbis Zone, LZ: Liasicus Zone, AZ: Angulata zone.

4.8 Summary

The St Audrie's Bay shows a complete record (preservation) of the marine fauna through the Tr/ J boundary. In this section, the samples from mudstone and limestone, records a significant loss of the species number through the Cotham Member (>90%). The richness estimated from limestone samples reaches a maximum peak during the Planorbis Zone and later the richness decreases slightly, whilst the taxon richness obtained from mudstone samples, like limestone samples reach the maximum species richness in the Planorbis Zone, the richness drops slightly and tend to increase top of the section.

Kurtosis (dominance values) tends to decrease from the Westbury Formation to the Liasicus Zone. The dominance index indicates that the Cotham and the Langport members are the assemblages with dominant species, compared to other stratigraphical units. In contrary, the assemblages associate mudstone samples shows more evenness. The rank abundance curves, mainly fitted lognormal distributions, however during the extinction event (the Cotham and Langport members) the distribution of the rank abundance in these assemblages tend to fit to the Geometric and Broken Stick models.

In term of composition, largest change occurs during the Cotham and Langport members. Whilst during the Blue Lias Formation and the Westbury Formation the assemblage remains in relative stasis.

Ecospace tends to expand from the Westbury Formation to the Liasicus Zone occupying 14 modes of life at the top of the section. However, the ecospace decreases to 3 modes of life during the Cotham Member. During this sequence the proportional abundance of semi infaunal modes of life decreases >50% compare with other stratigraphic units.

The body size of the bivalve assemblage seems increases through the study section. The richness of ichnogenerateda, abundance and burrow diameter tend to increase through the Blue Lias Formation, however. These variables reach a maximum peak during the Planorbis Zone. After this level, the ichno-parameters tend to decreases gradually, except by mean burrow diameter, which increase staidly to top of the section.

Chapter 5 Pinhay Bay section

5.1 Geological setting

The Tr/J section studied at Pinhay Bay ranges from the end of the Rhaetian to the Early Jurassic (Hettangian) (see Chapter 2 for locality details). The Rhaetian Stage in Pinhay is represented by the Langport Member of the Lilstock Formation formerly known as the “White Lias” (Swift 1999; Wignall 2001).

5.1.1 The Langport Member

This unit is made up mainly by micritic limestone with a series of complex sedimentary features, which reaches 6.90 m thickness in the Pinhay Bay section (Fig. 5.1). The first metre near to the base is made up of slumped limestone separated by porcellanous hardground surfaces (Beds 1a to 1b). From one to three m above the base of the section (Beds 2 to 3), the sequence consists of modular limestone with marl partings, where a channel system is filled in with slumps and dewatering structures (Fig. 5.1). From 3 to 4.20 m above the base of the section (Beds 4 - 8) the sequence is made up of laminated limestone, parallel bedded remobilised limestone with clasts that include shells and bored pebbles.

From 4.8 to 5.80 m above the base, the section consists of a slumped limestone bed (Bed 9) (Fig. 5.1), with abundant clasts up to boulder size; with a high clast concentration at the base of the bed. From 6 m above the base to the top of the Langport Member (Beds 10 to 11), the sequence comprises finely, wavy laminated limestone with marl partings. The topmost bed (Bed 12) consists of an intra-formational conglomerate, with *Diplocraterion* burrows.

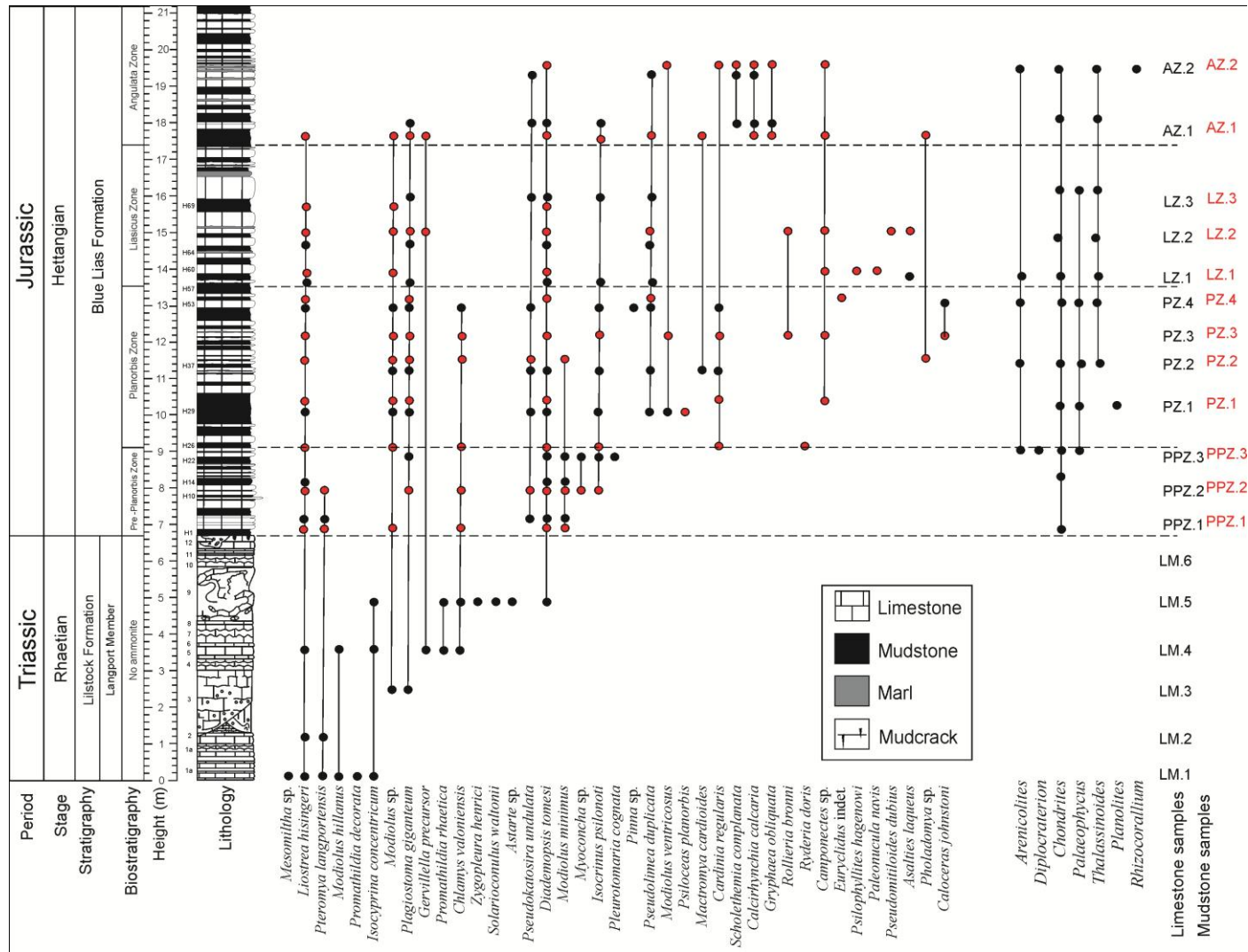


Figure 5.1 Lithostratigraphic log of the Lilstock Formation and basal Blue Lias Formation exposed at Pinhay Bay. Occurrences (limestone ● and mudstone ●) and ranges (black lines) of taxa recorded from 30 samples taken from the Pinhay Bay section.

The Langport Member has been interpreted as representing an abnormal system with varying salinity, deposited in a shallow, warm, lagoonal marine environment (Hallam 1960 ; Wignall 2001; Hesselbo *et al.* 2004). In the same time, slumped horizons observed at 6 m above the sections is attributed to earthquake activity (Gallois 2007). The fauna in this unit includes bivalves, gastropods, corals, echinoderms, rare conodonts and ostracods (Swift 1999). Ammonites are not present. However, as the system apparently records variable salinities, the presence of fossils of stenohaline organisms could suggest that their occurrence could be the result of transport or re-worked, rather than salinity control (Hesselbo *et al.* 2004).

4.1.2 The Blue Lias Formation

The base of the Blue Lias Formation lies close to the base of the Jurassic System in Britain (Page 2010, p.39; see Introduction: Stratigraphical framework). The Blue Lias Formation in Pinhay Bay represents a relatively condensed sequence (compared to St Audrie's Bay), around 18 m thick from the base of Lias Group to the top of the Angulata Zone. The detailed stratigraphy of the Blue Lias Formation of the Lyme Regis area was first described by Lang (1924) who allocated the lower part of the sequence to his beds H1-H91 (The Pre-Planorbis Zone to lower Angulata Zone), with Beds 1 to 18 representing the middle and upper Angulata Zone above. Lang's original zonation of the sequence has been revised most recently by Page (2010), whose scheme is used here.

The Blue Lias Formation consists by sedimentary rhythms of homogeneous and inhomogeneous limestone beds and marls to shales (Moghadam and Paul 2000; Wignall and Bond 2008). Limestone beds are mostly impure micrite mud- to wackestones and are 10 to 20 cm thick with extremes up to 50 cm. The limestone facies consists of fine-grained, predominantly clay grade sediments containing varying proportions of siliciclastic clay minerals and micrite (Paul *et al.* 2008). Limestones are interspersed by

siliciclastic marl and shale intervals, which are a few centimetres up to several meters in thickness. These beds mainly consist of pale-grey marls, dark-grey marls and organic-rich laminated black-shales (Paul *et al.* 2008). Siliciclastic sediments consist of (land-derived) clay minerals and marine and terrestrial organic matter (Weedon 1986).

Sedimentary rhythms in the Blue Lias Formation consist of a laminated black-shale that grades into a dark-grey marl, and a pale-grey marl commonly with concretionary to tabular (cemented) micritic limestone, which on top turns back into dark-grey marls and shales (Paul *et al.* 2008). These rhythms appear not always symmetrical because (organic-rich) shales or marls/limestones did not always develop or carbonate-rich sediments were diagenetically altered (Ruhl *et al.* 2010).

The Blue Lias Formation represents an offshore sedimentary setting, where the depositional environment was susceptible to anoxia, as well as the formation of laminated, organic-rich shales (Hallam 1995; Hallam 1997; Wignall 2001; Barras and Twitchett 2007). Carbonate-rich lithologies generally reflect well-oxygenated conditions whereas organic-rich lithologies generally reflect oxygen depletion (Hesselbo *et al.* 2004; Mander *et al.* 2008). The fauna of the lower Blue Lias is marine, although the first 2.5 m lacks ammonites. From the base of the sequence, environmental controls lead to successive faunal changes, although diversity is often high with records of fish remains, marine reptiles and marine invertebrates, mainly ammonites and bivalves. In addition, towards the upper part of this sequence, trace fossils begin to be more common, increasing in abundance as well as diversity although usually associated with episodic oxygen supply events (Moghadam and Paul 2000; Martin 2004; Barras and Twitchett 2007).

The first part of The Blue Lias Formation, approximately 2.7 m, corresponds to The Pre-Planorbis Zone and includes at least the higher part of Bed H1 to Bed H24 – based

on available carbon isotope excursion data (Clemence *et al.* 2010). No ammonites have been recorded in this interval in the Lyme Regis area, although *Psiloceras erugatum* (Phillips), which has been recorded in the upper part of the Zone, has been recorded in West Somerset at bed number H24 (Page 2010).

The base of the succeeding Planorbis Zone is placed at the first occurrence of *Neophyllites* in Bed H25 and the Zone ranges up to Bed H56, a total of 3.67m. The Liasicus Zone succeeds the Planorbis Zone, and is around 3.7 m thick, ranging from Bed H57 to Bed H83. Finally, the Angulata Zone spans beds H84 to 18 and is 4 m thick. (Page 2010) (Fig. 5.1).

5.2 Richness

865 individuals corresponding to 39 species, grouped in 26 families, 20 orders, 7 classes and 4 phyla were recorded from 30 samples taken from Tr/J section at Pinhay Bay. The Bivalvia represent 56% of all species recorded; followed by Gastropoda and Ammonoidea each with 14%. Groups such as crinoids, echinoids, brachiopods and chordates were represented by a single taxon (Appendix 5.1).

5.2.1 Limestone samples

The number of taxa increases significantly through the Tr/J section at Pinhay Bay. Thirty-one species were recorded from limestone samples. Fifteen of these were recorded from the Langport Member, representing 27% of the total number of species recorded. Through the Langport Member, species richness was variable, fluctuating from zero to seven taxa (with a mean of four) (Fig. 5.2A, Appendix 5.3).

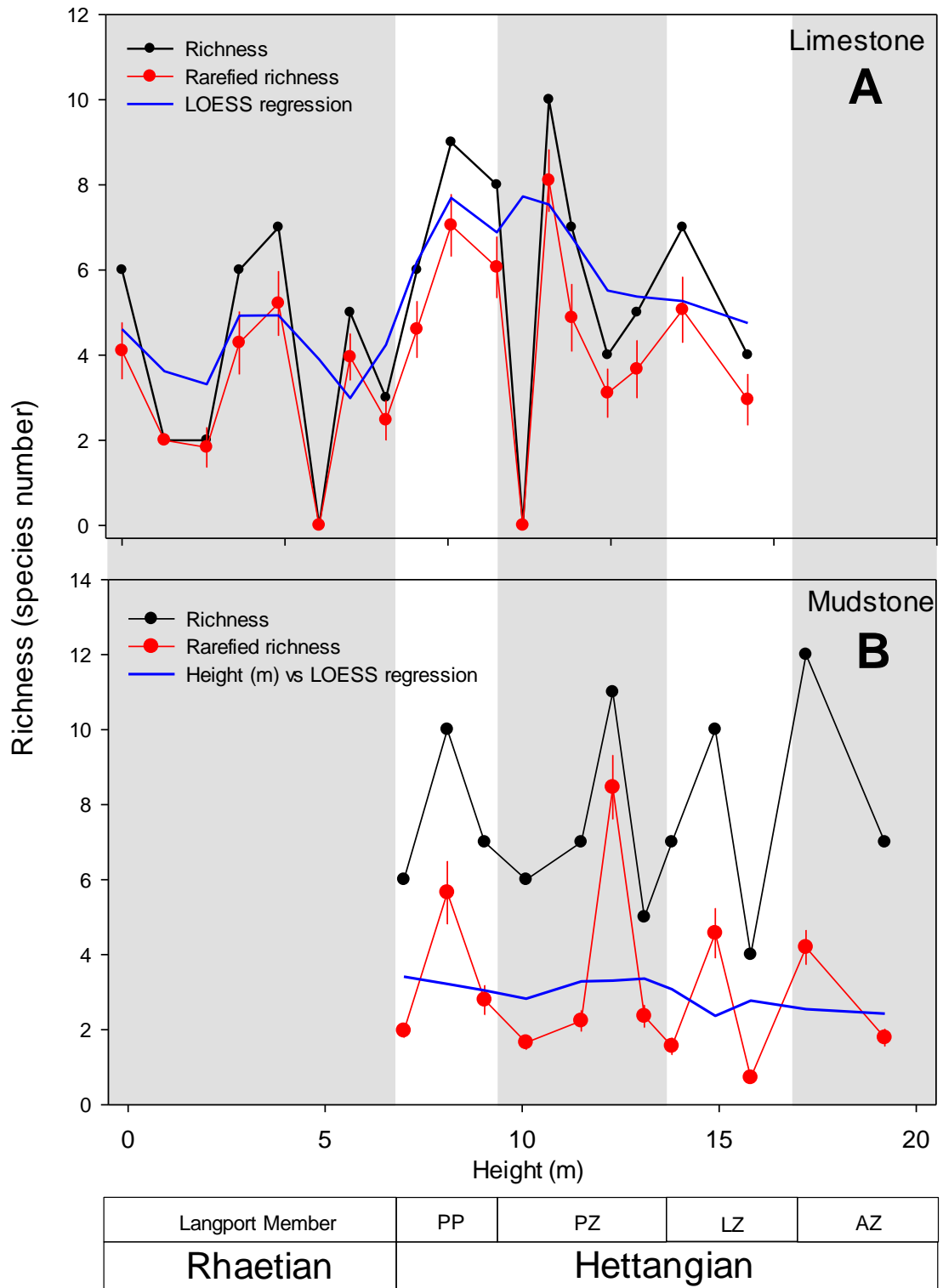


Figure 5.2 Raw (black line) and mean species richness (red line \pm 2 S.D.) recorded for each sample collected. The mean species richness represents the rarefied within-sample marine invertebrate richness estimated by 10,000 iterations. The blue line is the LOESS regression through the data point ($\alpha=0.3$). PPZ: Pre-Planorbis Zone, PZ: Planorbis Zone, LZ: Liasicus Zone, AZ: Angulata zone.

Through the Pre-Planorbis to Planorbis Zone, the average species richness tends to increase rapidly until 10.6 m above the base. This segment is characterised by an initial exponential increase in the number of species present, followed by a decrease in the rate of appearance (Fig. 5.2A, Appendix 5.2).

In contrast, from the base of the Liasicus Zone to the Angulata Zone, the average species richness tended to decrease slowly. Through this interval, the number of species recorded in samples is highly variable. In both the Liasicus Zone and the Angulata Zone eight species are recorded; however, the average species number per sample decreases through the Angulata Zone (Fig. 5.2A, Appendix 5.2).

5.2.2 Mudstone samples

Thirty species were identified from mudstone samples, but the average richness does not record a significant change through the section. However, there was a high variation in the observed richness between samples (Fig. 5.2B). Thirteen species were identified from the Pre-Planorbis Zone; the richness trajectory through this interval showing a maximum peak of 10 species at 8.1 m above the base. In the Planorbis Zone, sixteen species were identified and the highest peak recorded was at 12.3 m above the base. Fourteen species were recorded from the Liasicus Zone, with the highest peak of 10 species at 14.9 m. Finally, the Angulata Zone with 15 species, records the highest peak of 12 species at 17.20 m - above the base of the Blue Lias (Fig. 5.2B, Appendix 5.2 and 5.3).

Sample rarefaction was performed by increasing the sampling size in limestone samples, indicated that Langport Member record the highest richness following by the Planorbis, the Liasicus, and the Angulata Zone, while Pre-Planorbis recorded the lowest richness (Fig. 5.3A). Richness estimate from mudstone samples show a different

pattern. The species richness is higher in the Planorbis Zone, following by the Angulata, the Liasicus and the Pre-Planorbis Zone (Fig. 5.3B).

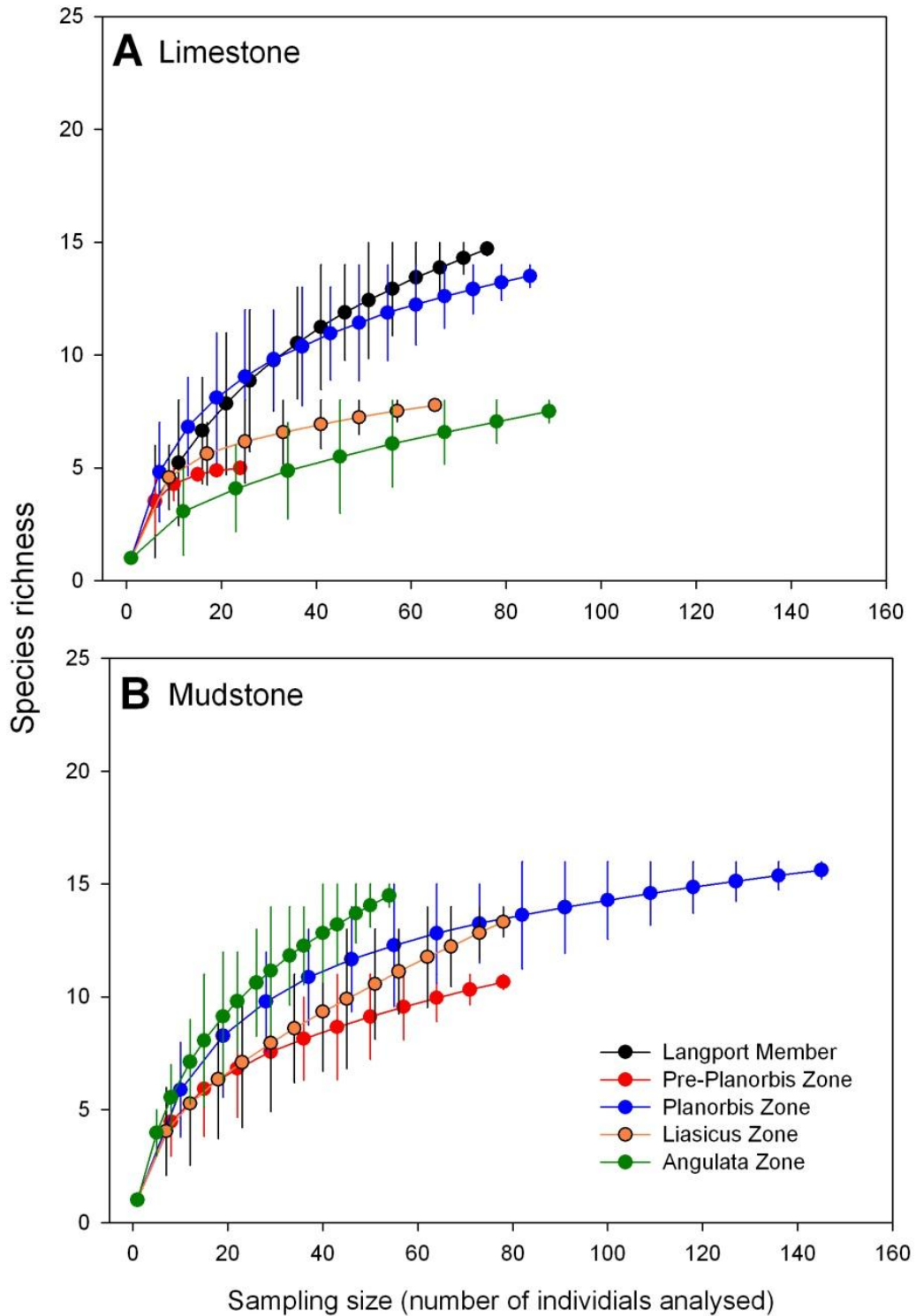


Figure 5.3 Average values (\pm 95% confidence intervals) of species richness estimated as sampling size increases through the Tr/J section in Pinhay Bay. Significant differences were assumed if 95% confidence intervals did not overlap.

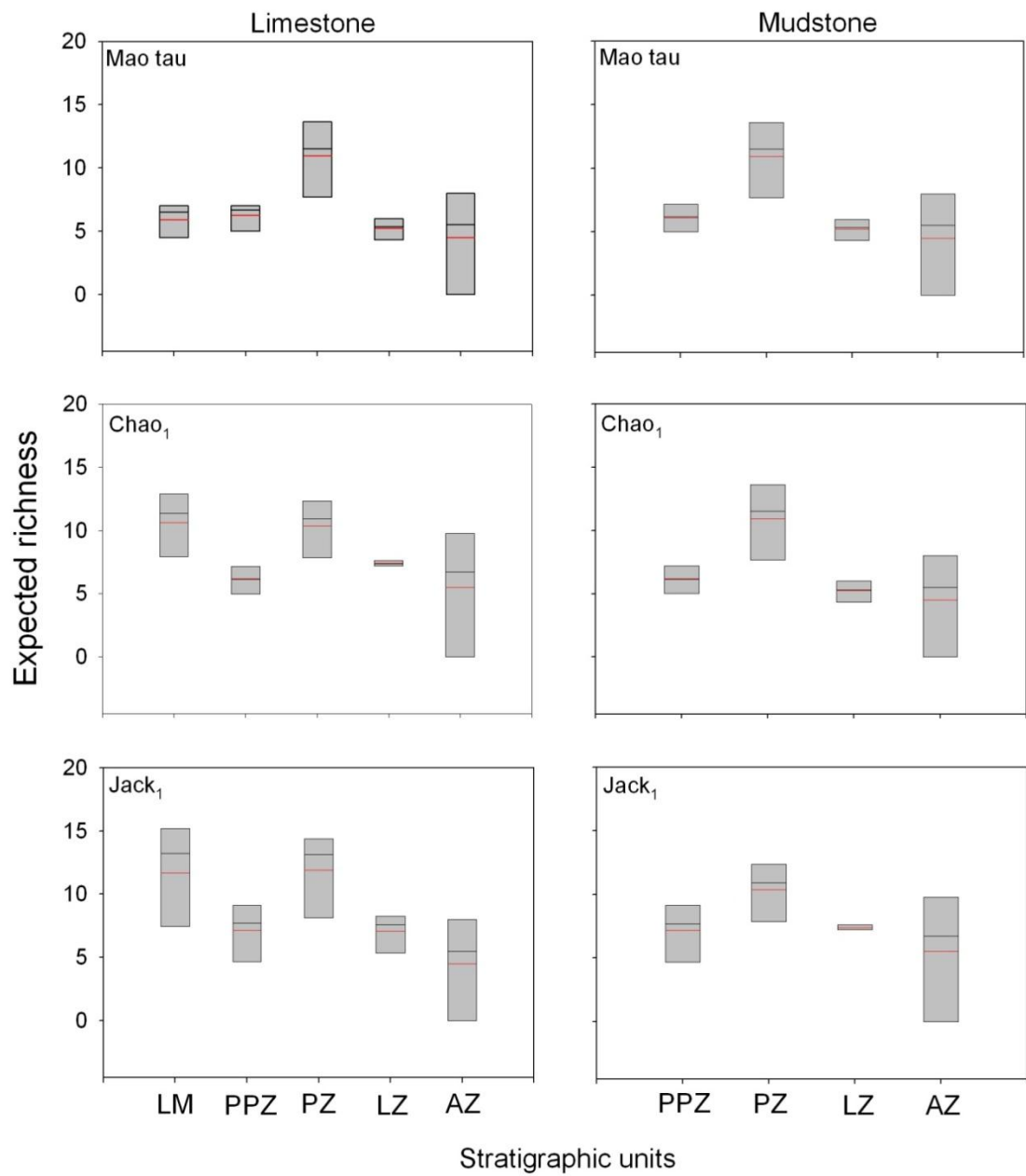


Figure 5.4 Boxplot of the rarefied within-sample marine fauna (Mao Tau, Chao₁ and Jack₁) during the study interval in Pinhay Bay section. Each box represents the 95% confidence interval. The median is shown by an inner black line and the mean by a red line. LM: Langport Member, PPZ: Pre-Planorbis Zone, PZ: Planorbis Zone, LZ: Liasicus Zone, AZ: Angulata Zone.

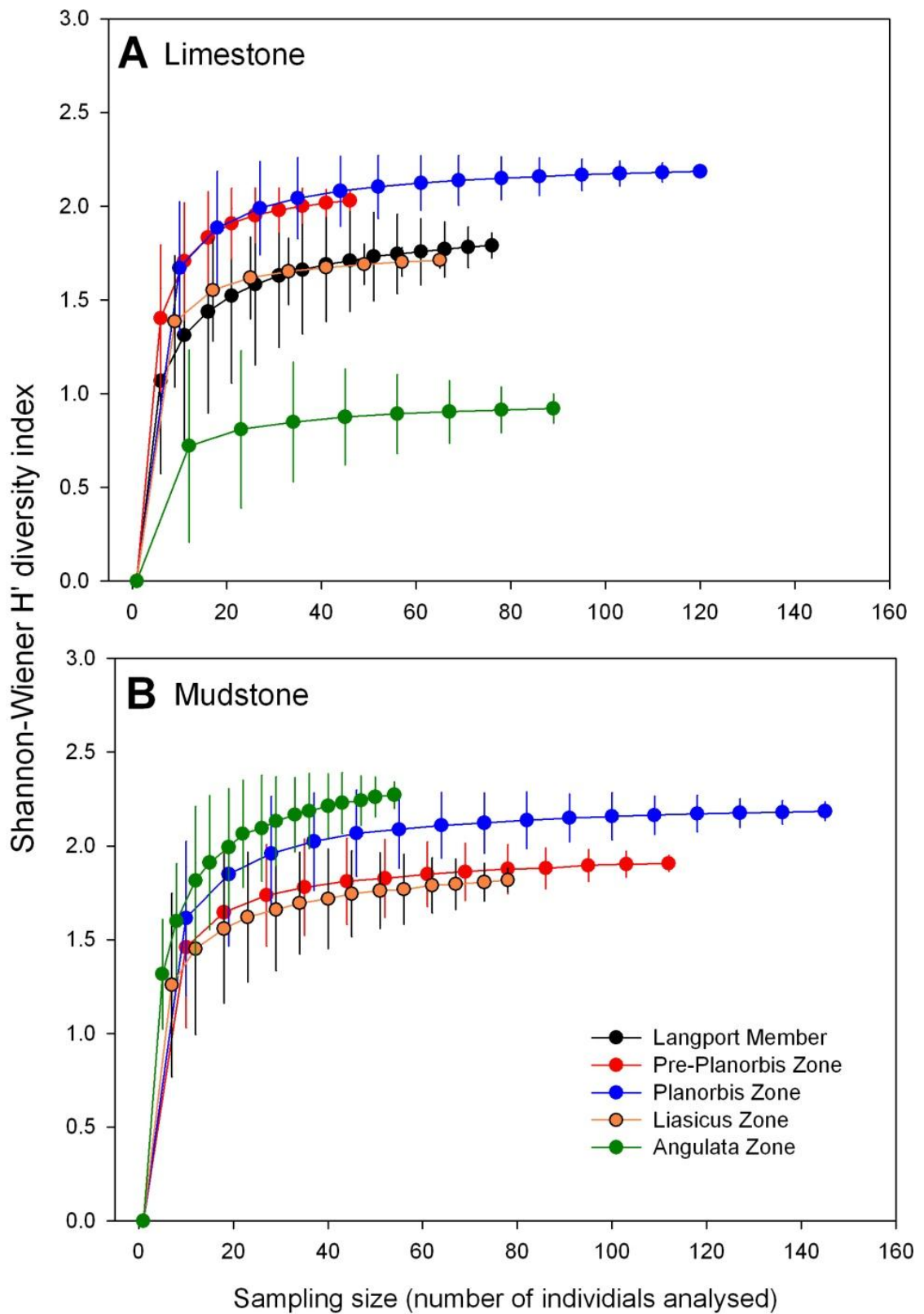


Figure 5.5 Average values ($\pm 95\%$ confidence intervals) of Shannon-Wiener diversity estimated as sampling size increased during the study interval. Significant differences were assumed if 95% confidence intervals did not overlap.

Sample rarefaction estimates by Mao Tau, Chao₁, and Jackknife₁ metrics shows that the species richness decreases significantly from the Langport Member to the Pre-Planorbis Zone and reaches a maximum in the Planorbis Zone (Fig. 5.4). Afterwards the richness decreases toward the Angulate Zone (Fig. 5.4). Estimation of the richness based on samples from mudstone, indicated that the species number increases from the Langport Member to the Planorbis Zone, however afterward, the diversity decreases toward the Angulata Zone (Fig. 5.4).

In contrast, estimates of the Shannon-Wiener index [H'] performed by increasing the sampling size in limestone, show three significantly different groupings (Fig. 5.5A).

The Planorbis and Pre-Planorbis zones recorded the highest richness values. In the second place, the Langport Member and the Liasicus Zone. Finally, the Angulata Zone recorded the lowest diversity values. In mudstone samples, the pattern is different (Fig. 5.5B). The Pre-Planorbis and Liasicus zones present the lowest H' index values and did not record significant differences between them. On the other hand, the Angulata Zone recorded the highest diversity followed by the Planorbis Zone.

5.3 Abundance

5.3.1 Limestone samples

Kurtosis values estimated from limestone samples, decrease from within the Langport Member (mean = 25.6 ± 1.27) to 10.1 m above the base of the Blue Lias Formation, within the Planorbis Zone (mean = 7.38 ± 3.64) and remain low until 13 m above the base. Later, the dominance (kurtosis) increases rapidly up to the Angulata Zone (mean = 30 ± 01) (Fig. 5.6A; Appendix 5.2).

Fifteen species are recorded in limestone samples from the Langport Member, the most dominant being *I. concentricum* (>50%). Three species comprised between 10- 5% of the assemblage (*P. rhaetica*, *S. waltonii* and *M. hillanus*) and eleven species record

densities at < 5% (Fig. 5.7A; Appendix 5.3). Examination of the shape of the rank abundance model using an Akaike weighting, shows that a Zipf–Mandelbrot provides the best fit for the invertebrate community of the Langport Member (Table 5.1). Zipf, Zipf-Mandelbrot and Lognormal model, are associated with assemblages with high richness and low dominance, generally relating to undisturbed systems or “*normal condition*”. Whilst the geometric model is related to systems with high dominance, generally associated with ecosystems that are highly disrupted. The broken stick model, supposes an even distribution of the species in the communities and is also referred to as a “null model” (See Chapter 2 for details).

Nine species are recorded in the Pre-Planorbis Zone, their relative abundance, however, never exceeding 20%. *L. hisingeri* and *P. giganteum* are the dominant species in assemblages at this level, both with relative abundance of around 18%. Three species have relative abundances of between 10 and 18% (*I. psilonoti*, *D. tomesi* and *P. langportiensis*) and four additional species are present at between 10 and 2% (Fig. 5.7A; Appendix 5.3). As for the Langport Member, the Zipf–Mandelbrot model was the best fit for this invertebrate assemblage (Table 5.1).

Fourteen species are recorded in the Planorbis Zone, *I. psilonoti* being the most abundant at ~25%; four species have abundances between 15-10%, five species between <10 - 1% and four species < 1% (Fig. 5.7; Appendix 5.3). Like the previous sequence, the Zipf–Mandelbrot model, is the best fit to the Planorbis assemblage (Table 5.1).

The Zipf–Mandelbrot model provides the best fit for the invertebrate community of the Liasicus Zone. Seventy-nine specimens are grouped into eight species. *P. undulate* has the highest abundance (30.14%), followed by *D. tomesi* (21.92%), *I. psilonoti* (17.81%) and *P. giganteum* (16.44%). The remaining species recorded have abundance between 8.22% and 1.37% (Fig. 5.7; Table 5.1; Appendix 5.3).

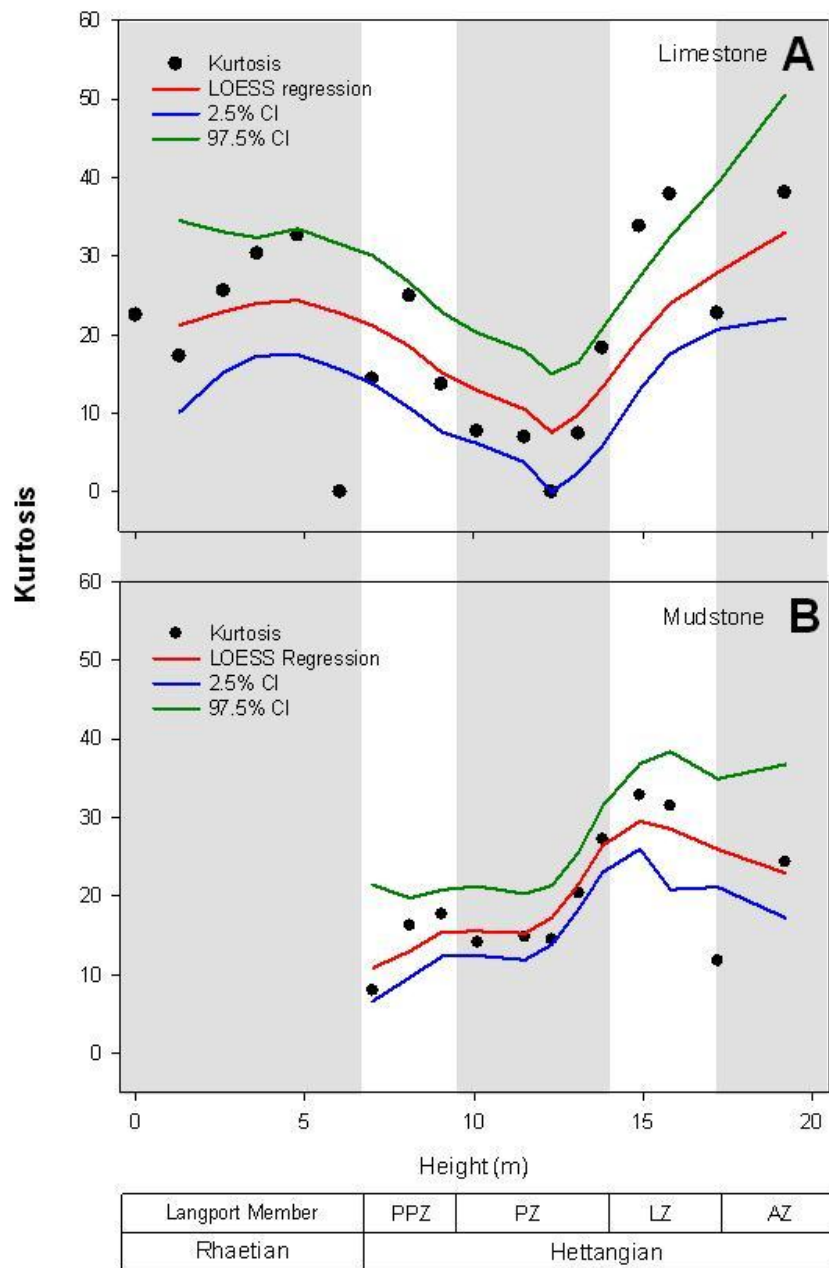


Figure 5.6 Dominance (Kurtosis \pm 95% confidence intervals) of marine fossils assemblages through Tr/J section in Pinhay Bay. The red line is the LOESS regression through the data point estimated with an alpha 0.3. PPZ: Pre-Planorbis Zone, PZ: Planorbis Zone, LZ: Liasicus Zone, AZ: Angulata Zone.

Despite the Angulata Zone having a low species richness (8 species), the relative abundance per species was relatively uniform. This species abundance distribution fits a Broken Stick model (Fig. 5.7; Table 5.1; Appendix 5.3). *Calcirhynchia calcaria* are

very abundant at >50%, follow by *P. undulate*, at ~16%. The remaining species abundance sharply drops to <5%, which is characteristic of the Broken Stick model.

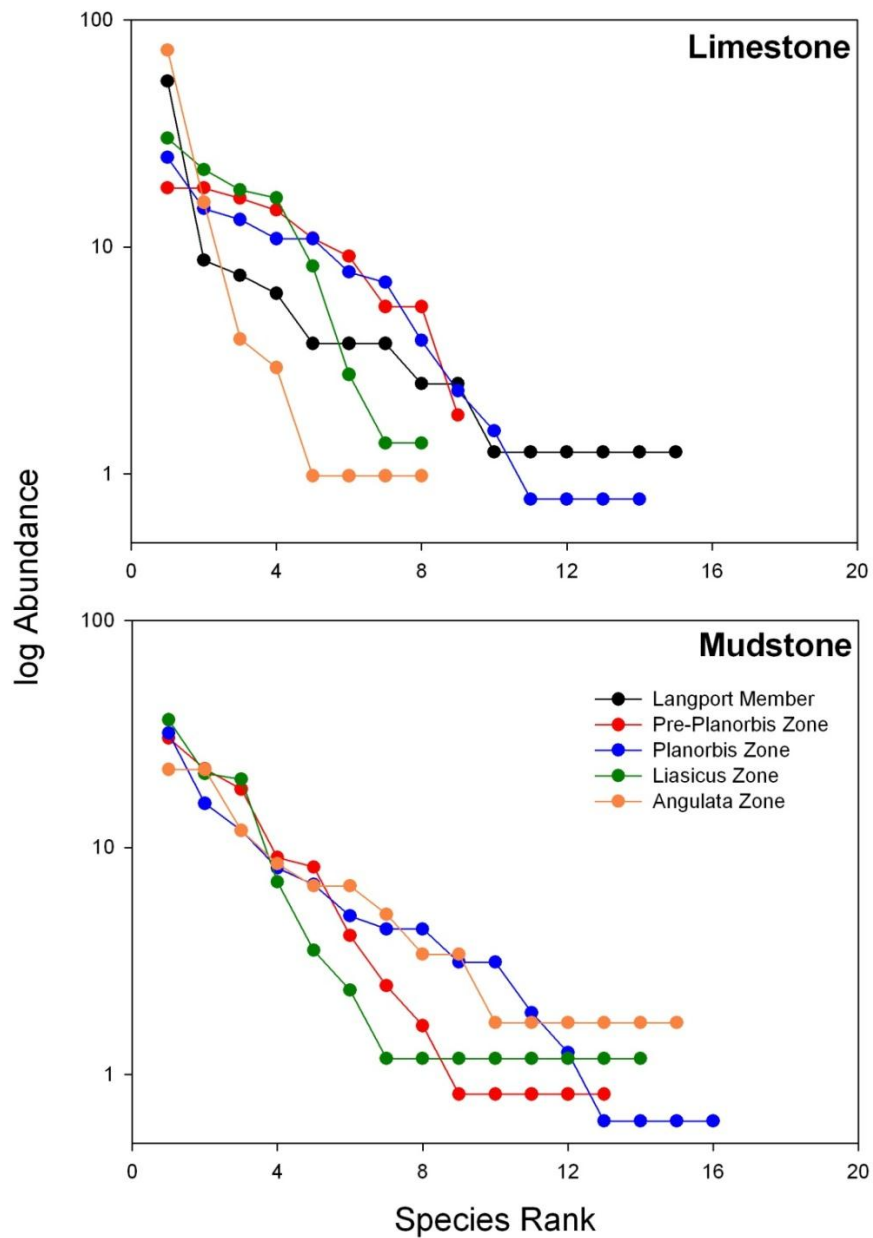


Figure 5.7 RACs derived from the abundance of marine invertebrate fossil communities through the Tr/J study interval. Y-axis on $\log(n)$ scale.

5.3.2 Mudstone samples

The kurtosis values estimated from mudstone samples increase significantly and rapidly up to the Liasicus Zone (at 15 m above the base of the section). Towards the Angulata

Zone, however, the kurtosis values tend to decrease slightly up to a level 19 m above the base of the section (Sample = AZ2; Fig. 5.6B; Appendix 5.2).

All the rank abundance distribution obtained from mudstone samples fits the Zipf–Mandelbrot model, which are interpreted as systems with high diversity (Fig. 5.7; Table 5.1). The Pre-Planorbis Zone contains 13 species, represented by 122 specimens. The rank distribution of the abundance decays smoothly, with *D. tomesi* the dominant species (proportional abundance >30%), followed by *L. hisingeri* with 22% and *Modiolus* sp. with 18%. The rank abundance of the remaining species drops to between 10% and 0.8%, but includes 70% of the total number of species recorded in this horizon (Fig. 5.7, Appendix 5.3 and 5.4).

Sixteen species were recorded through the Planorbis Zone: *D. tomesi* is dominant (32% proportional abundance), followed by *Modiolus* sp. (15%) and *L. hisingeri* (12%). Nine species have an abundance of between 9 and 1% (within the latter range, abundance decreases smoothly) and four species occur at <1% (Fig. 5.7, Appendix 5.3 and 5.4).

The Liasicus Zone records almost the same pattern as the Planorbis Zone, with *D. tomesi* the most abundant at ~36%, two further species at 20-22% and eleven species at a proportional abundance of only 1–7%, (Fig. 5.7, Appendix 5.3 and 5.4).

The Angulata Zone recorded a drastic change in composition. Fifteen species are recorded in this assemblage, which shows a more even distribution (Table 5.1). *C. calcaria* and *G. obliquata* were the most abundant species (22%), followed by *Modiolus* sp. (11%). The relative abundance of the rest of the species decreases gradually from 9-6% to 5-1% (Fig. 5.7, Appendix 5.3 and 5.4).

Table 5.1 Comparison of RAD models derived from abundance distribution of marine invertebrates through the Tr/J interval. The models were ranked based on Akaike's weights (ω_i) following Burnham and Anderson's (2002) recommendation. AICc sample-size corrected was estimated as $AICc = AIC + (2K/[K+1]) / (n-K-1)$. AIC is reported only for completeness. K is the number of parameters; T is the number of taxa; n is the number of specimens. The highest ω_i gives the best fit (**In bold**).

				Limestone				
				RAD models				
	T	n	AIC	Broken stick	Geometric	Lognormal	Zipf	Zipf – Mandelbrot
Parameters (K)				0	1	2	2	3
Langport Member	15	80	AIC	83.373	76.085	60.169	52.498	54.498
			AICc	6.798	6.237	6.431	5.792	8.318
			ω_i	0.188	0.142	0.156	0.113	0.401
Pre - Planorbis Zone	9	55	AIC	38.554	36.585	38.061	41.147	39.486
			AICc	6.222	5.941	9.177	9.691	15.297
			ω_i	0.009	0.008	0.042	0.054	0.887
Planorbis Zone	14	129	AIC	40.087	42.216	45.738	51.054	46.036
			AICc	3.757	3.935	5.703	6.187	8.304
			ω_i	0.056	0.061	0.149	0.189	0.545
Liasicus Zone	8	73	AIC	49.227	47.691	53.825	60.919	51.647
			AICc	6.367	6.758	11.296	12.604	19.105
			ω_i	0.002	0.002	0.019	0.036	0.941
Angulata Zone	8	102	AIC	88.956	45.589	47.126	47.285	44.960
			AICc	17.668	7.647	10.550	9.472	17.340
			ω_i	0.526	0.004	0.015	0.009	0.447

				Mudstone				
	T	n	AIC	Broken stick	Geometric	Lognormal	Zipf	Zipf – Mandelbrot
Parameters (K)				0	1	2	2	3
Pre - Planorbis Zone	13	122	AIC	63.513	48.291	58.703	67.522	52.251
			AICc	6.228	4.845	7.570	8.452	9.917
			ω_i	0.078	0.039	0.153	0.237	0.493
Planorbis Zone	16	160	AIC	70.694	66.545	62.452	69.225	66.755
			AICc	5.407	5.110	6.112	6.633	8.646
			ω_i	0.098	0.085	0.140	0.181	0.496
Liasicus Zone	14	85	AIC	78.158	56.910	53.179	53.103	53.158
			AICc	6.930	5.159	6.380	6.373	9.016
			ω_i	0.173	0.072	0.132	0.131	0.492
Angulata Zone	15	59	AIC	47.329	47.401	50.468	51.707	50.452
			AICc	4.025	4.031	5.622	5.726	7.950
			ω_i	0.073	0.073	0.162	0.171	0.520

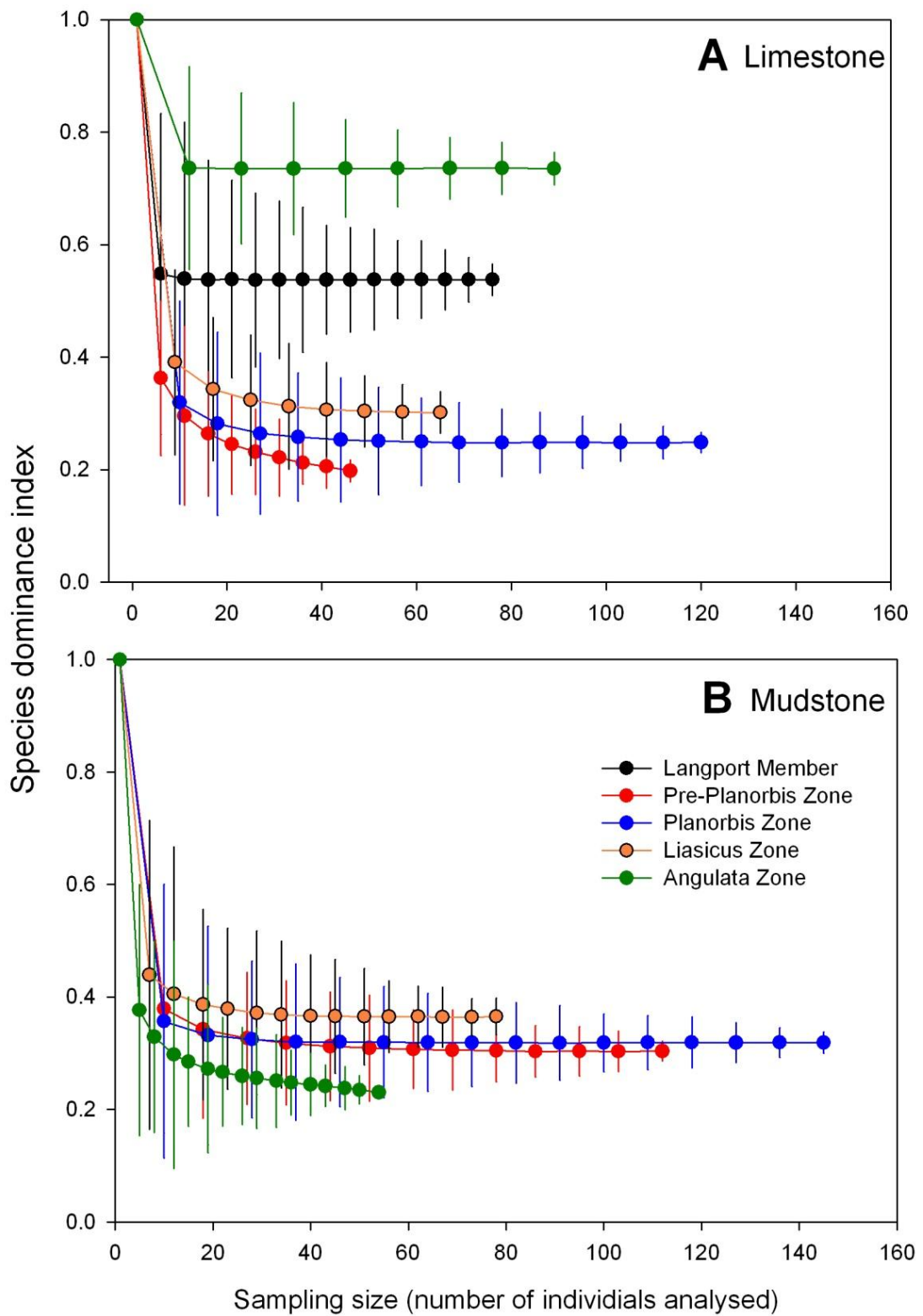


Figure 5.8 Average values ($\pm 95\%$ confidence intervals) of species dominance index estimated as sampling size increased during the Tr/J section in Pinhay Bay. Significant differences were assumed if 95% confidence intervals did not overlap.

5.3.3 Species dominance index

Sample rarefaction of the “species dominance index” from limestone samples (Fig. 5.8A), shows that the Angulata Zone assemblage record on average a high dominance. Assemblage of the Pre-Planorbis, Planorbis and Liasicus zones recorded lower dominance values of <0.5 (more even), whilst, samples from the Langport Member showed intermediate dominance values of ~ 0.5 . In contrast, assemblages recorded in mudstone samples show that communities from the Lias Group recorded very low dominance of < 0.5 (Fig. 5.8B), which is consistent with the RAD model, Zipf–Mandelbrot model (all data are shown in Appendix 5.3 and 5.4).

5.4 Composition

5.4.1 Limestone samples

Non-metric multidimensional scaling separates the limestone samples of the Langport Member from those of the younger stratigraphic units (Fig 4.9A). One-Way ANOSIM indicated significant differences in composition between the Langport and the higher levels ($R= 0.329$; $p = 0.012$). The SIMPER analysis shows that the dissimilarity is higher in samples from the Langport Member (87.85%) than at higher levels in the Blue Lias Formation (Appendix 5.5). This latter analysis indicates changes in the relative abundance of each species by stratigraphic unit and by the number of shared species across all stratigraphic units (dissimilarity).

The Langport Member records 15 species, 67% of them being exclusive to this stratigraphic unit; five species range through to the Blue Lias Formation, with just *P. langportiensis* disappearing within the Pre-Planorbis Beds and not reappearing higher in the Pinhay Bay sequence (Appendix 5.6). Within Langport Member assemblages, only

I. concentricum, *P. rhaetica* and *M. hillanus* are species that became regionally extinct, despite their abundance in the Member (Appendix 5.6). The Pre-Planorbis and the

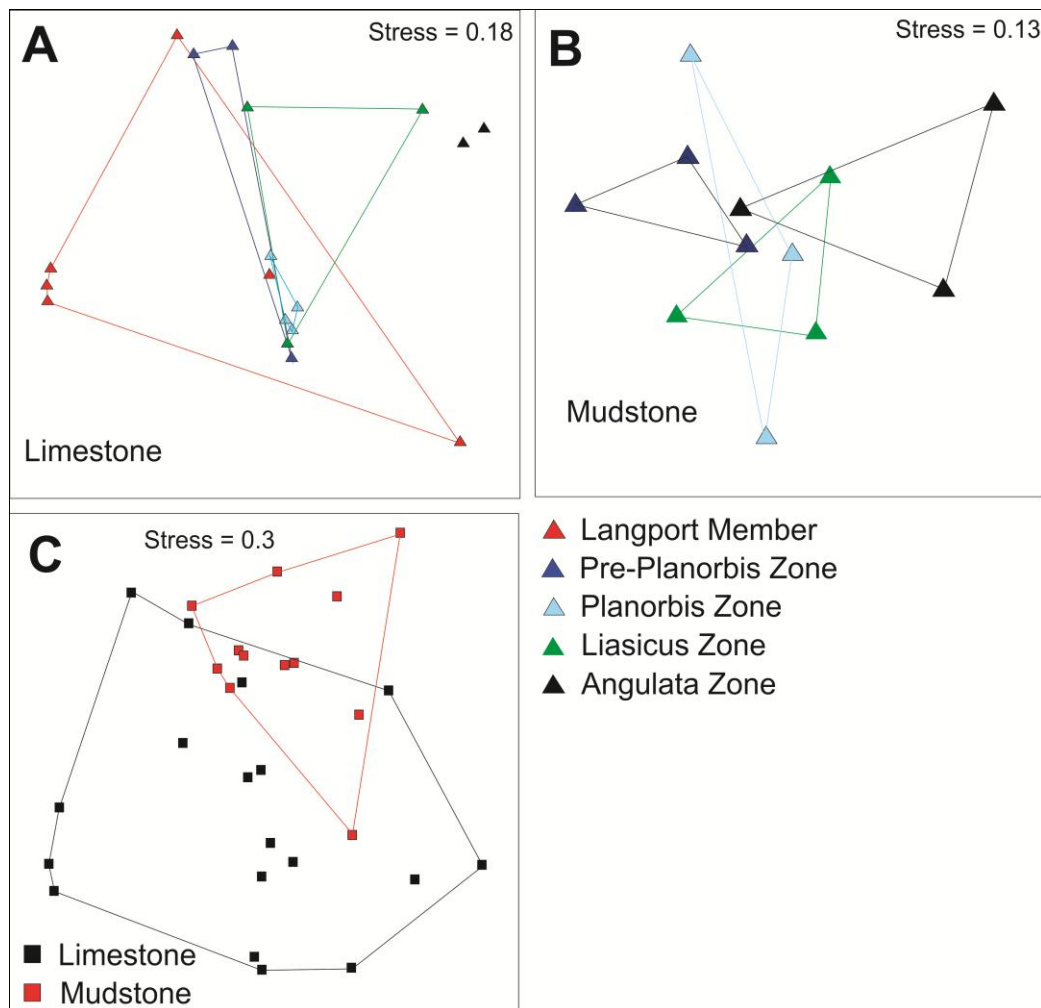


Figure 5.9 Non-metric multidimensional scaling (NMDS) plot resulting from the ordination analysis (Chord distance) of the marine invertebrate fauna from the Pinhay Bay section, using abundance data transformed by taking the fourth root of [×].

Planorbis zones show a dissimilarity of 77.12% (Appendix 5.5). Three taxa recorded occur uniquely in the Pre-Planorbis Zone (*M. minimus*, *Myoconcha* sp. and *P. cognate*), whilst *P. undulata* and *I. psilonoti* appear for the first time at this level and persist until the Angulata Zone (Appendix 5.6).

The assemblage of the Planorbis and the Liasicus zones records a dissimilarity of 59.04% with seven shared species (Appendix 5.5 and 5.6). The Planorbis Zone contains 14 species, six of which show an average contribution of >1%. Of these, three are present in the assemblages from the Langport Member (Appendix 5.6), two from the Pre-Planorbis Zone and one species first occurs at this unit. Seven species first appear in this unit, although five are represented by single specimens (with contribution <1%), whilst two species, *M. ventricosus* and *L. hisingeri*, range upwards into the Liasicus Zone and the Angulata Zone, respectively (Appendix 5.6). *Modiolus* sp. and *C. valoniensis* reappear, although, with an abundance of $\leq 1\%$.

The Liasicus and the Angulata zones record the same species richness (8 species), but show a high dissimilarity of 66.45% in terms of species composition. The Liasicus Zone sample includes three unique records, *L. hisingeri*, *M. ventricosus* and *A. laqueus*; the last represented by a single specimen (Appendix 5.6). Similarly, the Angulata Zone includes three unique species records, *C. calcaria*, *S. complanata* and *G. obliquata*. However, there is no significant difference between the Liasicus and the Angulata zone (Appendix 5.5 and 5.6).

5.4.2 Mudstone samples

In contrast to the limestones, the samples from the mudstones do not record significant differences in composition between stratigraphic units ($R = -0.049$, $p = 0.508$) (Fig. 5.9B), but there are significant differences between the two different lithologies ($R = 0.289$; $P < 0.001$) (Fig. 5.9C). Mudstone and limestone samples record differences of 80%. SIMPER analysis shows that nine species only occur in limestone samples (Appendix 5.7), whilst 13 species are exclusively recorded in mudstone samples (Appendix 5.7).

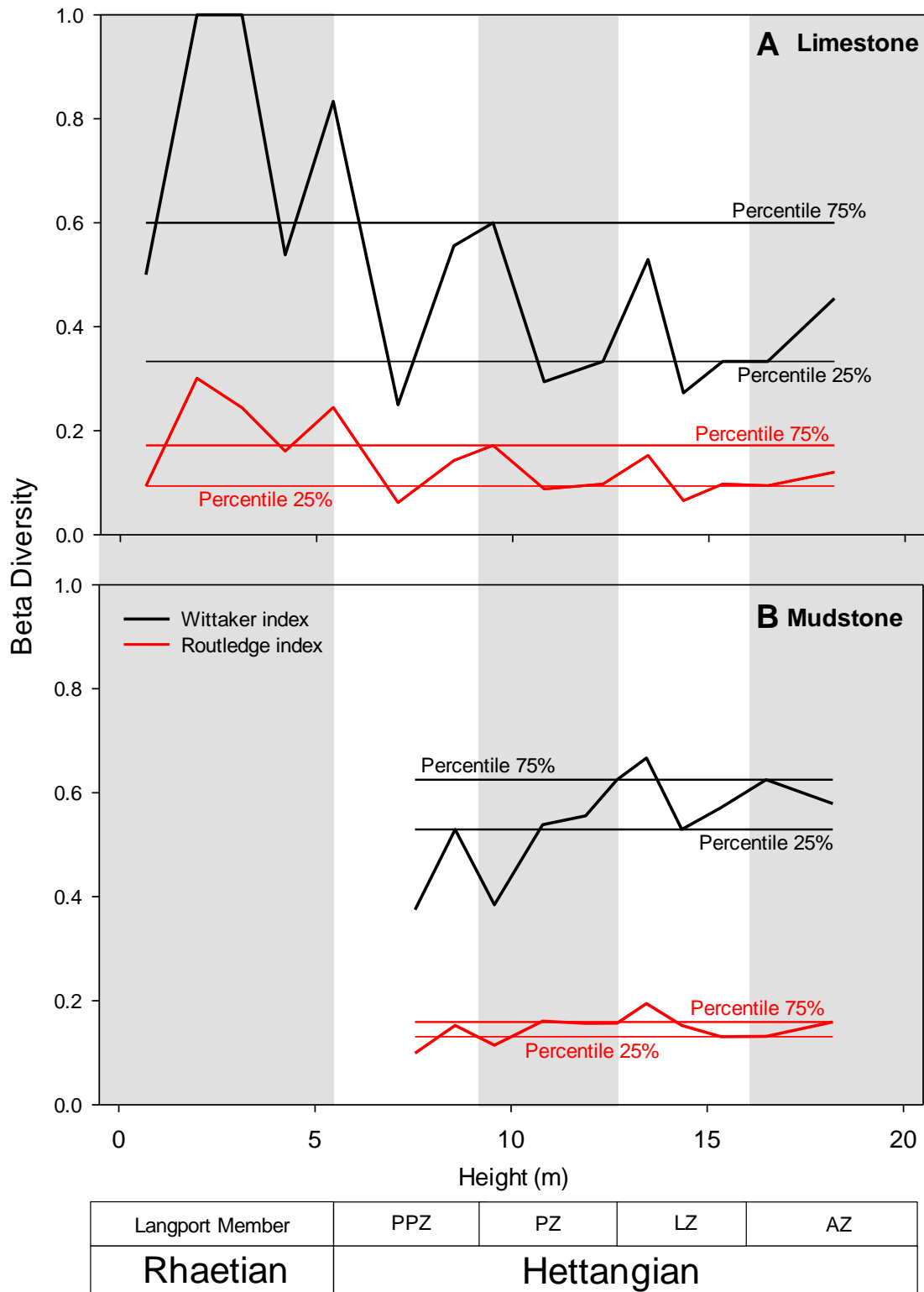


Figure 5.10 Beta diversity (β) estimated by Whittaker and Routledge indices. These indices reflect the temporal difference in species composition between samples. The percentiles represent the 95% confidence intervals calculated by bootstrap procedure (number of iterations = 10,000). PPZ: Pre-Planorbis Zone, PZ: Planorbis Zone, LZ: Liasicus Zone, AZ: Angulata zone. (See data appendix 5.2).

Like previous results (NMDS), the Whittaker and Routledge Beta indices show a significant peak at 2 m above the base of the section (i.e. within the Langport Member) (Fig. 5.10A), which decreases smoothly to a minimum value at 7 m – above this level the beta values (species composition) do not show significant changes. This indicates that the greatest turnover happens within the Langport Member, the faunal composition subsequently remaining in relative stasis. In contrast, the species composition estimated from mudstone samples, does not record significant differences. This indicates that the species composition does not change drastically through the Blue Lias Formation (Fig. 5.10B, Appendix, 5.2).

5.5 Ecospace

The marine fauna identified from limestone and mudstone samples used thirteen modes of life through the study interval, which corresponds to 6% of theoretical ecospace (Fig.5.10). In this case, samples of different lithologies were grouped by stratigraphic unit with the aim to observe potential interaction networks (e.g. predator-prey relationships) and the ecological complexity in each assemblage.

The number of modes of life increased from the Langport Member (8 modes of life) to the Liasicus Zone (10 modes of life) and later decreased to nine modes of life in the Angulata Zone. The relative abundance in Figure 5.10 was estimated as the number of species that use each mode of life as a percentage of the total number of species observed in each specific stratigraphic units. i.e. The Langport Member. (See data at Appendix 5.8; 5.9 and 5.10).

Three tiering categories were used by the marine assemblage of the Langport Member; surficial, semi-infaunal and shallow-infaunal. The surficial group: was made up by five modes of life. Three of which have slow or facultative motility (Fig. 5.10).

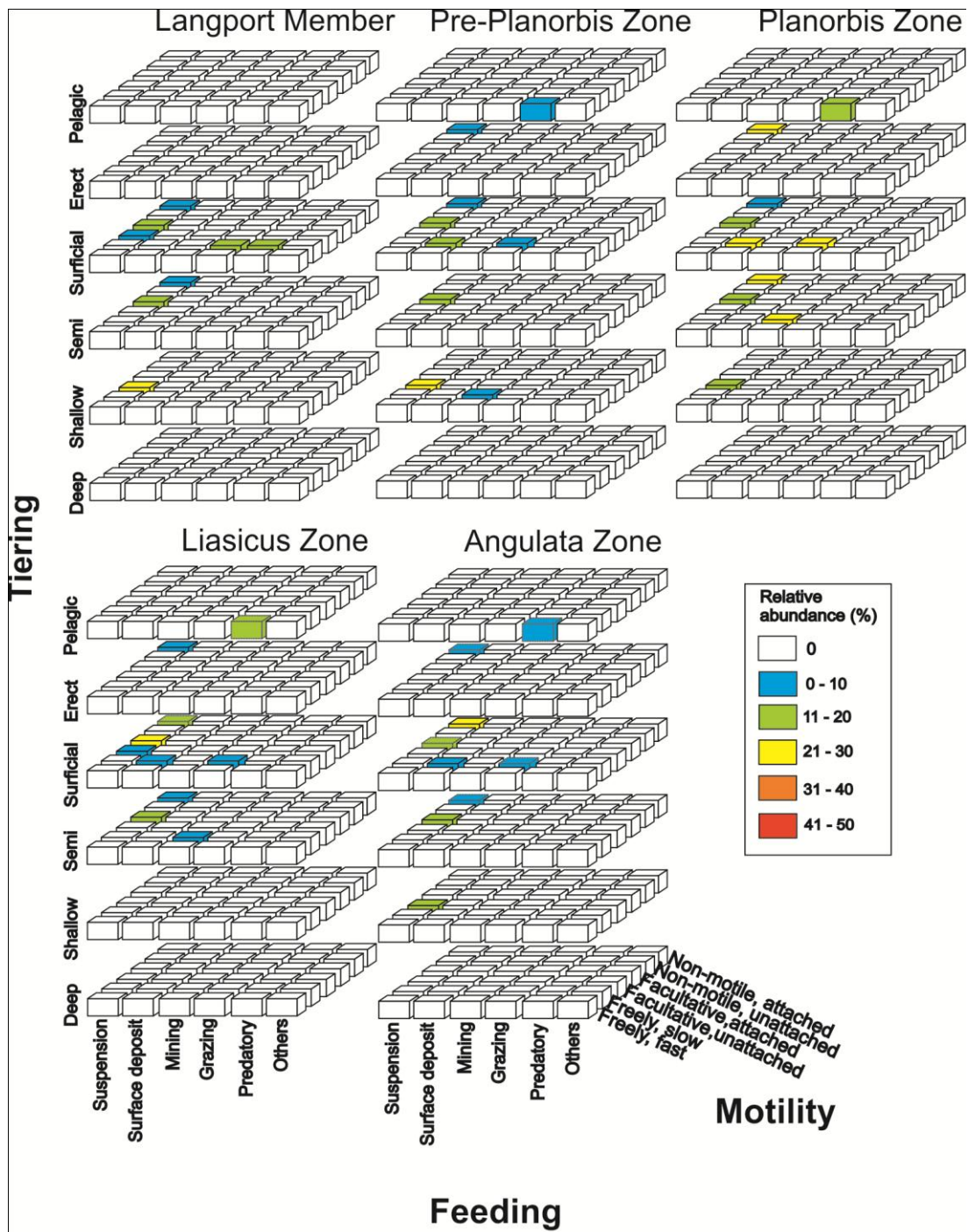


Figure 5.11 Ecospace occupations by the marine invertebrate assemblages of the Tr/J interval at Pinhay Bay.

Those categories were filled by echinoids, herbivorous gastropods and predatory gastropods, whilst facultative moving is occupied by *Z. henrici* (gastropod). The other two modes of life were made up by *P. giganteum* and *C. valoniensis* (facultative attached suspension feeders), and the stationary suspension feeders (*L. hisingeri*). The

semi-infaunal group was made up by three species; *G. precursor* (no motile) and two species of *Modiolus* (Facultative motile attached). The shallow-infaunal group was occupying by suspension feeders bivalves with facultative motility. The Langport assemblage represents a slightly complex benthic ecosystem, with restrictive motility (> 20% moving species) and with three trophic levels; suspension feeders (~70% of the species), herbivores and intermediate carnivores (both ~15%) (Figure 5.11) (Appendices 5.8, 5.9 and 5.10).

The Pre-Planorbis Zone assemblage comprises nine modes of life, four new modes being occupied in comparison to the Langport Member fauna (Fig. 5.10). Crinoids (*I. psilonoti*) represent erect forms; pelagic predators (*P. erugatum*) appear at the end of the Zone; deposit feeders were represented by *Pseudokatosira undulata* and *Pleurotomaria cognata*; and slow moving forms appeared for the first time in the shallow tier (*R. doris*). Three modes of life disappeared from the previous interval: Non-motile-semi-infaunal and epifaunal-facultative-motile-unattached, both modes of life that occupied by *G. precursor* and *Z. henrici*, respectively; and the epifaunal slow moving predators, which is occupied by two gastropod species, *P. decorata* and *P. rhaetica* (Appendix 4.9). The Pre-Planorbis assemblages are dominated by epifaunal species, whilst shallow and semi-infaunal modes of life are subordinate (Fig. 5.11, Appendix 5.8, 5.9 and 5.10).

The Planorbis fauna includes 10 modes of life, two new modes of life are using; the semi-infaunal slow moving miner appears in the study section for first time, represented by *R. bronni* and the semi infaunal, non-motile attached, suspension feeders which is occupying by *Pinna* sp. The shallow infaunal slow moving mining feeders disappear (*R. doris*). More predatory species (4 spp.) are incorporated into the trophic network and marine reptiles are recorded as being part of this marine assemblage (Fig. 5.10 and Fig. 5.11).

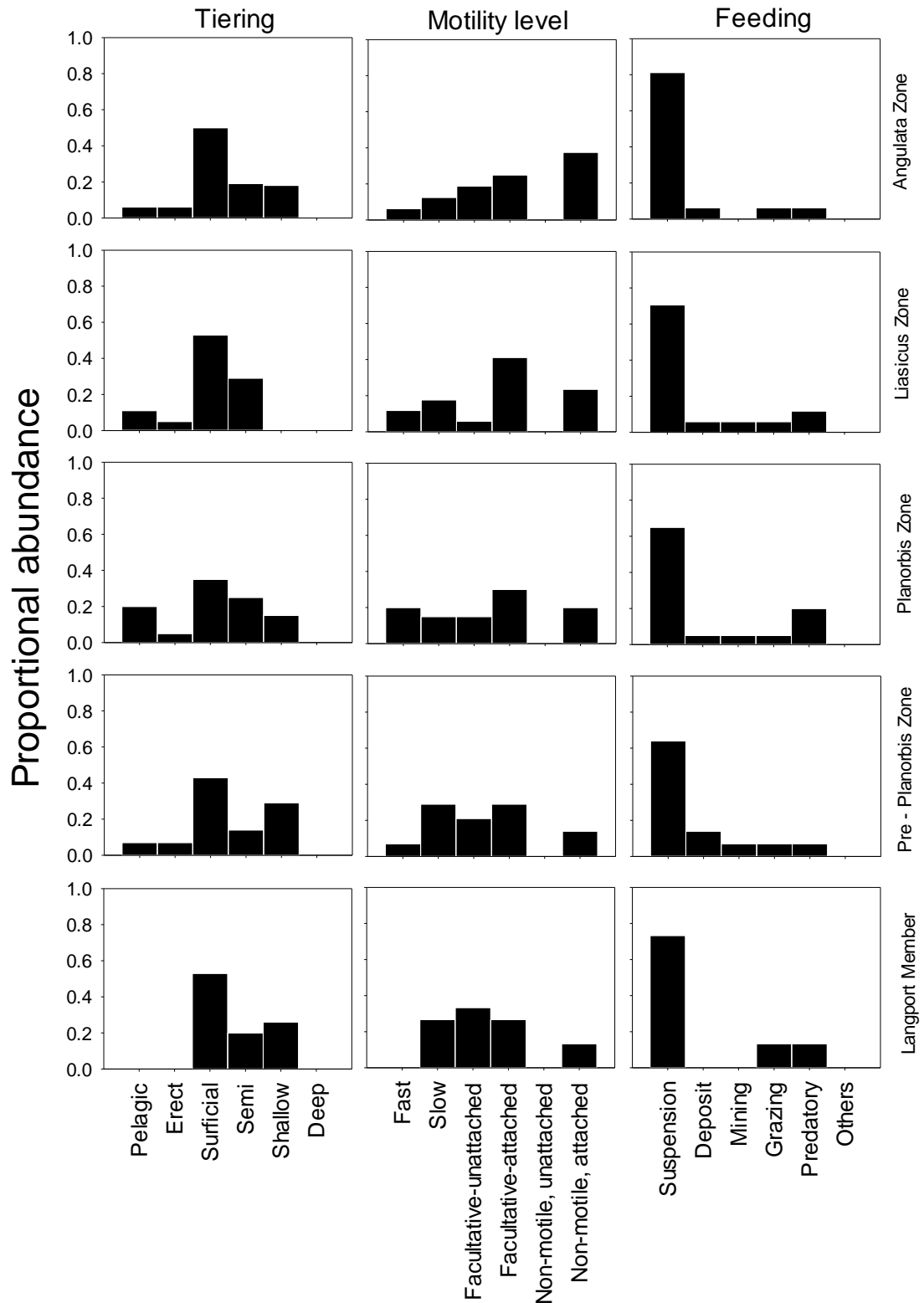


Figure 5.12 Mean proportional abundance of tiering, motility and feeding mechanisms based on the number of species in the Langport Member to the Angulata Zone of the Blue Lias Formation.

Crinoids represent the erect forms. The epifaunal facultatively motile attached

suspension feeder guild records one more genus (*Camponectes*), while the species

occupying the shallow facultative motile unattached suspension feeder group change completely (Appendix 5.8, 5.9 and 5.10). In terms of the proportional abundance, pelagic and semi-infaunal categories increase to ~50%, surficial and erect forms remain constant, while shallow forms tend to decrease (Fig. 5.11). In term of motility, slow and facultatively attached forms decrease on average by ~28%, while the other categories increase by ~50%. Suspension feeders increase by ~5%, predatory forms increase (double), surface miners and grazers decrease by ~5%, while deposit decrease > 50% (Fig. 5.11, Appendix 5.10).

The Liasicus Zone assemblage occupied 10 modes of life (Fig. 5.10). Surficial, facultatively motile, unattached suspension feeders are added into the assemblage, which is using by *P. navis*. In contrast, shallow facultatively motile unattached suspension feeders disappear. The Fast pelagic predator group is filled by just two species. Surficial-facultatively motile, attached suspension feeders incorporate one new species (*P. dubius*) whereas the semi-infaunal, non-motile suspension feeders record a complete compositional change. The rest of the modes of life do not record any changes (Fig. 5.10, Appendix 5.9).

Surficial and semi-infaunal groups increase their proportional abundance by ~9% compared to the Planorbis Zone. The pelagic tier decreases by ~10%, while shallow infaunal organisms disappear. In terms of motility, although 50% of the fauna have some level of motility, their relative abundance dropped on average by ~15%, while the stationary fauna increased by the same percentage. In terms of feeding, suspension feeders are the most abundant category, and increased by ~6% compared to the Planorbis Zone unit, while predators decreased by ~8% (Fig. 5.11, Appendix 5.10).

The Angulata Zone records nine modes of life (Fig. 5.10). Pelagic fast moving predators feeder are represented by just *S. complanata*. The surficial, facultative motile attached suspension and semi-infaunal, facultative motile attached suspension feeder are occupying by *P. giganteum* and *G. precursor*, respectively. The latter mode lost 50% of species compared to the Liasicus Zone. The stationary epifaunal suspension feeders incorporate two new species (*C. calcaria* and *G. obliquata*). Shallow, facultatively motile unattached suspension feeders newly appear, and are represented by *M. cardioides*, *C. regularis* and *Pholadomya* sp. The semi-infaunal miners, which were used by *R. bronni* disappear at the Liasicus Zone (Fig. 5.10, Appendix 5.9). Compare with the Liasicus Zone, the proportion of pelagic forms in the Angulata Zone decreases by ~5%, semi infaunal forms decrease by 10% and superficial categories by 3%, whilst erect forms remain constant. In terms of motility, this increases by ~3%, whilst the non-motile proportion decreases by ~8%, when compared to the Liasicus Zone. Suspension feeders are the only group that increases during the Angulata Zone. Grazing and deposit feeders do not change, whilst predation decreases by ~5% and miners disappear from the assemblage (Fig. 5.11, Appendix 5.10).

5.6 Body Size

Figure 5.12 shows the trajectory of the body size and the rate of change of the body size of bivalves through the study interval. From the Langport Member to the Angulata Zone the mean body size tends to increase smoothly, although with a low increase rate and high variation associate (~60%).

The Langport Member records a mean body size of $\sim 13.18 \pm 11.21$ mm. Of this, 80% of the measurements corresponded to *I. concentricum* (mean = 8.28 ± 2.57 mm) and the residual percentage was made up by seven species (Appendix 5.13). The body size values do not change significantly through this stratigraphic unit, except by one outlier value recorded by *Plagiostoma* sp. (33 mm) at 1.3 m. Toward the top of the Langport

Member, species with large body sizes appear, but their occurrences are low. For example, *C. valoniensis* (13.07 ± 8.87 mm), *P. langportiensis* (11.34 ± 6.09 mm) and *Plagiostoma* sp.

Through the Pre-Planorbis and Planorbis zones, species composition changes and the mean size tends to increase quickly until reaching a value of 29.17 mm at 11.5 m as result of high occurrences of species such as *M. minimus*, *L. hisingeri*, *C. valoniensis*, *C. regularis* and *P. giganteum* (Appendix 5.11).

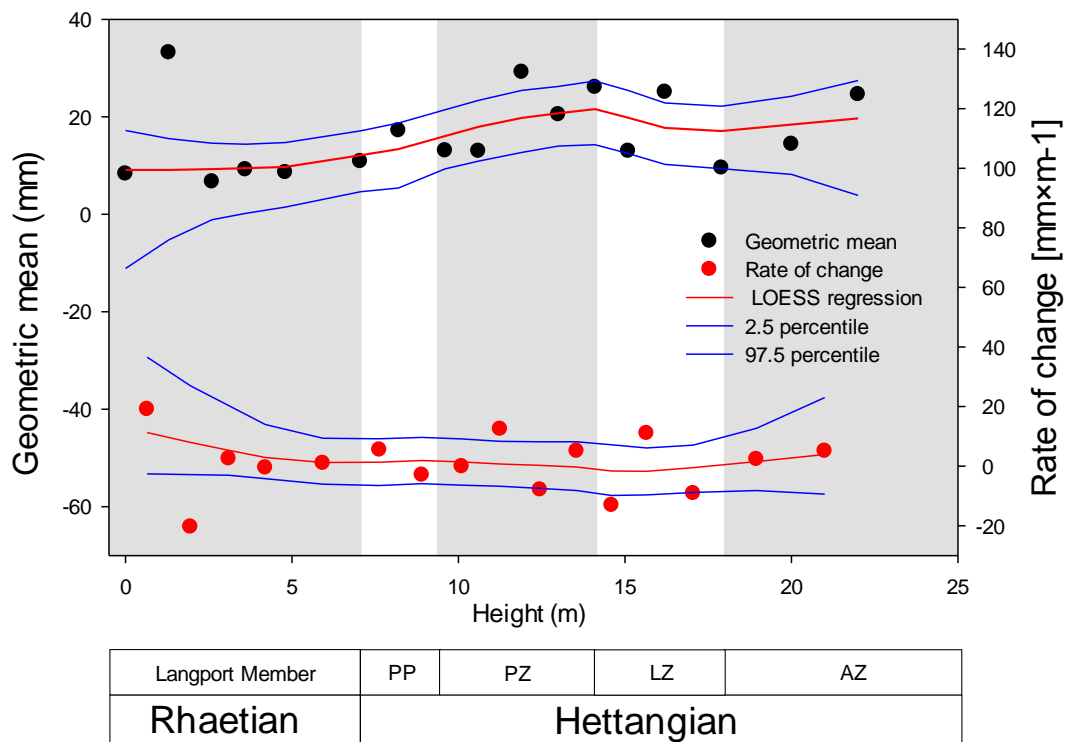


Figure 5.13 The average body size (●) and rate of change (●) of the bivalve assemblage sampled through the Triassic-Jurassic boundary at Pinhay Bay section. The red line is the LOESS regression through the data point estimated with an alpha 0.3. PPZ: Pre-Planorbis Zone, PZ: Planorbis Zone, LZ: Liasicus Zone, AZ: Angulata zone.

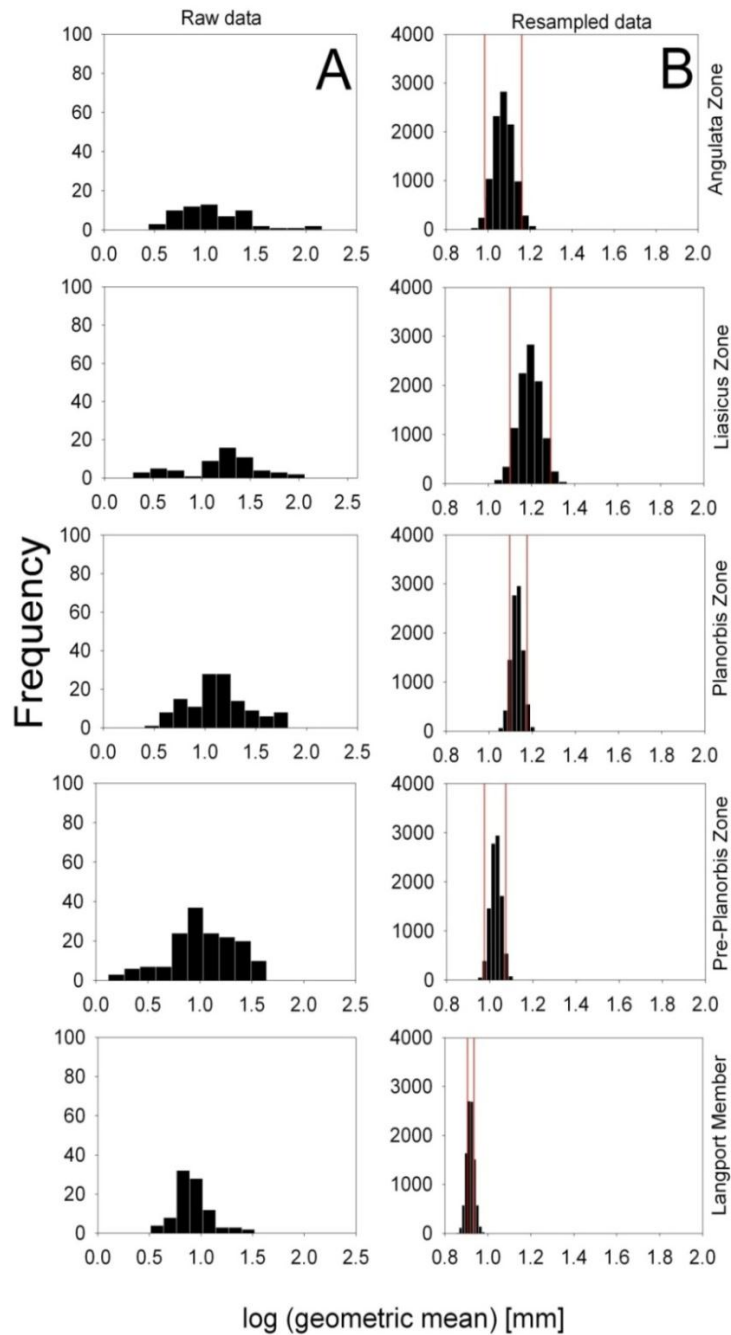


Figure 5.14 Frequency distribution of log geometric mean of bivalve size sampled through Tr/J boundary at Pinhay Bay section. (A) Shows the distribution frequency of raw data by each lithostratigraphy (B) Shows the distribution frequency of resampled data by bootstrapping procedure (10,000 iterations with replacement). The red lines indicate the percentiles of 2.5% and 97.5% around the mean.

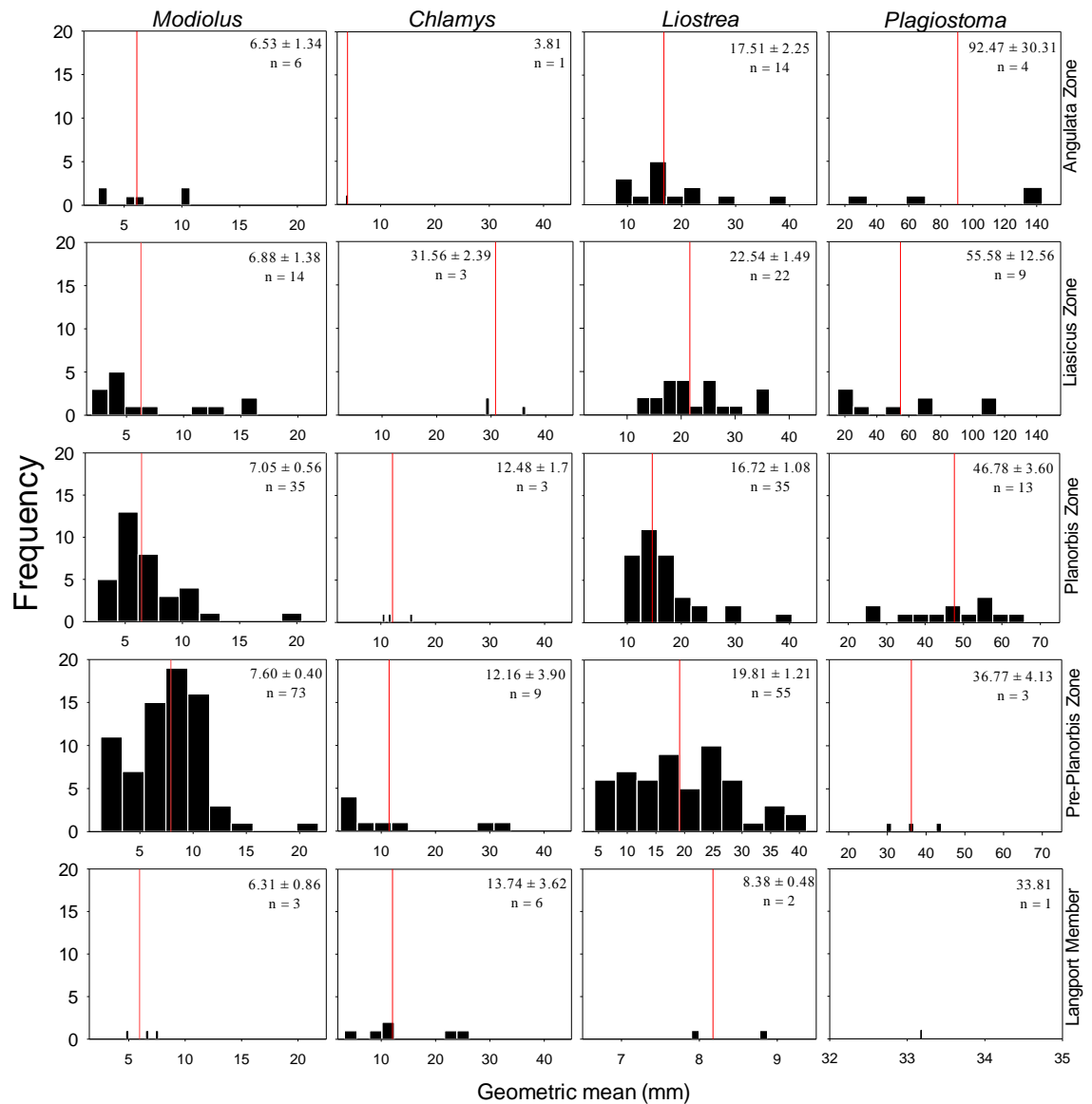


Figure 5.15 Frequency distribution of geometric mean of the four most common bivalve genera found through the study section at Pinhay Bay. The red line indicates the average values. Average values, standard error (\pm) and sample size (n) are indicated in the upper right corner of each histogram.

Through the Liasicus Zone, average body size decreases significantly at 15.8 m (10 ± 0.35 mm). In the Angulata Zone, the body sizes tend to increase again towards the top of the section, reaching average values of 24 mm (Fig. 5.13, Appendix 5.2). From the top of the Liasicus Zone to the Angulata Zone, species composition changes and bigger species are integrated to the community. (i.e. *Pholadomya* sp. *M. cardioides*). In the Angulata Zone, *L. hisingeri* decreases in abundance, *C. valoniensis* disappears and is

replaced by *Camponectes* sp. *G. obliquata* and *C. calcarea*, and *P. giganteum* increases in occurrence (Appendix 4.11).

In contrast, the rate of change of body size indicates that there is no significant change in the rate of change along the study section (Fig. 4.13, Appendix 4.2). A linear model fitted to rate of changes confirm the absence of trends ($F_{(1,14)} = 0.0005$; $P > 0.05$). Size-frequency distribution based on 449 individual measurements of bivalves from the studied section at Pinhay Bay, shows a significant increase in body size from the Langport Member to the Liasicus Zone. However, at the Angulata Zone the average body size tended to decrease slightly (Fig. 5.14). As well as the average size change, the variance also increases through the section (mainly the Liasicus and Angulata zones), which reflects the appearance of new species of different sizes.

Frequency distributions of the more common genera through the study interval were plotted to observe the trajectory of the body sizes of those taxon (Fig. 5.15). This figure shows that *Plagiostoma* ($F_{(3,28)} = 2.54$; $p < 0.05$) and *Liostrea* ($F_{(4,127)} = 2.98$; $p < 0.05$) increase significantly its body sizes from the Langport Member to the Angulata Zone for *Liostrea* and. However, the mean size of *Liostrea* recorded more fluctuations through the section. The mean body size of *Chlamys* also increases significantly, but only in the Liasicus Zone ($F_{(3,20)} = 3.38$; $p < 0.05$). From the Langport Member to the Planorbis Zone mean body size did not record significant changes (Fig. 5.15). In contrast, *Modiolus* did not record significant changes through the section ($F_{(4,130)} = 0.57$; $p > 0.05$) (Fig. 5.15, Table 5.2).

The changes in the minimum and maximum body sizes of *Chlamys*, *Modiolus*, *Liostrea* and *Plagiostoma* through the Langport Member and Blue Lias Formation are visualized using Jablonski target plots (Fig. 5.16), which record the percentage change in

maximum and minimum size and are useful for determining whether the changes are simply due to changes in variance (Jablonski, 1996). In this case, *Chlamys* increases the body size only between the Planorbis Zone and the Liasicus Zone, whilst between the Langport Member and the Pre-Planorbis Zone and between the Pre-Planorbis to the Planorbis Zone, the body size shows increases and decreases their variance, respectively. *Modiolus* tends to increase its body size between the Langport Member and the Pre-Planorbis Zone, However, towards younger assemblages; the body size tends to decrease the variance (decrease in the largest size and an increase in the smallest size) and decreases in body size (lower left quadrant).

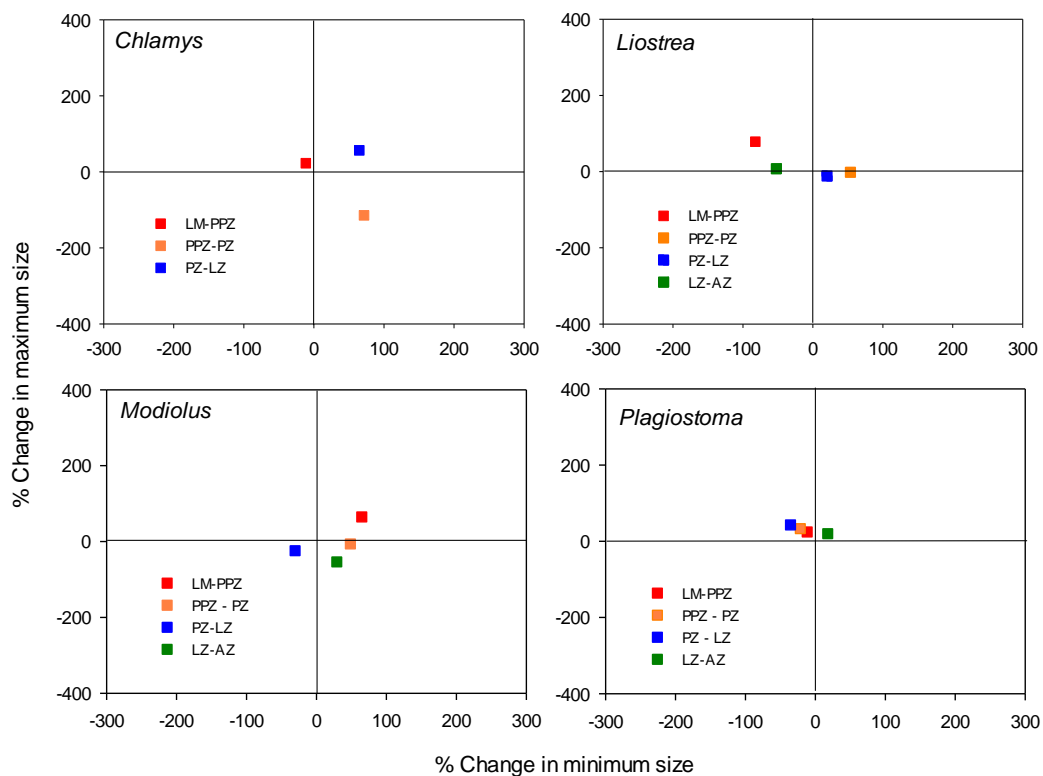


Figure 5.16 Change in size in four bivalve genera through the Pinhay Bay section. Top left and bottom right indicate variance in size whilst the top right and lower left represent Cope's Rule and size decrease, respectively. (After Jablonski 1996).

Liostrea, like its mean body size values did not show a clear pattern and just tend to increase or well decreases in variance through the section. In contrast, *Plagiostoma* tends constantly use upper left quadrant, which means an increase in variance (increase in the largest size and a decrease in the smallest size). Although through the Liasicus

Zone and the Angulata Zone, *Plagiostoma* is plotted within the upper right quadrant, which indicates an increase in size, or a directional trend toward larger body sizes (Fig. 5.16, Table 5.2).

Table 5.2 Body size parameters of four bivalve's genera with high occurrences trough the Tr/J interval in Pinhay Bay. LM: The Langport Member, PP: The Pre-Planorbis Zone, PZ: The Planorbis Zone, LZ: The Liasicus Zone, AZ: Angulata Zone. (*): just one data point was recorded.

	LM	PP	PZ	LZ	AZ
<i>Chlamys</i>					
Mean	13.74	12.16	12.48	31.563	3.811*
Stand. Error	3.624	3.904	1.708	2.3989	0
<i>n</i>	6	9	3	3	1
Min. size	3.24	2.904	10.21	28.954	0
Max. size	26.25	33.92	15.82	36.354	0
<i>Liostrea</i>					
Mean	8.386	19.81	16.72	22.544	17.51
Stand. Error	0.487	1.215	1.083	1.4981	2.254
<i>n</i>	2	55	35	22	14
Min. size	7.899	4.331	9.37	11.745	7.72
Max. size	8.873	41.22	40.47	36.333	39.38
<i>Plagiostoma</i>					
Mean	33.18*	36.77	46.78	55.584	92.47
Stand. Error	0	4.133	3.602	12.562	30.31
<i>n</i>	1	3	13	9	4
Min. size	33.18	29.67	24.4	17.992	21.81
Max. size	33.18	43.99	65.9	115.1	143.6
<i>Modiolus</i>					
Mean	6.351	7.607	7.058	6.8811	6.538
Stand. Error	0.867	0.409	0.56	1.3836	1.345
<i>n</i>	3	73	35	14	6
Min. size	4.71	1.313	2.552	1.9542	2.753
Max. size	7.65	21.77	20.45	16.471	10.71

Finally, the mean body size of bivalves was significantly higher than the null model values, which assumed a random distribution of the body sizes through the study

interval. This suggests that overall the bivalves show a directional trend to larger body size throughout the section (t-value = 5.16, d.f. = 32; $p < 0.001$) (Fig. 5.16, Appendix 5.13).

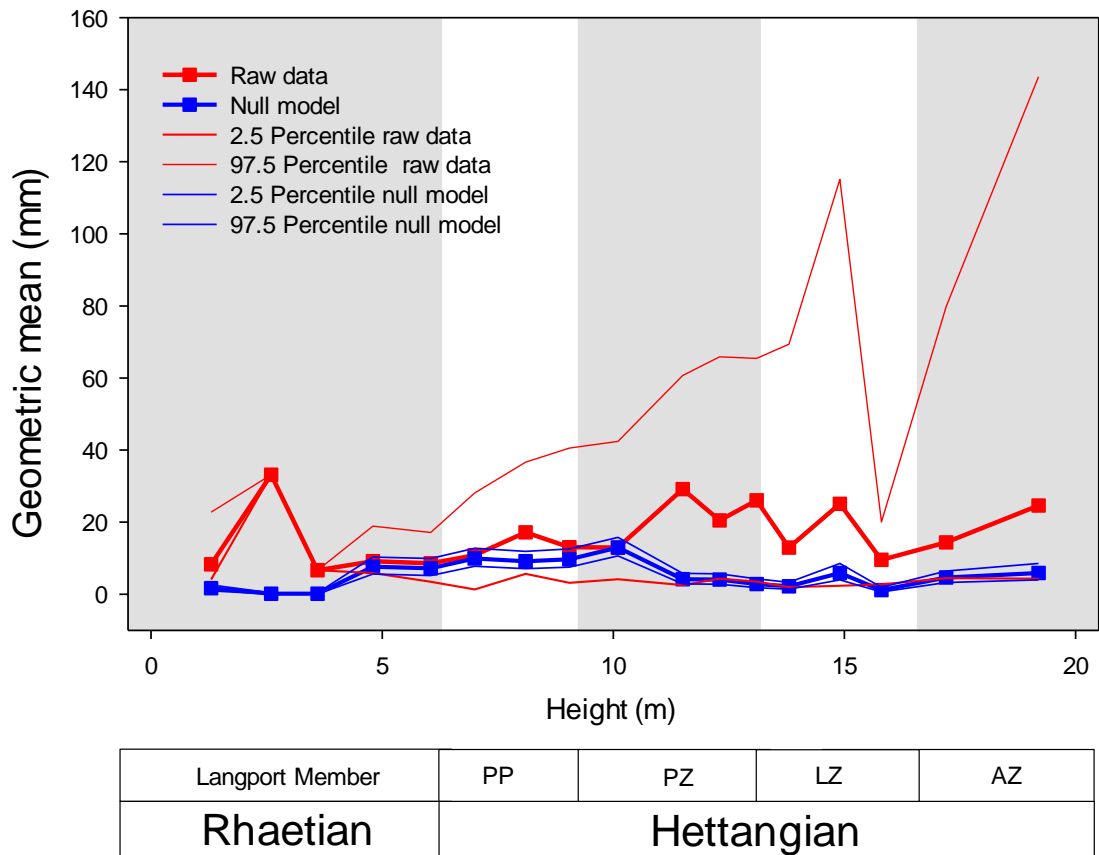


Figure 5.17 The average size of bivalves sampled through the study interval at Pinhay Bay (Red Line: raw data \pm percentile 2.5 % and 97.5 %). Null model (blue line \pm percentile 2.5 % and 97.5 %) was calculated by row-permutation (number of iterations = 10000) of the geometric mean of each individual by species through 36 samples (see Appendix 4.11). PPZ: Pre-Planorbis Zone, PZ: Planorbis Zone, LZ: Liasicus Zone, AZ: Angulata zone.

5.7 Trace Fossils

The number of ichnotaxa increased from the Top of the Langport Member to the Angulata Zone (Fig. 5.11) (see methodology for sampling). Through the Pre-Planorbis Zone, four ichnogenera were identified: *Chondrites*, *Diplocraterion*, *Palaeophycus* and *Arenicolites*, of which *Chondrites* was the first taxon recorded at the base of the Blue Lias Formation, while the remaining taxa were identified at 8.80 m – above the base of section (Fig.5.1) (See appendices 5.2 for ichno-parameters and 5.14 for trace fossils).

In the Planorbis Zone, five ichnogenera were identified, including two new appearances: *Planolites*, which was recorded at 10.10 m and *Thalassinoides* at 11.40 m. In the Liasicus Zone, *Thalassinoides*, *Chondrites*, *Arenicolites* and *Palaeophycus* were recorded at 13.8 m, of which *Thalassinoides* and *Chondrites* were the most frequent. In the Angulata Zone, *Rhizocorallium* contributed a single record at 19.50 m. While at the same height, the last occurrences of *Thalassinoides*, *Chondrites* and *Arenicolites* are recorded in this study (Fig. 5.1).

Burrow diameter and ichnofabric index both increase sharply from the base of Blue Lias Formation to the base of the Planorbis Zone. However, both variables remain “relatively constant” from the Planorbis to the Angulata Zone (Fig. 5.18). An apparently “ceiling” is reached at 10.4 m from the base of the Blue Lias Formation, which point, the maximum taxonomic richness of marine invertebrates’ recorded in this work is reached. On the other hand, the percentage of cover of each ichnotaxa tends to increase through the section without reaching any “ceiling”.

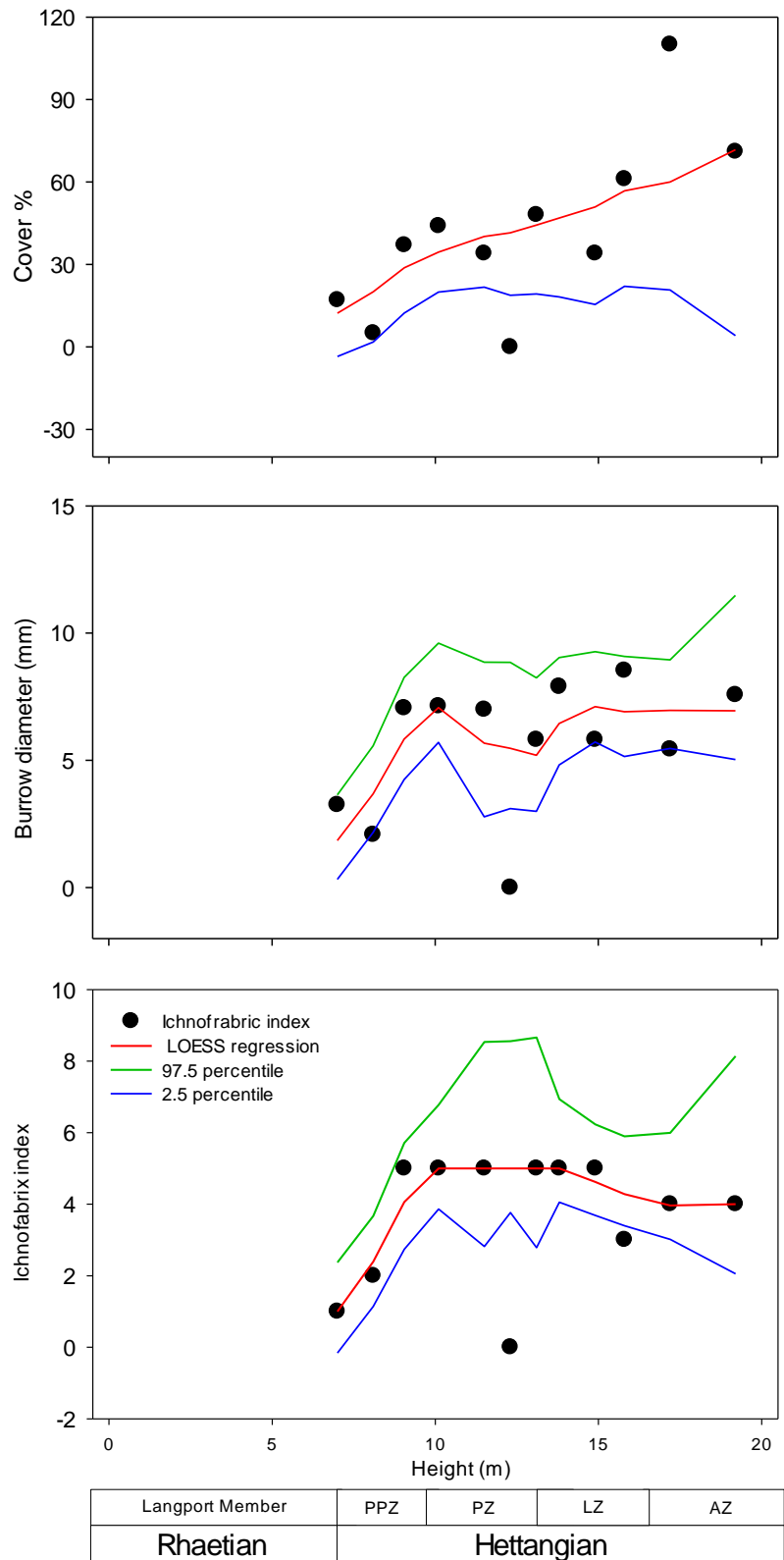


Figure 5.18 Response of the bioturbation estimates through three methodologies along the Tr/J boundary in Pinhay Bay.

5.8 Summary

The assemblages sampled through the study section at the Pinhay Bay, represent the recovery of ecosystems after the Tr/J mass extinction event (Barras and Twitchett 2007; Mander *et al.* 2008; Wignall and Bond 2008). Species richness estimated from limestone samples increases significantly from the Langport Member toward the Liasicus zone, and later drops in the Angulata Zone. In contrast, species richness estimated from mudstone samples does not seem to change through the study section. The limestone samples record higher species richness than the mudstone samples.

The assemblages describe in this section shows a high evenness, which is confirmed the RACs models, Zipf – Mandelbrot and Broken stick. However, dominance was lower in assemblages associated with the Pre-Planorbis, the Planorbis and the Liasicus zones.

The assemblages from mudstone samples have lower dominance than those from limestone samples.

In terms of composition, the samples show significant differences between lithologies.

When the limestone samples are binned in stratigraphic units, however, only the Langport Member is significantly different and only in the limestone samples (the Langport Member has not mudstone samples). In contrast, when mudstone samples are binned in stratigraphic units (from the Pre-Planorbis Zone to the Angulata Zone), do not record significant differences between stratigraphic units. The beta index shows a slight compositional turnover between the Langport Member and assemblages associated with the Lias Group. Later, the assemblages seem to be very similar in composition.

Finally, ecospace expanded quickly from the Langport Member to the Angulata Zone, in the same time, as more species appeared, the number of species by mode of life also increased, which generated communities that are more complex. At the same time, the

mean body sizes of bivalve species and the abundance occurrence and sizes of ichnofossils increase significantly from the Langport Member to the Angulata Zone.

Chapter 6 Larne section

6.1 Geological setting

6.1.1 The Westbury Formation

The Larne section consists of the same stratigraphic units as Somerset (England), the Penarth Group is a thin, but widely distributed and distinctive unit, consisting of the Westbury Formation and Lilstock Formation (Fig. 6.1). The Westbury Formation is constituted predominantly a dark grey mudstone, shale and subordinate sandstone. The Westbury Formation fauna is a low diversity, marine fauna, dominated by bivalves. Subordinate sandstones commonly contain vertebrate debris and a rich ichnofauna.

About 7.5 m of the Westbury Formation are absent in the Larne section, although they are present in The Larne borehole and at the outcrop at Whitehead and Cloghfin Port (Simms and Jeram 2007) (Fig. 6.1). The Westbury Formation comprises a series of coarsening-up and fining-up cycles (Macquaker, 1999). Simms and Jeram (2007) suggest that the Larne Basin is related to 4th order cyclicity. They based this assumption in apparent initial transgression in the lower 9 m of the Larne Basin succession, whilst the upper part (5m) generally coarsens-upward into the Lilstock Formation. Evidence of deposition above storm wave-base is ubiquitous in the Westbury Formation (Simms and Jeram 2007) (Fig. 6.1).

6.1.2 The Cotham Member

The Cotham Member overlies the Westbury Formation and is divided into a lower part, which is dominated by finely interbedded (mm-scale) mudstone and siltstone (= heterolith); and an upper part, with limestones, calcareous marls, mudstone, and more thickly-bedded heterolith. The lower Cotham Member is commonly cross-bedded, with rippled surfaces, and represents a very shallow shoreface facies. It exhibits frequent, and

locally intense, soft sediment deformation (Simms and Jeram 2007). A prominent dark grey shale bed indicates transgressive phase of a 4th order cycle, and suggests that the entire lower part was deposited during within two 4th order cycle. A desiccation-cracked emergent surface occurs near the top of the lower Cotham Member (Simms and Jeram 2007) (Fig. 6.1). However there is no evidence of erosion at the surface. Macrofossils and bioturbation are largely absent (Simms and Jeram 2007).

The Upper Cotham fines up, indicating deep water environments above the emergent surface. Three distinctive, laminated micritic limestones occur just above this surface and can be correlated to other sites in the basin (Simms and Jeram 2007). Above the limestones, abundant bivalves reappear in marly siltstone and dark shale of similar facies to the underlying Westbury Formation. Bioturbation is present in the thicker-bedded heterolith at the top of the member, along with convex-up shell pavements on discontinuous siltstone laminae.

6.1.3 The Langport Member

The Cotham Member is overlain by the Langport Member, which is divided into lower and upper part. The part of The Langport Member consists of inter-bedded siltstone and micaceous mudstone, with the frequency and thickness of the siltstones decreasing up-section. The next half generally coarsens-upward, with siltstones and the heterolith facies. The upper part of The Langport Member is characterised by a distinctive series of thin micritic limestone ribs and laminae, containing rounded and angular clasts of mudstone (Simms and Jeram 2007).

6.1.4 The Lias Group

Above the Langport Member a 1m thick, dark grey, shaly mudstone is taken to mark the base of Lias Group. This unit is pyrite-rich and can be correlated with the “paper shale” found throughout Southwest of Britain (Wignall, 2000, Simms and Jeram 2007), which reflects rapid deepening (Fig. 6.1). The base of the Lias Group is generally referred to as the ‘Pre-Planorbis Beds’ in the UK. Bivalves are abundant throughout the basal Lias Group at Larne but, in contrast to those in the Penarth Group, convex-up shell pavements do not occur, suggesting deeper water. The Waterloo Mudstone Formation was deposited primarily as hemipelagic marine mudstone in the extensive, but relatively shallow, north-western European seaway. It consists of rhythmically-bedded mudstone, marl and shale, with variable organic carbon and silt content, and with a diverse, fully marine fauna (Simms and Jeram 2007).

6.2 Richness

A total of 1,561 individuals corresponding to 42 species, grouped in 26 families, 14 orders, 5 classes and 2 phyla were identified from 36 samples taken along the Jurassic-Triassic section at Larne (Appendix 6.1).

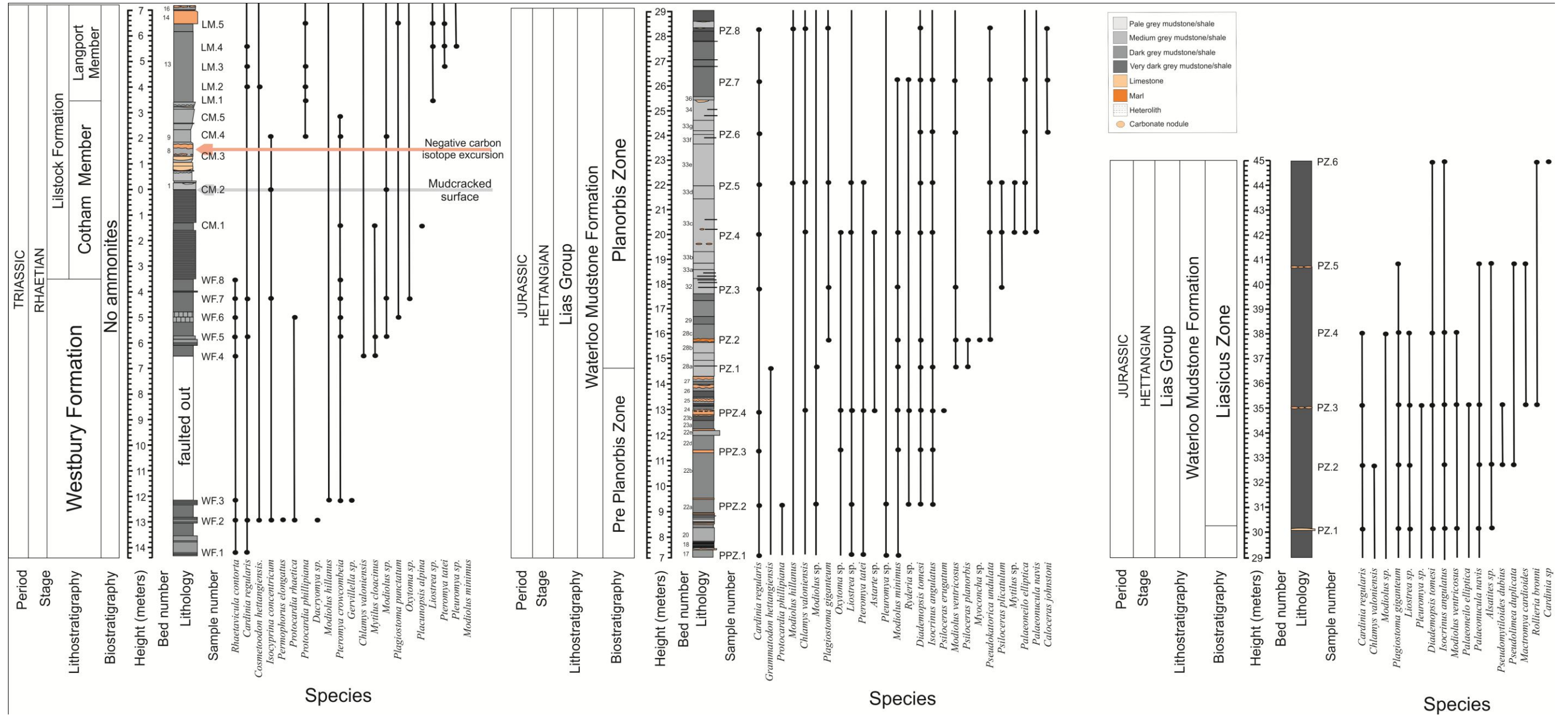


Figure 6.1 Lithostratigraphic log of the Penarth Group and basal Lias Group exposed at Waterloo Bay. Occurrences (●) and ranges (black lines) of taxa recorded from 36 samples taken from the Larne section. The author would like to extend a big thank you to A. Jeram for his support in drawing-up this log.

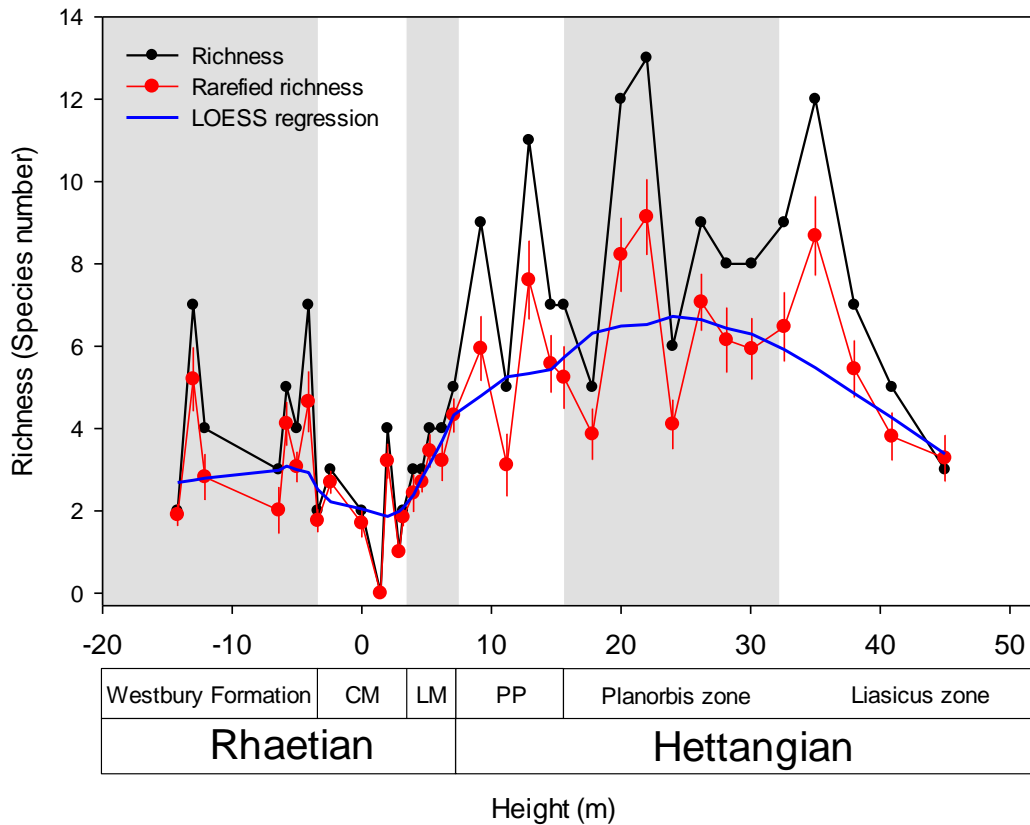


Figure 6.2 Raw (black line) and Mean species richness (red line \pm 2 S.D.) recorded for each sample collected. The mean represents the rarefied within-sample marine invertebrate richness estimated by 10000 iterations. The blue line is the LOESS regression through the data point estimated with an alpha 0.3. CM: Cotham Member, LM: Langport Member, PP: Pre-Planorbis Zone.

Fifteen species were recorded from the Westbury Formation, which represent the 36% of the total species recorded through the section (Appendix 6.2). Mean taxonomic diversity through this unit remained constant (Fig. 6.2, Blue line), although the minimum and maximum values of species number fluctuated between 2 and 7 species per sample (mean \sim 4). The minimum values were observed at -14.2 and -3.4 m from the mud-cracked surface of the mid-Cotham Member (0 m; Fig. 6.1), whilst the two highest peak (7 species) were recorded at -13 and -4.1 m, respectively (Fig. 6.2).

The Cotham Member contained 14% (6 sp.) of the total species observed along the section, which indicates a decrease of 20% with respect to the taxonomic diversity

observed in the Westbury Formation. Through the Cotham Member, species number fluctuates between samples (mean ~2), with peaks at -1.2 m (3 spp.) and 2 m (4 spp.). The minimum richness value (0 occurrences) was observed at 1.45 m (Sample CM3) after the mud-cracked surface (MCS) (0 m). Above this horizon, the number of species fluctuated between 4 and 1 species before cross through the Langport Member (Fig. 6.2).

The number of species increases through the Langport Member reaching a maximum of 4 spp. at 5.2 and 6.2 m above the base of the MCS. Despite this, the Langport Member still records comparatively a low taxonomic diversity through the section with a total of just 7 spp. representing 17% of all species found in this section. Despite this, the Langport Member records the onset of ecosystem recovery and the biggest composition turnover after the Tr/J boundary (Fig. 6.2).

From the base of the Pre-Planorbis Zone (7.10 m above the MCS) to the highest sample in the Planorbis Zone (28.15 m) 26 spp. (63% of the total) were recorded. Throughout this interval species number increases although at a lower rate than observed in the Langport Member. From the base of the Pre-Planorbis Zone to 22 metres above the MCS, the species richness shows three biggest peaks at 9.1, 12.9 and 22.8 m with 9, 11 and 13 spp. respectively. The lowest richness (5 spp.) values were recorded at 7.1 m, 11.2 m, and 17.8 m above the MCS (Fig. 6.2). Between 24 and 35 m above the MCS, species number increases rapidly and reaches a maximum of 12 species. From 35 to 45 m above the MCS, the species number drops to the same values than observed in the Pre-Planorbis Zone (mean ~7 spp.). The Liasicus Zone contains 40% (17 spp.) of all the species observed throughout the section (Appendix 5.2).

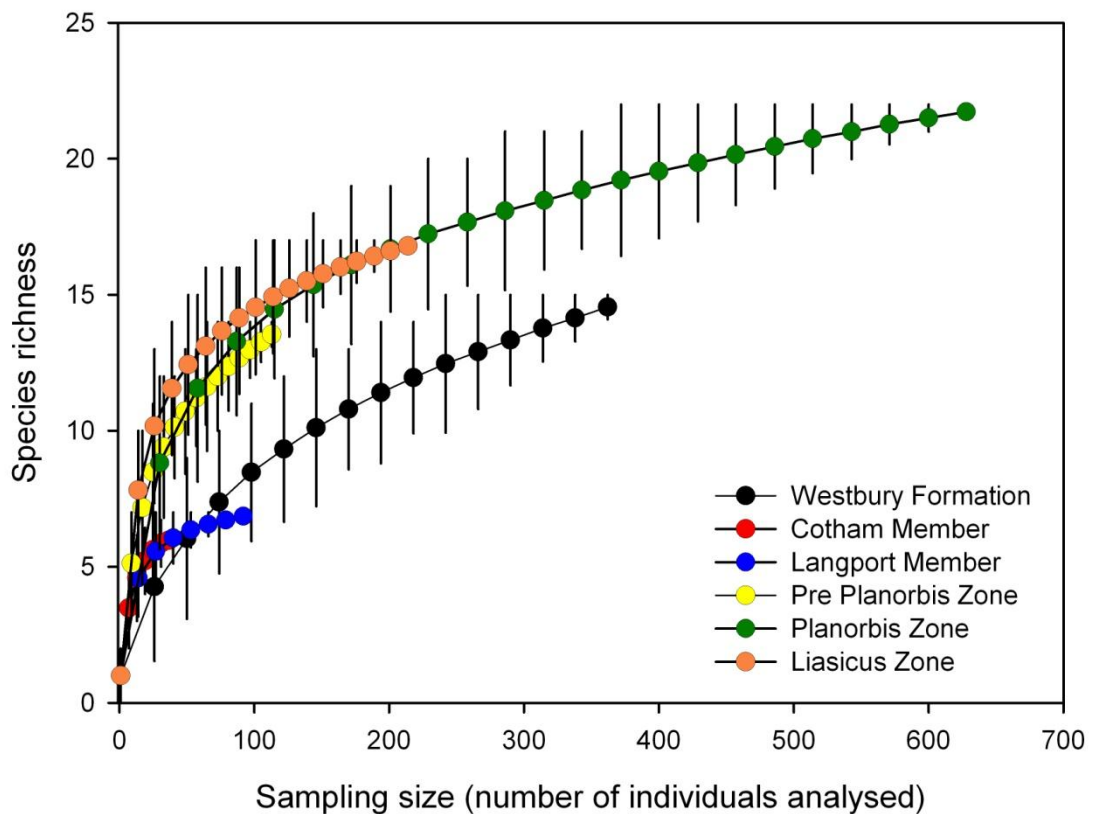


Figure 6.3 Average values ($\pm 95\%$ confidence intervals) of species richness estimated as sampling size increases through the Tr/J boundary in the Larne section. Significant differences were assumed if 95% confidence intervals did not overlap.

Sample rarefaction, performed by increasing the sampling size (see Chapter 2), showed that the number of species drops from the Westbury Formation (15 sp. 362 individuals) to the Cotham Member (6 sp. 37 individuals) and increases significantly throughout the Hettangian, reaching a maximum species richness on Planorbis Zone (22 spp. 628 individuals) (Fig. 6.3). Estimations based on among-sample richness using Mao Tau, Chao₁ and Jackknife₁ metrics (Fig. 6.4) confirm the decrease of taxonomic diversity from the Westbury Formation to the Cotham Member and the later, the richness increase from the Langport Member to the Planorbis Zone. However the species number tends throughout the Liasicus Zone (Fig. 6.4).

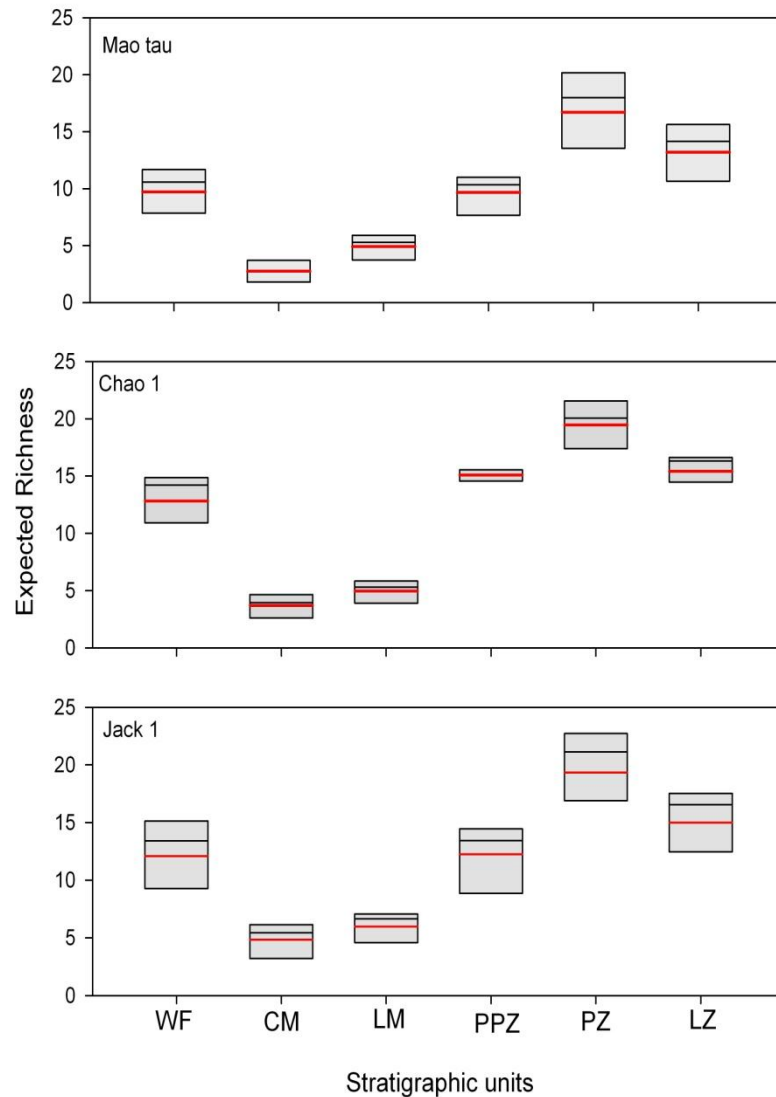


Figure 6.4 Boxplot of the rarefied within-sample marine fauna (Mao Tau, Chao₁ and Jackknife₁) during the study interval in Larne section. Each box represents the 95% confidence interval. The median is indicated by inner black line and the mean by a red line. WF: Westbury Formation, CM: Cotham Member, LM: Langport Member, PPZ: Pre-Planorbis Zone, PZ: Planorbis Zone, LZ: Liasicus Zone.

Alternatively, estimates of the Shannon-Wiener index [H'] with increasing sampling size (Fig. 6.5) indicates that mean diversity [H'] is lower in the Westbury Formation.

The fauna associate with the Cotham Member and the Langport Member did not record differences in mean diversity [H'] values, equally the Pre-Planorbis and the Planorbis faunas did not show significant differences; however records higher diversity [H'] values that observed during the Cotham and the Langport members. The Liasicus Zone

shows the higher mean diversity [H'] values throughout the section. The discrepancies observed between the Shannon-Wiener index [H'] and the rarefied expected richness are due to the fact that the [H'] index weights abundance values rather than just the number of the species when it is performed.

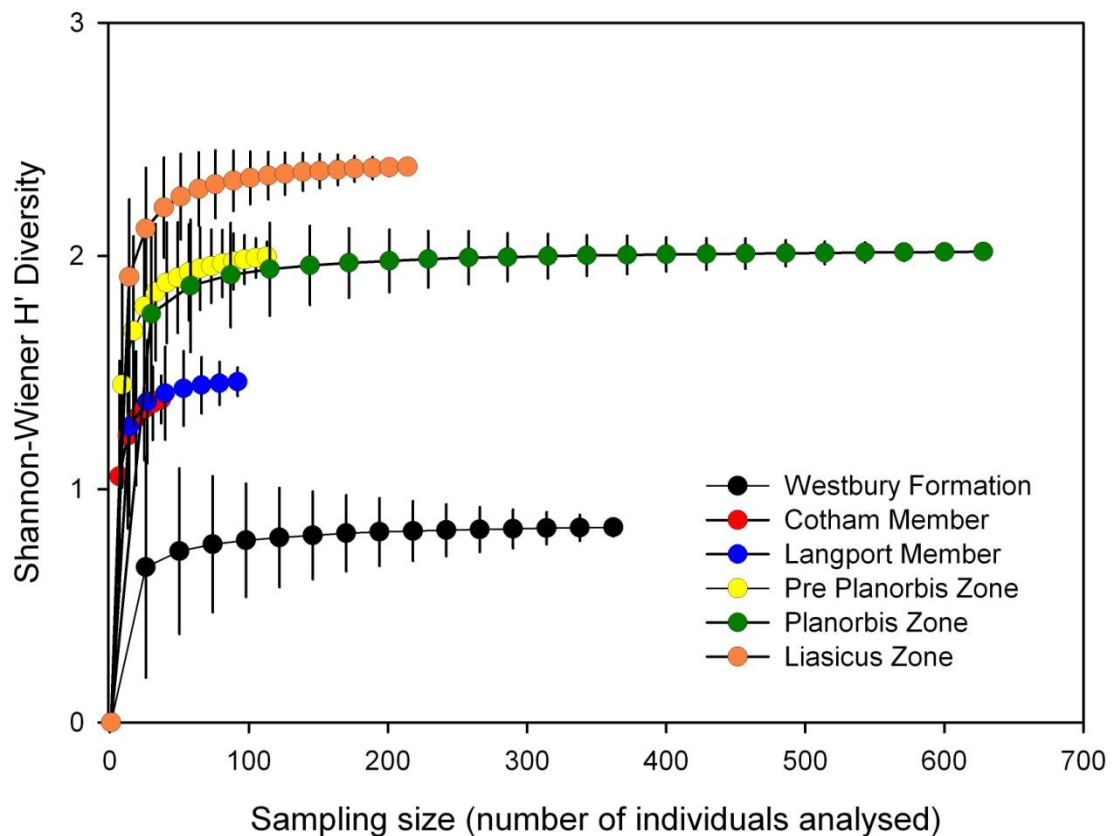


Figure 6.5 Average values ($\pm 95\%$ confidence intervals) of Shannon-Wiener diversity estimated as sampling size increases before, during the Tr/J interval. Significant differences are assumed if 95% confidence intervals did not overlap.

6.3 Abundance

The kurtosis tends to decrease along the Tr/J section at Larne (slope = - 0.19). Despite this the assemblages shows high variation in term of dominance (Fig. 6.6). Through the Westbury Formation the mean dominance tends to decrease until the base of the Cotham Member. Above this, the mean values increase quickly until 4 m in the Langport Member. Later, the kurtosis decrease to the base of the Pre-Planorbis Zone.

That increase in dominance coincides with the loss of species and with the negative carbon isotope excursion (Fig 6.1 for isotope excursion). Through the Hettangian, the assemblage records more even communities (average $\sim 18.8 \pm 2.14$), although at the end of the Pre-Planorbis Zone, the dominance increase significantly (Fig 6.6, Appendix 6.2).

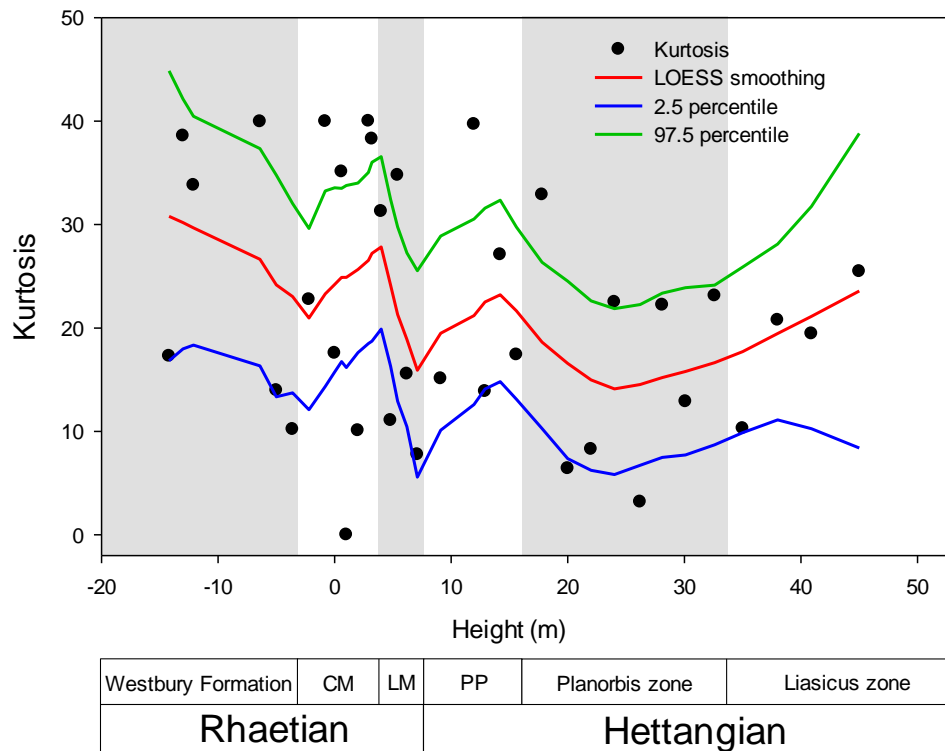


Figure 6.6 Dominance (Kurtosis \pm 95% confidence intervals) of marine fossils assemblages through the Tr/J boundary in the Larne section. The red line is the LOESS regression through the data point estimated with an alpha 0.3. CM: Cotham Member, LM: Langport Member, PP: Pre-Planorbis Zone.

From 15 species identified during the Westbury Formation, *Rhaetavicula contorta* was the most abundant, comprising 82% of the individuals. *Pteromya crowcombeia* comprised 8%, *Dacryomya* sp. 3% and *Cardinia regularis* ~2%. Five taxa showed abundance greater than 0.3% and 6 species show singleton occurrences with abundances <0.3% (Appendix 6.3 and 6.4). Examination of the shape of the rank abundance curves through Akaike's weight showed that the Zipf Model provided the best fit to the invertebrate community the Westbury Formation (Fig. 6.7; Table 6.1).

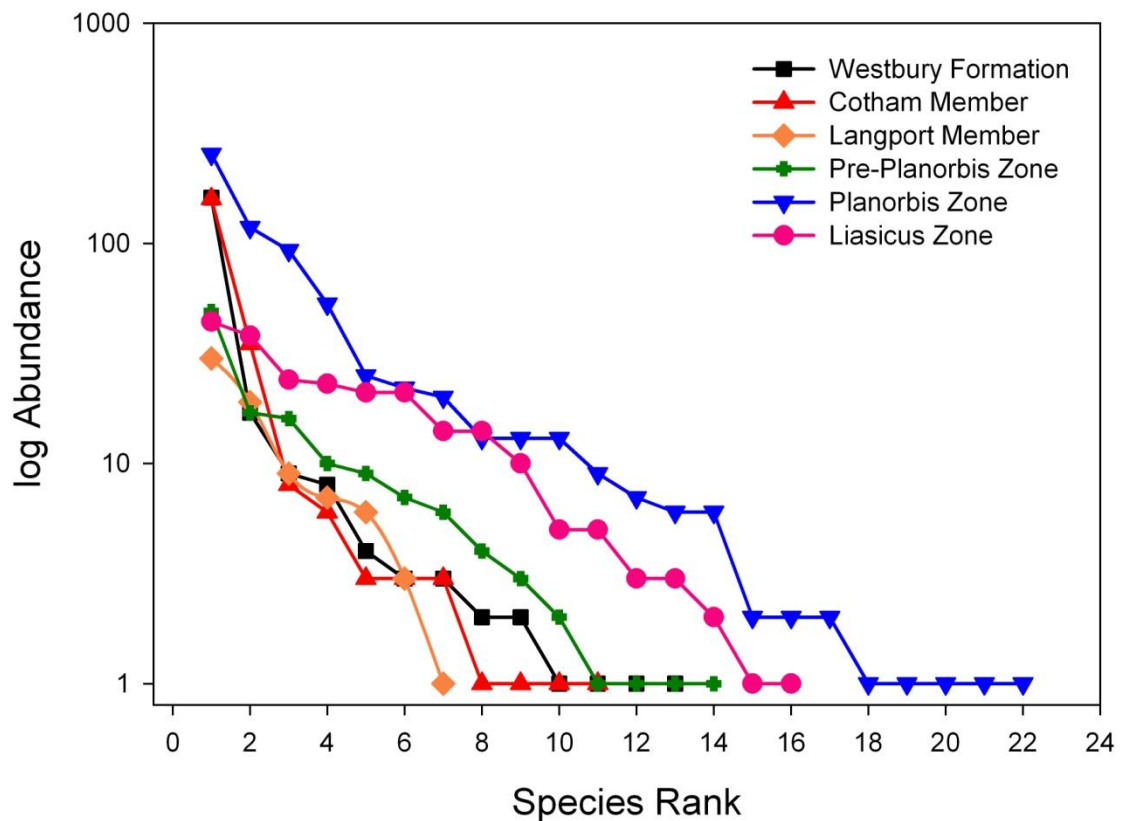


Figure 6.7 Rank abundance curves derived from the abundance of marine invertebrate fossil assemblages throughout the Tr/J boundary. Y-axis on $\log(n)$ scale.

The assemblages sampled in the Cotham Member record on average a high dominance. *P. crowcombeia* was the most dominant species (52%), followed by *Modiolus* sp. (17%) and *P. alpina* (14%). The remainder of the species recorded a relative abundance less than 8% (Appendix 6.3 and 6.4). The geometric model was the best fit of this RACs distribution through this stratigraphic unit (Fig. 6.7; Table 6.1).

During the Langport Member the assemblages display a more even abundance distribution (Fig. 6.6; Appendix 6.3 and 6.4). *P. philippiana* was the super-dominant reaching 44% of all species, follow by *P. tatei* (28%) and *Liostrea* sp. (10%). *C. regularis*, *P. punctatus* and *C. hettangiensis* reappear with an abundance of 8%, 6% and 1%, respectively. Finally, *Pleuromya* sp. recorded a single occurrence with a relative abundance ~3% (Appendix 6.3 and 6.4). Finally, the broken stick model was the best

descriptor of the rank abundance distribution (Fig. 6.7; Table 6.1). This model indicates that the abundance of the species are equally distributed.

Table 6.1 Comparison of RAD models derived from abundance distribution of marine invertebrates through the End Triassic mass extinction event. The models were ranked based on Akaike's weight (ω_i) following Burnham & Anderson's recommendation. AICc sample-size corrected was estimated as $AICc = AIC + (2K[K+1]) / (n-K-1)$. AIC is report only for completeness. K is the number of parameters; T is the number of taxa; n is the number of specimens. The highest ω_i gives the best fit (**In bold**).

	T	n	RAD models					
			AIC	Broken stick	Geometric	Log normal	Zipf	Zift Mandelbrot
Parameters (K)				0	1	2	2	3
			AIC	75.839	75.319	87.817	111.987	79.187
Liasicus Zone	17	230	AICc	4.739	5.421	7.701	9.427	9.322
			ω_i	0.468	0.333	0.106	0.044	0.047
			AIC	412.950	153.735	111.503	143.003	108.269
Planorbis Zone	23	663	AICc	19.664	7.986	6.921	8.579	8.348
			ω_i	6.797×10^{-4}	0.233	0.397	0.173	0.194
			AIC	65.796	59.554	54.851	58.535	58.999
Pre-Planorbis Zone	14	127	AICc	5.0612	5.462	6.804	7.139	10.099
			ω_i	0.374	0.306	0.156	0.132	0.030
			AIC	35.556	36.174	38.151	44.469	40.093
Langport Member	7	107	AICc	5.926	8.4349	14.537	16.117	27.364
			ω_i	0.766	0.218	0.010	0.004	1.695×10^{-5}
			AIC	24.117	25.257	26.410	25.231	27.231
Cotham Member	6	42	AICc	7.291	7.204	14.776	14.984	34.040
			ω_i	0.478	0.498	0.011	0.010	7.439×10^{-7}
			AIC	698.305	238.036	104.859	74.454	76.454
Westbury Formation	15	392	AICc	49.878	18.772	10.404	7.871	10.768
			ω_i	4.96×10^{-10}	0.002	0.185	0.657	0.154

The number of species recorded in the Pre-Planorbis Zone is relatively high (14 sp.), although the differences in relative abundance between species decrease smoothly (range: 39% - 0.8%). In this assemblage the dominant species are *Modiolus minimus*, *Diademopsis tomesi*, *Cardinia regularis*, *Liostrea* sp. and *P. tatei* abundance (Appendix 6.3). Like the Langport Member the broken stick model best fits this RAC (Fig. 6.7; Table 6.1).

More even assemblages were recorded in the Planorbis Zone, in which 23 species were recorded, within (> 5%) are *M. minimus*, *M. ventricosus*, *C. regularis*, *Modiolus* sp. Within this unit, the crinoid *I. angulatus* appears for first time and pelagic carnivores such as *P. planorbis* and *C. johnstoni* recorded relative average abundance ~1.8 %. In this unit, the lognormal RACs distribution model best fits recorded rank abundances as a majority of the assemblages are associated with highest evenness (Fig. 6.7; Table 6.1; Appendix 6.3).

During the Liasicus Zone, kurtosis values increase slightly. Through this zone the species number remains relatively high (17 sp.), although the RACs of this assemblage best fit to the broken stick model (Fig. 6.7; Table 6.1; Appendix 6.3). Sample rarefaction of the “species dominance index” (Fig. 6.8), also shows a decrease of dominance from the Westbury Formation to the Liasicus Zones of the Waterloo Mudstone Formation. Five groups were identified (see confidence intervals, Fig. 5.8). The first group comprising the Westbury Formation, which shows a highest dominance (average = 0.87 ± 0.014) (Fig. 6.8). The second group correspond to assemblages associate with the Cotham Member (Fig. 6.8). The third group, a less dominant assemblage, is made up by the Langport Member (0.55 ± 0.048). The fourth group is made up by the Pre-Planorbis and the Planorbis Zones (0.41 ± 0.022) (Fig. 5.8). Finally, The Liasicus Zone constitutes the fifth group with the lowest dominance values (0.24 ± 0.044) (Fig. 6.8).

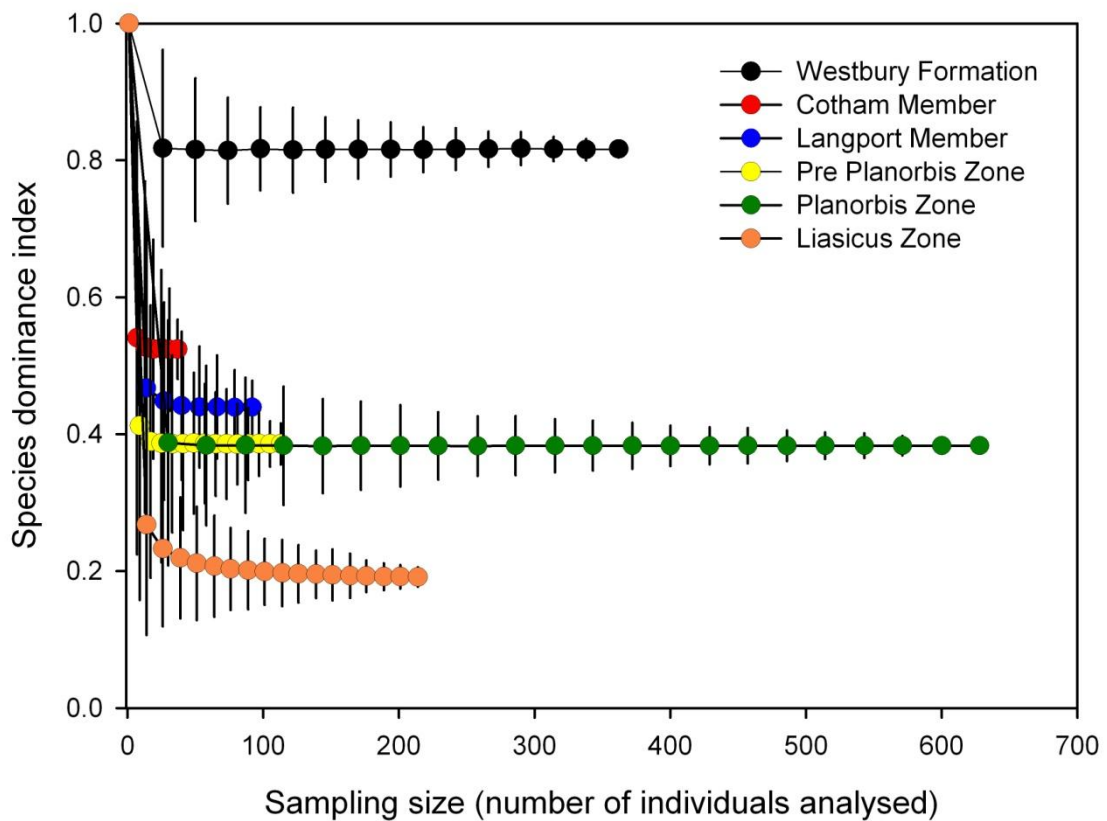


Figure 6.8 Average values ($\pm 95\%$ confidence intervals) of dominance estimated as sampling size increases through the Tr/J interval at Larne section. Significant differences are assumed if 95% confidence intervals do not overlap.

6.4 Composition

The Non-Metric Multidimensional scaling ordination shows that the samples from the Triassic are significantly separate from the Jurassic, perhaps due to major richness showed during the Hettangian Stage (Fig. 6.9). One-way ANOSIM shows significant differences between the composition fauna from each unit ($R = 0.633$; $p = 0.0001$). SIMPER analysis reveals that assemblages associate with the Cotham Member records higher dissimilarity compare to assemblage relate to the Westbury Formation, the Langport Member and the Waterloo Formation (Appendix 6.5).

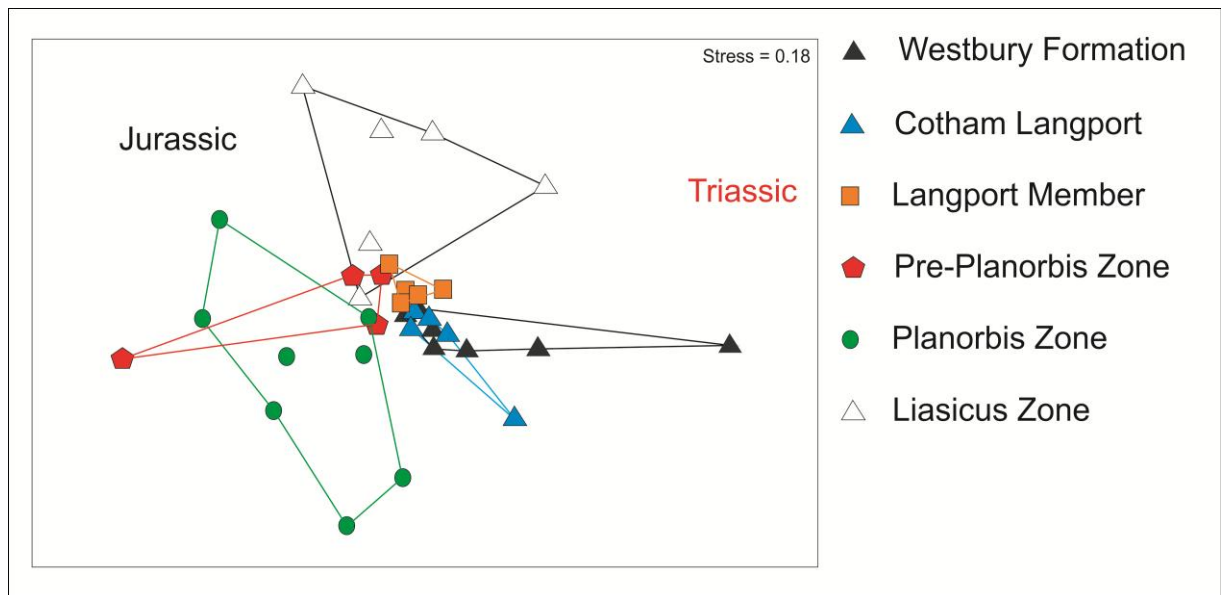


Figure 6.9 No metric multidimensional scaling (NMDS) plot resulting from the ordination analysis (Euclidean distance) of the marine invertebrate fauna from the from Larne section, using abundance data.

The faunal composition from the Westbury Formation to the Cotham Member records an average dissimilarity of 89.2% (Appendix 6.5). From the 15 species recorded in the Westbury Formation, seven species recorded singleton occurrences (Fig. 6.1), eleven species disappeared (Appendix 6.6) and just three species cross into the Cotham Member (Appendix 6.5). *Gervillella* sp. *Permophorus elongatus*, *R. contorta* and *Dacryomya* sp. became extinct, while seven other species reappeared from the Langport Member (Appendix 6.6).

The Cotham and Langport members record an average dissimilarity ~94% (Appendix 6.5). During the Cotham Member, 4 species disappear: *I. concentricum*, *P. alpina*, *M. cloacinus* and *P. crowcombeia*, while just *Modiolus* sp. and *P. philippiana* cross into the Langport Member. During the Cotham Member two species shows unique occurrences (Fig. 6.1, Appendix 6.6).

The dissimilarity between the Langport Member to the Pre-Planorbis Zone dropped to ~84%. Within the Langport Member just two species disappeared: *P. punctatum* and *C. hettangiensis*. Three new species appear and *Cardinia* re-appears into the assemblage, while *P. philippiana* is the only species that crosses into the Pre-Planorbis Zone (Appendix 6.6). Though the Langport Member 5 species showed singleton occurrences (Fig. 5.1).

From the Pre-Planorbis to the Planorbis Zone two species disappeared at the boundary, 12 new species appeared, two genera re-appear (*C. hettangiensis* and *M. hillanus*), 10 species cross through the Liasicus zone and 9 species occurred in both zones. The mean dissimilarity between both units decreased to ~82%, showing a high similarity between periods (Appendix 6.5 and 6.6) (Fig. 6.1).

The dissimilarity increases 88% between the Planorbis and the Liasicus zones, both stratigraphic units sharing 10 species (Appendix 6.3). The Planorbis Zone recorded 13 unique occurrences, whilst the Liasicus Zone recorded 7 single species, perhaps due to colonisation of new species. In addition, the Liasicus Zone underwent one of the biggest decreases in species richness; however it was not enough for generating significant differences in composition (Appendix 6.6).

In summary, 82% of the Westbury Formation assemblage disappears at the base of the Cotham Member. From the residual fauna, 67% underwent extinction before to reach the base of the Langport Member. In addition, dissimilarity percentage of the marine assemblage increases within the Cotham Member (94%; Appendix 6.5), which confirmed the compositional turnover estimates by B_w and B_r indices (Fig. 6.10; Appendix 6.2), which suggest that the extinction could be placed at the Cotham Member.

On the other hand, the random disappearance of some taxa and the high frequency of singleton occurrences through the Larnie section could reflect facies changes, sampling bias or well, biological process as, migration and/or dispersal. For that, stratigraphic ranges of taxa recorded in this study were compared with stratigraphic ranges of previous studies in the way to confirms global or regional extinction of some species (see Appendix 6.6).

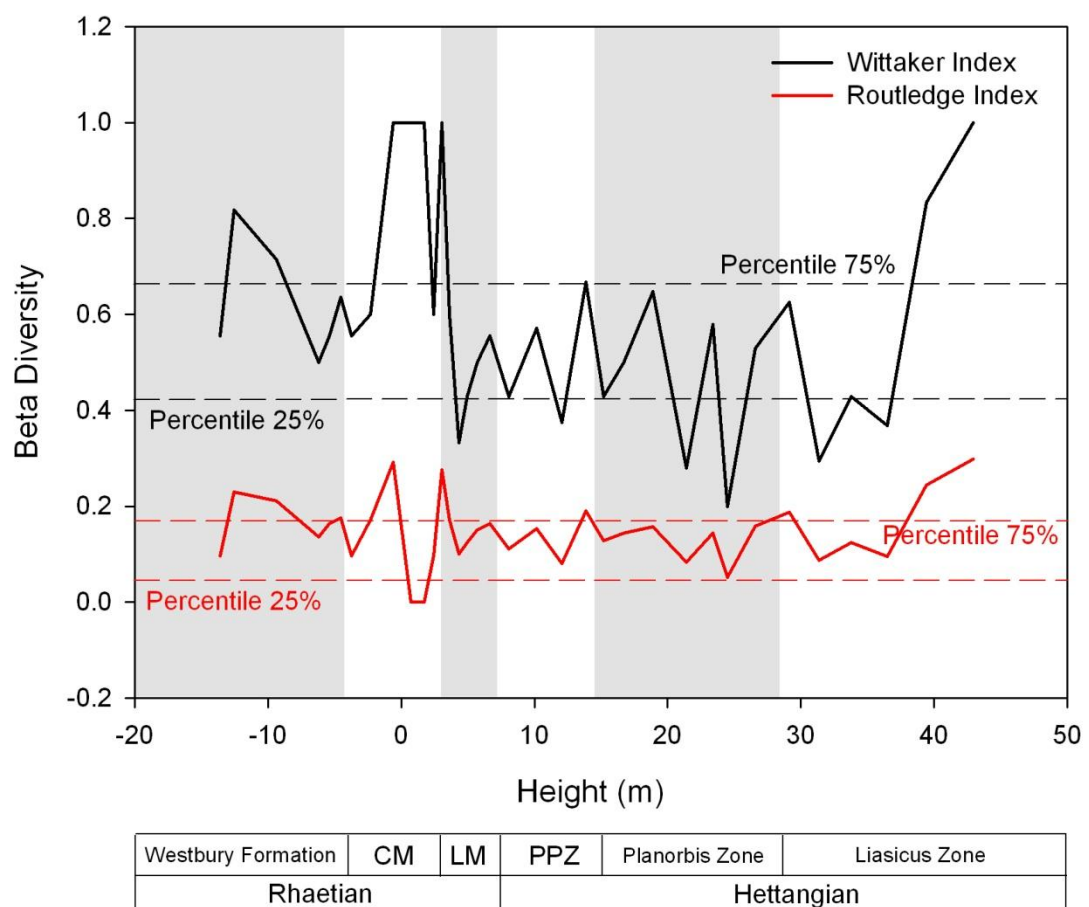


Figure 6.10 Beta diversity (β) estimated by Whittaker and Wilson-Shmida indices. Those indices reflect the temporal difference in species composition between samples. The percentiles represent the 95% confidence intervals calculated by bootstrap procedure (number of iterations = 10000). CM: Cotham Member, LM: Langport Member, PPZ: Pre-Planorbis Zone.

Of the taxa recorded of this locality, just three genera show global extinction, *Permophorus*, *Rhaetavicula* and *Pteromya*. *Permophorus* and *Rhaetavicula* disappear at the top of the Westbury Formation. While *Pteromya*, disappears at the base of the Planorbis Zone (Appendix 6.6). On the other hand, five species shows regional extinction; *P. alpina*, *M. cloacinus*, *I. concentricum*, *P. rhaetica*. Although, *Mytilus*, re-appear in the Planorbis Zone.

6.5 Ecospace

A total of 10 modes of life are occupied by the marine invertebrate fauna within the study interval (Fig. 6.11). The fauna found in the Westbury Formation include four modes of life, occupying 1.1% of the theoretically available ecospace. The fauna was made up almost completely by facultative attached suspension feeders as surficial (6 species), semi-infaunal (4 species) and shallow infaunal (4 species) (Appendix 6.6). *Dacryomya* sp. was the only species that records slow motility (Fig. 6.11, Appendix 6.6). The fauna of the Westbury Formation, contains high number of species, but its ecological categories are restricted to just benthic filters species with low motility (Fig. 6.12, Appendix 6.6 and 6.7).

Although three modes of life are recorded in the Cotham Member, the relative proportion of the modes of life associated to semi-infaunal and surficial categories drops in average ~10% and the composition of each ecological category changed drastically (Fig. 6.12, Appendix 6.6 and 6.7). The fauna of the Langport Member records just three modes of life; (1) surficial, sessile, suspension feeders, which appeared for the first time and are represented just by one genus, *Liostrea* (Fig. 6.11); (2) Surficial, facultatively attached, suspension feeders, which recorded a complete compositional change from underlying strata (Appendix 6.6); and (3) shallow infaunal,

facultatively unattached, suspension feeders which increase the species number and record high compositional change from the Westbury Formation and the Cotham Member assemblages (Fig. 6.12; Appendix 6.6 and 6.7).

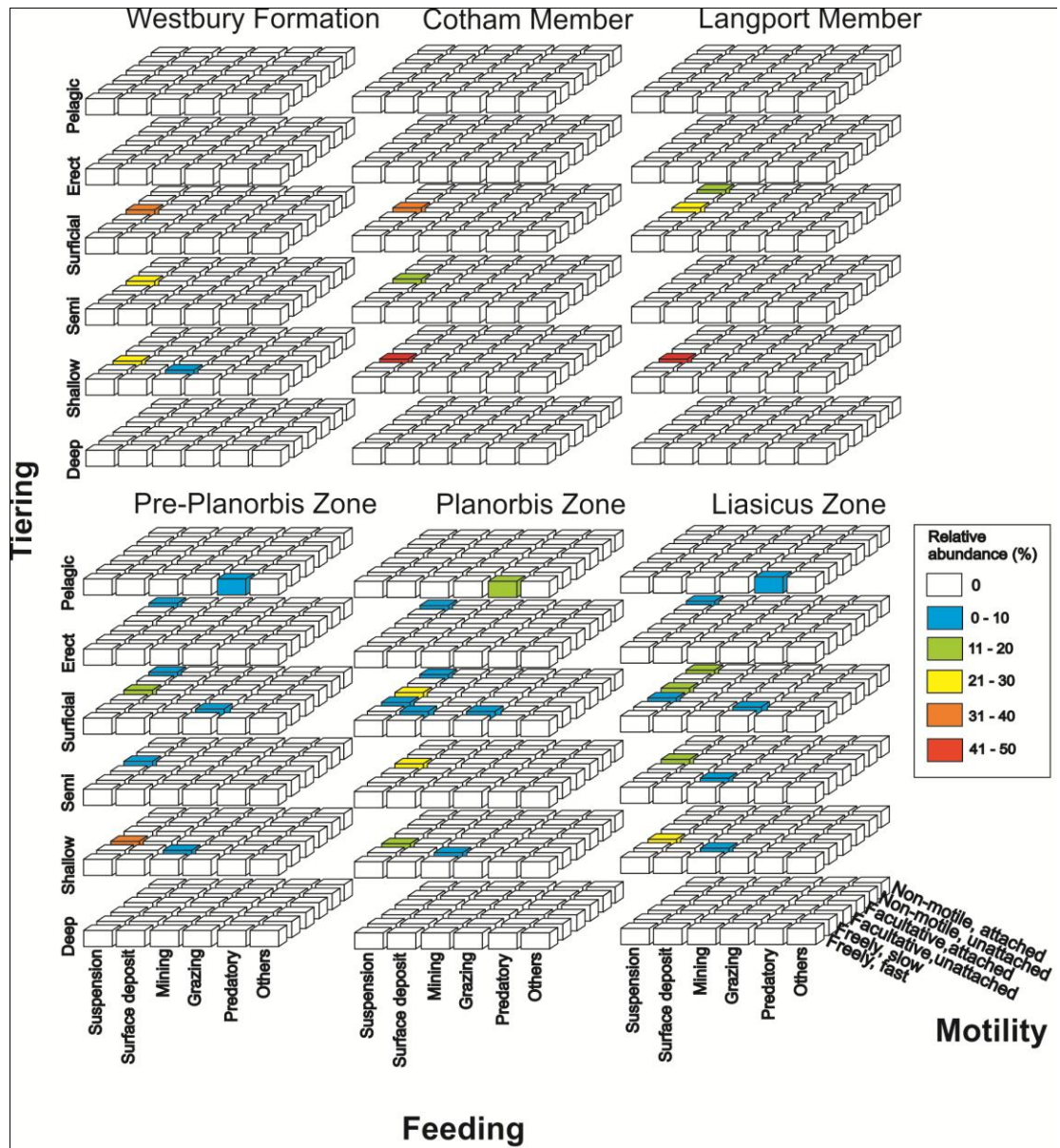


Figure 6.11 Theoretical ecospace occupations through the Tr/J interval at Larne section.

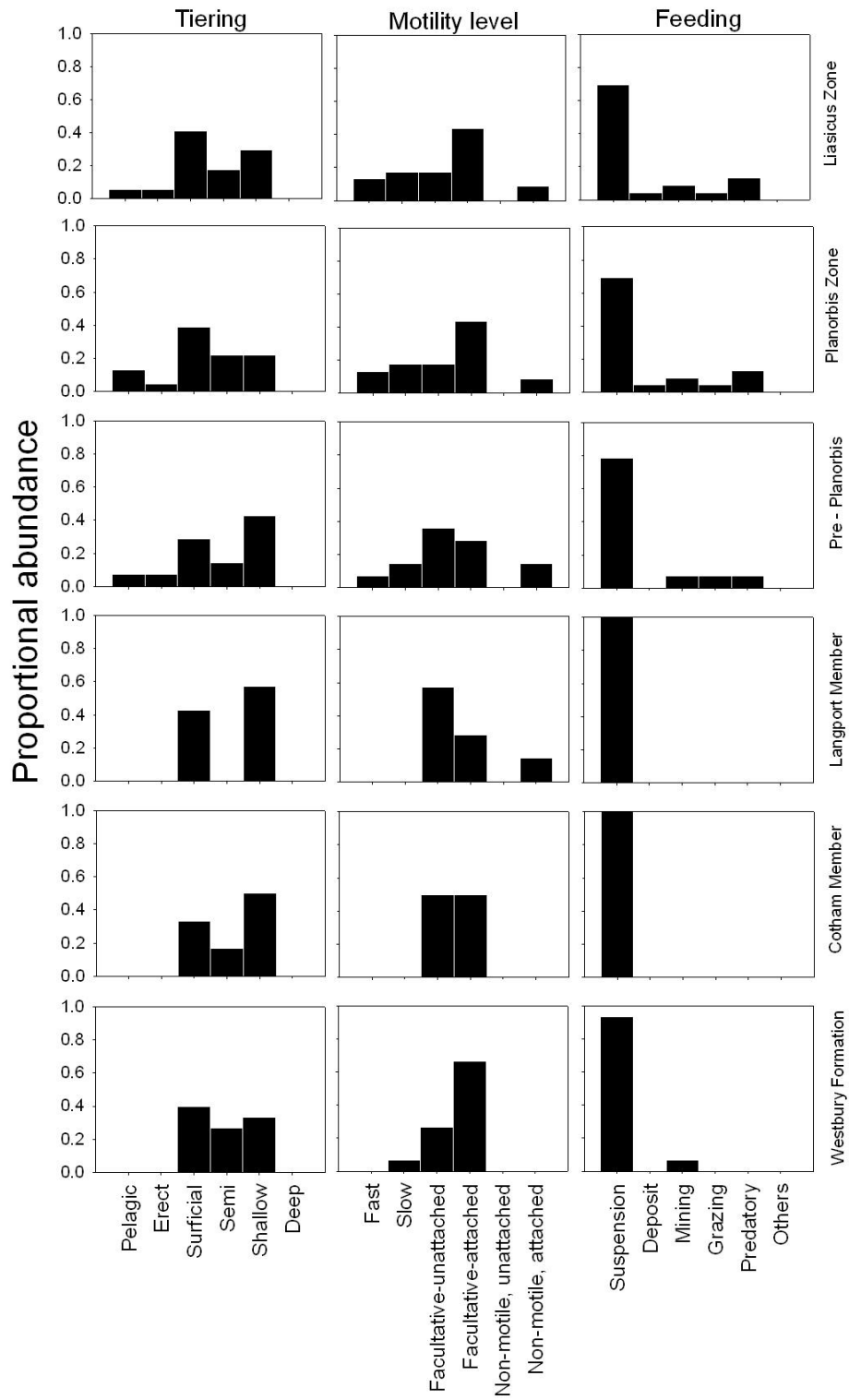


Figure 6.12 Proportional abundance of tiering, motility and feeding mechanisms based on species occurrences from the Westbury Formation to the Liasicus Zone.

From the Westbury Formation to the Langport Member there was a “gradual” disappearance of semi-infaunal genera such as *Modiolus*, *Permophorus* and *Gervillella* and a decrease in the abundance of shallow infaunal taxa (*Dacromya* sp. *Cardinia* sp. *Isocyprina* sp. *Protocardia* sp. and *Pteromya* sp.), which would suggest a selective extinction of taxa associated with semi- and shallow infaunal lifestyle during these intervals (see Semi-infaunal Fig. 6.12).

Through the Pre-Planorbis Zone the ecospace utilisation expanded. Eight modes of life were used by the Hettangian marine fauna including three new modes of life: fast pelagic predators (*Psiloceras* spp.), sessile erect suspension feeders (*Isocrinus angulatus*) and slow-moving epifaunal herbivores (*Diademopsis tomesi*) (Fig. 6.11) (Appendix 6.4). The semi faunal suspension feeder re-appears comprising the genus *Modiolus*, whilst *Ryderia* on the other hand, occupies a new category of slow-moving shallow miners mode of life (Fig. 6.11). Surficial, facultatively attached, suspension feeders and shallow infaunal, facultatively unattached, suspension feeders continue to occupy the ecospace. However, only the shallow-infaunal category records an increase in species occurrences (Fig. 6.12).

In the Planorbis Zone, the marine invertebrate fauna occupy 10 modes of life, eight modes in the previous assemblages. Two new modes of life are incorporated into the assemblage: surficial, facultative-unattached, filter feeders and epifaunal slow-moving deposit feeders (Fig. 6.11). Surficial, facultatively unattached, filter feeders made up by *Palaeonucula navis* (Bivalvia), while the slow-moving epifaunal was made up by the gastropod *Pseudokatosira undulata*. The abundance of groups as surficial, semi- and shallow-infaunal, decreases slightly in comparison to the Pre-Planorbis Zone (Fig. 6.12, Appendix 6.7).

Finally, 10 modes of life are used by the Liasicus Zone assemblage. Nine modes of life were used by the previous fauna, where slow moving, epifaunal, deposit feeders (*P. undulata*) is replaced by shallow slow-moving miners (*Rollieria bronni*) (Appendix 6.6). During this time the number of species per mode of life increases (packing) in the surficial and semi-infaunal categories (> 10%, Fig. 6.11).

6.6 Body Size

Figure 6.13 shows the trajectory of the body size and the rates of the change of body size of bivalves through the study interval. Through the Westbury Formation to the Cotham Member the mean body size did not change until the base of the Cotham Member (mean $\sim 7.84 \pm 0.56$). Mean body size then increase to a maximum peak at the base of the Pre-Planorbis Zone (mean $\sim 17.29 \pm 1.72$) due to the appearance of genera like *Cardinia* (15.94 ± 4.9 mm), *Plagiostoma* (27.74 ± 11.75 mm), *Liostrea* (18 ± 7.17 mm) and *Protocardia* (14.76 ± 3.5 mm) (Appendix 6.8). Later, the mean body size decrease significantly before to cross into the Planorbis Zone; species recorded in this level were *Chlamys valoniensis* (5.52 ± 1.14 mm), *Cardinia regularis* (12.50 ± 3.14 mm), *Liostrea hisingeri* (14.31 ± 3.14) and *Modiolus minimus* (4.81 ± 1.56 mm).

The second highest peak of the average mean body size is observed at the base of the Liasicus Zone (31.99 mm) at 32.6 m (Appendix 6.3). Above this the average size decreases to reach an average size of 8.76 ± 4.98 mm. At this level the fauna were constitutes mainly by *Plagiostoma giganteum* (27.90 ± 13.67 mm) and *Cardinia* sp. (9.46 ± 5.06 mm) (Appendix 6.8). In addition, the rate of change of body size shows that through the Cotham Member, the rate increase 68% respect from previous levels (Fig. 6.13). From the Langport Member to the Liasicus Zone the rate of changes did not record variation, which indicates that there was not variation in body size.

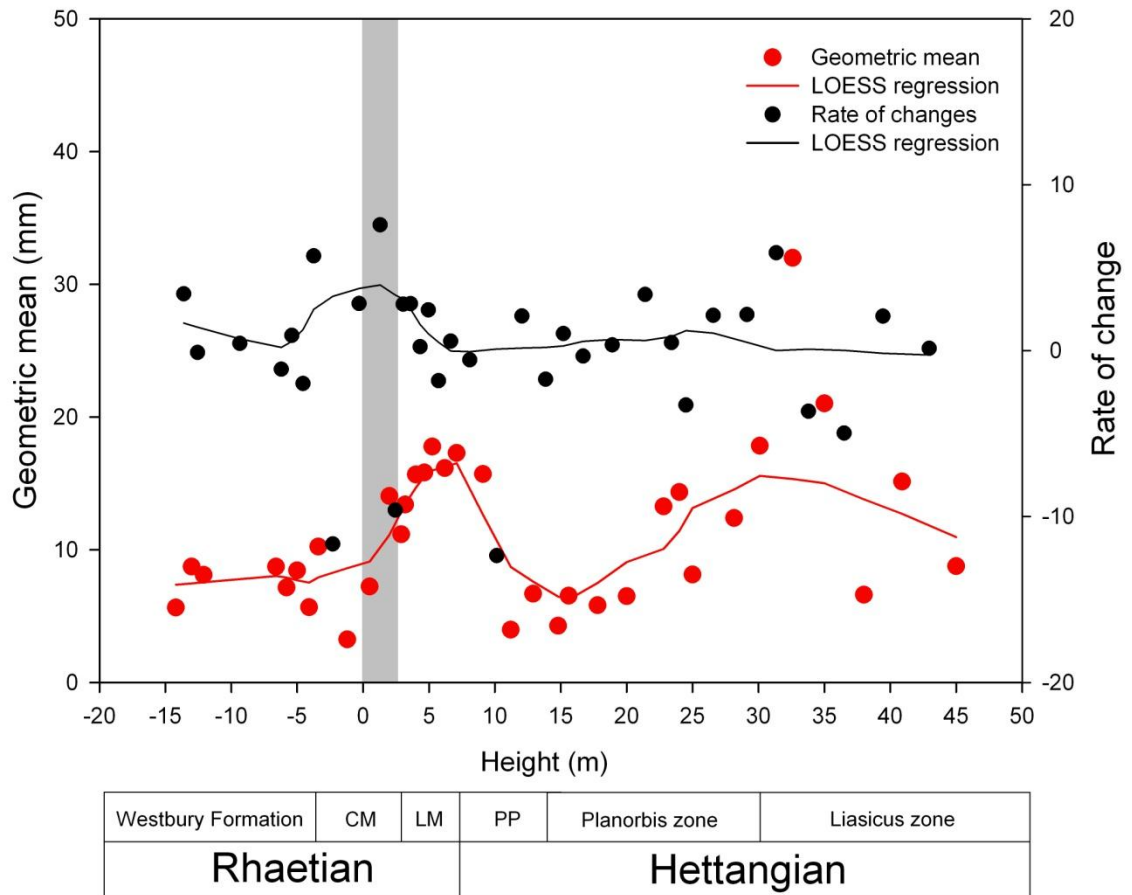


Figure 6.13 Time series of the average size (red dots) and rate of change (black dot) of bivalve's assemblage sampled through the Tr/J boundary from Larne section. The shading is used to indicate the negative carbon excursion. The red line is the LOESS regression through the data point estimated with an alpha 0.3. CM: Cotham Member, LM: Langport Member, PP: Pre-Planorbis Zone.

Size-frequency distribution based on 926 individuals measurements of bivalves from the studied section at Larne show a significant increase in size from the Westbury Formation to the Liasicus Zone, with a significant reduction of body size between the Pre-Planorbis and the Planorbis zones (Fig. 6.14). The variance associated with the mean body size increases throughout the section, which is related to the incorporation of new species of small size (Fig. 6.14, Appendix 6.8).

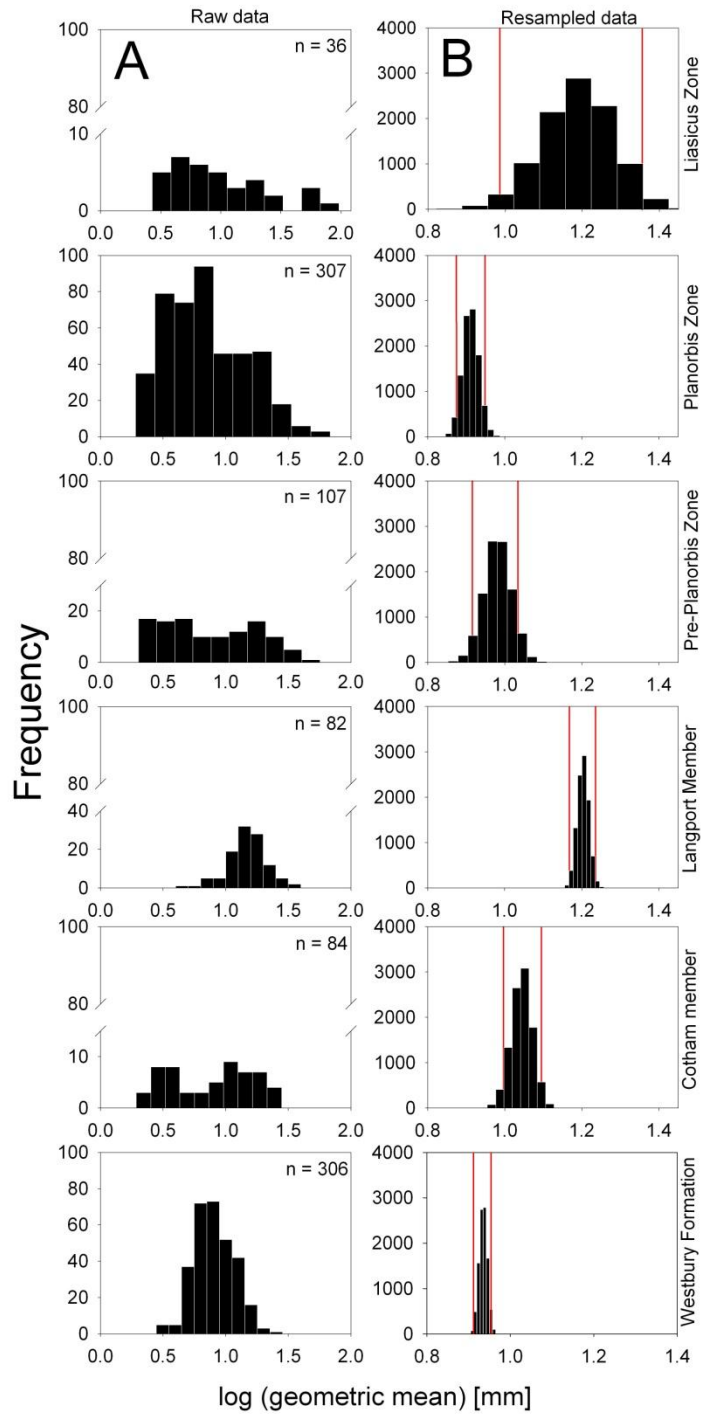


Figure 6.14 Frequency distribution of log mean of bivalve size sampled through the Tr/J interval at Larne section. (A) Shows the distribution frequency of raw data by each stratigraphic unit. (B) Shows the distribution frequency of re-sampled data by bootstrapping produce (10,000 iterations with replacement). The red lines indicate the percentiles of 2.5 and 97.5% around the mean.

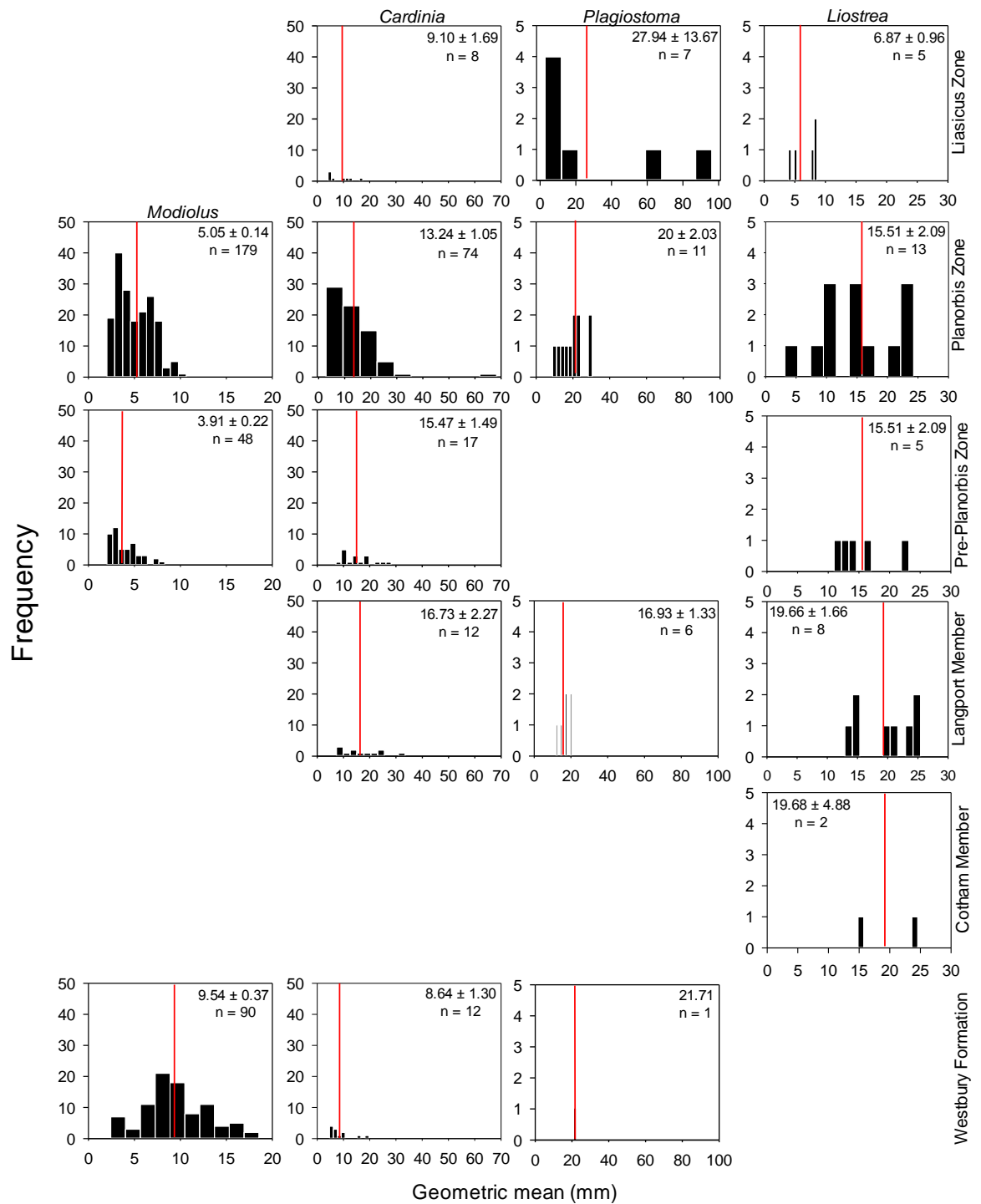


Figure 6.15 Frequency distributions of four bivalve genera commonly found through the study interval at Larne section. The red line indicates the average value. Average values, standard error (\pm) and number of individuals (n) are indicated in each graph.

Table 6.2 Body size parameters of four bivalve genera with frequent occurrences along the study interval at Larne section. WF: Westbury Formation, CM: Cotham Member, LM: Langport Member, PP: Pre-Planorbis Zone, PZ: Planorbis Zone, LZ: Liasicus Zone (Appendix 3.9).

	WF	CM	LM	PP	PZ	LZ
<i>Liostrea</i>						
Mean	---	19.686	19.666	15.511	15.346	6.873
Stand. Error	---	4.886	1.667	2.097	1.846	0.964
<i>n</i>	---	2	8	5	13	5
Max	---	24.571	25.458	23.145	24.279	8.613
Min	---	14.800	12.893	10.937	3.150	3.970
<i>Plagiostoma</i>						
Mean	21.71	---	---	16.932	20.007	27.947
Stand. Error	---	---	---	1.334	2.031	13.672
<i>n</i>	1	---	---	6	11	7
Max	21.71	---	---	20.408	30.497	96.317
Min	21.71	---	---	11.809	8.981	2.694
<i>Modiolus</i>						
Mean	9.562	---	---	3.919	5.055	---
Stand. Error	0.372	---	---	0.221	0.140	---
<i>n</i>	90	---	---	48	179	---
Max	18.546	---	---	8.304	10.644	---
Min	2.428	---	---	2.007	2.000	---
<i>Cardinia</i>						
Mean	8.864	---	16.731	15.470	13.246	9.107
Stand. Error	1.304	---	2.276	1.492	1.059	1.698
<i>n</i>	12	---	12	17	74	8
Max	19.684	---	33.483	28.265	68.350	17.382
Min	4.672	---	7.289	7.086	2.773	4.132

Figure 6.15 shows the size distribution of 4 genera that are highly represented in the succession in Larne. The size trajectory of each taxon seems to be highly variable. *Modiolus* records a high occurrence through the interval (309 individuals). Mean body size through the section decreases significantly from the Westbury Formation 9.56 ± 0.37 mm to the Pre-Planorbis ($F_{(2,316)} = 3.18 \times 10^{-41}$; $p < 0.05$). However from the Pre-Planorbis to the Planorbis Zone the body size increases from 3.19 ± 0.21 to 5.05 ± 0.14 mm, respectively.

The mean size of *Cardinia* increases from the Westbury Formation (8.86 ± 1.30 mm) to the Langport Member (16.73 ± 2.27 mm) and continues without significant changes to reach the Liasicus Zone where the body size drops to 9.10 ± 1.69 mm ($F_{(4,122)} = 3.65$; $p < 0.05$) (Table 6.2). On the contrary, the mean size of *Plagiostoma* did not record significant difference between assemblages ($F_{(2,23)} = 0.65$; $p > 0.05$). The mean size of *Liostrrea* decreases significantly only from the Planorbis Zone (15.51 ± 2.09 mm) to the Liasicus Zone (6.87 ± 0.96 mm). The body size did not show a difference from previous assemblages ($F_{(4,28)} = 0.01$; $p < 0.05$) (Fig. 6.15, Table 6.2).

Graphically, changes in the minimum and maximum body sizes of *Plagiostoma*, *Cardinia*, *Liostrrea* and *Modiolus* through the study interval (Rhaetian to Hettangian) can be visualised best by using Jablonski target plot (Fig. 6.16), which record the percentage of change in maximum and minimum size and are useful for determining whether the changes are simply due to changes in variance (Jablonski 1996).

The size trends in *Modiolus* did not experimentally change from the Westbury Formation to the Pre-Planorbis Zone the maximum and minimum sizes. However from the Pre-Planorbis to the Planorbis Zone, *Modiolus* tends to occupy the plot within the upper left quadrant, which indicates that body size tends to increase in variance (increase in the largest size and a decrease in the smallest size) (Fig. 6.16, Table 6.2).

From the Westbury Formation to the Langport Member the body size of *Cardinia* tends to increase (upper right quadrant) (Fig. 6.16, Table 6.2). From the Langport Member to the Planorbis Zone, the body size decreases. While from the Pre-Planorbis zone to the Planorbis Zone the body size tends to increase in variance and between the Planorbis to Liasicus Zones the *Cardinia* body size decreases in variance (increase in smallest the size and a decrease in the largest size) (Fig. 6.16, Table 6.2).

The body size of *Plagiostoma* tend to occupy the plot within the upper left quadrant, which indicates that body size tend to increase in variance (Fig. 6.16, Table 6.2). In contrary *Liostrea*, tend to shows an increase in variance (upper left quadrant) between the Langport Member and the Pre-Planorbis Zone and between, the Pre-Planorbis Zone and the Planorbis Zone. However at the Liasicus Zone the body size tend to decrease which is reflected by using the lower left quadrant (Fig. 6.16, Table 6.2).

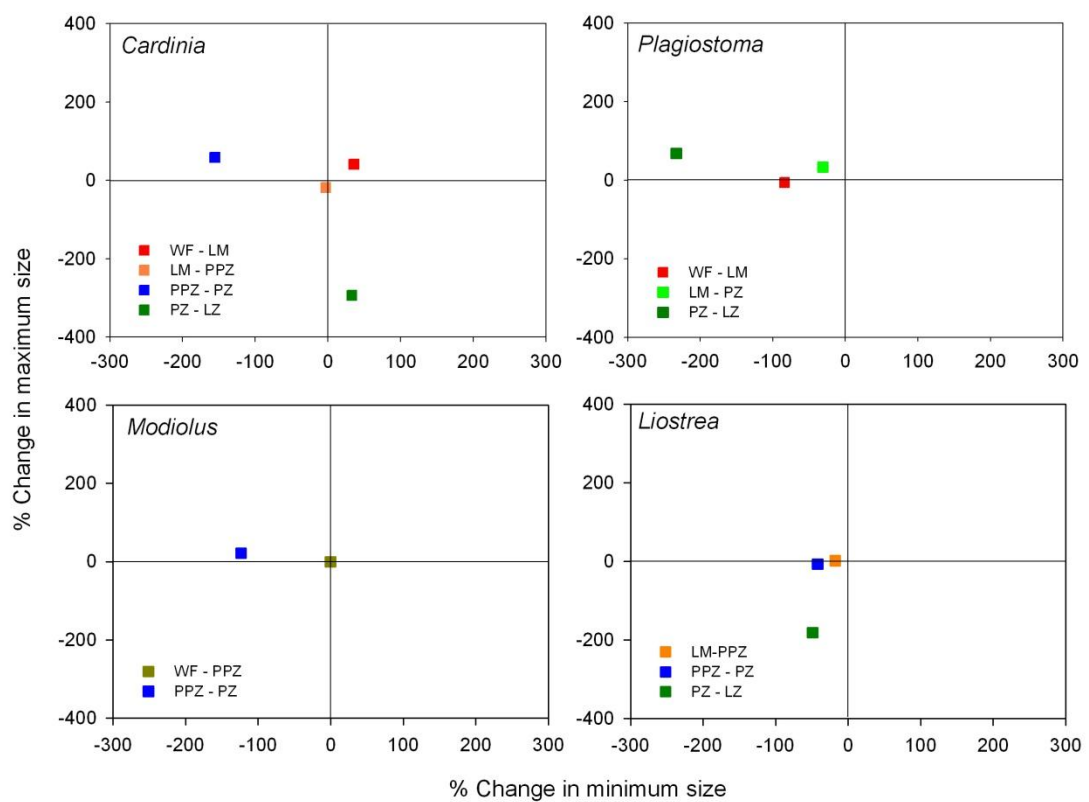


Figure 6.16 Change in frequency size in four bivalves genera through Late Triassic extinction event (after Jablonski, 1996). Top left and bottom right indicate variance in size whilst the top right and lower left represent Cope's Rule and size decrease, respectively.

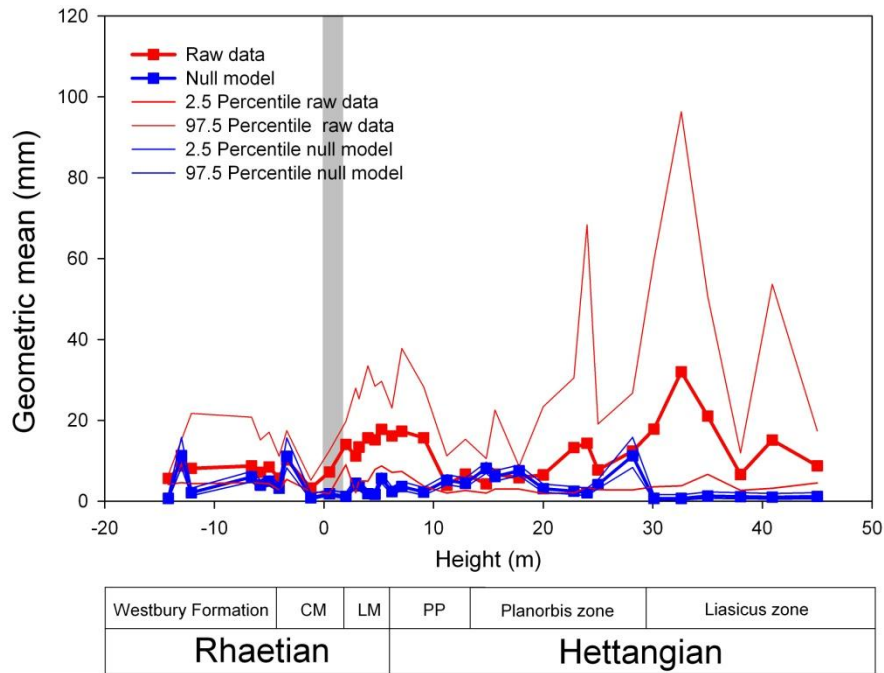


Figure 6.17 The average size of bivalves sampled through the study interval (red line, raw data \pm percentile 2.5 % and 97.5 %). Null model (blue line \pm percentile 2.5 % and 97.5 %) was calculated by row-permutation (number of iterations = 10000) of the geometric mean of each individual by specie through 35 samples (see appendix 6.10). The shading is used to indicate the negative carbon excursion. CM: Cotham Member, LM: Langport Member, PP: Pre-Planorbis Zone.

Finally, the mean body size of bivalves was significantly higher than the null model values that assume a random distribution of body sizes through the study interval. This indicates that overall bivalves show a directional trend to increase body size through the section (t -value = 6.56, df = 68; p < 0.001) (Fig. 6.17).

6.7 Summary

Sixty percent of the species disappear during the Cotham Member and the Langport Member, representing the onset of the recovery in which the number of the species reaches a maximum richness in the Planorbis Zone. In terms of abundance, the Cotham Member represents assemblages with few species and high dominant, condition reflected by Geometric model, which suggests to disturbed environments. On the other

hand, assemblages sampled from the Westbury Formation, the Langport Member and the Lias Group, present low dominance, which the rank abundance distribution tended to fit to lognormal or broken stick models, which reflect “normal communities”.

The marine fauna shows a constant, but low turnover of species composition through the study interval at Larne. However from the Cotham Member to the Langport Member the compositional differences reached 94%.

Ten modes of life were used by the marine fauna through the Tr/J boundary succession. In the Cotham Member, 3 modes of life were occupied by the marine fauna and the number of species per mode of life decrease >50%. Ecological categories as infaunal suffered a gradual decreases until disappear in the Langport Member. However from the Pre-Planorbis Zone to the Liasicus Zone, the number of modes of life used by the marine fauna increase and in the same time the abundance by mode of life.

Finally, the body size of marine bivalves did not decrease during the extinction event (The Cotham Member). Although the body size through the Tr/J in the Larne section seems highly variable between species and through the stratigraphic units, the general trend indicates that the marine bivalves tend to increase the body size.

Chapter 7 Portezuelo Providencia section

7.1 Geological setting

The sedimentary marine rocks of the Antofagasta region constitute a discontinuous band of outcrops located between 23°00'S and 26°30'S. These rocks were deposited from the Middle Triassic to the Middle Jurassic in a sedimentary basin of approximately 10,500 km². The lower part consists of intermediate to acid volcanic rocks of 1000 m thickness, while the upper part is constituted mainly by sedimentary rocks, which reach 100-150 m in thickness (Chong and Hillebrandt 1985).

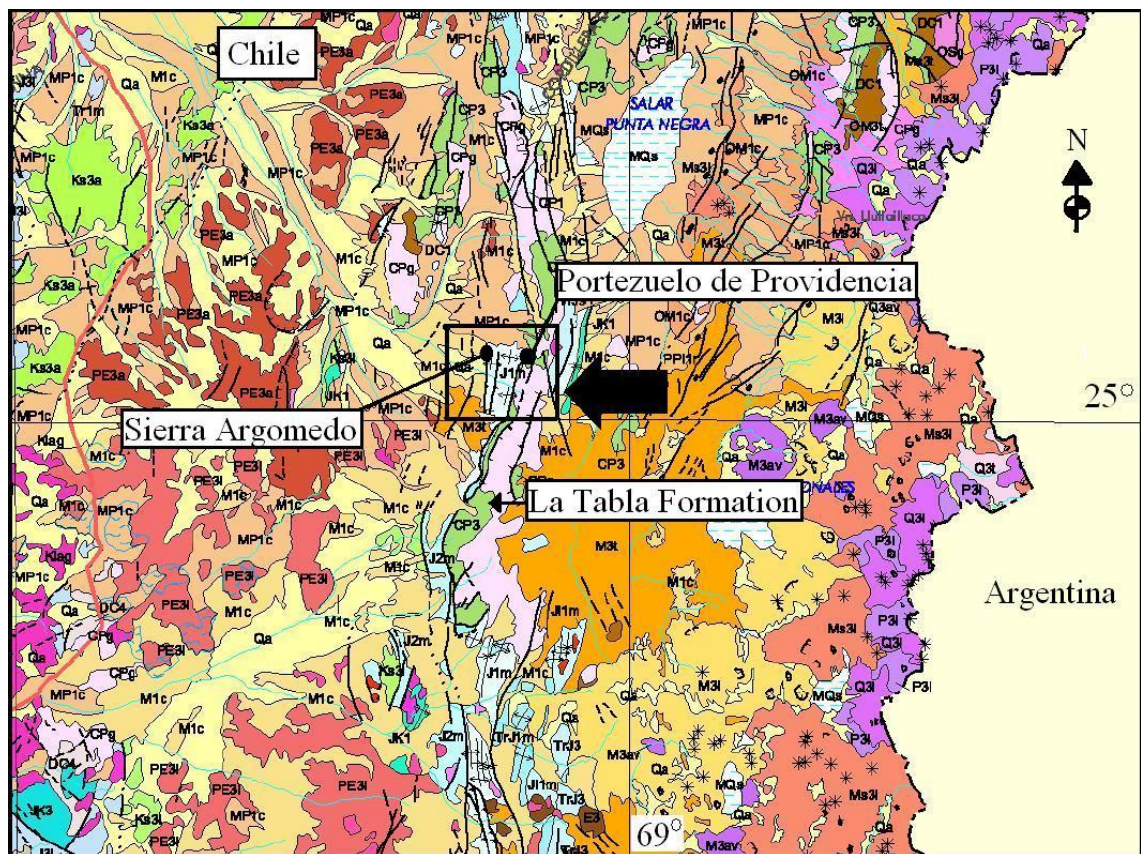


Figure 7.1 Sedimentary sequences of Northern Chile. The black square indicates the location of the study, Portezuelo Providencia, which is located at “El Profeta Formation” in pale blue [J1m]. In green is denoted La Table Formation [CP3]. Scale = 1:1.000.000 (Sernageomin 2003). El Profeta Formation is a sedimentary marine sequence comprising clastic and carbonate rocks: limestone, lutite, calcareous sandstone, conglomerate, gypsum and subordinate intercalations of clastic volcanic sediments (Sernageomin 2003). More details see Chapter 2.

The Tr/J units of northern Chile are mainly arranged in erosive unconformity on Palaeozoic intrusive rocks (granites), or in tectonic contact through faults with rocks of different ages. The Tr/J boundary is made up of relatively deep-water facies, without discordance with Hettangian sediments. From the west part of Sierra Argomedo to the Portezuelo Providencia a long band of outcrops range in age from the Middle Triassic to the Upper Jurassic, which are known as the El Profeta Formation. Towards the north-west, this sequence overlies with angular unconformity volcanic rocks from the Carboniferous-Permian, which are called the La Tabla Formation (Hervé *et al.* 1991) (Fig. 7.1).

The study site was located in a section named Portezuelo Providencia (for details see Chapter 2). This section was measured from the lower half of the north-western part of the syncline, which constitute the outcrops of the Profeta Formation (Fig. 7.2). It is made up mainly by fine grained sandstones and siltstones in the lower part, gradually changing to silty mudstones and bioclastic packstones in the upper part. The section measures more than 100 m in thickness, and ranges from the Upper Triassic to the Upper Jurassic (Hillebrandt 1994; 1990; 2000).

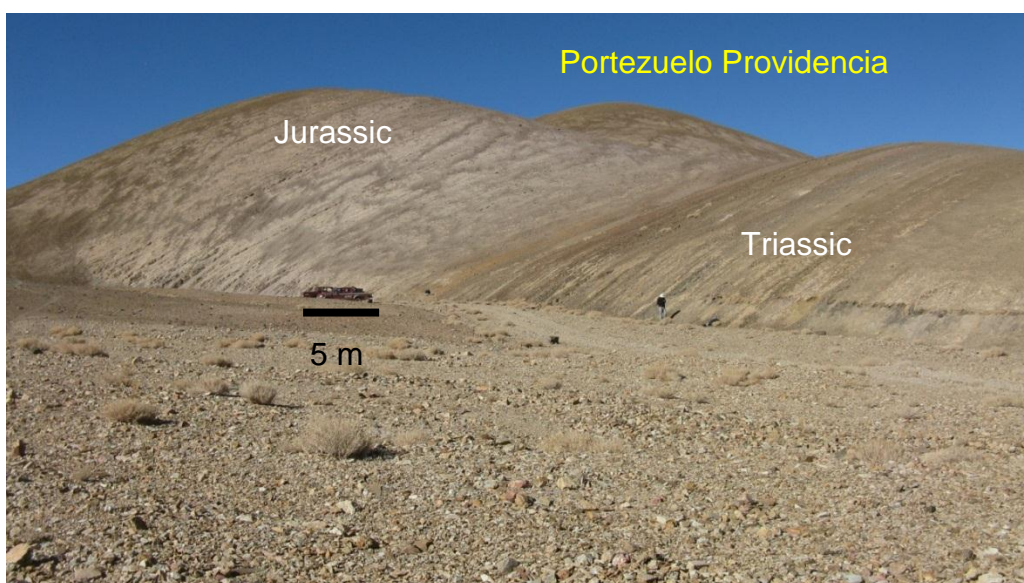


Figure 7.2 Study site; Portezuelo de Providencia. More details see Chapter 2.

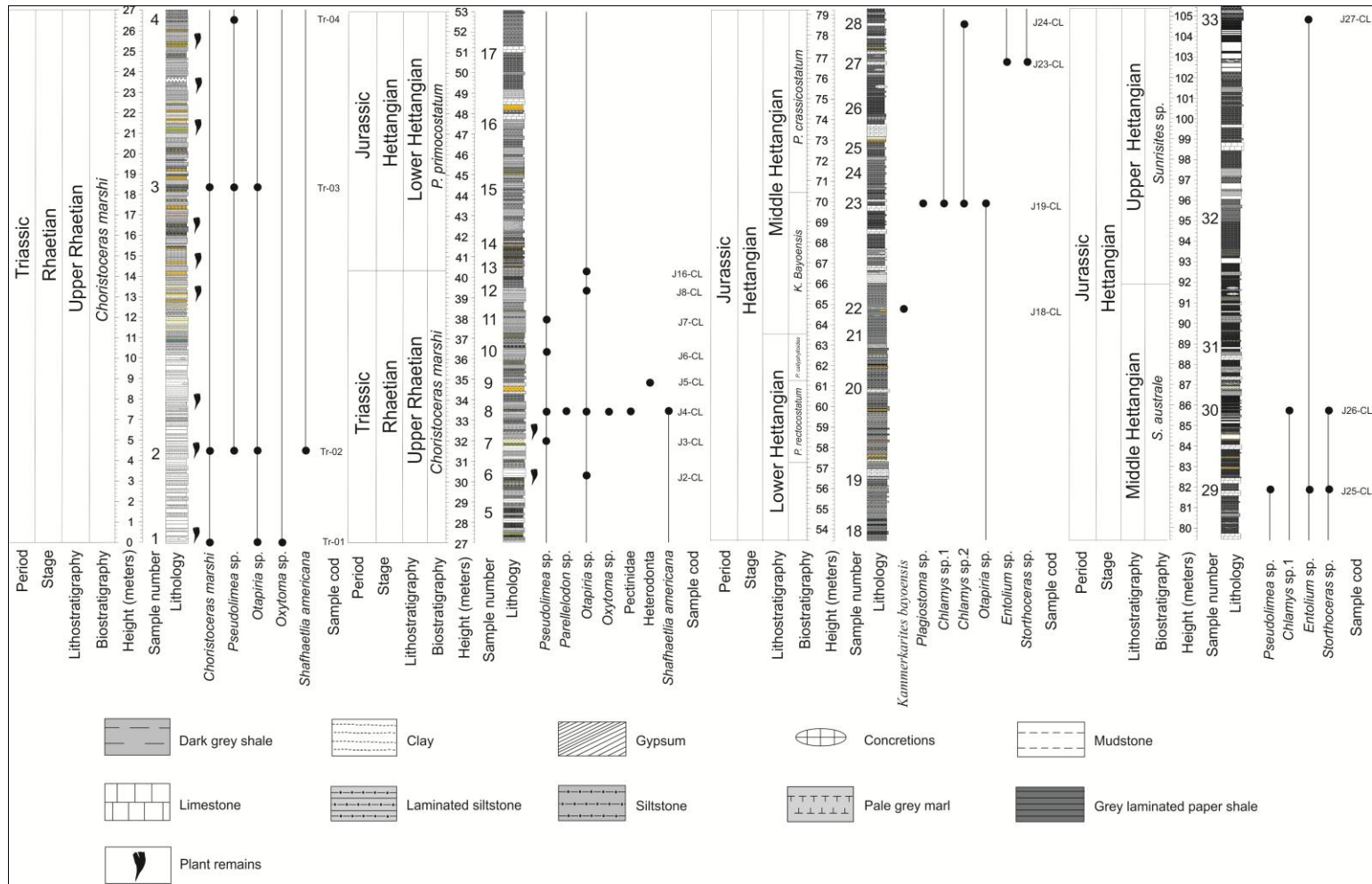


Figure 7.3 Lithostratigraphical log of the Triassic-Jurassic section in Chile. Occurrences (●) and ranges (black lines) of taxa recorded from 33 samples taken from Portezuelo Providencia. Log drew by R. Twitchett and the ammonites determinations were performed by A. Mourgues (*pers. comm.* 2010).

Chong and Hillebrandt (1985; pag. 176) described the sedimentary succession of this locality and defined the Tr/J boundary based on the last appearance of the ammonite genus *Choristoceras* and the first records of the first genera *Psiloceras* (Hillebrandt 1990; 1994; 2000). The outcrop is characterised by a monotonic succession more than 200 m thick (Fig. 7.2).

In the first 46 m of the section, dark grey siltstones dominate (Fig. 7.3). They alternate with blocky muddy silts, thin beds of fine grained sandstones, and grey siltstones with small intercalations of carbonate concretions. Small slumps (cm-scale) affect muddy silts from 17.71 to 21.31 m. At 0.55 m above the base of the section the first specimen of *Choristoceras marshi* was found. Plant remains of *Dicroidium zuberi* are frequent between 4.81 to 45.28 m. At 39.80 m above the section, the genus *Choristoceras* recorded the last appearance (LA), while 6.97 m afterwards, a purple–orange mottled layer of crumbly claystone. The bivalve fauna is relatively poor; however specimens such as *Schafhaeutlia*, *Parellodon*, *Otapiria* and *Pseudolimea* are common through the first 40 m above the section (Fig. 7.3).

At 49.54 m above the base of the section, the first appearance (FA) of *Psiloceras* is recorded. From this level to 56 m above the base of the section, the units comprise of phosphatic concretions with limestones, pale to grey paper shale with finely bedded siltstones and fine beds of gypsum and black organic mudstone. At the top, a series of 30 cm thickness limestone beds are intercalated among thin bedded siltstone and paper shales (Fig. 7.3).

At 56.82 m above the base, *Psiloceras rectocostatum* Hillebrandt recorded the FA on a laminated grey siltstone bed. Above this level, 12 cm of volcanic ash was observed (Fig. 7.3). From this level to the FA of *Psiloceras callyphylloides* (Pompeck), the unit

comprising almost completely of dark grey to black shale composed of thin layers, with thin beds of clay, calcareous siltstone and some phosphatic concretions. From *P. callyphylloides* to the first record of *Kammerkarites bayoensis* (Hillebrandt) (Fig. 7.3). The sequence is made up by intercalated paper shales, laminated siltstones and thin limestone beds. From *K. bayoensis* to the FA of *Psiloceras crassicostratum* (Guex), the sequence comprises black paper shale, siltstone, grey-mudstone, laminate mudstone and concretions of limestone. The *P. crassicostratum* units are made up of paper shale interbedded by limestone layers and calcareous concretions. From the FA of *Storhoceras australe* (Hillebrandt) to top of the section, phosphatic concretions and limestone beds are more frequent, although paper shales and laminated siltstones are dominant lithologies throughout the sequence.

From the LA of *C. marshi* to the top of the section, the plant remains are absent. The diversity of the marine fauna is low; bivalves are scarce through this segment, while ammonites are more diverse, but record a low abundance. The high occurrences of ammonites and the high proportion of siltstone and silt shale would suggest that the beds were deposited under conditions in which winnowing currents were rare or absent, which suggests that the deposits originated from pelagic suspension or turbidity currents. In this sense, Chong and Hillebrandt (1985) mention that these sections could be interpreted as a distal submarine fan. Parallel, in the region of the Pre-Cordillera, several sections with continuous sedimentation are found, some of them without significant facies changes from the Upper Triassic through the Upper Jurassic (Hillebrandt 1990).

To correlate the Chilean section with other Tr/J sections around the world; bed by bed sampling was performed throughout the Portezuelo Providencia section. The ammonite

fauna recorded was correlated and fit to the zonal terminology obtained from Hillebrandt's biostratigraphy framework (1990; 1994; 2000) (See appendix 1.2). In this work, the Portezuelo Providencia section is subdivided into four ages: the Upper Rhaetian, which is defined by the LA of *C. marshi*; the Lower Hettangian, which is defined by the FA of *Psiloceras tilmanni* (Lange) and corresponds to the *Planorbis* Zone; the Middle Hettangian, which is correlated to the Liasicus zone and is defined by the FA of *Kammerkarites bayoensis* (Hillebrandt); and the Upper Hettangian was defined by the FA of *Sunrisites* sp. and is correlated with the upper part of the *Peruvianus* Zone and *Extranodosa* Subzone from the Angulata Zone, see also Riccardi (2008).

7.2 Species Richness

A total of 261 individuals were recorded from 33 samples taken along the Tr/J section at Portezuelo Providencia (Appendix 7.1). Of these, two were identified to the species level (Appendix 6.1), eleven to genus level, one to family and one to subclass level.

The curve of species richness throughout the study interval at Portezuelo Providencia did not exceed 6 taxa per sample (Fig. 7.4). From the base to the top of the section, the trajectory of the average richness shows a progressive decrease of the number of taxa, reaching the minimum value at 32 m above the base of the section. From this point to 64.8 m above the base of the section the species richness remains constant to reach 70 m above the base; except for the biggest peak (5 taxa) observed at 33.40. From 70 m to 104.9 m above the base the species number decreases slightly reaching a mean ~2 taxa (Appendix 7.1).

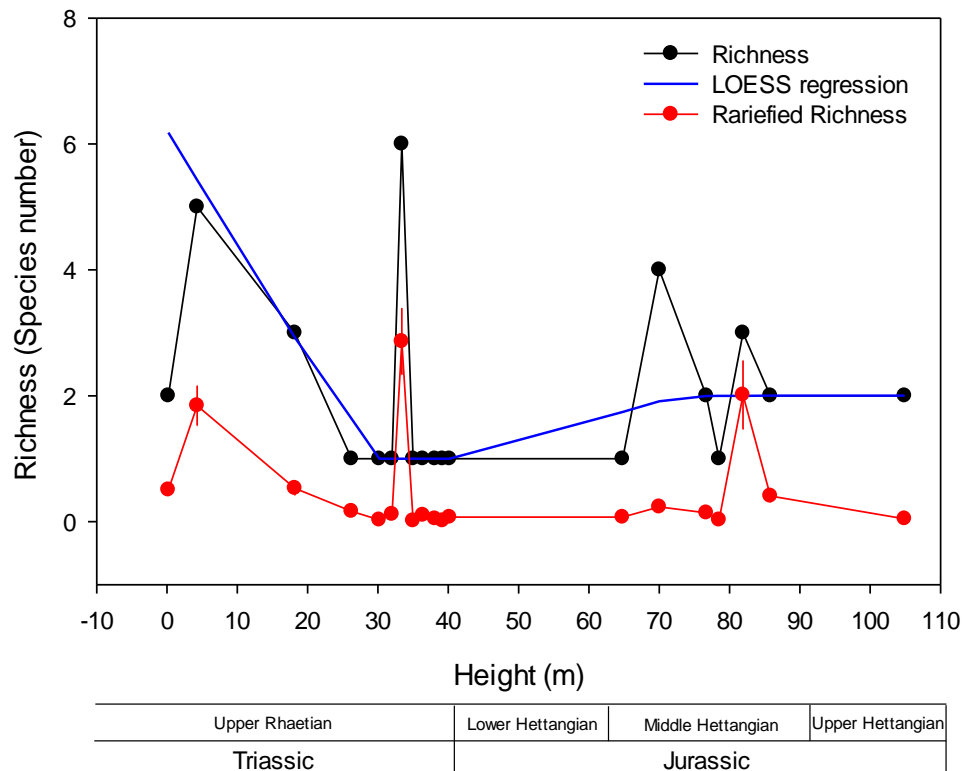


Figure 7.4 Raw (black line) and Mean species richness (red line \pm 2 S.D.) recorded for each sample collected. The mean represents the rarefied within-sample marine invertebrate richness estimated by 10000 iterations. The blue line is the LOESS regression through the data point ($\alpha= 0.3$).

The rarefied curve performed by increasing the sample size (Fig. 7.5) shows that there is no significant difference in the number of taxa sampled in the Triassic and Jurassic assemblages. The Triassic fauna reached a maximum richness value of 8.52 (95% Conf. High: 10.05 - Conf. Low: 2.00), whereas the Jurassic fauna recorded a richness of 8.79 (95% Conf. High: 9.59 – Conf. Low: 1.00). Estimates of the Shannon-Wiener index [H'] with increasing sampling size (Fig. 7.6) indicate that the mean diversity [H'] is significantly lower in Jurassic assemblages than in those of the Triassic.

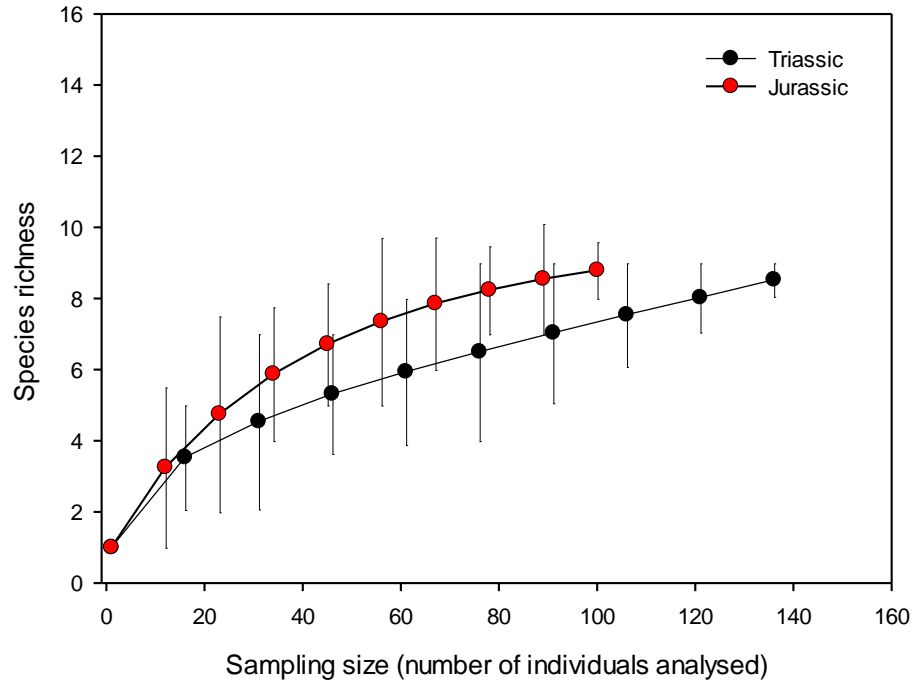


Figure 7.5 Average values ($\pm 95\%$ confidence intervals) of species richness estimated as sampling size increases during study interval at Portezuelo Providencia section. Significant differences were assumed if 95% confidence intervals did not overlap.

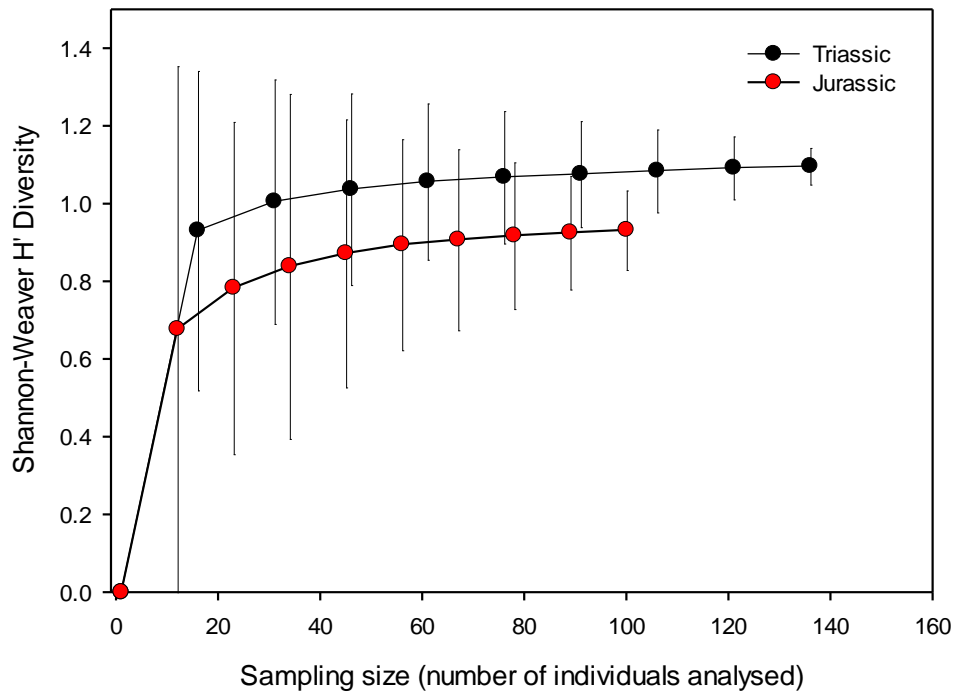


Figure 7.6 Average values ($\pm 95\%$ confidence intervals) of Shannon-Wiener diversity estimated as sampling size increases during the Tr/J interval. Significant differences were assumed if 95% confidence intervals did not overlap.

7.3 Abundance

The assemblages sampled through the study interval at Portezuelo Providencia did not record significant differences in the kurtosis values (overall mean $\sim 13.45 \pm 0.72$) (Fig. 7.7; Appendix 7.2). However, the rank abundance curves indicate that the Triassic assemblages show higher dominance compared to the Jurassic ones (Fig. 7.8 and Table 7.1).

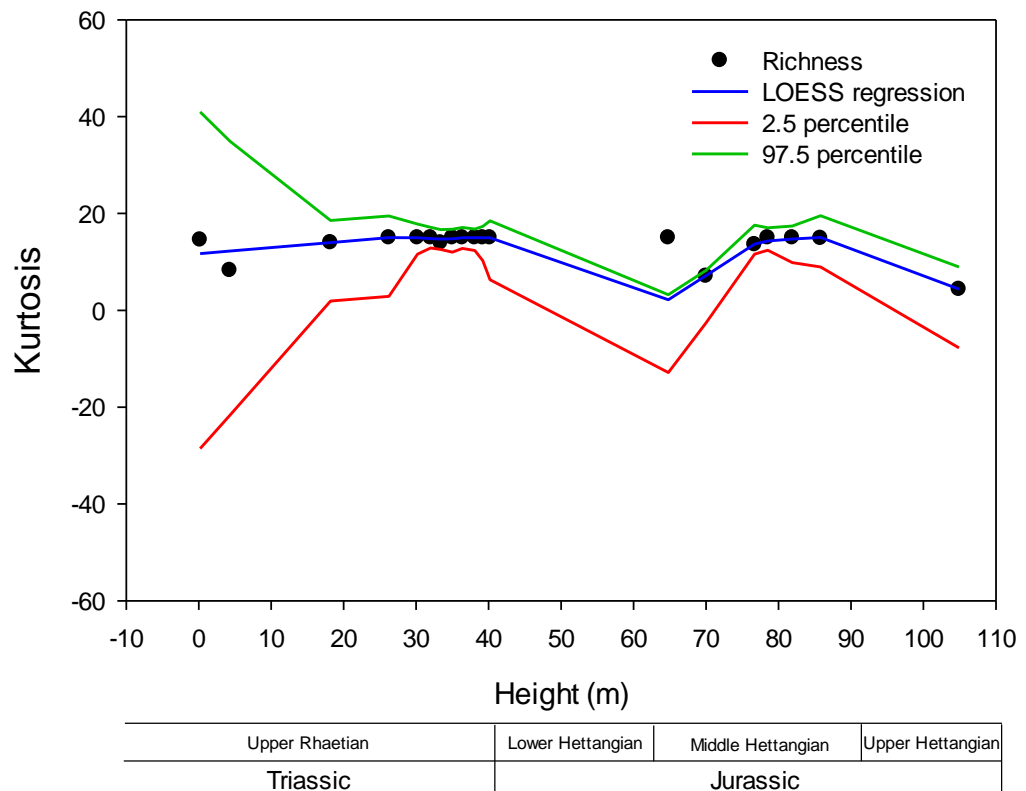


Figure 7.7 Dominance (Kurtosis \pm 95% confidence intervals) of marine fossils assemblages through the study interval at Portezuelo Providencia section. The blue line is the LOESS regression through the data point ($\alpha= 0.3$).

The assemblages from the Triassic are best described by the geometric RAD model, or well, communities with high dominance (Table 7.1). The rank abundance curve shows a

high slope, which reflects big differences in the proportional abundances of the taxa. For example, just four genera show high dominance: *Pseudolimea* (58%), *Otapiria* (31%), *Schafhaeutlia* (5%) and *Choristoceras* (3.3%), whereas more than half of the taxa (5 genera) recorded abundance less than 1% (Appendix 7.3).

The Jurassic samples showed a more even distribution. *Storthoceras* is the only taxon that is well represented (78% relative abundance), while the rest of the genera (8 genera) show abundances between 2 and 5% (Appendix 7.3). The ranking based on Akaike's weight indicates that the Zipf model is the best candidate to explain the rank distribution observed during the Jurassic (Fig. 7.8 and Table 7.1).

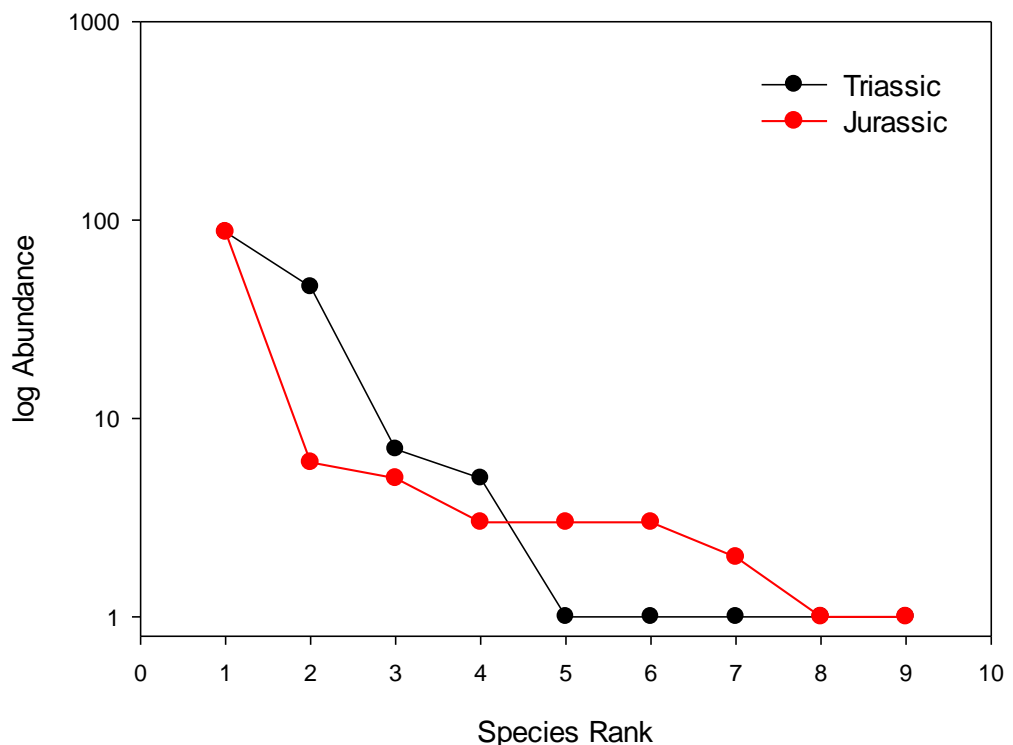


Figure 7.8 Rank Abundance Curves derived from the abundance of marine invertebrate fossil communities during the Tr/J interval. Y-axis on $\log(n)$ scale.

Table 7.1 Comparison of RAD models derived from abundance distribution of marine invertebrates through the Tr/J interval. The models were ranked based on Akaike's weight (ω_i) following Burnham & Anderson's (2002) recommendation. AICc sample-size corrected was estimated as $AICc = AIC + (2K[K+1]) / (n-K-1)$. AIC is report only for completeness. K is the number of parameters; T is the number of taxa; n is the number of specimens. The highest ω_i gives the best fit (**In bold**).

				RAD models				
	T	n	AIC	Broken stick	Geometric	Log normal	Zipf	Zift Mandelbrot
Parameters (K)				0	1	2	2	3
Triassic	9	150	AIC	128.47	46.13	53.25	56.65	47.43
			AICc	16.05	7.44	12.20	12.77	17.88
			ω_i	0.010	0.79	0.073	0.05	0.061
Jurassic	9	111	AIC	134.06	80.62	59.7	46.07	48.07
			AICc	16.75	12.37	13.28	11.01	18.01
			ω_i	0.029	0.264298	0.168	0.52	0.015

The dominance index estimates by increasing the sample size (Fig. 7.9), shows that the Jurassic assemblages are significantly more dominant than those observed during the Triassic. Both assemblages show a high dominance (>50%), but in the Triassic assemblages two taxa record a dominance of >30%: *Pseudolimea* sp. and *Otapiria* sp. whereas in Jurassic assemblages, *Storhoceras* sp. was the only dominant taxon (> 60%) (Appendix 7.3).

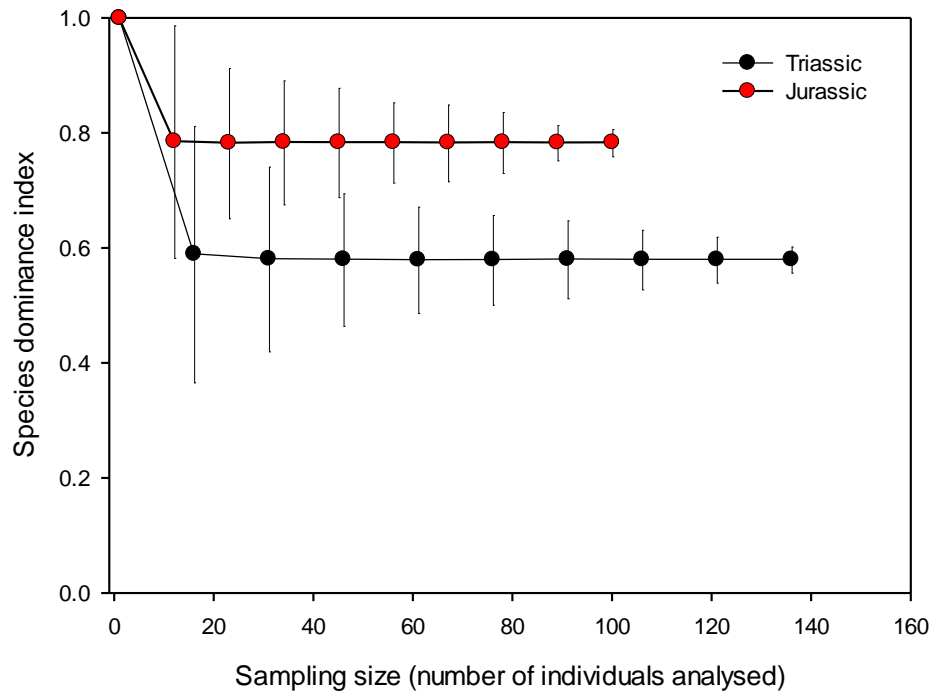


Figure 7.9 Average values ($\pm 95\%$ confidence intervals) of dominance estimated as sampling size increases through the Tr/J interval at lo Providencia. Significant differences are assumed if 95% confidence intervals do not overlap.

7.4 Composition

The Non-Metric Multidimensional scaling ordination showed that the samples from the Triassic are significantly separated from the Jurassic ones (Fig. 7.10). One-way ANOSIM shows significant differences between the faunal composition of each period ($R = 0.299$; $p < 0.001$). SIMPER analysis reveals a dissimilarity of 96.41% (Appendix 6.4), with just three taxa shared by both assemblages: *Pseudolimea*, *Otapiria* and *Chlamys* (Appendix 7.4).

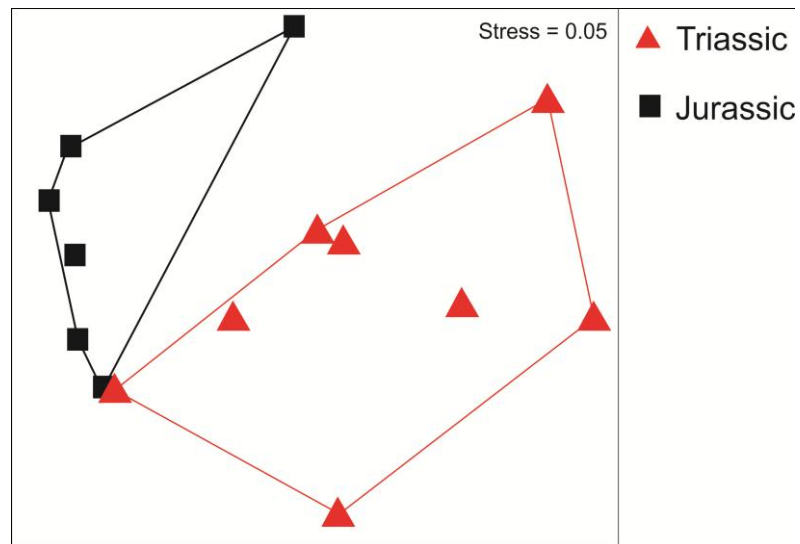


Figure 7.10 No metric multidimensional scaling (NMDS) plot resulting from the ordination analysis (Euclidean distance) of the marine invertebrate fauna from the Tr/J section from Portezuelo Providencia section, using abundance data.

Along the Portezuelo Providencia section, the transition from the Triassic to the Jurassic is abrupt. Between 36 to 40 m, 40% of all recorded taxa disappear and just *Otapiria* crosses the Tr/J boundary (Figure 7.1 and Appendix 7.1), whereas *Pseudolimea* disappears at 38.1 m and reappears just at 81.9 m in the Jurassic. 58% of the taxa are singletons, four of them appear at 33.4 m and one specimen of *Heterodonta* at 35 m above the base of the section. Despite the big species turnover through the Tr/J interval, only *Choristoceras* records a pattern of global extinction.

7.5 Ecospace

A total of 5 modes of life were used by the marine fauna within the study interval (Fig. 7.11). The fauna found in the Late Triassic use 5 modes of life, occupying 1.8% of the theoretically available ecospace. In this period, the fauna was made up by fast moving pelagic carnivores (1 taxon), surficial filters feeding forms (5 taxa), facultative motile attached (3 taxa) and motile unattached forms (2 taxa). Finally, semi-infaunal forms comprising 2 taxa: facultative motile attached chemo-symbiotic feeders and motile unattached filter feeders (Appendix 7.5).

Despite the marine Late Triassic fauna having low numbers of taxa associated with each mode of life, the assemblage has a relatively high ecological complexity. 10 ecological categories were used by the marine fauna, 75% of the taxa showed some degree of motility, the trophic spectrum spanned from carnivorous to chemotrophic taxa and 50% of the tiering categories were occupied (Figure 7.12, Appendix 7.6).

During the Tr/J, all the semi-infaunal forms disappeared and the marine fauna just recorded three modes of life (Fig. 7.11; Appendix 7.5). The abundance of each mode of life increases by an average ~20%, of which surficial, facultative-unattached suspension feeders record >50% of the relative abundance. Despite this, the ecological complexity is low and just 7 ecological categories are used (Fig 7.12, Appendix 7.6).

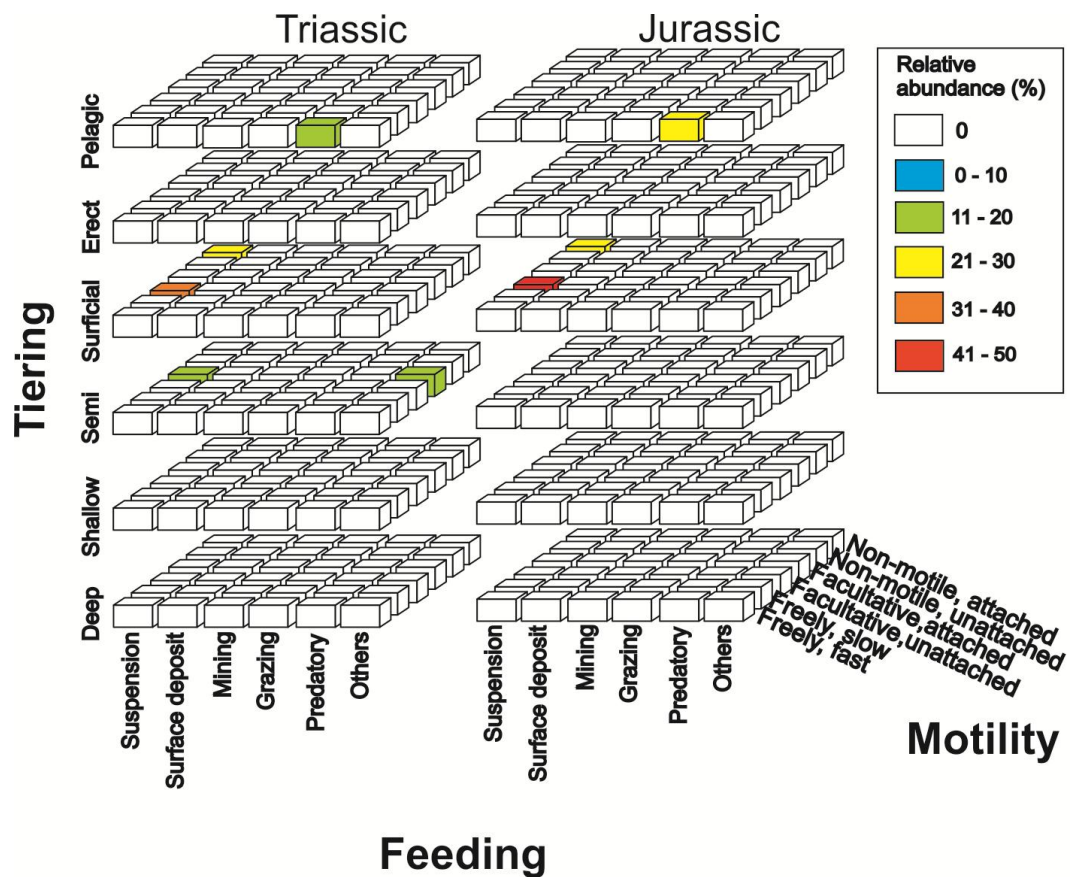


Figure 7.11 Theoretical ecospace occupations during the Tr/J boundary at Portezuelo Providencia, Chile.

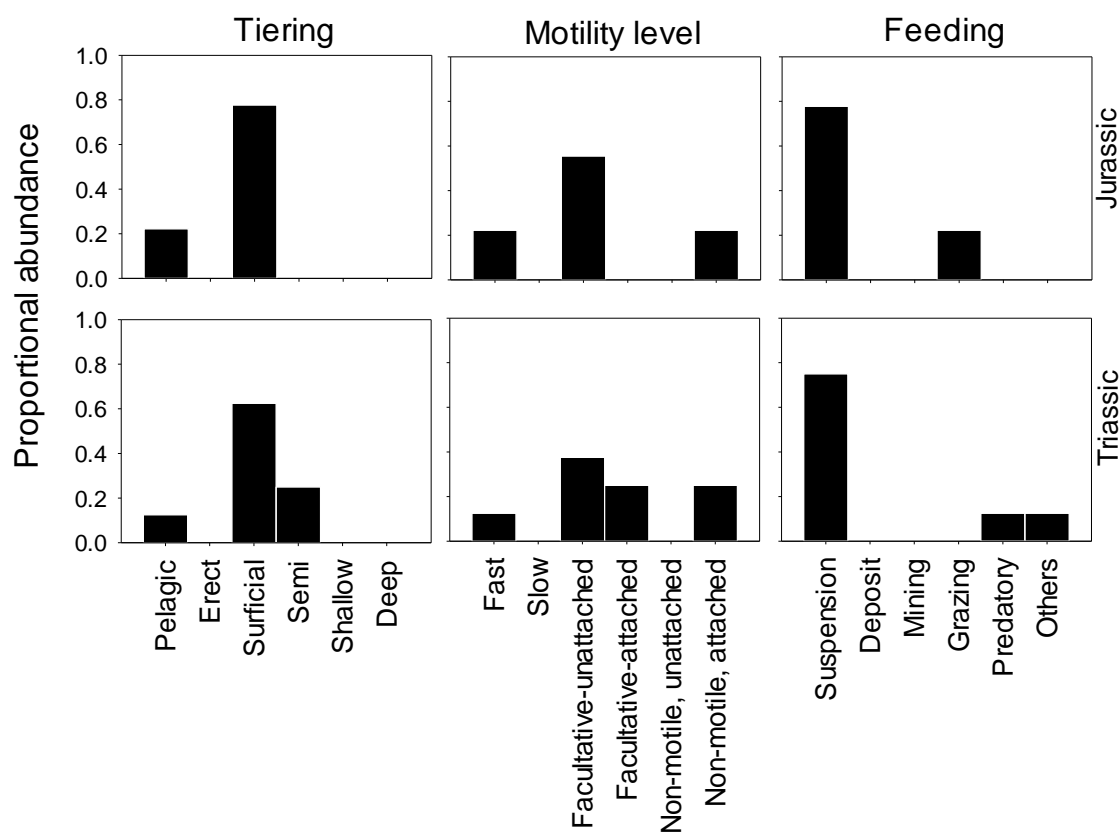


Figure 7.12 Proportional abundance of tiering, motility and feeding mechanisms, based on taxa occurrences across the Tr/J section at the Portezuelo Providencia section.

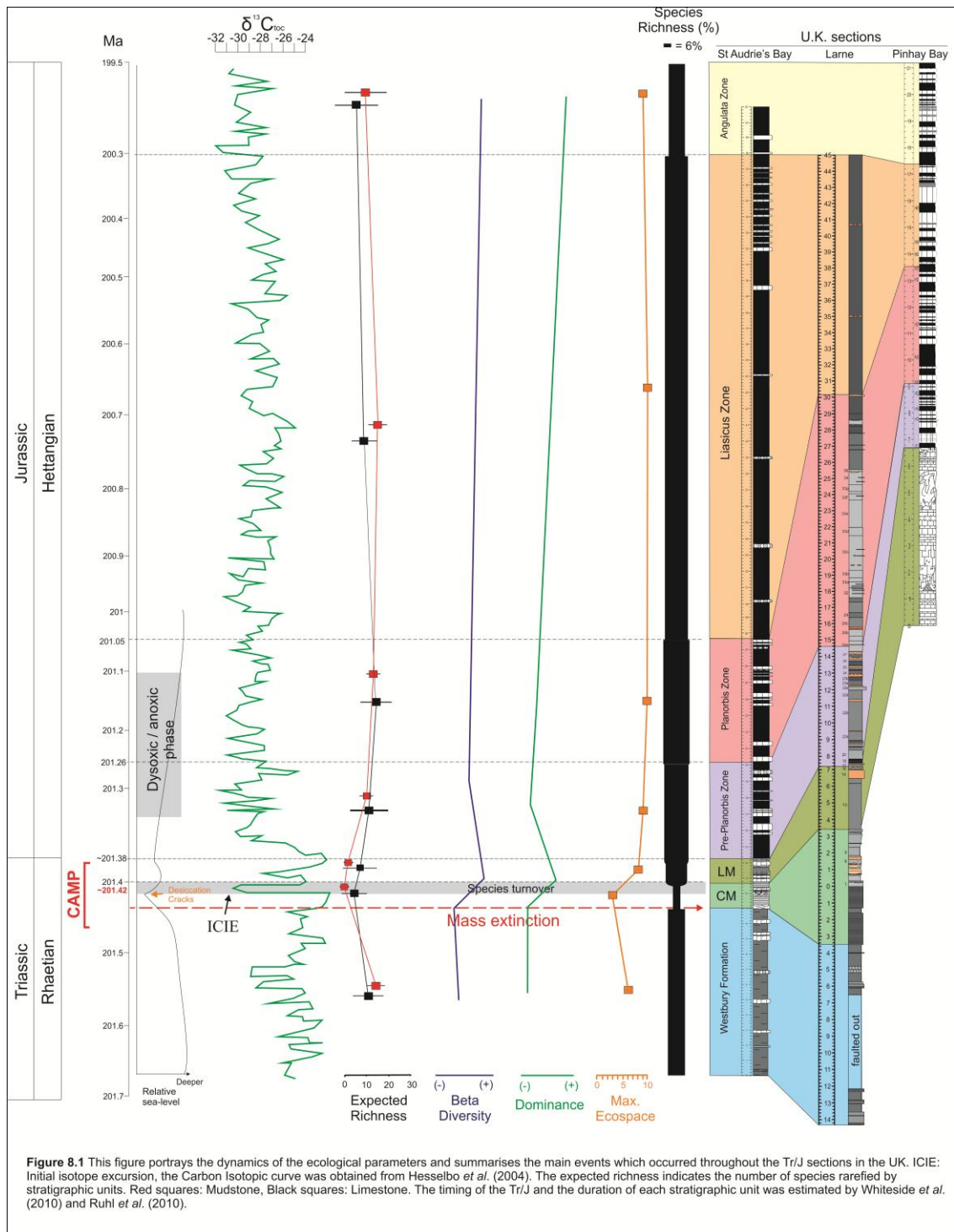
In summary, despite the fact that the number of taxa recorded during the Rhaetian and Hettangian (9 taxa) was the same, the number of taxa fluctuated significantly between samples. The Tr/J assemblage, in general, recorded high dominance values, but the assemblage associated with the Hettangian stage is highly dominant. The taxon composition changes abruptly from the Triassic to the Jurassic, generating a turnover of more than 95% of the entire fauna. Finally, during the Jurassic all the taxa associated with the semi-infaunal mode of life disappear, decreasing the ecological diversity by ~40% compared to the previous period.

Chapter 8 Discussion

8.1 Timing, recovery and species richness patterns through the Tr/J mass extinction event.

The St Audrie's Bay and Larne sections both show a complete trajectory of the marine fauna through the Tr/J boundary. In these successions the disappearance of the marine fauna occurred in the stratigraphic interval spanning the top of the Westbury Formation and the lower Lilstock Formation (the Cotham Member). During this interval, the species richness on average dropped to ~52%. Three modes of life were used by the Tr/J assemblages and high ecological dominance values are recorded and a sharp compositional turnover was detected by the beta index. Later, from the Langport Member to the middle of the Planorbis Zone, taxonomical and ecological richness reaches a maximum, but with a low compositional turnover. From this level and throughout the Liasicus Zone and the Angulata Zone, the number of species decreases and the ecological richness remains constant although with low compositional changes. In addition, the Pinhay Bay section also shows the same recovery pattern as the Larne and St Audrie's Bay sections (Fig. 4.2, 5.2 and 6.2).

The results observed in this work correspond with previous studies on U.K. sections (e.g. Hallam 2002; Mander *et al.* 2008; Wignall and Bond 2008), which indicate an elevated extinction rate (>50%) at the top the Westbury Formation and the base of the Cotham Member. For example, Wignall and Bond (2008) report that of 26 bivalve species present in the Westbury Formation, 20 became extinct (77% species extinction), while Mander *et al.* (2008), through a more exhaustive analysis, report an extinction of 65% across the Westbury Formation/Cotham Member boundary. In the present work, a total of 12 species (all bivalves) passed through the Cotham Member, where the extinction level was



demonstrated to be less severe at generic level. According to Mander and Twitchett (2008), *Rhaetavicula*, *Cassianella*, *Permophorus* and *Lyriomyophoria* were the only genera that experienced regional extinction, whilst other genera failed to survive into the Jurassic, except for *Isocyprina* and *Mesomiltha*, which underwent extinction during the Langport Member.

Another pattern observed across the Westbury Formation/Cotham Member boundary is the extinction of the infaunal forms (see appendices 4.11 and 6.11). Of 23 infaunal species recorded during the present study, only *Modiolus* spp., *Cardinia regularis* and *Protocardia philippiana* continued into the Jurassic, although during this interval, they kept a very low abundance (Appendices 4.3 and 6.3). In addition, *Protocardia rhaetica* and *Isocyprina* were also infaunal taxa that crossed the Westbury Formation/Cotham Member boundary, although they went extinct during the Langport Member. These observations are consistent with studies by Wignall and Bond (2008), Mander *et al.* (2008) and Mander and Twitchett (2008), which confirm the pattern of the Tr/J extinction event within marine faunas and the preferential decreases of the infaunal bivalves.

The Cotham Member and the Langport Member were interpreted as possible “extinction zones” immediately after the extinction event (Mander *et al.* 2008). In the present study, the main disappearance took place at two levels: across the Westbury Formation/Cotham Member boundary and during the Cotham Member. However, from the Langport Member onward, the number of species increased rapidly, which at this level could be considered as the onset of the recovery phase. Harries *et al.* (1996) state that the first stage of the marine recovery is characterised by a very diverse and very rapid increase of the marine fauna (over 100-500 ka). In this context, Wignall and Bond (2008) mention that the re-diversification began rapidly in the Langport Member, estimating an origination rate of ~39%. The present study confirms Wignall and Bond’s observation. An estimation based on the Langport Member fauna indicates that the mean rate of origination increases to ~30%, of which ~26% of all taxa recorded in this work (25 spp.) corresponding to bivalves, ~9% to gastropods and 2% to echinoids (Appendix 4.1, 5.1 and 6.1).

Despite the compositional changes of species between samples and lithologies, however, the recovery patterns are very similar and consistent between localities (Fig. 4.4; 5.4 and 6.4). This is strongly demonstrated by the three sample-rarefied estimations (Mao tau, Chao₁ and Jack₁), which indicate that the species richness decays through the Westbury Formation and Cotham Member and increases rapidly from the Langport Member to the Planorbis Zone. This could suggest that the timing of the extinction and the recovery event does not seem to vary between different UK sections.

The Planorbis Zone is characterised by reaching a maximum richness, low dominance, high compositional similarity and high ecological complexity (Fig. 8.1). Following the recovery model of Twitchett (2006), the Planorbis Zone could be classified as Stage 3. In this interval, crinoids (*I. psilonoti*), infaunal bivalves and epibenthic forms (herbivores, carnivores, miners) show high occurrences (Ecospace: Fig.4.11; 5.10; 6.11). However, burrow diameters do not exceed 20 mm, as in St Audrie's Bay as well as in the Pinhay Bay section (see Fig. 4.17 and 5.18), which is a condition that can be categorised as Stage 4 (mature assemblages). Younger assemblages such within the Bucklandi Zone (Lower Sinemurian), potentially record a burrow diameter of > 20 mm (Barras and Twitchett 2007). Hallam (1996) mentions that the recovery of assemblages after the Tr/J event is slow and it could have taken place in the Pliensbachian Stage. This contradicts ecospace values, since the ecological complexity does not change much from the Planorbis Zone to the Angulata Zone (between 10 to 9 modes of life) (Fig. 4.11; 5.10; 6.11). This would indicate that despite the species' expansion across the ecospace (high ecological complexity), the number of species by mode of life is still low, which is recorded by the low packing.

From the Planorbis Zone to the top of the Hettangian, the species richness estimated from limestone samples decreased gradually, while the richness calculated from mudstone samples through this sequence increased to the top of the Hettangian (Fig. 4.4; 5.4 and 6.4). These differences could be a consequence of taphonomical factors rather than biological control, however. For example, through the limestone samples the specimens were difficult to identify due to high fragmentation. In addition, assemblages were commonly made up of specimens of large size, but with low abundance, i.e.: *Mactromya cardioides*, *Cardinia regularis*, *Pleuromya* spp., *Gryphea* spp., *Calcirhynchia calcarea*, *Plagiostoma giganteum* and *Pinna* spp. (Appendices 4.3; 5.3 and 6.3). Another important associated factor is the proportion of limestone and mudstone through the section. Through the Planorbis Zone to the top of the Hettangian, mudstone dominates with 75%, which in St Audrie's Bay is more evident (see figure 4.1 and 5.1). This would produce a potential sampling-bias, which would explain the differences in richness in mudstone and limestone (Fig. 5.4 limestone/mudstone).

Figure 8.1 summarises the trajectory and the dynamic of the diversity through the Tr/J sections. This graph shows the timing of the Tr/J event and the duration of each stratigraphic unit. In this sense, it would allow an understanding of the velocity of response of marine communities to the mass extinction event. The Triassic part of UK Tr/J sections have a duration of ~1.37 Ma, which spans from 201.67 Ma at the base of the Westbury Formation to the top of the Langport Member at 200.3 ± 0.1 Ma (the Tr/J boundary), where the carbon isotope excursion would take place at 201.42 Ma, with a length of ~20-40kyr. In addition, estimates by Whiteside *et al.* (2010) and Ruhl *et al.* (2010), indicate that the Cotham and Langport members would both have a duration of ~120 kyr., of which the separation would be located at 201.4 Ma. Finally, the Hettangian/Sinemurian boundary is placed at 199.5 Ma, with the Hettangian having a

duration of 1.8 Ma (Whiteside *et al.* 2010), whereas the Pre-Planorbis interval has a duration of ~100 kyr. The Lower Jurassic ammonite zones, therefore, appear to be unequal in duration: Planorbis Zone ~250 kyr, Liasicus Zone ~750 kyr and the Angulata Zone ~800 kyr (Ruhl *et al.* 2010; Whiteside *et al.* 2010).

The results indicate that extirpation of the palaeocommunity during this extinction event was extremely rapid, which happened at 201.44 Ma, clearly before the first negative carbon excursion (201.43 Ma and with a length of ~20-40 kyr). The duration of the Dead Zone spanned ~100 kyr without recording any speciation event. The recovery, on the other hand, apparently took over ~120 kyr, before reaching the ceiling at the Planorbis Zone (Ruhl *et al.* 2010). Compared to the End-Permian or End-Cretaceous, the recovery of the End-Triassic ecosystems was very rapid and could be compared to the End-Ordovician mass extinction (Sole *et al.* 2010).

The recovery is an interval which is succeeded by the diversification of new species and eventual rebuilding of communities (Erwin 2008). The detailed studies of individual recovery events have demonstrated the variety of roads to success, and these models have explored the possible range of ecologic strategies that could aid survival and trigger the recovery process (Kauffman and Erwin 1994; Kauffman and Erwin 1995; Erwin and HuaZhang 1996; Harries *et al.* 1996; Erwin 1998; Erwin 2001; Sole *et al.* 2002; Benton and Twitchett 2003; Erwin 2008). Generally, those models describe increases in diversity after the mass extinction, with opportunistic blooms of some species, presumably taking advantage of empty ecological niches.

Previously, it was suggested that this data fits very well into a model, as proposed by Twitchett (2006), which divides the recovery phase after an extinction event into four

stages. However, the recovery stage observed through the Tr/J section in this work reaches Stage 3, which means that the assemblages have high richness, low dominance and a well-developed tier level. However, this data shows that burrow diameters remain small (< 20 mm) (Fig 4.17 and 5.18), which indicates that these assemblages are successional-early.

Kauffman and Harries (1996) show a model of extinction and recovery divided into three stages: (a) background conditions, or the assemblages associated with the Westbury Formation, which have a relative high number of species, low dominance and low ecological complexity; (b) the extinction interval (the Cotham Member), divided into three stages (early, mid and late extinction) and (c) repopulation which involves internal survival, characterised by blooms of disaster and opportunistic species and the first radiation of the progenitor taxa (assemblages from Langport Member to the Planorbis Zone). The second stage of the repopulation is the internal recovery by species that evolve from surviving lineages and the radiation of new lineages. In addition, Kauffman and Harries (1996) add survival mechanisms, which give specific strategies to the species that went through the extinction event. *Cardinia*, *Plagiostoma*, *Modiolus*, *L. hisingeri* and *C. valoniensis* were the only species that went through the extinction zone, while *Cardinia*, *Plagiostoma* and *Modiolus* show a strategy of rapid evolution (e.g. *M. hillanus*→*M. minimus*) (Kauffman and Harries 1996). *C. valoniensis* and *L. hisingeri* would have generalist strategies (eurytopes), i.e. high abundance before and after the extinction event (Appendices 4.3, 5.3 and 6.3).

From the Langport Member to the Planorbis Zone, the assemblage is characterised by a high colonisation of opportunistic species, which probably explains the high richness peak during the Planorbis Zone. However, during this stage there is no radiation of new

lineages. In terms of time and intensity, the Tr/J extinction event could be labelled as a catastrophic mass extinction. Generalist species or taxa with rapid evolution apparently could survive. The first stage of the ecosystem recovery was very rapid, however, as noted by Hallam (1996), although the complete recovery of the system is very slow, probably related to a slow rate of evolution of the survivor taxa as a result of environmental stress. This observation corresponds with studies carried out by Barras and Twitchett (2007), which suggest that late succession of the recovery stage could be located within the Sinemurian Stage.

8.2 Abundance and species composition

Through the Tr/J sections in Northern Ireland and St Audrie's Bay, the kurtosis values from limestone samples decreases significantly until the Planorbis Zone (Fig. 4.6 and 6.6). From this level to the Angulata Zone, the kurtosis tends to increase slightly, but significantly (Fig. 4.6, 5.6 and 6.6). Through the extinction event (i.e. within the Cotham Member) the kurtosis reached maximum values, which indicates: (1) structural changes in the assemblage and (2) high dominance by a few species. The kurtosis values estimated through mudstone samples records a variable response. Through the Tr/J section in St Audrie's Bay (Fig. 5.6B), the kurtosis decreases significantly from the Westbury Formation to the base of Blue Lias Formation, but through the entire Hettangian the assemblage did not record significant changes. Through the Pinhay Bay section, however, the kurtosis tends to increase only during the Liasicus Zone.

Webb *et al.* (2009) use the kurtosis values as a measure of the dominance and a proxy of the RADs to evaluate the ecological response of micro-benthic organisms through the Palaeocene-Eocene extinction event. As in this example, kurtosis detects the change in ecological structure through the Tr/J mass extinction, which is associated with increases

in dominance through the extinction zone. As the RADs proxy indicates, high kurtosis would be related to geometric models (assemblages under stress or under extinction). In contrast, low kurtosis could be related to background and recovery assemblages, with high ecological complex scenarios, where RADs models as Zipf or Lognormal are to be expected. In contrast, assemblages associated with the extinction zone (the Cotham Member), show a relatively “simple” ecological scenario in which RADs fit to a geometric or broken stick model. In addition, the dominance index values confirm the trend and indicate that assemblages of the “extinction zone” (i.e. the Lilstock Formation) recorded high dominance (>50%, Fig. 4.8, 5.8 and 6.8). Through the Cotham Member, not only does the taxonomical richness decrease, the structure and ecological complexity are also affected.

Applications of the Rank-Abundance Distributions (RADs) show that the Westbury Formation, the Langport Member, the Pre-Planorbis ‘Zone’ and the Planorbis Zone fit generally to Log-normal, Zipf or Zipf-Mandelbrot Models (Table 4.1, 5.2 and 6.1). Additionally, the assemblages from the Cotham Member in the Larne section was the only one that fitted to Geometric RADs during the extinction event. The geometric model is found primarily in species-poor environments of very early stages of a succession (Magurran 2004). Conversely, the assemblage of the Cotham Member in the St Audrie’s Bay section fits the Broken Stick model, which predicts a very uniform RADs, where the group of species have the same competitive ability jostling for niche space (Magurran 2004).

Several studies have evaluated RADs through palaeoassemblages (Peters and Bork 1999; Buzas and Hayek 2005; Wagner *et al.* 2006; McElwain *et al.* 2009; Webb *et al.* 2009). However, only Wagner *et al.* (2006) and McElwain *et al.* (2009) used Akaike’s

information criteria to evaluate the increase of complexity after the Permian extinction and changes in RADs of fossil plants after the Late Triassic extinction. In both cases, the results agree almost completely with the present study. These results indicate that during the extinction event the community shifts from ecologically complex scenarios (RADs: Zipf or Lognormal) to ecologically “simple” RADs (geometric or broken stick models). Later, assemblages return to normal conditions or ecologically complex scenarios during the recovery stages.

The geometric series occur in situations where one or a few factors dominate the ecology of a community (Magurran, 1988). For example, Magurran (1981) demonstrated that understory plants in a conifer forest - where light is the single most important factor controlling diversity - fit a geometric-series distribution. Miller (1986) showed that some Pleistocene fossil assemblages also approached log-series and geometric distributions in estuarine environments, where salinity and substrate were chiefly responsible for controlling diversity.

In this work, it is observed that probably the diversity seems to be controlled by factors, such as oxygen-concentration and sea level changes. During the Westbury Formation the marine fauna is associated with deep water environment dominated by infaunal organisms (i.e. *P. elongatus*, *M. sodburiensis*, *G. precursor*, *I. concentricum*, *I. ewaldi*, *C regularis*), although with a diverse epibenthic community (i.e. *P. rhaetica*, *R. contorta*, *P. alpina*, *C. valoniensis*, *M. cloacinus*, *P. punctatum*, *L. hisingeri*). The high abundance of infaunal filter feeders would reflect ecosystems of high productivity, with well-oxygenated conditions and high environmental heterogeneity due to infaunalisation effects (bulldozer effect). Through this ecological scenario, the resources cannot be a limiting factor under a log normal model.

On the other hand, the assemblages from the Cotham Member (extinction event), represent very shallow conditions, with a possibly lower-oxygen environment, where the habitat heterogeneity was minimal and disturbance was limited to quiet water; thus, uniform soft substrate predominated. Biodiversity in this environment was low (± 6 species) and superficial bivalves were numerically dominant (i.e. *P. crowcombeia*, *Modiolus* sp. *P. alpina*, *M. cloacinus*, *I. concentricum* and *P. philippiana*) (Appendix 6.3). However, in some cases, as the Cotham and Langport Members in St Audrie's Bay and the Langport Member in the Larne section, the evenness was quite high because of equitable allocation of abundant niche space between species. That rank abundance curve tends to decrease slightly, which indicates that the abundance between species tends to be similar (Appendices 4.3 and 6.3). Although too few species are present in those communities, the observed distribution of bivalves most closely matches the broken stick model. This distribution is most commonly found in communities where resources are shared rather equally among species. In the Cotham and Langport Members communities, harsh environmental factors may have limited the number of successful species, but offered plenty of resources to those few that were able to survive (Peters and Bork 1994).

The environmental conditions during the recovery stage improved significantly (the Pre-Planorbis Zone, the Planorbis Zone, the Liasicus Zone and the Angulata Zone). The sea level rose and the bioturbation re-appeared (Fig. 4.18 and 5.18) as a consequence of increases in oxygen concentrations and with them, an enhancement of the habitats' heterogeneity. During this scenario the resources are often more abundant, partitioned more equitably in a community; variation in the habitat is greater and sources of environmental stress are fewer. Through the recovery stage, 54% of the assemblages fit the log normal, Zipf or Mandelbrot distribution models. Of these, 28% of the

assemblages fit to log normal model when they reach the maximum species richness (Planorbis Zone at St Audrie's Bay and Larne section, Table 4.1 and 6.1), while the rest of the assemblages (72%) fit to Zipf and Mandelbrot models (Table 4.1, 5.1 and 6.1). Those models (Zipf and Mandelbrot models) have been interpreted as reflecting successional processes (like early recovery), in which later colonists have more specific requirements and hence are rarer than the first species to arrive (Magurran 2004).

Apparently the gradual environmental modification through the Tr/J boundary resulted mainly in a sea level fall and decreases in oxygen concentrations, which generated an ecological filter with a loss of biodiversity. The ecological changes in the Tr/J involved several of the processes mentioned by Mander *et al.* (2008) and Barras and Twitchett (2007), which included: (1) expansion and contraction of the relative abundance of dominant species, (2) exchange of rank-abundance among less dominant species, (3) rapid demotion and promotion of minor taxonomic components, and (4) deletion of less abundant taxa. In this sense, the ecological response suggests that reorganisation of the Tr/J assemblages was driven by organism-environment interactions, of which sea level changes and oxygen levels could have been factors that strongly modulate the structure of the local palaeocommunities.

NMDS ordination indicates that pre-extinction assemblages (i.e. of the Westbury Formation), during-extinction assemblages (in the Cotham and Langport members) were compositionally different from post-extinction assemblages (e.g. of the Blue Lias Formation). Beta diversity confirms the high species turnover into the Lilstock Formation, mainly within the Cotham Member.

Pooling all the data from the figures 4.9, 5.9 and 6.9 and the centroids of each stratigraphic unit are plotted and joins each centroid with a line; summarises the

trajectory of palaeocommunity change through the Tr/J boundary (Appendix 8.1). This axis, reflects a general depth gradient, meaning that the compositional changes observed through the Tr/J section obey related to sea level fall (Holland *et al.* 2001; Webber 2002; Holland and Patzkowsky 2004; Layou 2009).. The fauna associated with the Westbury Formation is mainly related to a relatively deep water environment with high dominance of infaunal forms, whilst the fauna associated with the Lilstock Formation is related to very shallow marine systems (Hesselbo *et al.* 2004). The Blue Lias Formation, however, represents a system with a high compositional similarity, in which the species composition represents an assemblage of moderate depth (Hesselbo *et al.* 2004). This work agrees with previous observations by Tomašových and Siblik (2007); Mander *et al.* (2008), Tomasovych (2006) and Hesselbo *et al.* (2004), which suggest that during the end Triassic, sea level changes produced one of the largest turnovers in marine assemblages during the Phanerozoic. During the sea level fall, more than 80% of the fauna associated with surficial environments disappear (see Appendix 4.11 and 6.7) while >60 % of the infaunal taxa range through to the Cotham Member.

This indicates that composition changes of the assemblages were abrupt and substantial, although consistent through different sections in UK. At the generic level, ~33% of the genera disappear, whilst at family level ~25% disappear. Families such as the Gryphaeidae and Pectinidae show local extinction. During the Langport Member, Arcticidae and Pteriidae disappear, with nine families disappearing between the Westbury Formation and the Cotham Member - of these, however, only Anomiidae, Limidae, Astartidae and Mathildidae show a global extinction. At a generic level, only six taxa show global extinction. In addition, the beta diversity increases slightly across the extinction boundary and then declines into the base of the Lias Group (Fig. 4.10, 5.10 and 6.10). This suggests that the assemblages should be more distinct immediately

following the extinction. This peak is repetitive through the section that records the Westbury Formation and Cotham Member interval. In contrast, the Blue Lias assemblages are characterised by the highest rate of incorporation of new taxa and high compositional similarity. This could suggest that environmental conditions through this sequence remained relatively stable, driving a relative stasis.

In term of spatial differences (Appendix 7), the fauna records significant differences between the sections of Pinhay Bay, St. Audrie's Bay and Larne. That could be explained by the Larne and Pinhay Bay sections representing environments with shallower conditions than St. Audrie's Bay, which could, therefore be deeper. Although the St. Audrie's Bay section recorded more richness, probably due to the greater thickness and high number of species found in the Westbury Formation (Appendix 7). However, most of the fauna associated with the Lias Group shows more affinity to deep-water conditions. For example, St. Audrie's Bay records a low abundance of bivalves, but a dominance of ammonites. In contrast, the assemblages of Pinhay Bay records high richness with assemblages being more complex. e.g. echinoids, crinoids, brachiopods, marine reptiles, bivalves, ammonites (Appendix 5.1). In addition, the Larne section, records a high diversity, although just restricted to bivalves, ammonites and echinoderms (appendices 4.1, 5.1 and 6.1). In summary, the spatial and temporal analysis of the marine fauna through the Tr/J boundary shows significant differences between localities due to environmental conditions. However, through the three sections there is a large turnover of species during the extinction event (i.e. across the Cotham and Langport members), with both regional and local extinctions.

8.3 Ecospace

A total of 10 modes of life were used by the Tr/J marine assemblages through the UK sections. The number of modes of life used by the marine fauna decreases during Cotham Member, however, from the Langport Member to the Blue Lias Formation, the number of modes of life increased gradually until a total of 10 modes of life were recorded.

Ecospace is a measurement of ecological complexity and can be used complementarily to describe palaeoecological patterns before, during and after an extinction event, because it describes the dynamics of the diversification into empty niches (Bambach *et al.* 2007; Bush *et al.* 2007; Novack-Gottshall 2007; Villegger *et al.* 2011). In this context, the recovery model proposed by Twitchett (2006) and Sole *et al.* (2010), will be used to categorise the information derivate from the ecospace studies.

The Westbury Formation can be defined as a background condition or pre-extinction condition (Harries *et al.* 1996), which presents a relatively high richness, however, with a low packing (number of species by mode of life) and low ecological complexity (number of feeding groups). This assemblage records herbivorous and carnivorous gastropods with restrictive moving and three suspension feeder categories that occupying surficial, semi and shallow infaunal modes of life. One important point through this analysis is that the observations are based only on standardised samples by stratigraphic units, which represent a value of local scale or alpha level, i.e. many papers describe the fauna associated with the Westbury Formation as including fish remains, reptile bones, bivalves and trace fossils (which expand the occupied ecospace). The incorporation of such information into the database overestimates the comparison scale,

however, and published studies are often only useful for comparing different scales i.e. regional versus local.

The Cotham Member represents the “Dead Zone” in which only 3 or 4 modes of life are used by species that explored basal trophic levels (see ecospace plots). Within this unit, two or three species fill each mode of life, resulting in a system with low packing, and ecologically very simple. Generally, this assemblage has high dominance, low richness and high values of beta diversity. The Langport Member, like the previous assemblage, shows few numbers of modes of life, however, the species packing increases, making the assemblage more robust, although the ecological complexity is low. In agreement with Twitchett’s model, this unit corresponds to Recovery Stage 1, with a low richness, high dominance (High kurtosis, fitting Geometric or Broken Stick models) and limited tiering (shallow and semi filter feeders). At this level, small traces fossils (*Chondrites* and *Diplocraterion*) are observed in the last beds of this Member (see St Audrie’s Bay and Pinhay Bay sections).

The Pre-Planorbis ‘Zone’ marks the Recovery Stage 2 (Mander *et al.* 2008), and in this level the fauna increases the number of trophic groups with the incorporation of pelagic predators (ammonites), miners and herbivores (echinoids), which indicates an influx of primary productivity into the assemblage. In terms of tiering, the species packing increases and almost all categories are used by the marine fauna (excepting deep-infaunal). At this level, the burrow diameter of ichnogenera (e.g. *Chondrites* and *Palaeophycus*) increases significantly through the sequence. In addition, the crinoid, *I. psilonoti* occupied for first time the erect category. At this time, the assemblage presents a high species richness, low kurtosis and a log normal distribution is presented by the species rank (i.e. mature and stable communities).

The Planorbis Zone represents Stage 3 or 4 of the recovery, which marks the return of the normal marine conditions. With high richness, the rank abundance distribution fits to Log normal models, with high species packing, wide expansion of the fauna through different axis of the ecospace and high ecological complexity. On average, 10 modes of life are used by the marine fauna at this level. Mining feeders, herbivores and pelagic carnivorous - as marine reptiles and ammonites - are found in this level. The burrow diameter of ichnofossils reaches a maximum point in this level.

The Liasicus and Angulata zones represent, in many cases, the same ecological structure that was observed in the Planorbis Zone and potentially could represent Stage 4 of the recovery stage - the complexity, however, at this level is high. Trace fossils are also present through these levels, with constant records of the number of ichnogenera and burrow diameter.

The results obtained by the present study are concurrent with previous observations by Twitchett and Barras (2004), Barras and Twitchett (2007) and Mander *et al.* (2008). The Planorbis Zone could be considered the final stage of the recovery, representing a ceiling in the species richness, the number of modes of life and the maximum values reached by ichno-parameters. The dynamic of the diversification after the extinction event was less intense (more genera extinct than upper taxa). It is probable that the rapid recovery (~125 kya) and occupation of ecospace was by closely related clades, meaning that the taxa were more likely to use the same mode of life, increasing the packing, redundancy and functional ecology.

Future studies could analyse the filling of the ecospace, considering the phylogenetic diversity of the ecospace and, in addition, measure complexity, functionality and

ecological redundancy (Villegger *et al.* 2011). This would allow a comparison of extinction events and generate a ranking base on a true biological index.

8.4 Environmental factors related to the extinction event: Sea level fall, CO₂ increase, or factor combinations.

When changes to the guild abundance structure are examined between stratigraphic units, environmental variation within the basin is apparent (see NMDS). The same pattern was previously observed by Hesselbo *et al.* (2004) in a detailed sedimentological analysis of the Tr/J section in St. Audrie's Bay. Hesselbo *et al.* (2004) interpreted the main facies changes across the Tr/J boundary using sequence stratigraphy. According to this study, the Cotham Member was deposited during a regression of the sea level, representing a low-stand system track.

Afterwards, the sea level started to rise again during the deposition of the Langport Member. As a consequence, the Cotham Member represents a sequence boundary, as the base of a sequence form when the relative sea level is falling at its most rapid rate. As shown by Holland (1995), the clustering of first and last occurrences of taxa is expected at sequence boundaries, indicating that changes in sea levels may trigger ecological collapse and reorganisation. As a matter of fact, the first main changes in faunal composition in the Tr/J in the UK sections are linked to sea level falls and occurred at the base of the Cotham Member.

Close to the top of the Cotham Member is a second major environmental disturbance, expressed by a raise in the CO₂ levels (Ruhl *et al.* 2011), generating a bio-calcification crisis and collapse of the productivity (Ward *et al.* 2001). This CO₂ change apparently did not affect the marine macrofauna immediately (Mander and Twitchett 2008), but rapidly affected marine photosynthetic phytoplankton and benthic foraminifers, through

the extinction and malformation of calcareous nannoplankton and with the apparition of blooms of organic-walled, green algal ‘disaster’ species (acritarchs and prasinophytes) (van de Schootbrugge *et al.* 2007; 2008; Clémence *et al.* 2010).

Consequently, the response of the macrofauna to ocean acidification (Hautmann 2004, 2006, Hautmann *et al.* 2008) is observed throughout the Tr/J section from the Langport Member to the Pre-Planorbis Beds, with a selective extinction of infaunal bivalves. This data concords with observations by McRoberts (1995), Hallam (2002), Mander and Twitchett (2008) and Kiessling *et al.* (2007), indicating the selective extinction of infaunal organisms during the Early Jurassic (See ecospace results). As indicated by Hautmann *et al.* (2008), hyper-calcifying organisms with an aragonitic or high-Mg calcitic skeletal mineralogy and little physiological control of biomineralisation are predicted to suffer most.

In addition, the shell mineralogy co-varies with the substrate relationship, where burrowing bivalves are exclusively aragonitic, whereas the vast majority of epifaunal and semi-infaunal Triassic bivalves had calcitic outer shell layers. In addition to this environmental scenario, a potentially localised anoxic phase is present in north-west European sections. Under benthic anoxic conditions, the redox boundary may be close to the sediment-water interface, resulting in the presence of toxic H₂S within the sediment. This model has been invoked to explain the apparent absence of infaunal suspension-feeders from other Early Jurassic low-oxygen bivalve assemblages (Aberhan and Baumiller 2003; Twitchett and Barras 2004; Barras and Twitchett 2007).

Ecological variable estimates in this study have a high probability of fit with the trajectory of physical variables such as sea level change, CO₂ increase and oxygen depletion observed across the Tr/J boundary. However, sea level changes led to the

greatest turnover of the fauna between the Westbury Formation and the Cotham Member. Later, ocean acidification and anoxic events directly affected the primary productivity and in addition, generated a selective extinction front for infaunal organisms, for which it can be stated that the Tr/J is a clear case of mass extinction, although related with two stages of extinction that acted a-synchronously.

8.5 Body size

The results of the analysis in body size indicate that the bivalve assemblage does not show a reduction in body size throughout the Tr/J study sections, whilst the mean body size tends to increase or remain constant throughout the sequence.

The ‘Lilliput effect’ is a term used to describe the temporary appearance of a subnormal phenotype (small body size) in surviving taxa in the immediate aftermath of an extinction event. This phenomenon has been widely documented over different extinction events and for different organisms (Jablonski and Raup 1995; Twitchett 2006; Twitchett 2007; Keller and Abramovich 2009; Wade and Twitchett 2009; Brayard *et al.* 2010; Huang *et al.* 2010; Bosetti *et al.* 2011; Song *et al.* 2011).

However, during the Tr/J extinction event only Hautmann (2004, 2006) and Mander *et al.* (2008) have observed this phenomenon, although from a holistic point of view. Mander *et al.* (2008) studied the St Audrie’s Bay section, defining the extinction between the Westbury Formation and Cotham Member and suggested that the reduction in body size of bivalve assemblage occurs after the extinction event, but without an exhaustive analysis. Hautmann (2004) generated a more elaborate explanation for body size reduction, and proposed that the reduction was caused by changes in the seawater chemistry (e.g. changes from aragonite to calcite). Infaunal bivalves are invariably

aragonite-shelled and were slightly more affected by the Tr/J extinction event than epifaunal bivalves, which frequently had partly calcitic shells (McRoberts 2001). In addition, Hautmann concluded that the largest and thickest shelled bivalve clades retained their aragonitic shell, but reduced their body size distinctly, as a way to compensate the metabolic cost of dissolution, e.g. within the Megalodontoidea (Hippuritoida).

In the present study, ~30% of the bivalve species recorded went through from the Westbury Formation to the Cotham Member and ~17% of this assemblage comprises infaunal bivalves. Despite this, none of the species recorded decreased their body size through the extinction event. Differences in aforementioned observations could be due to the fact that Hautmann (2004; 2006) based his conclusion on the fauna from the Kendelbach Gorge of the Alps (Austria), the species composition of which differs from that observed in the United Kingdom. For example, he extrapolated his conclusion based on the reduction of the size of taxa associated with the Megalodontoidea, however, representatives of these taxa are not present in the U.K. sections.

In parallel, epifaunal taxa did not experience a reduction in body size and are over-represented through the studied section, which masks the reduction in size of certain groups. Similarly, groups, such as Pectinidae, Plicatulidae, Ostreidae and Gryphaeidae, are recurrent taxa throughout the section and it has been documented that they tend to increase their body size between 25-100% across the Tr/J boundary (McRoberts and Carter 1994, Hautmann 2001, 2004). The Rhaetian fauna (from the Westbury Formation, the Cotham Member and the Langport Member) does not present specimens of large size (< 20 mm), even specimens of genera such as *Chlamys*, *Cardinia* and

Plagiostoma show a reduced body size. The species that went through the Tr/J extinction event, therefore, already have a small size (*see* histogram by species).

In addition, the evaluation of the change in body size through the Jablonski target plot (Jablonski *et al.* 1996) allows the separation of (a) directional trends (Lilliput effect and Cope Rule) from (b) trends that simply result from changes in variance (Metcalf *et al.* 2011).

These plots demonstrate that size changes through the extinction event in basically two ways: (1) towards an increase in body size and (2) an increase and decrease in variance. The observed increases in body size are driven by *Chlamys*, *Cardinia*, *Mytilus* and *Plagiostoma* and this phenomenon is most frequently to observed from the Langport Member to the top the Blue Lias Formation - although directional trends towards a reduction of the body size were not observed during the extinction event (from the Westbury Formation to the Cotham Member). Conversely, in most cases, *Modiolus* showed a more restrictive response; either a directional trend in reduction of the body size, or towards a decrease in variance (i.e., a decrease in the maximum size co-occurring with an increase in minimum size).

Most probably, the decrease of body size and increased variance in body size could be related to: (1) quality of the data, i.e., the sample size is not “big enough” to represent the general trend that happened to the assemblage through time (i.e., low occurrence of some taxa: *Mytilus*, *Plagiostoma* and *Chlamys*) and (2) a biological response, which could affect the change in variance, i.e. in other extinction events, an increase in variance has been described as coinciding with intervals of lowered diversity and abundance (Morten and Twitchett 2009) and as a result of reduced interspecific pressures (Metcalf *et al.* 2011).

The increase in body size of the assemblage is highly evident in specimens of the genus *Plagiostoma*, which could be explained by an improvement of environmental conditions. One of the major controls upon the body size is food supply (Twitchett 2007) and productivity and oxygen are two of the potential factors that control the ecological parameters. Twitchett and Barras (2004) and Barras and Twitchett (2007) demonstrated an increase in productivity and oxygen levels through the increase of burrow diameter and the intensity of bioturbation using trace fossils.

This was the first detailed study that incorporated systematic measurement of several species through the Tr/J section in the UK. However, it is necessary to increase the sampling intensity by species and by stratigraphic horizon in order to obtain a best representation of the distribution of size of each species. This will allow for a determination of certainty: firstly, to establish whether the changes in variance are due to biotic (intraspecific pressures) or abiotic factors (terrigenous input or even taphonomic biases) and secondly, to confirm the directional trends of increases in body size across the Tr/J boundary.

The different methods used to evaluate the reduction in body size in bivalve assemblages indicates that it is not possible to observe a Lilliput Effect through the section in the UK and that, in agreement with Hautmann's conclusions, this is most probably only a local phenomenon associated with a "calcification crisis", which involved some bivalve clades. Similarly, the body size tends to show high variations between different temporal assemblages (i.e. from the Langport Member to the Pre-Planorbis 'Zone'), which drive reductions and increases in variance, which in turn may be associated with physical or biological factors.

Finally, the increase in body size at the top of the section could be related to an improvement of the environmental condition, as productivity and oxygen availability are increased. More detailed observations are necessary; not only of body size, but also of morphological features, possibly spanning a wider period of time (i.e. Norian to Hettangian) as well as different clades. This will allow the relationships between disparity (morphological diversity), the extinction event and clade selection to be determined. In parallel, it is of high importance to correlate palaeo-proxies (temperature, oxygen, carbon and nitrogen) in order to determine with which variable the body size is associated and which of these variables has more effect on the organisms and the assemblage.

8.6 Tr/J in Chile

The section of the Portezuelo Providencia records a very low number of taxa (33) compare with the UK sections. Of 33 samples taken from the section, just 57% of the samples contained species, and of these, 12 samples came from the Rhaetian (*Marshi Zone*) and seven samples from the Hettangian (Fig. 7.3). In addition, the specimens were not scattered uniformly through the section, which made it difficult to pool the samples by biozone in such a way that they could be compare with other sections. For this reason, the numbers of specimens were pooled in two assemblages: Triassic and Jurassic. The separation between both periods was established by the FA of the ammonite of the genus *Psiloceras*, which was recorded in the field (Appendix 5.8). The genus *Psiloceras* recorded in this study indicated the base of the *Tilmanni Zone* (Table 7.4; South America), which correlates with the base of the Blue Lias in the UK sections (Page 2010).

Despite the low number of specimens recorded in this section, the number of taxa did not record differences between assemblages (Triassic and Jurassic) (Fig. 7.4). However, the trajectory of the mean taxonomic richness tended to decrease from the base (Triassic) to the top of the section (Jurassic) (Fig. 7.2). This diversity drop seemingly coincides stratigraphically with the diversity drop observed in the UK sections (the Cotham Member and the Langport Member). However, the richness curve through the section records high fluctuation.

In terms of composition, the fauna recorded a drastic turnover from the Triassic assemblage to the Jurassic assemblage. The Triassic assemblages are made up by taxa with high affinity to relatively shallow systems with high richness of bivalves (see appendix 7.4) which is replaced by a fauna dominated by ammonites and composed of just 3 genera; *Chlamys* sp., *Pseudolimea* sp. and *Otapiria* sp. (see fig. 7.8).

Previous observations, based on Hillebrandt (1990) and Chong and Hillebrandt (1985), indicate that the upper Triassic was made up by a very rich fauna, which includes species of the genus *Schafhaeutlia*, *Gryphea*, *Liostrea*, *Septocardia*, *Paleocardita*, *Pseudolimea* and *Oxytoma*. The cosmopolitan ammonite, *Choristoceras marshi*, and gastropods such as *Planospirina* and *Chartronella* were very common. Brachiopods such as *Zugmayerella* and *Clavigera* were typical in the Upper Triassic. Even in closer localities (Punta del Viento and Quebrada Vaquillas), conodonts genera such as *Epigondella* and *Neogondolella* have been described, as well as ichthyoliths associated with the genus *Glabisubcorona* sp. (Samson 2000). As additional information, remains of marine reptiles were found in the beds associated with the upper Triassic (“ex situ”). This can give an idea of how complex the End-Triassic assemblages were. In contrast, the Early Hettangian was constituted by a very poor assemblage, with genera like

Pseudolimea, *Chlamys*, *Entolium* and *Plagiostoma*, being most common through the assemblages, yet dominated by ammonites.

In contrast to the previous description, the ecological complexity of this assemblage is very poor. The fauna is restricted to pelagic, surficial and semi faunal forms, with just one specimen as a pelagic form. Just 2% of the ecospace is used by the Tr/J fauna in Chile. Five modes of life are used by the Triassic assemblages, whilst 3 modes are used by the Jurassic assemblages. Comparatively, ten modes of life were recorded from the UK sections. Of these, a minimum of 3 modes of life were occupied by the Cotham member assemblages (Figure. 3.11; 4.11; 5.11), but none of these assemblages shared any modes of life. Despite the fact that this Triassic assemblage from Chile records the first pelagic forms in the Triassic seascape, it is in agreement with the selective extinction of the infaunal bivalves (Hallam 1981; McRoberts 2001; Hallam 2002; Aberhan and Baumiller 2003; Hautmann 2004; Kiessling *et al.*, 2007; Mander and Twitchett 2008; Mander *et al.*, 2008). The Jurassic section does not record infaunal bivalve taxa, which suggests that the selectivity of the extinction against infaunal bivalves was potentially in response to a global phenomenon.

Aberhan and Baumiller (2003) performed a comparative study of the marine fauna from the early Jurassic between the Andean base and northwestern Europe. In this study, they made two important observations: that the richness of the marine fauna in the Andean basin is much lower than the richness observed in Europe and that the extinction rates are higher than observed in the Andean basin. They relate this drop to an anoxic event, adding that this extinction could change as a function of the geographic range.

In this work, it is observed that the richness, composition and structure of the assemblage changes abruptly through the Tr/J boundary. Many of the studied fossils are

poorly preserved due to heavily altered thin beds of silty clay shale. However, the results of this work are consistent with previous studies, which demonstrate a disruption in the marine assemblages. This is the first palaeoecological description performed in the Triassic/Jurassic section in Chile, which confirms the sudden change in the marine fauna.

The sample size used in this assemblage is not sufficient for an accurate representation, due to the low preservation quality of the fossil record in the Andean basin. This implicates that it is necessary to increase the sampling intensity in spatial terms. This could give a better approach to the effect of the Tr/J extinction event in terms of intensity and would also generate a more appropriate biological model for the factors that control the turnover and richness in the fauna. On the other hand, it is necessary to perform a detailed study of the ammonite fauna through the Tr/J boundary, even though Hillebrandt (2000) analysed the ammonite fauna in detail, because there is not a clear fit between the South America zones and the Northwest Europe subzones (i.e.: the correlation The *Tilmanni* Subzone with the *Planorbis* Zone).

8.7 Geographical variation of the Tr/J extinction event

The Tr/J palaeocommunities sampled in St Audrie's Bay, Larne and Pinhay Bay recorded a higher diversity than the ones observed in Chile. However, the dynamics of changes in each sampled community showed a drastic change in each ecological parameter. The Tr/J palaeocommunities in the UK have been well documented (Hallam 1960; Hallam 1996; Hallam and Wignall 2000; Twitchett and Barras 2004; Hesselbo et al. 2004; Barras and Twitchett 2007; Mander et al. 2008; Wignall and Bond 2008; Mander and Twitchett 2008; Korte et al. 2009; Clémence et al. 2010). However, an ecological approach has not been seen in detail until now. This work shows that the

dynamic of change of the biodiversity in St Audrie's Bay, Larné and Pinhay Bay is very similar. Despite that there are few differences in the species composition; all the localities described a significant and simultaneous drop in species richness from the Cotham Member to the Langport Member and a very similar recovery process (from the Pre-Planorbis Zone to the Angulata Zone).

The assemblages from the northern hemisphere recorded a selective disappearance of the infaunal bivalves; the species composition changed from deep systems to shallow-water conditions and the species dominance increased during the extinction regime. All the changes have been observed equally in other studies. However, those works were made in localities situated in the north of Pangaea.

The assemblages from Tr/J communities in Chile and the UK are ecologically not compatible. The section from Chile represents a deep-sea environment with poor-species, low ecological complexity and high dominance (Fig. 7.1 and Table 7.1); on which the sea level change had little or no effect in terms of the ecological structure of the assemblage. On the other hand, the assemblages from the UK represent a more shallow condition with high complexity and taxonomical diversity; however, they were strongly modulated by changes in sea level (list of taxa in appendices 4.1, 5.1, 6.1 and 7.1). This point is very important, because probably other environmental factors (apart from the sea level) could modulate the ecological replacement (i.e. Anoxia, CO₂, temperature).

Additionally, it is difficult to establish the simultaneity of the extinction due to absence of a good correlation (See appendix 1.2). Figure 1.3 summarises the correlations between the Chile (Portezuelo Providencia), the UK and the Austria (Kuhjoch) sections (the Austrian stratotype section). The Tr/J boundary through the Chilean and Austrian

section seems to be well correlated due to FA of *Psiloceras* (Appendix 7.8). However, unlike St Audrie's Bay, the Chilean sections do not have an isotopic analysis that allows linking one of the main CO₂ disturbance events with the onset of the extinction event (which is related to LA of *C. crickmayi* in Austria). This is another important point, because it does not allow comparison and a precise estimation of the response time and the intensity of the ecological changes in local assemblages (See section 7.1). In this sense, it is difficult to infer if the low biodiversity observance in the Chilean palaeoassemblages is the result of the extinction regime caused by increases in CO₂ concentrations.

The studies through the Tr/J boundary in South America has been mostly descriptive and focused on the establishment of a stratigraphical framework (Hillebrandt 1990, 1994, 2000, Riccardi and Llanos 1999, Riccardi 2008). In this sense, the palaeontological knowledge of the biotic crisis, especially during the Tr/J extinction event still remains unclear. This work is one of the first palaeoecological studies performed in South America, however, the information records in this work do not allow to establish the intensity and time span in which this event occurred. The data suggest a significant dynamic of changes of the species composition and a selective extinction of certain modes of life (infaunal forms), similar to observations through the UK sections (St Audrie's Bay, Larne).

Future investigation through the Chilean section should increase the sampling intensity and to incorporate other localities. Besides, for that would be necessary to develop isotopic analysis which permits identified environmental factors related to this extinction, correlated precisely with another section and determine the response times of the communities through the Tr/J extinction event.

Conclusions

Quantitative, palaeocommunity-level analyses of assemblages across Tr/J boundary sections clearly suggest a marked disruption in the evolution of marine fauna taxa and emphasise the variability of the ecological response to the extinction. Based on these analyses, the following aspects of this event may be highlighted:

- 1) More than 60% of the species disappear during the Cotham Member interval, whilst the Langport Member represents the onset of the recovery with the maximum taxonomical richness being reached in the Planorbis Zone.
- 2) Rapid sea level fall established the sudden disappearance of the marine fauna associated with the Westbury Formation. Through the Cotham Member and the Langport Member, ocean acidification produced a selective extinction of infaunal and aragonitic-shell organisms.
- 3) The extirpation of the palaeocommunity during this extinction event was extremely rapid, which happened at 201.44 Ma, clearly before the first negative carbon excursion (201.43 Ma and with a length of ~20-40 kyr). The duration of the Dead Zone spanned ~100 kyr without recording any speciation event.
- 4) In term of abundance, the Cotham Member represents assemblages with few species and high dominance, generally associated with RADs that fit a geometric or broken stick model. In contrast, assemblages sampled from the Westbury Formation, Langport Member and Blue Lias Formation, have a low dominance, and their RADs generally fit to a Lognormal, Zipf or Mandelbrot model, reflecting species-rich assemblages or assemblages from late successional stages.

- 5) NMDS ordination confirms that pre-extinction communities (of the Westbury Formation) were compositionally different from post-extinction communities (of the Blue Lias Formation). Similarly, examining the response of the beta diversity in all the section confirms the high species turnover into the Lilstock Formation, mainly within the Cotham Member.
- 6) Compositional analysis indicates that the extinction event acted significantly at a generic level rather than at family, order, or class level. This indicates that the ecological modifications were high; however, the phylogenetic structure did not show significant changes into the Early Jurassic.
- 7) The number of modes of life used by the marine fauna decreased during the Cotham Member. However, from the Langport Member to the Blue Lias Formation, the numbers of modes of life increased gradually, until a total of 10 were recorded; those changes in the ecospace are closely relating with the ecological complexity of the Tr/J assemblages.
- 8) The recovery of the Tr/J mass extinction was relatively quick (~1.8 Ma), compared to other mass extinctions (e.g. End-Permian), and spanned from the Pre-Planorbis Zone to the Angulata Zone. During the recovery stage the ichno-parameters, such as borrow diameter, cover and ichnofabric index increases from the Pre-Planorbis Zone to Angulata Zone, however, the increase was faster from the base to the top of the Pre-Planorbis Zone. Additionally, the ichno-parameter values increase simultaneously with the increase of the ecological variables.
- 9) Body size of marine bivalves did not decrease during the extinction event within the Cotham Member). Although the general trend indicates that the

marine bivalves tend to increase their body size, the trajectory of each body size seems high through the stratigraphic sequence.

10) The palaeoassemblages from the Portezuelo Providencia section recorded very low species richness (7 species). However, variables, such as abundance, demonstrate that the dominance increased in the assemblage; that the marine fauna suffered a compositional change of more than 90% and that diversity (Shannon-Weaver index) decreased after the Tr/J mass extinction event. Those parameters (composition and abundance) would suggest a Tr/J mass extinction effect. The Portezuelo Providencia section and the UK section do not show ecological compatibility. The Chilean section represents deep-water environment with a low richness, whilst all UK sections represent species-rich environments with deep-shallow water conditions.

11) The low number species in the Chilean section, the lack of a precise correlation of ammonites and the absence isotopic analysis do not allow correlation and comparison of the ecological response with the UK sections through the Tr/J mass extinction event.

References

- Aberhan, M. 1994. Guild–structure and evolution of Mesozoic benthic shelf communities. *Palaios* **9**, 516–545.
- Aberhan, M. and Baumiller, T. K. 2003. Selective extinction among Early Jurassic bivalves: A consequence of anoxia. *Geology*, **31**, (12) 1077–1080.
- Aberhan, M., 1992. Palökologie und zeitliche Verbreitung benthischer Faunengemeinschaften im Unterjura von Chile. *Beringeria* **5**, 1–174.
- Aberhan, M., 1994. Guild–structure and evolution of Mesozoic benthic shelf communities. *Palaios*, **9**, 516–545.
- Aberhan, M., Kiessling, W. and Fursich, F. T. 2006. Testing the role of biological interactions in the evolution of mid–Mesozoic marine benthic ecosystems. *Paleobiology*, **32**, (2) 259–277.
- Alessandrello, A., Arduini, P., Pinna, P., and Teruzzi, G., 1991. New observations on the Thylacocephala (Arthropoda, Crustacea). In: A. M. Simonetta & S. Conway Morris, *The Early Evolution of Metazoa and the Significance of Problematic Taxa*. Cambridge University Press, Cambridge. pp. 245–251.
- Alroy, J. 2008. Dynamics of origination and extinction in the marine fossil record. *Proceedings of the National Academy of Sciences of the United States of America*, **105**, 11536–11542.
- Alroy, J. *et al.*, 2008. Phanerozoic Trends in the Global Diversity of Marine Invertebrates. *Science*, **321**, 97 – 100.
- Anderson, J.R., Hoare, R.D., and Sturgeon, M.T., 1990. The Pennsylvanian gastropods *Donaldina* Knight in the Appalachian basin, eastern U.S.A. *Journal of Paleontology*, **64**, 557–562.
- Arias, C. 2008. Palaeoceanography and biogeography in the Early Jurassic Panthalassa and Tethys Oceans. *Gondwana Research*, **14**, 306–315.
- Arratia, G., 1996. The Jurassic and the early history of teleosts. In: G. Arratia & G. Viohl (Eds.), *Mesozoic Fishes: Systematics and Paleoecology*. Verlag Dr. F. Pfeil, München, 243–259 pp.
- Arratia, G., and Tintori, A., 2004. *Mesozoic Fishes 3: Systematics and Paleoecology*. Verlag Dr. F. Pfeil, München, Germany.
- Ausich, W.I., and Bottjer, D.J., 1982. Tiering in suspension feeding communities on soft substrata throughout the Phanerozoic. *Science*, **216**, 173–174.
- Ausich, W.I., and Bottjer, D.J., 2001, Sessile invertebrates, in Briggs, D.E.G., and Crowther, P.R., eds., *Palaeobiology II*: Oxford, Blackwell Science, p. 384–386.
- Ausich, W.I., and Bottjer, D.J., 2003. Infauna and Epifauna. In: *Palaeobiology: A Synthesis*, D. Briggs and P. Crowther (Eds.), Blackwell Scientific Publications, Oxford, p. 41–49.

- Bacon, K. L., Belcher, C. M., Hesselbo, S. P. and McElwain, J. C. 2011. The Triassic–Jurassic Boundary Carbon–Isotope Excursions Expressed in Taxonomically Identified Leaf Cuticles. *Palaios*, **26**, (7–8) 461–469.
- Bambach, R. K., Bush, A. M. and Erwin, D. H. 2007. Autecology and the filling of ecospace: Key metazoan radiations. *Palaeontology*, **50**, 1–22.
- Bambach, R. K., Knoll, A. H. and Sepkoski, J. J. 2002. Anatomical and ecological constraints on Phanerozoic animal diversity in the marine realm. *Proceedings of the National Academy of Sciences of the United States of America*, **99**, (10) 6854–6859.
- Bambach, R. K., Knoll, A. H. and Wang, S. C. 2004. Origination, extinction, and mass depletions of marine diversity. *Paleobiology*, **30**, (4) 522–542.
- Bambach, R.K., 1977. Species Richness in marine benthic habitats through the Phanerozoic. *Paleobiology*, **3**: 152–167.
- Bambach, R.K., 1983. Ecospace utilization and guilds in marine communities through the Phanerozoic. *Biotic interactions in Recent and fossil benthic communities*: pp. 719–746.
- Bambach, R.K., 1985. Classes and Adaptive Variety: The Ecology of Diversification in Marine Faunas Through the Phanerozoic. in Valentine, J.W. (Eds) *Phanerozoic Diversity Patterns: Profiles in Macroevolution*. Princeton University Press. pp. 191–253
- Bambach, R.K., 1986. Phanerozoic marine communities. Patterns and processes in the history of life. Report of the Dahlem workshop, Berlin: 407–428.
- Bambach, R.K., 2002. Supporting predators: changes in the global ecosystem inferred from changes in predator diversity. In: M. Kowalewski and P.H. Kelley, (Eds), *The Fossil Record of Predation*, Paleontological Society Papers, pp. 319–351.
- Bambach, R.K., and Knoll, A.H., 2001. Is there a separate class of "mass" extinctions? Program and Abstracts Geological Society of America Annual Meeting (Boston, 2001), session 58.
- Bambach, R.K., Bush, A.M., and Erwin, D.H., 2007. Autoecology and the filling of ecospace: key metazoan radiations. *Palaeontology*, **50**, 1–22.
- Bambach, R.K., Knoll, A.H., and Sepkoski, J.J., 2002. Anatomical and Ecological Constraints on Phanerozoic Animal Diversity in the Marine Realm. *Proceedings of the National Academy of Sciences, U. S. A.* **99**, 6854–6859.
- Bambach, R.K., Knoll, A.H., and Wang, S.C., 2004. Origination, extinction, and mass depletions of marine diversity. *Paleobiology*, **30**, 522 – 542.
- Barras, C. G. and Twitchett, R. J. 2007. Response of the marine infauna to Triassic–Jurassic environmental change: Ichnological data from southern England. *Palaeogeography, Palaeoclimatology, Palaeoecology*, **244**, (1–4) 223–241.
- Beauvais, L., 1984. Evolution and diversification Scleractinia. *Palaeontographica Americana*, **54**, 219– 224.

- Beerling, D.J., and Berner, R.A., 2002. Biogeochemical constraints on the Triassic–Jurassic boundary carbon cycle event. *Global Biogeochemical Cycles*, **16**: 101–113.
- Begon, M., Townsend, C. and Harper J.L., 2006. *Ecology: from individuals to ecosystems*. Blackwell publishing, 4th edition, Oxford, 738 pp.
- Belcher, C. M., Mander, L., Rein, G., Jervis, F. X., Haworth, M., Hesselbo, S. P., Glasspool, I. J. and McElwain, J. C. 2010. Increased fire activity at the Triassic/Jurassic boundary in Greenland due to climate–driven floral change. *Nature Geoscience*, **3**, (6) 426–429.
- Bellwood, D.R., 2003. Origins and escalation of herbivory in fishes: a functional perspective. *Paleobiology*, **29**(1): 71–83.
- Benton, M. J. 1995. Diversification and extinction in the history of life. *Science*, **268**, 52–58.
- Benton, M. J. and Twitchett, R. J. 2003. How to kill (almost) all life: the end-Permian extinction event. *Trends in Ecology & Evolution*, **18**, (7) 358–365.
- Benton, M.J., (ed.) 1993. *The Fossil Record 2*. Chapman & Hall, London: 845pp.
- Berke, S. K. 2010. Functional Groups of Ecosystem Engineers: A Proposed Classification with Comments on Current Issues. *Integrative and Comparative Biology*, **50**, (2) 147–157.
- Berner, R.A., and Beerling, D.J., 2007. Volcanic degassing necessary to produce a CaCO₃ undersaturated ocean at the Triassic–Jurassic boundary. *Palaeogeography, Palaeoclimatology, Palaeoecology*, **244**(1–4): 368–373.
- Blake, D.B., and Hagdorn, H., 2003. The Asteroidea (Echinodermata) of the Muschelkalk (Middle Triassic of Germany). *Palaontologische Zeitschrift*, **77**: 23–58.
- Bloos, G. 1990. Sea–level changes in the upper Keuper and in the lower Lias of Central Europe. *Cahiers de l' Université catholique de Lyon, Serie Scientifique*, **3**, 5–16.
- Bloos, G. and Page, K. N. (Eds) 2000. *The basal Jurassic ammonite succession in the north–west European province—review and new results*. Advances in Jurassic Research. Tran Tech Publications, Zurich. 105– 117 pp.
- Bloos, G. and Page, K. N. 1998. The Basal Jurassic Ammonite succession in the North–West European Province – review and new results. *GeoResearch Forum*, **6**, 27–40.
- Boomer, I. D., Duffin, C. J. and Swift, A. 1999. Arthropods 1: crustaceans. In: Swift, A. and Martill, D.M. (Eds). *Fossils of the Rhaetian Penarth Group*. The Palaeontological Association, Special Publication, London. pp 129–148.
- Bosetti, E. P., Grahn, Y., Horodyski, R. S., Mauller, P. M., Breuer, P. and Zabini, C. 2011. An earliest Givetian "Lilliput Effect" in the Parana Basin, and the collapse of the Malvinokaffric shelly fauna. *Palaeontologische Zeitschrift*, **85**, (1) 49–65.

- Bottjer, D.J., Schubert, J.K., and Droser, M.L., 1996. Comparative evolutionary palaeoecology: Assessing the changing ecology of the past. In Hart, M. (ed.), *Biotic Recovery from Mass Extinction Events*, Geological Society of London Special Publication No. 102, pp. 1–13.
- Bray, R.J. and Curtis, J.T., 1957. An ordination of the upland forest communities of southern Wisconsin. *Ecological Monograph*, **27**, 325–349.
- Brayard, A., Nutzelt, A., Stephen, D. A., Bylund, K. G., Jenks, J. and Bucher, H. 2010. Gastropod evidence against the Early Triassic Lilliput effect. *Geology*, **38**, (2) 147-150.
- Brayard, A., Vennin, E., Olivier, N., Bylund, K. G., Jenks, J., Stephen, D. A., Bucher, H., Hofmann, R., Goudemand, N. and Escarguel, G. 2011. Transient metazoan reefs in the aftermath of the end-Permian mass extinction. *Nature Geoscience*, **4**, (10) 693–697.
- Brenchley, P. J., Marshall, J. D. and Underwood, C. J. 2001. Do all mass extinctions represent an ecological crisis? Evidence from the Late Ordovician. *Geological Journal*, **36**, 329–340.
- Brown–Saracino, J., Peckol, P., Curran, H. A. and Robbart, M. L. 2007. Spatial variation in sea urchins, fish predators, and bioerosion rates on coral reefs of Belize. *Coral Reefs*, **26**, (1) 71–78.
- Buatois, L.A., and Mangano, M.G., 1993. Ecospace utilization, paleoenvironmental trends, and the evolution of early nonmarine biotas. *Geology*, **21**(7): 595–598.
- Burnham, K. P. and Anderson, D. R. 2002. *Model Selection and Multimodel Inference: A Practical Information-Theoretic Approach*. (2nd Edition ed) Springer-Verlag, New York.
- Burnham, K.P. and Overton, W.S., 1978. Estimation of the size of a closed population when capture probabilities vary among animals. *Biometrika*, **65**, 623–633.
- Burnham, K.P. and Overton, W.S., 1979. Robust estimation of population size when capture probabilities vary among animals. *Ecology*, **60**, 927–936.
- Bush, A. M. and Bambach, R. K. 2011. Paleoecologic Megatrends in Marine Metazoa. *Annual Review of Earth and Planetary Sciences, Vol 39*, **39**, 241–269.
- Bush, A. M., Bambach, R. K. and Daley, G. M. 2007. Changes in theoretical ecospace utilization in marine fossil assemblages between the mid-Paleozoic and late Cenozoic. *Paleobiology*, **33**, (1) 76-97.
- Bush, A.M., and Bambach, R.K., 2004. Did alpha diversity increase during the phanerozoic? Lifting the veils of taphonomic, latitudinal, and environmental biases. *Journal of Geology*, **112**(6): 625–642.
- Buzas, M. A. and Hayek, L. A. C. 2005. On richness and evenness within and between communities. *Paleobiology*, **31**, (2) 199-220.

- Carroll, R.L., 1988. Vertebrate Paleontology and Evolution. W. H. Freeman and Company, New York, pp. 1–698.
- Chamberlin, T. C. and Moulton, F. R. 1909. The development of the planetesimal hypothesis. *Science*, **30**, 642–645.
- Chao, A., 1984. Non–parametric estimation of the number of classes in a population. *Scandinavian Journal of Statistics*, **11**, 265–270.
- Chao, A., 1987. Estimating the population size for capture–recapture data with unequal catchability. *Biometrics*, **43**, 783–791.
- Chazottes, V., Lecampionsumard, T. and Peyrotclausade, M. 1995. Bioerosion Rates on Coral–Reefs – Interactions between Macroborers, Microborers and Grazers (Moorea, French–Polynesia). *Palaeogeography Palaeoclimatology Palaeoecology*, **113**, (2–4) 189–198.
- Chong, G. and Hillebrandt, A., 1985. El Triásico preandino de Chile entre los 23° 30' y 26° 00' de latitud Sur, 4th Congreso Geológico Chileno, **1**, 1–62.
- Clarke, K.R., 1993. Non–parametric multivariate analysis of changes in community structure. *Australian Journal of Ecology*, **18**, 117–143.
- Clarke, K.R. and Gorley, R.N., 2006. PRIMER v6: User Manual/Tutorial. PRIMER–E, Plymouth.
- Clémence, M. E., Bartolini, A., Gardin, S., Paris, G., Beaumont, V. and Page, K. N. 2010. Early Hettangian benthic–planktonic coupling at Doniford (SW England) Palaeoenvironmental implications for the aftermath of the end–Triassic crisis. *Palaeogeography Palaeoclimatology Palaeoecology*, **295**, (1–2) 102–115.
- Clemmensen, L. B., Kent, D. V. and Jenkins, F. A. 1998. A Late Triassic lake system in East Greenland: facies, depositional cycles and palaeoclimate. *Palaeogeography, Palaeoclimatology, Palaeoecology*, **140**, 135–159.
- Coddington, J.A., Young, L.H., and Coyle, F.A., 1996. Estimating spider species richness in a southern Appalachian cove hardwood forest. *Journal of Arachnology*, **24**, 111–128.
- Colbert, E. H. 1958. Triassic tetrapod extinction at the end of the Triassic period. *Proceedings of the National Academy of Sciences*, **44**, 973– 977.
- Coleman, B.D., Mares, M.A., Willig, M.R. and Hsieh., Y.–H., 1982. Randomness, area, and species richness. *Ecology*, **63**, 1121–1133.
- Colwell, R. K., Mao, C. X., and Chang, J., 2004. Interpolating, extrapolating, and comparing incidence–based species accumulation curves. *Ecology*, **85**, 2717–2727
- Colwell, R.K., 2000. EstimateS: Statistical Estimation of Species Richness and Shared Species from Samples (Software and User's Guide), Version 6.
<http://viceroy.eeb.uconn.edu/estimates>

- Colwell, R.K., and Coddington, J.A., 1994. Estimating terrestrial biodiversity through extrapolation. *Philosophical Transactions of the Royal Society of London B*, **345**, 101–118.
- Cope, J. C. W., Getty, T. A., Howarth, M. K., Morton, N. and Torrens, H. S. 1980. *A correlation of Jurassic rocks in the British Isles. Part One: Introduction and lower Jurassic*. Geological Society of London, London. 73 pp.
- Crne, A. E., Weissert, H., Gorican, S. and Bernasconi, S. M. 2011. A biocalcification crisis at the Triassic–Jurassic boundary recorded in the Budva Basin (Dinarides, Montenegro). *Geological Society of America Bulletin*, **123**, (1–2) 40–50.
- Deenen, M. H. L., Ruhl, M., Bonis, N. R., Krijgsman, W., Kuerschner, W. M., Reitsma, M. and van Bergen, M. J. 2010. A new chronology for the end–Triassic mass extinction. *Earth and Planetary Science Letters*, **291**, (1–4) 113–125.
- Deng, S. H., Lu, Y. Z. and Xu, D. Y. 2005. Progress and review of the studies on the end–Triassic Mass extinction event. *Science in China Series D–Earth Sciences*, **48**, (12) 2049–2060.
- Dietl, G.P., 2003. The Escalation Hypothesis: One Long Argument. *Palaios*, **18**(2): 83–86
- Dietl, G.P., and Kelley, P.H., 2002. The fossil record of predator–prey arms races: Coevolution and escalation hypotheses. In: *The Fossil Record of Predation*, Kowalewski, M., & Kelley, P. (eds.). *Paleontological Society Papers*, **8**: 353–374.
- Droser, M. L., Bottjer, D. J., Sheehan, P. M. and McGhee, G. R. 2000. Decoupling of taxonomic and ecologic severity of Phanerozoic marine mass extinctions. *Geology*, **28**, (8) 675–678.
- Droser, M.L., and Bottjer, D.J., 1986. A semiquantitative field classification of ichnofabric. *Journal of Sedimentary Petrology*, **56**, 558–559.
- Droser, M.L., and Bottjer, D.J., 1991. Trace fossils and ichnofabric in leg 119 cores. *Proceedings of the Ocean Drilling Program, Scientific Results*, **119**, 635–641.
- Droser, M.L., and Bottjer, D.J., 1993. Trend and patterns of Phanerozoic Ichnofabrics. *The Annual Review of Earth and Planetary Sciences*, **21**, 205–225.
- Droser, M.L., and Finnegan, S., 2003. The Ordovician radiation: A follow–up to the Cambrian explosion? *Integrative and Comparative Biology*, **43**(1): 178–184.
- Droser, M.L., Bottjer, D.J., and Sheehan, P.M., 1997. Evaluating the ecological architecture of major events in the Phanerozoic history of marine invertebrate life. *Geology*, **25**(2): 167–170.
- Droser, M.L., Bottjer, D.J., Sheehan, P.M., and McGhee, G.R.J., 2000. Decoupling of taxonomic and ecologic severity of Phanerozoic marine mass extinctions. *Geology*, **28**(8): 675–678.

- Dubiel, R. F., Parrish, J. T., Parrish, J. M. and Good, S. C. 1991. The Pangaeian megamonsoon: evidence from the Upper Triassic Chinle Formation, Colorado Plateau. *Palaios*, **6**, 347–370.
- Erwin, D. H. 1998a. The end and the beginning: recoveries from mass extinctions. *Trends in Ecology & Evolution*, **13**, (9) 344–349.
- Erwin, D. H. 1998b. Evolution – After the end: Recovery from extinction. *Science*, **279**, (5355) 1324–1325.
- Erwin, D. H. 2001. Lessons from the past: Biotic recoveries from mass extinctions. *Proceedings of the National Academy of Sciences of the United States of America*, **98**, (10) 5399–5403.
- Erwin, D. H. 2008. Extinction as the loss of evolutionary history. *Proceedings of the National Academy of Sciences of the United States of America*, **105**, 11520–11527.
- Erwin, D. H. and HuaZhang, P. 1996. Recoveries and radiations: Gastropods after the Permo–Triassic mass extinction. *Biotic Recovery from Mass Extinction Events*, (102) 223–229.
- Erwin, D.H., 2006. *Extinction! How Life Nearly Ended 250 Million Years ago*. Princeton University Press..
- Erwin, D.H., Valentine, J.W., and Sepkoski, J.J., 1987. A comparative study of diversification events: the early Paleozoic versus the Mesozoic. *Evolution*, **41**(6): 1177–1186.
- Ezcurra, M. D. 2010. Biogeography of Triassic tetrapods: evidence for provincialism and driven sympatric cladogenesis in the early evolution of modern tetrapod lineages. *Proceedings of the Royal Society B–Biological Sciences*, **277**, (1693) 2547–2552.
- Faith, D. P., Minchin, P. R., and Belbin, L., 1987. Compositional dissimilarity as a robust measure of ecological distance. *Vegetatio*, **69**, 57–68.
- Fastovsky, D.E., Huang, Y., Hsu, J., Martin–McNaughton, J., Sheehan, P.M., and Weishampel, D.B., 2004. Shape of Mesozoic dinosaur richness. *Geology*, **32**: 877–880.
- Feldmann, R.M., and Goolaert, S., 2005. *Palaega rugosa*, a new species of fossil isopod (crustacea) from maastrichtian rocks of tunisia. *Journal of Paleontology*, **79**(5): 1031–1035.
- Foggo, A., Attrill, M.J., Frost, M.T. and Rowden, A.A., 2003. Estimating marine species richness: an evaluation of six extrapolative techniques. *Marine Ecology Progress Series*, **248**, 15–26.
- Fraiser, M.L., and Bottjer, D.J., 2005. Restructuring in benthic level–bottom shallow marine communities due to prolonged environmental stress following the end–Permian mass extinction. *Comptes Rendus – Palevol*, **4**(6–7): 515–523.

- Frakes, L. A., Francis, J. E. and Syktus, J. L. 1992. *Climate Modes of the Phanerozoic: The History of the Earth's Climate over the Past 600 Million Years*. Cambridge University Press, Cambridge. 274 pp.
- Fraser, N.M., Bottjer, D.J., and Fischer, A.G., 2004. Dissecting “Lithiotis” Bivalves: Implications for the Early Jurassic Reef Eclipse. *Palaios*, **19**: 51–67.
- Frontier, S. 1987. Applications of fractal theory to ecology. In: Legendre, P. (editor) *Developments in Numerical Ecology*, Springer–Verlag, Berlin, pp. 357–378.
- Frontier, S., 1985. Diversity and structure in aquatic ecosystems. *Oceanography and Marine Biology Annual Review*, **23**, 253–312.
- Gallois, R. W. 2007. The stratigraphy of the Penarth Group (Late Triassic) of the east Devon coast. *Geoscience in south-west England*, **11**, 287–297
- George, N. T. 1969. Recommendations on stratigraphical usage. *Proceeding Geological Society of London*, **1656**, 139– 166.
- Gerhard, L. C., Anderson, S. B., Lefever, J. A. and Carlson, C. G. 1982. Geological development, origin, and energy mineral resources of Williston Basin, North Dakota. *American Association of Petroleum Geologists* **66**, 989–1020.
- Golonka, J. 2004. Plate tectonic evolution of the southern margin of Eurasia in the Mesozoic and Cenozoic *Tectonophysics*, **381**, 235–273.
- Golonka, J. 2007. Late Triassic and Early Jurassic paleogeography of the world *Palaeogeography, Palaeoclimatology, Palaeoecology*, **244**, 297–307.
- Gotelli, N. J. and Graves, G. R., 1996. *Null models in ecology*. Smithsonian Institution Press. Washington. 368 pp.
- Gotelli, N.J. and Entsminger, G.L., 2011. EcoSim: Null models software for ecology. Version 7. Acquired Intelligence Inc. & Kesity–Bear. Jericho, VT 05465. <http://garyentsminger.com/ecosim.htm>.
- Gotelli, N.J., 2006. Null versus neutral models: what’s the difference? *Ecography*, **29**, 793–800.
- Gould, S.J., and Calloway, C.B., 1980. Clams and brachiopods — ships that pass in the night, *Paleobiology*, **6**: 383–396.
- Gradstein, F., Ogg, J., and Smith, A., 2005. *A Geologic Time Scale*, Cambridge University Press, Cambridge.
- Grossmann, S., and Reichardt, W., 1991. Impact of *Arenicola marina* on bacteria in intertidal sediments. *Marine Ecology Progress Series*, **77**: 85–93.
- Guex, J., Bartolini, A., Atudorei, V. and Taylor, D. 2004. High–resolution ammonite and carbon isotope stratigraphy across the Triassic–Jurassic boundary at New York Canyon (Nevada). *Earth and Planetary Science Letters*, **225**, (1–2) 29–41.

- Hallam, A. 1960 A sedimentary and faunal study of the Blue Lias of Dorset. *Philosophical Transaction of the Royal Society, London*, **B243**, 1-44.
- Hallam, A. 1981. The end- Triassic bivalve extinction event. *Palaeogeography, Palaeoclimatology, Palaeoecology*, **35**, (1) 1-44.
- Hallam, A. 1990. The End–Triassic Mass Extinction Event. *Global Catastrophes in Earth History : An Interdisciplinary Conference on Impacts, Volcanism, and Mass Mortality*. pp 577–583.
- Hallam, A. 1995. Oxygen-restricted facies of the basal Jurassic of North West Europe. *Historical Biology*, **10** 247–257.
- Hallam, A. 1995. Oxygen–restricted facies of the basal Jurassic of North West Europe. *Historical Biology*, **10**, 247–257.
- Hallam, A. 1996. Recovery of the marine fauna in Europe after the end-Triassic and early Toarcian mass extinctions. *Biotic Recovery from Mass Extinction Events*, (102) 231-236.
- Hallam, A. 1997. Estimates of the amount and rate of sea–level change across the Rhaetian–Hettangian and Pliensbachian–Toarcian boundaries (latest Triassic to early Jurassic). *Journal of Geological Society*, **154**, 773–779.
- Hallam, A. 2002. How catastrophic was the end-Triassic mass extinction? *Lethaia*, **35**, 147-157.
- Hallam, A. and Wignall, P. B. 1997. *Mass extinctions and their aftermath*. Oxford University Press, New York.
- Hallam, A. and Wignall, P. B. 1999. Mass extinctions and sea–level changes. *Earth Science Reviews*, **48**, (4) 217–250.
- Hallam, A. and Wignall, P. B. 2000. Facies changes across the Triassic–Jurassic boundary in Nevada, USA. *Journal of the Geological Society*, **157**, 49–54.
- Hammer, Ø., and Harper, D.A.T., 2006. Paleontological Data Analysis. Blackwell, pp. 351.
- Hammer, Ø., Harper, D.A.T., and Ryan, P. D., 2001. PAST: Paleontological Statistics Software Package for Education and Data Analysis. *Palaeontologia Electronica*, **4**,1–9.
- Harper, E.M., 2003. The Mesozoic Marine Revolution. In Kelley, P., Kowalewski, M., and Hansen T.A., Kluwer (Eds) *Predator–prey interaction in the fossil record*, Academic/Plenum Publishers, New York, pp. 433–455.
- Harries, P. J., Kauffman, E. G. and Hansen, T. A. 1996. Models for biotic survival following mass extinction. *Biotic Recovery from Mass Extinction Events*, (102) 41-60.
- Hautmann, M. 2001. Taxonomy and phylogeny of cementing Triassic Bivalves (Families Prospondylidae, Plicatulidae, Dimyidae and Ostreidae). *Palaeontology* **44** (2) 339-373.

- Hautmann, M. 2004. Effect of end-Triassic CO₂ maximum on carbonate sedimentation and marine mass extinction. *Facies*, **50**, (2) 257-261.
- Hautmann, M. 2006. Shell mineralogical trends in epifaunal Mesozoic bivalves and their relationship to seawater chemistry and atmospheric carbon dioxide concentration. *Facies*, **52**, 417-433.
- Hautmann, M. and Golej, M. 2004. *Terquemia* (*Dentiterquemia*) *eudesdeslongchampsii* new subgenus and species, an interesting cementing bivalve from the Lower Jurassic of the western Carpathians (Slovakia). *Journal of Paleontology*, **78**, (6) 1086-1090.
- Hautmann, M., Benton, M. J. and Tomasovych, A. 2008. Catastrophic ocean acidification at the Triassic-Jurassic boundary. *Neues Jahrbuch für Geologie und Paläontologie, Abhandlungen*, **249** (1)119-127.
- Hautmann, M., Stiller, F., Huawei, C. and Jingeng, S. 2008b. Extinction-recovery pattern of level-bottom faunas across the Triassic-Jurassic boundary in Tibet: implications for potential killing mechanisms. *Palaios*, **23**, (711-718)
- Hayek, L.C., and Buzas. M. A., 1997. Surveying natural populations. Columbia University Press, New York, 563 pp.
- He, W.-H. Twitchett, R. J., Zhang, Y., Shi, G. R., Feng, Q.-L., Yu, J.-X., Wu, S.-B., Peng, X.-F., 2010. Controls on body size during the Late Permian mass extinction event. *Geobiology*, **8**, 391-402.
- Hendy, A., Aberhan, M., Alroy, J., Clapham, M., Kiessling, W., Lin, A., and LaFlamme, M., 2009: A 600 million year record of ecological diversification. Unpublished ecological data in support of GSA 2009, Abstract.
- Hesselbo, S. P., Mcroberts, C. A. and Palfy, J. 2007. Triassic-Jurassic boundary events: problems, progress, possibilities. *Palaeogeography, Palaeoclimatology, Palaeoecology*, **244** 1-10.
- Hesselbo, S. P., Robinson, S. A. and Surlyk, F. 2004. Sea-level change and facies development across potential Triassic-Jurassic boundary horizons, SW Britain. *Journal of the Geological Society*, **161**, (3)365-379.
- Hesselbo, S. P., Robinson, S. A., Surlyk, F. and Piasecki, S. 2002. Terrestrial and marine extinction at the Triassic-Jurassic boundary synchronized with major carbon-cycle perturbation: a link to initiation of massive volcanism? . *Geology*, **30**, 251-254.
- Hillebrandt, A. V. 1990. The Triassic-Jurassic boundary in the northern of Chile. *Cahiers de l' Université catholique de Lyon, Serie Scientifique*, **3**, 27-53.
- Hillebrandt, A. V. 1994. The Triassic-Jurassic boundary and Hettangian Biostratigraphy in the area of the Utcubamba (Northern Peru). *Geobios*, **17**, 297- 307.
- Hillebrandt, A. V. 2000. Die Ammoniten-Fauna des südamerikanischen Hettangium (basaler Jura). *Teil I. Palaeontographica A*, **257**, 85-189.

Hillebrandt, A. V., Krystyn, L. and Kueschner, W. M. 2007. A candidate GSSP for the base of the Jurassic in the Northern Calcareous Alps (Kuhjoch section; Karwendel Mountains, Tyrol, Austria). *ISJS Newsletter* **34**, (1) 2–20.

Hodges, P., 2000. The early Jurassic Bivalvia from the Hettangian and lower Sinemurian of south–west Britain: part 1. *Palaeontographical Society Monograph*, 154 pp.

Hodych, J. P. and Dunning, G. R. 1992. Did the Manicouagan impact trigger end–of–Triassic mass extinction? *Geology* **20**, 51–54.

Holland, S. M. 1995. The Stratigraphic Distribution of Fossils. *Paleobiology*, **21**, (1) 92–109.

Huang, B., Harper, D. A. T., Zhan, R. B. and Rong, J. Y. 2010. Can the Lilliput Effect be detected in the brachiopod faunas of South China following the terminal Ordovician mass extinction? *Palaeogeography Palaeoclimatology Palaeoecology*, **285**, (3–4) 277–286.

Hunt, G. and Carrano, M.T., 2010. Models and methods for analyzing phenotypic evolution in lineages and clades. In : J. Alroy and G., Hunt (Editors), *Quantitative Methods in Paleobiology*. The Paleontological Society papers, pp. 245–269.

Ivimey-Cook, H. C., Hodges, P., Swift, A. and Radley, J. D. 1999. Bivalves. In: Swift, A. and Martill, D.M. (Eds). *Fossils of the Rhaetian Penarth Group*. The Palaeontological Association, Special Publication, London. pp 83–128.

Jablonski, D. 1986. Evolutionary consequences of mass extinctions. *Raup, D. M. And D. Jablonski*. pp 313–330.

Jablonski, D. 1989. The biology of mass extinction – a paleontological view *Philosophical Transactions of the Royal Society of London Series B–Biological Sciences*, **325**, (1228) 357–368.

Jablonski, D. and Raup, D. M. 1995. Selectivity of end-cretaceous marine bivalve extinctions. *Science*, **268**, (5209) 389–391.

Jablonski, D., Erwin, D. H. and Lipps, J. H. (Eds) 1996. *Evolutionary Paleobiology*. Body size and Macroevolution. Evolutionary Paleobiology, Chicago. 484 pp.

Jablonski, D., 1996. Body size and macroevolution. In: D. Jablonski, D.H. Erwin and J.H. Lipps (Editors), *Evolutionary Paleobiology* University of Chicago Press, Chicago, pp. 256–289.

Johnson, J.B. and Omland, K.S., 2004. Model selection in ecology and evolution. *Trends in Ecology and Evolution*, **2**, 101–108.

Kauffman, E. G. and Erwin, D. H. 1994. Igcp-335 - Biotic Recoveries from Mass Extinction - Initial Meetings. *Episodes*, **17**, (3) 68–73.

- Kauffman, E. G. and Erwin, D. H. 1995. Surviving Mass Extinctions. *Geotimes*, **40**, (3) 14-17.
- Kauffman, E. G. and Harries, P. J. 1996. The importance of crisis progenitors in recovery from mass extinction. *Biotic Recovery from Mass Extinction Events*, (102) 15-39.
- Keller, G. and Abramovich, S. 2009. Lilliput effect in late Maastrichtian planktic foraminifera: Response to environmental stress. *Palaeogeography Palaeoclimatology Palaeoecology*, **284**, (1-2) 47-62.
- Kelly, S. P. and Spray, J. G. 1997. A Late Triassic age for the Rochechouart impact structure, France. *Meteoritics & Planetary Science*, **32**, 629–636.
- Kent, D. V. and Olsen, P. E. 1998. Impacts on Earth in the Late Triassic: discussion. *Nature*, **395**, 126.
- Kent, D. V. and Olsen, P. E. 2000. *Implications of a new astronomical time scale for the Late Triassic*. Zentralblatt für Geologie und Paläontologie. 1463–1474 pp.
- Kidwell, S.M., and Brenchley, P.J., 1996. Evolution of the fossil record: thickness trends in marine skeletal accumulations and their implications. In: J. Jablonski, Erwin, D.H., and Lipps, J.H., (Eds), *Evolutionary Paleobiology*, University of Chicago Press, Chicago, 336–399 pp.
- Kiessling, W. and Aberhan, M. 2007a. Environmental determinants of marine benthic biodiversity dynamics through Triassic–Jurassic time. *Paleobiology*, **33**, (3) 414–434.
- Kiessling, W. and Aberhan, M. 2007b. Geographical distribution and extinction risk: lessons from Triassic–Jurassic marine benthic organisms. *Journal of Biogeography*, **34**, (9) 1473–1489.
- Kiessling, W., 2001. Phanerozoic reef trends based on the Paleoreefs database. In: Stanley, G.D. (Ed.), *The History and Sedimentology of Ancient Reef Systems*. Plenum Press, New York: 41–88 pp.
- Kiessling, W., Aberhan, M., Brenneis, B. and Wagner, P. J. 2007. Extinction trajectories of benthic organisms across the Triassic–Jurassic boundary. *Palaeogeography, Palaeoclimatology, Palaeoecology*, **244**, (1–4) 201–222.
- Kiessling, W., Flügel, E., Golonka, J., 2003. Patterns of Phanerozoic carbonate platform sedimentation. *Lethaia*, **36** (3): 195–225.
- Knight, K. B., Nomade, S., Renne, P. R., Marzoli, A., Bertrand, H. and Youbi, N. 2004. The Central Atlantic magmatic province at the Triassic–Jurassic boundary: paleomagnetic and ⁴⁰Ar/³⁹Ar evidence from Morocco for brief, episodic volcanism. *Earth and Planetary Science Letters* **228**, 143–160.
- Knopf, F., Koenemann, S., Schram, F.R., and Wolff, C., 2006. The urosome of the Pan- and Peracarida. *Contributions to Zoology*, **75**(1/2): 1–21

- Kohn, B. P., Osadeta, K. G. and Bezys, R. K. 1995. Apatite fission-track dating of two crater structures in the Canadian Williston basin. *Bulletin of Canadian Petroleum Geology*, **43**, 54–64.
- Koleff, P., Gaston, K.J. and Lennon, J.J., 2003. Measuring beta diversity for presence absence data. *Journal of Animal Ecology*, **72**, 367–382.
- Korte, C., Hesselbo, S. P., Jenkyns, H. C. Rickaby, R. E. M., and C. Spotl, 2009. Palaeoenvironmental significance of carbon - and oxygen - isotope stratigraphy of marine Triassic–Jurassic boundary sections in SW Britain. *Journal of Geological Society*, **166**, 431–445.
- Kosnik, M.A., 2005. Changes in Late Cretaceous–early Tertiary benthic marine assemblages: analyses from the North American coastal plain shallow shelf. *Paleobiology*, **31**: 459–479.
- Kowalewski, M., and Novack–Gottshall, P., 2010. Resampling Methods in Paleontology, In: J. Alroy and G. Hunt (Editors), *Quantitative Methods in Paleobiology*. The Paleontological Society papers, pp. 19–54.
- Kowalewski, M., Dulai, A., and Fürsich, F.T., 1998. A fossil record full of holes: The Phanerozoic history of drilling predation. *Geology*, **26**: 1091–1094.
- Kowalewski, M., Kiessling, W., Aberhan, M., Fürsich, F.T., Scarponi, D., Barbour Wood, S. L., and Hoffmeister, A.P., 2006. Ecological, taxonomic, and taphonomic components of the post–Paleozoic increase in sample–level species diversity of marine benthos. *Paleobiology*, **32**: 533–561.
- Kowalewski, M., Simões, M.G., Torello, F.F., Mello, L.H.C., and Ghilardi, R.P., 2000. Drill holes in shells of Permian benthic invertebrates. *Journal of Paleontology*, **74**: 532–543.
- Layout, K. M. 2009. Ecological restructuring after extinction: The Late Ordovician (Mohawkian) of the eastern United States. *Palaios*, **24**, 118–130.
- Leighton, L.R., 2002. Inferring predation intensity in the marine fossil record. *Paleobiology*, **28**(3): 328–324.
- Lethiers, F., and Whatley, R., 1995. Oxygenation des eaux et ostracodes filtreurs: application au Devonien–Dinantien. *Geobios*, **28** (2): 199–207.
- Lloyd, A. J. 1964 The Luxembourg Colloquium and the revision of the stages of the Jurassic System. *Geological Magazine*, **101**, 249–259.
- Longridge, L. M., Palfy, J., Smith, P. L., Howard, W. and Tipper, H. W. 2008. Middle and late Hettangian (Early Jurassic) ammonites from the Queen Charlotte Islands, British Columbia, Canada. *Revue de Paléobiologie, Genève*, **27**, (1) 191–248.
- Longridge, L.M., Carter, E.S., Haggart, J.W., and Smith, P.L., 2007. The Triassic–Jurassic transition at Kunga Island, Queen Charlotte, British Columbia, Canada. *ISJS Newsletter*, **34**, 21–23.

- Lord, A.R. and Davis, P.G., 2010. *Fossils from the Lower Lias of the Dorset Coast*. The Palaeontological Association, London, 436 pp.
- Lucas, S. G. 1999. Tetrapod-based correlation of the nonmarine Triassic, *Zentralblatt für Geologie und Paläontologie*, Teil 1: Allgemeine, Angewandte, Regionale und Historische. *Geologie*, **7–8**, 497–521.
- Lucas, S.G., Taylor, D.G., Guex, J., Tanner, L.H. and Krainer, K., 2007. Updated proposal for global Stratotype section and point for the base of the Jurassic system in the New York Canyon, Nevada, USA. *ISJS Newsletter*, **34**, 34–42.
- Macquaker, J. H. S. 1994. Paleoenvironmental Significance of Bone-Beds in Organic-Rich Mudstone Successions - an Example from the Upper Triassic of South-West Britain. *Zoological Journal of the Linnean Society*, **112**, (1-2)285-308.
- Macquaker, J. H. S. 1999. Aspects of the sedimentology of the Westbury Formation. In: Swift, A. and Martill, D.M. (Eds). *Fossils of the Rhaetian Penarth Group*. The Palaeontological Association, Special Publication, London. pp 39–48.
- Madin, J.S., Alroy, J., Aberhan, M., Fürsich, F.T., Kiessling, W., Kosnik, M.A., and Wagner, P.J., 2006. Statistical independence of escalatory ecological trends in Phanerozoic marine invertebrates. *Science*, **312**: 897–900.
- Magnusson, K., Agrenius, S., and Ekelund, R., 2003. Distribution of a tetrabrominated diphenyl ether and its metabolites in softbottom sediment and macrofauna species. *Marine Ecology Progress Series*, **255**: 155–170.
- Magurran, A. 2004. *Measuring Biological Diversity*. Blackwell Publishing, Oxford. 256 pp.
- Manceñido, M. O. 2000. A systematic summary of the stratigraphic distribution of Jurassic rhynchonellid genera (Brachiopoda). *Georesearch Forum*, **6**, 387–396.
- Mander, L. and Twitchett, R. J. 2008. Quality of the triassic-jurassic bivalve fossil record in Northwest Europe. *Palaeontology*, **51**, (6) 1213-1223. .
- Mander, L., Twitchett, R. J. and Benton, M. J. 2008. Palaeoecology of the Late Triassic extinction event in the SW UK. *Journal of the Geological Society*, **165**, (1) 319–332.
- Martill, D. M. 1999. Bone beds of the Westbury Formation. In: Swift, A. and Martill, D.M. (Eds). *Fossils of the Rhaetian Penarth Group*. The Palaeontological Association, Special Publication, London. pp 49–64.
- Martin, K. D. 2004. In: McIlroy, D. (Ed). *The Application of the Ichnology to Palaeoenvironmental and Stratigraphic Analysis*. Geological Society of London Special Publication, London. pp 145-166.
- Marzoli, A., Bertrand, H., Knight, K. B., Cirilli, S., Burati, N., Verati, C., Nomade, S., Renne, P. R., Youbi, N., Martini, R., Allenbach, K., Neuwerth, R., Rapaille, C., Zaninetti, L. and Bellieni, G. 2004. Synchrony of the Central Atlantic magmatic province and the Triassic–Jurassic boundary climatic and biotic crisis. *Geology*, **32**, 973–976.

- Marzoli, A., Jourdan, F., Bertrand, H., Renne, P. R., Cirilli, S., Tanner, L., Kontak, D., McHone, G. and Bellieni, G. 2007. Ar-40/Ar-39 ages of CAMP in North America (Hartford, Deerfield and Fundy basins). *Geochimica Et Cosmochimica Acta*, **71**, (15) A632–A632.
- Marzoli, A., Renne, P. R., Picirillo, E. M., Ernesto, M., Belieni, G. and Demin, A. 1999. Extensive 200-million-year-old continental flood basalts of the central Atlantic Magmatic province. *Science*, **284**, 616 – 618.
- Masaitis, V. L. 1999. Impact structures of northeastern Eurasia: the territories of Russia and adjacent countries. *Meteoritics & Planetary Science*, **34**, 691–711.
- Maubeuge, P. L. (Ed) 1964. *Colloque du Jurassique à Luxembourg*. Résolutions du colloque. Ministère des Arts et des Sciences, Luxembourg.
- May, R. M., 1975. Patterns of species abundance and diversity. In: Cody, M.L. and Diamond, M.J. (Editors) *Ecology and Evolution of Communities*, Harvard University Press, Cambridge, pp. 81–120.
- McElwain, J. C. 2004. Climate-independent paleoaltimetry using stomatal density in fossil leaves as a proxy for CO₂ partial pressure. *Geology*, **32**, (12) 1017–1020.
- McElwain, J. C. and Punyasena, S. W. 2007. Mass extinction events and the plant fossil record. *Trends in Ecology and Evolution*, **22**, (10) 548–557.
- McElwain, J. C., Beerling, D. J. and Woodward, F. I. 1999. Fossil plants and global warming at the Triassic–Jurassic boundary. *Science*, **285**, 1386–1390.
- McElwain, J. C., Popa, M. E., Hesselbo, S. P., Haworth, M. and Surlyk, F. 2007. Macroecological responses of terrestrial vegetation to climatic and atmospheric change across the Triassic/Jurassic boundary in East Greenland. *Paleobiology*, **33**, (4) 547–573.
- McElwain, J. C., Wagner, P. J. and Hesselbo, S. P. 2009. Fossil Plant Relative Abundances Indicate Sudden Loss of Late Triassic Biodiversity in East Greenland. *Science*, **324**, (5934) 1554–1556.
- McElwain, J.C., Beerling, D.J., and Woodward, F.I., 1999. Fossil plants and global warming at the Triassic–Jurassic boundary, *Science*, **285**: 1386–1390.
- McGhee, G. R., Sheehan, P. M., Bottjer, D. J. and Droser, M. L. 2004. Ecological ranking of Phanerozoic biodiversity crises: ecological and taxonomic severities are decoupled. *Palaeogeography Palaeoclimatology Palaeoecology*, **211**, (3–4) 289–297.
- McGhee, J.R., Sheehan, P.M., Bottjer, D.J., and Droser, M.L., 2004. Ecological ranking of Phanerozoic biodiversity crises: Ecological and taxonomic severities are decoupled. *Palaeogeography, Palaeoclimatology, Palaeoecology*, **211**(3–4): 289–297.
- McHone, J. G. 1996. Broad-terrane Jurassic flood basalts across northeastern North America. *Geology*, **24**, 319–322.
- McHone, J. G. 2000. Non-plume magmatism and rifting during the opening of the central Atlantic Ocean. *Tectonophysics* **316**, 287– 296.

- Mclaren, D. J. 1990. Geological and Biological Consequences of Giant Impacts. *Annual Review of Earth and Planetary Sciences*, **18**, 123–171.
- McRoberts, C. A. 2001. Triassic bivalves and the initial marine Mesozoic revolution: A role for predators? *Geology*, **29**, (4) 359–362.
- McRoberts, C. A. and Carter, J. G. 1994. Nacre in an early gryphaeid bivalve (Mollusca). *Journal of Paleontology*, **68**, (6) 1405-1408.
- McRoberts, C.A. and Newton, C.R., 1995. Selective extinction among end–Triassic European bivalves. *Geology*, **23**,102–104.
- McRoberts, C.A., 2001. Triassic bivalves and the initial marine Mesozoic revolution: A role for predators? *Geology*, **29**(4): 359–362.
- McRoberts, C.A., and Aberhan, M., 1997. Marine diversity and sea–level changes: Numerical tests for association using Early Jurassic bivalves. *Geologische Rundschau*, **86**(1): 160–167.
- McRoberts, C.A., and Newton, C.R., 1995. Selective extinction among end–Triassic European bivalves. *Geology*, **23**: 102–104.
- McRoberts, C.A., Ward, P.D. and Hesselbo, S., 2007. A proposal for the base Hettangian stage (=base Jurassic System) GSSP at New York Canyon, Nevada, USA using carbon isotopes. *ISJS Newsletter*, **34**, 43–49.
- Metcalf, B., Twitchett, R. J. and Price-Lloyd, N. 2011. Changes in size and growth rate of 'Lilliput' animals in the earliest Triassic. *Palaeogeography Palaeoclimatology Palaeoecology*, **308**, (1-2) 171-180.
- Miller, A., 1998. Biotic Transitions in Global Marine Diversity. *Science*, **281**: 1157–1160.
- Moghadam, H. V. and Paul, C. R. C. 2000. Trace Fossils of the Jurassic, Blue Lias, Lyme Regis, Southern England. *Ichnos*, **7**, (4) 283-306.
- Morten, S. D. and Twitchett, R. J. 2009. Fluctuations in the body size of marine invertebrates through the Pliensbachian-Toarcian extinction event. *Palaeogeography Palaeoclimatology Palaeoecology*, **284**, (1-2) 29-38.
- Morton, N. 1974. The definition of standard Jurassic stages in Colloque du Jurassique, Luxembourg, 1967. *Mémoires du Bureau de Recherches Géologiques et Minières*, **75**, 83–95.
- Motani, R. 2005. Evolution of fish–shaped reptiles (Reptilia : Ichthyopterygia) in their physical environments and constraints. *Annual Review of Earth and Planetary Sciences*, **33**, 395–420.
- Motomura, I. 1932. A statistical treatment of associations. *Japanese Journal of Zoology*, **44**, 379–383.

- Motomura, I. 1947. Further notes on the law of geometrical progression of the population density in animal association. *Physiological Ecology*, **1**, 55–60.
- Mudil, R., Palfy, J. and Matzel, J. 2005. *New constraints on the timing of the Triassic–Jurassic extinction and recovery*. Geological Society of America pp 187.
- Müller, J., 2005. The anatomy of *Askeptosaurus italicus* from the Middle Triassic of Monte San Giorgio and the interrelationships of thalattosaurs (Reptilia, Diapsida), *Canadian Journal of Earth Sciences*, **42**(7): 1347–1367.
- Müller, J., 2007. First record of a Thalattosaur from the upper Triassic of Austria. *Journal of Vertebrate Paleontology*, **27**(1): 236–240.
- Mutter, R.J., and Herzog, A., 2004. A new genus of Triassic actinopterygian with an evaluation of depend flank scales in fusiform fossil fishes, *Journal of Vertebrate Paleontology*, **24** (4):794–801.
- Newell, N. D. 1962. Paleontological gaps and geochronology. *Journal of Paleontology*, **36** 592–610.
- Newell, N. D. 1967. *Paraconformities*. Univ. Kansas Press, Lawrence, KS. 349– 367 pp.
- Nomade, S., Knight, K. B., Renne, P. R., Verati, C., Feraud, G., Marzoli, A., Youbi, N. and Bertrand, H. 2007. The chronology of CAMP: relevance for the central Atlantic rifting processes and the Triassic–Jurassic biotic crisis. *Palaeogeography, Palaeoclimatology, Palaeoecology* **244**, 326–344.
- Novack-Gottshall, P. M. 2007. Using a theoretical ecospace to quantify the ecological diversity of Paleozoic and modern marine biotas. *Paleobiology*, **33**, (2) 273-294.
- Nutzel, A. 2002. The Late Triassic species *Cryptaulax? bittneri* (Mollusca: Gastropoda: Procerithiidae) and remarks on early aspects of the Mesozoic revolution. *Paläontologische Zeitschrift*, **76**, 57–63.
- Olsen, P. E. 1997. Stratigraphic record of the early Mesozoic breakup of Pangea in the Laurasia–Gondwana rift system. *Annual Reviews of Earth and Planetary Science*, **25**, 337–401.
- Olsen, P. E. 1999. Giant lava flows, mass extinctions, and mantle plumes. *Science*, **284**, 604– 605.
- Olsen, P. E. and Rainforth, E. C. 2002. The "Age of Dinosaurs" in the Newark Basin. *American Paleontologist*, **10**, 2–5.
- Olsen, P. E., Kent, D. V., Sues, H.–D., Koeberl, C., Huber, H., Montanari, A., Rainforth, E. C., Fowell, S. J., Szajna, M. J. and Hartline, B. W. 2002. Ascent of dinosaurs linked to an iridium anomaly at the Triassic–Jurassic boundary. *Science*, **296**, 1305–1307.

- Olsen, P. E., Shubin, N. H. and Anders, M. H. 1987. New early Jurassic tetrapod assemblages constrain Triassic– Jurassic tetrapod extinction event. *Science*, **237**, (4818) 1025–1029.
- Olszewski, T.D., 2010. Diversity Partitioning Using Shannon’s Entropy and its Relationship to Rarefaction, In: J. Alroy and G. Hunt (Eds), *Quantitative Methods in Paleobiology*. The Paleontological Society papers, pp. 95 –116.
- Page, K. N. 2004. Biostratigraphy of invertebrate macrofossils and microfossils: Macrofossils – Ammonites. In: Simms, M.J., Chidlaw, N., Morton, N. and Page, K.N. (Eds). *British Lower Jurassic Stratigraphy*. Joint Nature Conservation Committee, Peterborough. pp 28-31.
- Page, K. N. 2010. Stratigraphical framework. In: Lord, A. and Davis, P. (Eds). *Fossils from the Lower Lias of the Dorset Coast*. The Palaeontological Association, London. pp 33-53.
- Palfy, J., Demeny, A., Haas, J., Htenyi, M., Orchard, M. J. and Veto, I. 2001. Carbon isotope anomaly at the Triassic– Jurassic boundary from a marine section in Hungary. *Geology* **29**, 1047–1050.
- Palfy, J., Mortensen, J. K., Carter, E. S., Smith, P. L., Friedman, R. M. and Tipper, H. W. 2000. Timing the end–Triassic mass extinction: First on land, then in the sea? *Geology*, **28**, (1) 39–42.
- Palmer, C. P. 1972. Lower Lias (Lower Jurassic) between Watchet and Lilstock in North Somerset (UK). *Newsletters on Stratigraphy*, **2**, (1)1-30.
- Paris, G., Beaumont, V., Bartolini, A., Clémence, M. E., Gardin, S. and Page, K. 2010. Nitrogen isotope record of a perturbed paleoecosystem in the aftermath of the end–Triassic crisis, Doniford section, SW England. *Geochemistry Geophysics Geosystems*, **11**, 1–15.
- Parrish, J. T. 1993. Climate of the supercontinent Pangea. *The Journal of Geology*, **101**, 215–253.
- Paul , C.R.C., Allison P.A., and Brett, C.E. 2008.The occurrence and preservation of ammonites in the Blue Lias Formation (lower Jurassic) of Devon and Dorset, England and their palaeoecological, sedimentological and diagenetic significance. *Palaeogeography, Palaeoclimatology, Palaeoecology*, **270**, 258–272.
- Payne, J. L. and Finnegan, S. 2007. The effect of geographic range on extinction risk during background and mass extinction. *Proceedings of the National Academy of Sciences of the United States of America*, **104**, (25) 10506–10511.
- Payne, J. L., Truebe, S., Nutzelt, A. and Chang, E. T. 2011. Local and global abundance associated with extinction risk in late Paleozoic and early Mesozoic gastropods. *Paleobiology*, **37**, (4) 616–632.
- Payne, J.L., and Van De Schootbrugge, B., 2007. Ocean life in the Triassic: Links between benthic and planktonic recovery and radiation. In: Falkowski, P.G., Knoll,

- A.H. (Eds.), *Evolution of Primary Producers in the Sea*, Elsevier, Amsterdam, 165–189 pp.
- Peters, S. E. and Bork, K. B. 1999. Species-abundance models: An ecological approach to inferring paleoenvironment and resolving paleoecological change in the Waldron Shale (Silurian). *Palaios*, **14**, (3) 234-245.
- Phillips, J. 1860. *Life on the Earth: Its Origin and Succession* Macmillan, Cambridge.
- Plotnick, R.E., and Baumiller, T.K., 2000. Invention by evolution: Functional analysis in paleobiology. *Paleobiology*, **26**(4): 305–323.
- Porter, S.D. and Savignano, D.A., 1990. Invasion of polygyne fire ants decimates native ants and disrupts arthropod community. *Ecology*, **71**, 2095–2106.
- Preston, F., 1948. The commonness and rarity of species. *Ecology*, **29**, 254–283.
- R Development Core Team., 2006. R: A Language and Environment for Statistical Computing, R Foundation for Statistical Computing, Vienna, <http://www.R-project.org>.
- Raup, D. M. 1982. Large Body Impacts and Terrestrial Evolution Meeting, October 19–22, 1981. *Paleobiology*, **8**, (1) 1–3.
- Raup, D. M. 1995. The role of extinction in evolution. *Tempo and Mode in Evolution: Genetics and Paleontology 50 Years after Simpson*. pp 109–124.
- Raup, D. M. and Sepkoski, J. J. 1982. Mass Extinctions in the Marine Fossil Record. *Science*, **215**, 1501–1502.
- Raup, D. M., and Sepkoski, J.J., 1986. Periodic extinction of families and genera. *Science*, **231**: 833–836.
- Raup, D.M., 1979. Taxonomic Diversity during the Phanerozoic, *Science*, **177**: 1065 – 1071.
- Raup, D.M., and Sepkoski, J.J., 1982. Mass extinctions in the marine fossil record. *Science*, **215**: 1501 – 1503.
- Retallack, G. J. 2002. Triassic–Jurassic atmospheric CO₂ spike. *Nature*, **415**, 387–388.
- Rhoads, D. L. and Morse, J. W. 1971. Evolutionary and Ecologic Significance of Oxygen–deficient Marine Basins *Lethaia*, **4**, 413–428.
- Rhoads, D.L., and Morse, J.W., 1971. Evolutionary and Ecologic Significance of Oxygen–deficient Marine Basins. *Lethaia*, **4**: 413–428.
- Riccardi, A. C. 2008. The marine Jurassic of Argentina: a biostratigraphic framework. *Episodes*, **31**, (3) 326-335.
- Rieppel, O., 2002. Feeding mechanics in Triassic stem–group sauropterygians: the anatomy of a successful invasion of Mesozoic seas. *Zoological Journal of the Linnean Society*, **135**: 33–63.

- Rohr, D., and Blodgett, R.B., 1985. Upper Ordovician gastropoda from west-central Alaska, *Journal of paleontology*, **59**(3): 667–673.
- Roy, K., Jablonski, D. and Martien, K. K. 2000. Invariant size–frequency distributions along a latitudinal gradient in marine bivalves. *Proceedings of the National Academy of Sciences of the United States of America*, **97**, (24) 13150–13155.
- Royer, D. L., Wing, S. L., Beerling, D. J., Jolley, D. W., Koch, P. L., Hickey, L. J. and Berner, R. A. 2001. Paleobotanical evidence for near present–day levels of atmospheric CO₂ during part of the Tertiary. *Science*, **292**, 2310–2313.
- Ruhl, M. and Kurschner, W. M. 2011. Multiple phases of carbon cycle disturbance from large igneous province formation at the Triassic–Jurassic transition. *Geology*, **39**, (5) 431–434.
- Ruhl, M., Bonis, N. R., Reichart, G. J., Damste, J. S. S. and Kurschner, W. M. 2011. Atmospheric Carbon Injection Linked to End–Triassic Mass Extinction. *Science*, **333**, (6041) 430–434.
- Ruhl, M., Deenen, M. H. L., Abels, H. A., Bonis, N. R., Krijgsman, W. and Kurschner, W. M. 2010. Astronomical constraints on the duration of the early Jurassic Hettangian stage and recovery rates following the end–Triassic mass extinction (St Audrie's Bay/East Quantoxhead, UK). *Earth and Planetary Science Letters*, **295**, (1–2) 262–276.
- Ruhl, M., Kurschner, W. M. and Reichart, G. J. 2009. Global carbon cycle turnover at the Triassic–Jurassic boundary. *Geochimica Et Cosmochimica Acta*, **73**, (13) A1131–A1131.
- Samson, I.J., 2000. Late Triassic (Rhaetian) conodonts and ichthyofauna from Chile. *Geological magazine*, **137**, 129–135.
- Saucède, T., Mooi, R., and Davis, B., 2007. Phylogeny and origin of Jurassic irregular echinoids (Echinodermata: Echinoidea). *Geological magazine*, **144**, 1–28.
- Schaller, M. F., Wright, J. D. and Kent, D. V. 2011. Response to Comment on "Atmospheric PCO₂ Perturbations Associated with the Central Atlantic Magmatic Province". *Science*, **334**, 6056
- Schaltegger, U., Guex, J., Bartolini, A., Schoene, B. and Ovtcharova, M. 2008. Precise U–Pb age constraints for end–Triassic mass extinction, its correlation to volcanism and Hettangian post–extinction recovery. *Earth and Planetary Science Letters*, **267**, (1–2) 266–275.
- Schindewolf, O. H. 1963. Neokatastrophismus? Zeits. *Deutsche geologische Recherchen* **114**, 430–435.
- Schoene, B., Guex, J., Bartolini, A., Schaltegger, U. and Blackburn, T. J. 2010. Correlating the end–Triassic mass extinction and flood basalt volcanism at the 100 ka level. *Geology*, **38**, (5) 387–390.

- Schoener, T.W., 1974. Resource Partitioning in Ecological Communities. *Science*, **185**: 27 – 39.
- Schubert, J. K., Bottjer, D. J. and Simms, M. J. 1992. Paleobiology of the Oldest Known Articulate Crinoid. *Lethaia*, **25**, (1) 97–110.
- Schubert, J.K., and Bottjer, D.J., 1995. Aftermath of the Permian–Triassic mass extinction event: Palaeoecology of Lower Triassic carbonates in the western U.S. *Palaeogeography, Palaeoclimatology, Palaeoecology*, **116**: 1–39.
- Schweigert, G., 2007. *Juracyclus posidoniae* n. Gen. and sp., the first cycloid arthropod from the jurassic. *Journal of Paleontology*, **81**(1), 213–215.
- Scotese, C.R., 2002. <http://www.scotese.com>, (PALEOMAP website).
- Sepkoski, J. J. 1996. Patterns of Phanerozoic extinction: a perspective from global data bases In: Walliser, O.H. (Ed). *Global Events and Event Stratigraphy*. Springer, Berlin. pp 35–51.
- Sepkoski, J. J. 1997. Biodiversity: past, present, and future. *Journal of Paleontology*, **71**, 533–539.
- Sepkoski, J.J Jr., 1982. A Compendium of Fossil Marine Families, Contributions to Biology and Geology, Milwaukee Public Museum, **51**, 1–125.
- Sepkoski, J.J Jr., 1992. Phylogenetic and ecologic patterns in the Phanerozoic history of marine biodiversity. In: N. Eldredge (Eds), *Systematics, Ecology and the Biodiversity Crisis*, Columbia University Press, New York.
- Sepkoski, J.J.Jr., 1979. A kinetic model of Phanerozoic taxonomic diversity: II Early Phanerozoic families and multiple equilibria. *Paleobiology*, **5**: 222–251.
- Sepkoski, J.J.Jr., 1981. A factor analytic description of the Phanerozoic marine fossil record. *Paleobiology*, **7**(1): 36–53.
- Sepkoski, J.J.Jr., 1984. A kinematic model of Phanerozoic taxonomic diversity: III. Post–Paleozoic families and mass extinctions, *Paleobiology*, **10**: 246–267.
- Sepkoski, J.J.Jr., 1990. The taxonomic structure of periodic extinction. pp. 33–44. In: V. Sharpton, and Warda, P., (eds.), *Global Catastrophes in Earth History*. Geological Society of America Special Paper **247**.
- Sepkoski, J.J.Jr., 1996. Patterns of Phanerozoic extinction: a perspective from global data bases. In: O.H. Walliser, (Eds). *Global Events and Event Stratigraphy*. Springer, Berlin: 35–51.
- Sepkoski, J.J.Jr., 2002. A compendium of fossil marine animal genera. *Bulletins of American Paleontology*, **363**: 1–560.
- Sernageomin 2003. Mapa Geológico de Chile: versión digital. Servicio Nacional de Geología y Minería, Santiago. Publicación Geológica Digital, No. 4.
- Sheehan, P. M. 1996. A new look at Ecologic Evolutionary Units (EEUs) *Palaeogeography, Palaeoclimatology, Palaeoecology*, **127**, (1–4), 21–32.

- Sheehan, P.M., 1996. A new look at Ecologic Evolutionary Units (EEUs). *Palaeogeography, Palaeoclimatology, Palaeoecology*, **127**: 21–32.
- Sheehan, P.M., 2001. History of marine biodiversity. *Geological Journal*, **36** (3–4), 231–249.
- Shubin, N. H. and Sues, H. D. 1991. Biogeography of Early Mesozoic Continental Tetrapods – Patterns and Implications. *Paleobiology*, **17**, (3), 214–230.
- Signor III, C.E., and Brett, P.W., 1984. The mid–Paleozoic precursor to the Mesozoic marine revolution. *Paleobiology*, **10**: 229–245.
- Simberloff, D., and Dayan, T., 1991. The guild concept and the structure of ecological communities. *Annual Review of Ecology and Systematics*, **22**: 115–143.
- Simms, M. J. 2003. Uniquely extensive seismite from the latest Triassic of the United Kingdom: Evidence for bolide impact? *Geology*, **31**, (6) 557–560.
- Simms, M. J. and Ruffel, A. H. 1990. Climatic and biotic change in the Late Triassic. *Journal of Geological Society, London*, **147**, 321–327.
- Simms, M.J. and Jeram, A.J., 2007. Waterloo Bay, Larne, Northern Ireland: a candidate Global stratotype section and the point for the base of the Hettangian stage and Jurassic system. *ISJS Newsletter*, **34**, 50–68.
- Smith, A.B., and McGowan, A.J., 2007. The shape of the Phanerozoic diversity curve. How much can be predicted from the sedimentary rock record of Western Europe? *Palaeontology*, **50**: 765–777.
- Smith, A.M., Key, M.M., and Gordon, D.P., 2006. Skeletal mineralogy of bryozoans: Taxonomic and temporal patterns. *Earth–Science Reviews*, **78**(3–4): 287–306.
- Smith, C.D. and Pontius, J.S, 2006. Jackknife estimator of species Richness with S–Plus. *Journal of statistical software*, **15**, 1–12.
- Sole, R. V., Montoya, J. M. and Erwin, D. H. 2002. Recovery after mass extinction: evolutionary assembly in large-scale biosphere dynamics. *Philosophical Transactions of the Royal Society B-Biological Sciences*, **357**, (1421) 697–707.
- Sole, R. V., Saldana, J., Montoya, J. M. and Erwin, D. H. 2010. Simple model of recovery dynamics after mass extinction. *Journal of Theoretical Biology*, **267**, (2) 193–200.
- Song, H. J., Tong, J. A. and Chen, Z. Q. 2011. Evolutionary dynamics of the Permian–Triassic foraminifer size: Evidence for Lilliput effect in the end-Permian mass extinction and its aftermath. *Palaeogeography Palaeoclimatology Palaeoecology*, **308**, (1–2) 98–110.
- Spray, J. G., Kelley, S. P. and Rowley, D. B. 1998. Evidence for a Late Triassic multiple impact event on Earth. *Nature*, **392**, 171– 173.
- Stanley, S. M. 2006. Influence of seawater chemistry on biomineralization throughout Phanerozoic time: Paleontological and experimental evidence. *Palaeogeography, Palaeoclimatology, Palaeoecology*, **232**, 214–236.

- Stanley, S. M. 2008. *Earth System History*. (3rd Edition edition ed) W. H. Freeman, San Francisco.
- Stanley, S.M., 1972. Functional morphology and evolution of byssally attached bivalve mollusks. *Journal of Paleontology*, **46**: 165–212.
- Stanley, S.M., 1977. Coadaptation in the Trigoniidae, a remarkable family of burrowing bivalves. *Paleontology*, **20**: 869–899.
- Stanley, S.M., 2007. An analysis of the history of marine animal diversity. *Paleobiology*, **33**(4): 1–55.
- Stanley, S.M., 2008. Predation defeats competition on the seafloor. *Paleobiology*, **34**(1): 1–21.
- StatSoft, Inc. (1997). STATISTICA for Windows [Computer program manual]. Tulsa, OK: StatSoft, Inc., <http://www.statsoft.com>.
- Steneck, R.S., 1983. Quantifying herbivory on coral reefs: just scratching the surface and biting off more than we can chew. In: Reaka M.L. (Eds.) *The ecology of deep and shallow coral reefs*. NOAA Symp Ser Undersea Res, Vol 3, Silver Spring, MD, p 103–111.
- Stripmple, H.L., and Nassichuk, W.W., 1974. Pennsylvanian crinoids from ellesmere island, Artic Canada, *Journal of Paleontology*, **18** (6), 1149–1155.
- Swift, A. 1999. Stratigraphy. In: Swift, A. and Martill, D.M. (Eds). *Fossils of the Rhaetian Penarth Group*. The Palaeontological Association Field Guides to Fossils, London. pp 15–30.
- Swift, A. and Martill, D.M., 1999. *Fossils of the Rhaetian Penarth Group*. The Palaeontological Association, London, 311 pp.
- Tanner, L. H., Lucas, S. G. and Chapman, M. G. 2004. Assessing the record and causes of Late Triassic extinctions. *Earth–Science Reviews*, **65**, (1–2) 103–139..
- Taylor, D. G., Boelling, K. and Guex, J. 2000. The Triassic/Jurassic System Boundary in the Gabbs Formation, Nevada. *GeoResearch Forum* **6**, 225–235.
- Taylor, D., Guex, J. and Rakus, M. 2001. Hettangian and Sinemurian ammonoid zonation for the Western Cordillera of North America, . *Société Vaudoise des Sciences Naturelles*, **87**, (4) 381–421.
- Teichert, C. 1988. Main Features of Cehalopod Evolution. In: Clarke, M.R. and E.R. Trueman (Eds). *The Mollusca Paleontology and Neontology of Cephalopods*. Academic Press, Inc., San Diego, CA. pp 355.
- Thayer, C.W., 1979. Biological bulldozers and the evolution of marine benthic communities. *Science*, **203**: 458–461.
- Thayer, C.W., 1983. Sediment–mediated biological disturbance and the evolution of marine benthos. In: M. J. S. Tevesz & P. L. McCall, (Ed.) *Biotic interactions in Recent and fossil benthic communities*, Plenum Press, New York and London, 479–625 pp.

- Thorne, P. M., Ruta, M. and Benton, M. J. 2011. Resetting the evolution of marine reptiles at the Triassic–Jurassic boundary. *Proceedings of the National Academy of Sciences of the United States of America*, **108**, (20) 8339–8344.
- Tintori, A. 1998. Fish biodiversity in the marine Norian (Late Triassic) of northern Italy: the first Neopterygian radiation. *Italian Journal of Zoology*, **65**, 193–198.
- Tintori, A., 1990. The Actinopterygian fish Prohalecites from the Triassic of Northern Italy. *Paleontology*, **31**(1): 155–174.
- Tokeshi, M., 1993. Species abundance patterns and community structure. *Advance in Ecological Research*, **24**, 112–186.
- Tomasovych, A. 2006. Brachiopod and bivalve ecology in the Late Triassic (Alps, Austria): Onshore–offshore replacements caused by variations in sediment and nutrient supply. *Palaios*, **21**, (4) 344–368.
- Tomasovych, A. and Siblík, M. 2007. Evaluating compositional turnover of brachiopod communities during the end–Triassic mass extinction (Northern Calcareous Alps): Removal of dominant groups, recovery and community reassembly. *Palaeogeography, Palaeoclimatology, Palaeoecology*, **244**, (1–4) 170–200.
- Tracey, S., J.A., T. and Erwin., D. H. 1993. Mollusca: Gastropoda. . In: Benton, M.J. (Ed). *The Fossil Record 2*. Chapman and Hall, London. pp 131–167.
- Tracey, S., Todd, J.A., and Erwin, D.H., 1993. Mollusca: Gastropoda. In: M.J. Benton, Editor, *The Fossil Record 2*, Chapman and Hall, London, 131–167.
- Tucker, M. E. and Benton, M. J. 1982. Triassic environments, climates, and reptile evolution. . *Palaeogeography, Palaeoclimatology, Palaeoecology* **40**, 361– 379.
- Tucker, M.E., and Benton, M.J., 1982. Triassic environments, climates, and reptile evolution. *Palaeogeography, Palaeoclimatology, Palaeoecology*, **40**: 361– 379.
- Turnsek, D., 1997. Mesozoic corals of Slovenia. ZRC SAZU, Ljubljana 1–512
- Tverdokhlebov, V.P., Tverdokhlebova, G.I., Surkov, M.V., and Benton, M.J., 2002. Tetrapod localities from the Triassic of the SE of European Russia. *Earth–Science Reviews*, **60**: 1–66.
- Twitchett, R. J. 2001. Incompleteness of the Permian–Triassic fossil record: a consequence of productivity decline? *Geological Journal*, **36**, 341–353.
- Twitchett, R. J. 2006. The palaeoclimatology, palaeoecology and palaeoenvironmental analysis of mass extinction events. . *Palaeogeography, Palaeoclimatology, Palaeoecology*, , **232**, (2–4) 190–213. .
- Twitchett, R. J. 2007. The Lilliput effect in the aftermath of the end-Permian extinction event. *Palaeogeography Palaeoclimatology Palaeoecology*, **252**, (1-2) 132-144.
- Twitchett, R. J. and Barras, C. G. 2004. Trace fossils in the aftermath of mass extinction events.

- Twitchett, R. J., Krystyn, L., Baud, A., Wheeley, J. R. and Richoz, S. 2004. Rapid marine recovery after the end-Permian mass extinction event in the absence of marine anoxia. *Geology*, **32**, (805–808)
- Twitchett, R.J. and Barras, C.G., 2004. Trace fossils in the aftermath of mass extinction events. *Geological Society, London, Special Publications*, **228**, 397–418.
- Twitchett, R.J., 2007. The Lilliput effect in the aftermath of the end-Permian extinction event. *Palaeogeography, Palaeoclimatology, Palaeoecology*, **252**, 132–144.
- Twitchett, R.J., and Barras, C.G., 2004. Trace Fossils in the aftermath of mass extinction events. In: McIlroy, D. (Ed) *The application of the Ichnology to paleoenvironmental and Stratigraphic analysis*. Geological Society, London Special publications, **228**: 397–481.
- Ulrichs, M. 1972. Ostracoden aus den Ko'ssener Schichten und ihre Abhängigkeit von der Ökologie. *Mitt. Ges. Geol. Bergbaustud.*, **21**, 661–710.
- Underwood, C. J. 2006. Diversification of the Neoselachii (Chondrichthyes) during the Jurassic and Cretaceous. *Paleobiology*, **32**, (2) 215–235.
- Urbanek, A. 1993. Biotic crises in the history of Upper Silurian graptoloids: a Palaeobiological model. *Historical Biology*, **7**, 29–50.
- van de Schootbrugge, B., Payne, J. L., Tomasovych, A., Pross and J. Fiebig, J., Benbrahim, M., Follmi, K. B. and Quan, T. M. 2008. Carbon cycle perturbation and stabilization in the wake of the Triassic-Jurassic boundary mass-extinction event. *Geochemistry Geophysics Geosystems*, **9**, (4) 1-16.
- van de Schootbrugge, B., Payne, J. L., Tomasovych, A., Pross, J., Fiebig, J., Benbrahim, M., Foellmi, K. B. and Quan, T. M. 2008. Carbon cycle perturbation and stabilization in the wake of the Triassic–Jurassic boundary mass–extinction event. *Geochemistry Geophysics Geosystems*, **9**, 1–16.
- van de Schootbrugge, B., Tremolada, F., Rosenthal, Y., Bailey, T. R., Feist-Burkhardt, S., Brinkhuis, H., Pross, J., Kent, D. V. and Falkowski, P. G. 2007. End-Triassic calcification crisis and blooms of organic-walled 'disaster species'. *Palaeogeography Palaeoclimatology Palaeoecology*, **244**, (1-4) 126-141.
- Vannier, J., Chen, J., Huang, D., Charbonnier, S., and Wang, X., 2006. The Early Cambrian origin of thylacocephalan arthropods, *Acta Palaeontologica Polonica*, **51** (2): 201–214.
- Verati, C., Rapaille, C., Feraud, G., Marzoli, A., Bertrand, H. and Youbi, N. 2007. ⁴⁰Ar/³⁹Ar ages and duration of the Central Atlantic Magmatic Province volcanism in Morocco and Portugal and its relation to the Triassic–Jurassic boundary. *Palaeogeography, Palaeoclimatology, Palaeoecology*, **244**, 308–325.
- Vermeij G.J., and Lindberg, D.R., 2003. Delayed herbivory and the assembly of marine benthic ecosystems. *Paleobiology*, **26** (3): 419–430.

- Vermeij, G. J. 2008. Escalation and its role in Jurassic biotic history. *Palaeogeography Palaeoclimatology Palaeoecology*, **263**, (1–2) 3–8.
- Vermeij, G. J., 1982. Unsuccessful predation and evolution, *American Naturalist*, **120**: 701–720.
- Vermeij, G.J., 1977. The Mesozoic marine revolution: evidence from snails, predators and grazers. *Paleobiology*, **3**: 245–258.
- Vermeij, G.J., 1978. Biogeography and adaptation: patterns of marine life. Harvard University Press, Cambridge.
- Vermeij, G.J., 1987. Evolution and Escalation: an Ecological History of Life, Princeton University Press, Princeton.
- Vermeij, G.J., 1995. Economics, volcanoes, and Phanerozoic revolutions. *Paleobiology*, **21**: 125–152.
- Vermeij, G.J., 1999. Inequality and the directionality of the history. *American Naturalist*, **153**: 243–253.
- Vermeij, G.J., and Herbert, G.S., 2004. Measuring relative abundance in fossil and living assemblages. *Paleobiology*, **30**: 1–4
- Vermeij, G.J., and Leighton, L.R., 2003. Does global diversity mean anything? *Paleobiology*, **29**: 3–7
- Villegier, S., Novack-Gottshall, P. M. and Mouillot, D. 2011. The multidimensionality of the niche reveals functional diversity changes in benthic marine biotas across geological time. *Ecology Letters*, **14**, (6) 561-568.
- Villier, L., Neraudeau, D., Clavel, B., Neumann, and David, B., 2004. Phylogeny and early Cretaceous spatangoids (Echinodermata: Echinoidea) and taxonomic implications. *Palaeontology*, **47**: 265–92.
- Wade, B. S. and Twitchett, R. J. 2009. Extinction, dwarfing and the Lilliput effect Preface. *Palaeogeography Palaeoclimatology Palaeoecology*, **284**, (1-2) 1-3.
- Wagner, P. J., Kosnik, M. A. and Lidgard, S. 2006. Abundance distributions imply elevated complexity of post-Paleozoic marine ecosystems. *Science*, **314**, (5803) 1289-1292.
- Wainwright, P.C., and Reilly, S.M., 1994. Ecological morphology: integrative organismal biology. University of Chicago Press, Chicago.
- Wang, S.C., 2010. Principles of Statistical Inference: Likelihood and the Bayesian Paradigm, In : J. Alroy and G. Hunt (Eds), *Quantitative Methods in Paleobiology*. The Paleontological Society papers, pp. 1 –18.
- Ward, P. D., Haggart, J. W., Carter, E. S., Wilbur, D., Tipper, H. W. and Evans, T. 2001. Sudden productivity collapse associated with the Triassic-Jurassic boundary mass extinction. *Science*, **292**, (5519) 1148-1151.

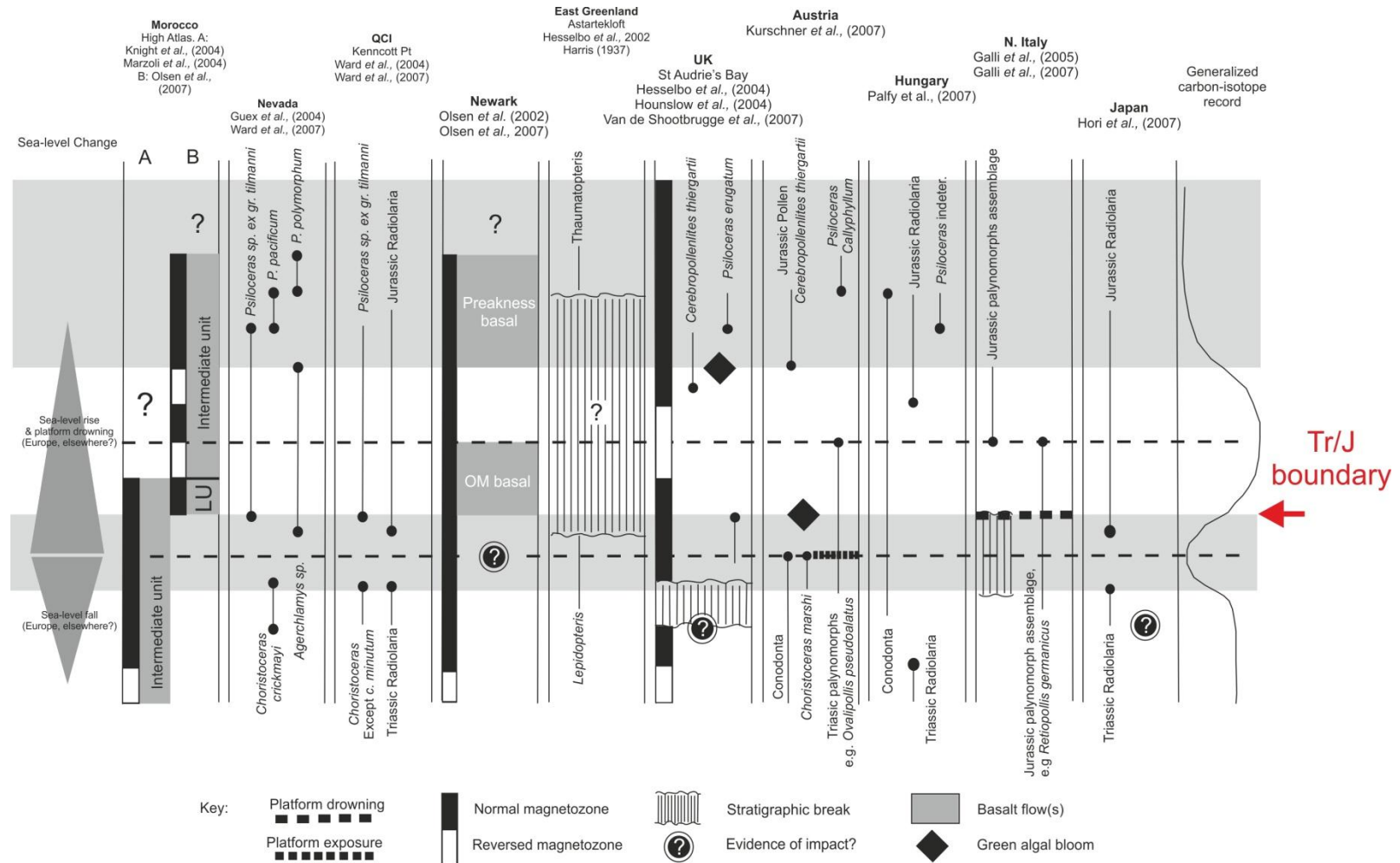
- Warrington, G., Cope, J. C. W. and Ivimey-Cook, H. C. 2008. The St Audrie's Bay – Doniford Bay section, Somerset, England: Updated proposal for a candidate Global stratotype section and point for the base of the Hettangian stage, of the Jurassic system. *International subcommission on Jurassic Stratigraphy Newsletter*, **35**, 1-74.
- Webb, A. E., Leighton, L. R., Schellenberg, S. A., Landau, E. A. and Thomas, E. 2009. Impact of the Paleocene-Eocene thermal maximum on deep-ocean microbenthic community structure: Using rank-abundance curves to quantify paleoecological response. *Geology*, **37**, (9) 783-786.
- Weedon, G. P. 1986. Hemipelagic Shelf Sedimentation and Climatic Cycles - the Basal Jurassic (Blue Lias) of South Britain. *Earth and Planetary Science Letters*, **76**, (3-4) 321-335.
- Whiteside, J. H., Grogan, D. S., Olsen, P. E. and Kent, D. V. 2011. Climatically driven biogeographic provinces of Late Triassic tropical Pangea. *Proceedings of the National Academy of Sciences of the United States of America*, **108**, (22) 8972–8977.
- Whiteside, J. H., Olsen, P. E., Eglinton, T., Brookfield, M. E. and Sambrotto, R. N. 2010. Compound-specific carbon isotopes from Earth's largest flood basalt eruptions directly linked to the end-Triassic mass extinction. *Proceedings of the National Academy of Sciences of the United States of America*, **107**, (15) 6721–6725.
- Whittaker, A. and Green, G. W. 1983. *Geology of the Country around Weston-Super-Mare. Memoirs of the Geological Survey of Great Britain*. HMSO, London.
- Whittaker, R., 1965. Dominance and diversity in plant communities. *Science*, **147**, 250–260.
- Wignall, P. B. 2001a. Large igneous provinces and mass extinctions. *Earth-Science Reviews*, **53**, (1–2) 1–33.
- Wignall, P. B. 2001b. Sedimentology of the Triassic–Jurassic boundary beds in Pinhay Bay (Devon, SW England). *Proceedings of the Geologists Association*, **112**, 349–360.
- Wignall, P. B. 2009. Carbon isotope excursions at times of mass extinction. *Geochimica Et Cosmochimica Acta*, **73**, (13) A1441–A1441.
- Wignall, P. B. and Bond, D. P. G. 2008. The end-Triassic and Early Jurassic mass extinction records in the British Isles. *Proceedings of the Geologists Association*, **119**, 73-84.
- Wignall, P.B., 2001. Sedimentology of the Triassic–Jurassic boundary beds in Pinhay Bay (Devon, SW England). *Proceedings of the Geologists' Association*, **112**, 349–360.
- Wilson, G.D., and Edgecombe, G.D., 2003. The Triassic Isopod *Protamphisopus wianamattensis* (chilton) and comparison with extant taxa (Crustacea, Phreatoicidea). *Journal of Paleontology*, **77**(3): 454 – 470.
- Wilson, J. B., 1991. Methods for fitting dominance/diversity curves. *Journal of Vegetation Science*, **2**, 35–46.

Winemiller, K.O., 1994. Ecomorphological Diversification in Lowland Freshwater Fish Assemblages from Five Biotic Regions. *Ecological Monographs*, **61** (4): 343–365.

Woodin, S. A., Wethey, D. S. and Volkenborn, N. 2010. Infaunal Hydraulic Ecosystem Engineers: Cast of Characters and Impacts. *Integrative and Comparative Biology*, **50**, (2) 176–187.

Zar, J.H. 1999. *Biostatistical Analysis*. 4th Edition. Prentice–Hall, New Jersey, pp. 931.

Appendix 1.1 Major events around the Tr/J boundary observed in key sections. Successions are correlated on the basis of: 1) carbon isotope stratigraphy; 2) ammonite biostratigraphy; 3) radiolarian biostratigraphy, and; 4) magnetostratigraphy. QCI=Queen Charlotte Islands; OM=Orange Mountain; LU=Lower Unit. [Obtained from Hesselbo *et al.*, 2007].



Appendix 1.2 Correlation of Early Hettangian ammonites zones, subzones and horizons (grey). Broken Lines = approximated correlations (obtained from Hillebrandt *et al.*, 2007; Tanner *et al.*, 2004; Clémence 2008). This section summarise the Hillebrandt *et al.*, (2007) and Tunner *et al.*, (2004) works. However, complementary works can be observed in Hesselbo *et al.*, (2007), Bloos & Page, (2000), Bloos, (2000); Wignall (2001); Simms, (2006), Hillebrandt, (1990), (1994), Riccardi *et al.*, (2004); Schaltegeer *et al.*, (2008); McRoberts *et al.*, (1997); Ward *et al.*, (2007); Longridge *et al.*, (2007). ?= not ammonite record.

		Northern Calcareous Alps	NW Europe (Great Britain)	North America (Nevada)	South America (Chilingote)
Lower Hettangian	Tilmanni	<i>P. naumanni</i>	<i>C. johnstoni</i>	<i>C. crassicosatum</i>	<i>P. cf. calliphyloides</i>
		<i>P. costosum + P. calliphyllum</i>	<i>P. plicatulum</i>	<i>C. polymorphum</i>	<i>P. rectocostatum</i>
		Neophyllites	<i>P. psilonotum</i>		<i>P. primocostatum</i>
			<i>P. planorbis</i>		<i>P. planocostatum</i>
			Neophyllites	<i>P. erugatum</i>	<i>P. pacificum</i>
		<i>P. cf. pacificum</i>	?	<i>P. marcouxii</i>	<i>P. tilmanni</i>
	<i>P. ex. gr. P. tilmanni</i>	<i>P. spelae</i>		<i>Psiloc. cf. spelae</i>	
<i>Psiloc. Cf. spelae</i>					
Rhaetian	Marshi	<i>Choristoceras marshi</i>		<i>Choristoceras crickmayi</i>	<i>Choristoceras marshi + crickmayi</i>

Appendix 1.3 Other marine sections

Europe: The best studied marine sections that are relevant to the Tr/J extinctions are concentrated in Western Europe, North America, and the Andes Cordillera (Fig.1.10). St Audrie's Bay, Somerset, England in north-western Europe was proposed by Warrington *et al.*, (1994) as GSSP for the base of the Hettangian, and Bed 13 (thought to represent the first occurrence of the genus *Psiloceras* – at that time *P. planorbis*) as definition of the stratotype point. Later results (Bloos and Page, 2000) demonstrated, however, that the oldest psiloceratid of NW Europe (Great Britain) is *Psiloceras erugatum*, with the first occurrence (FO) in Bed 8 at Doniford Bay (near St Audrie's Bay), followed closely above by *Psiloceras planorbis* in the upper part of Bed 9. Though *P. erugatum* has inner whorls with nodes ('Knoetchenstadium'), like most of the *Psiloceras* of the Northern Calcareous Alps, it has never been found there and therefore cannot be fitted into the Alpine *Psiloceras* sequence.

Considering the more or less pronounced ribbing on the inner whorls, and the occurrence closely below *Neophyllites* in NW Europe, *P. erugatum* should be younger than any of the Karwendel ammonites found below the Calliphyllum Zone, in which *Neophyllites* occurs in the Northern Calcareous Alps (Bloos, 2004; von Hillebrandt *et al.*, 2007).

North America: Tr/J sections in New York Canyon (Nevada, USA) have been described and show an almost complete ammonite record (Guex 1995; Guex *et al.*, 1998; Guex *et al.*, 2002; Guex *et al.*, 2003). This locality has been proposed as the Tr/J GSSP in various ways: an initial negative isotope excursion (McRoberts *et al.*, 1997; Fraser *et al.*, 2004; Ward 2007), the FO of *Psiloceras* (Guex *et al.*, 1998). However, the section seems to be complicated in a tectonic sense.

The GSSP horizon proposed by Guex *et al.*, (1998), with the FO of *Psiloceras spelae* as boundary event, can be correlated with ammonite level (2) of the Karwendel Syncline. The beds with *Choristoceras minutum*, *Odoghertyceras deweveri*, *Psiloceras marcouxii*, *P. tilmanni* and cf. *Neophyllites* (Guex *et al.* 2002; Lucas *et al.*,) occurring 7.2 m higher in the section, may be correlated with ammonite level (3), but choristoceratids and psiloceratids similar to *Psiloceras marcouxii* do not occur in the Hettangian of Europe, and the determination of *Neophyllites* is doubtful.

The lower part of the beds with *Psiloceras pacificum* (excluding specimens with ribbed inner whorls) may correlate with ammonite horizon (4). The pelecypod *Agerchlamys* occurs slightly earlier than *Psiloceras spelae*, mirroring the situation in the NCA. Hettangian microfossils of biostratigraphic value were not found in the Nevada sections.

South America: The Andes section in the Utcubamba Valley of northern Peru was also proposed as GSSP candidate for the Tr/J (Hillebrandt 2000), but the proposal was withdrawn in 2006. The first Hettangian ammonite bed is characterised by a species of *Psiloceras* that is distinguished from *Psiloceras tilmanni* by a steeper umbilical wall. *Odoghertyceras* was also found in this bed. Above follow several beds with *Psiloceras tilmanni*. Below this bed, a limestone sample contains radiolarians transitional to basal Hettangian radiolarians, with just a few Rhaetian holdovers. The radiolarian turnover is probably older than the ammonite turnover (Lucas *et al.*, 2005).

There are other complete Tr/J sections in the Utcubamba Valley (Hillebrandt, 2000), but the ammonites are mostly compressed and not yet studied in detail. Recently, Guex (Guex *et al.* 2004) discovered *Psiloceras cf. spelae* close to a section described by Hillebrandt (1994). *P. cf. spelae* was found just above *Choristoceras crickmayi* and 10 m below *Psiloceras tilmanni*. The Utcubamba Valley could eventually provide the

possibility of a correlation of ammonite and radiolarian biostratigraphy. (Guex *et al.* 2004)

Other Tr/J sections are found in northern Chile, but the lowest Hettangian ammonite horizons are missing (Hillebrandt 1990; Hillebrandt 2000). However, Chong (personal comm.) indicated that there are more complete marine sections of the Tr/J close to those reported by Chong and Hillebrandt, (Chong and Hillebrandt 1985). The oldest ammonite level can be correlated with part of the beds with *Psiloceras polymorphum* in Nevada and the Planorbis and Calliphylum Zones in Europe.

Appendix 2.1 List of Index richness estimator described in the Chapter 2.

Richness Estimator	Calculation	Elements	Concept
Individual-based Rarefaction (Coleman curves)	$S_m = \sum_{i=1}^s \left[1 - \frac{\binom{N-n_i}{m}}{\binom{N}{m}} \right]$	S_m : is the total number of species expected; n_i is the number of individuals of the i th species; m is the subsample of the entire collection of size N .	This tool estimates how many taxa you would expect to find in a sample with a smaller total number of individuals. With this method, it is possible to compare the number of taxa in samples of different size. Using rarefaction analysis on the largest sample, it is possible to read out the number of expected taxa for any smaller sample size (including that of the smallest sample) (Coleman <i>et al.</i> , 1982; Olszewski 2010; Magurran 2004; Hammer and Harper, 2006).
Sample-based Rarefaction (Mao Tau = expected species accumulation curves)	$S_a = \sum_{i=1}^{S_{total}} \left[1 - \frac{\binom{A-o_i}{a}}{\binom{A}{a}} \right]$	A : number of total collections; a : number of the collection in the subset; O_i : number of the number collection in which the taxon i occurs, and S_a : expected richness at a collections.	(Also called) Collector's curves are conceptually very similar to individual-based rarefaction. However, Sample-based Rarefaction depicts the trajectory of richness as a series of the entire collection is added successively. The collection can be replicated from a single sampling location or a set of sampling units from different locations in a region or different beds in a stratigraphic succession (Gotelli and Colwell, 2001; Olszewski 2010).
Chao ₁	$S_{Chao1} = S_{obs} \frac{F_1^2}{2F_2}$	S_{obs} : number of species observed in the sample; F_1 : the number of observed species represented by a single individual (singletons); F_2 : number of observed species represented by two individuals (doubletons).	Richness estimator of the absolute number of species in assemblage. Chao ₁ is non-parametric, but also requires relative abundance data. It is based on the number of rare species in the sample. The richness estimation produced by Chao ₁ is a function of the ratio of singletons and doubletons and will exceed observed species richness by ever greater margin as the relative frequency of singletons increases. (Coddington <i>et al.</i> , 1996; Magurran 2004; Colwell 2005)
Chao ₂	$S_{Chao2} = S_{obs} \frac{Q_1^2}{2Q_2}$	Q_1 : the number of species that occur in one sample (unique species); Q_2 : the number of species that occur in two samples.	Chao ₂ is a richness estimator using an incidence-based approach. The disadvantage of Chao ₁ is that it requires abundance data (Magurran 2004). However, Chao ₂ is a modified estimator that uses presence/absence data. In this case, it is only necessary to know the number of species found in just one and two samples (Magurran, 2004; Foggo <i>et al.</i> , 2003).
Jackknife ₁	$S_{Jack1} = S_{obs} + Q_1 \left(\frac{m-1}{m} \right)$	S_{obs} : number of species observed Q_1 : number of species found in one sample; m : number of samples.	Jackknife ₁ is a first order estimator that employs the number of species that occur in only a single sample (Magurran 2004). It is based on presence/absence data rather than species abundances. It is useful to reduce bias and estimates species richness. It has a closed form (Smith and Pontius 2006).

Appendix 2.2 List of Rank abundance Models and of the estimators used for inferred the most competence model.

Estimator	Calculation	Elements	Concept
Broken stick model	$n_i = \frac{Nt}{S} \sum_{n=1}^s \frac{1}{n}$	Where n_i : the abundance of the i th species; Nt : is the total number of individuals (site total) and S is the total number of species in the community.	Developed by MacArthur (1957), broken stick is the closest nature gets to maximal evenness. MacArthur likened the subdivision of niche space within a community to a stick broken randomly and simultaneously into S pieces. It is the most uniform distribution ever found in natural communities. The model could be viewed as representative of a group of species of equal competitive ability jostling for niche space (Tokeshi 1993; Magurran, 2004).
Geometric series	$n_i = NC_k k(1 - k)^{i-1}$	Where the n_i : the total number of individuals in the i th species; N : the total number of individuals; k : the proportion of the remaining niche space occupied by each successively colonizing species (k is the constant); $C_k = [1-(1-k)^S]^{-1}$ and is a constant that insures that $\sum n_i = N$.	The Geometric model (Motomura 1932, 1947; Whittaker 1965) suggests that the 'most successful species' (presumably the one with the highest competitive ability) takes fraction k of the resources, and therefore forms approximately (Whittaker 1965) fraction k of the abundance. The ratio of abundance of each species to the abundance of its predecessor is constant through the ranked list, so that the plot of abundance/species rank appears like a straight line that decays. Empirical data showed that this model is found in species-poor (and often harsh) environments or early stages of a succession (Magurran 2004).
Log normal	$S(R) = S_0 e^{-a^2 R^2}$	$S(R)$: is the number of species in the R th octave to the right, and to the left, of the symmetric curve; S_0 : the number of species in the modal octave; and $a = (2\sigma^2)^{-\frac{1}{2}}$: the inverse width of the distribution.	The majority of the largest assemblages studied by ecologists appear to follow a log normal pattern of specie abundance. Preston (1948) proposed the use of a Lognormal dominance/diversity distribution for empirical reasons. " <i>The organism growth is affected by several species, and by several environmental factors. The result will tend to a normal distribution. Since organisms have intrinsic logarithmic growth, effects will tend to be proportional, and the result will be a General Lognormal distribution</i> " (May 1975; Wilson 1991; Magurran 2004). In summary, the log normal distribution presents a shallower slope, which is associated with the highest evenness, generally associated with more "stable" ecosystems (Magurran 2004).
Zipf-Mandelbrot	$A_i = A_1 i^{-\gamma}$	Where: A_i : the fitted abundance of the most abundant species and represents the average probability of the appearance of a species, all previous conditions necessary for this species being realised. Graphically, it is the slope of log abundance on log rank, so near 1 gives greater evenness of abundance; it is rarely less than 1 (Frontier 1985).	It reflects successional process in which the later colonists have more specific requirements and hence are rarer than the first species that arrive. The Mandelbrot model related originally to information systems assesses the cost of information. "Applied to plant communities, the presence of a species can be seen as dependent on previous physical conditions and previous species presences - the costs. Pioneer species have low cost, requiring few prior conditions. Late successional species have a high cost, viz. the energy, time, and organisation of the ecosystem required before they can invade. On this basis they will be rare" (Frontier 1987; Wilson 1991).

Appendix 2.3 Statistical tools

Estimator	Calculation	Elements	Concept
Whittaker (β_w)	$\beta_w = S/\bar{\alpha}$	Where S: the total number of species recorded in the system, and α : is the average sample diversity, where the samples are standardised and the diversity is measured as like species richness.	Beta reflects the biotic change or species replacement. That means, beta diversity is a measure of the extent to which the diversity of two or more spatial units differs (Magurran 2004). For more information about the performance of each index, see Wilson and Shmida (1984), Koleff <i>et al.</i> , (2003); and Magurran (2004).
Wilson and Shmida's index (β_T)	$\beta_T = \frac{S[g(H)+1(H)]}{2\bar{S}}$	$g(H)$: is the number of species gained; $1(H)$: is the number of the species lost and \bar{S} : is the total number of species recorded in the system.	
ANOSIM (Analysis of similarities)	$R = \frac{\bar{r}_b - \bar{r}_w}{N(N-1)/4}$	Its statistic is based on the mean ranks of within group (\bar{r}_w) and between group (\bar{r}_b) dissimilarities, scaled into the rank $-1 \dots +1$, and $R = 0$: indicating independence.	Analysis of similarities (ANOSIM) evaluates if the groups generated by NMDS are different. ANOSIM is often represented as a non-parametric variant of analysis of variance. The statistic uses only rank-order information, and is conceptually related to NMDS. The significance is based on permutation test.
Euclidean distance	$ED_{i,h} = \sqrt{\sum_{j=1}^p (a_{ij} - a_{hj})^2}$	This formula is the Pythagorean theorem applied to p dimension rather than the usual two dimensions. Each element of the matrix, a_{ij} , is the abundance of species j in sample unit i or h .	This is probably the most commonly chosen type of distance. It simply is the geometric distance in the multidimensional space.
SIMPER	SIMPER (Similarity Percentage) is a method for assessing which taxa are primarily responsible for an observed difference between groups of samples (Clarke 1993). "The overall significance of the difference is often assessed by ANOSIM". The Bray-Curtis similarity measure (multiplied by 100) is implicit to SIMPER. The description is based on the program PAST (Hammer and Harper 2006).		

Appendix 2.4 Definitions

2.41 Species dominance index estimation: This is simply the fraction of the collection that is represented by the most common species. Dominance can be a useful index of resource monopolization by a superior competitor, particularly in communities that have been invaded by exotic species (e.g., Porter and Savignano 1990). Like species richness, dominance is sensitive to sample size. In the extreme case of a collection of only 1 individual, dominance would always equal 1.0” (Gotelli and Entsminger 2011).

2.42 Kurtosis: A statistical measure used to describe the distribution of observed data around the mean. The fourth power of the deviations from the mean, provide a measure of kurtosis. Kurtosis \approx “peakedness” or “tailed-ness, but in fact, is the dispersion around $\mu - \sigma$ and $\mu + \sigma$. A *leptokurtic* distribution has values highly concentrated around the mean. The *platykurtic* distribution records a great variation around the mean or a more inflated curve. Finally, *mesokurtic* reflects a “normal” distribution.

2.43 Null Models: Gotelli and Graves (1996: 3) provide an operational definition of a null model as it has been applied in community ecology: ... “*A null model is a pattern-generating model that is based on randomization of ecological data or random sampling from a known or specified distribution. The null model is designed with respect to some ecological or evolutionary process of interest. Certain elements of the data are held constant, and others are allowed to vary stochastically to create new*”. See also Gotelli (2006).

2.44 Randomisation (permutation): A Nonparametric resampling method applied solely to a particular data set (i.e., not generalisable to the sampled population) that involves re-assigning observations without replacement to the probability of observing some outcome (Kowalewski and Novack-Gottshall 2010).

2.45 Non-metric Multidimensional scaling (nMDS): Is a method that groups elements (samples) based on a Similarity matrix. In this case the matrix built was based on Euclidian distance. The nMDS attempts to place the data points in a two- or three-dimensional coordinate system such that the *ranked differences* are preserved (Clarke and Gorley 2006; Hammer 2001; Clarke 1993).

Appendix 3.1 Occurrences average per stage and continent from Sepkoski Compendium, data obtained from Paleobiology Database.

Continent / Gradstein: Stages	Wordian	Capitanian	Wuchiapingian	Changhsingian	Induan	Olenekian	Anisian	Ladinian	Carnian	Norian	Rhaetian	Hettangian	Sinemurian
Antarctica	0	0	0	0	0	0	0	0	0	0	0	0	0
Indian Ocean	0	0	2	0	0	0	0	0	0	0	0	0	0
Africa	5.6	2.5	0	0	0	0	0	3	1	1	2.2	0	3
North America	4.7	2.3	2	4	2.4	4.3	2.7	3.2	4.7	3.4	4.3	2.3	2.4
South America	0	0	0	0	0	0	0	0	0	4.5	27.2	3.2	8.4
Asia	3.7	4.8	6.5	4.4	4.1	4.4	15.7	4.3	6.6	6	5	4.7	3.4
Europe	11.4	1.5	8.1	6.7	2.3	3.6	4.7	4.5	8.6	9.7	4.4	6.7	5.8
Oceania	15.8	3.7	5.3	2.7	1	2.9	1.5	1.9	9.3	6.3	23.8	6	0
AVERAGE	5.15	1.85	2.9875	2.225	1.225	1.9	3.075	2.1125	3.775	3.8625	8.3625	2.8625	2.875
SUM	41.2	14.8	23.9	17.8	9.8	15.2	24.6	16.9	30.2	30.9	66.9	22.9	23
%	12.18	4.37	7.06	5.26	2.89	4.49	7.27	4.99	8.93	9.139	19.78	6.77	6.80

Appendix 3.2 Number of genera and mode of life recorded through P/Tr and Tr/J obtain from Sepkoski's data base. Cog: Codification of each mode of life based in the the numeration of the table 7.1. This code is made up by 3 numbers. The first one, indicate tiering level (listed at table 7.1). The second, indicate the level of motility and third one indicate the feeding mechanism. Example, 111 mean Pelagic-Fast-Filter feeders.

Cog	Modes of life	Number of Genera
111	Pelagic, Freely-Fast, Suspension	(7)
ARTRHPODA		
Malacostraca		
Cumacea		
Mysidacea		
Ostracoda		
Myocopida		
114	Pelagic, Freely-Fast, Grazing	(31)
CHORDATA		
Osteichthyes		
Pachycormiformes		
115	Pelagic, Freely-Fast, Predatory	(876)
MOLLUSCA		
Cephalopoda		
Ammonoidea		
Anarcestida		
Aulacocerida		
Belemnitida		
Ceratitida		
Goniatitida		
Nautilida		
Orthocerida		
Phragmoteuthida		
Phylloceratida		
Prolecanitida		
Teuthida		
ARTHROPODA		
Malacostraca		
Lophogastrida		
Thylacocephala		
Concavicularida		
Conchyliocarida		
CHORDATA		
Amphibia		
Temnospondyli		
Chondrichthyes		
Chimaeriformes		
Ctenacanthida		
Eugeneodontida		
Galeomorphii Incertae Sedis		
Hexanchiformes		
Holocephali Incertae Sedis		

Orectolobiformes

Petalodontida

Osteichthyes

Amiiformes

Bobasatraniformes

Cephaloxeniformes Coelocanthiformes

Macrosemiiformes

Peltopleuriformes

Perleidiformes

Pholidopleuriformes

Ptycholepiformes

Pycnodontiformes

Saurichthyiformes

Semionotiformes

Reptilia

Crocodylia

Ichthyosauria

Notosauria

Placodontia

Plesiosauria

Thalattosauria

261 Erect, Non-motile-attached, Suspension (135)

ECHINODERMATA

Crinoidea

Cladida

Comatulida

Disparida

Encrinida

Isocrinida

Millericrinida

Monobathrida

Roveacrinida

Sagenocrinida

311 Surficial, Freely-Fast, Suspension

(10)

ARTHROPODA

Malacostraca

Leptostraca

Ostracoda

Metacopida

312 Surficial, Freely-Fast, Deposit

(8)

ARTHROPODA

Malacostraca

Isopoda

Tanaidacea

313 Surficial, Freely-Fast, Mining

(24)

ARTHROPODA

Marrelomorpha

Cyclina

Trilobita

Proetida

- 315 Surficial, Freely-Fast, Predatory (16)**
ARTHROPODA
 Malacostraca
 Decapoda
- 321 Surficial, Freely-Slow, Suspension (108)**
ARTHROPODA
 Ostracoda
 Platicopida
MOLLUSCA
 Gastropoda
 Cephalaspida
 Heterostrophia
 Neotaenioglossa
- 322 Surficial, Freely-Slow, Surface deposit (39)**
ECHINODERMATA
 Ophiuroidea
 Ophiurida
MOLLUSCA
 Gastropoda
 Architaenoglossa
 Cephalaspida
 Heterostrophia
 Neotaenioglossa
- 323 Surficial, Freely-Slow, Mining (92)**
ARTHROPODA
 Ostracoda
 Podocopida
ECHINODERMATA
 Echinoidea
 Disasteroidea
 Echinocystitoida
 Pedinoidea
- 324 Surficial, Freely-Slow, Grazing (257)**
ECHINODERMATA
 Echinoidea
 Cidaroida
 Diadematoidea
 Hemicidaroida
 Phymosomatoida
 Plesiocidaroida
MOLLUSCA
 Gastropoda
 Archaeogastropoda
 Architaenoglossa
 Cephalaspida
 Neotaenioglossa
 Polyplacophora
 Neoloricata

Paleoloricata
Tergomya
Patellogastropoda
325 Surficial, Freely-Slow, Predatory (55)

ANNELIDA

Polychaeta
Eunicemorpha

ARTHROPODA

Merostomata
Xiphosurida

ECHINODERMATA

Asteroidea
Forcipulatida
Notomyotida
Trichasteropsida
Valvatida

MOLLUSCA

Gastropoda
Bellerophonitida
Cephalaspida
Heterostrophia
Neotaenioglossa

331 Surficial, Facultative-Unattached, Suspension (10)

MOLLUSCA

Bivalvia
Arcoidea
Pterioidea
Hyalitha
Hyalithida

334 Surficial, Facultative-Unattached, Grazing (13)

MOLLUSCA

Gastropoda
Euomphalina

361 Surficial, Non-motiles, attached, Suspension (1254)

ANNELIDA

Polychaeta
Serpulimorpha

ARTHROPODA

Cirripedia
Pedunculata
Acrothoracica
Scalpelliformes

BRACHIOPODA

Craniata
Craniida
Rhynchonellata
Orthida
Rhynchonellida

Spiriferida
Terebratulida
Thecideida
Athyridida

Strophomenata

Orthotetida
Productida
Strophomenida

BRYOZOA

Gymnolaemata

Ctenostomata

Stenolaemata

Cryptostomata
Cyclostomata
Cystoporata
Fenestrata
Trepotomata

CNIDARIA

Anthozoa

Alcyonacea
Pennatulacea
Rugosa
Scleractina
Tabulata

Scyphozoa

Conulariida

Hydrozoa

Hydroida
Lemniscaterina
Milleporina

ECHINODERMATA

Blastoidea

Fissiculata
Spiraculata

HEMICHORDATA

Pterobranchia

Rhabdopleurida
Order uncertain (genus: Megaderaion)

MOLLUSCA

Bivalvia

Arcoida
Hippuritoida
Pectinoida
Pholadomyoida
Pterioida

Gastropoda

Neotaenioglossa

PORIFERA

Calcarea

Pharetronida
Sycones

Demospongea

Agelasida
Astrophorida
Axinellida

Guadalupiida
Hadromerida
Haplosclerida
Lithistida
Permosphincta
Poecilosclerida
Tabulospongida
Verticillitida

SILICISPONGEA

Hexactinellida

Amphidiscosa
Hexactinosa
Lychniscosa
Lyssacinosida
Reticulosa

HEMICHORDATA

Enteropneusta

Megaderaion

- 362** **Surficial, Non-motiles, Attached, Surface-Deposit** **(1)**
ANNELIDA
 Polychaeta
 Order uncertain (genus: Microtubus)
- 411** **Semi-infaunal, Freely-Fast, Suspension** **(23)**
ARTHROPODA
 Ostracoda
 Palaeocopida
- 422** **Semi-infaunal, Freely-Slow, surface deposit** **(3)**
MOLLUSCA
 Scaphopoda
 Dentaliida
- 424** **Semi-infaunal, Freely-Slow, Grazing** **(1)**
ECHINODERMATA
 Echinoidea
 Pygasteroidea
- 425** **Semi-infaunal, Freely-Slow, Predatory** **(1)**
ECHINODERMATA
 Asteroidea
 Velatida
- 431** **Semi-infaunal, Facultative-Unattached, Suspension** **(10)**
MOLLUSCA
 Bivalvia
 Arcoida
 Order uncertain (genus: Cruciella)
 Order uncertain (genus: Laubeia)
 Order uncertain (genus: Taeniodon)

- 435 Semi-infaunal, Facultative-Unattached, Predatory (4)**
 ANNELIDA
 Polychaeta
 Phyllodoceomorpha
- 441 Semi-infaunal, Facultative-Attached, Suspension (53)**
 MOLLUSCA
 Bivalvia
 Pterioida
 ECHINODERMATA
 Holothuroidea
 Apodida
 Aspidochirotida
 Dactylochirotida
 Dendrochirotida
 Elasipodida
 Molpadiida
 Order uncertain (genus: Acanthocaudina)
 Order uncertain (genus: Calclyra)
 Order uncertain (genus: Conisia)
 Order uncertain (genus: Crucivirga)
 Order uncertain (genus: Curvatella)
 Order uncertain (genus: Semperites)
 Order uncertain (genus: Triradites)
 Order uncertain (genus: Uniramosa)
 BRACHIOPODA
 Lingulata
 Lingulida
- 451 Semi-infaunal, Non-motile-Unattached, Suspension (2)**
 MOLLUSCA
 Rostrochonchia
 Conocardioida
- 461 Semi-infaunal, Non-motile-Attached, Suspension (16)**
 MOLLUSCA
 Bivalvia
 Mytiloida
 Pterioida
 Hippuritoida
- 531 Shallow-infaunal, Facultative-Unattached, Suspension (53)**
 MOLLUSCA
 Bivalvia
 Trigonioida
 Arcoida
 Pholadomyoida
 Nuculoida
- 532 Shallow-infaunal, Facultative-Unattached, Surfacedeposit (6)**
 MOLLUSCA
 Bivalvia
 Nuculoida

535	Shallow-infaunal, Facultative-Unattached, Predator	(1)
	MOLLUSCA	
	Bivalvia	
	Pholadomyoidea	
541	Shallow-infaunal, Facultative-attached, Suspension	(33)
	MOLLUSCA	
	Bivalvia	
	Veneroidea	
546	Shallow-infaunal, Facultative-attached, Chemotrophic	(5)
	MOLLUSCA	
	Bivalvia	
	Solemyoidea	
561	Shallow-infaunal, Non-motile-attached, Suspension	(32)
	MOLLUSCA	
	Bivalvia	
	Pholadomyoidea	
	Myoidea	
	Veneroidea	
	Unionoidea	
	Nuculoidea	
633	Deep-infaunal, Facultative-Unattached, Mining	(1)
	MOLLUSCA	
	Bivalvia	
	Drilomorpha	

Appendix 3.3 Number of genera per mode of life present before and after an extinction event.

T	M	F	Changhsingian				Taxa that cross to Induan				Rhaetian				Taxa that cross to Hettangian			
			Phylum	Class	Order	Genera	Phylum	Class	Order	Genera	Phylum	Class	Order	Genera	Phylum	Class	Order	Genera
1	1	1	1	1	1	1	0	0	0	0	0	0	0	0	0	0	0	0
1	1	4	1	1	1	6	1	1	1	1	1	1	2	6	1	1	2	2
1	1	5	2	3	13	36	2	3	11	16	3	5	22	90	3	5	16	25
2	6	1	1	1	2	2	0	0	0	0	1	1	5	13	1	1	2	7
3	1	1	1	1	1	3	1	1	1	2	1	1	1	4	1	1	1	4
3	1	2	1	1	2	2	1	1	1	2	1	1	2	2	1	1	1	1
3	1	3	1	2	2	3	1	1	1	1	1	1	1	3	0	0	0	0
3	1	5	1	1	1	1	0	0	0	0	1	1	1	2	1	1	1	1
3	2	1	1	1	3	8	1	1	3	7	2	2	3	45	2	2	3	24
3	2	2	1	1	3	7	1	1	2	3	1	1	4	17	1	1	4	8
3	2	3	1	1	1	28	1	1	1	3	2	2	2	19	2	2	2	14
3	2	4	2	4	7	44	2	4	5	25	2	4	6	74	2	4	5	33
3	2	5	2	2	4	21	2	2	4	13	3	3	5	12	3	3	4	11
3	3	1	1	1	1	1	0	0	0	0	1	1	1	6	1	1	1	5
3	3	4	1	1	1	6	1	1	1	4	1	1	1	4	1	1	1	1
3	6	1	8	13	27	221	8	12	21	65	9	13	29	296	9	12	22	105
3	6	2	0	0	0	0	0	0	0	0	1	1	1	1	0	0	0	0
4	1	1	1	1	1	13	1	1	1	2	1	1	1	1	1	1	1	1
4	2	4	0	0	0	0	0	0	0	0	0	0	0	0	0	0	0	0
4	2	5	0	0	0	0	0	0	0	0	0	0	0	0	0	0	0	0
4	3	1	1	1	1	2	1	1	1	2	1	1	1	3	1	1	1	3
4	3	5	1	1	1	2	1	1	1	2	2	2	3	5	2	2	3	4
4	4	1	2	2	5	11	2	2	5	11	3	3	7	23	3	3	7	21
4	5	1	0	0	0	0	0	0	0	0	0	0	0	0	0	0	0	0
4	6	1	1	1	2	2	1	1	2	2	1	1	3	8	1	1	2	4
5	3	1	1	1	3	5	1	1	3	4	1	1	3	14	1	1	3	6
5	3	2	0	0	0	0	0	0	0	0	1	1	1	2	1	1	1	1
5	3	5	0	0	0	0	0	0	0	0	1	1	1	1	1	1	1	1
5	4	1	2	2	2	3	0	0	0	0	1	1	1	12	1	1	1	5
5	4	6	1	1	1	1	1	1	1	1	1	1	1	1	1	1	1	1
5	6	1	1	1	2	3	1	1	2	2	1	1	4	13	1	1	4	8
6	3	3	0	0	0	0	0	0	0	0	1	1	1	1	0	0	0	0
Average			1.48	1.84	3.52	17.28	1.24	1.52	2.72	6.72	1.709	3.61	3.61	21.83	1.34	1.56	2.81	9.25

Appendix 4.2 Summary of palaeoecological parameters estimated in this study. SC: Sample cog; H: Height (m), R: Richness, MR: Mean Richness, K: Kurtosis, B_w: Whittaker index, B_R: Routledge index; AC: Average cover %; II: Ichnofabric indices; NM = mean values of null model (mm); GM = Geomean of body size (mm), RT = Rate of change in body size, BD=Burrow diameter (mm), CI: Carbon isotope data, (0.00) = No Data.

Limestone														Mudstone						
Sample Code	H	R	MR	K	B _w	B _R	AC	II	NM	GM	RT	BD	CI	Sample code	H	R	MR	K	B _w	B _R
WF1	1.90	6.00	3.97	51.11	0.00	0.00	0.00	2.00	5.12	9.79	0.00	0.00	-25.4	WF1	2.4	3	0.14	45.87	0	0
WF2	2.90	7.00	5.38	22.14	0.38	0.11	0.00	1.00	4.76	16.85	7.06	0.00	-25.8	WF2	3.8	3	0.07	23.53	0.33	0.10
WF3	4.90	8.00	5.73	15.31	0.47	0.14	0.00	3.00	3.94	8.63	-4.11	0.00	-26.2	WF3	6	4	0.39	49.62	0.71	0.21
WF4	6.80	8.00	5.07	23.31	0.50	0.15	0.00	4.00	6.99	11.46	1.49	0.00	-26.7	WF4	8.2	4	0.20	40.05	0.50	0.15
WF5	9.00	8.00	5.80	21.75	0.38	0.11	0.00	3.00	7.29	16.42	2.25	0.00	-26.5	WF5	9.7	7	3.06	21.23	0.64	0.18
WF6	10.20	5.00	3.89	39.50	0.38	0.10	0.00	4.00	12.48	9.74	-5.56	0.00	-25.9	WF6	10.5	6	5.32	16.50	0.69	0.21
CM1	11.00	4.00	2.78	27.60	1.00	0.30	0.00	1.00	1.05	7.70	-2.55	0.00	-26.4	LM 1	13	0	0.00	0.00	1.00	0.28
CM2	11.40	0.00	0.00	0.00	0.00	0.21	0.00	0.00	0.00	0.00	0.00	0.00	-24.6	LM 2	13.3	3	0.11	48.75	0.00	0.12
CM3	12.00	3.00	2.38	38.90	0.71	0.00	0.00	0.00	1.24	13.13	5.43	0.00	-28.6	PPZ1	14.8	4	0.34	26.83	0.43	0.10
CM4	12.40	0.00	0.00	0.00	0.00	0.29	0.00	0.00	0.00	0.00	0.00	0.00	-29.2	PPZ2	16.6	5	1.99	14.20	0.33	0.06
LM1	12.90	0.00	0.00	0.00	0.00	0.00	0.00	1.00	3.68	10.55	-2.86	0.00	-29	PPZ3	18	8	1.78	28.23	0.23	0.12
LM2	13.30	5.00	3.96	28.35	1.00	0.00	10.00	3.00	2.73	17.00	16.11	3.00	-26.2	PPZ4	19.25	6	0.73	38.02	0.43	0.16
LM3	14.00	4.00	2.77	43.19	0.56	0.16	11.00	3.00	5.03	17.12	0.17	3.53	-26.8	PZ1	20.8	7	0.58	14.88	0.54	0.04
LM4	14.20	6.00	4.87	41.26	0.60	0.17	60.00	3.00	0.00	0.00	0.00	4.91	-26.6	PZ2	22	5	0.38	44.01	0.17	0.14
PPZ1	15.80	7.00	5.21	17.71	0.54	0.16	65.00	4.00	5.92	14.05	-1.70	4.04	-26.4	PZ3	23.2	6	0.47	12.10	0.45	0.14
PPZ2	17.20	7.00	5.74	11.98	0.43	0.13	96.00	3.00	12.83	13.42	-0.45	4.98	-27	PZ4	24.6	5	0.12	11.51	0.45	0.16
PPZ3	18.40	9.00	7.65	4.44	0.50	0.15	80.00	4.00	3.04	13.56	0.11	4.63	-27.2	PZ5	26.7	10	2.34	49.81	0.60	0.15
PPZ4	19.60	7.00	5.54	31.00	0.25	0.07	78.00	3.00	0.78	13.58	0.02	6.97	-29.3	LZ1	28.1	7	0.77	29.10	0.53	0.14
PZ1	20.30	5.00	4.44	20.41	0.33	0.09	56.00	4.00	3.43	10.97	-3.73	7.87	-29.1	LZ2	32.6	8	0.59	17.70	0.47	0.09
PZ2	21.20	10.00	8.24	6.59	0.47	0.12	35.00	4.00	5.55	14.28	3.68	3.82	-28.9	LZ3	36.2	3	0.10	39.76	0.45	0.14
PZ3	23.70	8.00	5.51	28.02	0.44	0.13	78.00	5.00	1.48	8.14	-2.45	10.49	-28	LZ4	41.6	4	0.38	27.98	0.50	0.15
PZ4	25.00	7.00	5.15	18.43	0.60	0.18	80.00	4.00	0.43	12.23	3.15	10.02	-28.1	LZ5	46.7	10	1.17	19.70	0.57	0.15
PZ5	25.90	10.00	7.21	34.88	0.41	0.12	90.00	3.00	3.77	39.54	30.34	7.79	-27.4	LZ6	52.25	5	0.33	20.48	0.57	0.20
PZ6	27.60	10.00	7.51	18.11	0.20	0.06	60.00	3.00	1.46	8.87	-18.04	6.82	-28.2	LZ7	58.6	9	2.26	15.73	0.71	0.09
LZ1	32.00	5.00	3.85	21.18	0.33	0.08	45.00	4.00	3.15	22.61	3.12	5.48	0.00	AZ1	61.5	8	0.66	44.09	0.29	0.14
LZ2	35.50	6.00	4.02	50.96	0.45	0.14	70.00	3.00	2.09	9.17	-3.84	5.06	0.00							
LZ3	40.90	5.00	3.58	19.69	0.45	0.14	75.00	3.00	0.69	6.17	-0.56	5.51	0.00							
LZ4	46.00	6.00	3.80	15.32	0.45	0.14	56.00	4.00	0.23	10.27	0.80	6.80	0.00							
LZ5	51.30	3.00	2.43	24.21	1.00	0.28	47.00	4.00	1.14	12.49	0.42	4.20	0.00							
LZ6	58.00	6.00	5.01	10.08	0.78	0.21	50.00	3.00	1.96	11.35	-0.17	11.21	0.00							
AZ1	61.00	5.00	3.96	24.66	0.45	0.14	40.00	2.00	3.53	16.17	1.61	10.01	0.00							

Appendix 4.3 Total species abundance (%) by Lithology and lithostratigraphy: WF: Cotham Member, CM: Cotham Member, LM Langport Member, PPZ: Pre-Planorbis Zone, PZ: Planorbis zone, LZ: Liasicus zone, AZ: angulate zone.

Limestone											
Species	WF	Species	CO	Species	LANG	Species	PPZ	Species	PZ	Species	LZ
<i>Isocyprina concentricum</i>	32.48	<i>Chlamys valoniensis</i>	48.15	<i>Liostrea hisingeri</i>	46.61	<i>Liostrea hisingeri</i>	35.82	<i>Diademopsis tomes</i>	32.32	<i>Modiolus ventricosus</i>	34.44
<i>Isocyprina ewaldi</i>	29.91	<i>Modiolus</i> sp.	22.22	<i>Pholadomya</i> sp.	14.41	<i>Modiolus minimus</i>	23.28	<i>Liostrea hisingeri</i>	16.41	<i>Diademopsis tomes</i>	26.67
<i>Permophorus elongatus</i>	17.26	<i>Isocyprina concentricum</i>	14.81	<i>Myoconcha</i> sp.	10.17	<i>Diademopsis tomes</i>	15.52	<i>Isocrinus psilonoti</i>	12.88	<i>Isocrinus psilonoti</i>	16.67
<i>Placunopsis alpina</i>	8.72	<i>Protocardia rhaetica</i>	7.41	<i>Modiolus hillanus</i>	8.47	<i>Modiolus</i> sp.	6.87	<i>Plagiostoma giganteum</i>	12.12	<i>Plagiostoma giganteum</i>	7.22
<i>Chlamys valoniensis</i>	5.13	<i>Cardinia regularis</i>	3.70	<i>Pteromya langportensis</i>	6.78	<i>Modiolus hillanus</i>	3.58	<i>Modiolus minimus</i>	9.60	<i>Modiolus</i> sp.	6.11
<i>Mytilus cloacinus</i>	2.22	<i>Rhaetavicula contorta</i>	3.70	<i>Grammatodon hettangiensis</i>	5.93	<i>Isocrinus psilonoti</i>	2.99	<i>Pteromya langportensis</i>	4.80	<i>Pseudolimea duplicata</i>	3.33
<i>Liostrea hisingeri</i>	0.85			<i>Modiolus</i> sp.	2.54	<i>Plagiostoma giganteum</i>	2.99	<i>Cardinia regularis</i>	3.28	<i>Liostrea hisingeri</i>	2.78
<i>Modiolus</i> sp.	0.85			<i>Cardinia regularis</i>	2.54	<i>Chlamys valoniensis</i>	2.69	<i>Modiolus</i> sp.	3.03	<i>Psilophyllites hagenowi</i>	1.11
<i>Plagiostoma punctatum</i>	0.68			<i>Plagiostoma giganteum</i>	1.69	<i>Mytilus</i> sp.	1.79	<i>Chlamys valoniensis</i>	1.01	<i>Cardinia regularis</i>	0.56
<i>Liriomyophoria postera</i>	0.51			<i>Chlamys valoniensis</i>	0.84	<i>Cardinia regularis</i>	1.49	<i>Modiolus ventricosus</i>	1.01	<i>Chlamys valoniensis</i>	0.56
<i>Astarte</i> sp.	0.34					<i>Oxytoma inequivalvis</i>	1.49	<i>Pinna</i> sp.	0.76	<i>Pseudokatosira undulata</i>	0.56
<i>Cardinia regularis</i>	0.34					<i>Pseudolimea duplicata</i>	0.60	<i>Caloceras johnstoni</i>	0.51		
<i>Rhaetavicula contorta</i>	0.34					<i>Pteromya langportensis</i>	0.60	<i>Pholadomya</i> sp.	0.51		
<i>Isocyprina depressum</i>	0.17					<i>Parellodon</i> sp.	0.30	<i>Pseudolimea duplicata</i>	0.51		
<i>Promathilda rhaetica</i>	0.17							<i>Briozoa</i>	0.25		
								<i>Paleonucula navis</i>	0.25		
								<i>Pseudokatosira undulata</i>	0.25		
								<i>Psiloceras planorbis</i>	0.25		
								<i>Rollieria bronni</i>	0.25		

Mudstone											
Species	WF	Species	CO	Species	LANG	Species	PPZ	Species	PZ	Species	LZ
<i>Rhaetavicula contorta</i>	35.04			<i>Pteromya langportensis</i>	80	<i>Diademopsis tomes</i>	28.93	<i>Caloceras johnstoni</i>	37.06	<i>Diademopsis tomes</i>	21.5
<i>Isocyprina concentricum</i>	17.66			<i>Modiolus</i> sp.	10	<i>Modiolus</i> sp.	18.78	<i>Liostrea hisingeri</i>	13.99	<i>Modiolus</i> sp.	16.5
<i>Isocyprina ewaldi</i>	14.81			<i>Liostrea hisingeri</i>	10	<i>Liostrea hisingeri</i>	14.72	<i>Pteromya langportensis</i>	13.99	<i>Cardinia regularis</i>	14.5
<i>Promathilda rhaetica</i>	11.68					<i>Pteromya langportensis</i>	9.137	<i>Diademopsis tomes</i>	9.091	<i>Waehnoceras portlocki</i>	9
<i>Modiolus sodburiensis</i>	7.692					<i>Psilocoas erugatum</i>	8.629	<i>Modiolus minimus</i>	6.294	<i>Asalties laqueus</i>	6.5
<i>Cassianella</i> sp.	4.558					<i>Cardinia regularis</i>	6.599	<i>Modiolus</i> sp.	4.895	<i>Psilophyllites hagenowi</i>	5.5
<i>Protocardia rhaetica</i>	2.849					<i>Asalties laqueus</i>	5.584	<i>Psiloceras planorbis</i>	4.196	<i>Palaeoneilo elliptica</i>	4.5
<i>Chlamys valoniensis</i>	1.14					<i>Antiquilima</i> sp.	3.553	<i>Pseudomitiloides dubius</i>	2.797	<i>Pseudomitiloides dubius</i>	4.5
<i>Isocyprina depressum</i>	1.14					<i>Astarte</i> sp.	1.015	<i>Modiolus hillanus</i>	2.098	<i>Plagiostoma giganteum</i>	4
<i>Modiolus</i> sp.	1.14					<i>Modiolus minimus</i>	1.015	<i>Isocrinus psilonoti</i>	1.399	<i>Paleonucula navis</i>	3.5
<i>Diademopsis tomes</i>	0.855					<i>Caloceras johnstoni</i>	0.508	<i>Psiloceras sampsoni</i>	1.399	<i>Modiolus ventricosus</i>	3
<i>Gervillella precursor</i>	0.57					<i>Chlamys valoniensis</i>	0.508	<i>Antiquilima</i> sp.	0.699	<i>Camptonectes</i> sp.	2.5
<i>Mytilus cloacinus</i>	0.57					<i>Isocrinus psilonoti</i>	0.508	<i>Camptonectes</i> sp.	0.699	<i>Rollieria bronni</i>	1.5
<i>Plagiostoma giganteum</i>	0.285					<i>Pholadomya</i> sp.	0.508	<i>Plagiostoma giganteum</i>	0.699	<i>Liostrea hisingeri</i>	0.5
								<i>Rollieria bronni</i>	0.699	<i>Myoconcha</i> sp.	0.5
										<i>Ryderia doris</i>	0.5
										<i>Modiolus minimus</i>	0.5
										<i>Bositra</i> sp.	0.5
										<i>Pholadomya</i> sp.	0.5

Appendix 4.4 Total species abundance by Lithology and lithostratigraphy: WF: Westbury Formation, CM: Cotham Member, LM Langport Member, PPZ: Pre-Planorbis Zone, PZ: Planorbis zone, LZ: Liasicus zone.

	Limestone						Mudstone				
	WF	CM	LM	PPZ	PZ	LZ	WF	LM	PPZ	PZ	LZ
	101	0	0	0	0	0	123	0	0	0	0
	190	4	0	0	0	0	3	0	57	13	43
	175	0	0	0	0	0	4	1	48	7	33
	13	0	0	0	0	0	62	0	0	0	0
	2	1	0	0	0	0	0	0	0	53	0
	3	0	0	0	0	0	0	8	25	20	0
	1	0	0	0	0	0	52	0	0	0	0
	30	13	0	9	4	1	0	1	29	20	1
	5	6	3	23	12	11	0	0	15	0	29
	2	1	3	5	13	1	41	0	0	0	0
	4	0	0	0	0	0	27	0	0	0	0
	51	0	0	0	0	0	0	0	17	0	0
	5	0	55	120	65	5	16	0	0	0	0
	2	0	0	0	0	0	0	0	0	0	14
	1	0	0	0	0	0	0	0	0	0	13
	0	0	7	0	0	0	0	0	3	9	1
	0	0	8	2	19	0	0	0	0	4	9
	0	0	17	0	2	0	0	0	0	0	11
	0	0	2	0	0	0	1	0	0	1	8
	0	0	1	2	2	6	10	0	0	0	0
	0	0	2	10	48	13	0	0	0	0	9
	0	0	10	12	0	0	0	0	0	0	7
	0	0	12	0	0	0	0	0	0	1	5
	0	0	0	52	128	48	0	0	0	0	6
	0	0	0	5	0	0	0	0	0	6	0
	0	0	0	78	38	0	4	0	1	0	0
	0	0	0	6	0	0	4	0	0	0	0
	0	0	0	10	51	30	0	0	0	1	3
	0	0	0	1	0	0	0	0	0	0	4
	0	2	0	0	1	0	0	0	1	2	0
	0	0	0	0	3	0	0	0	0	3	0
	0	0	0	0	1	0	2	0	0	0	0
	0	0	0	0	1	0	2	0	0	0	0
	0	0	0	0	1	0	0	0	1	0	1
	0	0	0	0	1	1	0	0	0	2	0
	0	0	0	0	1	0	0	0	0	1	0
	0	0	0	0	4	62	0	0	0	0	1
	0	0	0	0	2	0	0	0	0	0	1
	0	0	0	0	0	2	0	0	0	0	1
	0	0	0	0	0	2	0	0	0	0	1
Individuals	585	27	120	335	397	180	351	10	197	143	200
Species	15	6	11	14	20	11	14	3	10	15	20

Appendix 4.5 Pairwise comparisons of the faunal composition of each stratigraphic units taken from limestone samples. The values showed were estimated by Bray Curtis dissimilarity index. WF: Westbury Formation, CM: Cotham Member, LM: Langport Member, PPZ: Pre-Planorbis Zone, PZ: Planorbis Zone, LZ: Liasicus Zone. Overall average dissimilarity between stratigraphic units = 81.15%.

Taxa	WF	CM	LM	PPZ	PZ	LZ
	87.3					
		84.6				
			81			
<i>% Dissimilarity</i>				50		
					54.2	

Appendix 4.6 SIMPER analysis. C: Percentage contribution = average contribution/average dissimilarity between stratigraphic units. AC%: represents the average contribution of the taxon *i* to the average dissimilarity between lithostratigraphy (overall average = 71.40%. See appendix 4.4). Mean abundance of each taxon by stratigraphic units. WF: Westbury Formation, CM: Cotham Member, LM: Langport Member, PPZ: Pre-Planorbis Zone, PZ: Planorbis Zone, LZ: Liasicus Zone, §: Taxa with regional extinction, †: Taxa with global extinction.

Taxon	Contribution	Cumulative %	WF	CM	LM	PPZ	PZ	PZ
<i>Diademopsis tomesi</i>	7.541	9.247	0	0	0	1.72	2.01	1.4
<i>Liostrea hisingeri</i>	7.143	18.01	0.563	0	1.08	2.2	1.69	0.553
<i>Isocrinus psilonoti</i>	5.539	24.8	0	0	0	0.445	1.58	1.18
<i>Modiolus</i> sp.	4.976	30.9	0.698	0.624	0.329	1.17	1.02	0.622
<i>Plagiostoma giganteum</i>	4.651	36.6	0	0	0.297	0.445	1.21	0.84
<i>Modiolus minimus</i>	4.542	42.17	0	0	0	1.95	1.01	0
<i>Chlamys valoniensis</i>	4.501	47.69	1.04	0.475	0	0.67	0.386	0.167
<i>Isocyprina concentricum</i> §	3.9	52.47	1.56	0.354	0	0	0	0
<i>Modiolus ventricosus</i>	3.543	56.82	0	0	0	0	0.386	1.17
<i>Cardinia regularis</i>	3.342	60.91	0.198	0.25	0.329	0.604	0.71	0.167
<i>Permophorus elongatus</i> †	3.043	64.65	1.41	0	0	0	0	0
<i>Placunopsis alpina</i>	2.722	67.98	1.09	0	0	0	0	0
<i>Mytilus cloacinus</i>	2.711	71.31	1.17	0	0	0	0	0
<i>Pteromya langportensis</i>	2.567	74.46	0	0	0.891	0.297	0.348	0
<i>Isocyprina ewaldi</i> §	2.397	77.4	1.21	0	0	0	0	0
<i>Pseudolimea duplicata</i>	2.255	80.16	0	0	0.25	0.297	0.333	0.434
<i>Pholadomya</i> sp.	1.775	82.34	0	0	0.75	0	0.198	0
<i>Modiolus hillanus</i>	1.745	84.48	0	0	0.445	0.78	0	0
<i>Oxytoma inequivalvis</i>	1.235	85.99	0	0	0	0.829	0	0
<i>Rhaetavicula contorta</i> †	1.161	87.41	0.333	0.25	0	0	0	0
<i>Protocardia rhaetica</i> §	0.8938	88.51	0	0.297	0	0	0.167	0
<i>Psilophyllites hagenowi</i>	0.8896	89.6	0	0	0	0	0	0.333
<i>Plagiostoma punctatum</i>	0.8292	90.62	0.386	0	0	0	0	0
<i>Pseudokatosira undulata</i>	0.7591	91.55	0	0	0	0	0.167	0.167
<i>Grammatodon hettangiensis</i>	0.7529	92.47	0	0	0.407	0	0	0
<i>Myoconcha</i> sp.	0.7286	93.37	0	0	0.465	0	0	0
<i>Mytilus</i> sp.	0.6753	94.19	0	0	0	0.391	0	0
<i>Promathilda rhaetica</i> †	0.4384	95.41	0.167	0	0	0	0	0
<i>Astarte</i> sp.	0.4337	95.94	0.198	0	0	0	0	0
<i>Rollieria bronni</i>	0.4124	96.44	0	0	0	0	0.167	0
<i>Psiloceras planorbis</i>	0.4124	96.95	0	0	0	0	0.167	0
<i>Liriomyophoria postera</i> †	0.4069	97.45	0.219	0	0	0	0	0
<i>Bryozoa</i>	0.3922	97.93	0	0	0	0	0.167	0
<i>Pinna</i> sp.	0.3611	98.37	0	0	0	0	0.219	0
<i>Caloceras johnstoni</i>	0.3588	98.81	0	0	0	0	0.198	0
<i>Parellodon</i> sp.	0.3502	99.24	0	0	0	0.25	0	0
<i>Paleonucula navis</i>	0.3097	99.62	0	0	0	0	0.167	0
<i>Isocyprina depressum</i> §	0.3092	100	0.167	0	0	0	0	0

Appendix 4.7 Pairwise comparisons of the faunal composition of each stratigraphic units taken from mudstone samples. The values showed were estimated by Bray Curtis dissimilarity index. WF: Westbury Formation, CM: Cotham Member, LM: Langport Member, PPZ: Pre-Planorbis Zone, PZ: Planorbis Zone, LZ: Liasicus Zone. Overall average dissimilarity between stratigraphic units = 89.81%.

Taxa	WF	LM	PPZ	PZ	LZ
	97.52				
		85.54			
<i>% Dissimilarity</i>			79.56		
				86.55	

Appendix 4.8 SIMPER analysis of mudstone samples. C: Percentage contribution = average contribution/average dissimilarity between stratigraphic units. AC%: represents the average contribution of the taxon *i* to the average dissimilarity between lithostratigraphy (overall average = 81.15%. See appendix 4.4). Mean abundance of each taxon by stratigraphic units. WF: Westbury Formation, LM: Langport Member, PPZ: Pre-Planorbis Zone, PZ: Planorbis Zone, LZ: Liasicus Zone, §: Taxa with regional extinction, †: Taxa with global extinction.

Taxon	Contribution	Cumulative %	WF	LM	PPZ	PZ	LZ
<i>Antiquilima</i> sp.	0.08482	99.83	0	0	0	0.2	0
<i>Asalties laqueus</i>	1.032	90.41	0	0	0	0	1.86
<i>Caloceras johnstoni</i>	4.496	65.53	0	0	0	10.6	0
<i>Camptonectes</i> sp.	0.9997	92.63	0	0	0	0.2	0.714
<i>Cardinia regularis</i>	4.589	60.54	0	0.667	4.33	0	4.14
<i>Cassianella</i> sp.	1.586	80.19	2.67	0	0	0	0
<i>Chlamys valoniensis</i>	0.427	98.33	0.667	0	0.333	0	0
<i>Diademopsis tomesi</i>	12.02	13.34	0.5	0	19	2.6	6.14
<i>Gervillella precursor</i>	0.07229	100	0.333	0	0	0	0
<i>Isocrinus psilonoti</i>	0.4962	97.86	0	0	0.333	0.4	0
<i>Isocyprina concentricum</i> §	2.241	74.02	10.3	0	0	0	0
<i>Isocyprina depressum</i> §	0.2574	99.37	0.667	0	0	0	0
<i>Isocyprina ewaldi</i> §	8.141	31.47	8.67	0	0	0	0
<i>Liostrrea hisingeri</i>	5.834	55.45	0	0.333	9.67	4	0.143
<i>Modiolus hillanus</i>	0.5512	97.31	0	0	0	0.6	0
<i>Modiolus minimus</i>	1.943	78.43	0	0.333	0.667	1.8	0.143
<i>Modiolus sodburiensis</i>	1.371	86.65	4.5	0	0	0	0
<i>Modiolus</i> sp.	8.2	22.44	0.667	4	12.3	1.4	4.71
<i>Modiolus ventricosus</i>	1.003	91.52	0	0	0	0	0.857
<i>Myoconcha</i> sp.	0.07937	99.92	0	0	0	0	0.143
<i>Mytilus cloacinus</i>	0.4109	98.79	0.333	0	0	0	0
<i>Bositra</i> sp.	0.1654	99.55	0	0	0	0	0.143
<i>Palaeoneilo elliptica</i>	1.183	87.97	0	0	0	0	1.29
<i>Paleonucula navis</i>	0.8101	94.43	0	0	0	0	1
<i>Pholadomya</i> sp.	0.2669	99.08	0	0	0.333	0	0.143
<i>Plagiostoma giganteum</i>	1.556	81.92	0.167	0	0	0.2	1.14
<i>Promathilda rhaetica</i> §	1.482	83.56	6.83	0	0	0	0
<i>Protocardia rhaetica</i> §	0.6436	96.7	1.67	0	0	0	0
<i>Pseudomitiloides dubius</i>	2.397	71.53	0	0	0	0.8	1.29
<i>Psiloeas erugatum</i>	3.011	68.87	0	0	5.67	0	0
<i>Psiloceras planorbis</i>	1.17	89.26	0	0	0	1.2	0
<i>Psiloceras sampsoni</i>	0.6693	95.98	0	0	0	0.4	0
<i>Psilophyllites hagenowi</i>	1.417	85.13	0	0	0	0	1.57
<i>Pteromya langportensis</i>	8.12	40.48	0	5	6	4	0
<i>Rhaetavicula contorta</i> †	7.651	48.97	20.5	0	0	0	0
<i>Rollieria bronni</i>	0.8129	93.53	0	0	0	0.2	0.429
<i>Ryderia doris</i>	0.1654	99.74	0	0	0	0	0.143
<i>Scholethemia complanata</i>	0.7263	95.24	0	0	0	0	0.571
<i>Waehnoceras portlocki</i>	2.034	76.27	0	0	0	0	2

Appendix 4.9 SIMPER analysis. AC: represents the average contribution of the taxon *i* to the average dissimilarity between lithology (overall average = 89.35 %). C%: Percentage contribution = average contribution/average dissimilarity between lithologies. Mean abundance of each taxa by lithology.

Taxon	Contribution	Cumulative %	Limestone	Mudstone
<i>Diademopsis tomesi</i>	11.35	12.71	7.6	4.8
<i>Liostraea hisingeri</i>	9.924	23.81	8.33	2.68
<i>Isocyprina ewaldi</i>	5.896	30.41	5.83	2.08
<i>Modiolus</i> sp.	5.715	36.81	2	3.76
<i>Isocyprina concentricum</i>	5.235	42.67	6.47	2.48
<i>Pteromya langportensis</i>	4.478	47.68	0.967	2.12
<i>Isocrinus pylonoti</i>	4.202	52.38	3.03	0.12
<i>Modiolus minimus</i>	3.698	56.52	3.87	0.52
<i>Modiolus ventricosus</i>	3.554	60.5	2.2	0.28
<i>Rhaetavicula contorta</i>	3.548	64.47	0.1	4.92
<i>Plagiostoma giganteum</i>	3.459	68.34	2.43	0.44
<i>Chlamys valoniensis</i>	3.314	72.05	1.9	0.2
<i>Cardinia regularis</i>	2.936	75.34	0.833	1.8
<i>Placunopsis alpina</i>	2.38	78	1.7	0
<i>Caloceras johnstoni</i>	1.994	80.23	0.0667	2.12
<i>Permophorus elongatus</i>	1.614	82.04	3.37	0
<i>Pholadomya</i> sp.	1.186	83.37	0.633	0.08
<i>Pseudomitiloides dubius</i>	1.135	84.64	0	0.52
<i>Psiloceas erugatum</i>	1.083	85.85	0	0.68
<i>Waehnoceras portlocki</i>	0.9429	86.91	0	0.56
<i>Cassianella</i> sp.	0.824	87.83	0.0667	0.64
<i>Psilophyllites hagenowi</i>	0.8078	88.73	0.0667	0.44
<i>Mytilus cloacinus</i>	0.8074	89.64	0.433	0.08
<i>Modiolus hillanus</i>	0.7938	90.52	0.733	0.12
<i>Promathilda rhaetica</i>	0.7273	91.34	0.0333	1.64
<i>Modiolus sodburiensis</i>	0.6212	92.03	0	1.08
<i>Palaeoneilo elliptica</i>	0.5513	92.65	0	0.36
<i>Protocardia rhaetica</i>	0.5506	93.27	0.1	0.4
<i>Psiloceras planorbis</i>	0.5468	93.88	0.0333	0.24
<i>Pseudolimea duplicata</i>	0.5134	94.45	0.367	0
<i>Asalties laqueus</i>	0.496	95.01	0	0.52
<i>Myoconcha</i> sp.	0.4882	95.55	0.4	0.08
<i>Camptonectes</i> sp.	0.4659	96.08	0	0.24
<i>Rollieria bronni</i>	0.4469	96.58	0.0333	0.16
<i>Paleonucula navis</i>	0.4152	97.04	0.0333	0.28
<i>Grammatodon hettangiensis</i>	0.4117	97.5	0.233	0
<i>Mytilus</i> sp.	0.3837	97.93	0.2	0
<i>Scholethemia complanata</i>	0.334	98.3	0	0.16
<i>Psiloceras sampsoni</i>	0.2947	98.63	0	0.08
<i>Oxytoma inequivalvis</i>	0.2028	98.86	0.167	0
<i>Pseudokatosira undulata</i>	0.1567	99.04	0.0667	0
<i>Ryderia doris</i>	0.1471	99.2	0	0.08
<i>Isocyprina depressum</i>	0.1291	99.35	0.0333	0.16
<i>Plagiostoma punctatum</i>	0.1256	99.49	0.133	0
<i>Astarte</i> sp.	0.1052	99.6	0.0667	0
<i>Bositra</i> sp.	0.07625	99.69	0	0.04
<i>Pinna</i> sp.	0.07263	99.77	0.1	0
<i>Briozoa</i>	0.07017	99.85	0.0333	0
<i>Liriomyophoria postera</i>	0.04388	99.9	0.1	0
<i>Antiquilima</i> sp.	0.03661	99.94	0	0.04
<i>Gervillella precursor</i>	0.03344	99.98	0	0.08
<i>Parellodon</i> sp.	0.02052	100	0.0333	0

Appendix 4.10 Modes of life, number of species and relative abundance of each mode of life by stratigraphic unit. WF: Westbury Formation, CM: Cotham Member, LM: Langport Member, PPZ: Pre-Planorbis Zone, PZ: Planorbis Zone, LZ: Liasicus Zone. Modes of Life; T: Tiering, M: Motility level; FM: Feeding Mechanism.

Modes of life			Number of species						Proportional abundance					
T	M	FM	WF	CM	LM	PPZ	PZ	LZ	WF	CM	LM	PPZ	PZ	LZ
1	1	5				1	3	3	0.00	0.00	0.00	0.06	0.12	0.14
2	6	1				1	1	1	0.00	0.00	0.00	0.06	0.04	0.05
3	4	1	6	2	2	4	6	5	0.30	0.33	0.20	0.25	0.24	0.23
3	6	1	1		2	2	2	2	0.05	0.00	0.20	0.13	0.08	0.09
3	2	2					1	1	0.00	0.00	0.00	0.00	0.04	0.05
3	6	3							0.00	0.00	0.00	0.00	0.00	0.00
3	2	4	1			1	1	1	0.05	0.00	0.00	0.06	0.04	0.05
3	2	5	1						0.05	0.00	0.00	0.00	0.00	0.00
4	4	1	4	1	3	5	5	4	0.20	0.17	0.30	0.31	0.20	0.18
4	6	1					1		0.00	0.00	0.00	0.00	0.04	0.00
4	4	2							0.00	0.00	0.00	0.00	0.00	0.00
4	2	3					2	3	0.00	0.00	0.00	0.00	0.08	0.14
5	3	1	7	3	3	2	3	2	0.35	0.50	0.30	0.13	0.12	0.09

Appendix 4.11 Modes of life used by species of each stratigraphy unit. WF: Westbury Formation, CM: Cotham Member, LM: Langport Member, PPZ: Pre-Planorbis Zone, PZ: Planorbis Zone, LZ: Liasicus Zone.

WF	T	M	F
<i>D. tomesi</i>	Surficial	Slow	Grazing
<i>P. rhaetica</i>	Surficial	slow	Predatory
<i>R. contorta</i>	Surficial	Facultative Motile Attached	Suspension
<i>P. alpina</i>	Surficial	Facultative Motile Attached	Suspension
<i>C. valoniensis</i>	Surficial	Facultative Motile Attached	Suspension
<i>Cassianella</i> sp.	Surficial	Facultative Motile Attached	Suspension
<i>M. cloacinus</i>	Surficial	Facultative Motile Attached	Suspension
<i>P. punctatum</i>	Surficial	Facultative Motile Attached	Suspension
<i>L. hisingeri</i>	Surficial	Non-Motile Attached	Suspension
<i>P. elongatus</i>	Semi-faunal	Facultative Motile Attached	Suspension
<i>M. sodburienensis</i>	Semi-faunal	Facultative Motile Attached	Suspension
<i>Modiolus</i> sp.	Semi-faunal	Facultative Motile Attached	Suspension
<i>G. precursor</i>	Semi-faunal	Facultative Motile Attached	Suspension
<i>Astarte</i> sp.	Shallow-infaunal	Facultative Motile Unattached	Suspension
<i>I. concentricum</i>	Shallow-infaunal	Facultative Motile Unattached	Suspension
<i>I. ewaldi</i>	Shallow-infaunal	Facultative Motile Unattached	Suspension
<i>P. rhaetica</i>	Shallow-infaunal	Facultative Motile Unattached	Suspension
<i>I. depressum</i>	Shallow-infaunal	Facultative Motile Unattached	Suspension
<i>L. postera</i>	Shallow-infaunal	Facultative Motile Unattached	Suspension
<i>C. regularis</i>	Shallow-infaunal	Facultative Motile Unattached	Suspension

CM	T	M	F
<i>C. valoniensis</i>	Surficial	Facultative Motile Attached	Suspension
<i>R. contorta</i>	Surficial	Facultative Motile Attached	Suspension
<i>Modiolus</i> sp.	Semi-faunal	Facultative Motile Attached	Suspension
<i>I. concentricum</i>	Shallow-infaunal	Facultative Motile Unattached	Suspension
<i>P. rhaetica</i>	Shallow-infaunal	Facultative Motile Unattached	Suspension
<i>C. regularis</i>	Shallow-infaunal	Facultative Motile Unattached	Suspension

LM	T	M	F
<i>G. hettangiensis</i>	Surficial	Facultative Motile Attached	Suspension
<i>P. giganteum</i>	Surficial	Facultative Motile Attached	Suspension
<i>L. hisingeri</i>	Surficial	Non-Motile Attached	Suspension
<i>P. duplicata</i>	Surficial	Non-Motile Attached	Suspension
<i>Myoconcha</i> sp.	Semi-infaunal	Facultative Motile Attached	Suspension
<i>M. hillanus</i>	Semi-infaunal	Facultative Motile Attached	Suspension
<i>Modiolus</i> sp.	Semi-infaunal	Facultative Motile Attached	Suspension
<i>Pholadomya</i> sp.	Shallow-infaunal	Facultative Motile Unattached	Suspension
<i>P. langportensis</i>	Shallow-infaunal	Facultative Motile Unattached	Suspension
<i>C. regularis</i>	Shallow-infaunal	Facultative Motile Unattached	Suspension

PPZ	T	M	F
<i>P. erugatum</i>	Pelagic	Fast	Predatory
<i>I. psilonoti</i>	Erect	Non-Motile Attached	Suspension
<i>D. tomesi</i>	Surficial	Slow	Grazing
<i>C. valoniensis</i>	Surficial	Facultative Motile Attached	Suspension
<i>P. giganteum</i>	Surficial	Facultative Motile Attached	Suspension
<i>Mytilus</i> sp.	Surficial	Facultative Motile Attached	Suspension
<i>O. inequivalvis</i>	Surficial	Facultative Motile Attached	Suspension
<i>P. duplicata</i>	Surficial	Non-Motile Attached	Suspension
<i>L. hisingeri</i>	Surficial	Non-Motile Attached	Suspension
<i>M. minimus</i>	Semi-faunal	Facultative Motile Attached	Suspension
<i>Modiolus</i> sp.	Semi-faunal	Facultative Motile Attached	Suspension
<i>P. langportensis</i>	Semi-faunal	Facultative Motile Attached	Suspension
<i>M. hillanus</i>	Semi-faunal	Facultative Motile Attached	Suspension
<i>Parrellodon</i> sp.	Semi-faunal	Facultative Motile Attached	Suspension
<i>C. regularis</i>	Shallow-infaunal	Facultative Motile Unattached	Suspension
<i>Pholadomya</i> sp.	Shallow-infaunal	Facultative Motile Unattached	Suspension

PZ	T	M	F
<i>C. johnstoni</i>	Pelagic	Fast	Predatory
<i>P. planorbis</i>	Pelagic	Fast	Predatory
<i>P. sampsoni</i>	Pelagic	Fast	Predatory
<i>I. psilonoti</i>	Erect	Non-Motile Attached	Suspension
<i>P. undulata</i>	Surficial	Slow	Surface deposit
<i>D. tomesi</i>	Surficial	Slow	Grazing
<i>P. giganteum</i>	Surficial	Facultative Motile Attached	Suspension
<i>C. valoniensis</i>	Surficial	Facultative Motile Attached	Suspension
<i>P. dubius</i>	Surficial	Facultative Motile Attached	Suspension
<i>Antiquilima</i> sp.	Surficial	Facultative Motile Attached	Suspension
Bryozoa	Surficial	Facultative Motile Attached	Suspension
<i>Camptonectes</i> sp.	Surficial	Facultative Motile Attached	Suspension
<i>L. hisingeri</i>	Surficial	Non-Motile Attached	Suspension
<i>P. duplicata</i>	Surficial	Non-Motile Attached	Suspension
<i>R. bronni</i>	Semi-infaunal	Slow	Mining
<i>P. navis</i>	Semi-infaunal	Slow	Mining
<i>M. minimus</i>	Semi-infaunal	Facultative Motile Attached	Suspension
<i>P. langportensis</i>	Semi-infaunal	Facultative Motile Attached	Suspension
<i>Modiolus</i> sp.	Semi-infaunal	Facultative Motile Attached	Suspension
<i>M. ventricosus</i>	Semi-infaunal	Facultative Motile Attached	Suspension
<i>M. hillanus</i>	Semi-infaunal	Facultative Motile Attached	Suspension
<i>Pinna</i> sp.	Semi-infaunal	Non-Motile Attached	Suspension
<i>C. regularis</i>	Shallow-infaunal	Facultative Motile Unattached	Suspension
<i>Pholadomya</i> sp.	Shallow-infaunal	Facultative Motile Unattached	Suspension

LZ	T	M	F
<i>W. portlocki</i>	Pelagic	Fast	Predatory
<i>A. laqueus</i>	Pelagic	Fast	Predatory
<i>P. hagenowi</i>	Pelagic	Fast	Predatory
<i>I. pylonoti</i>	Erect	Non-Motile Attached	Suspension
<i>P. undulata</i>	Surficial	Slow	Surface deposit
<i>D. tomesii</i>	Surficial	Slow	Grazing
<i>P. giganteum</i>	Surficial	Facultative Motile Attached	Suspension
<i>P. dubius</i>	Surficial	Facultative Motile Attached	Suspension
<i>Camptonectes</i> sp.	Surficial	Facultative Motile Attached	Suspension
<i>C. valoniensis</i>	Surficial	Facultative Motile Attached	Suspension
<i>Bositra</i> sp.	Surficial	Facultative Motile Attached	Suspension
<i>L. hisingeri</i>	Surficial	Non-Motile Attached	Suspension
<i>P. duplicata</i>	Surficial	Non-Motile Attached	Suspension
<i>P. navis</i>	Semi-infaunal	Slow	Mining
<i>P. elliptica</i>	Semi-infaunal	Slow	Mining
<i>R. bronni</i>	Semi-infaunal	Slow	Mining
<i>Ryderia doris</i>	Semi-infaunal	Slow	Mining
<i>M. ventricosus</i>	Semi-infaunal	Facultative Motile Attached	Suspension
<i>Modiolus</i> sp.	Semi-infaunal	Facultative Motile Attached	Suspension
<i>M. minimus</i>	Semi-infaunal	Facultative Motile Attached	Suspension
<i>Myoconcha</i> sp.	Semi-infaunal	Facultative Motile Attached	Suspension
<i>C. regularis</i>	Shallow-infaunal	Facultative Motile Unattached	Suspension
<i>Pholadomya</i> sp.	Shallow-infaunal	Facultative Motile Unattached	Suspension

Appendix 4.12 Proportion of mode of life. WF: Westbury Formation, CM: Cotham Member, LM: Langport Member, PPZ: Pre-Planorbis Zone, PZ: Planorbis Zone, LZ: Liasicus Zone.

Ecological Categories	Stratigraphy					
	WF	CM	LM	PPZ	PZ	LZ
Pelagic	0.00	0.00	0.00	0.06	0.12	0.14
Erect	0.00	0.00	0.00	0.06	0.04	0.05
Surficial	0.45	0.33	0.40	0.44	0.48	0.55
Semi-infaunal	0.20	0.17	0.30	0.31	0.32	0.32
Shallow-infaunal	0.35	0.50	0.30	0.13	0.12	0.09
Deep-infaunal	0.00	0.00	0.00	0.00	0.00	0.00
Fast	0.00	0.00	0.00	0.06	0.12	0.14
Slow	0.10	0.00	0.00	0.06	0.16	0.23
Facultative, unattached	0.35	0.50	0.30	0.13	0.12	0.09
Facultative, attached	0.50	0.50	0.50	0.56	0.44	0.41
Non-Motile unattached	0.00	0.00	0.00	0.00	0.00	0.00
Non-Motile Attached	0.05	0.00	0.20	0.19	0.16	0.14
Suspension	0.90	1.00	1.00	0.88	0.72	0.64
Surface deposit	0.00	0.00	0.00	0.00	0.04	0.05
Mining	0.00	0.00	0.00	0.00	0.08	0.14
Grazing	0.05	0.00	0.00	0.06	0.04	0.05
Predatory	0.05	0.00	0.00	0.00	0.00	0.00
Other	0.00	0.00	0.00	0.00	0.00	0.00

Appendix 4.13 Geometric mean (mm) by species through the Tr/J section in Audrie's Bay. WF: Westbury Formation, CM: Cotham Member, LM: Langport Member, PPZ: Pre-Planorbis Zone, **SP**: species. IC: *I. concentricum*; PG: *P. giganteum*; CV; *C. valoniensis*; MESO: *Mesomiltha* sp.; MH: *M. hillanus*; G; *Gervillella* sp.; M; *Modiolus* sp.; MM: *M. minimus*; CR: *C. regularis*; PH: *Pholadomya* sp.; PT: *P. langportiensis*; L: *Liostrea*; MY; *Myoconcha* sp.; MC: *M. cardioides*; PD: *P. duplicata*; GRE: *G. obliquata*; CC: *C. calcarea*; CA: *Camponectes* sp.; RB: *R. bronni*.

SP	WF1	SP	WF2	SP	WF3	SP	WF4	SP	WF5	SP	WF6	SP	CM1	SP	CM3	SP	LM1	SP	LM2	SP	LM3	SP	PPZ1	SP	PPZ 2	SP	PPZ3	SP	PPZ4
CV	9.38	CR	15.98	CAS	3.57	IC	7.59	RC	6.26	CAS	2.57	PR	12.35	CV	28.13	M	5.33	PHO	25.52	MYT	16.81	M	28.29	PT	12.44	OXY	38.60	M	9.23
IC	5.78	CV	6.76	CAS	2.63	IC	8.74	RC	4.59	CAS	4.85	PR	7.82	CV	12.88	M	4.83	COS	14.33	L	23.60	LH	8.53	LH	16.30	CR	2.72	CR	22.16
IC	3.87	CV	6.66	IC	7.34	IC	9.34	RC	5.58	CV	13.35	PR	6.72	CV	2.82	M	5.59	CR	15.71	L	19.52	LH	1.98	LH	9.50	PG	33.29	CR	12.49
IC	3.95	CV	4.98	IC	4.46	IC	6.57	RC	3.17	CV	14.54	CR	14.59	M	4.77	M	3.65	CR	24.49	L	23.64	PL	1.46	MM	8.26	PG	27.18	CR	12.72
IC	3.75	CV	1.23	IC	6.76	IC	8.49	PG	24.59	CV	13.26	M	4.95	M	4.40	M	7.89	PHO	18.70	L	14.55	PL	22.65	CR	16.80	CV	14.86	L	21.75
IC	4.55	CV	8.69	IC	7.87	IC	5.75	RC	2.91	CV	14.90	IC	4.32	RC	8.79	M	4.50	PHO	21.68	MYT	14.57	PL	11.40	LH	23.27	CV	1.87	L	15.22
IC	5.34	CV	22.64	IC	6.47	IC	6.26	RC	3.46	CV	9.12	IC	4.12	CV	5.77	M	8.33	PHO	11.58	MH	2.00	CR	1.90	LH	9.34	RD	3.84	MH	6.79
L	1.55	CV	9.26	IC	11.16	IC	9.96	PA	25.58	CV	11.25	IC	5.22	CV	16.83	MM	5.66	PHO	14.49	MH	8.48	LH	13.28	MM	4.79	MM	6.26	MH	8.27
L	13.93	CV	14.84	IC	5.37	IC	8.45	CV	11.94	CV	19.99	IC	1.33	M	5.82	M	4.45	PHO	2.46	MH	18.48	CR	8.73	MM	5.98	CV	8.23	0	0
M	4.33	CV	11.57	IC	27.45	IC	4.87	CV	2.32	CV	16.55	0	0	M	5.76	CR	1.77	CR	14.45	MH	1.42	CR	2.61	LH	14.99	PG	15.60	0	0
M	2.79	CV	7.88	IC	7.12	IC	1.94	CV	26.46	CV	5.43	0	0	CV	31.16	M	4.97	PHO	21.89	MH	13.12	CR	18.83	LH	9.17	PG	44.69	0	0
M	4.56	CV	4.48	IC	6.91	IC	5.85	PA	18.22	CV	8.64	0	0	0	0	CR	9.63	PD	11.75	L	23.76	PT	12.49	LH	5.78	CV	5.45	0	0
MH	12.67	CV	2.93	IC	9.25	IC	6.58	MH	13.24	CV	17.13	0	0	0	0	M	4.25	P	14.18	CR	19.84	PT	14.12	LH	5.25	MM	7.44	0	0
PE	13.53	CV	34.80	IC	7.53	CV	6.12	CV	17.86	IC	1.42	0	0	0	0	PT	1.36	P	29.46	m	16.70	MM	3.79	MM	4.59	PG	15.69	0	0
PE	11.96	IC	1.15	IC	6.82	IC	5.67	CV	23.30	IC	8.48	0	0	0	0	PT	9.60	P	11.92	L	12.37	MM	8.45	LH	16.59	LH	15.65	0	0
PE	9.78	L	11.23	IC	6.65	IC	5.98	L	15.68	IC	1.13	0	0	0	0	PT	6.18	P	24.67	MH	7.63	MYO	2.49	MM	7.31	CV	1.88	0	0
PE	8.24	L	11.38	IC	5.23	IC	8.88	CV	16.29	IC	9.27	0	0	0	0	PT	11.12	P	19.62	L	15.75	LH	14.17	MH	1.50	MM	5.50	0	0
PE	13.42	L	18.33	IC	8.51	RC	1.25	CV	23.34	IC	8.76	0	0	0	0	M	9.53	CR	1.25	M	7.16	MYO	11.57	CR	17.65	CV	14.62	0	0
PE	1.73	M	5.87	IC	7.15	RC	1.68	CV	29.52	IC	7.93	0	0	0	0	M	1.16	P	18.97	L	16.40	LH	19.90	PT	16.42	M	3.69	0	0
PE	8.39	M	9.78	IC	7.84	IC	4.39	CV	18.44	IC	6.91	0	0	0	0	M	5.76	PG	13.92	L	24.13	LH	21.59	PHO	27.92	PT	6.54	0	0
PE	13.65	MCL	7.87	IC	8.29	MYT	7.53	CV	2.39	IC	8.24	0	0	0	0	PT	11.45	P	19.53	CR	12.75	LH	17.29	M	12.60	PT	8.47	0	0
PE	11.45	MM	5.77	IC	9.99	CV	17.28	CV	2.11	IC	8.37	0	0	0	0	L	13.65	PT	8.96	MH	16.32	OXI	9.19	PT	8.96	PT	8.53	0	0
PE	9.79	MYO	17.95	IC	6.68	L	13.78	M	11.22	IC	5.86	0	0	0	0	PT	11.64	PT	11.43	MYT	14.64	LH	13.41	M	6.38	PT	1.54	0	0
PE	1.80	PA	15.57	IE	1.26	CV	16.78	CV	26.42	IC	9.64	0	0	0	0	PT	8.45	P	15.75	L	16.66	LH	12.87	CR	16.97	PT	12.63	0	0
PE	6.48	PA	36.41	IE	7.77	L	16.95	CV	25.20	IC	8.40	0	0	0	0	PT	18.65	P	14.23	L	23.68	MYT	21.45	CR	11.23	PT	8.16	0	0
PE	9.31	PA	1.36	IE	1.41	PG	18.88	CV	12.54	IC	6.79	0	0	0	0	L	13.19	0	0	MH	12.00	PHO	16.28	CR	24.95	PT	8.54	0	0
PE	11.12	PA	7.77	IE	5.94	CV	26.85	CV	18.43	IC	8.34	0	0	0	0	PT	11.78	0	0	L	2.69	LH	18.22	CR	13.93	PT	7.49	0	0
PE	15.15	PA	1.52	M	5.85	IC	8.00	L	8.92	IC	14.31	0	0	0	0	L	13.50	0	0	L	2.32	L	16.86	CR	11.48	PT	6.94	0	0
PE	13.62	PA	12.75	MCL	14.80	CV	1.16	CV	24.84	IC	5.66	0	0	0	0	L	24.23	0	0	MYT	18.97	L	2.15	MM	4.54	0	0	0	0

PE	13.58	PA	26.75	PA	2.47	PA	26.88	PA	3.21	IC	8.21	0	0	0	0	PG	29.33	0	0	L	17.68	PT	1.28	MM	7.30	0	0	0	0
PE	11.67	PA	15.45	PE	9.77	PA	17.16	CV	2.57	IC	8.81	0	0	0	0	PG	23.23	0	0	L	2.74	L	13.87	LH	7.86	0	0	0	0
PE	11.52	PA	28.25	PE	1.26	PG	24.63	CV	23.45	IC	6.27	0	0	0	0	L	17.42	0	0	L	22.83	L	1.11	MM	5.29	0	0	0	0
PE	1.17	PA	16.85	PE	12.31	MH	26.36	PA	25.46	IC	5.49	0	0	0	0	L	11.69	0	0	L	15.57	CR	39.81	LH	19.52	0	0	0	0
PE	9.58	PA	7.52	PR	6.16	PE	19.23	CV	21.68	IC	8.86	0	0	0	0	0	0	0	0	CR	17.32	CR	18.86	MM	8.96	0	0	0	0
PE	14.62	PA	38.69	RC	9.60	PA	35.45	CV	34.29	IC	5.00	0	0	0	0	0	0	0	0	L	21.37	M	13.68	MM	9.88	0	0	0	0
PE	12.76	PA	22.62	0	0	MS	4.37	LH	19.29	IC	9.42	0	0	0	0	0	0	0	0	L	17.77	M	11.74	LH	8.16	0	0	0	0
PE	16.20	PA	36.84	0	0	IC	8.87	CV	16.42	IC	8.27	0	0	0	0	0	0	0	0	MM	7.30	M	1.97	MM	2.96	0	0	0	0
PE	15.38	PA	5.25	0	0	IC	8.15	CV	15.69	IC	9.24	0	0	0	0	0	0	0	0	MM	12.90	M	5.57	MM	6.34	0	0	0	0
PE	8.33	PE	17.37	0	0	IC	8.95	CV	18.98	IC	5.43	0	0	0	0	0	0	0	0	MYT	2.54	L	1.29	LH	7.60	0	0	0	0
PE	8.73	PE	13.37	0	0	IC	9.27	CV	17.23	IC	1.39	0	0	0	0	0	0	0	0	PG	22.83	L	12.77	LH	23.14	0	0	0	0
PE	11.72	PE	2.93	0	0	IC	7.99	CV	22.80	IC	8.94	0	0	0	0	0	0	0	0	L	26.58	L	14.95	LH	19.19	0	0	0	0
PE	11.27	PE	12.72	0	0	IC	8.75	PR	7.19	IC	6.76	0	0	0	0	0	0	0	0	L	16.54	L	13.28	MM	8.60	0	0	0	0
PE	1.68	RC	1.56	0	0	IC	11.46	PG	11.74	IC	8.63	0	0	0	0	0	0	0	0	L	22.57	M	12.26	LH	8.59	0	0	0	0
PE	7.82	0	0	0	0	IC	1.14	MS	5.48	IE	9.54	0	0	0	0	0	0	0	0	L	24.64	M	12.34	MM	7.22	0	0	0	0
PE	1.13	0	0	0	0	IC	8.68	PE	13.82	IE	3.82	0	0	0	0	0	0	0	0	PT	9.87	MM	14.46	OXI	7.60	0	0	0	0
PE	8.76	0	0	0	0	PE	19.76	PE	18.47	IE	9.30	0	0	0	0	0	0	0	0	L	19.69	L	8.30	MM	9.13	0	0	0	0
PE	6.95	0	0	0	0	PE	6.92	PR	14.78	IE	11.79	0	0	0	0	0	0	0	0	0	0	PT	7.47	LH	11.85	0	0	0	0
0	0	0	0	0	0	PE	18.26	PE	8.12	IE	8.38	0	0	0	0	0	0	0	0	0	0	MM	11.62	LH	14.52	0	0	0	0
0	0	0	0	0	0	PE	4.54	M	1.43	IE	4.86	0	0	0	0	0	0	0	0	0	0	MM	11.79	LH	12.75	0	0	0	0
0	0	0	0	0	0	PE	1.19	M	1.52	IE	9.22	0	0	0	0	0	0	0	0	0	0	MM	4.26	LH	11.53	0	0	0	0
0	0	0	0	0	0	IC	9.77	M	12.93	IE	4.79	0	0	0	0	0	0	0	0	0	0	MM	12.82	LH	2.24	0	0	0	0
0	0	0	0	0	0	IC	8.35	MS	6.22	L	17.59	0	0	0	0	0	0	0	0	0	0	PT	14.25	LH	13.65	0	0	0	0
0	0	0	0	0	0	IC	12.18	MS	6.71	L	17.22	0	0	0	0	0	0	0	0	0	0	PT	15.52	LH	18.82	0	0	0	0
0	0	0	0	0	0	CR	9.32	PR	6.92	M	11.89	0	0	0	0	0	0	0	0	0	0	L	13.26	LH	14.50	0	0	0	0
0	0	0	0	0	0	IC	5.37	PR	11.69	M	12.52	0	0	0	0	0	0	0	0	0	0	L	15.94	LH	19.82	0	0	0	0
0	0	0	0	0	0	CR	7.87	PR	13.84	M	13.31	0	0	0	0	0	0	0	0	0	0	L	11.79	LH	18.74	0	0	0	0
0	0	0	0	0	0	PE	13.14	M	5.93	M	1.64	0	0	0	0	0	0	0	0	0	0	0	0	MM	7.73	0	0	0	0
0	0	0	0	0	0	PE	26.73	PE	11.25	MC	6.18	0	0	0	0	0	0	0	0	0	0	0	0	LH	13.54	0	0	0	0
0	0	0	0	0	0	PE	4.25	PR	14.98	MCL	1.58	0	0	0	0	0	0	0	0	0	0	0	0	MM	7.14	0	0	0	0
0	0	0	0	0	0	PE	5.23	MH	3.31	MCL	7.22	0	0	0	0	0	0	0	0	0	0	0	0	LH	11.76	0	0	0	0
0	0	0	0	0	0	MS	8.71	MH	5.87	MCL	6.18	0	0	0	0	0	0	0	0	0	0	0	0	MM	6.67	0	0	0	0
0	0	0	0	0	0	IC	5.77	MH	7.96	MCL	11.56	0	0	0	0	0	0	0	0	0	0	0	0	LH	11.54	0	0	0	0
0	0	0	0	0	0	IC	36.91	PG	3.73	MH	7.15	0	0	0	0	0	0	0	0	0	0	0	0	LH	6.77	0	0	0	0
0	0	0	0	0	0	IC	6.83	L	15.74	MS	16.86	0	0	0	0	0	0	0	0	0	0	0	0	LH	29.54	0	0	0	0
0	0	0	0	0	0	PE	13.54	L	28.24	MS	5.86	0	0	0	0	0	0	0	0	0	0	0	0	MM	8.38	0	0	0	0
0	0	0	0	0	0	CR	12.11	L	25.95	MS	1.95	0	0	0	0	0	0	0	0	0	0	0	0	MM	8.61	0	0	0	0
0	0	0	0	0	0	IC	8.75	PG	13.67	MS	13.99	0	0	0	0	0	0	0	0	0	0	0	0	MM	6.92	0	0	0	0

0	0	0	0	0	0	MY	11.74	PA	29.39	MS	7.95	0	0	0	0	0	0	0	0	0	0	0	0	MYO	8.90	0	0	0	0
0	0	0	0	0	0	0	0	PG	23.36	MS	8.84	0	0	0	0	0	0	0	0	0	0	0	0	LH	21.12	0	0	0	0
0	0	0	0	0	0	0	0	L	31.39	MS	8.73	0	0	0	0	0	0	0	0	0	0	0	0	LH	13.58	0	0	0	0
0	0	0	0	0	0	0	0	0	0	MS	8.13	0	0	0	0	0	0	0	0	0	0	0	0	LH	15.87	0	0	0	0
0	0	0	0	0	0	0	0	0	0	MS	9.24	0	0	0	0	0	0	0	0	0	0	0	0	MYO	8.56	0	0	0	0
0	0	0	0	0	0	0	0	0	0	MS	7.75	0	0	0	0	0	0	0	0	0	0	0	0	MM	7.28	0	0	0	0
0	0	0	0	0	0	0	0	0	0	MS	11.83	0	0	0	0	0	0	0	0	0	0	0	0	MYO	4.45	0	0	0	0
0	0	0	0	0	0	0	0	0	0	MS	4.32	0	0	0	0	0	0	0	0	0	0	0	0	MYO	8.26	0	0	0	0
0	0	0	0	0	0	0	0	0	0	MS	6.18	0	0	0	0	0	0	0	0	0	0	0	0	M	11.73	0	0	0	0
0	0	0	0	0	0	0	0	0	0	MS	7.42	0	0	0	0	0	0	0	0	0	0	0	0	M	6.39	0	0	0	0
0	0	0	0	0	0	0	0	0	0	MS	6.98	0	0	0	0	0	0	0	0	0	0	0	0	MYO	1.21	0	0	0	0
0	0	0	0	0	0	0	0	0	0	MS	4.88	0	0	0	0	0	0	0	0	0	0	0	0	LH	1.75	0	0	0	0
0	0	0	0	0	0	0	0	0	0	PA	31.75	0	0	0	0	0	0	0	0	0	0	0	0	MM	6.43	0	0	0	0
0	0	0	0	0	0	0	0	0	0	PA	17.85	0	0	0	0	0	0	0	0	0	0	0	0	M	7.61	0	0	0	0
0	0	0	0	0	0	0	0	0	0	PC	9.36	0	0	0	0	0	0	0	0	0	0	0	0	M	7.91	0	0	0	0
0	0	0	0	0	0	0	0	0	0	PC	11.13	0	0	0	0	0	0	0	0	0	0	0	0	MM	5.73	0	0	0	0
0	0	0	0	0	0	0	0	0	0	PE	7.75	0	0	0	0	0	0	0	0	0	0	0	0	MM	5.15	0	0	0	0
0	0	0	0	0	0	0	0	0	0	PE	12.70	0	0	0	0	0	0	0	0	0	0	0	0	L	18.54	0	0	0	0
0	0	0	0	0	0	0	0	0	0	PE	11.52	0	0	0	0	0	0	0	0	0	0	0	0	L	13.27	0	0	0	0
0	0	0	0	0	0	0	0	0	0	PE	7.85	0	0	0	0	0	0	0	0	0	0	0	0	L	14.26	0	0	0	0
0	0	0	0	0	0	0	0	0	0	PE	12.75	0	0	0	0	0	0	0	0	0	0	0	0	L	17.14	0	0	0	0
0	0	0	0	0	0	0	0	0	0	PE	9.86	0	0	0	0	0	0	0	0	0	0	0	0	L	14.58	0	0	0	0
0	0	0	0	0	0	0	0	0	0	PE	11.58	0	0	0	0	0	0	0	0	0	0	0	0	L	11.26	0	0	0	0
0	0	0	0	0	0	0	0	0	0	PE	16.36	0	0	0	0	0	0	0	0	0	0	0	0	M	9.26	0	0	0	0
0	0	0	0	0	0	0	0	0	0	PE	13.90	0	0	0	0	0	0	0	0	0	0	0	0	L	8.92	0	0	0	0
0	0	0	0	0	0	0	0	0	0	PE	13.72	0	0	0	0	0	0	0	0	0	0	0	0	L	1.54	0	0	0	0
0	0	0	0	0	0	0	0	0	0	PE	15.43	0	0	0	0	0	0	0	0	0	0	0	0	L	1.68	0	0	0	0
0	0	0	0	0	0	0	0	0	0	PE	7.64	0	0	0	0	0	0	0	0	0	0	0	0	L	12.97	0	0	0	0
0	0	0	0	0	0	0	0	0	0	PE	15.36	0	0	0	0	0	0	0	0	0	0	0	0	CR	2.53	0	0	0	0
0	0	0	0	0	0	0	0	0	0	PE	11.58	0	0	0	0	0	0	0	0	0	0	0	0	CR	19.95	0	0	0	0
0	0	0	0	0	0	0	0	0	0	PE	12.46	0	0	0	0	0	0	0	0	0	0	0	0	MYT	2.23	0	0	0	0
0	0	0	0	0	0	0	0	0	0	PG	21.73	0	0	0	0	0	0	0	0	0	0	0	0	OXY	4.87	0	0	0	0
0	0	0	0	0	0	0	0	0	0	PR	17.47	0	0	0	0	0	0	0	0	0	0	0	0	PHO	26.73	0	0	0	0
0	0	0	0	0	0	0	0	0	0	PR	11.57	0	0	0	0	0	0	0	0	0	0	0	0	MH	17.16	0	0	0	0
0	0	0	0	0	0	0	0	0	0	RC	1.14	0	0	0	0	0	0	0	0	0	0	0	0	MH	16.84	0	0	0	0
0	0	0	0	0	0	0	0	0	0	RC	4.32	0	0	0	0	0	0	0	0	0	0	0	0	L	21.47	0	0	0	0
0	0	0	0	0	0	0	0	0	0	RC	11.32	0	0	0	0	0	0	0	0	0	0	0	0	MYT	2.47	0	0	0	0
0	0	0	0	0	0	0	0	0	0	RC	9.18	0	0	0	0	0	0	0	0	0	0	0	0	LH	12.11	0	0	0	0

0	0	0	0	0	0	0	0	0	0	RC	4.88	0	0	0	0	0	0	0	0	0	0	0	0	LH	8.22	0	0	0	0
0	0	0	0	0	0	0	0	0	0	RC	8.83	0	0	0	0	0	0	0	0	0	0	0	0	PHO	14.62	0	0	0	0
0	0	0	0	0	0	0	0	0	0	RC	11.38	0	0	0	0	0	0	0	0	0	0	0	0	PHO	23.52	0	0	0	0
0	0	0	0	0	0	0	0	0	0	RC	1.86	0	0	0	0	0	0	0	0	0	0	0	0	CR	24.13	0	0	0	0
0	0	0	0	0	0	0	0	0	0	RC	7.85	0	0	0	0	0	0	0	0	0	0	0	0	MH	15.71	0	0	0	0
0	0	0	0	0	0	0	0	0	0	RC	7.49	0	0	0	0	0	0	0	0	0	0	0	0	GER	16.47	0	0	0	0
0	0	0	0	0	0	0	0	0	0	RC	8.22	0	0	0	0	0	0	0	0	0	0	0	0	GER	21.96	0	0	0	0
0	0	0	0	0	0	0	0	0	0	RC	6.41	0	0	0	0	0	0	0	0	0	0	0	0	CR	18.21	0	0	0	0
0	0	0	0	0	0	0	0	0	0	RC	8.36	0	0	0	0	0	0	0	0	0	0	0	0	GER	16.29	0	0	0	0
0	0	0	0	0	0	0	0	0	0	RC	6.68	0	0	0	0	0	0	0	0	0	0	0	0	L	11.76	0	0	0	0
0	0	0	0	0	0	0	0	0	0	RC	6.39	0	0	0	0	0	0	0	0	0	0	0	0	L	2.53	0	0	0	0
0	0	0	0	0	0	0	0	0	0	RC	4.45	0	0	0	0	0	0	0	0	0	0	0	0	CR	2.16	0	0	0	0
0	0	0	0	0	0	0	0	0	0	RC	18.14	0	0	0	0	0	0	0	0	0	0	0	0	CR	2.31	0	0	0	0
0	0	0	0	0	0	0	0	0	0	RC	9.94	0	0	0	0	0	0	0	0	0	0	0	0	PHO	31.96	0	0	0	0
0	0	0	0	0	0	0	0	0	0	RC	4.50	0	0	0	0	0	0	0	0	0	0	0	0	L	14.72	0	0	0	0
0	0	0	0	0	0	0	0	0	0	RC	7.41	0	0	0	0	0	0	0	0	0	0	0	0	L	13.83	0	0	0	0
0	0	0	0	0	0	0	0	0	0	RC	6.76	0	0	0	0	0	0	0	0	0	0	0	0	GER	2.27	0	0	0	0
0	0	0	0	0	0	0	0	0	0	RC	6.90	0	0	0	0	0	0	0	0	0	0	0	0	MH	14.79	0	0	0	0
0	0	0	0	0	0	0	0	0	0	RC	5.84	0	0	0	0	0	0	0	0	0	0	0	0	CR	16.15	0	0	0	0
0	0	0	0	0	0	0	0	0	0	RC	6.15	0	0	0	0	0	0	0	0	0	0	0	0	CR	19.93	0	0	0	0
0	0	0	0	0	0	0	0	0	0	RC	9.34	0	0	0	0	0	0	0	0	0	0	0	0	CR	16.20	0	0	0	0
0	0	0	0	0	0	0	0	0	0	RC	7.76	0	0	0	0	0	0	0	0	0	0	0	0	GER	19.37	0	0	0	0
0	0	0	0	0	0	0	0	0	0	0	0	0	0	0	0	0	0	0	0	0	0	0	0	CR	2.78	0	0	0	0
0	0	0	0	0	0	0	0	0	0	0	0	0	0	0	0	0	0	0	0	0	0	0	0	MH	18.96	0	0	0	0
0	0	0	0	0	0	0	0	0	0	0	0	0	0	0	0	0	0	0	0	0	0	0	0	PHO	24.35	0	0	0	0
0	0	0	0	0	0	0	0	0	0	0	0	0	0	0	0	0	0	0	0	0	0	0	0	PHO	23.48	0	0	0	0

Appendix 4.13 (Continuation) Geometric mean (mm) by species through the Tr/J section in Audrie's Bay. PZ: Planorbis Zone, LZ: Liasicus Zone; SP: species. IC: *I. concentricum*; PG: *P. giganteum*; CV; *C. valoniensis*; MESO: *Mesomiltha* sp.; MH: *M. hillanus*; G; *Gervillella* sp.; M; *Modiolus* sp.; MM: *M. minimus*; CR: *C. regularis*; PH: *Pholadomya* sp.; PT: *P. langportiensis*; L: *Liostrea*; MY; *Myoconcha* sp.; MC: *M. cardioides*; PD: *P. duplicata*; GRE: *G. obliquata*; CC: *C. calcarea*; CA: *Camponectes* sp.; RB: *R. bronni*.

SP	PZ1	SP	PZ2	SP	PZ3	SP	PZ4	SP	PZ5	SP	PZ6	SP	LZ1	SP	LZ2	SP	LZ3	SP	LZ4	SP	LZ5	SP	LZ6	SP	AZ1
L	12.68	L	7.26	M	5.47	PT	8.54	L	37.16	MV	6.47	PG	7.47	MV	3.72	PE	6.92	L	12.24	CR	43.47	MV	3.42	MYT	19.54
L	9.96	PG	17.95	M	11.27	RB	2.64	L	19.26	PG	17.45	L	2.23	MV	4.71	PA	9.17	MV	8.52	CR	11.94	MV	6.27	L	15.85
L	15.79	PG	26.58	L	6.52	M	5.22	MM	4.96	PNA	2.45	L	13.45	MV	2.97	MS	7.39	0	0	M	8.93	CA	7.89	L	16.18
L	11.84	PG	33.93	L	14.56	LH	14.73	PG	52.46	PH	14.22	PG	63.54	MV	8.28	PE	5.17	0	0	CV	1.70	CR	14.26	MV	6.73
L	1.76	CR	1.90	L	1.46	0	0	L	18.34	MV	3.52	M	14.82	PE	2.93	CO	6.45	0	0	CA	6.67	PE	3.86	MV	6.32
L	9.92	PG	8.19	L	2.23	0	0	PG	19.40	P	8.39	PG	51.46	MV	2.24	MS	4.55	0	0	CA	12.00	PE	4.78	CR	16.29
L	6.89	CV	18.49	M	6.65	0	0	CR	21.55	CR	19.58	PG	33.24	PH	11.57	PE	3.67	0	0	CA	9.27	CR	13.44	CR	18.25
L	18.29	L	7.65	PD	6.24	0	0	L	2.77	CR	7.19	M	1.22	PH	18.54	0	0	0	0	MS	3.15	CR	11.72	MYO	15.36
MM	1.78	L	9.48	M	4.35	0	0	CR	69.76	CA	9.85	PG	29.50	PH	4.92	0	0	0	0	CA	13.32	MV	5.39	CR	15.42
MM	6.43	L	13.13	CR	6.12	0	0	PG	21.57	CR	5.93	CR	11.94	PE	4.93	0	0	0	0	MS	6.59	CR	14.32	CR	24.92
MM	8.50	L	13.25	CR	4.19	0	0	PG	1.63	MM	5.96	PG	33.88	PE	5.51	0	0	0	0	0	0	MV	2.00	CR	19.69
LH	22.35	CR	13.36	M	3.17	0	0	L	29.39	CR	6.20	PG	32.25	MV	2.28	0	0	0	0	0	0	CR	13.97	MYO	34.93
MM	14.53	L	13.73	LH	6.98	0	0	L	35.72	M	8.53	RD	31.99	MV	7.14	0	0	0	0	0	0	CR	12.32	MYO	19.76
LH	19.92	PT	7.82	0	0	0	0	L	28.52	0	0	RD	22.22	MV	7.81	0	0	0	0	0	0	CR	23.88	MYO	14.77
MM	6.23	PT	8.13	0	0	0	0	L	2.39	0	0	L	11.23	PE	3.22	0	0	0	0	0	0	CV	14.43	CR	17.58
MM	7.47	PT	1.35	0	0	0	0	CR	23.38	0	0	M	4.40	PE	5.39	0	0	0	0	0	0	MV	15.96	L	13.14
M	5.83	CV	16.90	0	0	0	0	CR	42.15	0	0	PG	37.12	MV	2.28	0	0	0	0	0	0	MV	14.59	MV	6.45
MM	5.21	PG	22.27	0	0	0	0	CV	26.40	0	0	M	9.49	MV	1.97	0	0	0	0	0	0	MV	14.47	L	15.63
L	1.59	PG	32.96	0	0	0	0	CR	16.22	0	0	CR	14.83	PG	73.83	0	0	0	0	0	0	0	0	L	12.83
L	24.63	MM	17.56	0	0	0	0	L	12.74	0	0	CR	24.29	0	0	0	0	0	0	0	0	0	0	L	17.83
MM	13.39	L	18.15	0	0	0	0	L	11.36	0	0	PG	25.72	0	0	0	0	0	0	0	0	0	0	L	8.97
L	6.26	L	11.56	0	0	0	0	PN	15.82	0	0	L	19.85	0	0	0	0	0	0	0	0	0	0	L	18.94
LH	1.85	L	11.24	0	0	0	0	PN	23.11	0	0	M	1.62	0	0	0	0	0	0	0	0	0	0	CR	19.65
MM	6.76	L	15.79	0	0	0	0	PN	20.00	0	0	PD	6.52	0	0	0	0	0	0	0	0	0	0	MYO	17.18
L	4.23	L	1.93	0	0	0	0	PN	15.19	0	0	MC	28.25	0	0	0	0	0	0	0	0	0	0	L	12.32
MM	1.25	L	9.96	0	0	0	0	PG	47.65	0	0	MC	17.72	0	0	0	0	0	0	0	0	0	0	MYO	28.95
MH	7.69	L	11.86	0	0	0	0	L	12.93	0	0	PD	6.60	0	0	0	0	0	0	0	0	0	0	L	14.59
MM	6.97	L	15.57	0	0	0	0	L	2.47	0	0	PD	6.44	0	0	0	0	0	0	0	0	0	0	CR	15.78
L	9.54	CV	8.74	0	0	0	0	MM	14.42	0	0	PD	4.23	0	0	0	0	0	0	0	0	0	0	M	9.77
PL	8.33	PG	37.64	0	0	0	0	L	25.13	0	0	0	0	0	0	0	0	0	0	0	0	0	0	MYO	13.98
L	17.95	PT	8.16	0	0	0	0	MM	1.61	0	0	0	0	0	0	0	0	0	0	0	0	0	0	L	16.79

0	0	PT	9.44	0	0	0	0	PT	2.35	0	0	0	0	0	0	0	0	0	0	0	0	0	0	L	14.99
0	0	PT	9.12	0	0	0	0	L	17.27	0	0	0	0	0	0	0	0	0	0	0	0	0	0	0	0
0	0	PT	6.97	0	0	0	0	CV	2.79	0	0	0	0	0	0	0	0	0	0	0	0	0	0	0	0
0	0	CR	2.98	0	0	0	0	0	0	0	0	0	0	0	0	0	0	0	0	0	0	0	0	0	0
0	0	CR	19.49	0	0	0	0	0	0	0	0	0	0	0	0	0	0	0	0	0	0	0	0	0	0
0	0	CR	17.60	0	0	0	0	0	0	0	0	0	0	0	0	0	0	0	0	0	0	0	0	0	0
0	0	MM	5.12	0	0	0	0	0	0	0	0	0	0	0	0	0	0	0	0	0	0	0	0	0	0
0	0	CR	16.99	0	0	0	0	0	0	0	0	0	0	0	0	0	0	0	0	0	0	0	0	0	0
0	0	CR	18.44	0	0	0	0	0	0	0	0	0	0	0	0	0	0	0	0	0	0	0	0	0	0
0	0	MM	13.00	0	0	0	0	0	0	0	0	0	0	0	0	0	0	0	0	0	0	0	0	0	0
0	0	MM	8.23	0	0	0	0	0	0	0	0	0	0	0	0	0	0	0	0	0	0	0	0	0	0
0	0	CR	21.71	0	0	0	0	0	0	0	0	0	0	0	0	0	0	0	0	0	0	0	0	0	0
0	0	CR	15.19	0	0	0	0	0	0	0	0	0	0	0	0	0	0	0	0	0	0	0	0	0	0
0	0	MM	4.77	0	0	0	0	0	0	0	0	0	0	0	0	0	0	0	0	0	0	0	0	0	0
0	0	MM	1.48	0	0	0	0	0	0	0	0	0	0	0	0	0	0	0	0	0	0	0	0	0	0
0	0	CR	13.79	0	0	0	0	0	0	0	0	0	0	0	0	0	0	0	0	0	0	0	0	0	0
0	0	CR	11.11	0	0	0	0	0	0	0	0	0	0	0	0	0	0	0	0	0	0	0	0	0	0
0	0	CR	9.78	0	0	0	0	0	0	0	0	0	0	0	0	0	0	0	0	0	0	0	0	0	0
0	0	CR	17.80	0	0	0	0	0	0	0	0	0	0	0	0	0	0	0	0	0	0	0	0	0	0
0	0	CR	15.19	0	0	0	0	0	0	0	0	0	0	0	0	0	0	0	0	0	0	0	0	0	0
0	0	MM	8.13	0	0	0	0	0	0	0	0	0	0	0	0	0	0	0	0	0	0	0	0	0	0

Appendix 4.14 Data used to build the frequency distribution and Jablonski plot target.
 LM: Langport Member, PPZ: Pre-Planorbis Zone, PZ: Planorbis zone, LZ: Liasicus zone.
 Average values **in bold**.

<i>Modiolus</i>						<i>Cardinia</i>					<i>Chlamys</i>				
WF	CM	LM	PPZ	PZ	LZ	WF	LM	PPZ	PZ	LZ	WF	CM	PPZ	PZ	LZ
4.33	4.10	5.33	28.29	5.80	14.82	15.98	10.77	10.90	6.12	11.94	9.38	28.13	14.85	18.49	10.70
2.79	4.77	4.83	13.61	5.47	10.22	9.30	9.06	8.70	4.11	14.83	6.76	12.88	10.86	16.90	14.43
4.56	4.40	5.51	11.74	11.27	4.31	7.87	15.71	20.06	10.90	24.29	6.66	20.82	8.23	8.74	
5.87	5.82	3.65	10.91	6.60	9.05	12.11	24.49	18.83	13.36	16.00	4.98	5.77	5.45	26.04	
9.78	5.76	7.89	5.57	4.35	1.62		14.45	39.81	20.98	18.25	10.23	16.83	10.88	20.79	
5.85		4.00	12.26	3.17	9.08		10.25	18.86	19.49	15.42	8.69	31.16	14.62		
11.22		8.33	12.34	5.02	8.93		19.84	16.70	17.60	24.92	22.64				
10.43		4.45	12.51	8.53	7.39		12.75	17.65	16.99	19.69	9.26				
10.51		4.96	6.38	7.69	4.50		17.32	16.97	18.40	17.58	14.84				
12.93		4.21	11.73	10.78	3.15			11.02	21.71	19.65	11.57				
5.93		9.53	6.39	6.00	6.01			24.95	15.19	15.70	7.80				
11.88		10.11	7.61	8.50	6.73			13.93	13.79	43.00	40.48				
12.52		5.76	7.91	14.53	6.32			11.48	11.11	11.94	20.93				
13.31		16.61	9.26	6.23	6.45			20.53	9.78	14.03	34.79				
10.64		7.16	3.68	7.47	3.72			19.91	17.80	13.40	6.12				
12.67		10.10	9.23	5.20	4.71			24.13	15.19	11.72	17.28				
26.36		8.48	10.49	13.39	2.96			18.21	19.58	14.32	16.71				
13.20		18.48	17.16	6.76	8.28			20.16	7.19	13.97	26.85				
3.31		10.41	16.84	10.25	2.24			20.03	5.93	12.32	10.16				
5.87		13.00	15.71	6.97	2.28			16.15	6.20	23.88	11.94				
7.96		7.63	14.08	17.56	7.10			19.09	21.55		20.32				
7.15		16.32	18.96	5.10	7.81			16.20	609.76		26.46				
5.77		11.99	6.79	13.00	2.28			20.78	23.38		17.86				
4.04		5.07	8.27	8.20	1.97			20.07	42.01		23.29				
8.70		7.30	3.79	4.77	8.52			22.16	16.22		16.29				
5.48		12.81	8.45	10.48	3.42			12.49			23.34				
6.22			14.46	8.13	6.27			12.72			29.05				
6.71			11.62	5.96	5.39		11.32	14.96	18.24	39.37	17.84	18.44			
16.86			11.79	4.91	11.00						20.39				
5.86			4.21	14.42	15.96						20.11				
10.95			12.82	10.61	14.06						26.42				
13.99			8.26	6.47	14.47						25.20				
7.94			4.79	3.52							12.54				
8.84			5.01								18.40				
8.72			4.59								24.84				
8.13			7.00								20.57				
9.02			4.53								23.45				
7.75			7.29								21.68				
11.83			5.29								34.29				
4.32			8.96								16.42				
6.18			9.88								15.69				
7.04			2.95								18.98				
6.97			6.30								17.23				
4.87			8.60								22.08				
			7.22								13.30				
			9.13								14.54				
			7.70								13.26				
			7.14								14.09				
			6.67								9.12				
			8.38								11.25				
			8.61								19.99				
			6.92								16.06				
			7.21								5.43				
			6.43								8.64				
			5.70								17.13				
			5.15								17.35	19.27	10.81	18.19	12.56
			6.25												
			7.44												
			5.50												
8.76	4.97	8.61	9.05	8.09	6.91										

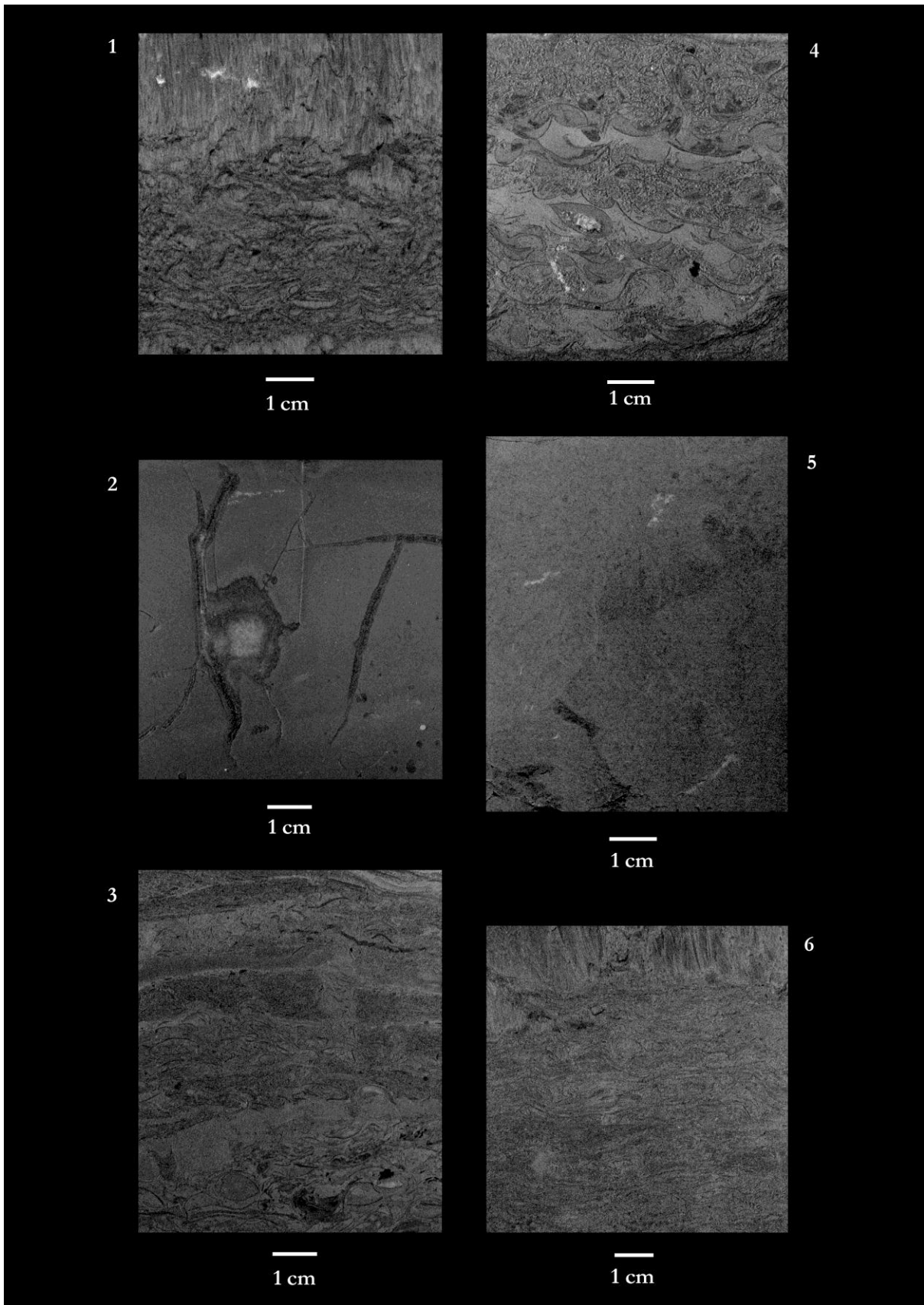
Appendix 4.14 (*Continuation*) Data used to build the frequency distribution and Jablonski plot target. LM: Langport Member, PPZ: Pre-Planorbis Zone, PZ: Planorbis zone, LZ: Liasicus zone. Average values **in bold**.

<i>Liostrrea</i>					<i>Mytilus</i>			<i>Plagiostoma</i>				
WF	LM	PPZ	PZ	LZ	WF	LM	PPZ	WF	LM	PPZ	PZ	LZ
10.55	13.07	16.86	12.68	20.20	6.18	16.81	21.45	18.88	29.32	33.29	17.95	70.05
13.92	13.19	20.14	9.96	13.45	7.87	14.57	20.20	24.63	23.23	27.18	26.58	63.54
11.20	13.50	13.87	15.79	11.23	14.80	14.64	20.47	24.59	13.92	15.60	33.90	51.45
11.38	24.23	10.11	11.84	19.85	10.58	18.97		11.74	22.83	44.69	8.19	33.02
18.33	17.42	10.03	10.76	15.85	7.22	20.54		30.73		15.69	22.27	29.50
13.78	11.69	12.77	9.92	16.18	6.18			13.67			32.96	33.88
16.95	23.60	14.95	6.89	13.13	11.56			23.36			37.60	32.25
15.68	19.50	13.03	18.21	15.63	11.74			21.73			17.45	37.10
8.92	23.64	8.30	10.59	12.80	7.53						52.46	25.72
15.74	14.55	13.26	24.63	17.83	9.29	17.11	20.71				19.31	73.82
28.24	23.08	15.94	6.26	8.97							21.57	
25.10	12.37	11.79	4.23	18.94							10.63	
31.38	15.07	18.54	9.54	12.30							47.65	
17.59	16.40	13.27	17.95	14.51				21.16	22.32	27.29	26.81	45.03
17.22	24.13	14.26	6.52	16.71								
19.29	16.66	17.14	14.55	14.99								
	23.68	14.58	10.46	12.02								
	20.69	11.26	20.23									
	20.30	8.92	7.03									
	17.68	10.54	7.65									
	20.74	10.68	9.48									
	22.83	12.97	13.13									
	15.57	21.47	13.25									
	21.31	11.76	13.73									
	17.77	20.52	18.15									
	26.58	14.72	11.56									
	16.54	13.83	11.24									
	22.06	21.75	15.79									
	24.64	15.22	10.93									
	19.69	8.53	9.96									
		10.98	11.86									
		13.28	15.57									
		14.16	37.15									
		19.81	19.26									
		21.06	18.30									
		17.02	20.77									
		13.40	29.39									
		12.87	35.72									
		18.22	28.51									
		16.30	20.39									
		9.50	12.74									
		23.27	11.36									
		9.34	12.93									
		14.99	20.47									
		9.17	25.13									
		5.78	17.27									
		5.02	22.04									
		16.51	19.92									
		7.09	10.85									
		19.52	6.98									
		8.16	14.73									
		7.51										
		23.14										
		19.19										
		8.59										
		11.85										
17.21	19.07	14.17	15.18	14.98								

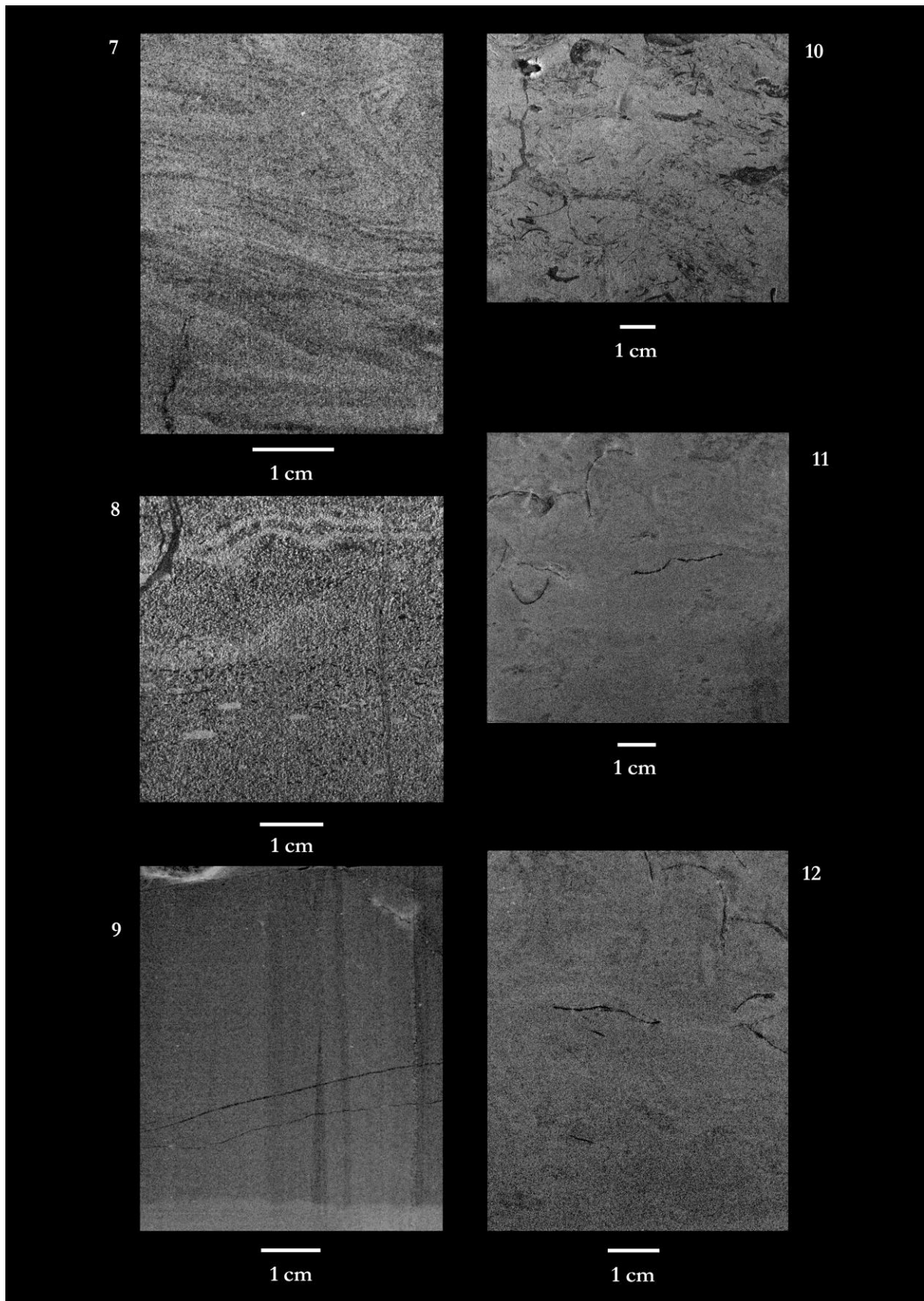
Appendix 4.15 Matrix used to generate null model.

S	WF1	WF2	WF3	WF4	WF5	WF6	CM1	CM3	LM1	LM2	LM3	PPZ1	PPZ 2	PPZ3	PPZ4	PZ1	PZ2	PZ3	PZ4	PZ5	PZ6	LZ1	LZ2	LZ3	LZ4	LZ5	LZ6	AZ1
H	1.9	2.9	4.9	6.8	9	10.2	11	12	12.9	13.3	14	15.8	17.2	18.4	19.6	20.3	21.2	23.7	25	25.9	27.6	32	35.5	40.9	46	51.3	58	61
1	9.38	15.98	3.51	7.59	6.26	31.70	12.35	28.13	5.33	25.52	16.81	28.29	12.44	38.60	9.23	12.68	7.03	5.47	8.54	37.15	6.47	70.05	3.72	6.92	12.02	43.00	3.42	19.05
2	5.78	6.76	2.63	8.07	4.59	10.42	7.82	12.88	4.83	14.33	23.60	8.53	16.30	20.07	22.16	9.96	17.95	11.27	20.64	19.26	17.45	20.20	4.71	9.16	8.52	11.94	6.27	15.85
3	3.87	6.66	7.34	9.34	5.58	11.88	6.72	20.82	5.51	15.71	19.50	10.98	9.50	33.29	12.49	15.79	26.58	6.52	5.02	4.91	2.45	13.45	2.96	7.39	0.00	8.93	7.01	16.18
4	3.95	4.98	4.46	6.57	3.17	16.86	14.59	4.77	3.65	24.49	23.64	10.46	8.26	27.18	12.72	11.84	33.90	14.55	14.73	52.46	14.20	63.54	8.28	5.17	0.00	10.70	14.03	6.73
5	3.75	10.23	6.07	8.49	24.59	8.41	4.10	4.40	7.89	18.70	14.55	22.65	16.70	14.85	21.75	10.76	10.90	10.46	0.00	18.30	3.52	14.82	2.93	6.45	0.00	6.67	3.86	6.32
6	4.55	8.69	7.87	5.75	2.91	12.52	4.32	8.08	4.00	21.68	14.57	11.31	23.27	10.86	15.22	9.92	8.19	20.23	0.00	19.31	8.04	51.45	2.24	4.50	0.00	11.91	4.78	16.00
7	5.34	22.64	6.47	6.26	3.46	13.30	4.12	5.77	8.33	11.58	10.10	10.90	9.34	3.84	6.79	6.89	18.49	6.60	0.00	21.55	19.58	33.02	11.57	3.61	0.00	9.27	13.40	18.25
8	10.55	9.26	11.16	9.91	25.58	17.59	5.22	16.83	5.07	14.49	8.48	13.28	4.79	6.25	8.27	18.21	7.65	6.02	0.00	20.77	7.19	10.22	18.54	0.00	0.00	3.15	11.72	15.31
9	13.92	14.84	5.37	8.41	11.94	10.12	10.03	5.82	4.45	20.46	18.48	8.70	5.01	8.23	0.00	10.78	9.48	4.35	0.00	609.76	9.80	29.50	4.92	0.00	0.00	13.32	5.39	15.42
10	4.33	11.57	27.05	4.87	20.32	10.58	0.00	5.76	10.77	14.45	10.41	20.06	14.99	15.60	0.00	6.00	13.13	6.12	0.00	21.57	5.93	11.94	4.93	0.00	0.00	6.01	14.32	24.92
11	2.79	7.80	7.12	1.94	26.46	9.27	0.00	31.16	4.96	21.09	13.00	18.83	9.17	44.69	0.00	8.50	13.25	4.11	0.00	10.63	5.96	33.88	5.51	0.00	0.00	0.00	11.00	19.69
12	4.56	40.48	6.91	5.85	18.22	21.73	0.00	0.00	9.06	11.07	23.08	12.49	5.78	5.45	0.00	22.04	13.36	3.17	0.00	29.39	6.20	32.25	2.28	0.00	0.00	0.00	13.97	34.93
13	12.67	20.93	9.02	6.58	13.20	10.14	0.00	0.00	4.21	14.18	19.84	14.12	5.02	7.44	0.00	14.53	13.73	6.98	0.00	35.72	8.53	31.99	7.10	0.00	0.00	0.00	12.32	19.71
14	13.50	34.79	7.05	6.12	17.86	8.71	0.00	0.00	10.31	29.46	16.61	3.79	4.59	15.69	0.00	19.92	7.80	0.00	0.00	28.51	0.00	22.22	7.81	0.00	0.00	0.00	23.88	14.77
15	11.96	10.01	6.82	5.67	23.29	7.90	0.00	0.00	9.60	11.92	12.37	8.45	16.51	15.65	0.00	6.23	8.10	0.00	0.00	20.39	0.00	11.23	3.22	0.00	0.00	0.00	14.43	17.58
16	9.78	11.20	6.65	5.98	15.68	6.91	0.00	0.00	6.18	24.67	7.63	20.49	7.00	10.88	0.00	7.47	10.35	0.00	0.00	23.38	0.00	4.31	5.39	0.00	0.00	0.00	15.96	13.13
17	8.24	11.38	5.23	8.88	16.29	8.24	0.00	0.00	11.10	19.06	15.07	14.16	10.49	5.50	0.00	5.80	16.90	0.00	0.00	42.01	0.00	37.10	2.28	0.00	0.00	0.00	14.06	6.45
18	13.42	18.33	8.51	10.25	23.34	5.86	0.00	0.00	9.53	10.25	7.16	11.57	17.65	14.62	0.00	5.20	22.27	0.00	0.00	26.04	0.00	9.05	1.97	0.00	0.00	0.00	14.47	15.63
19	10.73	5.87	7.15	10.68	29.05	4.32	0.00	0.00	10.11	18.10	16.40	19.81	16.40	3.68	0.00	10.59	32.96	0.00	0.00	16.22	0.00	14.83	73.82	0.00	0.00	0.00	0.00	12.80
20	8.30	9.78	7.84	4.39	18.44	8.37	0.00	0.00	5.76	13.92	24.13	21.06	27.92	6.05	0.00	24.63	17.56	0.00	0.00	12.74	0.00	24.29	0.00	0.00	0.00	0.00	0.00	17.83
21	13.64	7.87	8.29	7.53	20.39	7.22	0.00	0.00	11.45	19.50	12.75	17.02	12.51	8.47	0.00	13.39	18.15	0.00	0.00	11.36	0.00	25.72	0.00	0.00	0.00	0.00	0.00	8.97
22	11.40	5.77	9.10	17.28	20.11	14.54	0.00	0.00	13.07	8.96	16.32	9.19	8.96	8.53	0.00	6.26	11.56	0.00	0.00	15.08	0.00	19.85	0.00	0.00	0.00	0.00	0.00	18.94
23	9.78	17.95	6.68	13.78	11.22	13.26	0.00	0.00	11.64	11.43	14.64	13.40	6.38	10.54	0.00	10.85	11.24	0.00	0.00	23.11	0.00	1.62	0.00	0.00	0.00	0.00	0.00	19.65
24	10.80	15.57	10.26	16.71	26.42	5.86	0.00	0.00	8.45	15.70	16.66	12.87	16.97	12.63	0.00	6.76	15.79	0.00	0.00	20.00	0.00	6.52	0.00	0.00	0.00	0.00	0.00	17.18
25	6.48	36.41	7.77	16.95	25.20	6.18	0.00	0.00	18.65	14.23	23.68	21.45	11.02	8.15	0.00	4.23	10.93	0.00	0.00	15.19	0.00	28.25	0.00	0.00	0.00	0.00	0.00	12.30
26	9.31	10.36	10.41	18.88	12.54	9.64	0.00	0.00	13.19	0.00	11.99	16.28	24.95	8.54	0.00	10.25	9.96	0.00	0.00	47.65	0.00	17.71	0.00	0.00	0.00	0.00	0.00	28.95
27	11.12	7.71	5.94	26.85	18.40	11.56	0.00	0.00	11.78	0.00	20.69	18.22	13.93	7.49	0.00	7.69	11.86	0.00	0.00	12.93	0.00	6.06	0.00	0.00	0.00	0.00	0.00	14.51
28	15.15	10.52	5.85	7.90	8.92	14.09	0.00	0.00	13.50	0.00	20.30	16.86	11.48	6.94	0.00	6.97	15.57	0.00	0.00	20.47	0.00	6.44	0.00	0.00	0.00	0.00	0.00	15.70
29	13.62	12.75	14.80	10.16	24.84	8.31	0.00	0.00	24.23	0.00	18.97	20.14	4.53	0.00	0.00	9.54	8.74	0.00	0.00	14.42	0.00	4.23	0.00	0.00	0.00	0.00	0.00	9.08
30	13.58	26.75	20.47	26.88	30.21	17.22	0.00	0.00	29.32	0.00	17.68	10.20	7.29	0.00	0.00	8.33	37.60	0.00	0.00	25.13	0.00	0.00	0.00	0.00	0.00	0.00	0.00	13.98
31	11.67	15.45	9.77	17.16	20.57	9.12	0.00	0.00	23.23	0.00	20.74	13.87	7.09	0.00	0.00	17.95	8.15	0.00	0.00	10.61	0.00	0.00	0.00	0.00	0.00	0.00	0.00	16.71
32	11.05	28.25	10.26	24.63	23.45	11.25	0.00	0.00	17.42	0.00	22.83	10.11	5.29	0.00	0.00	0.00	9.44	0.00	0.00	20.35	0.00	0.00	0.00	0.00	0.00	0.00	0.00	14.99
33	10.02	16.85	12.30	26.36	25.46	10.95	0.00	0.00	11.69	0.00	15.57	39.81	19.52	0.00	0.00	0.00	9.12	0.00	0.00	17.27	0.00	0.00	0.00	0.00	0.00	0.00	0.00	0.00
34	9.58	7.52	6.16	19.20	21.68	6.79	0.00	0.00	0.00	0.00	17.32	18.86	8.96	0.00	0.00	0.00	6.97	0.00	0.00	20.79	0.00	0.00	0.00	0.00	0.00	0.00	0.00	0.00

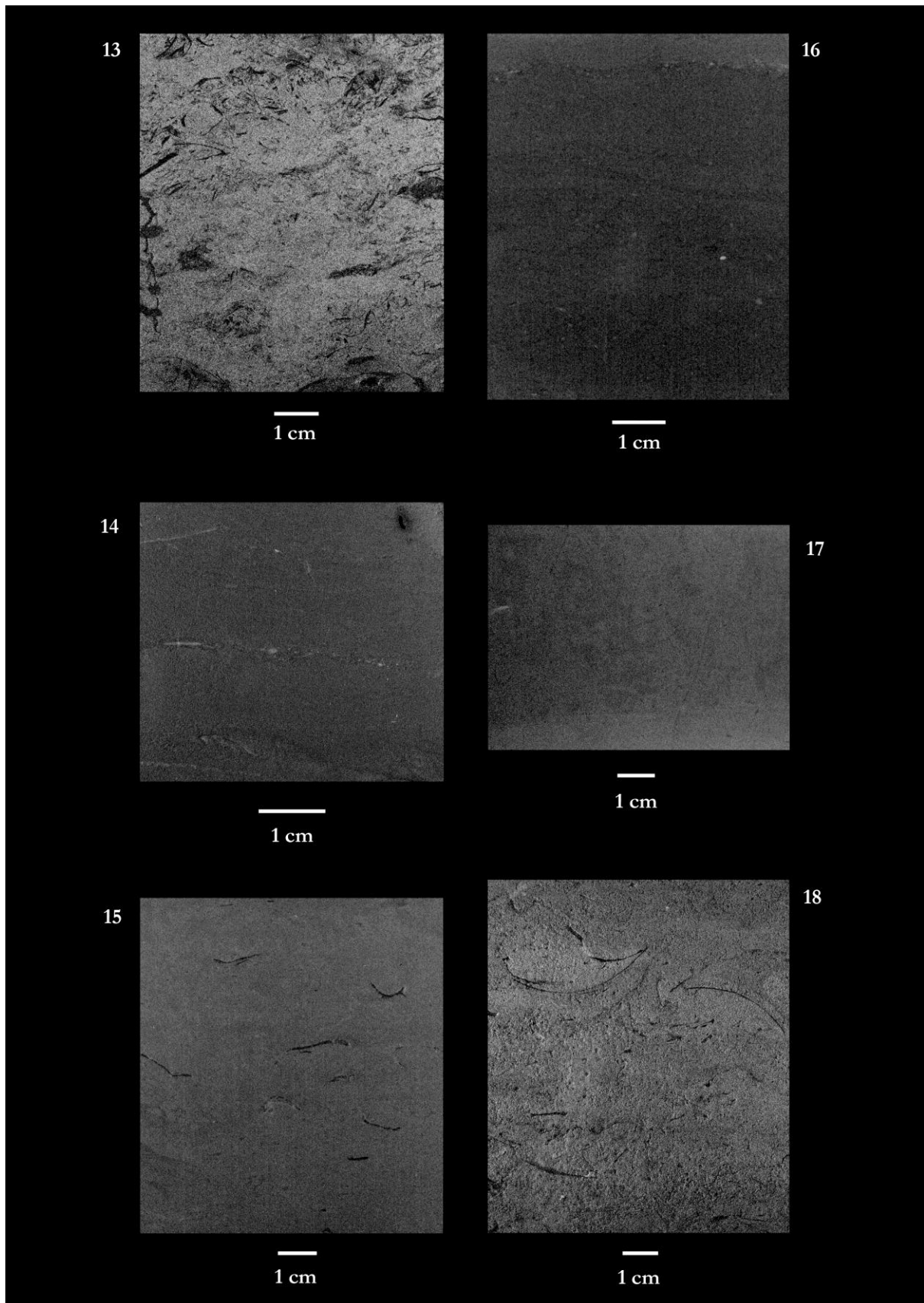
Appendix 4.16 Trace Fossils: Plates 1 to 6 (Westbury Formation).



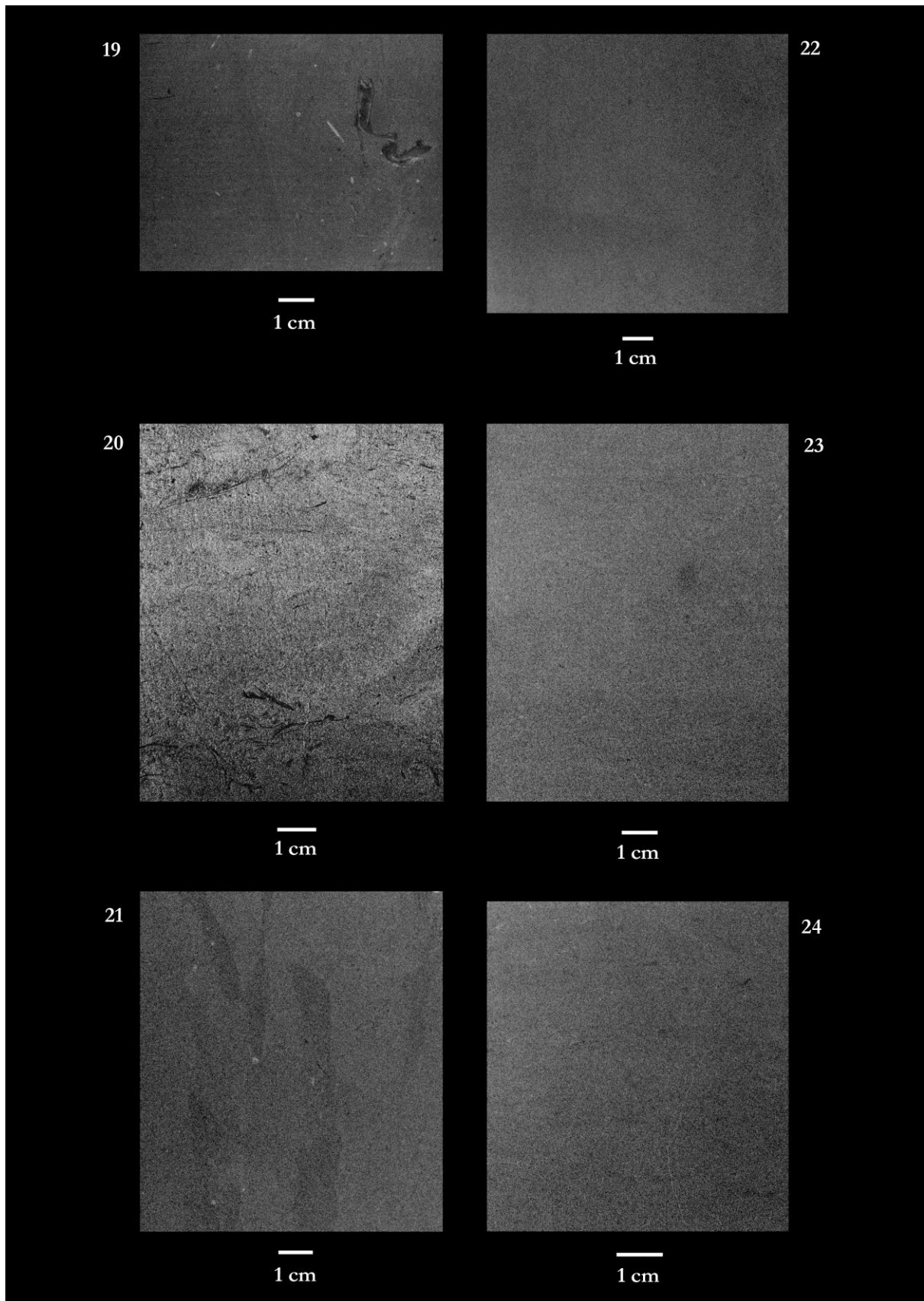
Appendix 4.16 Trace fossils: Plates 7 - 8 (The Cotham Member); Plates 9 to 11 (the Langport Member); Plate 12 (Pre-Planorbis Zone).



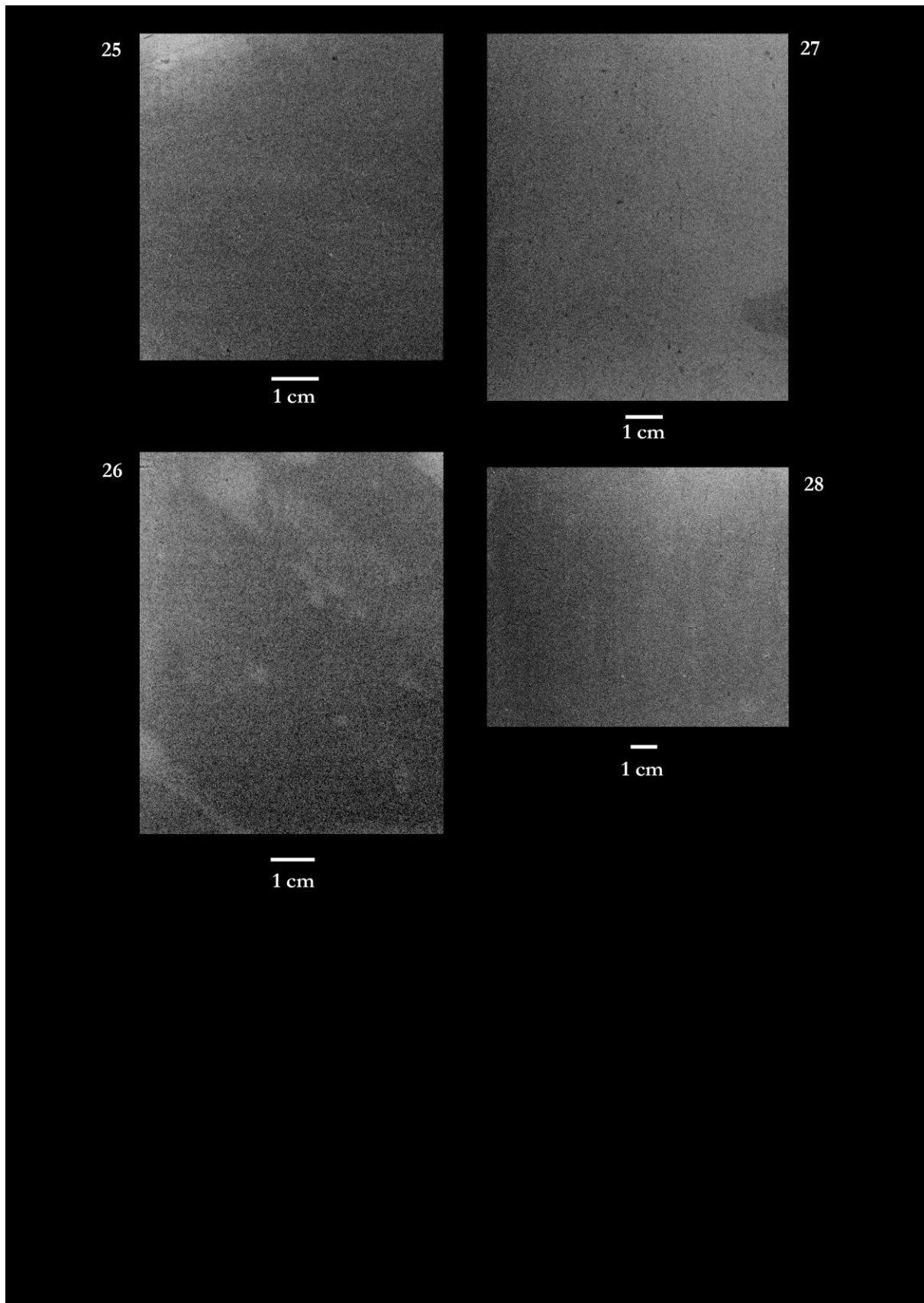
Appendix 4.16 Trace fossils: Plates 13 - 14 (Pre-Planorbis Zone); Plate 15 - 18 (Planorbis Zone).



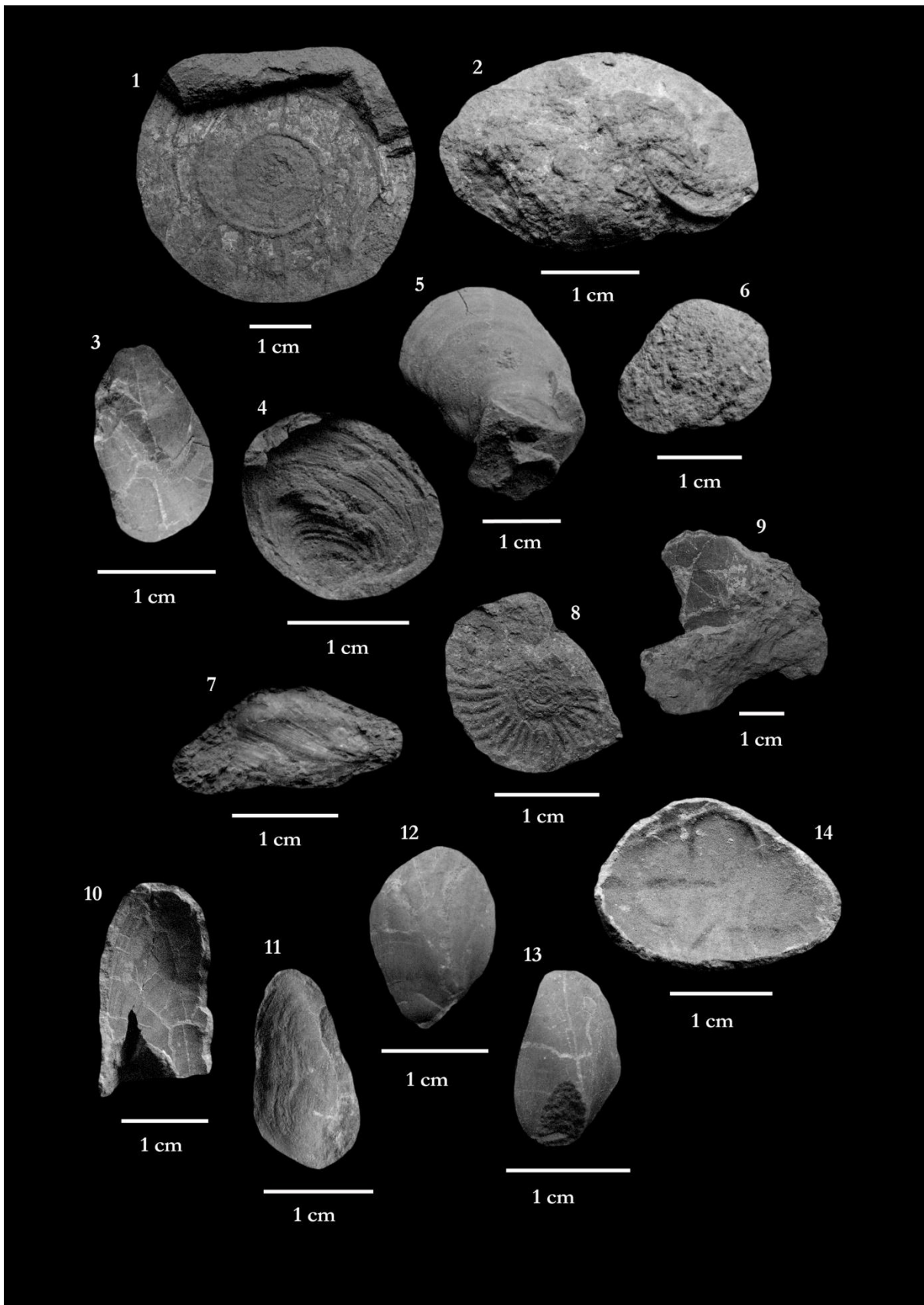
Appendix 4.16 Trace fossils: Plates 19 - 20 (Planorbis Zone); Plate 21-24 (Liasicus Zone).



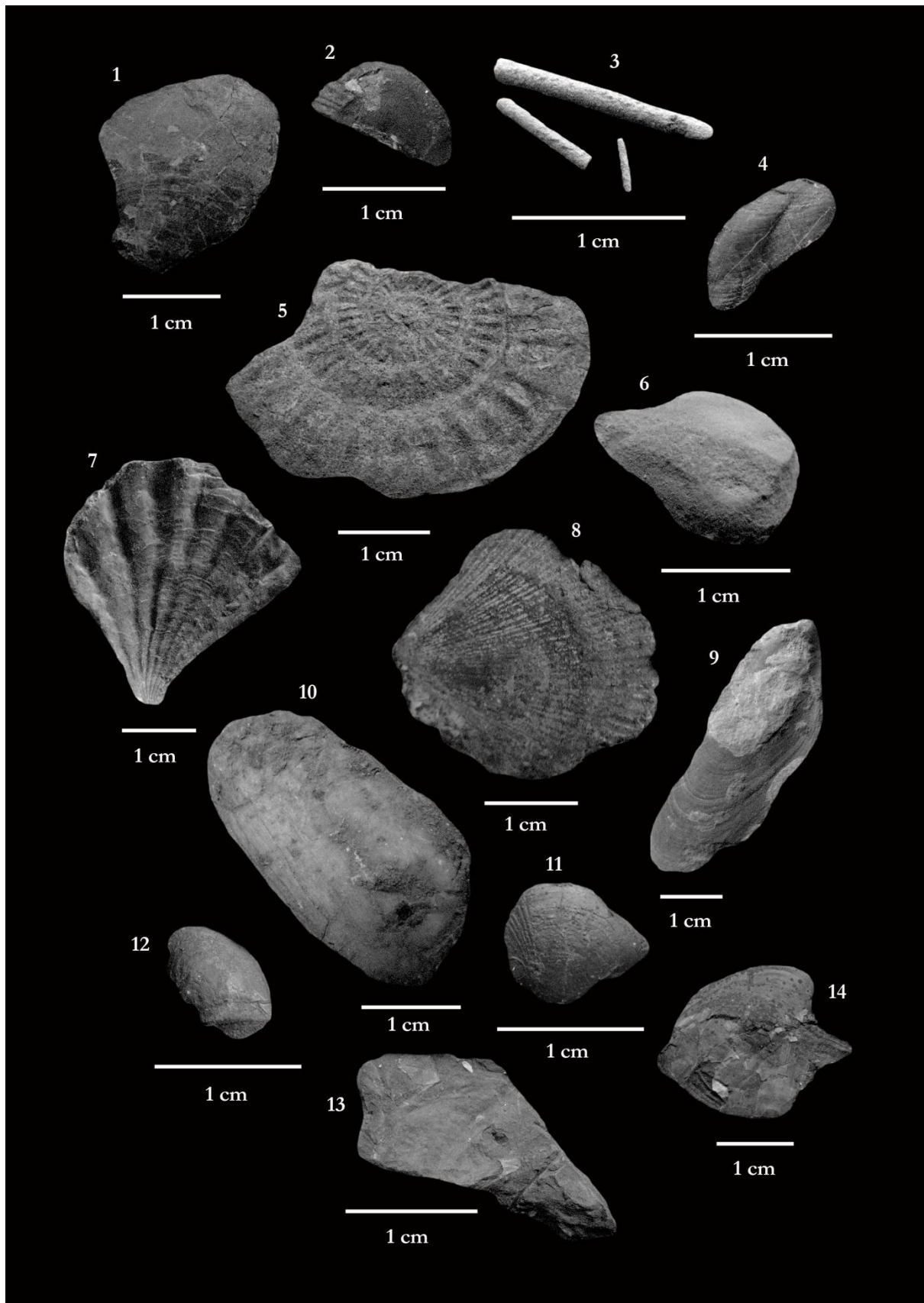
Appendix 4.16 Trace fossils: Plates 25 - 26 (Liasicus Zone); Plate 28 (Angulata Zone).



Appendix 4.17 Specimens found through the St Audrie's Bay section.



Appendix 4.18 Specimens found through the St Audrie's Bay section.



Appendix 4.17: 1. *Psilophyllites hagenowi* (Dunker); 2. *Cassianella* sp; 3. *Modiolus* sp; 4. *Cardinia regularis* (Terquem); 5. *Liostrea hisingeri* (Nilsson); 6. *Pteromya langportensis* (Richardson and Tutcher); 7. *Permophorus elongatus* (Moore); 8. *Waehnoceras portlocki* (Wright); 9. *Modiolus ventricosus* (Roener); 10. *Myoconcha* sp.; 11. *Modiolus minimus* (J. Sowerby); 12. *Modiolus sodburiensis* (Vaughan); 13. *Liostrea hisingeri* (Nilsson); 14. *Pholadomya* sp.

Appendix 4.18: 1. *Plagiostoma giganteum* (Sowerby); 2. *Paleonucula navis* (Piette); 3. *Diademopsis tomesi* (Wright); 4. *Mytilus cloacinus* (Tutcher); 5. *Caloceras johnstoni* (Sowerby); 6. *Pteromya langportensis* (Richardson and Tutcher); 7. *Camptonectes* sp; 8. *Chlamys valoniensis* (Defrance); 9. *Gervillella precursor* (Quenstedt); 10. *Permophorus elongatus* (Moore); 11. *Protocardia rhaetica* (Merian); 12. *Isocyprina depressum* (Moore); 13. *Chlamys valoniensis* (Defrance); 14. *Mytilus* sp.

Appendix 5.1 Lists of taxa and abundance of each species by lithology recorded at each sample along the Pinhay Bay section.

						Limestone																	
Meters above Langport Member(m)						0	1.3	2.6	3.6	4.8	6.05	7	8.1	8.9	10.1	11.5	12.3	13.1	13.8	14.9	15.8	17.2	19.2
Species	Phylum	Class	Order	Family		LLM1	LLM2	LLM3	LLM4	LLM5	LLM6	PP1	PP2	PP3	PZ1	PZ2	PZ3	PZ4	LZ1	LZ2	LZ3	AZ1	AZ2
<i>Mesomiltha</i> sp.	Mollusca	Bivalvia	Lucinoidea	Lucinidae		1	0	0	0	0	0	0	0	0	0	0	0	0	0	0	0	0	0
<i>Liostrea hisingeri</i> (Nilsson)	Mollusca	Bivalvia	Pterioidea	Gryphaeidae		1	1	0	1	0	0	2	8	0	3	0	0	11	1	1	0	0	0
<i>Pteromya langportensis</i> (Richardson and Tutchter)	Mollusca	Bivalvia	Pholadomyoidea	Pholadomyidae		1	1	0	0	0	0	6	0	0	0	0	0	0	0	0	0	0	0
<i>Modiolus hillanus</i> (Sowerby)	Mollusca	Bivalvia	Mytiloidea	Mytilidae		2	0	0	3	0	0	0	0	0	0	0	0	0	0	0	0	0	0
<i>Promathildia decorata</i> (Moore)	Mollusca	Gastropoda	Heterostrophoidea	Mathildidae		1	0	0	0	0	0	0	0	0	0	0	0	0	0	0	0	0	0
<i>Isocyprina concentricum</i> (Moore)	Mollusca	Bivalvia	Veneroidea	Arcticidae		5	0	0	14	24	0	0	0	0	0	0	0	0	0	0	0	0	0
<i>Modiolus</i> sp.	Mollusca	Bivalvia	Mytiloidea	Mytilidae		0	0	2	0	0	0	0	0	0	5	2	0	3	0	0	0	0	0
<i>Plagiostoma giganteum</i> (Sowerby)	Mollusca	Bivalvia	Limnoidea	Limidae		0	0	1	0	0	0	0	0	10	5	3	0	11	7	3	2	4	0
<i>Gervillia precursor</i> (Quenstedt)	Mollusca	Bivalvia	Pterioidea	Bakevelliidae		0	0	0	1	0	0	0	0	0	0	0	0	0	0	0	0	0	0
<i>Promathildia rhaetica</i> (Moore)	Mollusca	Gastropoda	Heterostrophoidea	Mathildidae		0	0	0	4	3	0	0	0	0	0	0	0	0	0	0	0	0	0
<i>Chlamys valoniensis</i> (Defrance)	Mollusca	Bivalvia	Pectinoidea	Pectinidae		0	0	0	1	2	0	0	0	0	0	0	0	3	0	0	0	0	0
<i>Zygopleura henrici</i> (Martin)	Mollusca	Gastropoda	Apogastropoda	Zygopleuridae		0	0	0	0	3	0	0	0	0	0	0	0	0	0	0	0	0	0
<i>Solaricoconulus waltonii</i> (Moore)	Mollusca	Gastropoda	Archaeogastropoda	Trochidae		0	0	0	0	6	0	0	0	0	0	0	0	0	0	0	0	0	0
<i>Astarte</i> sp.	Mollusca	Bivalvia	Carditoida	Astartidae		0	0	0	0	1	0	0	0	0	0	0	0	0	0	0	0	0	0
<i>Pseudokatosira undulata</i> (Benz)	Mollusca	Gastropoda	Murchisoniina	Zygopleuridae		0	0	0	0	0	0	3	0	0	10	1	0	6	0	0	22	7	9
<i>Diademopsis tomesi</i> (Wright)	Echinodermata	Echinoidea	Pedinoidea	Pedinidae		0	0	0	0	1	0	3	4	1	3	6	0	0	1	13	2	1	0
<i>Modiolus minimus</i> (J. Sowerby)	Mollusca	Bivalvia	Mytiloidea	Mytilidae		0	0	0	0	0	0	1	1	3	0	0	0	0	0	0	0	0	0
<i>Myoconcha</i> sp.	Mollusca	Bivalvia	Pholadomyoidea	Permophoridae		0	0	0	0	0	0	0	0	3	0	0	0	0	0	0	0	0	0
<i>Isocrinus psilonoti</i> (Quenstedt)	Echinodermata	Crinoidea	Articulata	Isocrinidae		0	0	0	0	0	0	0	0	9	10	7	0	15	11	0	2	1	0
<i>Pleurotomaria cognata</i> (Chapuis and Dewalque)	Mollusca	Gastropoda	Vetigastropoda	Pleurotomariidae		0	0	0	0	0	0	0	0	1	0	0	0	0	0	0	0	0	0
<i>Pinna</i> sp.	Mollusca	Bivalvia	Pterioidea	Pinnidae		0	0	0	0	0	0	0	0	0	0	0	0	2	0	0	0	0	0
<i>Pseudolimea duplicata</i> (Sowerby)	Mollusca	Bivalvia	Limnoidea	Limidae		0	0	0	0	0	0	0	0	0	3	7	0	4	3	2	1	0	1
<i>Modiolus ventricosus</i> (Roener)	Mollusca	Bivalvia	Mytiloidea	Mytilidae		0	0	0	0	0	0	0	0	0	1	0	0	0	1	0	0	0	0
<i>Psilocoeras erugatum</i> (Phillips)	Mollusca	Cephalopoda	Ammonoidea	Psiloceratidae		0	0	0	0	0	0	0	0	0	1	0	0	0	0	0	0	0	0
<i>Mactromya cardioides</i> (Phillips)	Mollusca	Bivalvia	Veneroidea	Mactromyidae		0	0	0	0	0	0	0	0	0	0	1	0	0	0	0	0	0	0
<i>Cardinia regularis</i> (Terquem)	Mollusca	Bivalvia	Carditoida	Cardiniidae		0	0	0	0	0	0	0	0	0	2	0	0	3	0	0	0	0	0
<i>Caloceras johnstoni</i> (Sowerby)	Mollusca	Cephalopoda	Ammonoidea	Psiloceratidae		0	0	0	0	0	0	0	0	0	0	0	0	1	0	0	0	0	0
<i>Scholethemia complanata</i>	Mollusca	Cephalopoda	Ammonoidea	Psiloceratidae		0	0	0	0	0	0	0	0	0	0	0	0	0	0	0	0	2	1
<i>Calcirhynchia calcaria</i> (Buckman)	Brachiopoda	Rhynchonellata	Rhynchonellida	Wellerellidae		0	0	0	0	0	0	0	0	0	0	0	0	0	0	0	0	15	60
<i>Gryphaea obliquata</i> (Sowerby)	Mollusca	Bivalvia	Pterioidea	Gryphaeidae		0	0	0	0	0	0	0	0	0	0	0	0	0	0	0	0	1	0
<i>Asatrics laqueus</i> (Quenstedt)	Mollusca	Cephalopoda	Ammonoidea	Psiloceratidae		0	0	0	0	0	0	0	0	0	0	0	0	1	0	0	0	0	0

Appendix 5.1 (Continuation).

						Mudstone												
Meters above Langport Member(m)						7	8.1	9.05	10.1	11.5	12.3	13.1	13.8	14.9	15.8	17.2	19.2	
Species	Phylum	Class	Order	Family		PP1	PP2	PP3	PZ1	PZ2	PZ3	PZ4	LLZ1	LLZ3	LLZ4	AZ1	AZ2	
<i>Liostrea hisingeri</i> (Nilsson)	Mollusca	Bivalvia	Pterioida	Gryphaeidae		3	20	4	5	3	2	9	1	6	10	4	0	
<i>Pteromya langportensis</i> (Richardson and Tutcher)	Mollusca	Bivalvia	Pholadomyoidea	Pholadomyidae		2	1	0	0	0	0	0	0	0	0	0	0	
<i>Modiolus hillanus</i> (Sowerby)	Mollusca	Bivalvia	Mytiloidea	Mytilidae		0	0	0	0	0	0	0	1	0	0	0	0	
<i>Modiolus</i> sp.	Mollusca	Bivalvia	Mytiloidea	Mytilidae		6	0	16	3	6	16	0	11	5	2	7	0	
<i>Plagiostoma giganteum</i> (Sowerby)	Mollusca	Bivalvia	Limoida	Limidae		0	1	0	1	1	4	7	0	1	0	1	0	
<i>Gervillia precursor</i> (Quenstedt)	Mollusca	Bivalvia	Pterioida	Bakevelliidae		0	0	0	0	0	0	0	0	1	0	1	0	
<i>Chlamys valoniensis</i> (Defrance)	Mollusca	Bivalvia	Pectinoidea	Pectinidae		8	1	1	0	2	6	0	0	0	2	0	0	
<i>Pseudokatosira undulata</i> (Benz)	Mollusca	Gastropoda	Murchisoniina	Zygopleuridae		0	2	0	0	11	0	0	0	0	0	0	0	
<i>Diademopsis tomesi</i> (Wright)	Echinodermata	Echinoidea	Pedinoidea	Pedinidae		3	24	10	9	0	23	19	2	27	2	1	3	
<i>Modiolus minimus</i> (J. Sowerby)	Mollusca	Bivalvia	Mytiloidea	Mytilidae		5	6	0	0	1	0	0	0	0	0	0	0	
<i>Myoconcha</i> sp.	Mollusca	Bivalvia	Pholadomyoidea	Permophoridae		0	1	0	0	0	0	0	0	0	0	0	0	
<i>Isocrinus psilonoti</i> (Quenstedt)	Echinodermata	Crinoidea	Articulata	Isocrinidae		0	1	4	0	0	2	0	0	0	0	2	0	
<i>Pseudolimea duplicata</i> (Sowerby)	Mollusca	Bivalvia	Limoida	Limidae		0	0	0	0	0	3	0	1	0	3	0	0	
<i>Modiolus ventricosus</i> (Roener)	Mollusca	Bivalvia	Mytiloidea	Mytilidae		0	0	0	0	0	7	0	0	0	0	0	1	
<i>Psiloeas erugatum</i> (Phillips)	Mollusca	Cephalopoda	Ammonoidea	Psiloceratidae		0	1	0	0	0	0	0	0	0	0	0	0	
<i>Mactromya cardioides</i> (Phillips)	Mollusca	Bivalvia	Veneroidea	Mactromyidae		0	0	0	0	0	0	0	0	0	0	1	0	
<i>Cardinia regularis</i> (Terquem)	Mollusca	Bivalvia	Carditoida	Cardiniidae		0	0	1	3	0	4	0	0	0	0	0	1	
<i>Caloceras johnstoni</i> (Sowerby)	Mollusca	Cephalopoda	Ammonoidea	Psiloceratidae		0	0	0	0	0	1	0	0	0	0	0	0	
<i>Scholethemia complanata</i>	Mollusca	Cephalopoda	Ammonoidea	Psiloceratidae		0	0	0	0	0	0	0	0	0	0	0	2	
<i>Calcirhynchia calcaria</i> (Buckman)	Brachiopoda	Rhynchonellata	Rhynchonellida	Wellerellidae		0	0	0	0	0	0	0	0	0	0	10	3	
<i>Gryphaea obliquata</i> (Sowerby)	Mollusca	Bivalvia	Pterioidea	Gryphaeidae		0	0	0	0	0	0	0	0	0	0	2	11	
<i>Rollieria bronni</i> (Ander)	Mollusca	Bivalvia	Nuculanoidea	Yoldiidae		0	0	0	0	0	1	0	0	1	0	0	0	
<i>Ryderia doris</i> (d'Orbigny)	Mollusca	Bivalvia	Nuculanoidea	Nuculanidae		0	0	1	0	0	0	0	0	0	0	0	0	
<i>Camptonectes</i> sp.	Mollusca	Bivalvia	Pectinoidea	Pectinidae		0	0	0	3	0	2	0	3	3	0	2	3	
<i>Euryclidus</i> sp.	Chordata	Reptilia	Plesiosauria	Plesiosauridae		0	0	0	0	0	0	1	0	0	0	0	0	
<i>Psilophyllites hagenowi</i> (Dunker)	Mollusca	Cephalopoda	Ammonoidea	Psiloceratidae		0	0	0	0	0	0	3	0	0	0	0	0	
<i>Paleonucula navis</i> (Piette)	Mollusca	Bivalvia	Nuculoidea	Nuculidae		0	0	0	0	0	0	0	1	0	0	0	0	
<i>Pseudomitiloides dubius</i> (Sowerby)	Mollusca	Bivalvia	Pterioidea	Inoceramidae		0	0	0	0	0	0	0	1	0	0	0	0	
<i>Asalties laqueus</i> (Quenstedt)	Mollusca	Cephalopoda	Ammonoidea	Psiloceratidae		0	0	0	0	0	0	0	0	1	0	0	0	
<i>Pholadomya</i> sp	Mollusca	Bivalvia	Pholadomyoidea	Pholadomyidae		0	0	0	0	5	0	0	0	0	0	1	0	

Appendix 5.2 Summary of palaeoecological parameters estimated in this study. SC: Sample cog; H: Height (mm), R: Richness, MR: Mean Richness, K: Kurtosis, B_w: Whittaker index, B_R: Routledge index; AC: Average cover %; II: Ichnofabric indices; NM = mean values of null model; GM = Geomean of body size, RT = Rate of change in body size, BD=Burrow diameter, (0.00) = No Data.

Limestone													Mudstone							
SC	H	R	MR	K	B _w	B _R	AC	II	NM	GM	RT	BD	N	H	R	MR	K	B _w	B _R	
LM1	0.00	6.00	4.10	22.50	0.00	0.00	0.00	0.00	1.67	8.32	19.12	0.00	0.00	0.00	0.00	0.00	0.00	0.00	0.00	0.00
LM2	1.30	2.00	2.00	17.28	0.5	0.09	0.00	0.00	0.16	33.18	-20.38	0.00	0.00	1.30	0.00	0.00	0.00	0.00	0.00	0.00
LM3	2.60	2.00	1.83	25.61	1	0.30	0.00	0.00	0.16	6.69	2.49	0.00	0.00	2.60	0.00	0.00	0.00	0.00	0.00	0.00
LM4	3.60	6.00	4.29	30.31	1	0.24	0.00	0.00	7.64	9.17	-0.49	0.00	0.00	3.60	0.00	0.00	0.00	0.00	0.00	0.00
LM5	4.80	7.00	5.21	32.68	0.53	0.16	0.00	0.00	7.18	8.58	1.01	0.00	0.00	4.80	0.00	0.00	0.00	0.00	0.00	0.00
LM6	6.05	0.00	0.00	0.00	0.00	0.00	0.00	0.00	0.00	0.00	0.00	0.00	0.00	6.05	0.00	0.00	0.00	0.00	0.00	0.00
PPZ1	7.00	5.00	3.96	14.38	0.83	0.24	17.00	1.00	9.94	10.85	5.50	3.25	PP1	7.00	6.00	1.97	8.01	0.00	0.00	0.00
PPZ2	8.90	3.00	2.47	24.94	0.25	0.06	5.00	2.00	9.17	17.18	-2.95	2.08	PP2	8.10	10.00	5.65	16.28	0.37	0.09	0.09
PPZ3	9.05	6.00	4.60	13.68	0.55	0.14	37.00	5.00	9.69	13.06	-0.08	7.06	PP3	8.90	7.00	2.79	17.71	0.52	0.15	0.15
PZ1	10.10	9.00	7.05	7.73	0.6	0.17	44.00	5.00	12.95	12.97	12.47	7.13	PZ1	10.10	6.00	1.66	14.11	0.38	0.11	0.11
PZ2	11.50	8.00	6.06	6.98	0.29	0.08	34.00	5.00	4.19	29.18	-7.90	7.00	PZ2	11.50	7.00	2.23	14.81	0.53	0.16	0.16
PZ3	12.30	0.00	0.00	0.00	0.00	0.00	0.00	0.00	4.07	20.49	5.07	0.00	PZ3	12.30	11.00	8.46	14.44	0.55	0.15	0.15
PZ4	13.10	10.00	8.10	7.43	0.33	0.09	48.00	5.00	2.84	26.06	-13.09	5.81	PZ4	13.10	5.00	2.36	20.33	0.62	0.15	0.15
LLZ1	13.80	7.00	4.88	18.31	0.52	0.15	125.00	5.00	2.20	12.97	11.02	7.89	LLZ1	13.80	7.00	1.56	27.21	0.66	0.19	0.19
LLZ2	14.90	4.00	3.11	33.81	0.27	0.06	34.00	5.00	5.91	25.09	-9.15	5.81	LLZ2	14.90	10.00	4.57	32.81	0.52	0.15	0.15
LLZ3	15.80	5.00	3.67	37.89	0.33	0.09	61.00	3.00	1.17	9.53	2.32	8.53	LLZ3	15.80	4.00	0.72	31.49	0.57	0.13	0.13
AZ1	17.20	7.00	5.06	22.74	0.33	0.09	110.00	4.00	4.68	14.40	5.10	5.44	AZ1	17.20	12.00	4.19	11.75	0.62	0.13	0.13
AZ2	19.20	4.00	2.95	38.08	0.00	0.00	71.00	4.00	5.90	24.60	0.00	7.57	AZ2	19.20	7.00	1.79	24.31	0.57	0.15	0.15

Appendix 5.3 Total species abundance (%) by Lithology and lithostratigraphy: LM Langport Member, PPZ: Pre-Planorbis Zone, PZ: Planorbis zone, LZ: Liasicus zone, AZ: Angulate Zone.

Limestone									
Species	LM	Species	PPZ	Species	PZ	Species	LZ	Species	AZ
<i>I. concentricum</i>	53.75	<i>L. hisingeri</i>	18.18	<i>I. psilonoti</i>	24.81	<i>P. undulata</i>	30.14	<i>C. calcaria</i>	73.53
<i>P. rhaetica</i>	8.75	<i>P. giganteum</i>	18.18	<i>P. giganteum</i>	14.73	<i>D. tomesi</i>	21.92	<i>P. undulata</i>	15.69
<i>S. waltonii</i>	7.5	<i>I. psilonoti</i>	16.36	<i>P. undulata</i>	13.18	<i>I. psilonoti</i>	17.81	<i>P. giganteum</i>	3.92
<i>M. hillanus</i>	6.25	<i>D. tomesi</i>	14.55	<i>L. hisingeri</i>	10.85	<i>P. giganteum</i>	16.44	<i>S. complanata</i>	2.94
<i>L. hisingeri</i>	3.75	<i>P. langportensis</i>	10.91	<i>P. duplicata</i>	10.85	<i>P. duplicata</i>	8.22	<i>D. tomesi</i>	0.98
<i>C. valoniensis</i>	3.75	<i>M. minimus</i>	9.09	<i>Modiolus</i> sp.	7.75	<i>L. hisingeri</i>	2.74	<i>I. psilonoti</i>	0.98
<i>Z. henrici</i>	3.75	<i>P. undulata</i>	5.45	<i>D. tomesi</i>	6.98	<i>M. ventricosus</i>	1.37	<i>P. duplicata</i>	0.98
<i>P. langportensis</i>	2.5	<i>Myoconcha</i> sp.	5.45	<i>C. regularis</i>	3.88	<i>A. laqueus</i>	1.37	<i>G. obliquata</i>	0.98
<i>Modiolus</i> sp.	2.5	<i>P. cognata</i>	1.82	<i>C. valoniensis</i>	2.33				
<i>Mesomiltha</i> sp.	1.25			<i>Pinna</i> sp.	1.55				
<i>P. decorata</i>	1.25			<i>M. ventricosus</i>	0.78				
<i>P. giganteum</i>	1.25			<i>P. planorbis</i>	0.78				
<i>G. precursor</i>	1.25			<i>M. cardioides</i>	0.78				
<i>Astarte</i> sp.	1.25			<i>W. portlocki</i>	0.78				
<i>D. tomesi</i>	1.25								

Mudstone							
Species	PPZ	Species	PZ	Species	LZ	Species	AZ
<i>D. tomesi</i>	30.33	<i>D. tomesi</i>	31.88	<i>D. tomesi</i>	36.47	<i>C. calcaria</i>	22.03
<i>L. hisingeri</i>	22.13	<i>Modiolus</i> sp.	15.63	<i>Modiolus</i> sp.	21.18	<i>G. obliquata</i>	22.03
<i>Modiolus</i> sp.	18.03	<i>L. hisingeri</i>	11.88	<i>L. hisingeri</i>	20.00	<i>Modiolus</i> sp.	11.86
<i>M. minimus</i>	9.02	<i>P. giganteum</i>	8.13	<i>Camptonectes</i> sp.	7.06	<i>Camptonectes</i> sp.	8.47
<i>C. valoniensis</i>	8.20	<i>P. undulata</i>	6.88	<i>P. hagenowi</i>	3.53	<i>L. hisingeri</i>	6.78
<i>I. psilonoti</i>	4.10	<i>C. valoniensis</i>	5.00	<i>C. valoniensis</i>	2.35	<i>D. tomesi</i>	6.78
<i>P. langportensis</i>	2.46	<i>M. ventricosus</i>	4.38	<i>M. hillanus</i>	1.18	<i>P. duplicata</i>	5.08
<i>P. undulata</i>	1.64	<i>C. regularis</i>	4.38	<i>P. giganteum</i>	1.18	<i>I. psilonoti</i>	3.39
<i>P. giganteum</i>	0.82	<i>Camptonectes</i> sp.	3.13	<i>G. precursor</i>	1.18	<i>S. complanata</i>	3.39
<i>Myoconcha</i> sp.	0.82	<i>Pholadomya</i> sp.	3.13	<i>P. duplicata</i>	1.18	<i>P. giganteum</i>	1.69
<i>P. planorbis</i>	0.82	<i>P. duplicata</i>	1.88	<i>R. bronni</i>	1.18	<i>G. precursor</i>	1.69
<i>C. regularis</i>	0.82	<i>I. psilonoti</i>	1.25	<i>P. navis</i>	1.18	<i>M. ventricosus</i>	1.69
<i>R. doris</i>	0.82	<i>M. minimus</i>	0.63	<i>P. dubius</i>	1.18	<i>M. cardioides</i>	1.69
		<i>R. bronni</i>	0.63	<i>A. laqueus</i>	1.18	<i>C. regularis</i>	1.69
		<i>Plesiosaurus</i> sp.	0.63			<i>Pholadomya</i> sp.	1.69
		<i>C. johnstoni</i>	0.63				

Appendix 5.4 Total species abundance by Lithology and lithostratigraphy: LM Langport Member, PPZ: Pre-Planorbis Zone, PZ: Planorbis zone, LZ: Liasicus zone, AZ: angulate zone.

	Limestone					Mudstone			
	LM	PPZ	PZ	LZ	AZ	PPZ	PZ	LZ	AZ
1	0	0	0	0	0	0	0	0	0
3	10	14	2	0	0	27	19	17	4
2	6	0	0	0	0	3	0	0	0
5	0	0	0	0	0	0	0	1	0
1	0	0	0	0	0	0	0	0	0
43	0	0	0	0	0	0	0	0	0
2	0	10	0	0	0	22	25	18	7
1	10	19	12	4	4	1	13	1	1
1	0	0	0	0	0	0	0	1	1
7	0	0	0	0	0	0	0	0	0
3	0	3	0	0	0	10	8	2	0
3	0	0	0	0	0	0	0	0	0
6	0	0	0	0	0	0	0	0	0
1	0	0	0	0	0	0	0	0	0
0	3	17	22	16	16	2	11	0	0
1	8	9	16	1	1	37	51	31	4
0	5	0	0	0	0	11	1	0	0
0	3	0	0	0	0	1	0	0	0
0	9	32	13	1	1	5	2	0	2
0	1	0	0	0	0	0	0	0	0
0	0	2	0	0	0	0	0	0	0
0	0	14	6	1	1	0	3	1	3
0	0	1	1	0	0	0	7	0	1
0	0	1	0	0	0	1	0	0	0
0	0	1	0	0	0	0	0	0	1
0	0	5	0	0	0	1	7	0	1
0	0	1	0	0	0	0	0	0	0
0	0	0	0	3	3	0	0	0	2
0	0	0	0	75	75	0	0	0	13
0	0	0	0	1	1	0	0	0	13
0	0	0	0	0	0	0	1	1	0
0	0	0	0	0	0	1	0	0	0
0	0	0	0	0	0	0	5	6	5
0	0	0	0	0	0	0	1	0	0
0	0	0	0	0	0	0	0	3	0
0	0	0	0	0	0	0	0	1	0
0	0	0	0	0	0	0	0	1	0
0	0	0	1	0	0	0	0	1	0
0	0	0	0	0	0	0	5	0	1
0	0	0	0	0	0	0	1	0	0
Total individuals	80	55	129	73	102	122	160	85	59
Species	15	9	14	8	8	13	16	14	15

Appendix 5.5 Pairwise comparisons of the faunal composition of each stratigraphic unit. The values showed were estimated by Bray Curtis dissimilarity index. LM: Langport Member, PPZ: Pre-Planorbis Zone, PZ: Planorbis Zone, LZ: Liasicus Zone. Overall average dissimilarity between stratigraphic units = 81.15%.

Taxa	LM	PPZ	PZ	LZ	AZ
	87.85				
		77.12			
<i>% Dissimilarity</i>			59.04		
				66.45	

Appendix 5.6 SIMPER analysis. C: Percentage contribution = average contribution/average dissimilarity between stratigraphic units. AC%: represents the average contribution of the taxon *i* to the average dissimilarity between lithostratigraphy (overall average = 81.15%. See appendix 4.4). Mean abundance of each taxon by stratigraphic units. LM: Langport Member, PPZ: Pre-Planorbis Zone, PZ: Planorbis Zone, LZ: Liasicus Zone, AZ: Angulata Zone, §: Taxa with regional extinction.

Taxon	C	AC %	LM	PPZ	PZ	LZ	AZ
<i>Diademopsis tomesi</i>	7.553	9.307	0.167	1.24	0.72	1.36	0.5
<i>Pseudokatosira undulata</i>	7.379	18.4	0	0.439	1.09	0.722	1.68
<i>Plagiostoma giganteum</i>	7.262	27.35	0.167	0.593	1.16	1.38	0.707
<i>Isocrinus psilonoti</i>	6.599	35.48	0	0.577	1.34	1	0.5
<i>Liostrea hisingeri</i>	6.416	43.39	0.5	0.957	0.784	0.667	0
<i>Pseudolimea duplicata</i>	5.861	50.61	0	0	1.09	1.17	0.5
<i>Calcirhynchia calcaria</i>	4.772	56.49	0	0	0	0	2.38
<i>Isocyprina concentricum</i> §	3.667	61.01	0.941	0	0	0	0
<i>Modiolus</i> sp.	3.602	65.45	0.198	0	1	0	0
<i>Modiolus minimus</i>	3.539	69.81	0	1.11	0	0	0
<i>Pteromya langportensis</i>	3.334	73.92	0.333	0.522	0	0	0
<i>Scholethemia complanata</i>	2.136	76.55	0	0	0	0	1.09
<i>Chlamys valoniensis</i>	1.941	78.94	0.365	0	0.329	0	0
<i>Modiolus hillanus</i> §	1.74	81.08	0.418	0	0	0	0
<i>Promathildia rhaetica</i> §	1.714	83.2	0.455	0	0	0	0
<i>Cardinia regularis</i>	1.565	85.12	0	0	0.626	0	0
<i>Modiolus ventricosus</i>	1.395	86.84	0	0	0.25	0.333	0
<i>Myoconcha</i> sp.	1.158	88.27	0	0.439	0	0	0
<i>Solariiconulus waltonii</i>	0.9137	89.4	0.261	0	0	0	0
<i>Pleurotomaria cognata</i>	0.88	90.48	0	0.333	0	0	0
<i>Gryphaea obliquata</i>	0.8741	91.56	0	0	0	0	0.5
<i>Asalties laqueus</i>	0.8464	92.6	0	0	0	0.333	0
<i>Zygopleura henrici</i>	0.7683	93.55	0.219	0	0	0	0
<i>Promathildia decorata</i>	0.7232	94.44	0.167	0	0	0	0
<i>Mesomiltha</i> sp.	0.7232	95.33	0.167	0	0	0	0
<i>Mactromya cardioides</i>	0.704	96.2	0	0	0.25	0	0
<i>Gervillella precursor</i>	0.6687	97.02	0.167	0	0	0	0
<i>Pinna</i> sp.	0.6576	97.83	0	0	0.297	0	0
<i>Psiloeas planorbis</i>	0.6235	98.6	0	0	0.25	0	0
<i>Astarte</i> sp.	0.5838	99.32	0.167	0	0	0	0
<i>Caloceras johnstoni</i>	0.553	100	0	0	0.25	0	0

Appendix 5.7 SIMPER analysis. AC: represents the average contribution of the taxon *i* to the average dissimilarity between lithology (overall average = 80 %). C%: Percentage contribution = average contribution/average dissimilarity between lithologies. Mean abundance of each taxa by lithology.

Taxon	AC	C %	Limestone	Mudstone
<i>Modiolus</i> sp.	1.697	10.21	0.288	1.21
<i>Diademopsis tomesi</i>	1.515	19.32	0.706	1.52
<i>Liostraea hisingeri</i>	1.229	26.71	0.612	1.36
<i>Pseudokatosira undulata</i>	1.12	33.45	0.621	0.251
<i>Isocrinus psilonoti</i>	1.015	39.55	0.618	0.399
<i>Calcirhynchia calcaria</i>	0.9172	45.07	0.264	0.258
<i>Plagiostoma giganteum</i>	0.908	50.53	0.72	0.67
<i>Chlamys valoniensis</i>	0.8251	55.49	0.195	0.635
<i>Camptonectes</i> sp.	0.8131	60.38	0	0.637
<i>Pseudolimea duplicata</i>	0.7142	64.67	0.492	0.303
<i>Isocyprina concentricum</i>	0.6043	68.31	0.314	0
<i>Modiolus minimus</i>	0.5565	71.65	0.184	0.338
<i>Cardinia regularis</i>	0.5427	74.92	0.139	0.394
<i>Gryphaea obliquata</i>	0.4219	77.45	0.0556	0.251
<i>Pteromya langportensis</i>	0.3761	79.72	0.198	0.182
<i>Modiolus ventricosus</i>	0.3663	81.92	0.111	0.219
<i>Pholadomya</i> sp.	0.2697	83.54	0	0.208
<i>Modiolus hillanus</i>	0.2349	84.95	0.139	0.0833
<i>Scholethemia complanata</i>	0.2279	86.32	0.122	0.0991
<i>Promathildia rhaetica</i>	0.2073	87.57	0.152	0
<i>Gervillella precursor</i>	0.2037	88.79	0.0556	0.167
<i>Myoconcha</i> sp.	0.1674	89.8	0.0731	0.0833
<i>Rollieria bronni</i>	0.1667	90.8	0	0.167
<i>Psilophyllites hagenowi</i>	0.1443	91.67	0	0.11
<i>Solariconulus waltonii</i>	0.1361	92.49	0.0869	0
<i>Caloceras johnstoni</i>	0.1296	93.27	0.0556	0.0833
<i>Mactromya cardioides</i>	0.1296	94.05	0.0556	0.0833
<i>Psiloeas planorbis</i>	0.1296	94.83	0.0556	0.0833
<i>Asalties laqueus</i>	0.1296	95.61	0.0556	0.0833
<i>Zygopleura henrici</i>	0.0962	96.19	0.0731	0
<i>Pseudomitiloides dubius</i>	0.0833	96.69	0	0.0833
<i>Paleonucula navis</i>	0.0833	97.19	0	0.0833
<i>Plesiosaurus</i> sp.	0.0833	97.69	0	0.0833
<i>Ryderia doris</i>	0.0833	98.19	0	0.0833
<i>Pinna</i> sp.	0.0786	98.66	0.0661	0
<i>Astarte</i> sp.	0.0556	99	0.0556	0
<i>Pleurotomaria cognata</i>	0.0556	99.33	0.0556	0
<i>Promathildia decorata</i>	0.0556	99.67	0.0556	0
<i>Mesomiltha</i> sp.	0.0556	100	0.0556	0

Appendix 5.8 Modes of life, number of species and relative abundance of each mode of life by stratigraphic unit. LM: Langport Member, PPZ: Pre-Planorbis Zone, PZ: Planorbis Zone, LZ: Liasicus Zone, AZ: Angulata Zone. Modes of Life; T: Tiering, M: Motility level; FM: Feeding Mechanism.

Modes of life			Number of species					Proportional abundance				
T	M	FM	LM	PPZ	PZ	LZ	AZ	LM	PPZ	PZ	LZ	AZ
1	1	5			4	2	1	0.00	0.00	20.00	11.76	6.25
2	6	1		1	1	1	1	0.00	7.69	5.00	5.88	6.25
3	2	2		2	1	1	1	0.00	15.38	5.00	5.88	6.25
3	2	4	2	1	1	1	1	13.33	7.69	5.00	5.88	6.25
3	2	5	2					13.33	0.00	0.00	0.00	0.00
3	3	1	1			1		6.67	0.00	0.00	5.88	0.00
3	4	1	2	2	3	4	2	13.33	15.38	15.00	23.53	12.50
3	6	1	1	1	2	2	4	6.67	7.69	10.00	11.76	25.00
4	2	3			1	1		0.00	0.00	5.00	5.88	0.00
4	4	1	2	2	3	3	2	13.33	15.38	15.00	17.65	12.50
4	6	1	1		1	1	1	6.67	0.00	5.00	5.88	6.25
5	2	3		1				0.00	7.69	0.00	0.00	0.00
5	3	1	4	3	3		3	26.67	23.08	15.00	0.00	18.75

Appendix 5.9 Modes of life used by species of each stratigraphy unit.

Langport member			
	Tiering	Motility	Feeding mechanism
<i>S. waltonii</i>	Surficial	Slow	Grazing
<i>D. tomesi</i>	Surficial	Slow	Grazing
<i>P. decorata</i>	Surficial	slow	Predatory
<i>P. rhaetica</i>	Surficial	slow	Predatory
<i>Z. henrici</i>	Surficial	Facultative Motile Unattached	Suspension
<i>P. giganteum</i>	Surficial	Facultative Motile Attached	Suspension
<i>C. valoniensis</i>	Surficial	Facultative Motile Attached	Suspension
<i>L. hisingeri</i>	Surficial	Non-Motile Attached	Suspension
<i>M. hillanus</i>	Semi-infaunal	Facultative Motile Attached	Suspension
<i>Modiolus</i> sp.	Semi-infaunal	Facultative Motile Attached	Suspension
<i>G. precursor</i>	Semi-infaunal	Non-Motile Attached	Suspension
<i>Mesomiltha</i> sp.	Shallow-infaunal	Facultative Motile Unattached	Suspension
<i>P. langportensis</i>	Shallow-infaunal	Facultative Motile Unattached	Suspension
<i>I. concentricum</i>	Shallow-infaunal	Facultative Motile Unattached	Suspension

Pre-Planorbis			
<i>P. erugatum</i>	Pelagic	Fast	Predatory
<i>I. psilonoti</i>	Erect	Non-Motile Attached	Suspension
<i>P. undulata</i>	Surficial	Slow	Surface deposit
<i>P. cognata</i>	Surficial	slow	Surface deposit
<i>D. tomesi</i>	Surficial	Slow	Grazing
<i>P. giganteum</i>	Surficial	Facultative Motile Attached	Suspension
<i>C. valoniensis</i>	Surficial	Facultative Motile Attached	Suspension
<i>L. hisingeri</i>	Surficial	Non-Motile Attached	Suspension
<i>Modiolus</i> sp.	Semi-infaunal	Facultative Motile Attached	Suspension
<i>M. minimus</i>	Semi-infaunal	Facultative Motile Attached	Suspension
<i>R. doris</i>	Shallow-infaunal	Slow	Mining
<i>P. langportensis</i>	Shallow-infaunal	Facultative Motile Unattached	Suspension
<i>Myoconcha</i> sp.	Shallow-infaunal	Facultative Motile Unattached	Suspension
<i>C. regularis</i>	Shallow-infaunal	Facultative Motile Unattached	Suspension

Planorbis Zone

<i>P. planorbis</i>	Pelagic	Fast	Predatory
<i>W. portlocki</i>	Pelagic	Fast	Predatory
<i>Eurycleidus</i> sp.	Pelagic	Fast	Predatory
<i>C. johnstoni</i>	Pelagic	Fast	Predatory
<i>I. psilonoti</i>	Erect	Non-Motile Attached	Suspension
<i>P. undulata</i>	Surficial	Slow	Surface deposit
<i>D. tomesi</i>	Surficial	Slow	Grazing
<i>P. giganteum</i>	Surficial	Facultative Motile Attached	Suspension
<i>C. valoniensis</i>	Surficial	Facultative Motile Attached	Suspension
<i>Camptonectes</i> sp.	Surficial	Facultative Motile Attached	Suspension
<i>L. hisingeri</i>	Surficial	Non-Motile Attached	Suspension
<i>P. duplicata</i>	Surficial	Non-Motile Attached	Suspension
<i>R. bronni</i>	Semi-infaunal	Slow	Mining
<i>Modiolus</i> sp.	Semi-infaunal	Facultative Motile Attached	Suspension
<i>M. minimus</i>	Semi-infaunal	Facultative Motile Attached	Suspension
<i>M. ventricosus</i>	Semi-infaunal	Facultative Motile Attached	Suspension
<i>Pinna</i> sp.	Semi-infaunal	Non-Motile Attached	Suspension
<i>M. cardioides</i>	Shallow-infaunal	Facultative Motile Unattached	Suspension
<i>C. regularis</i>	Shallow-infaunal	Facultative Motile Unattached	Suspension
<i>Pholadomya</i> sp.	Shallow-infaunal	Facultative Motile Unattached	Suspension

Liasicus Zone

<i>P. hagenowi</i>	Pelagic	Fast	Predatory
<i>A. laqueus</i>	Pelagic	Fast	Predatory
<i>I. psilonoti</i>	Erect	Non-Motile Attached	Suspension
<i>P. undulata</i>	Surficial	Slow	Surface deposit
<i>D. tomesi</i>	Surficial	Slow	Grazing
<i>P. navis</i>	Surficial	Facultative Motile Unattached	Suspension
<i>P. giganteum</i>	Surficial	Facultative Motile Attached	Suspension
<i>C. valoniensis</i>	Surficial	Facultative Motile Attached	Suspension
<i>Camptonectes</i> sp.	Surficial	Facultative Motile Attached	Suspension
<i>P. dubius</i>	Surficial	Facultative Motile Attached	Suspension
<i>L. hisingeri</i>	Surficial	Non-Motile Attached	Suspension
<i>P. duplicata</i>	Surficial	Non-Motile Attached	Suspension
<i>R. bronni</i>	Semi-infaunal	Slow	Mining
<i>M. hillanus</i>	Semi-infaunal	Facultative Motile Attached	Suspension
<i>Modiolus</i> sp.	Semi-infaunal	Facultative Motile Attached	Suspension
<i>M. ventricosus</i>	Semi-infaunal	Facultative Motile Attached	Suspension
<i>G. precursor</i>	Semi-infaunal	Non-Motile Attached	Suspension

Angulata Zone			
<i>S. complanata</i>	Pelagic	Fast	Predatory
<i>I. psilonoti</i>	Erect	Non-Motile Attached	Suspension
<i>P. undulata</i>	Surficial	Slow	Surface deposit
<i>D. tomesii</i>	Surficial	Slow	Grazing
<i>P. giganteum</i>	Surficial	Facultative Motile Attached	Suspension
<i>C. valoniensis</i>	Surficial	Facultative Motile Attached	Suspension
<i>Camptonectes</i> sp.	Surficial	Facultative Motile Attached	Suspension
<i>L. hisingeri</i>	Surficial	Non-Motile Attached	Suspension
<i>P. duplicata</i>	Surficial	Non-Motile Attached	Suspension
<i>C. calcaria</i>	Surficial	Non-Motile Attached	Suspension
<i>G. obliquata</i>	Surficial	Non-Motile Attached	Suspension
<i>Modiolus</i> sp.	Semi-infaunal	Facultative Motile Attached	Suspension
<i>M. ventricosus</i>	Semi-infaunal	Facultative Motile Attached	Suspension
<i>G. precursor</i>	Semi-infaunal	Non-Motile Attached	Suspension
<i>M. cardioides</i>	Shallow- infaunal	Facultative Motile Unattached	Suspension
<i>C. regularis</i>	Shallow- infaunal	Facultative Motile Unattached	Suspension
<i>Pholadomya</i> sp.	Shallow- infaunal	Facultative Motile Unattached	Suspension

Appendix 5.10 Proportion of mode of life. LM: Langport Member, PP: Pre-Planorbis Zone, PZ: Planorbis zone, LZ: Liasicus Zone, AZ : Angulata Zone.

Ecological Categories	Stratigraphy				
	LM	PP	PZ	LZ	AZ
Pelagic	0	0.07	0.2	0.11	0.06
Erect	0	0.07	0.05	0.05	0.06
Surficial	0.53	0.43	0.35	0.53	0.50
Semi-infaunal	0.20	0.14	0.25	0.29	0.19
Shallow-infaunal	0.26	0.29	0.15	0	0.18
Deep-infaunal	0	0	0	0	0
Fast	0	0.07	0.2	0.11	0.06
Slow	0.27	0.29	0.15	0.18	0.13
Facultative, unattached	0.33	0.21	0.15	0.06	0.19
Facultative, attached	0.27	0.29	0.30	0.41	0.25
Non-Motile unattached	0.00	0.00	0.00	0.00	0.00
Non-Motile Attached	0.13	0.14	0.20	0.24	0.38
Suspension	0.73	0.64	0.65	0.71	0.81
Surface deposit	0.00	0.14	0.05	0.06	0.06
Mining	0.00	0.07	0.05	0.06	0.00
Grazing	0.13	0.07	0.05	0.06	0.06
Predatory	0.13	0.07	0.2	0.11	0.06
Other	0.00	0.00	0.00	0.00	0.00

Appendix 5.11 Geometric mean (mm) by species through the Tr/J section in Pinhay Bay. **Tr1-Tr5:** Samples from Langport Member; **PPZ:** Pre-Planorbis; **PZ:** Planorbis Zone; **LZ:** Liassic Zone and **AZ:** Angulata Zone; **SP:** species. **IC:** *I. concentricum*; **PG:** *P. giganteum*; **CV:** *C. valoniensis*; **MESO:** *Mesomiltha* sp.; **MH:** *M. hillanus*; **G:** *Gervillella* sp.; **M:** *Modiolus* sp.; **MM:** *M. minimus*; **CR:** *C. regularis*; **PH:** *Pholadomya* sp.; **PT:** *P. langportiensis*; **L:** *Liostraea*; **MY:** *Myoconcha* sp.; **MC:** *M. cardioides*; **PD:** *P. duplicata*; **GRE:** *G. obliquata*; **CC:** *C. calcarea*; **CA:** *Camponectes* sp.; **RB:** *R. bronni*.

Sp	LM1	Sp	LM2	Sp	LM3	Sp	LM4	Sp	LM5	Sp	PP1	Sp	PP2	Sp	PP3	Sp	PZ1	Sp	PZ2	Sp	PZ3	Sp	PZ4	Sp	LZ1	Sp	LZ2	Sp	LZ3	Sp	AZ1	Sp	AZ2
CV	22.8	PG	33.17	M	6.69	CV	11.3	IC	10.6	CV	4.56	CV	33.9	CR	13.9	CA	17.9	CR	20.2	CA	30.5	CV	29.4	CA	10.4	CA	14.9	CV	3.81	CA	9.6	CA	4.33
CV	8.46	0	0	0	0	CV	26.2	IC	8	CV	2.9	CV	14.7	CR	11.1	CA	15.7	CV	11.4	CV	15.8	CV	36.4	CA	6.48	CA	11.3	L	20	CA	8.68	CA	10.6
IC	5.7	0	0	0	0	CV	10.3	IC	3.45	CV	3.43	CV	28.8	CV	7.15	CR	12.4	L	19.3	L	22.6	CV	29	CA	13.4	GE	19.5	L	13.7	CA	79.8	CC	7.65
IC	7.92	0	0	0	0	CV	3.24	IC	6.43	CV	2.44	L	8.28	CV	11.5	CR	13.5	L	40.5	L	30.3	L	18.7	M	3.64	GE	17.9	L	15	CC	9.64	CR	10.5
IC	4.07	0	0	0	0	G	6.09	IC	6.54	L	7.19	L	7.34	L	25	CR	19.2	M	6.46	L	19.2	L	19.7	M	1.95	L	27.6	L	8	CC	10.4	CR	22.1
IC	7.49	0	0	0	0	IC	12.1	IC	6.04	L	35.9	L	23	L	29.3	CR	15.2	M	9.18	L	30.5	L	15.7	M	3.65	L	36.3	M	3.42	CC	11	GRE	28.6
IC	5.18	0	0	0	0	IC	7.72	IC	5.77	L	28.1	L	18.4	L	27.2	CR	12.9	M	2.55	L	12.1	L	17.6	M	1.98	L	14.1	M	2.75	CC	10	GRE	24.1
IC	10.4	0	0	0	0	IC	8.25	IC	8.54	L	24.9	L	7.43	L	40.5	CR	10.5	M	8	L	23.9	L	20.4	M	4.82	L	11.7	0	0	CC	8.32	GRE	7.07
MESO	6.56	0	0	0	0	IC	6.65	IC	6.1	L	24.2	L	9.61	L	17.2	CR	12.4	M	6.99	L	19.1	L	24.1	M	15.6	L	22.3	0	0	CC	4.49	GRE	4.69
MH	4.71	0	0	0	0	IC	7.23	IC	8.54	L	19.3	L	6.23	L	25.9	CR	23.9	PG	56.7	L	18.3	L	14.3	M	13.3	L	26.3	0	0	CC	11	GRE	5.91
0	0	0	0	0	0	IC	9.34	IC	5.1	L	7.67	L	15.7	L	29.5	CR	10.7	PG	25	L	17.8	L	21.5	M	7.58	L	17.7	0	0	CC	5.23	GRE	6.65
0	0	0	0	0	0	IC	8.96	IC	6.02	L	18.4	L	26.3	L	12.8	CR	22.7	PG	55.2	L	14.2	PD	3.52	M	16.5	L	36	0	0	CC	9.76	GRE	6.3
0	0	0	0	0	0	IC	7.55	IC	17.1	L	12.8	L	33.9	M	6.51	CR	11.2	PG	50	L	9.37	PG	51.9	PG	69.4	L	34.2	0	0	CR	25.7	GRE	4.6
0	0	0	0	0	0	IC	6.2	IC	10.5	L	14.3	L	22.7	M	5.76	CR	12.1	PG	60.7	L	11.3	PG	65.5	0	0	L	30.4	0	0	CR	21	GRE	4.68
0	0	0	0	0	0	IC	9.68	IC	13.7	L	10.8	L	23.9	M	3.15	CR	4.9	PG	56.6	M	4.3	PG	18	0	0	L	25.7	0	0	L	17	GRE	17.5
0	0	0	0	0	0	IC	9.77	IC	14.2	L	12.9	L	26	M	3	CR	10	PH	17.9	M	20.4	PG	31.4	0	0	L	24.4	0	0	L	21.5	GRE	42.9
0	0	0	0	0	0	IC	7.24	IC	12.2	L	4.33	L	26.6	M	6.56	CR	9.97	PH	33.6	MY	14.5	0	0	0	0	L	17.5	0	0	L	21.1	L	39.4
0	0	0	0	0	0	IC	7.47	IC	8.96	L	14.2	L	41.2	M	5.58	CR	4.68	PH	26.1	PG	65.9	0	0	0	0	L	19.8	0	0	L	7.72	L	14.3
0	0	0	0	0	0	IC	8.96	IC	6.83	L	18.1	L	18.2	M	6.79	CR	4.18	PH	40	PG	24.4	0	0	0	0	M	4.33	0	0	L	8.03	L	27.4
0	0	0	0	0	0	IC	10.4	IC	7.24	L	19.1	L	9.93	M	7.53	CR	15.8	PH	33.6	PT	15.8	0	0	0	0	M	2.37	0	0	L	17.1	M	10
0	0	0	0	0	0	IC	8.67	IC	11.9	L	24.5	L	17.8	M	11.2	CR	12.4	PH	32.1	PT	8.61	0	0	0	0	M	3.78	0	0	L	14.9	M	6.46
0	0	0	0	0	0	IC	5.9	IC	5.06	LH	11.5	L	34	M	9.57	CR	15.3	PH	36.6	PT	21.8	0	0	0	0	M	12	0	0	M	5.85	M	10.7
0	0	0	0	0	0	IC	7.39	IC	8.71	M	2.64	L	23.3	M	9.45	CR	12.5	PT	22.4	0	0	0	0	0	0	M	4.95	0	0	PD	12.7	PD	7.83
0	0	0	0	0	0	IC	7.69	IC	14	M	2.38	L	19	M	8.24	CR	9.23	0	0	0	0	0	0	0	0	PD	5.48	0	0	PD	4.88	PD	12.3
0	0	0	0	0	0	IC	10.9	IC	10.2	M	3.76	L	28.4	M	11	CR	12.1	0	0	0	0	0	0	0	0	PG	15.5	0	0	PD	4.66	PD	6.93
0	0	0	0	0	0	IC	9.49	IC	11.4	M	3.52	L	14.7	M	8.7	CR	12.1	0	0	0	0	0	0	0	0	PG	110	0	0	0	0	PG	21.8
0	0	0	0	0	0	IC	7.16	IC	10	M	3.09	L	9.35	M	8.57	CR	25.1	0	0	0	0	0	0	0	0	PG	24	0	0	0	0	PG	144
0	0	0	0	0	0	IC	6.55	IC	8.52	M	7.3	L	20.8	M	11	CR	8.13	0	0	0	0	0	0	0	0	PG	115	0	0	0	0	PG	142

0	0	0	0	0	0	IC	6.9	IC	3.47	M	1.37	L	32.7	M	8.02	CV	10.2	0	0	0	0	0	0	0	0	0	0	0	0	PH	23.2	0	0	0	0	0	PG	62	
0	0	0	0	0	0	IC	7.82	IC	10.1	M	2.64	L	10.9	M	6.8	L	10.9	0	0	0	0	0	0	0	0	0	0	0	0	0	0	0	0	0	0	0	0	0	
0	0	0	0	0	0	IC	7.22	IC	6.27	M	4.58	L	18.3	M	8.56	L	16.1	0	0	0	0	0	0	0	0	0	0	0	0	0	0	0	0	0	0	0	0		
0	0	0	0	0	0	IC	10.6	IC	5.52	M	4.61	L	20.3	M	8.17	L	15.3	0	0	0	0	0	0	0	0	0	0	0	0	0	0	0	0	0	0	0	0		
0	0	0	0	0	0	IC	7.62	IC	5.85	M	1.46	M	9.9	M	8.07	L	14.6	0	0	0	0	0	0	0	0	0	0	0	0	0	0	0	0	0	0	0	0		
0	0	0	0	0	0	IC	6.07	L	8.87	M	2.58	M	15.1	M	9.58	L	9.42	0	0	0	0	0	0	0	0	0	0	0	0	0	0	0	0	0	0	0	0		
0	0	0	0	0	0	IC	7.66	M	7.65	M	1.31	M	5.66	M	10.2	L	10.5	0	0	0	0	0	0	0	0	0	0	0	0	0	0	0	0	0	0	0	0		
0	0	0	0	0	0	IC	9.18	PT	13.8	M	4.27	M	11.2	M	8.62	L	11.9	0	0	0	0	0	0	0	0	0	0	0	0	0	0	0	0	0	0	0	0		
0	0	0	0	0	0	IC	9.94	PT	5.33	M	4.75	M	10.6	M	10.8	L	17.8	0	0	0	0	0	0	0	0	0	0	0	0	0	0	0	0	0	0	0	0		
0	0	0	0	0	0	L	7.9	PT	7.42	M	5.63	M	8.12	M	6.07	L	15.6	0	0	0	0	0	0	0	0	0	0	0	0	0	0	0	0	0	0	0	0		
0	0	0	0	0	0	MESO	9.75	0	0	M	2.46	M	9.31	M	9.02	L	16.9	0	0	0	0	0	0	0	0	0	0	0	0	0	0	0	0	0	0	0	0		
0	0	0	0	0	0	MY	18.9	0	0	M	6.36	M	12.3	M	11.9	L	14.2	0	0	0	0	0	0	0	0	0	0	0	0	0	0	0	0	0	0	0	0		
0	0	0	0	0	0	MY	8.47	0	0	M	6.94	M	7.48	M	12	L	15.3	0	0	0	0	0	0	0	0	0	0	0	0	0	0	0	0	0	0	0	0		
0	0	0	0	0	0	PT	18.7	0	0	PT	18.5	M	5.13	MM	7.68	L	11.5	0	0	0	0	0	0	0	0	0	0	0	0	0	0	0	0	0	0	0	0		
0	0	0	0	0	0	0	0	0	0	PT	9.54	M	7.24	MM	10.9	L	14.5	0	0	0	0	0	0	0	0	0	0	0	0	0	0	0	0	0	0	0	0	0	
0	0	0	0	0	0	0	0	0	0	PT	26.7	M	10.2	MM	8.7	L	13.5	0	0	0	0	0	0	0	0	0	0	0	0	0	0	0	0	0	0	0	0	0	
0	0	0	0	0	0	0	0	0	0	PT	17.9	MM	9.82	MM	6.66	L	13.4	0	0	0	0	0	0	0	0	0	0	0	0	0	0	0	0	0	0	0	0	0	
0	0	0	0	0	0	0	0	0	0	PT	20.8	MM	7	MM	9.13	L	13.5	0	0	0	0	0	0	0	0	0	0	0	0	0	0	0	0	0	0	0	0	0	
0	0	0	0	0	0	0	0	0	0	PT	13	MM	10.7	MM	9.24	L	14.8	0	0	0	0	0	0	0	0	0	0	0	0	0	0	0	0	0	0	0	0	0	
0	0	0	0	0	0	0	0	0	0	PT	13.2	MM	21.8	MM	8.23	L	16.5	0	0	0	0	0	0	0	0	0	0	0	0	0	0	0	0	0	0	0	0	0	
0	0	0	0	0	0	0	0	0	0	PT	9.26	MM	10.7	MM	10.4	L	14.9	0	0	0	0	0	0	0	0	0	0	0	0	0	0	0	0	0	0	0	0	0	0
0	0	0	0	0	0	0	0	0	0	PT	15.4	PG	36.7	PG	29.7	L	15.7	0	0	0	0	0	0	0	0	0	0	0	0	0	0	0	0	0	0	0	0	0	
0	0	0	0	0	0	0	0	0	0	PT	11.1	PT	15.9	PG	44	M	5.97	0	0	0	0	0	0	0	0	0	0	0	0	0	0	0	0	0	0	0	0	0	0
0	0	0	0	0	0	0	0	0	0	PT	6.78	0	0	PT	20.4	M	5.39	0	0	0	0	0	0	0	0	0	0	0	0	0	0	0	0	0	0	0	0	0	0
0	0	0	0	0	0	0	0	0	0	PT	6.61	0	0	PT	40.5	M	5.28	0	0	0	0	0	0	0	0	0	0	0	0	0	0	0	0	0	0	0	0	0	0
0	0	0	0	0	0	0	0	0	0	PT	17.7	0	0	RB	8	M	5.69	0	0	0	0	0	0	0	0	0	0	0	0	0	0	0	0	0	0	0	0	0	0
0	0	0	0	0	0	0	0	0	0	PT	17.3	0	0	0	0	M	3.93	0	0	0	0	0	0	0	0	0	0	0	0	0	0	0	0	0	0	0	0	0	0
0	0	0	0	0	0	0	0	0	0	0	0	0	0	0	M	3.99	0	0	0	0	0	0	0	0	0	0	0	0	0	0	0	0	0	0	0	0	0	0	
0	0	0	0	0	0	0	0	0	0	0	0	0	0	0	M	4.45	0	0	0	0	0	0	0	0	0	0	0	0	0	0	0	0	0	0	0	0	0	0	
0	0	0	0	0	0	0	0	0	0	0	0	0	0	0	M	4.71	0	0	0	0	0	0	0	0	0	0	0	0	0	0	0	0	0	0	0	0	0	0	
0	0	0	0	0	0	0	0	0	0	0	0	0	0	0	M	7.74	0	0	0	0	0	0	0	0	0	0	0	0	0	0	0	0	0	0	0	0	0	0	
0	0	0	0	0	0	0	0	0	0	0	0	0	0	0	M	6.07	0	0	0	0	0	0	0	0	0	0	0	0	0	0	0	0	0	0	0	0	0	0	
0	0	0	0	0	0	0	0	0	0	0	0	0	0	0	M	5.1	0	0	0	0	0	0	0	0	0	0	0	0	0	0	0	0	0	0	0	0	0	0	
0	0	0	0	0	0	0	0	0	0	0	0	0	0	0	M	4.18	0	0	0	0	0	0	0	0	0	0	0	0	0	0	0	0	0	0	0	0	0	0	
0	0	0	0	0	0	0	0	0	0	0	0	0	0	0	M	8.71	0	0	0	0	0	0	0	0	0	0	0	0	0	0	0	0	0	0	0	0	0	0	

0	0	0	0	0	0	0	0	0	0	0	0	0	0	0	M	7	0	0	0	0	0	0	0	0	0	0	0	0	0	0	0	0	0	0	0	
0	0	0	0	0	0	0	0	0	0	0	0	0	0	0	M	9.8	0	0	0	0	0	0	0	0	0	0	0	0	0	0	0	0	0	0	0	0
0	0	0	0	0	0	0	0	0	0	0	0	0	0	0	MM	10.7	0	0	0	0	0	0	0	0	0	0	0	0	0	0	0	0	0	0	0	0
0	0	0	0	0	0	0	0	0	0	0	0	0	0	0	MM	5.19	0	0	0	0	0	0	0	0	0	0	0	0	0	0	0	0	0	0	0	0
0	0	0	0	0	0	0	0	0	0	0	0	0	0	0	MM	6.14	0	0	0	0	0	0	0	0	0	0	0	0	0	0	0	0	0	0	0	0
0	0	0	0	0	0	0	0	0	0	0	0	0	0	0	MM	6.21	0	0	0	0	0	0	0	0	0	0	0	0	0	0	0	0	0	0	0	0
0	0	0	0	0	0	0	0	0	0	0	0	0	0	0	MM	11.1	0	0	0	0	0	0	0	0	0	0	0	0	0	0	0	0	0	0	0	0
0	0	0	0	0	0	0	0	0	0	0	0	0	0	0	MM	5.41	0	0	0	0	0	0	0	0	0	0	0	0	0	0	0	0	0	0	0	0
0	0	0	0	0	0	0	0	0	0	0	0	0	0	0	MM	7.54	0	0	0	0	0	0	0	0	0	0	0	0	0	0	0	0	0	0	0	0
0	0	0	0	0	0	0	0	0	0	0	0	0	0	0	MM	12.8	0	0	0	0	0	0	0	0	0	0	0	0	0	0	0	0	0	0	0	0
0	0	0	0	0	0	0	0	0	0	0	0	0	0	0	MM	5.93	0	0	0	0	0	0	0	0	0	0	0	0	0	0	0	0	0	0	0	0
0	0	0	0	0	0	0	0	0	0	0	0	0	0	0	MM	11.4	0	0	0	0	0	0	0	0	0	0	0	0	0	0	0	0	0	0	0	0
0	0	0	0	0	0	0	0	0	0	0	0	0	0	0	MM	7.73	0	0	0	0	0	0	0	0	0	0	0	0	0	0	0	0	0	0	0	0
0	0	0	0	0	0	0	0	0	0	0	0	0	0	0	MM	5.99	0	0	0	0	0	0	0	0	0	0	0	0	0	0	0	0	0	0	0	0
0	0	0	0	0	0	0	0	0	0	0	0	0	0	0	MM	5	0	0	0	0	0	0	0	0	0	0	0	0	0	0	0	0	0	0	0	0
0	0	0	0	0	0	0	0	0	0	0	0	0	0	0	PG	48.4	0	0	0	0	0	0	0	0	0	0	0	0	0	0	0	0	0	0	0	0
0	0	0	0	0	0	0	0	0	0	0	0	0	0	0	PG	48.6	0	0	0	0	0	0	0	0	0	0	0	0	0	0	0	0	0	0	0	0
0	0	0	0	0	0	0	0	0	0	0	0	0	0	0	PG	37.5	0	0	0	0	0	0	0	0	0	0	0	0	0	0	0	0	0	0	0	0
0	0	0	0	0	0	0	0	0	0	0	0	0	0	0	PG	36.7	0	0	0	0	0	0	0	0	0	0	0	0	0	0	0	0	0	0	0	0
0	0	0	0	0	0	0	0	0	0	0	0	0	0	0	PG	42.4	0	0	0	0	0	0	0	0	0	0	0	0	0	0	0	0	0	0	0	0

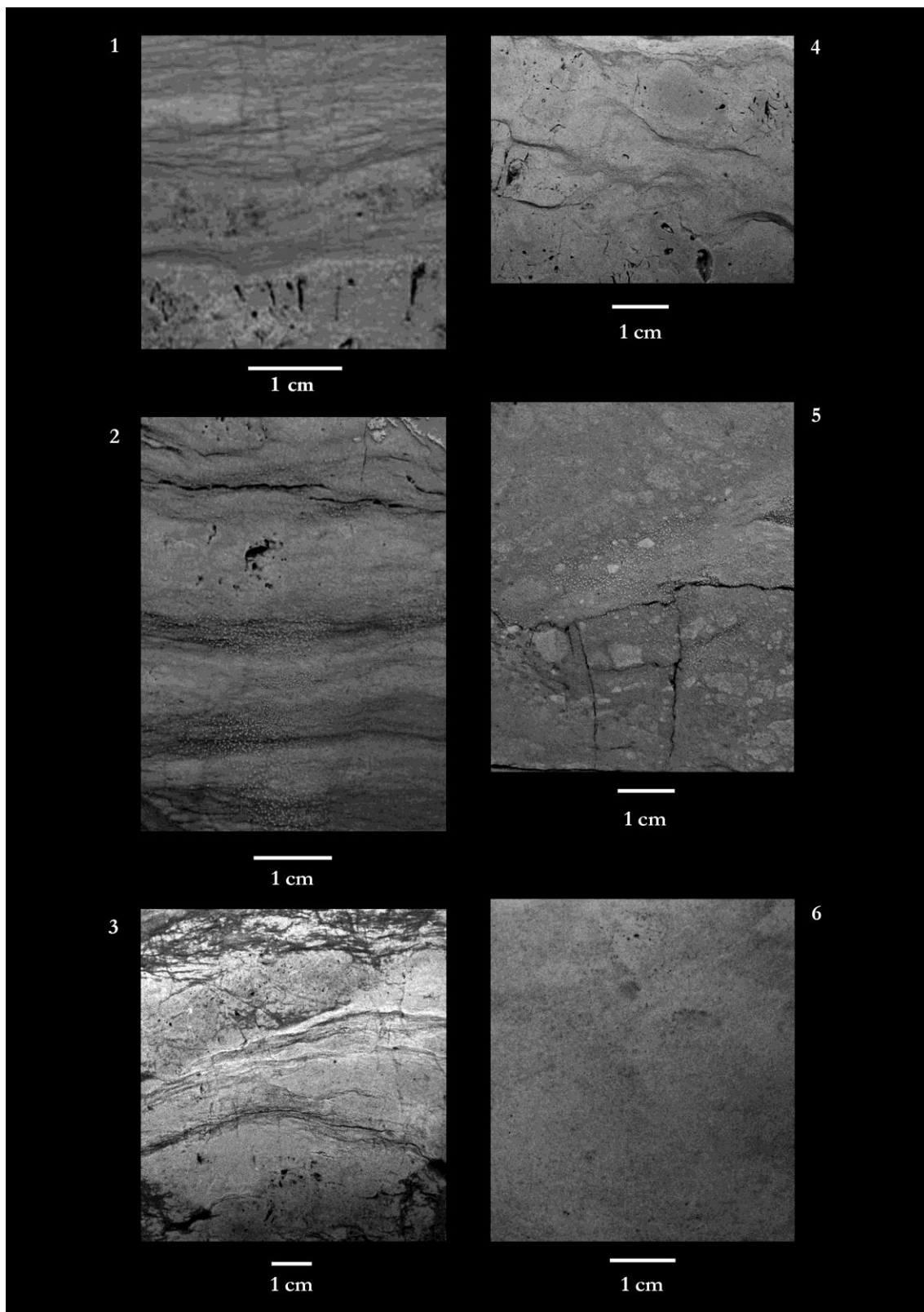
Appendix 5.12 Data used to build the frequency distribution and Jablonski plot target.
 LM: Langport Member, PP: Pre-Planorbis Zone, PZ: Planorbis zone, LZ: Liasicus zone.
 Average values **in bold**.

<i>Plagiostoma</i>					Chlamys				
LM	PP	PZ	LZ	AZ	LM	PP	PZ	LZ	AZ
33.2	36.7	24.4	51.9	21.8	LiasiLias	4.56	10.21	29.38	3.81
	29.7	25.0	65.5	143.6	8.46	2.90	11.40	36.35	
	44.0	36.7	18.0	142.4	11.33	3.43	15.82	28.95	
		37.5	31.4	62.0	26.25	2.44			
		42.4	69.4		10.34	33.92			
		48.4	15.5		3.24	14.69			
		48.6	109.5			28.82			
		50.0	24.0			7.15			
		55.2	115.1			11.49			
		56.6			11.922	12.156	12.4764	31.56	3.811
		56.7							
		60.7							
		65.9							
33.1783062	36.7723	46.77857	55.58	92.5					

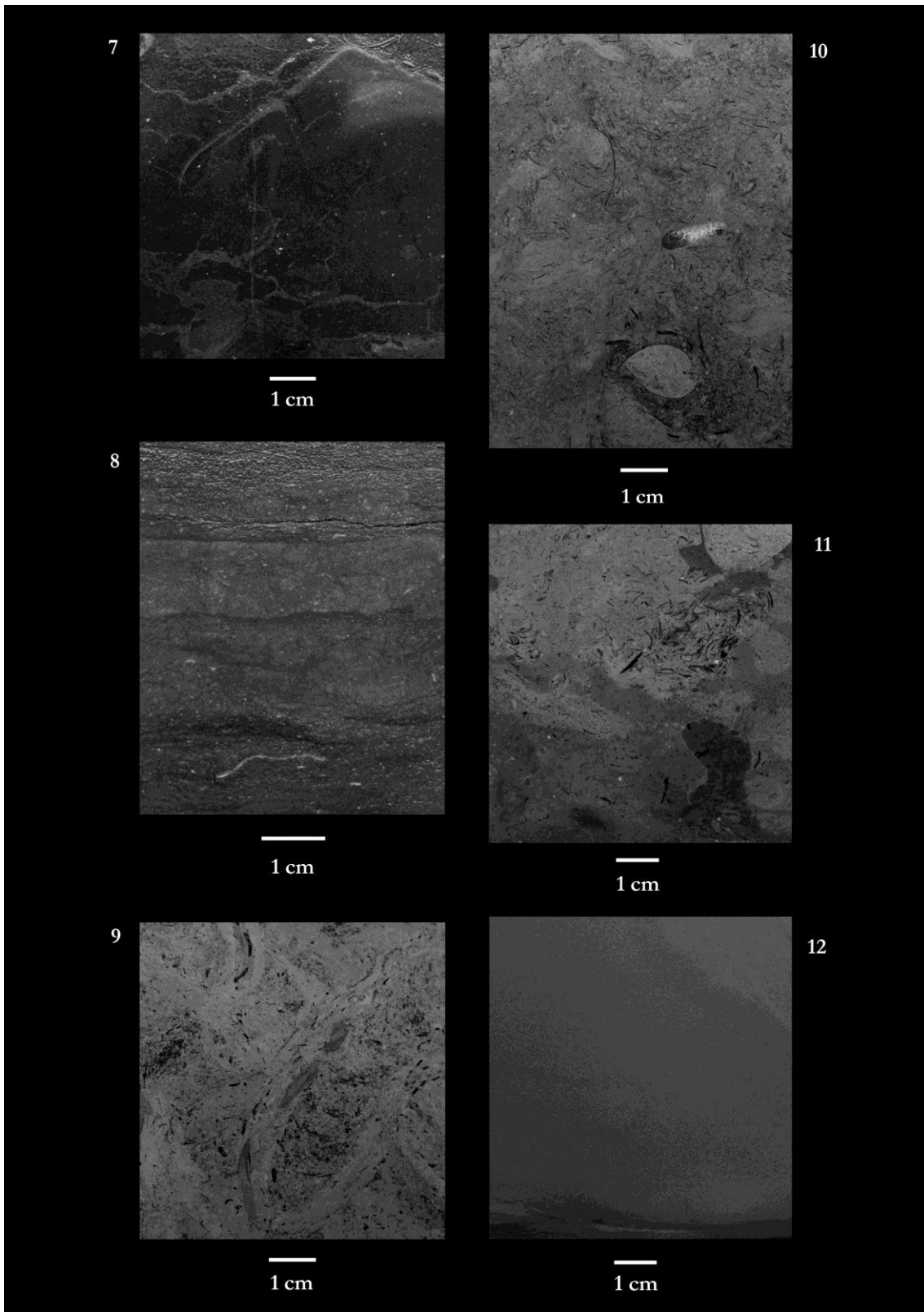
Appendix 5.12 (*Continuation*) Data used to build the frequency distribution and Jablonski plot target. LM: Langport Member, PP: Pre-Planorbis Zone, PZ: Planorbis zone, LZ: Liasicus zone. Average values **in bold**.

<i>Modiolus</i>					<i>Liostrea</i>				
LM	PP	PZ	LZ	AZ	LM	PP	PZ	LZ	AZ
6.69	1.31	2.55	1.95	2.75	7.90	4.33	9.37	11.75	7.72
7.65	1.37	3.93	1.98	3.42	8.87	6.23	9.42	14.05	8.00
4.71	1.46	3.99	2.37	5.85	7.19	10.55	14.26	8.03	
	2.38	4.18	3.64	6.46	7.34	10.93	15.70	13.75	
	2.46	4.30	3.65	10.04	7.43	11.25	17.49	14.32	
	2.58	4.45	3.78	10.71	7.67	11.45	17.64	14.89	
	2.64	4.71	4.33		8.28	11.93	17.75	14.97	
	2.64	5.00	4.82		9.35	12.11	18.71	16.96	
	3.00	5.10	4.95		9.61	13.39	19.70	17.08	
	3.09	5.19	7.58		9.93	13.50	19.77	20.04	
	3.15	5.28	11.97		10.76	13.52	20.40	21.14	
	3.52	5.39	13.29		10.90	14.16	21.51	21.48	
	3.76	5.41	15.56		11.52	14.21	22.25	27.36	
	4.27	5.69	16.47		12.82	14.45	24.11	39.38	
	4.58	5.93			12.85	14.63	24.37		
	4.61	5.97			12.89	14.78	25.69		
	4.75	5.99			14.17	14.87	26.27		
	5.13	6.07			14.33	15.32	27.60		
	5.58	6.14			14.71	15.34	30.40		
	5.63	6.21			15.66	15.61	34.21		
	5.66	6.46			17.20	15.68	36.00		
	5.76	6.99			17.80	16.11	36.33		
	6.07	7.00			18.11	16.52			
	6.36	7.54			18.23	16.91			
	6.51	7.73			18.29	17.81			
	6.56	7.74			18.38	17.83			
	6.66	8.00			18.43	18.33			
	6.79	8.71			19.01	19.11			
	6.80	9.18			19.14	19.19			
	6.94	9.80			19.27	19.29			
	7.00	10.69			20.25	22.57			
	7.24	11.10			20.80	23.89			
	7.30	11.35			22.66	30.26			
	7.48	12.82			22.97	30.53			
	7.53	20.45			23.25	40.47			
	7.68				23.93				
	8.02				24.20				
	8.07				24.45				
	8.12				24.88				
	8.17				24.97				
	8.23				25.90				
	8.24				26.02				
	8.56				26.27				
	8.57				26.58				
	8.62				27.21				
	8.70				28.10				
	8.70				28.35				
	9.02				29.30				
	9.13				29.45				
	9.24				32.66				
	9.31				33.91				
	9.45				34.00				
	9.57				35.89				
	9.58				40.48				
	9.82				41.22				
					8.39	19.81	16.72	22.54	17.51
9.90									
10.20									
10.20									
6.35	7.61	7.06	6.88	6.54					

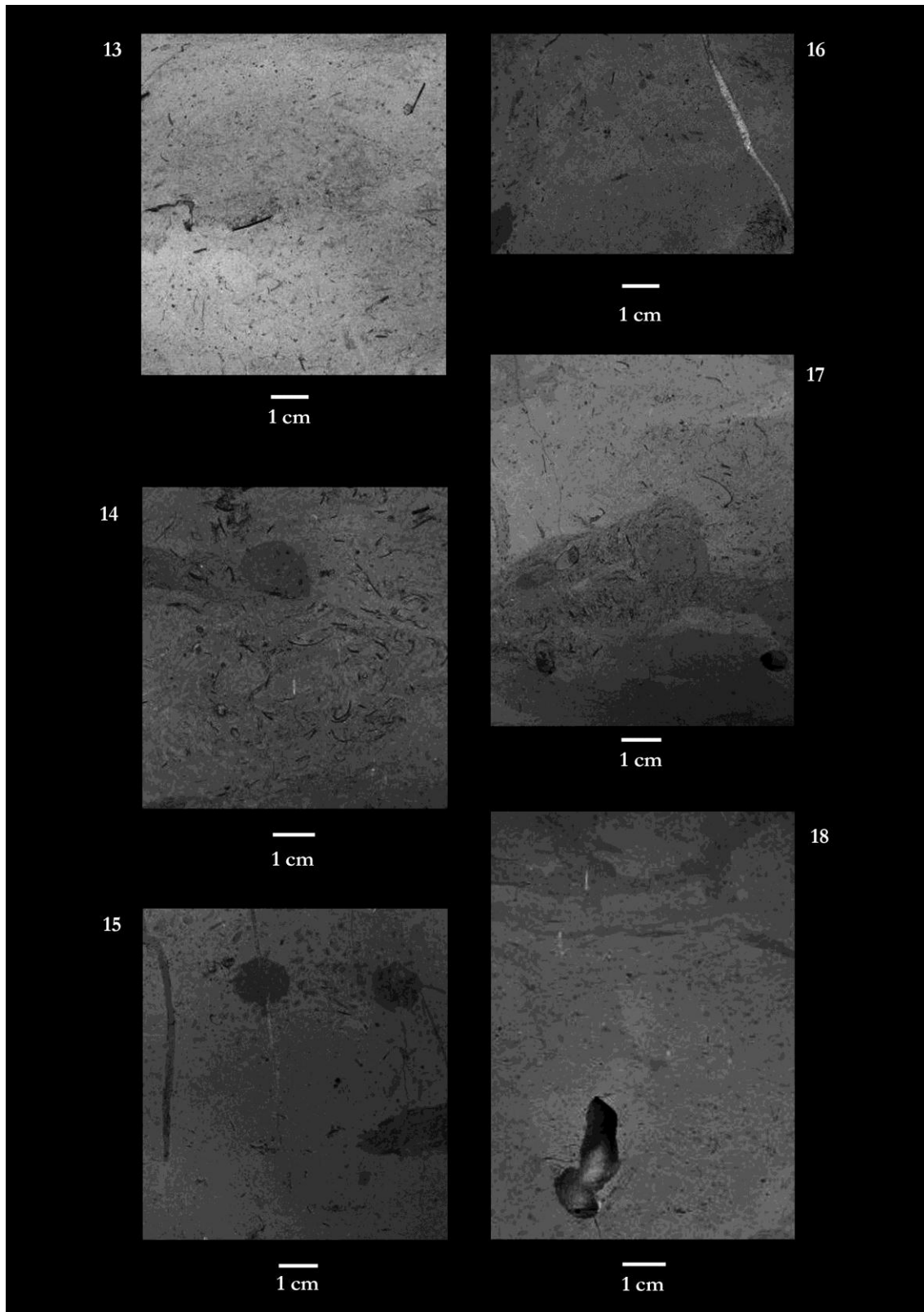
Appendix 5.14 Trace Fossils: Plates 1 to 6: LM1–LM6; LM: the Langport Member



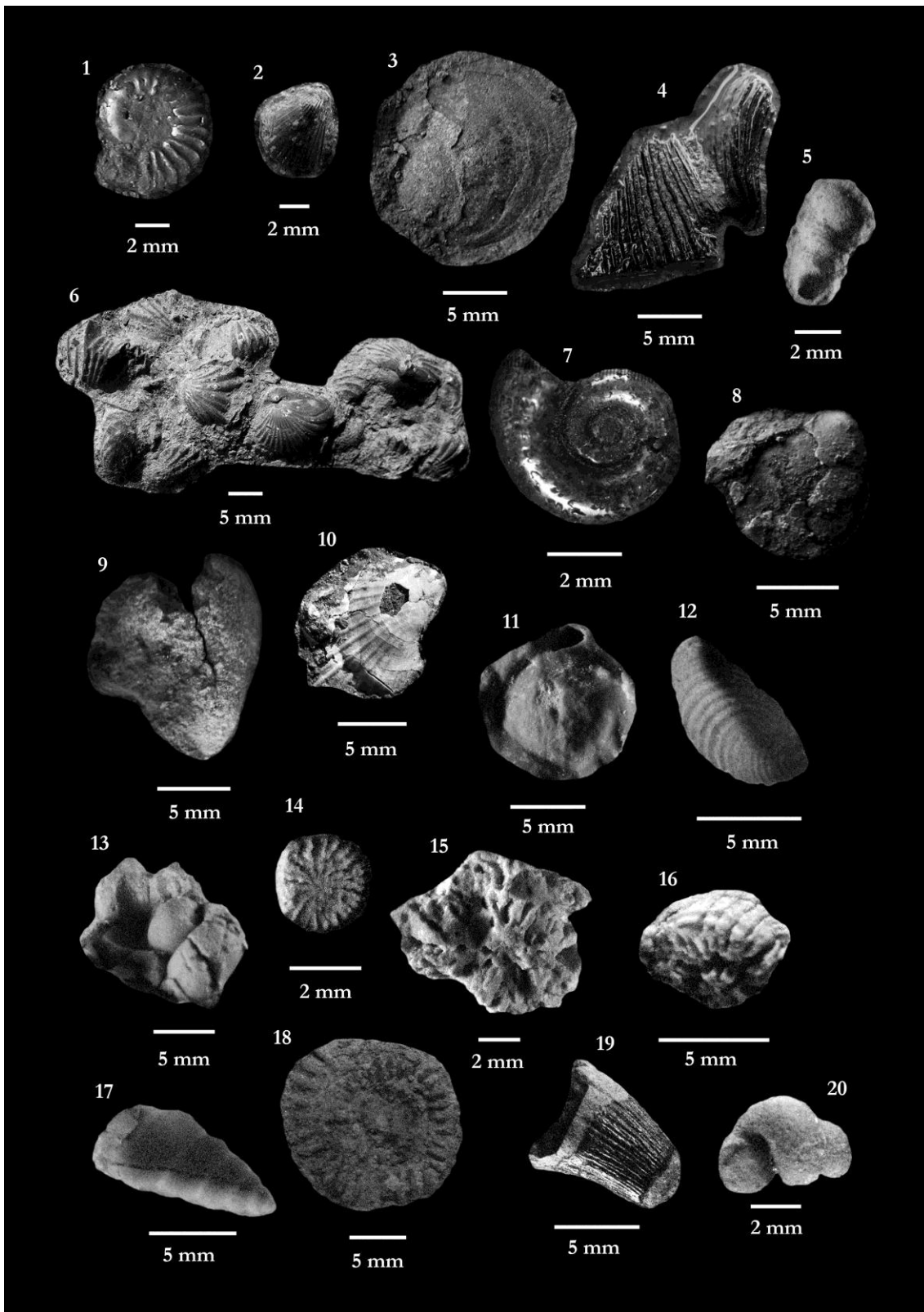
Appendix 5.14 (continuation) Plates 7 to 9: PPZ1-PPZ3; the Pre-Planorbis Zone. Plates 10 to 12: PZ1-PZ3; Planorbis Zone Plates.



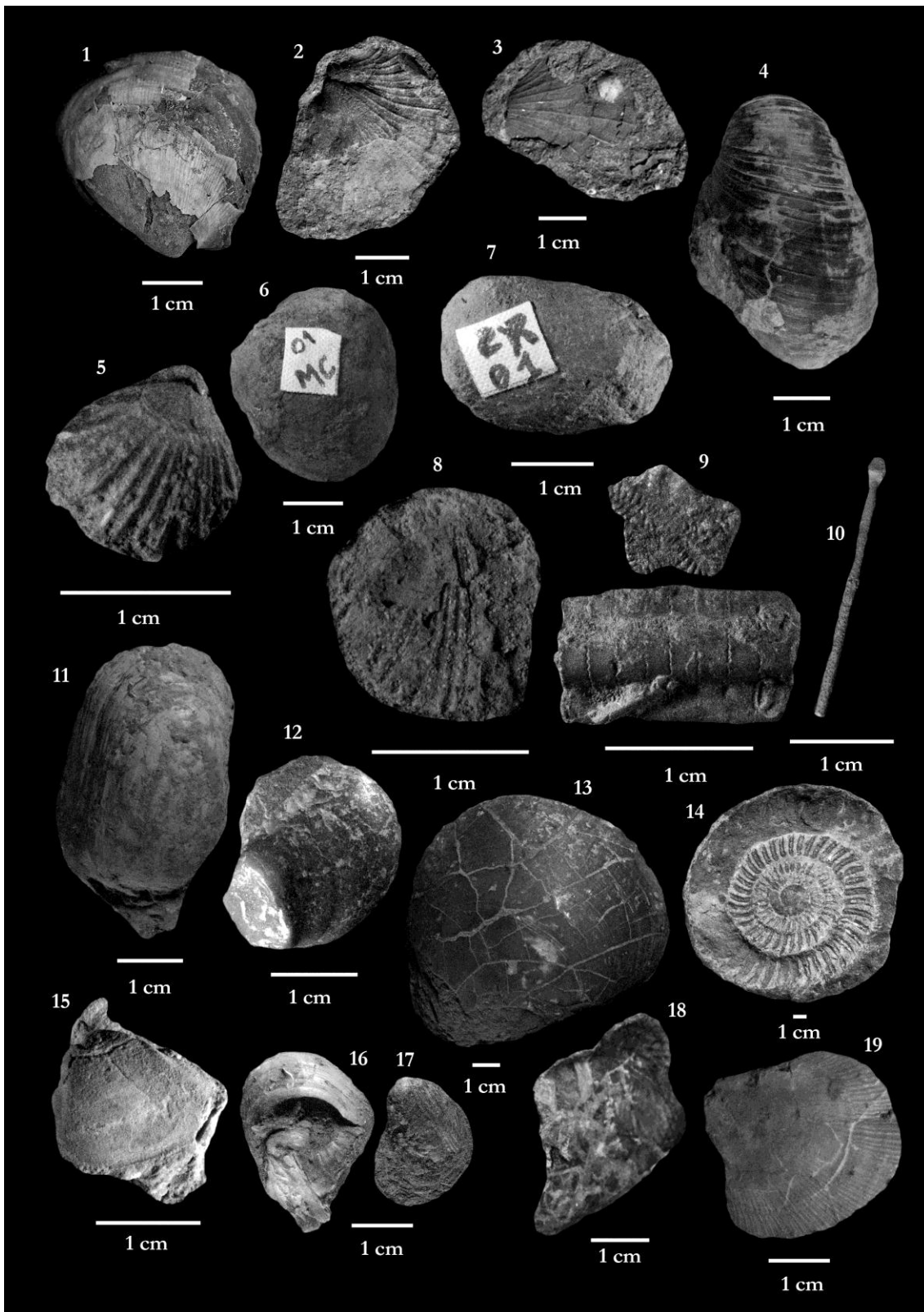
Appendix 5.14 (continuation) Plate 13 : PZ4. Planorbis Zone, 14-16: LZ1-LZ3; Angulata zone and Plates 17 to 18:AZ1-AZ2. Angulata zone



Appendix 5.15 Specimens found through Pinhay Bay section.



Appendix 5.16 Specimens found through Pinhay Bay section.



Appendix 5.15: 1. *Asaltites laqueus* (Quenstedt), 2. *Astarte* sp., 3. *Chlamys valoniensis* (Defrance), 4. *Pinna* sp., 5. *Modiolus* sp., 6. *Calcirhynchia calcaria* (Buckman), 7. *Asaltites laqueus* (Quenstedt), 8. *Pteromya langportensis* (Richardson and Tutcher), 9. *Isocyprina concentricum* (Moore), 10. *Chlamys valoniensis* (Defrance), 11. *Mesomiltha* sp., 12. *Isocyprina concentricum* (Moore), 13. *Pleurotomaria cognata* (Chapuis and Dewalque), 14. *Montivaltia* sp., 15. *Montivaltia* sp., 16. *Montivaltia* sp., 17. *Promathildia decorata* (Moore), 18. *Caloceras johnstoni* (Sowerby), 19. *Euryclidus* spp., 20. *Pseudokatosira undulata* (Benz).

Appendix 5.16: 1. *Plagiostoma punctatum* (Sowerby), 2. *Chlamys valoniensis* (Defrance), 3. *Oxytoma* sp., 4. *Gryphaea obliquata* (Sowerby), 5. *Calcirhynchia calcaria* (Buckman), 6. *Mactromya cardioides* (Phillips), 7. *Cardinia regularis* (Terquem), 8. *Pseudolimea duplicata* (Sowerby), 9. *Isocrinus psilonoti* (Quenstedt), 10. *Diademopsis tomesi* (Wright), 11. *Pholadomya* sp., 12. *Liostrea hisingeri* (Nilsson), 13. *Plagiostoma giganteum* (Sowerby), 14. *Scholethemia complanata*, 15. *Isocyprina concentricum* (Moore), 16. *Liostrea hisingeri* (Nilsson), 17. *Liostrea hisingeri* (Nilsson), 18. *Pleurotomaria cognata* (Chapuis and Dewalque), 19. *Chlamys valoniensis* (Defrance).

Appendix 6.1 List of taxa and abundance of each species recorded at each sample along the Larne section.

				Number sample																							
				1	2	3	4	5	6	7	8	9	10	11	12	13	14	15	16	17	18	19	20	21	22		
				Stratigraphic height (m)																							
Phyla	Class	Order	Family	Species	WF 1	WF 2	WF 3	WF 4	WF 5	WF 6	WF 7	WF 8	CM1	CM2	CM3	CM4	CM5	LM1	LM2	LM3	LM4	LM5	PPZ1	PPZ2	PPZ3	PPZ4	
Mollusca	Cephalopoda	Ammonoidea	Psiloceratidae	<i>Psiloceras erugatum</i> (Phillips)	0	0	0	0	0	0	0	0	0	0	0	0	0	0	0	0	0	0	0	0	0	1	
Mollusca	Cephalopoda	Ammonoidea	Psiloceratidae	<i>Psiloceras planorbis</i> (J. Sowerby)	0	0	0	0	0	0	0	0	0	0	0	0	0	0	0	0	0	0	0	0	0	0	
Mollusca	Cephalopoda	Ammonoidea	Psiloceratidae	<i>Psiloceras plicatulum</i> (Quenstedt)	0	0	0	0	0	0	0	0	0	0	0	0	0	0	0	0	0	0	0	0	0	0	
Mollusca	Cephalopoda	Ammonoidea	Psiloceratidae	<i>Caloceras johnstoni</i> (Sowerby)	0	0	0	0	0	0	0	0	0	0	0	0	0	0	0	0	0	0	0	0	0	0	
Mollusca	Cephalopoda	Ammonoidea	Psiloceratidae	<i>Alsatites</i> sp.	0	0	0	0	0	0	0	0	0	0	0	0	0	0	0	0	0	0	0	0	0	0	
Echinodermata	Crinoidea	Articulata	Isocrinidae	<i>Isocrinus angulatus</i> (Quenstedt)	0	0	0	0	0	0	0	0	0	0	0	0	0	0	0	0	0	0	0	3	1	2	
Mollusca	Gastropoda	Murchisoniina	Zygopleuridae	<i>Pseudokatosira undulata</i> (Benz)	0	0	0	0	0	0	0	0	0	0	0	0	0	0	0	0	0	0	0	0	0	0	
Echinodermata	Echinoidea	Pedinoida	Pedinidae	<i>Diademopsis tomesi</i> (Wright)	0	0	0	0	0	0	0	0	0	0	0	0	0	0	0	0	0	0	0	1	1	15	
Mollusca	Bivalvia	Nuculoidea	Nuculidae	<i>Palaeonucula navis</i> (Piette)	0	0	0	0	0	0	0	0	0	0	0	0	0	0	0	0	0	0	0	0	0	0	
Mollusca	Bivalvia	Pterioidea	Pteriidae	<i>Rhaetavicula contorta</i> (Portlock)	3	79	1	66	12	2	4	153	0	0	0	0	0	0	0	0	0	0	0	0	0	0	
Mollusca	Bivalvia	Arcoida	Parallelodontidae	<i>Cosmetodon hettangiensis</i> (Terquem)	0	1	0	0	0	0	0	0	0	0	0	0	0	0	1	0	0	0	0	0	0	0	
Mollusca	Bivalvia	Pectinoidea	Pectinidae	<i>Chlamys valoniensis</i> (Defrance)	0	0	0	1	0	0	0	0	0	0	0	0	0	0	0	0	0	0	0	0	0	4	
Mollusca	Bivalvia	Mytiloidea	Mytilidae	<i>Mytilus cloacinus</i> (Tutcher)	0	0	0	1	1	0	0	0	3	0	0	0	0	0	0	0	0	0	0	0	0	0	
Mollusca	Bivalvia	Limoida	Limidae	<i>Plagiostoma giganteum</i> (J. Sowerby)	0	0	0	0	0	0	0	0	0	0	0	0	0	0	0	0	0	0	0	0	0	0	
Mollusca	Bivalvia	Limoida	Limidae	<i>Plagiostoma punctatum</i> (J. Sowerby)	0	0	0	0	0	1	0	0	0	0	0	0	0	0	0	0	0	6	0	0	0	0	
Mollusca	Bivalvia	Pectinoidea	Oxytomidae	<i>Oxytoma</i> sp.	0	0	0	0	0	0	1	0	0	0	0	0	0	0	0	0	0	0	0	0	1	2	
Mollusca	Bivalvia	Pectinoidea	Anomiidae	<i>Placunopsis alpina</i> (Winkler)	0	0	0	0	0	0	0	0	6	0	0	0	0	0	0	0	0	0	0	0	0	0	
Mollusca	Bivalvia	Mytiloidea	Mytilidae	<i>Mytilus</i> sp.	0	0	0	0	0	0	0	0	0	0	0	0	0	0	0	0	0	0	0	0	0	0	
Mollusca	Bivalvia	Pterioidea	Inoceramidae	<i>Pseudomytiloides dubius</i> (Sowerby)	0	0	0	0	0	0	0	0	0	0	0	0	0	0	0	0	0	0	0	0	0	0	
Mollusca	Bivalvia	Pterioidea	Gryphaeidae	<i>Liostrrea</i> sp.	0	0	0	0	0	0	0	0	0	0	0	0	0	4	0	0	5	2	2	7	0	1	
Mollusca	Bivalvia	Limoida	Limidae	<i>Pseudolimea duplicata</i> (Sowerby)	0	0	0	0	0	0	0	0	0	0	0	0	0	0	0	0	0	0	0	0	0	0	
Mollusca	Bivalvia	Nuculanoida	Yoldiidae	<i>Rollieria bronni</i> (Ander)	0	0	0	0	0	0	0	0	0	0	0	0	0	0	0	0	0	0	0	0	0	0	
Mollusca	Bivalvia	Pholadomyoidea	Permophoridae	<i>Permophorus elongatus</i> (Moore)	0	4	0	0	0	0	0	0	0	0	0	0	0	0	0	0	0	0	0	0	0	0	
Mollusca	Bivalvia	Mytiloidea	Mytilidae	<i>Modiolus hillanus</i> (J. Sowerby)	0	0	1	0	0	0	0	0	0	0	0	0	0	0	0	0	0	0	0	0	0	0	
Mollusca	Bivalvia	Pterioidea	Bakevelliidae	<i>Gervillella</i> sp.	0	0	1	0	0	0	0	0	0	0	0	0	0	0	0	0	0	0	0	0	0	0	
Mollusca	Bivalvia	Mytiloidea	Mytilidae	<i>Modiolus</i> sp.	0	0	0	0	3	0	1	0	0	4	0	3	0	0	0	0	0	0	0	0	1	0	0
Mollusca	Bivalvia	Mytiloidea	Mytilidae	<i>Modiolus minimus</i> (J. Sowerby)	0	0	0	0	0	0	0	0	0	0	0	0	0	0	0	0	0	0	0	3	0	32	14
Mollusca	Bivalvia	Mytiloidea	Mytilidae	<i>Modiolus ventricosus</i> (Roener)	0	0	0	0	0	0	0	0	0	0	0	0	0	0	0	0	0	0	0	0	0	0	0
Mollusca	Bivalvia	Pholadomyoidea	Permophoridae	<i>Myoconcha</i> sp.	0	0	0	0	0	0	0	0	0	0	0	0	0	0	0	0	0	0	0	0	0	0	
Mollusca	Bivalvia	Nuculanoida	Nuculanidae	<i>Dacryomya</i> sp.	0	9	0	0	0	0	1	0	0	0	0	0	0	0	0	0	0	0	0	0	0	0	0
Mollusca	Bivalvia	Nuculanoida	Nuculanidae	<i>Ryderia</i> sp.	0	0	0	0	0	0	0	0	0	0	0	0	0	0	0	0	0	0	0	1	0	1	
Mollusca	Bivalvia	Nuculanoida	Malletiidae	<i>Palaeoneilo elliptica</i> (Goldfuss)	0	0	0	0	0	0	0	0	0	0	0	0	0	0	0	0	0	0	0	0	0	0	
Mollusca	Bivalvia	Carditoida	Cardiniidae	<i>Cardinia regularis</i> (Terquem)	3	1	0	0	4	0	1	0	0	0	0	0	0	3	3	3	0	7	4	1	4	4	
Mollusca	Bivalvia	Veneroidea	Arctiidae	<i>Isocyprina concentricum</i> (Moore)	0	3	0	0	0	0	1	0	0	1	0	1	0	0	0	0	0	0	0	0	0	0	
Mollusca	Bivalvia	Veneroidea	Cardiidae	<i>Protocardia rhaetica</i> (Merian)	0	2	0	0	0	1	0	0	0	0	0	0	0	0	0	0	0	0	0	0	0	0	
Mollusca	Bivalvia	Veneroidea	Cardiidae	<i>Protocardia philippiana</i> (Dunker)	0	0	0	0	0	0	0	0	0	0	0	2	0	28	9	3	0	7	0	1	0	0	
Mollusca	Bivalvia	Pholadomyoidea	Pholadomyidae	<i>Pteromya crowcombeia</i> (Moore)	0	0	6	0	11	2	8	3	3	0	0	3	16	0	0	0	0	0	0	0	0	0	
Mollusca	Bivalvia	Pholadomyoidea	Pholadomyidae	<i>Pteromya langportensis</i> (Richardson and Tutcher)	0	0	0	0	0	0	0	0	0	0	0	0	0	0	4	25	1	7	1	0	1	1	
Mollusca	Bivalvia	Carditoida	Astartidae	<i>Astarte</i> sp.	0	0	0	0	0	0	0	0	0	0	0	0	0	0	0	0	0	0	0	0	0	1	
Mollusca	Bivalvia	Pholadomyoidea	Pleuromyidae	<i>Pleuromya</i> sp.	0	0	0	0	0	0	0	0	0	0	0	0	0	0	0	3	0	6	1	0	0	0	
Mollusca	Bivalvia	Veneroidea	Mactromyidae	<i>Mactromya cardioides</i> (Phillips)	0	0	0	0	0	0	0	0	0	0	0	0	0	0	0	0	0	0	0	0	0	0	
Mollusca	Bivalvia	Carditoida	Cardiniidae	<i>Cardinia</i> sp.	0	0	0	0	0	0	0	0	0	0	0	0	0	0	0	0	0	0	0	0	0	0	

Appendix 6.1 (continuation) List of taxa and abundance of each species recorded at each sample along the Larne section.

				Number sample	23	24	25	26	27	28	29	30	31	32	33	34	35	36
				Stratigraphic height (m)	14.8	15.6	17.8	20	22.8	24	25	28.2	30	33	35	38	41	45
Phyla	Class	Order	Famliy	Species	PZ1	PZ2	PZ3	PZ4	PZ5	PZ6	PZ7	PZ8	LZ1	LZ2	LZ3	LZ4	LZ5	LZ6
Mollusca	Cephalopoda	Ammonoidea	Psiloceratidae	<i>Psiloceras erugatum</i> (Phillips)	0	0	0	0	0	0	0	0	0	0	0	0	0	0
Mollusca	Cephalopoda	Ammonoidea	Psiloceratidae	<i>Psiloceras planorbis</i> (J. Sowerby)	5	8	0	0	0	0	0	0	0	0	0	0	0	0
Mollusca	Cephalopoda	Ammonoidea	Psiloceratidae	<i>Psiloceras plicatulum</i> (Quenstedt)	0	0	6	7	1	0	0	0	0	0	0	0	0	0
Mollusca	Cephalopoda	Ammonoidea	Psiloceratidae	<i>Caloceras johnstoni</i> (Sowerby)	0	0	0	0	0	1	6	1	0	0	0	0	0	0
Mollusca	Cephalopoda	Ammonoidea	Psiloceratidae	<i>Alsatites</i> sp.	0	0	0	0	0	0	0	0	1	1	0	0	3	0
Echinodermata	Crinoidea	Articulata	Isocrinidae	<i>Isocrinus angulatus</i> (Quenstedt)	1	0	0	2	2	1	1	0	4	2	17	20	0	1
Mollusca	Gastropoda	Murchisoniina	Zygopleuridae	<i>Pseudokatosira undulata</i> (Benz)	0	1	0	4	1	0	4	3	0	0	0	0	0	0
Echinodermata	Echinoidea	Pedinoidea	Pedinidae	<i>Diademopsis tomesi</i> (Wright)	5	4	0	1	2	1	4	8	1	0	1	7	0	5
Mollusca	Bivalvia	Nuculoidea	Nuculidae	<i>Palaeonucula navis</i> (Piette)	0	0	0	0	2	0	0	0	3	7	6	0	8	0
Mollusca	Bivalvia	Pterioidea	Pteriidae	<i>Rhaetavicula contorta</i> (Portlock)	0	0	0	0	0	0	0	0	0	0	0	0	0	0
Mollusca	Bivalvia	Arcoidea	Parallelodontidae	<i>Cosmetodon hettangiensis</i> (Terquem)	1	0	0	0	0	0	0	0	0	0	0	0	0	0
Mollusca	Bivalvia	Pectinoidea	Pectinidae	<i>Chlamys valoniensis</i> (Defrance)	0	0	0	1	1	0	0	4	0	1	0	0	0	0
Mollusca	Bivalvia	Mytiloidea	Mytilidae	<i>Mytilus cloacinus</i> (Tutcher)	0	0	0	0	0	0	0	0	0	0	0	0	0	0
Mollusca	Bivalvia	Limoida	Limidae	<i>Plagiostoma giganteum</i> (J. Sowerby)	0	1	1	0	9	0	0	2	3	18	4	9	4	0
Mollusca	Bivalvia	Limoida	Limidae	<i>Plagiostoma punctatum</i> (J. Sowerby)	0	0	0	0	0	0	0	0	0	0	0	0	0	0
Mollusca	Bivalvia	Pectinoidea	Oxytomidae	<i>Oxytoma</i> sp.	0	0	0	1	0	0	0	0	0	0	0	0	0	0
Mollusca	Bivalvia	Pectinoidea	Anomiidae	<i>Placunopsis alpina</i> (Winkler)	0	0	0	0	0	0	0	0	0	0	0	0	0	0
Mollusca	Bivalvia	Mytiloidea	Mytilidae	<i>Mytilus</i> sp.	0	0	0	1	8	0	0	0	0	0	0	0	0	0
Mollusca	Bivalvia	Pterioidea	Inoceramidae	<i>Pseudomytiloides dubius</i> (Sowerby)	0	0	0	0	0	0	0	0	0	6	15	0	0	0
Mollusca	Bivalvia	Pterioidea	Gryphaeidae	<i>Liostraea</i> sp.	0	0	0	3	3	0	0	0	8	2	1	3	0	0
Mollusca	Bivalvia	Limoida	Limidae	<i>Pseudolimea duplicata</i> (Sowerby)	0	0	0	0	0	0	0	0	0	1	0	0	1	0
Mollusca	Bivalvia	Nuculanoida	Yoldiidae	<i>Rolleria bronni</i> (Andler)	0	0	0	0	0	0	0	0	0	0	1	0	0	9
Mollusca	Bivalvia	Pholadomyoidea	Permophoridae	<i>Permophorus elongatus</i> (Moore)	0	0	0	0	0	0	0	0	0	0	0	0	0	0
Mollusca	Bivalvia	Mytiloidea	Mytilidae	<i>Modiolus hillanus</i> (J. Sowerby)	0	0	0	0	1	0	0	1	0	0	0	0	0	0
Mollusca	Bivalvia	Pterioidea	Bakevelliidae	<i>Gervillella</i> sp.	0	0	0	0	0	0	0	0	0	0	0	0	0	0
Mollusca	Bivalvia	Mytiloidea	Mytilidae	<i>Modiolus</i> sp.	7	0	0	0	0	0	0	46	0	0	0	1	0	0
Mollusca	Bivalvia	Mytiloidea	Mytilidae	<i>Modiolus minimus</i> (J. Sowerby)	96	41	111	4	0	0	2	0	0	0	0	0	0	0
Mollusca	Bivalvia	Mytiloidea	Mytilidae	<i>Modiolus ventricosus</i> (Roener)	43	32	34	0	0	2	7	0	1	0	1	1	0	0
Mollusca	Bivalvia	Pholadomyoidea	Permophoridae	<i>Myoconcha</i> sp.	0	1	0	0	0	0	0	0	0	0	0	0	0	0
Mollusca	Bivalvia	Nuculanoida	Nuculanidae	<i>Dacryomya</i> sp.	0	0	0	0	0	0	0	0	0	0	0	0	0	0
Mollusca	Bivalvia	Nuculanoida	Nuculanidae	<i>Rydera</i> sp.	0	0	0	0	0	0	1	0	0	0	0	0	0	0
Mollusca	Bivalvia	Nuculanoida	Malletiidae	<i>Palaeoneilo elliptica</i> (Goldfuss)	0	0	0	7	2	5	6	0	0	0	5	0	0	0
Mollusca	Bivalvia	Carditoida	Cardiniidae	<i>Cardinia regularis</i> (Terquem)	0	0	1	1	5	1	7	78	11	2	7	3	0	0
Mollusca	Bivalvia	Veneroidea	Arctiidae	<i>Isocyprina concentricum</i> (Moore)	0	0	0	0	0	0	0	0	0	0	0	0	0	0
Mollusca	Bivalvia	Veneroidea	Cardiidae	<i>Protocardia rhaetica</i> (Merian)	0	0	0	0	0	0	0	0	0	0	0	0	0	0
Mollusca	Bivalvia	Veneroidea	Cardiidae	<i>Protocardia philippiana</i> (Dunker)	0	0	0	0	0	0	0	0	0	0	0	0	0	0
Mollusca	Bivalvia	Pholadomyoidea	Pholadomyidae	<i>Pteromya crowcombeia</i> (Moore)	0	0	0	0	0	0	0	0	0	0	0	0	0	0
Mollusca	Bivalvia	Pholadomyoidea	Pholadomyidae	<i>Pteromya langportensis</i> (Richardson and Tutcher)	0	0	0	0	2	0	0	0	0	0	0	0	0	0
Mollusca	Bivalvia	Carditoida	Astartidae	<i>Astarte</i> sp.	0	0	0	1	0	0	0	0	0	0	0	0	0	0
Mollusca	Bivalvia	Pholadomyoidea	Pleuromyidae	<i>Pleuromya</i> sp.	0	0	0	0	0	0	0	0	0	0	1	0	0	0
Mollusca	Bivalvia	Veneroidea	Mactromyidae	<i>Mactromya cardioides</i> (Phillips)	0	0	0	0	0	0	0	0	0	0	2	0	1	0
Mollusca	Bivalvia	Carditoida	Cardiniidae	<i>Cardinia</i> sp.	0	0	0	0	0	0	0	0	0	0	0	0	0	21

Appendix 6.2 Summary of palaeoecological parameters estimated in this study. N = number, GS = Lithostratigraphy, SC= Sample cog, H = Height (mm), R = Richness, MR = Mean Richness, A = Abundance, K = Kurtosis, B_W = Whittaker index, B_T = Wilson-Shmida index, MF = modes of life, GM = Geomean of body size, *n* = sample size used for estimate the geomean, Min = Minimum geomean, Max. = maximum geomean, σ^2 = Variance, NM = mean values of null model, (*) = Not recorded.

																	Body size parameters				
N	L	SC	H (m)	R	MR	A	K	B _W	B _T	MF	GM	<i>n</i>	Min.	Max.	σ^2	NM					
1	WF	I- W-1B	-14.2	2	1.90	6	17.29	7.8	4.4	2	5.64	4	4.16	6.50	1.06	0.70					
2	WF	I-W- 3A	-13	7	5.20	99	38.57	6.27	7.27	4	8.72	76	3.36	15.25	7.35	11.29					
3	WF	I-W- 4A	-12.1	4	2.82	9	33.80	10	17.143	3	8.12	14	4.37	21.72	19.83	2.12					
4	WF	W1A	-6.4	3	2.01	68	39.96	9	20	1	8.73	47	3.52	28.43	16.83	6.03					
5	WF	W2A1	-5	5	4.12	31	13.96	7.88	26.66	3	7.16	29	4.50	15.14	5.07	3.98					
6	WF	W3A1	-3.6	4	3.07	6	10.21	6.27	32.72	2	8.44	38	4.31	17.10	10.80	4.96					
7	WF	W4A1	-2.2	7	4.65	17	22.76	7.8	31.11	4	5.67	23	2.79	11.13	3.32	3.22					
8	WF	W5A1	-0.8	2	1.76	156	39.97	15	36	2	10.24	75	3.37	18.55	10.43	11.12					
9	CM	W6A1	0	3	2.69	12	17.57	15	40	2	3.25	5	2.43	5.20	1.28	0.86					
10	CM	W6-1A1	0.6	2	1.70	5	35.11	19	40	2	7.23	12	1.93	12.50	11.71	1.83					
11	CM	W6-2A1	1	0	0.00	0	0.00	9	40	0	*	*	*	*	*	0.00					
12	CM	W6-3A1	2	4	3.21	9	10.09	15	40	2	14.05	7	8.98	19.68	14.10	1.16					
13	CM	TopCot	2.9	1	1.00	16	40.00	25.66	40	1	11.17	33	2.13	27.96	60.42	4.43					
14	LM	Cot-Lan	3.2	2	1.85	32	38.29	15	40	2	13.41	27	5.03	25.31	19.56	3.76					
15	LM	L1B	4	3	2.42	13	31.28	12.33	40	2	15.67	12	4.95	33.48	58.41	1.84					
16	LM	L2B	4.8	3	2.70	10	11.07	10.42	40	1	15.82	11	7.86	28.45	47.41	1.72					
17	LM	L2-5B	5.4	4	3.45	36	34.78	9	40	2	17.78	44	7.29	38.74	34.52	5.64					
18	LM	L3A	6.2	4	3.22	16	15.56	7.88	35.55	3	16.15	16	7.12	23.05	13.65	2.37					
19	PP	10 PP	7.1	5	4.32	25	7.77	4.71	31.42	3	17.30	27	7.36	37.79	79.90	3.65					
20	PP	11 PP	9.1	9	5.94	20	15.10	4.71	31.42	6	15.71	15	3.74	28.26	58.58	2.26					
21	PP	12 PP	11.95	5	3.11	36	39.69	4	25	5	3.98	40	2.01	14.14	4.91	5.21					
22	PP	13 PP	12.9	11	7.61	46	13.88	3.4	24.44	8	6.69	25	2.65	15.31	15.29	4.43					
23	PZ	14 PZ	14.2	7	5.57	158	27.10	4.71	25.7	5	4.27	61	2.00	14.68	5.02	8.15					
24	PZ	15 PZ	15.6	7	5.24	88	17.42	5.66	30	5	6.54	44	2.80	24.28	23.00	6.13					
25	PZ	16 PZ	17.8	5	3.86	153	32.88	3.7	30.58	4	5.82	59	2.67	14.20	3.76	7.55					
26	PZ	17 PZ	20	12	8.22	33	6.41	2.2	25.6	9	6.51	16	1.90	23.38	44.30	3.08					
27	PZ	19 PZ	22	13	9.14	39	8.27	3.21	27.36	10	13.28	15	2.06	30.50	105.06	2.50					
28	PZ	20 PZ	24	6	4.10	11	22.50	4.3	26.66	6	14.35	13	3.41	68.35	338.99	2.13					
29	PZ	21 PZ	26.2	9	7.07	38	3.19	3.7	25.88	7	8.13	27	2.81	19.10	14.84	4.07					
30	PZ	22 PZ	28.1	8	6.15	143	22.23	4	30	6	12.39	75	2.77	28.52	35.01	11.22					
31	LZ	1 LZ	30.1	8	5.93	32	12.88	3.7	28.23	8	17.84	4	3.57	59.61	775.61	0.71					
32	LZ	2 LZ	32.6	9	6.47	40	23.12	2.8	28.57	6	31.99	4	3.82	96.32	1880.69	0.70					
33	LZ	3 LZ	35	12	8.68	61	10.29	3.21	29.47	9	21.03	8	6.66	50.69	238.50	1.30					
34	LZ	4 LZ	38	7	5.45	44	20.76	5.66	26.66	6	6.61	7	2.69	11.93	9.86	1.15					
35	LZ	5 LZ	40.9	5	3.81	17	19.45	7.88	20	5	15.14	6	3.21	53.68	381.99	0.99					
36	LZ	6 LZ	45	3	3.28	36	25.47	*	*	4	8.76	7	4.52	17.38	24.83	1.15					

Appendix 6.3

Relative species abundance (%) by Lithostratigraphy. WF: Westbury Formation, CM: Cotham Member, LM: Langport Member, PPZ: Pre-Planorbis Zone, PZ: Planorbis Zone, LZ: Liasicus Zone.

Species	WF	Species	CM	Species	LM	Species	PPZ	Species	PZ	Species	LZ
<i>R. contorta</i>	81.633	<i>P. crowcombeia</i>	52.381	<i>P. philippiana</i>	43.925	<i>M. minimus</i>	38.583	<i>M. minimus</i>	38.311	<i>I. angulatus</i>	19.1304
<i>P. crowcombeia</i>	7.653	<i>Modiolus</i> sp.	16.667	<i>P. tatei</i>	28.037	<i>D. tomesi</i>	13.386	<i>M. ventricosus</i>	17.798	<i>P. giganteum</i>	16.5217
<i>Dacryomya</i> sp.	2.551	<i>P. alpina</i>	14.286	<i>Liostrea</i> sp.	10.280	<i>C. regularis</i>	12.598	<i>C. regularis</i>	14.027	<i>P. navis</i>	10.4348
<i>C. regularis</i>	2.296	<i>M. cloacinus</i>	7.143	<i>C. regularis</i>	8.411	<i>Liostrea</i> sp.	7.874	<i>Modiolus</i> sp.	7.994	<i>C. regularis</i>	10
<i>P. elongatus</i>	1.020	<i>I. concentricum</i>	4.762	<i>P. punctatum</i>	5.607	<i>P. tatei</i>	7.087	<i>D. tomesi</i>	3.771	<i>P. dubius</i>	9.13043
<i>Modiolus</i> sp.	1.020	<i>P. philippiana</i>	4.762	<i>Pleuromya</i> sp.	2.804	<i>Pleuromya</i> sp.	5.512	<i>P. elliptica</i>	3.017	<i>Cardinia</i> sp.	9.13043
<i>I. concentricum</i>	1.020			<i>G. hettangiensis</i>	0.935	<i>I. angulatus</i>	4.724	<i>P. plicatulum</i>	2.112	<i>D. tomesi</i>	6.08696
<i>P. rhaetica</i>	0.765					<i>C. valoniensis</i>	3.150	<i>P. undulata</i>	1.961	<i>Liostrea</i> sp.	6.08696
<i>M. cloacinus</i>	0.510					<i>Oxytoma</i> sp.	2.362	<i>P. planorbis</i>	1.961	<i>R. bronni</i>	4.34783
<i>C. hettangiensis</i>	0.255					<i>Ryderia</i> sp.	1.575	<i>P. giganteum</i>	1.961	<i>Alsatites</i> sp.	2.17391
<i>C. valoniensis</i>	0.255					<i>P. erugatum</i>	0.787	<i>Mytilus</i> sp.	1.357	<i>P. elliptica</i>	2.17391
<i>P. punctatum</i>	0.255					<i>Modiolus</i> sp.	0.787	<i>C. johnstoni</i>	1.207	<i>M. ventricosus</i>	1.30435
<i>Oxytoma</i> sp.	0.255					<i>P. philippiana</i>	0.787	<i>I. angulatus</i>	1.056	<i>M. cardioides</i>	1.30435
<i>M. hillanus</i>	0.255					<i>Astarte</i> sp.	0.787	<i>Liostrea</i> sp.	0.905	<i>P. duplicata</i>	0.86957
<i>Gervillella</i> sp.	0.255							<i>C. valoniensis</i>	0.905	<i>C. valoniensis</i>	0.43478
								<i>P. navis</i>	0.302	<i>Modiolus</i> sp.	0.43478
								<i>P. tatei</i>	0.302	<i>Pleuromya</i> sp.	0.43478
								<i>M. hillanus</i>	0.302		
								<i>Ryderia</i> sp.	0.151		
								<i>Oxytoma</i> sp.	0.151		
								<i>Myoconcha</i> sp.	0.151		
								<i>G. hettangiensis</i>	0.151		
								<i>Astarte</i> sp.	0.151		

Appendix 6.4 Total species abundance by stratigraphy. WF: Westbury Formation, CM: Cotham Member, LM: Langport Member, PPZ: Pre-Planorbis Zone, PZ: Planorbis Zone, LZ: Liasicus Zone.

Taxa	WF	CM	LM	PPZ	PZ	LZ
<i>P. erugatum</i>	0	0	0	1	0	0
<i>P. planorbis</i>	0	0	0	0	13	0
<i>P. plicatulum</i>	0	0	0	0	14	0
<i>C. johnstoni</i>	0	0	0	0	8	0
<i>Alsatites</i> sp.	0	0	0	0	0	5
<i>I. angulatus</i>	0	0	0	6	7	44
<i>P. undulata</i>	0	0	0	0	13	0
<i>D. tomesi</i>	0	0	0	17	25	14
<i>P. navis</i>	0	0	0	0	2	24
<i>R. contorta</i>	320	0	0	0	0	0
<i>C. hettangiensis</i>	1	0	1	0	1	0
<i>C. valoniensis</i>	1	0	0	4	6	1
<i>M. cloacinus</i>	2	3	0	0	0	0
<i>P. giganteum</i>	0	0	0	0	13	38
<i>P. punctatum</i>	1	0	6	0	0	0
<i>Oxytoma</i> sp.	1	0	0	3	1	0
<i>P. alpina</i>	0	6	0	0	0	0
<i>Mytilus</i> sp.	0	0	0	0	9	0
<i>P. dubius</i>	0	0	0	0	0	21
<i>Liostrea</i> sp.	0	0	11	10	6	14
<i>P. duplicata</i>	0	0	0	0	0	2
<i>R. bronni</i>	0	0	0	0	0	10
<i>P. elongatus</i>	4	0	0	0	0	0
<i>M. hillanus</i>	1	0	0	0	2	0
<i>Gervillella</i> sp.	1	0	0	0	0	0
<i>Modiolus</i> sp.	4	7	0	1	53	1
<i>M. minimus</i>	0	0	0	49	254	0
<i>M. ventricosus</i>	0	0	0	0	118	3
<i>Myoconcha</i> sp.	0	0	0	0	1	0
<i>Dacryomya</i> sp.	10	0	0	0	0	0
<i>Ryderia</i> sp.	0	0	0	2	1	0
<i>P. elliptica</i>	0	0	0	0	20	5
<i>C. regularis</i>	9	0	9	16	93	23
<i>I. concentricum</i>	4	2	0	0	0	0
<i>P. rhaetica</i>	3	0	0	0	0	0
<i>P. philippiana</i>	0	2	47	1	0	0
<i>P. crowcombeia</i>	30	22	0	0	0	0
<i>P. tatei</i>	0	0	30	9	2	0
<i>Astarte</i> sp.	0	0	0	1	1	0
<i>Pleuromya</i> sp.	0	0	3	7	0	1
<i>M. cardioides</i>	0	0	0	0	0	3
<i>Cardinia</i> sp.	0	0	0	0	0	21
Total individuals	392	42	107	127	663	230

Appendix 6.5 Pairwise comparisons of the faunal composition of each stratigraphic unit. The values showed were estimated by Bray Curtis dissimilarity index. WF: Westbury Formation, CM: Cotham Member, LM: Langport Member, PPZ: Pre-Planorbis Zone, PZ: Planorbis Zone, LZ: Liasicus Zone. Overall average dissimilarity between stratigraphic units = 93.86%.

Taxa	WF	CM	LM	PPZ	PZ	LZ
	89.2					
		94.07				
<i>% Dissimilarity</i>			84.09			
				81.81		
					88.04	

Appendix 6.6 SIMPER analysis. AC: represents the average contribution of the taxon *i* to the average dissimilarity between habitats (overall average = 93.86%: See appendix 3.5). C%: Percentage contribution = average contribution/average dissimilarity between stratigraphic units. Mean abundance of each taxa by stratigraphic units. WF: Westbury Formation, CM: Cotham Member, LM: Langport Member, PPZ: Pre-Planorbis Zone, PZ: Planorbis Zone, LZ: Liasicus Zone. †: Taxa with global extinction, §: Taxa with regional extinction. **: Taxa with regional extinction, but were recorded in this data.

N	Taxon	AC	C %	WF	CM	LM	PPZ	PZ	LZ
1	<i>R. contorta</i> †	13.57	14.47	40	0	0	0	0	0
2	<i>M. minimus</i>	12.42	27.7	0	0	0	12.3	31.8	0
3	<i>C. regularis</i>	7.432	35.62	1.13	0	1.8	4	11.6	3.83
4	<i>P. philippiana</i>	5.877	41.88	0	0.4	9.4	0.25	0	0
5	<i>P. crowcombeia</i> †	5.765	48.03	3.75	4.4	0	0	0	0
6	<i>M. ventricosus</i>	4.81	53.15	0	0	0	0	14.8	0.5
7	<i>I. angulatus</i>	4.167	57.59	0	0	0	1.5	0.875	7.33
8	<i>P. tatei</i>	4.073	61.93	0	0	6	2.25	0.25	0
9	<i>P. giganteum</i>	4.017	66.21	0	0	0	0	1.63	6.33
10	<i>D. tomesi</i>	3.476	69.92	0	0	0	4.25	3.13	2.33
11	<i>Liostrea</i> sp.	3.438	73.58	0	0	2.2	2.5	0.75	2.33
12	<i>Modiolus</i> sp.	3.234	77.03	0.5	1.4	0	0.25	6.63	0.167
13	<i>P. navis</i>	2.505	79.7	0	0	0	0	0.25	4
14	<i>P. elliptica</i>	2.462	82.32	0	0	0	0	2.5	0.833
15	<i>Cardinia</i> sp.	1.881	84.33	0	0	0	0	0	3.5
16	<i>P. dubius</i>	1.428	85.85	0	0	0	0	0	3.5
17	<i>Pleuromya</i> sp.	1.131	87.06	0	0	0.6	1.75	0	0.167
18	<i>P. punctatum</i>	1.029	88.15	0.125	0	1.2	0	0	0
19	<i>P. undulata</i>	0.9425	89.16	0	0	0	0	1.63	0
20	<i>P. plicatulum</i>	0.9182	90.14	0	0	0	0	1.75	0
21	<i>R. bronni</i>	0.8679	91.06	0	0	0	0	0	1.67
22	<i>P. alpina</i> §	0.864	91.98	0	1.2	0	0	0	0
23	<i>Mytilus</i> sp.**	0.7682	92.8	0	0	0	0	1.13	0
24	<i>C. johnstoni</i>	0.7217	93.57	0	0	0	0	1	0
25	<i>C. valoniensis</i>	0.7073	94.32	0.125	0	0	1	0.75	0.167
26	<i>Alsatites</i> sp.	0.6046	94.97	0	0	0	0	0	0.833
27	<i>M. cloacinus</i>	0.561	95.57	0.25	0.6	0	0	0	0
28	<i>I. concentricum</i> §	0.5563	96.16	0.5	0.4	0	0	0	0
29	<i>P. planorbis</i>	0.5093	96.7	0	0	0	0	1.63	0
30	<i>Dacryomya</i> sp.	0.4831	97.22	1.25	0	0	0	0	0
31	<i>Oxytoma</i> sp.**	0.4419	97.69	0.125	0	0	0.75	0.125	0
32	<i>Ryderia</i> sp.	0.2889	97.99	0	0	0	0.5	0.125	0
33	<i>P. rhaetica</i> §	0.2782	98.29	0.375	0	0	0	0	0
34	<i>M. hillanus</i>	0.2733	98.58	0.125	0	0	0	0.25	0
35	<i>M. cardioides</i>	0.2652	98.86	0	0	0	0	0	0.5
36	<i>P. duplicata</i>	0.2249	99.1	0	0	0	0	0	0.333
37	<i>C. hettangiensis</i>	0.218	99.34	0.125	0	0.2	0	0.125	0
38	<i>Astarte</i> sp.	0.1691	99.52	0	0	0	0.25	0.125	0
39	<i>Gervillella</i> sp.	0.1685	99.7	0.125	0	0	0	0	0
40	<i>P. elongatus</i> †	0.1591	99.87	0.5	0	0	0	0	0
41	<i>P. erugatum</i>	0.07964	99.95	0	0	0	0.25	0	0
42	<i>Myoconcha</i> sp.	0.046	100	0	0	0	0	0.125	0

Appendix 6.7 Modes of life used by marine fauna record in each stratigraphy units.

Westbury Fomation			
Species	Mode of life		
	Tiering	Motility	Feeding
<i>Rhaetavicula contorta</i>	Surficial	Facultative Motile Attached	Suspension
<i>Cosmetodon hettangiensis</i>	Surficial	Facultative Motile Attached	Suspension
<i>Chlamys valoniensis</i>	Surficial	Facultative Motile Attached	Suspension
<i>Mytilus cloacinus</i>	Surficial	Facultative Motile Attached	Suspension
<i>Permophorus elongatus</i>	Semi-faunal	Facultative Motile Attached	Suspension
<i>Modiolus hillanus</i>	Semi-faunal	Facultative Motile Attached	Suspension
<i>Gervillella</i> sp.	Semi-faunal	Facultative Motile Attached	Suspension
<i>Modiolus</i> sp.	Semi-faunal	Facultative Motile Attached	Suspension
<i>Dacryomya</i> sp.	Shallow-infaunal	Slow	Mining
<i>Cardinia regularis</i>	Shallow-infaunal	Facultative Motile Unattached	Suspension
<i>Isocyprina concentricum</i>	Shallow-infaunal	Facultative Motile Unattached	Suspension
<i>Protocardia rhaetica</i>	Shallow-infaunal	Facultative Motile Unattached	Suspension
<i>P. punctatum</i>	Surficial	Facultative Motile Attached	Suspension
<i>Oxytoma</i> sp.	Surficial	Facultative Motile Attached	Suspension
<i>Pteromya crowcombeia</i>	Shallow-infaunal	Facultative Motile Unattached	Suspension

Cotham Member			
Species	Mode of life		
	Tiering	Motility	Feeding
<i>M. cloacinus</i>	Surficial	Facultative Motile Attached	Suspension
<i>P. alpina</i>	Surficial	Facultative Motile Attached	Suspension
<i>Modiolus</i> sp.	Semi-faunal	Facultative Motile Attached	Suspension
<i>I. concentricum</i>	Shallow-infaunal	Facultative Motile Unattached	Suspension
<i>P. philippiana</i>	Shallow-infaunal	Facultative Motile Unattached	Suspension
<i>P. crowcombeia</i>	Shallow-infaunal	Facultative Motile Unattached	Suspension

Langport Member			
Species	Mode of life		
	Tiering	Motility	Feeding
<i>P. punctatum</i>	Surficial	Facultative Motile Attached	Suspension
<i>C. hettangiensis</i>	Surficial	Facultative Motile Attached	Suspension
<i>Liostrea</i> sp.	Surficial	Non-Motile Attached	Suspension
<i>C. regularis</i>	Shallow-infaunal	Facultative Motile Unattached	Suspension
<i>P. philippiana</i>	Shallow-infaunal	Facultative Motile Unattached	Suspension
<i>P. tatei</i>	Shallow-infaunal	Facultative Motile Unattached	Suspension
<i>Pleuromya</i> sp.	Shallow-infaunal	Facultative Motile Unattached	Suspension

Pre-Planorbis Zone

Species	Mode of life		
	Tiering	Motility	Feeding
<i>P. erugatum</i>	Pelagic	Fast	Predatory
<i>I. angulatus</i>	Erect	Non-Motile Attached	Suspension
<i>D. tomesi</i>	Surficial	Slow	Grazing
<i>C. valoniensis</i>	Surficial	Facultative Motile Attached	Suspension
<i>Oxytoma</i> sp.	Surficial	Facultative Motile Attached	Suspension
<i>Liostrea</i> sp.	Surficial	Non-Motile Attached	Suspension
<i>Modiolus</i> sp.	Semi-faunal	Facultative Motile Attached	Suspension
<i>M. minimus</i>	Semi-faunal	Facultative Motile Attached	Suspension
<i>Ryderia</i> sp.	Shallow-infaunal	Slow	Mining
<i>C. regularis</i>	Shallow-infaunal	Facultative Motile Unattached	Suspension
<i>P. philipinana</i>	Shallow-infaunal	Facultative Motile Unattached	Suspension
<i>P. tatei</i>	Shallow-infaunal	Facultative Motile Unattached	Suspension
<i>Astarte</i> sp.	Shallow-infaunal	Facultative Motile Unattached	Suspension
<i>Pleuromya</i> sp.	Shallow-infaunal	Facultative Motile Unattached	Suspension

Planorbis Zone

Species	Mode of life		
	Tiering	Motility	Feeding
<i>P. planorbis</i>	Pelagic	Fast	Predatory
<i>C. johnstoni</i>	Pelagic	Fast	Predatory
<i>P. plicatulum</i>	Pelagic	Fast	Predatory
<i>I. angulatus</i>	Erect	Non-Motile Attached	Suspension
<i>P. undulata</i>	Surficial	Slow	Deposit
<i>D. tomesi</i>	Surficial	Slow	Grazing
<i>P. navis</i>	Surficial	Facultative Motile Unattached	Suspension
<i>C. valoniensis</i>	Surficial	Facultative Motile Attached	Suspension
<i>P. giganteum</i>	Surficial	Facultative Motile Attached	Suspension
<i>Oxytoma</i> sp.	Surficial	Facultative Motile Attached	Suspension
<i>Cosmetodon</i> sp.	Surficial	Facultative Motile Attached	Suspension
<i>Mytilus</i> sp.	Surficial	Facultative Motile Attached	Suspension
<i>Liostrea</i> sp.	Surficial	Non-Motile Attached	Suspension
<i>M. hillanus</i>	Semi-infaunal	Facultative Motile Attached	Suspension
<i>Modiolus</i> sp.	Semi-infaunal	Facultative Motile Attached	Suspension
<i>M. minimus</i>	Semi-infaunal	Facultative Motile Attached	Suspension
<i>M. ventricosus</i>	Semi-infaunal	Facultative Motile Attached	Suspension
<i>Myoconcha</i> sp.	Semi-infaunal	Facultative Motile Attached	Suspension
<i>Ryderia</i> sp.	Shallow-infaunal	Slow	Mining
<i>P. elliptica</i>	Shallow-infaunal	Slow	Mining
<i>C. regularis</i>	Shallow-infaunal	Facultative Motile Unattached	Suspension
<i>P. tatei</i>	Shallow-infaunal	Facultative Motile Unattached	Suspension
<i>Astarte</i> sp.	Shallow-infaunal	Facultative Motile Unattached	Suspension

Liasicus Zone

Species	Mode of life		
	Tiering	Motility	Feeding
<i>Alsatites sp.</i>	Pelagic	Fast	Predatory
<i>I. angulatus</i>	Erect	Non-Motile Attached	Suspension
<i>D. tomesi</i>	Surficial	Slow	Grazing
<i>P. navis</i>	Surficial	Facultative Motile Unattached	Suspension
<i>C. valoniensis</i>	Surficial	Facultative Motile Attached	Suspension
<i>P. giganteum</i>	Surficial	Facultative Motile Attached	Suspension
<i>P. dubius</i>	Surficial	Facultative Motile Attached	Suspension
<i>Liostrea sp.</i>	Surficial	Non-Motile Attached	Suspension
<i>P. duplicata</i>	Surficial	Non-Motile Attached	Suspension
<i>R. bronni</i>	Semi-infaunal	Slow	Mining
<i>Modiolus sp.</i>	Semi-infaunal	Facultative Motile Attached	Suspension
<i>M. ventricosus</i>	Semi-infaunal	Facultative Motile Attached	Suspension
<i>P. elliptica</i>	Shallow-infaunal	Slow	Mining
<i>C. regularis</i>	Shallow-infaunal	Facultative Motile Unattached	Suspension
<i>Pleuromya sp.</i>	Shallow-infaunal	Facultative Motile Unattached	Suspension
<i>M. cardioides</i>	Shallow-infaunal	Facultative Motile Unattached	Suspension
<i>Cardinia sp.</i>	Shallow-infaunal	Facultative Motile Unattached	Suspension

Appendix 6.8 Proportion of mode of life. WF: Westbury Formation, CM: Cotham Member, LM: Langport Member, PPZ: Pre-Planorbis Zone, PZ: Planorbis Zone, LZ: Liasicus Zone.

Ecological categories	Stratigraphy					
	WF	CM	LM	PPZ	PZ	LZ
Pelagic	0	0	0	0.07	0.1	0.1
Erect	0	0	0	0.07	0	0.1
Surficial	0.4	0.3	0.4	0.29	0.4	0.4
Semi-infaunal	0.27	0.2	0	0.14	0.2	0.2
Shallow-infaunal	0.33	0.5	0.6	0.43	0.2	0.3
Deep-infaunal	0	0	0	0	0	0
Fast	0	0	0	0.07	0.1	0.1
Slow	0.07	0	0	0.14	0.2	0.2
Facultative_unattached	0.27	0.5	0.6	0.36	0.2	0.3
Facultative-attached	0.67	0.5	0.3	0.29	0.4	0.3
No motile Unattached	0	0	0	0	0	0
No motile Attached	0	0	0.1	0.14	0.1	0.2
Suspension	0.93	1	1	0.79	0.7	0.8
Surface deposit	0	0	0	0	0	0
Mining	0.07	0	0	0.07	0.1	0.1
Grazing	0	0	0	0.07	0	0.1
Predatory	0	0	0	0.07	0.1	0.1
Other	0	0	0	0	0	0

Appendix 6.9 Geometric mean of the species recorded along the study interval at Larne section. WF: Westbury Formation, CM: Cotham Member, LM: Langport Member, PPZ: Pre-Planorbis Zone, PZ: Planorbis Zone, LZ: Liasicus Zone; PP: Pre Planorbis; PZ: Planorbis Zone; LZ: Liasicus Zone and AZ: Angulata Zone. Sp.: species. IC: *I. concentricum*; PG: *P. giganteum*; CV: *C. valoniensis*; MH: *M. hillanus*; G; *Gervillella* sp.; M; *Modiolus* sp.; MM: *M. minimus*; CR: *C. regularis*; PH: *Pholadomya* sp.; PT: *P. langportiensis*; LH: *Liostrea*; MY; *Myoconcha* sp.; MC: *M. cardioides*; PD: *P. duplicata*; GRE: *G. obliquata*; C: *C. calcarea*; CA: *Camponectes* sp.; RB: *R. bronni*.

Sp	WF1	Sp	WF2	Sp	WF3	Sp	WF4	Sp	WF5	Sp	WF6	Sp	WF7	Sp	C1	Sp	C2	Sp	C3	Sp	C4	Sp	C5	Sp	LM1	Sp	LM2	Sp	LM3	Sp	LM4	Sp	LM5
CR	6.50	CR	10.23	PG	21.72	RC	5.67	M	6.83	RC	17.10	PC	6.41	PC	9.04	IC	5.20	PC	8.75	PC	16.88	PL	24.96	LH	24.57	CR	10.40	PL	19.16	PL	18.60	LH	23.05
CR	6.13	D	5.96	PC	6.27	RC	10.55	RC	7.03	RC	6.68	PC	4.95	PC	9.99	M	3.24	PA	6.46	IC	8.98	PC	27.96	PR	15.41	PR	13.65	PL	28.45	PL	12.62	PG	17.73
CR	5.79	D	15.25	MH	11.14	RC	16.37	RC	6.78	RC	11.56	PC	7.15	RC	8.54	M	2.83	PA	6.41	PC	10.34	PL	13.46	PR	11.92	PR	19.07	A	8.83	PL	29.24	PG	20.41
RC	4.16	D	6.54	MH	7.65	RC	9.02	M	4.56	RC	9.78	PC	4.38	RC	10.15	M	2.43	PA	4.68	CR	19.68	PC	13.81	PR	25.31	PC	12.53	PR	11.25	PR	18.70	PG	11.81
	0.00	D	6.51	PC	10.71	RC	8.99	PC	4.90	PC	5.14	PC	4.49	RC	7.29	M	2.56	PC	12.50	PR	12.49	PC	6.33	PR	14.61	PR	15.66	PL	7.86	P	29.66	PG	19.74
	0.00	D	7.40	RC	9.76	RC	9.77	PC	6.45	PC	6.82	D	7.81	RC	7.91		0.00	MC	10.60	CR	15.78	PC	5.15	PR	5.03	CR	23.55	CR	21.00	CR	7.29	PG	17.47
	0.00	D	5.26	PC	4.64	RC	6.80	PC	5.69	PC	7.74	OX	5.18	RC	8.46		0.00	MC	2.96	PR	14.20	PC	23.91	PR	7.11	CR	33.48	PL	24.05	CR	15.31	LH	12.89
	0.00	D	7.73	PC	4.37	RC	20.78	PC	5.35	PC	6.84	OX	3.43	RC	8.00		0.00	MC	3.43		0.00	PC	17.00	PR	11.10	PR	13.53	PR	12.05	CR	24.80	PR	17.77
	0.00	D	4.65	PC	7.30	RC	4.59	PC	9.39	PC	6.38	PC	3.13	RC	6.13		0.00	PC	10.37		0.00	PC	14.50	PR	11.48	CR	19.07	PR	12.01	L	24.41	PR	7.12
	0.00	G	12.15	PC	5.92	RC	8.45	RC	6.40	PC	6.61	PC	5.18	RC	14.61		0.00	MC	1.93		0.00	PC	16.47	PR	8.97	PR	15.41	CR	9.15	L	15.18	PR	15.04
	0.00	IC	8.90	PC	6.50	RC	12.00	RC	15.14	PC	6.11	PC	5.18	RC	10.44		0.00	PA	9.37		0.00	PC	26.61	PR	9.14	PR	4.95	CR	13.17	PL	18.20	P	17.52
	0.00	IC	7.30	PC	4.94	RC	6.89	RC	5.93	PC	5.46	PC	2.79	RC	10.22		0.00	PA	9.30		0.00	PC	15.30	PR	14.24	PR	6.79		0.00	L	15.33	PR	15.14
	0.00	IC	5.77	PC	6.12	RC	6.77	RC	6.34	RC	9.50	RC	6.44	RC	15.79		0.00		0.00		0.00	PC	12.45	PR	13.21		0.00		0.00	PR	13.32	PG	14.43
	0.00	IC	4.94	PC	6.61	RC	8.38	PC	6.33	RC	12.24	RC	8.46	RC	7.94		0.00		0.00		0.00	PC	14.55	L	14.80		0.00		0.00	CR	14.72	PR	15.21
	0.00	IC	6.25		0.00	RC	8.69	PC	6.36	RC	11.24	PC	5.32	RC	7.21		0.00		0.00		0.00	PC	8.40	PR	17.59		0.00		0.00	P	38.74	PR	16.51
	0.00	IC	6.07		0.00	RC	7.18	PC	5.45	RC	11.56	CR	6.34	RC	9.09		0.00		0.00		0.00	PC	16.48	PR	10.14		0.00		0.00	PR	19.49	PR	16.55
	0.00	PE	10.65		0.00	RC	6.81	M	7.27	RC	7.76	IC	4.63	RC	9.23		0.00		0.00		0.00	PC	3.81	PR	16.53		0.00		0.00	PL	16.61		0.00
	0.00	PE	12.02		0.00	RC	8.33	PC	5.40	RC	5.56	RC	6.31	RC	7.66		0.00		0.00		0.00	PC	11.36	PR	13.11		0.00		0.00	PR	13.05		0.00
	0.00	PE	6.07		0.00	RC	8.98	PC	4.50	RC	4.31	PC	5.21	RC	7.86		0.00		0.00		0.00	PC	10.21	PR	16.83		0.00		0.00	PL	18.69		0.00
	0.00	PR	10.86		0.00	RC	5.82	CR	6.96	RC	5.86	PC	5.14	RC	7.60		0.00		0.00		0.00	PC	18.43	PR	11.33		0.00		0.00	PL	13.30		0.00
	0.00	PR	11.92		0.00	RC	6.40	RC	10.00	RC	8.64	RC	6.35	RC	6.49		0.00		0.00		0.00	PC	18.80	PR	15.21		0.00		0.00	PL	18.82		0.00
	0.00	RC	3.36		0.00	RC	8.47	RC	8.49	RC	10.15	PC	4.98	RC	9.40		0.00		0.00		0.00	PC	12.02	PR	12.23		0.00		0.00	PL	20.59		0.00
	0.00	RC	11.10		0.00	RC	9.27	RC	9.26	RC	10.15	RC	11.13	RC	13.86		0.00		0.00		0.00	PC	3.97	PR	12.26		0.00		0.00	PL	14.09		0.00
	0.00	RC	8.56		0.00	RC	8.68	RC	7.80	RC	14.27		0.00	RC	5.95		0.00		0.00		0.00	PC	2.54	PR	14.53		0.00		0.00	PL	23.41		0.00
	0.00	RC	6.62		0.00	RC	6.85	CR	8.75	RC	12.77		0.00	RC	8.88		0.00		0.00		0.00	PC	3.13	PR	11.86		0.00		0.00	L	25.46		0.00
	0.00	RC	11.32		0.00	RC	8.56	MC	10.05	RC	12.29		0.00	RC	9.19		0.00		0.00		0.00	PC	4.05	PR	10.01		0.00		0.00	L	21.51		0.00

	0.00	RC	12.42		0.00	RC	3.52	CR	6.11	RC	14.72		0.00	RC	8.64		0.00		0.00	PC	3.99	PR	13.43		0.00		0.00	PR	8.72		0.00
	0.00	RC	9.74		0.00	RC	11.97	CR	4.67	RC	9.21		0.00	RC	9.15		0.00		0.00	PC	3.56		0.00		0.00		0.00	L	19.51		0.00
	0.00	RC	14.14		0.00	RC	8.55	CR	9.43	RC	12.61		0.00	RC	6.74		0.00		0.00	PC	3.40		0.00		0.00		0.00	PR	15.11		0.00
	0.00	RC	11.78		0.00	RC	8.98		0.00	RC	6.22		0.00	RC	3.37		0.00		0.00	PC	3.82		0.00		0.00		0.00	PR	16.82		0.00
	0.00	RC	12.68		0.00	RC	4.83		0.00	RC	5.19		0.00	RC	5.60		0.00		0.00	PC	2.79		0.00		0.00		0.00	PR	11.45		0.00
	0.00	RC	10.55		0.00	CV	28.43		0.00	RC	5.39		0.00	RC	12.98		0.00		0.00	PC	2.13		0.00		0.00		0.00	PL	19.40		0.00
	0.00	RC	7.81		0.00	MC	11.47		0.00	RC	6.76		0.00	RC	15.43		0.00		0.00	PC	3.09		0.00		0.00		0.00	PL	16.08		0.00
	0.00	RC	8.62		0.00	RC	6.21		0.00	RC	4.52		0.00	RC	14.17		0.00		0.00		0.00		0.00		0.00		0.00	PL	22.76		0.00
	0.00	RC	9.87		0.00	RC	7.64		0.00	D	4.86		0.00	RC	7.87		0.00		0.00		0.00		0.00		0.00		0.00	PL	19.74		0.00
	0.00	RC	12.45		0.00	RC	8.43		0.00	PR	5.38		0.00	RC	11.43		0.00		0.00		0.00		0.00		0.00		0.00	PL	19.01		0.00
	0.00	RC	4.58		0.00	RC	8.24		0.00	IC	8.08		0.00	RC	7.76		0.00		0.00		0.00		0.00		0.00		0.00	PL	17.00		0.00
	0.00	RC	10.88		0.00	RC	5.77		0.00	PR	5.32		0.00	RC	9.51		0.00		0.00		0.00		0.00		0.00		0.00	PL	13.41		0.00
	0.00	RC	7.90		0.00	RC	6.50		0.00		0.00		0.00	RC	11.46		0.00		0.00		0.00		0.00		0.00		0.00	PL	15.64		0.00
	0.00	RC	8.16		0.00	RC	7.60		0.00		0.00		0.00	RC	7.19		0.00		0.00		0.00		0.00		0.00		0.00	PL	12.52		0.00
	0.00	RC	7.67		0.00	RC	8.46		0.00		0.00		0.00	RC	9.65		0.00		0.00		0.00		0.00		0.00		0.00	PL	17.68		0.00
	0.00	RC	5.68		0.00	RC	6.33		0.00		0.00		0.00	RC	6.62		0.00		0.00		0.00		0.00		0.00		0.00	PL	11.81		0.00
	0.00	RC	5.69		0.00	RC	7.59		0.00		0.00		0.00	RC	12.09		0.00		0.00		0.00		0.00		0.00		0.00	PL	12.88		0.00
	0.00	RC	6.57		0.00	RC	7.18		0.00		0.00		0.00	RC	5.40		0.00		0.00		0.00		0.00		0.00		0.00	PL	11.64		0.00
	0.00	RC	8.25		0.00	RC	6.51		0.00		0.00		0.00	PC	10.22		0.00		0.00		0.00		0.00		0.00		0.00		0.00		0.00
	0.00	RC	7.34		0.00	RC	6.49		0.00		0.00		0.00	RC	18.55		0.00		0.00		0.00		0.00		0.00		0.00		0.00		0.00
	0.00	RC	10.14		0.00	RC	10.35		0.00		0.00		0.00	RC	14.25		0.00		0.00		0.00		0.00		0.00		0.00		0.00		0.00
	0.00	RC	8.05		0.00		0.00		0.00		0.00		0.00	RC	13.47		0.00		0.00		0.00		0.00		0.00		0.00		0.00		0.00
	0.00	RC	6.72		0.00		0.00		0.00		0.00		0.00	RC	9.48		0.00		0.00		0.00		0.00		0.00		0.00		0.00		0.00
	0.00	RC	8.20		0.00		0.00		0.00		0.00		0.00	RC	13.59		0.00		0.00		0.00		0.00		0.00		0.00		0.00		0.00
	0.00	RC	7.02		0.00		0.00		0.00		0.00		0.00	RC	15.84		0.00		0.00		0.00		0.00		0.00		0.00		0.00		0.00
	0.00	RC	9.19		0.00		0.00		0.00		0.00		0.00	RC	7.19		0.00		0.00		0.00		0.00		0.00		0.00		0.00		0.00
	0.00	RC	7.41		0.00		0.00		0.00		0.00		0.00	RC	11.80		0.00		0.00		0.00		0.00		0.00		0.00		0.00		0.00
	0.00	RC	8.54		0.00		0.00		0.00		0.00		0.00	RC	17.45		0.00		0.00		0.00		0.00		0.00		0.00		0.00		0.00
	0.00	RC	9.76		0.00		0.00		0.00		0.00		0.00	RC	8.40		0.00		0.00		0.00		0.00		0.00		0.00		0.00		0.00
	0.00	RC	7.44		0.00		0.00		0.00		0.00		0.00	RC	11.52		0.00		0.00		0.00		0.00		0.00		0.00		0.00		0.00
	0.00	RC	8.13		0.00		0.00		0.00		0.00		0.00	RC	6.98		0.00		0.00		0.00		0.00		0.00		0.00		0.00		0.00
	0.00	RC	10.50		0.00		0.00		0.00		0.00		0.00	RC	16.47		0.00		0.00		0.00		0.00		0.00		0.00		0.00		0.00
	0.00	RC	7.02		0.00		0.00		0.00		0.00		0.00	RC	13.30		0.00		0.00		0.00		0.00		0.00		0.00		0.00		0.00
	0.00	RC	5.95		0.00		0.00		0.00		0.00		0.00	RC	12.80		0.00		0.00		0.00		0.00		0.00		0.00		0.00		0.00

	0.00	RC	12.44		0.00		0.00		0.00		0.00	RC	13.21		0.00		0.00		0.00		0.00		0.00		0.00		0.00
	0.00	RC	11.46		0.00		0.00		0.00		0.00	RC	8.54		0.00		0.00		0.00		0.00		0.00		0.00		0.00
	0.00	RC	15.16		0.00		0.00		0.00		0.00	RC	7.87		0.00		0.00		0.00		0.00		0.00		0.00		0.00
	0.00	RC	13.83		0.00		0.00		0.00		0.00	RC	16.57		0.00		0.00		0.00		0.00		0.00		0.00		0.00
	0.00	RC	6.08		0.00		0.00		0.00		0.00	RC	13.52		0.00		0.00		0.00		0.00		0.00		0.00		0.00
	0.00	RC	7.57		0.00		0.00		0.00		0.00	RC	6.49		0.00		0.00		0.00		0.00		0.00		0.00		0.00
	0.00	RC	4.85		0.00		0.00		0.00		0.00	RC	11.71		0.00		0.00		0.00		0.00		0.00		0.00		0.00
	0.00	RC	8.52		0.00		0.00		0.00		0.00	RC	12.53		0.00		0.00		0.00		0.00		0.00		0.00		0.00
	0.00	RC	11.46		0.00		0.00		0.00		0.00	RC	13.54		0.00		0.00		0.00		0.00		0.00		0.00		0.00
	0.00	RC	8.20		0.00		0.00		0.00		0.00	RC	8.41		0.00		0.00		0.00		0.00		0.00		0.00		0.00
	0.00	RC	7.55		0.00		0.00		0.00		0.00	RC	9.20		0.00		0.00		0.00		0.00		0.00		0.00		0.00
	0.00	RC	8.39		0.00		0.00		0.00		0.00	RC	12.29		0.00		0.00		0.00		0.00		0.00		0.00		0.00
	0.00	RC	8.53		0.00		0.00		0.00		0.00	RC	12.69		0.00		0.00		0.00		0.00		0.00		0.00		0.00
	0.00	RC	9.95		0.00		0.00		0.00		0.00	RC	10.27		0.00		0.00		0.00		0.00		0.00		0.00		0.00
	0.00	RC	5.16		0.00		0.00		0.00		0.00	RC	7.89		0.00		0.00		0.00		0.00		0.00		0.00		0.00
	0.00	RC	13.63		0.00		0.00		0.00		0.00	RC	0.00		0.00		0.00		0.00		0.00		0.00		0.00		0.00

Appendix 6.9 (Continuation) Geometric mean of the species recorded along the study interval at Larne section. WF: Westbury Formation, CM: Cotham Member, LM: Langport Member, PPZ: Pre-Planorbis Zone, PZ: Planorbis Zone, LZ: Liasicus Zone; PP: Pre Planorbis; PZ: Planorbis Zone; LZ: Liasicus Zone and AZ: Angulata Zone. Sp.: species. IC: *I. concentricum*; PG: *P. giganteum*; CV; *C. valoniensis*; MH: *M. hillanus*; G; *Gervillella* sp.; M; *Modiolus* sp.; MM: *M. minimus*; CR: *C. regularis*; PH: *Pholadomya* sp.; PT: *P. langportiensis*; LH: *Liostrea*; MY; *Myoconcha* sp.; MC: *M. cardioides*; PD: *P. duplicata*; GRE: *G. obliquata*; C: *C. calcarea*; CA: *Camponectes* sp.; RB: *R. bronni*.

Sp	PP1	Sp	PP2	Sp	PP3	Sp	PP4	Sp	PP5	Sp	PZ2	Sp	PZ3	Sp	PZ4	Sp	PZ5	Sp	PZ6	Sp	PZ7	Sp	PZ8	Sp	LZ1	Sp	LZ2	Sp	LZ3	Sp	LZ4	Sp	LZ5	Sp	LZ6
MM	8.50	PC	16.06	MM	4.33	PP	9.01	MV	4.43	MM	3.77	PG	18.23	CI	32.45	CR	2.92	CR	6.69	PE	5.58	CR	26.73	PG	59.61	PG	96.32	PN	7.14	LH	8.03	Mc	53.68	CR	10.49
PC	13.47	P	24.16	OX	5.00	MM	2.87	MV	6.33	MM	3.70	MV	6.60	CI	18.88	CR	14.77	CI	17.30	CI	59.46	CR	23.33	MV	3.57	LH	8.58	MC	20.36	PG	2.69	PG	7.36	CR	17.38
PL	12.14	CR	9.89	M	3.95	PP	19.73	MV	7.08	MM	7.39	MV	7.72	OX	2.19	CR	6.13	CR	3.78	CI	33.15	CR	11.51	PN	4.05	PG	19.24	PG	50.69	LH	3.97	AL	17.11	CR	4.56
PC	34.78	PC	19.08	MM	3.26	PL	5.42	MV	2.51	MV	8.43	MV	7.73	CI	22.82	PG	20.72	PE	3.41	CR	6.91	CR	13.28	CR	4.13	PN	3.82	CO	29.14	PG	5.88	PN	5.62	CR	6.50
P	22.37	CR	26.01	MM	5.65	MM	5.18	MV	8.50	LH	24.28	MV	6.64	PE	3.19	T	3.34	CR	26.50	MV	9.28	CR	15.45		0.00		0.00	RB	6.66	Cr	11.93	PN	3.84	CR	12.86
CR	11.23	CR	28.26	MM	4.04	MM	5.05	MV	7.33	PS	22.60	MV	7.59	CN	1.90	PG	8.98	CV	7.00	MV	6.27	CR	17.80		0.00		0.00	CO	12.98	LH	5.17	PN	3.21	CR	5.01
MN	56.62	L	16.23	MM	3.12	MM	4.23	MM	2.49	PS	18.48	MV	4.25	CR	9.91	PG	30.50	CR	8.31	MV	6.18	CR	20.61		0.00		0.00	MC	9.26	LH	8.61		0.00	PG	4.52
P	21.32	RY	19.51	MM	2.19	PP	18.91	MM	2.00	MV	3.48	MV	6.51	MM	3.09	CR	17.44	PE	4.38	RY	11.29	CR	12.92		0.00		0.00	P	32.03		0.00		0.00		0.00
P	12.69	PR	10.54	MM	2.19	PP	24.63	MM	3.15	MV	7.03	MV	3.74	T	4.85	PG	23.24	MM	7.85	MM	7.23	CR	28.52		0.00		0.00		0.00		0.00		0.00		0.00
PC	10.67	L	23.14	MM	3.07	MM	4.80	MM	4.95	MM	5.46	MV	7.16	PE	3.13	CR	23.81	CR	6.46	MV	5.38	CR	16.49		0.00		0.00		0.00		0.00		0.00		0.00
P	17.70	MM	3.81	MM	4.93	CV	4.99	MM	4.90	MV	2.80	MV	5.55	PE	4.82	PL	4.47	MM	7.39	PE	5.90	CR	22.59		0.00		0.00		0.00		0.00		0.00		0.00
CR	22.29	CR	16.37	CA	14.14	RY	12.32	MM	3.43	MM	5.57	MV	3.31	CI	10.29	PL	2.06	CR	4.72	RY	5.03	CR	15.70		0.00		0.00		0.00		0.00		0.00		0.00
CR	16.25	L	16.13	MM	3.46	PD	19.23	MM	3.39	MM	3.30	MV	5.18	MM	5.84	PE	5.71		0.00	CR	5.60	CR	13.83		0.00		0.00		0.00		0.00		0.00		0.00
L	37.79	PC	10.75	MM	2.94	MM	3.91	MM	5.26	M	5.58	MV	6.52	PE	3.36	M	3.64		0.00	CR	19.10	MM	7.19		0.00		0.00		0.00		0.00		0.00		0.00
P	10.21	M	3.74	MM	2.67	MM	4.88	MM	2.17	MM	3.65	CI	24.11	CR	3.66	M	4.62		0.00	CR	8.87	LH	11.57		0.00		0.00		0.00		0.00		0.00		0.00
CR	11.05		0.00	MM	3.67	OX	2.65	MM	2.00	MM	4.17	MV	7.70	CR	8.83	CI	13.22		0.00	PE	5.40	MH	7.01		0.00		0.00		0.00		0.00		0.00		0.00
PL	11.40		0.00	MM	4.73	CR	9.28	MV	3.49	MM	3.68	MV	6.91	CI	21.74	PG	30.13		0.00	PE	5.56	MH	6.50		0.00		0.00		0.00		0.00		0.00		0.00
CR	20.96		0.00	MM	2.57	CR	15.08	MM	2.42	MM	3.20	MV	5.02	MY	2.52		0.00		0.00	CR	16.68	PG	12.61		0.00		0.00		0.00		0.00		0.00		0.00
MM	7.36		0.00	CR	7.09	PP	20.42	MM	3.08	LH	7.71	MV	6.97	PE	3.43		0.00		0.00	CR	7.97	MH	2.81		0.00		0.00		0.00		0.00		0.00		0.00
CR	9.84		0.00	MM	2.13	MM	2.94	MM	3.97	MV	9.54	MV	6.51		0.00		0.00		0.00	CR	8.57	PG	16.69		0.00		0.00		0.00		0.00		0.00		0.00
PL	16.50		0.00	MM	3.55	OX	2.70	MV	2.45	MV	6.22	MV	4.82		0.00		0.00		0.00	CR	17.89	T	3.14		0.00		0.00		0.00		0.00		0.00		0.00
PC	14.72		0.00	MM	2.79	CV	4.35	PS	15.20	MV	5.26	MV	4.71		0.00		0.00		0.00	CR	6.91	PG	21.77		0.00		0.00		0.00		0.00		0.00		0.00
PL	15.36		0.00	MM	6.25	MM	2.94	PS	5.34	MV	4.34	MV	4.50		0.00		0.00		0.00	CR	6.58	PG	17.19		0.00		0.00		0.00		0.00		0.00		0.00
LH	25.92		0.00	M	8.30	CR	10.34	MV	3.72	MV	3.47	MV	4.67		0.00		0.00		0.00	CR	9.12	CR	7.20		0.00		0.00		0.00		0.00		0.00		0.00
PL	35.31		0.00	MM	5.87	CR	15.31	PS	23.54	MV	6.65	MV	3.69		0.00		0.00		0.00	CR	8.50	CR	12.44		0.00		0.00		0.00		0.00		0.00		0.00
MM	10.17		0.00	MM	5.22	MM	6.32	MM	2.02	PG	22.55	MV	6.62		0.00		0.00		0.00	MY	12.99	CR	18.11		0.00		0.00		0.00		0.00		0.00		0.00
	0.00		0.00	MM	2.47	PP	37.94	MV	4.06	MV	5.68	MV	3.77		0.00		0.00		0.00	CR	5.58	CR	16.38		0.00		0.00		0.00		0.00		0.00		0.00
	0.00		0.00	MM	4.76	LH	14.31	MV	3.91	MV	6.12	MV	3.01		0.00		0.00		0.00		0.00	CR	12.11		0.00		0.00		0.00		0.00		0.00		0.00
	0.00		0.00	MM	3.77	CV	5.74	MM	4.21	MM	4.10	MV	5.31		0.00		0.00		0.00		0.00	MH	7.57		0.00		0.00		0.00		0.00		0.00		0.00
	0.00		0.00	MM	2.62	MM	7.29	MM	3.64	MM	3.31	MV	4.65		0.00		0.00		0.00		0.00	M	10.64		0.00		0.00		0.00		0.00		0.00		0.00
	0.00		0.00	MM	2.10	CV	7.02	MM	3.50	MM	2.99	MV	3.17		0.00		0.00		0.00		0.00	CR	7.99		0.00		0.00		0.00		0.00		0.00		0.00

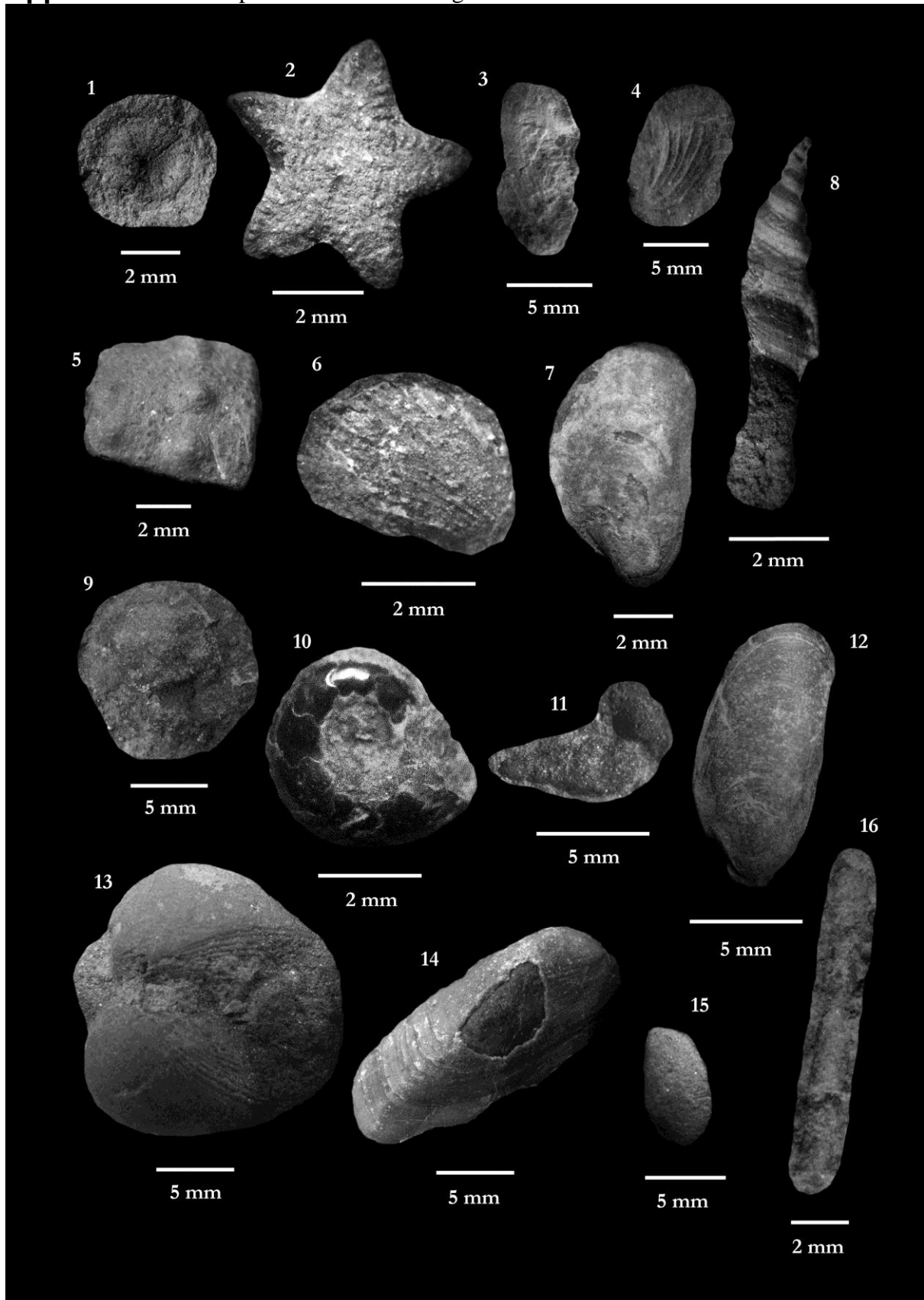
	0.00			MM	2.02	MM	7.32	MM	4.47	MM	4.25	MV	4.76		0.00		0.00		0.00	PT	12.53		0.00		0.00		0.00		0.00		0.00		0.00
	0.00		0.00	MM	4.94	PP	35.25	MM	2.77	MM	3.95	MV	3.97		0.00		0.00		0.00	CR	21.15		0.00		0.00		0.00		0.00		0.00		0.00
	0.00		0.00	OX	2.54		0.00	MV	2.84	MM	6.91	MV	3.52		0.00		0.00		0.00	MM	3.10		0.00		0.00		0.00		0.00		0.00		0.00
	0.00		0.00	MM	2.64		0.00	MM	2.51	MM	5.74	MV	3.46		0.00		0.00		0.00	MH	8.93		0.00		0.00		0.00		0.00		0.00		0.00
	0.00		0.00	MM	3.67		0.00	MM	2.38	MV	6.99	MV	3.46		0.00		0.00		0.00	CR	14.48		0.00		0.00		0.00		0.00		0.00		0.00
	0.00		0.00	MM	3.25		0.00	MM	2.10	PS	14.37	MM	7.24		0.00		0.00		0.00	MM	3.78		0.00		0.00		0.00		0.00		0.00		0.00
	0.00		0.00	MM	2.54		0.00	MM	4.53	MV	5.26	MM	7.58		0.00		0.00		0.00	CR	18.98		0.00		0.00		0.00		0.00		0.00		0.00
	0.00		0.00	MM	2.01		0.00	PS	34.52	MV	3.51	MM	5.27		0.00		0.00		0.00	CR	11.68		0.00		0.00		0.00		0.00		0.00		0.00
	0.00		0.00	MM	2.65		0.00	MM	7.45	LH	17.69	MM	6.65		0.00		0.00		0.00	CR	7.31		0.00		0.00		0.00		0.00		0.00		0.00
	0.00		0.00		0.00		0.00	M	3.67	MV	6.58	MV	6.14		0.00		0.00		0.00	MM	6.09		0.00		0.00		0.00		0.00		0.00		0.00
	0.00		0.00		0.00		0.00	MV	3.50	MV	3.67	MV	8.66		0.00		0.00		0.00	CR	14.90		0.00		0.00		0.00		0.00		0.00		0.00
	0.00		0.00		0.00		0.00	MM	4.37	MY	14.78	MV	5.49		0.00		0.00		0.00	CR	17.85		0.00		0.00		0.00		0.00		0.00		0.00
	0.00		0.00		0.00		0.00	MM	2.25	MM	4.15	MV	4.72		0.00		0.00		0.00	CR	14.84		0.00		0.00		0.00		0.00		0.00		0.00
	0.00		0.00		0.00		0.00	MM	3.45	PS	12.91	MV	6.70		0.00		0.00		0.00	CR	20.68		0.00		0.00		0.00		0.00		0.00		0.00
	0.00		0.00		0.00		0.00	MM	2.48	PS	18.54	MV	7.54		0.00		0.00		0.00	CV	6.81		0.00		0.00		0.00		0.00		0.00		0.00
	0.00		0.00		0.00		0.00	MV	4.03	MY	8.12	MV	5.89		0.00		0.00		0.00	CR	11.69		0.00		0.00		0.00		0.00		0.00		0.00
	0.00		0.00		0.00		0.00	CR	7.24	MM	6.34	MV	6.58		0.00		0.00		0.00	CV	6.03		0.00		0.00		0.00		0.00		0.00		0.00
	0.00		0.00		0.00		0.00	M	3.09		0.00	MV	3.23		0.00		0.00		0.00	M	6.78		0.00		0.00		0.00		0.00		0.00		0.00
	0.00		0.00		0.00		0.00	MM	3.33		0.00	MM	7.40		0.00		0.00		0.00	CR	14.39		0.00		0.00		0.00		0.00		0.00		0.00
	0.00		0.00		0.00		0.00	MM	2.43		0.00	MV	7.98		0.00		0.00		0.00	LH	14.53		0.00		0.00		0.00		0.00		0.00		0.00
	0.00		0.00		0.00		0.00	MV	4.47		0.00	CS	7.67		0.00		0.00		0.00	CR	7.54		0.00		0.00		0.00		0.00		0.00		0.00
	0.00		0.00		0.00		0.00	MM	7.52		0.00	MM	2.67		0.00		0.00		0.00	CR	9.84		0.00		0.00		0.00		0.00		0.00		0.00
	0.00		0.00		0.00		0.00	MV	6.19		0.00	CR	8.65		0.00		0.00		0.00	M	3.68		0.00		0.00		0.00		0.00		0.00		0.00
	0.00		0.00		0.00		0.00	MV	5.92		0.00	MV	6.16		0.00		0.00		0.00	M	9.37		0.00		0.00		0.00		0.00		0.00		0.00
	0.00		0.00		0.00		0.00	L	14.68		0.00	MM	3.70		0.00		0.00		0.00	M	9.17		0.00		0.00		0.00		0.00		0.00		0.00
	0.00		0.00		0.00		0.00	L	10.53		0.00	MM	6.54		0.00		0.00		0.00	CR	7.39		0.00		0.00		0.00		0.00		0.00		0.00
	0.00		0.00		0.00		0.00	MM	4.23		0.00	MM	4.83		0.00		0.00		0.00	CR	3.32		0.00		0.00		0.00		0.00		0.00		0.00
	0.00		0.00		0.00		0.00	PS	7.00		0.00	MV	6.96		0.00		0.00		0.00	CR	14.27		0.00		0.00		0.00		0.00		0.00		0.00
	0.00		0.00		0.00		0.00	MM	6.02		0.00	MV	5.90		0.00		0.00		0.00	CV	6.19		0.00		0.00		0.00		0.00		0.00		0.00
	0.00		0.00		0.00		0.00	MM	4.17		0.00	MV	7.05		0.00		0.00		0.00	CR	11.31		0.00		0.00		0.00		0.00		0.00		0.00
	0.00		0.00		0.00		0.00	MM	4.19		0.00		0.00		0.00		0.00		0.00	CR	2.77		0.00		0.00		0.00		0.00		0.00		0.00
	0.00		0.00		0.00		0.00	MM	3.42		0.00		0.00		0.00		0.00		0.00	M	4.46		0.00		0.00		0.00		0.00		0.00		0.00
	0.00		0.00		0.00		0.00	MM	3.91		0.00		0.00		0.00		0.00		0.00	CR	12.82		0.00		0.00		0.00		0.00		0.00		0.00
	0.00		0.00		0.00		0.00	MV	3.08		0.00		0.00		0.00		0.00		0.00	PG	18.96		0.00		0.00		0.00		0.00		0.00		0.00
	0.00		0.00		0.00		0.00	MV	3.13		0.00		0.00		0.00		0.00		0.00	CR	17.16		0.00		0.00		0.00		0.00		0.00		0.00
	0.00		0.00		0.00		0.00		0.00		0.00		0.00		0.00		0.00		0.00	MH	5.87		0.00		0.00		0.00		0.00		0.00		0.00
	0.00		0.00		0.00		0.00		0.00		0.00		0.00		0.00		0.00		0.00	LH	11.15		0.00		0.00		0.00		0.00		0.00		0.00
	0.00		0.00		0.00		0.00		0.00		0.00		0.00		0.00		0.00		0.00	CR	15.36		0.00		0.00		0.00		0.00		0.00		0.00

0.00		0.00		0.00		0.00		0.00		0.00		0.00		0.00		0.00		0.00	CR	10.01		0.00		0.00		0.00		0.00		0.00		0.00		0.00
0.00		0.00		0.00		0.00		0.00		0.00		0.00		0.00		0.00		0.00	CR	10.51		0.00		0.00		0.00		0.00		0.00		0.00		
0.00		0.00		0.00		0.00		0.00		0.00		0.00		0.00		0.00		0.00	CR	15.93		0.00		0.00		0.00		0.00		0.00		0.00		
0.00		0.00		0.00		0.00		0.00		0.00		0.00		0.00		0.00		0.00	CR	13.07		0.00		0.00		0.00		0.00		0.00		0.00		
0.00		0.00		0.00		0.00		0.00		0.00		0.00		0.00		0.00		0.00	CR	41.23		0.00		0.00		0.00		0.00		0.00		0.00		
0.00		0.00		0.00		0.00		0.00		0.00		0.00		0.00		0.00		0.00	LH	14.98		0.00		0.00		0.00		0.00		0.00		0.00		
0.00		0.00		0.00		0.00		0.00		0.00		0.00		0.00		0.00		0.00	CR	6.44		0.00		0.00		0.00		0.00		0.00		0.00		

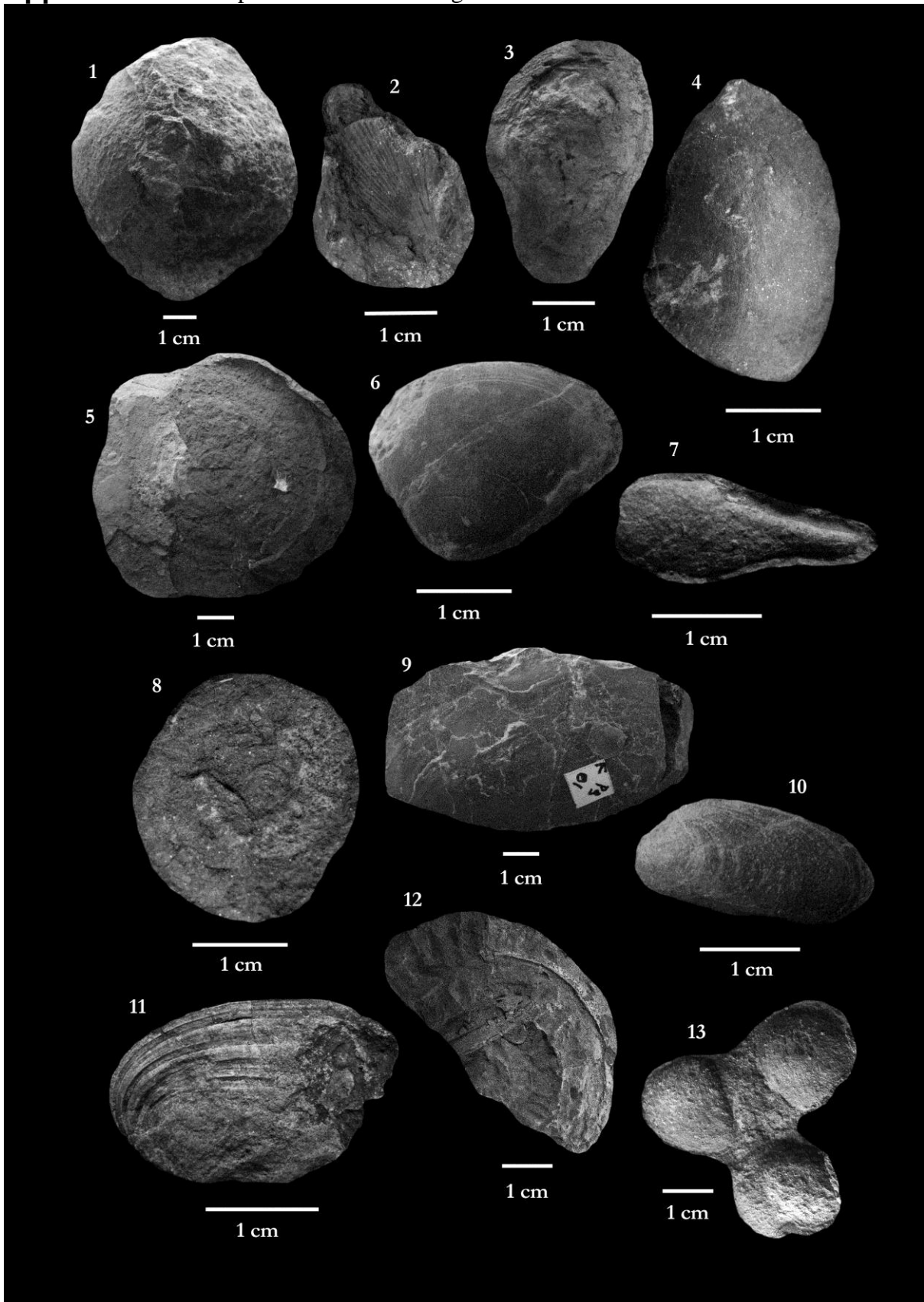
Appendix 6.10 Data used build the frequency distribution and Jablonski plot target. WF: Westbury Formation, LM: Langport Member, PPZ: Pre-Planorbis Zone, PZ: Planorbis Zone, LZ: Liasicus Zone.

<i>Cardinia</i>					<i>Modiolus</i>			<i>Plagiostoma</i>				<i>Liostrea</i>			
WF	LM	PPZ	PZ	LZ	W	PP	PZ	W	L	PZ	LZ	LM	PPZ	PZ	LZ
5.79	7.29	7.09	2.77	4.13	2.43	2.01	2.00	21.72	14.43	8.98	2.69	23.05	14.31	11.57	8.58
6.13	8.83	9.28	2.92	11.93	2.56	2.02	2.00		17.47	12.61	5.88	12.89	12.91	14.53	8.03
6.50	9.15	9.84	3.32	10.49	2.83	2.10	2.02		17.73	14.20	7.36	24.41	23.14	11.15	5.17
10.23	10.40	9.89	3.66	17.38	3.24	2.13	2.10		19.74	16.69	4.52	15.18	10.94	24.16	8.61
4.67	13.17	10.21	4.72	4.56	3.37	2.19	2.17		20.41	18.96	96.32	25.46	16.25	21.70	
6.11	14.72	10.34	4.77	6.50	3.74	2.19	2.25		11.81	20.72	59.61	21.51	25.92	23.38	
6.96	15.31	11.40	4.90	12.86	3.81	2.47	2.38			21.77		19.51	16.25	24.28	
8.75	19.07	14.14	5.00	5.01	4.56	2.54	2.42			22.28				7.71	
9.43	21.00	15.08	5.58		5.40	2.57	2.43			22.55				17.69	
6.34	23.55	15.31	5.60		5.60	2.62	2.43			23.24				14.68	
15.78	24.80	17.14	6.13		5.95	2.64	2.45			30.13				10.53	
19.68	33.48	17.70	6.44		6.13	2.65	2.49			30.50					
		19.47	6.46		6.49	2.67	2.51	21.72	16.93	20.22	29.40	20.29	17.10	16.49	7.60
		19.47	6.58		6.49	2.79	2.51								
		22.37	6.69		6.62	2.87	2.67								
		26.01	6.91		6.74	2.94	2.77								
		28.26	6.91		6.83	2.94	2.80								
			7.20		6.98	2.94	2.81								
			7.20		7.19	3.07	2.84								
			7.24		7.19	3.12	2.99								
			7.31		7.21	3.25	3.01								
			7.54		7.27	3.26	3.08								
			7.97		7.29	3.46	3.08								
			7.99		7.36	3.55	3.09								
			18.11		11.23		3.77								
			18.98		11.43		3.78								
			19.10		11.46		3.91								
			20.61		11.52		3.91								
			20.68		11.71		3.95								
			21.15		11.80		3.97								
			22.59		12.09		3.97								
			23.33		12.29		4.03								
			23.81		12.53		4.06								
			26.73		12.69		4.10								
			28.52		12.80		4.15								
			33.05		12.98		4.17								
			68.35		13.21		4.17								
8.86	16.73	15.47	13.25		13.30		4.19								
					13.47		4.23								
					9.56	3.92	5.05								

Appendix 6.12 Specimens found through in Larne section.



Appendix 6.13 Specimens found through in Larne section.



Appendix 6.12: 1. *Montivaltia* sp., 2. *Isocrinus psilonoti* (Quenstedt), 3. *Cardinia* sp., 4. *Rhaetavicula contorta* (Portlock), 5. *Diademopsis tomesi* (Wright), 6. *Chlamys valoniensis* (Defrance), 7. *Modiolus ventricosus* (Roener), 8. *Pseudokatosira undulata* (Benz), 9. *Placunopsis alpina* (Winkler), 10. *Alsatites* sp., 11. *Pseudokatosira undulata* (Benz), 12. *Mytilus cloacinus* (Tutcher), 13. *Protocardia rhaetica* (Merian), 14. *Permophorus elongatus* (Moore), 15. *Modiolus* sp., 16. *Diademopsis tomesi* (Wright).

Appendix 6.13 1. *Mactromya cardioides* (Phillips), 2. *Chlamys valoniensis* (Defrance), 3. *Liostraea* sp., 4. *Modiolus* sp., 5. *Psiloceras planorbis* (J. Sowerby), 6. *Plagiostoma giganteum* (J. Sowerby), 7. *Ryderia* sp., 8. *Psiloceras erugatum* (Phillips), 9. *Cardinia regularis* (Terquem), 10. *Mytilus cloacinus* (Tutcher), 11. *Cardinia regularis* (Terquem), 12. *Caloceras johnstoni* (Sowerby), 13. *Pteromya langportensis* (Richardson and Tutcher).

Appendix 7.1 List of taxa, modes of life and abundance of each species recorded at each sample along the Portezuelo Providencia section in Chile.

				Height (m)	0.2	4.3	18.2	26.25	30.2	32	33.4	35	36.4	38.1
				Samples	1	2	3	4	6	7	8	9	10	11
				Samples cod	TR-01	TR-02	TR-03	TR-04	J2-CL	J3-CL	J4-CL	J5-CL	J6-CL	J7-CL
Class	Order	Family	Genera and Species	TR1	TR2	TR3	TR4	TR5	TR6	TR7	TR8	TR9	TR10	
Cephalopoda	Ceratitida	Choristoceratidae	<i>Choristoceras</i> sp.	1	1	1	0	0	0	0	0	0	0	0
Cephalopoda	Ammonoidea	Psiloceratidae	<i>Psiloceras primocostatum</i> (Hillebrandt)	0	0	0	0	0	0	0	0	0	0	0
Cephalopoda	Ammonoidea	Psiloceratidae	<i>Storhoceras</i> sp.	0	0	0	0	0	0	0	0	0	0	0
Bivalvia		Oxytomidae	<i>Oxytoma</i> sp.	0	0	0	0	0	0	0	1	0	0	0
Bivalvia		Pectinidae	Pectinidae	0	0	0	0	0	0	0	1	0	0	0
Bivalvia	Pectinoida	Pectinidae	<i>Chlamys</i> sp.	0	1	0	0	0	0	0	0	0	0	0
Bivalvia	Pectinoida	Pectinidae	<i>Chlamys</i> sp 2	0	0	0	0	0	0	0	0	0	0	0
Bivalvia		Entoliidae	<i>Entolium</i> sp	0	0	0	0	0	0	0	0	0	0	0
Bivalvia	Pectinoida	Pectinidae	<i>Eopecten</i> sp.	0	0	0	0	0	0	0	0	0	0	0
Bivalvia		Limidae	<i>Plagiostoma</i> sp.	0	0	0	0	0	0	0	0	0	0	0
Bivalvia	Limoida	Limidae	<i>Pseudolimea</i> sp.	0	1	1	1	0	1	1	0	1	1	1
Bivalvia	Pterioida	Pteriidae	<i>Otapiria</i> sp.	1	1	1	0	1	0	1	0	0	0	0
Bivalvia	Arcoida	Parallelodontidae	<i>Parallelodon</i> sp.	0	0	0	0	0	0	1	0	0	0	0
Bivalvia	Veneroida	Fimbridae	<i>Schafhaeutlia americana</i> (Cox)	0	1	0	0	0	0	6	0	0	0	0
Bivalvia	??	??	Heterodonta	0	0	0	0	0	0	0	1	0	0	0

				Height (m)	39.2	40.2	64.8	70	76.7	78.5	81.9	85.8	104.9
				Samples	12	13	22	23	27	28	29	30	33
				Samples cod	J8-CL	J16-CL	J18-CL	J19-CL	J23-CL	J24-CL	J25-CL	J26-CL	J29-CL
Class	Order	Family	Genera and Species	TR11	JU1	JU2	JU3	JU4	JU5	JU6	JU7	JU8	
Cephalopoda	Ceratitida	Choristoceratidae	<i>Choristoceras</i> sp.	0	0	0	0	0	0	0	0	0	0
Cephalopoda	Ammonoidea	Psiloceratidae	<i>Psiloceras primocostatum</i> (Hillebrandt)	0	0	1	0	0	0	0	0	0	0
Cephalopoda	Ammonoidea	Psiloceratidae	<i>Storhoceras</i> sp.	0	0	0	0	1	0	1	1	0	0
Bivalvia		Oxytomidae	<i>Oxytoma</i> sp.	0	0	0	0	0	0	0	0	0	0
Bivalvia		Pectinidae	Pectinidae	0	0	0	0	0	0	0	0	0	0
Bivalvia	Pectinoida	Pectinidae	<i>Chlamys</i> sp.	0	0	0	1	0	0	0	1	0	0
Bivalvia	Pectinoida	Pectinidae	<i>Chlamys</i> sp 2	0	0	0	1	0	1	0	0	0	0
Bivalvia		Entoliidae	<i>Entolium</i> sp	0	0	0	0	1	0	1	0	1	0
Bivalvia	Pectinoida	Pectinidae	<i>Eopecten</i> sp.	0	0	0	0	0	0	0	0	0	1
Bivalvia	Limoida	Limidae	<i>Plagiostoma</i> sp.	0	0	0	1	0	0	0	0	0	0
Bivalvia	Limoida	Limidae	<i>Pseudolimea</i> sp.	0	0	0	0	0	0	1	0	0	0
Bivalvia	Pterioida	Pteriidae	<i>Otapiria</i> sp.	1	1	0	1	0	0	0	0	0	0
Bivalvia	Arcoida	Parallelodontidae	<i>Parallelodon</i> sp.	0	0	0	0	0	0	0	0	0	0
Bivalvia	Veneroida	Fimbridae	<i>Schafhaeutlia americana</i> (Cox)	0	0	0	0	0	0	0	0	0	0
Bivalvia	??	??	Heterodonta	0	0	0	0	0	0	0	0	0	0

Appendix 7.2 Summary of palaeoecological parameters estimated in this study. S: sample number, SC= Sample cog, Period = TR: Triassic, JU: Jurassic, H = Height (mm), R = Richness, RR: Rarefied richness, K = Kurtosis. LOESS = Loess regression values, 2.5% P = 2.5% Percentile, 97.5% P = 97.5% Percentile and St. Dev.= Standard deviations of the rarefied richness.

S	SC	Period	H	R	LOESS	2.5% P	97.5% P	RR	St. Dev.	K	LOESS	2.5% P	97.5% P
1	TR-01	TR	0.20	2	6.18	5.88	11.37	0.51	0.09	14.54	11.70	-28.58	40.95
2	TR-02	TR	4.30	5	5.43	4.99	9.73	1.84	0.32	8.26	12.22	-21.66	34.94
3	TR-03	TR	18.20	3	2.93	0.71	5.55	0.53	0.11	13.98	13.99	1.92	18.54
4	TR-04	TR	26.25	1	1.64	-0.08	2.86	0.16	0.00	15.00	15.01	2.90	19.48
6	J2-CL	TR	30.20	1	1.00	-1.04	1.80	0.03	0.00	15.00	14.99	11.58	17.83
7	J3-CL	TR	32.00	1	1.00	-1.12	1.70	0.12	0.00	15.00	14.81	12.88	17.14
8	J4-CL	TR	33.40	6	1.00	-1.17	1.73	2.86	0.53	13.94	14.71	12.56	16.66
9	J5-CL	TR	35.00	1	1.00	-0.72	1.62	0.01	0.00	15.00	14.75	12.01	16.73
10	J6-CL	TR	36.40	1	1.00	-0.43	1.74	0.10	0.00	15.00	15.00	12.77	17.09
11	J7-CL	TR	38.10	1	1.00	-0.48	2.04	0.04	0.00	15.00	15.00	12.35	16.77
12	J8-CL	TR	39.20	1	1.00	-0.60	2.45	0.01	0.00	15.00	15.00	10.24	17.31
13	J16-CL	JU	40.20	1	1.00	-0.82	2.78	0.07	0.00	15.00	15.00	6.29	18.46
22	J18-CL	JU	64.80	1	1.74	-1.80	5.74	0.07	0.00	15.00	2.19	-12.85	3.21
23	J19-CL	JU	70.00	4	1.91	-0.50	4.69	0.24	0.03	7.07	7.18	-2.59	8.25
27	J23-CL	JU	76.70	2	2.00	0.46	3.40	0.14	0.03	13.56	13.70	11.61	17.57
28	J24-CL	JU	78.50	1	2.00	0.48	3.23	0.03	0.00	15.00	14.31	12.42	17.04
29	J25-CL	JU	81.90	3	2.00	0.55	3.07	2.01	0.55	14.98	14.71	9.86	17.38
30	J26-CL	JU	85.80	2	2.00	0.31	3.23	0.41	0.10	14.87	15.07	8.94	19.52
33	J29-CL	JU	104.90	2	2.00	-2.35	5.55	0.04	0.00	4.35	4.38	-7.77	8.95

Appendix 7.3 Absolute and relative abundance by taxa (%). TR: Triassic, J: Jurassic.

Period	TR	J	TR (%)	J (%)
<i>Choristoceras</i> sp.	5	0	3.33	0
<i>Pseudolimea</i> sp.	87	1	58	0.90
<i>Otapiria</i> sp.	46	6	30.66	5.40
<i>Parellelodon</i> sp.	1	0	0.66	0
<i>Pectinidae</i>	1	0	0.66	0
<i>Oxytoma</i> sp.	1	0	0.66	0
<i>Shafhaetlia americana</i>	7	0	4.66	0
Heterodonta	1	0	0.66	0
<i>Psiloceras primocostatum</i>	0	5	0	4.50
<i>Chlamys</i> sp.	1	2	0.66	1.80
<i>Storthoceras</i> sp.	0	87	0	78.37
<i>Chlamys</i> sp. 2	0	3	0	2.70
<i>Entolium</i> sp.	0	3	0	2.70
<i>Eopecten</i> sp.	0	1	0	0.90
<i>Plagiostoma</i> sp.	0	3	0	2.70
Abundance	150	111		
Taxa	9	9		

Appendix 7.4 SIMPER analysis. AC: represents the average contribution of the taxon *i* to the average dissimilarity between habitats (overall average = 96.41%). C%: Percentage contribution = average contribution/average dissimilarity between stratigraphic units. Mean abundance of each taxa by period. TR: Triassic and J: Jurassic.

Taxon	AC	C %	TR	J
<i>Pseudolimea</i> sp.	29.2	30.29	7.91	0.125
<i>Storthoceras</i> sp.	23.06	54.21	0	10.9
<i>Otapiria</i> sp.	20.42	75.4	4.18	0.75
<i>Psiloceras primocostatum</i>	5.434	81.03	0	0.625
<i>Chlamys</i> sp2	4.505	85.71	0	0.375
<i>Plagiostoma</i> sp.	2.921	88.74	0	0.375
<i>Entolium</i> sp	2.899	91.74	0	0.375
<i>Eopecten</i> sp.	1.766	93.57	0	0.125
<i>Chlamys</i> sp.	1.546	95.18	0.0909	0.25
Heterodonta	1.538	96.77	0.0909	0
<i>Choristoceras</i> sp.	1.457	98.28	0.455	0
<i>Shafhaetlia americana</i>	1.174	99.5	0.636	0
<i>Oxytoma</i> sp.	0.1604	99.67	0.0909	0
Pectinidae	0.1604	99.83	0.0909	0
<i>Parellelodon</i> sp.	0.1604	100	0.0909	0

Appendix 7.5 Modes of life used by marine fauna recorded in each Period.

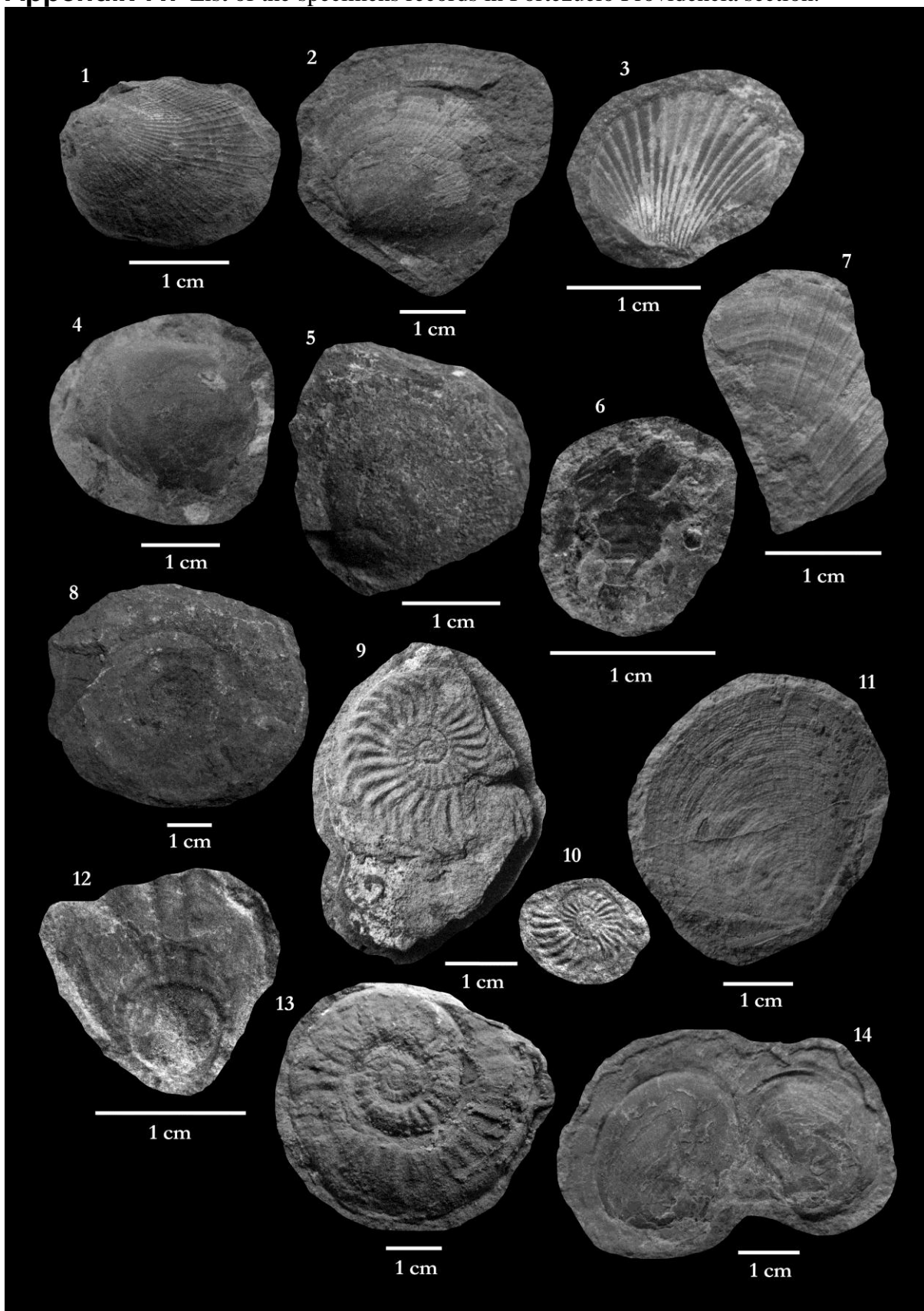
Triassic			
Mode of life			
Taxa	Tiering	Motility	Feeding mechanism
<i>Choristoceras</i> sp.	Pelagic	Fast	Predatory
<i>Oxytoma</i> sp.	Surficial	Facultative Motile Attached	Suspension
Pectinidae	Surficial	Facultative Motile Attached	Suspension
<i>Chlamys</i> sp.	Surficial	Facultative Motile Attached	Suspension
<i>Pseudolimea</i> sp.	Surficial	No motile Attached	Suspension
<i>Otapiria</i> sp.	Surficial	Non-Motile Attached	Suspension
<i>Parallelodon</i> sp.	Semi-infaunal	Facultative No-Motile Attached	Suspension
<i>S. americana</i>	Semi-Infaunal	Facultative Motile Attached	chemosymbiotic
Heterodonta	??	??	??

Jurassic			
Mode of life			
Taxa	Tiering	Taxa	Tiering
<i>P. primocostatum</i>	Pelagic	Fast	Predatory
<i>Storhoceras</i> sp.	Pelagic	Fast	Predatory
<i>Chlamys</i> sp.	Surficial	Facultative Motile Attached	Suspension
<i>Chlamys</i> sp 2	Surficial	Facultative Motile Attached	Suspension
<i>Entolium</i> sp	Surficial	Facultative Motile Attached	Suspension
<i>Eopecten</i> sp.	Surficial	Facultative Motile Attached	Suspension
<i>Plagiostoma</i> sp.	Surficial	Facultative Motile Attached	Suspension
<i>Pseudolimea</i> sp.	Surficial	No motile Attached	Suspension
<i>Otapiria</i> sp.	Surficial	Non-Motile Attached	Suspension

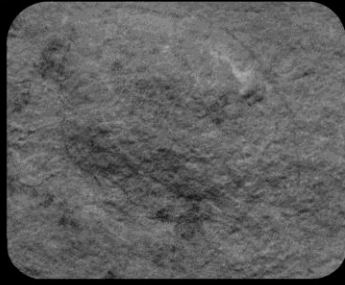
Appendix 7.6 Proportion of mode of life by period. TR: Triassic, J: Jurassic.

Ecological categories	TR	J
Pelagic	0.125	0.2222
Erect	0	0
Surficial	0.625	0.777
Semi-infaunal	0.25	0
Shallow-infaunal	0	0
Deep-infaunal	0	0
Fast	0.125	0.2222
Slow	0	0
Facultative-unattached	0.375	0.5556
Facultative-attached	0.25	0
No motile Unttached	0	0
No motile Attached	0.25	0.222
Suspension	0.75	0.7777
Surface deposit	0	0
Mining	0	0
Grazing	0	0.2222
Predatory	0.125	0
Other	0.125	0

Appendix 7.7 List of the specimens records in Portezuelo Providencia section.

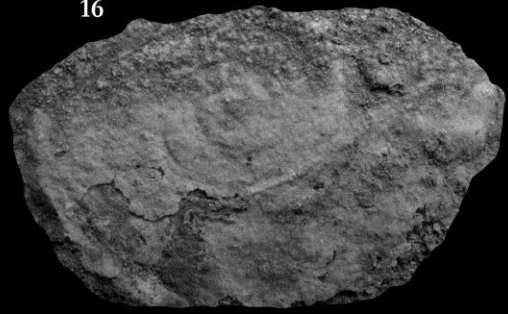


15



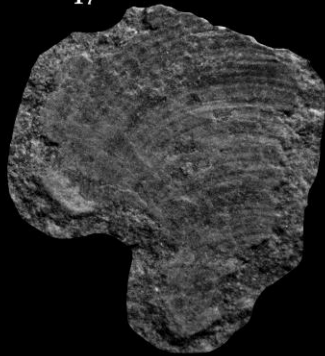
1 cm

16



1 cm

17



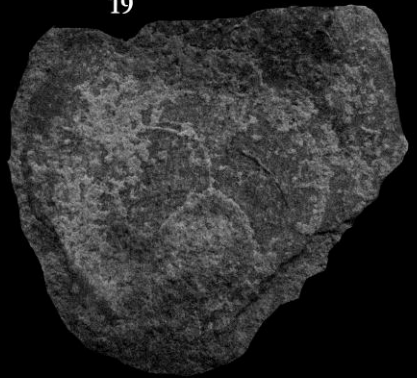
1 cm

18



1 cm

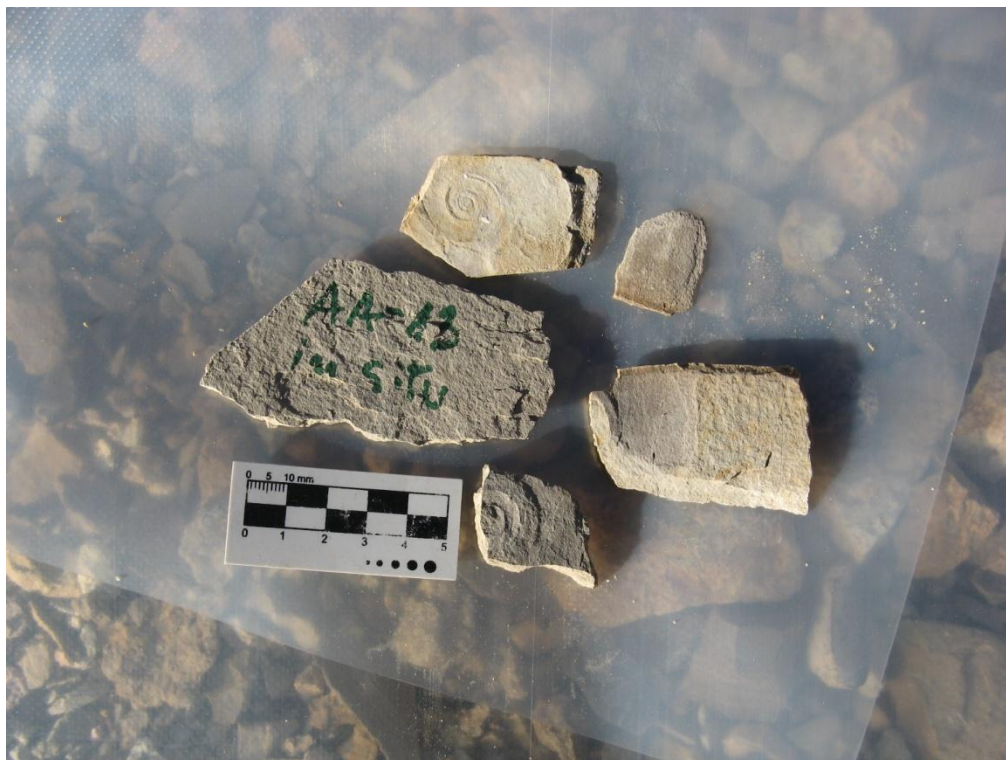
19



1 cm

Appendix 7.7 (Continuation) List of specimens: 1: *Pseudolimea* sp., 2: *Chlamys* sp.1., 3: *Pseudolimea* sp., 4-5: *Schafhaeutlia Americana* (cox, 1949), 6: *Otapiria* sp. , 7: *Oxytoma* sp., 8: *Psiloceras primocostatum* (Hillebrandt, 1988), 9-10: *Storhoceras* sp., 11: *Chlamys* sp.2., 12: *Eopecten* sp., 13: *Storhoceras* sp., 14: *Otapiria* sp., 15: *Heterodonta*, 16: *P. primocostatum*, 17: *Entolium* sp, 18: *Choristoceras* sp., 19: *Plagiostoma* sp.

Appendix 7.8 *Psiloceras* sp. recorded at 40.20 m above the base of the section.



Appendix 8.1 Compositional change of the Tr/J boundary marine palaeocommunities recorded in UK. The red line represents the trajectory of the community through the Tr/J boundary. This pattern indicates that changes in species composition could be due to changes in sea level. WF: The Westbury Formation; CM: The Cotham Member; LM: The Langport Member; PPZ: The Pre-Planorbis Zone; PZ: The Planorbis Zone; LZ: Liasicus Zone. Stars: Centroid of each stratigraphic unit.

